

# Targeting autophagy in cancer therapy: Focus on small-molecule modulators and new strategies

**Edited by**

Chen Yi, Ryszard Pluta, Guan Wang, Liang Ouyang and Bo Liu

**Published in**

Frontiers in Pharmacology

Frontiers in Oncology



## FRONTIERS EBOOK COPYRIGHT STATEMENT

The copyright in the text of individual articles in this ebook is the property of their respective authors or their respective institutions or funders. The copyright in graphics and images within each article may be subject to copyright of other parties. In both cases this is subject to a license granted to Frontiers.

The compilation of articles constituting this ebook is the property of Frontiers.

Each article within this ebook, and the ebook itself, are published under the most recent version of the Creative Commons CC-BY licence. The version current at the date of publication of this ebook is CC-BY 4.0. If the CC-BY licence is updated, the licence granted by Frontiers is automatically updated to the new version.

When exercising any right under the CC-BY licence, Frontiers must be attributed as the original publisher of the article or ebook, as applicable.

Authors have the responsibility of ensuring that any graphics or other materials which are the property of others may be included in the CC-BY licence, but this should be checked before relying on the CC-BY licence to reproduce those materials. Any copyright notices relating to those materials must be complied with.

Copyright and source acknowledgement notices may not be removed and must be displayed in any copy, derivative work or partial copy which includes the elements in question.

All copyright, and all rights therein, are protected by national and international copyright laws. The above represents a summary only. For further information please read Frontiers' Conditions for Website Use and Copyright Statement, and the applicable CC-BY licence.

ISSN 1664-8714  
ISBN 978-2-83251-574-7  
DOI 10.3389/978-2-83251-574-7

## About Frontiers

Frontiers is more than just an open access publisher of scholarly articles: it is a pioneering approach to the world of academia, radically improving the way scholarly research is managed. The grand vision of Frontiers is a world where all people have an equal opportunity to seek, share and generate knowledge. Frontiers provides immediate and permanent online open access to all its publications, but this alone is not enough to realize our grand goals.

## Frontiers journal series

The Frontiers journal series is a multi-tier and interdisciplinary set of open-access, online journals, promising a paradigm shift from the current review, selection and dissemination processes in academic publishing. All Frontiers journals are driven by researchers for researchers; therefore, they constitute a service to the scholarly community. At the same time, the *Frontiers journal series* operates on a revolutionary invention, the tiered publishing system, initially addressing specific communities of scholars, and gradually climbing up to broader public understanding, thus serving the interests of the lay society, too.

## Dedication to quality

Each Frontiers article is a landmark of the highest quality, thanks to genuinely collaborative interactions between authors and review editors, who include some of the world's best academicians. Research must be certified by peers before entering a stream of knowledge that may eventually reach the public - and shape society; therefore, Frontiers only applies the most rigorous and unbiased reviews. Frontiers revolutionizes research publishing by freely delivering the most outstanding research, evaluated with no bias from both the academic and social point of view. By applying the most advanced information technologies, Frontiers is catapulting scholarly publishing into a new generation.

## What are Frontiers Research Topics?

Frontiers Research Topics are very popular trademarks of the *Frontiers journals series*: they are collections of at least ten articles, all centered on a particular subject. With their unique mix of varied contributions from Original Research to Review Articles, Frontiers Research Topics unify the most influential researchers, the latest key findings and historical advances in a hot research area.

Find out more on how to host your own Frontiers Research Topic or contribute to one as an author by contacting the Frontiers editorial office: [frontiersin.org/about/contact](https://frontiersin.org/about/contact)

# Targeting autophagy in cancer therapy: Focus on small-molecule modulators and new strategies

## Topic editors

Chen Yi — Sichuan University, China

Ryszard Pluta — Laboratory of Ischemic and Neurodegenerative Brain Research, Mossakowski Medical Research Institute (PAS), Poland

Guan Wang — Sichuan University, China

Liang Ouyang — Sichuan University, China

Bo Liu — Sichuan University, China

## Citation

Yi, C., Pluta, R., Wang, G., Ouyang, L., Liu, B., eds. (2023). *Targeting autophagy in cancer therapy: Focus on small-molecule modulators and new strategies*. Lausanne: Frontiers Media SA. doi: 10.3389/978-2-83251-574-7

# Table of contents

- 04 **Editorial: Targeting autophagy in Cancer Therapy: Focus on small-molecule modulators and new strategies**  
Ryszard Pluta
- 06 **AMTDB: A comprehensive database of autophagic modulators for anti-tumor drug discovery**  
Jiahui Fu, Lifeng Wu, Gaoyong Hu, Qiqi Shi, Ruodi Wang, Lingjuan Zhu, Haiyang Yu and Leilei Fu
- 16 **Inhibiting Cytoprotective Autophagy in Cancer Therapy: An Update on Pharmacological Small-Molecule Compounds**  
Lijuan Zhang, Yuxuan Zhu, Jiahui Zhang, Lan Zhang and Lu Chen
- 35 **The crosstalk between sonodynamic therapy and autophagy in cancer**  
Yujie Zhang, Yuanru Zhao, Yuanyuan Zhang, Qingguang Liu, Mingzhen Zhang and Kangsheng Tu
- 58 **Upregulation of nuclear division cycle 80 contributes to therapeutic resistance *via* the promotion of autophagy-related protein-7-dependent autophagy in lung cancer**  
Xi Chen, Qingchun He, Shuangshuang Zeng and Zhijie Xu
- 73 **Review of various NAMPT inhibitors for the treatment of cancer**  
Yichen Wei, Haotian Xiang and Wenqiu Zhang
- 96 **Deconvoluting the complexity of autophagy in colorectal cancer: From crucial pathways to targeted therapies**  
Liming Qiang, Hongpeng Li, Zhaohui Wang, Lin Wan and Guangfu Jiang
- 106 **Suppression of endoplasmic reticulum stress-dependent autophagy enhances cynaropicrin-induced apoptosis via attenuation of the P62/Keap1/Nrf2 pathways in neuroblastoma**  
Randong Yang, Shurong Ma, Ran Zhuo, Lingqi Xu, Siqi Jia, Pengcheng Yang, Ye Yao, Haibo Cao, Liya Ma, Jian Pan and Jian Wang
- 122 **Unravelling the roles of Autophagy in OSCC: A renewed perspective from mechanisms to potential applications**  
Qitong Gou, Ling-Li Zheng and Haixia Huang
- 134 **Discovery of novel anti-tumor compounds targeting PARP-1 with induction of autophagy through *in silico* and *in vitro* screening**  
Danfeng Shi, Qianqian Pang, Qianyu Qin, Xinsheng Yao, Xiaojun Yao and Yang Yu
- 149 **Targeting autophagy in pancreatic cancer: The cancer stem cell perspective**  
Dimitrios Troumpoukis, Adriana Papadimitropoulou, Chrysanthi Charalampous, Paraskevi Kogionou, Kostas Palamaris, Panagiotis Sarantis and Ioannis Serafimidis





## OPEN ACCESS

EDITED AND REVIEWED BY  
Olivier Feron,  
Université catholique de Louvain, Belgium

## \*CORRESPONDENCE

Ryszard Pluta,  
✉ [pluta@imdik.pan.pl](mailto:pluta@imdik.pan.pl),  
✉ [pluta2018@wp.pl](mailto:pluta2018@wp.pl)

## SPECIALTY SECTION

This article was submitted to  
Pharmacology of Anti-Cancer Drugs,  
a section of the journal  
Frontiers in Pharmacology

RECEIVED 15 January 2023

ACCEPTED 23 January 2023

PUBLISHED 01 February 2023

## CITATION

Pluta R (2023), Editorial: Targeting  
autophagy in Cancer Therapy: Focus on  
small-molecule modulators and  
new strategies.  
*Front. Pharmacol.* 14:1145255.  
doi: 10.3389/fphar.2023.1145255

## COPYRIGHT

© 2023 Pluta. This is an open-access  
article distributed under the terms of the  
[Creative Commons Attribution License](https://creativecommons.org/licenses/by/4.0/)  
(CC BY). The use, distribution or  
reproduction in other forums is permitted,  
provided the original author(s) and the  
copyright owner(s) are credited and that  
the original publication in this journal is  
cited, in accordance with accepted  
academic practice. No use, distribution or  
reproduction is permitted which does not  
comply with these terms.

# Editorial: Targeting autophagy in Cancer Therapy: Focus on small-molecule modulators and new strategies

Ryszard Pluta\*

Ecotech-Complex Analytical and Programme Centre for Advanced Environmentally-Friendly Technologies,  
University of Marie Curie-Skłodowska, Lublin, Poland

## KEYWORDS

cancer, autophagy, therapy, small-molecule modulators, new strategies

## Editorial on the Research Topic

[Targeting autophagy in Cancer Therapy: Focus on small-molecule modulators and new strategies](#)

Cancers are one of the deadliest and most difficult to treat diseases in the world. The incidence of tumors in humans is constantly increasing and is one of the main challenges facing the health service. During the last 2 decades, remarkable advances have been made in diagnosing and developing new drugs to treat cancers through the use of genomics and high-throughput screening. Among them, autophagy plays an important role in tumors. Originally described as the phenomenon of removal and recovery of intracellular waste, autophagy has become a key biological process closely related to many types of cancer, suggesting that autophagy intervention is a promising therapeutic strategy in the development of anti-cancer drugs. Therefore, the discovery of cancer-related targets of autophagy and the related mechanisms of action of targeted small molecule drugs is of paramount importance. Autophagy plays a dynamic role in the inhibition or propagation of a tumor depending on its stage of development. In the early stages of tumor development, autophagy, as a survival and quality control phenomenon, prevents tumor formation. However, when cancers are at an advanced stage, autophagy, as a dynamic degradation and recycling system, contributes to the survival and growth of the tumors and promotes their spread through metastasis.

Although the pathology of cancer is fairly well understood, until recently we knew little about its molecular regulation. These mechanisms and their subsequent therapeutic orientation are the subject of our Research Topic. Of the 10 articles published on our Research Topic, four were original studies and six were reviews of currently known and emerging therapeutic targets for cancer treatment.

Thus, a high-quality database is crucial to elucidate the complicated relationship between autophagy and cancers, elucidate the crosstalk between key autophagy mechanisms and autophagy modulators with their remarkable anticancer activities. To achieve this goal, [Fu et al.](#) developed an extensive database of autophagic modulators that provided users with a high-quality practical online platform. Autophagic modulators database focuses on 153 tumor types, 1153 autophagic regulators including 903 activating, 191 inhibitory and 59 bidirectional compounds, 860 targets and 2046 signaling pathways ([Fu et al.](#)). Another original study by [Yang et al.](#) showed that cinaropicrin inhibited the growth of neuroblastoma cells *in vitro* and *in vivo*, through a mechanism involving endoplasmic reticulum stress/autophagy/NRF2 signaling/

apoptosis. They provided insights into the mechanisms by which cynaropicrin induces apoptosis and endoplasmic reticulum stress-mediated protective autophagy (Yang et al.). This study indicated that cynaropicrin may be a potential antitumor agent for neuroblastoma prevention and treatment (Yang et al.). This study provided a basis for future preclinical and clinical trial exploration to improve the efficacy of cynaropicrin in neuroblastoma treatment. Chen et al. study presented that nuclear division cycle 80 might be a diagnostic and prognostic biomarker in lung cancer. Furthermore, elevated nuclear division cycle 80 expressions were detected in ionizing radiation resistant non-small lung cancer cells, and was found to induce radiation resistance (Chen et al.). These findings provide novel insights into the effect of nuclear division cycle 80 on radioresistance in cancer cells, and suggest that nuclear division cycle 80 could serve as a drug target for improving radiosensitivity (Chen et al.). Last original work by Shi et al. discovered by *in silico* and *in vitro* screening four compounds 8012-0567, 8018-6529, 8018-7168 and 8018-7603 with inhibitory activities target PARP-1. Further cell assays showed that compounds 8018-6529 and 8018-7168 could inhibit the growth of the human colorectal cancer cell with an induced autophagy process and provide potential hit compounds for the development anti-cancer drug (Shi et al.).

Therefore, the autophagy pathway is highly drug-sensitive and has multiple drug targets. The inhibition of cytoprotective autophagy in the treatment of cancer is gaining importance as a potentially new therapeutic approach in the treatment of cancer (Zhang et al.). From a clinical perspective, new inhibitors targeting autophagy modulation are currently under investigation and small molecule inhibitors continue to show promise in cancer treatment (Zhang et al.). Review by Wei et al. summarizes the experimental validation and practical application of the strategies using specific and dual inhibitors, drug combinations and antibody-drug conjugates, with the intention of aiding and inspiring future research on nicotinamide phosphoribosyltransferase-targeted oncology drugs. The further development and design of novel, selective, highly efficient, low toxicity and low molecular weight nicotinamide phosphoribosyltransferase inhibitors will not only help basic pathology study, but also bring great hope for the clinical therapy of tumors involving nicotinamide phosphoribosyltransferase to the benefit of more patients (Wei et al.). A promising cancer treatment, which combines sonodynamic therapy with autophagy inhibition using a nanoparticle delivering system, is presented by Zhang et al. Authors speculated that the combination of targeted delivery of sonosensitizer and inhibition of autophagy can effectively kill cancer cells and also avoid the activation of protective-autophagy by increasing the production of reactive oxygen species (Zhang et al.). Autophagy connected genes,

miRNAs, lncRNAs, and circRNAs have been described as autophagy biomarkers. As well, developing specially designed drugs for the abovementioned autophagy-associated biomarkers by high-throughput screening, molecular docking, and molecular dynamic simulation may be promising in improving oral squamous cell carcinoma therapy (Gou et al.). Qiang et al. presented that modulating autophagy has been emerging as a promising strategy for colorectal tumor therapy, which can benefit the patients who are not suitable for traditional treatment, and can be used as adjuvant, polypeptides, and small-molecule compounds, photodynamic and non-coding RNAs chemotherapies to overcome drug resistance. New experimental facts, from *in vitro* and *in vivo* investigations, suggest a context-dependent anticancer manifestation of autophagy, mediated by an injurious consequence on cancer stem cell survival and metastasis (Troupoukis et al.). Even though autophagy is a process opposite to apoptosis, evident autophagic influx can in fact trigger apoptosis under certain conditions by activation of caspase eight and the reduction of endogenous apoptosis inhibitors (Troupoukis et al.).

Taken together, the identification of new drug targets and the development of new treatment strategies based on them offer the exciting prospect of more effective therapies in the treatment of cancers. I thank the authors for their contributions and hope that each article on this Research Topic will both inform and generate further interest in the effective treatment of tumors.

## Author contributions

RP prepared and approved manuscript for publication.

## Conflict of interest

The author declares that the research was conducted in the absence of any commercial or financial relationships that could be construed as a potential conflict of interest.

## Publisher's note

All claims expressed in this article are solely those of the authors and do not necessarily represent those of their affiliated organizations, or those of the publisher, the editors and the reviewers. Any product that may be evaluated in this article, or claim that may be made by its manufacturer, is not guaranteed or endorsed by the publisher.



## OPEN ACCESS

## EDITED BY

Jianxun Ding,  
Changchun Institute of Applied  
Chemistry (CAS), China

## REVIEWED BY

Yi Dai,  
Jinan University, China  
Xiaoxiao Huang,  
Shenyang Pharmaceutical University,  
China

## \*CORRESPONDENCE

Leilei Fu,  
leilei\_fu@163.com  
Haiyang Yu,  
hyu@tjutcm.edu.cn  
Lingjuan Zhu,  
zhulingjuanadele@163.com

\*These authors have contributed equally  
to this work

## SPECIALTY SECTION

This article was submitted to  
Pharmacology of Anti-Cancer Drugs,  
a section of the journal  
Frontiers in Pharmacology

RECEIVED 30 May 2022

ACCEPTED 11 July 2022

PUBLISHED 09 August 2022

## CITATION

Fu J, Wu L, Hu G, Shi Q, Wang R, Zhu L,  
Yu H and Fu L (2022), AMTDB: A  
comprehensive database of autophagic  
modulators for anti-tumor  
drug discovery.  
*Front. Pharmacol.* 13:956501.  
doi: 10.3389/fphar.2022.956501

## COPYRIGHT

© 2022 Fu, Wu, Hu, Shi, Wang, Zhu, Yu  
and Fu. This is an open-access article  
distributed under the terms of the  
[Creative Commons Attribution License](https://creativecommons.org/licenses/by/4.0/)  
(CC BY). The use, distribution or  
reproduction in other forums is  
permitted, provided the original  
author(s) and the copyright owner(s) are  
credited and that the original  
publication in this journal is cited, in  
accordance with accepted academic  
practice. No use, distribution or  
reproduction is permitted which does  
not comply with these terms.

# AMTDB: A comprehensive database of autophagic modulators for anti-tumor drug discovery

Jiahui Fu<sup>1†</sup>, Lifeng Wu<sup>2,3†</sup>, Gaoyong Hu<sup>4†</sup>, Qiqi Shi<sup>1</sup>, Ruodi Wang<sup>1</sup>,  
Lingjuan Zhu<sup>1\*</sup>, Haiyang Yu<sup>4\*</sup> and Leilei Fu<sup>2\*</sup>

<sup>1</sup>School of Traditional Chinese Materia Medica, Key Laboratory of Structure-Based Drug Design and Discovery, Ministry of Education, Shenyang Pharmaceutical University, Shenyang, China, <sup>2</sup>Sichuan Engineering Research Center for Biomimetic Synthesis of Natural Drugs, School of Life Science and Engineering, Southwest Jiaotong University, Chengdu, China, <sup>3</sup>State Key Laboratory of Biotherapy and Cancer Center, West China Hospital, Sichuan University, Chengdu, China, <sup>4</sup>State Key Laboratory of Component-based Chinese Medicine, Tianjin University of Traditional Chinese Medicine, Tianjin, China

Autophagy, originally described as a mechanism for intracellular waste disposal and recovery, has been becoming a crucial biological process closely related to many types of human tumors, including breast cancer, osteosarcoma, glioma, etc., suggesting that intervention of autophagy is a promising therapeutic strategy for cancer drug development. Therefore, a high-quality database is crucial for unraveling the complicated relationship between autophagy and human cancers, elucidating the crosstalk between the key autophagic pathways, and autophagic modulators with their remarkable antitumor activities. To achieve this goal, a comprehensive database of autophagic modulators (AMTDB) was developed. AMTDB focuses on 153 cancer types, 1,153 autophagic regulators, 860 targets, and 2,046 mechanisms/signaling pathways. In addition, a variety of classification methods, advanced retrieval, and target prediction functions are provided exclusively to cater to the different demands of users. Collectively, AMTDB is expected to serve as a powerful online resource to provide a new clue for the discovery of more candidate cancer drugs.

## KEYWORDS

AMTDB, database, autophagy, autophagic modulator, anti-tumor drug

**Abbreviations:** 3-MA, 3-methyladenine; AMTDB, a comprehensive database of autophagy regulators; AMPK, adenosine 5-monophosphate activated protein kinase; AJAX, asynchronous JavaScript and XML; CQ, chloroquine; GO, gene ontology; HCQ, hydroxychloroquine; HIFs, hypoxia-inducible factors; IUPAC, international union of pure and applied chemistry; LC3, microtubule-associated protein 1 light chain 3; ncRNAs, non-coding RNAs; ROS, reactive oxygen species; TFEB, transcription factor EB; ULK1, Unc-51-like kinase 1.

## Introduction

Autophagy is the process by which cells clean up abnormal and redundant substances, such as proteins, nucleic acids, and damaged organelles, and produce new substances for reuse by the body. Normally, autophagy is maintained within a reasonable range, which is beneficial to keep human cells healthy, resist aging and resist the invasion of diseases (Aman et al., 2021). Nonetheless, abnormal autophagy can have a significant impact on the occurrence and development of diseases, which are fully unraveled by tumor diseases. On the one hand, autophagy removes impaired mitochondria and attenuates the production of reactive oxygen species (ROS), thereby avoiding the accumulation of DNA damage, which may induce tumorigenesis and development and increase susceptibility to cancer. (Filomeni et al., 2015). In addition, activated autophagy induces programmed cell death and restrains tumor cell growth (Meyer et al., 2021). Similarly, autophagy together with ubiquitinated proteins can mediate the clearance of p62, an adaptor protein that binds microtubule-associated protein 1 light chain 3 (LC3) to ubiquitin on ubiquitin and is upregulated in cancer cells, and induction of autophagy can alleviate p62 accumulation and inhibit tumorigenesis (Mathew et al., 2009). On the other hand, autophagy provides sufficient energy and nutrients for the rapid division of cancer cells, especially in areas of low perfusion where nutrients and oxygen are limited. Activated autophagy protects tumor cells from the control of therapeutic drugs or increases drug resistance to interfere with the therapeutic effect (Zhang et al., 2015; Zhuang et al., 2022). Therefore, manipulating autophagy with compounds is a promising approach to tumor intervention, which plays the purpose of treating tumors by inhibiting autophagy and inducing autophagy to prevent the occurrence of tumors.

Recently, increasingly autophagy regulators have been reported, such as BL-918, NVP-BEZ235, perifosine, 3-methyladenine (3-MA), and so on. In particular, the successful use of chloroquine (CQ) and hydroxychloroquine (HCQ) in clinical practice have greatly stimulated the design and development of autophagy regulators (Fu et al., 2022). Protein kinases like adenosine 5-monophosphate activated protein kinase (AMPK), AKT, unc-51-like kinase 1 (ULK1), transcription factors such as transcription factor EB (TFEB), and hypoxia-inducible factors (HIFs), other “druggable” targets as Dopamine receptors, adrenergic receptors, etc. are all regulatory targets of autophagy compounds (Zhang et al., 2017; Li et al., 2021; Zhang et al., 2021). Herein, it is very important to establish a comprehensive information platform to collect the above information.

Although some online resources, including ACDB, HAMdb, and PubMed, have provided chemical information on autophagy regulators and autophagy-related genes, these databases only contain partial information and have not been effectively organized. The accumulating deposited autophagy compounds

and targets, the development of antitumor drugs, and the elucidation of the relationship between tumors and autophagy all urgently require the emergence of a new database. In such cases, we focused on compounds and targets, and constructed a comprehensive database of autophagy modulators (AMTDB), providing users with a high-quality and practical online platform. Information such as International Union of Pure and Applied Chemistry (IUPAC) Name, CAS, tumor type, and molecular mechanism are all covered comprehensively. Importantly, the AMTDB database also provides target prediction services, to provide potential targets for the discovery of autophagy regulators, paving a creditable avenue for the development of anti-tumor drugs.

## Materials and methods

### Data collection and curation

AMTDB is a comprehensive pool of compounds and proteins, and its total data collection and curation process is shown in Figure 1. Using “ [autophagy (Title/Abstract)] AND {[inhibitor (Title/Abstract) OR activator (Title/Abstract) OR agonist (Title/Abstract) OR antagonist (Title/Abstract)]}” as the search term, we performed text mining on 11,523 articles, collected from PubMed, including research articles and reviews, and manually typed in 1,153 autophagy regulators and 297 targets. Of course, in order to ensure the reliability of the data, a third person was allowed to verify the original data set. Notably, articles that did not introduce autophagy compounds were considered negatives, and repeated data were considered false positives, which were not recognized and included. Finally, after the above data processing is completed, a simple random sampling method is used to confirm the final data. The data number is obtained by the function “= RAND ()” in EXCEL. For these modulators, we have retained and supplemented information such as compound structure, SMILES, IUPAC Name, CAS numbers, and references. At the same time, we also summarized its effect on autophagy (e.g., activating/inhibiting), molecular mechanism, and tumor content. Importantly, the regulatory targets of compounds were the focus of our emphasis.

Two approaches were used to gather gene and protein information. One is based on the autophagy-related genes provided by the existing Gene Ontology (GO) and HADb databases, and the two data collections were summarized and eliminated to obtain 660 genes in total. Another way is to add new data from the compound targets that have been sorted out (i.e., reported in the literature). All the above gene/protein information was cleaned again with the ID provided by UniProt, and 860 key information was finally obtained. Notably, given that the database is intended to assist in the design and discovery of new anti-tumor drugs, here the UniProt ID corresponds to *Homo sapiens*, and homology mapping is required if other species are to be studied.

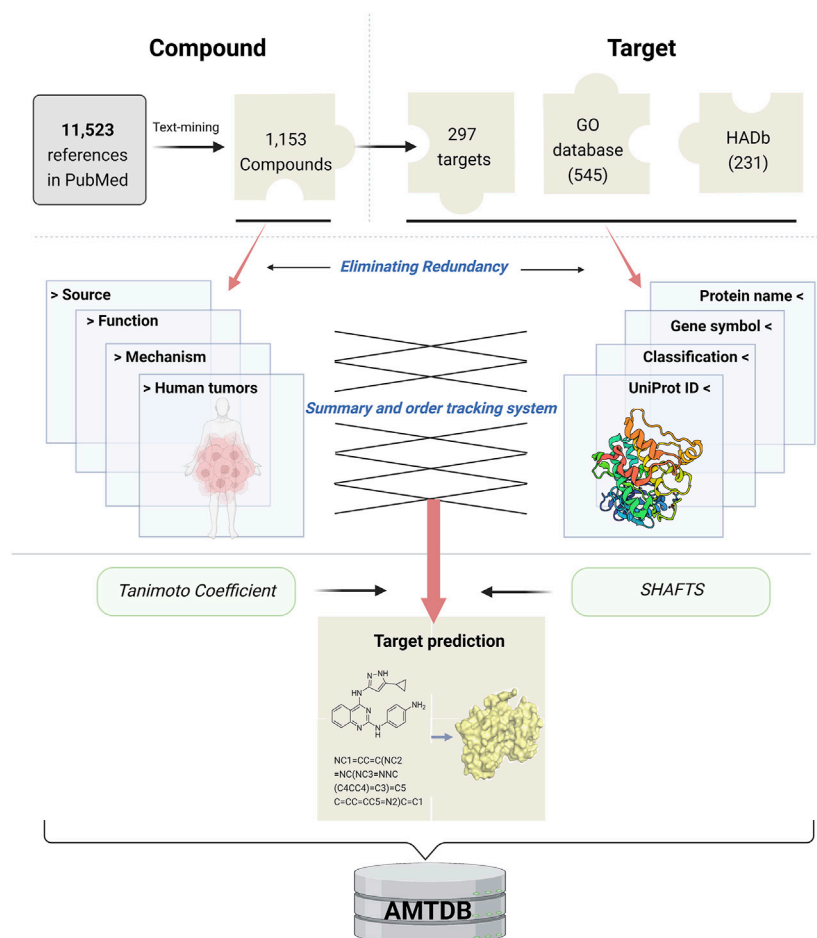


**FIGURE 1**  
A logical framework of AMTDB.

The above data are collected and collated using multiple databases, as shown below:

Chemical Book (<https://www.chemicalbook.com/>)  
 GO database (<http://geneontology.org/>)  
 HADb (<http://www.autophagy.lu/>)  
 MCE (<https://www.medchemexpress.cn/>)  
 PubChem (<https://pubchem.ncbi.nlm.nih.gov/>)  
 PubMed (<https://pubmed.ncbi.nlm.nih.gov/>)  
 UniProt (<https://www.uniprot.org/>)  
 Web of Science (<http://www.webofscience.com/>)  
 SciFinder (<https://scifinder.cas.org/>)

## Classification principles for data

To manage and account for the above data more clearly, we have implemented various classification standards for autophagy modulators and autophagy-related genes/proteins respectively,

which also provides convenient retrieval for users. First, compounds are divided into four categories based on their source: 1) compounds organically synthesized compounds; 2) monomers isolated from natural products; 3) derivatives and metabolites; 4) extracts and compound preparations. Notably, the derivatives included in AMTDB refer to the more complex products derived from the structure of monomers (obtained from natural products) in which hydrogen atoms or groups are replaced by other atoms or groups. For example, quinoline derivatives of tetrahydrocurcumin and zingerone, 3-Acetyl dihydroxy-olide oleanolic derivative, etc. Secondly, compounds are classified as activator and inhibitor according to their effects on autophagy. In this context, the above concept has been redefined, for example, activator means those that induce autophagy, promote autophagy or increase autophagosome/flux either directly or indirectly. Instead, compounds that block, inhibit, and reduce autophagy, a biological process, are defined as inhibitors. Notably, some compounds have different autophagy effects in different diseases. In terms of gene and protein, type I



TABLE 1 Similarity calculation formula.

	Formula	References
<i>Tanimoto Coefficient</i> <sup>a</sup>	<p>The formula for continuous variables</p> $S_{A,B} = \frac{\left[ \sum_{j=1}^n x_{jA} x_{jB} \right]}{\left[ \sum_{j=1}^n (x_{jA})^2 + \sum_{j=1}^n (x_{jB})^2 - \sum_{j=1}^n x_{jA} x_{jB} \right]}$	<p>The formula for dichotomous variables</p> $S_{A,B} = c/[a + b - c]$ <p>Bajusz et al. (2015)</p>
<i>SHAFTS</i> <sup>b</sup>	<p>Shape Score</p> $V_{AB} = \sum_{i \in A} \sum_{j \in B} \int d\vec{r} \rho_i(\vec{r}) \rho_j(\vec{r}) = \sum_{i \in A} \sum_{j \in B} p_i p_j \exp\left(-\frac{\gamma_i \gamma_j}{\gamma_i + \gamma_j}\right) \left(\frac{\pi}{\gamma_i + \gamma_j}\right)^{\frac{3}{2}}$ $\text{Shape Score} = \frac{V_{AB}}{\sqrt{V_A V_B}}$	<p>Feature Score</p> $F_{AB} = \sum_{f \in F} \sum_{i \in A} \sum_{j \in B} \exp\left[-2.5 \left(\frac{d_{ij}}{R_f}\right)^2\right]$ $\text{Feature Score} = \frac{F_{AB}}{\sqrt{F_A F_B}}$ <p>Liu et al. (2011)</p>
<b>Hybrid Score = Shape Score + <math>\omega</math> · Feature Score</b>		

<sup>a</sup> $x_{jA}$  means the  $j$ -th feature of molecule  $A$ .  $a$  is the number of *on* bits in molecule  $A$ ,  $b$  is number of *on* bits in molecule  $B$ , while  $c$  is the number of bits that are *on* in both molecules. <sup>b</sup> $i$  and  $j$  represent atoms  $A$  and  $B$  respectively;  $d_{ij}$ : the interatomic distance between atom  $i$  and  $j$ ;  $\gamma$ : is the width of a Gaussian which is relevant with atomic van der Waals radii, where  $i$  and  $j$  run over the feature points with the same type  $f$  in  $A$  and  $B$ , respectively,  $d_{ij}$  is the distance between point  $i$  and  $j$ , and  $R_f$  is the overlap tolerance with a default value of 0.8 Å.  $\omega$  default weighting factor of 1.0

refers to that the gene has been both reported in the literature and included in the autophagy-related database. Type II is only predicted by the database as autophagy-related genes, but there is no literature to support it, which is a potential target for designing autophagy modulators. Gene that do not fall into the above two categories are automatically classified as type III, which are mostly inherent targets of compounds and are later found to regulate autophagy.

### Similarity calculations

Compounds that can exert biological activity to achieve the purpose of treating diseases are mediated by the binding of their molecules to biological macromolecules such as proteins in the body, which requires the support of binding pockets. The more similar the compounds are, the more likely they are to act on the target with the same spatial configuration. It is well known that virtual screening based on molecular similarity is based on the “similarity hypothesis,” that is, compounds with similar structures have similar physical chemistry information and biological activities (Pavadai et al., 2017). Currently, molecular similarity can be evaluated using descriptors at both 2D and 3D levels. 2D descriptors are calculated from 2D molecular graphs or structural fragments, such as topological indices, molecular fingerprints, etc. For example, a fingerprint is a representation of the molecular structure of a binary format, in which the overlap between molecular fingerprints is used to calculate the Structural similarity between molecules (Maggiora et al., 2014). *Tanimoto Coefficient* is widely used in 2D molecular similarity calculation because of its fast and simple calculation speed (Racz et al., 2018).

Since compounds are essentially three-dimensional, the complex spatial conformation contains much richer information. Therefore, similarity assessment by 3D shape is also allowed, depending on the degree of molecular shape overlap. The *SHAFTS* algorithm uses the descriptor to calculate the shape

score and the feature score respectively, and the addition of the two is the final evaluation standard (Gong et al., 2013). Table 1.

### Website design

We have a detailed plan for long-term maintenance and changes to the database. AMTDB is deployed on a Linux server and integrates the collated valid data into a MySQL database. We adopted a lightweight Web server (Ngnix version 1.8.1) that alleviates memory pressure and supports responses up to 50,000 concurrent connections (Ma and Chi, 2022). In addition, the Django (version 3.2.13) framework, written in Python, is used to render the Graphical User Interface. The web front end consists of Bootstrap and Asynchronous JavaScript and XML (AJAX) to asynchronously update data and refresh portions of the page. Google Chrome, Safari, and Firefox all have friendly access to the AMTDB (<https://amtdb.vercel.app/>).

### Results

#### Contents of a comprehensive database of autophagy modulators

The AMTDB database, a comprehensive database of autophagy regulators and autophagy-related genes, is dedicated to elucidating the important role of autophagy as a biological process in tumors.

Through text mining of 11,523 published references, we finally obtained 1,153 autophagy regulators, 860 targets, 153 diseases, and involved 2,046 molecular mechanisms. Notably, autophagy-related genes in the GO database and HADb database were included in the AMTDB database as potential targets. The database provides the UniProt ID,

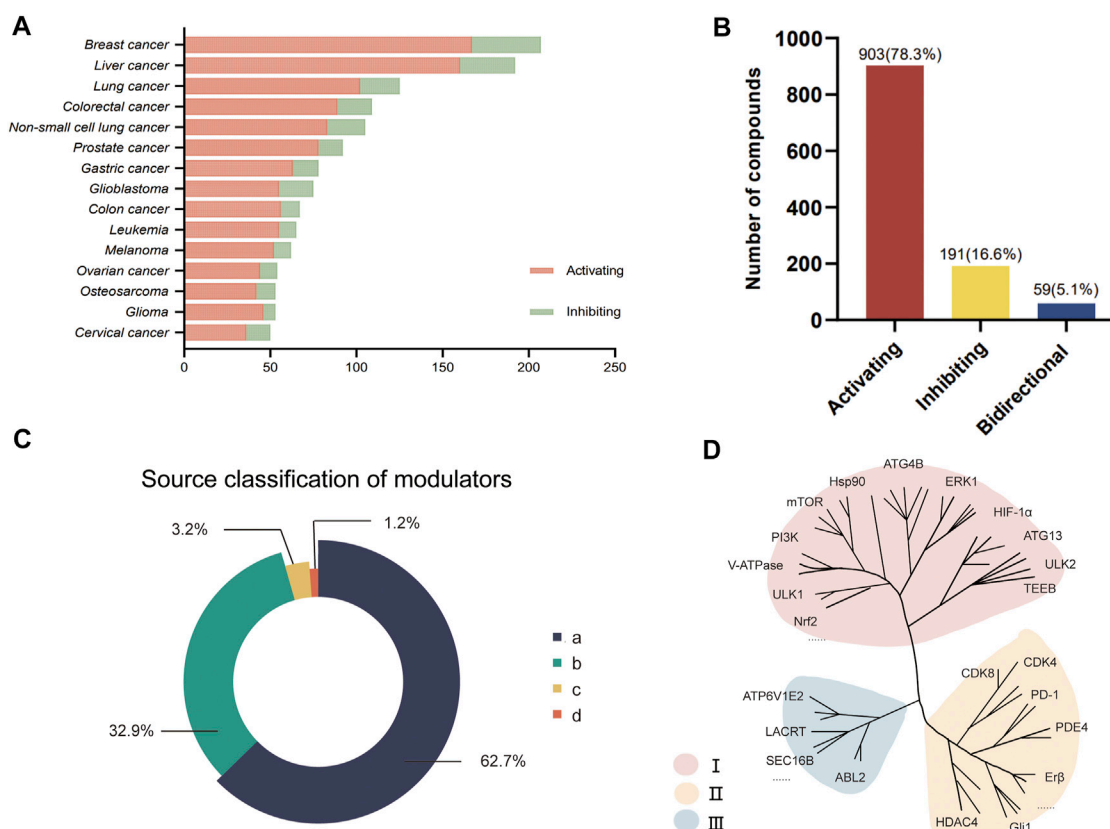


FIGURE 2

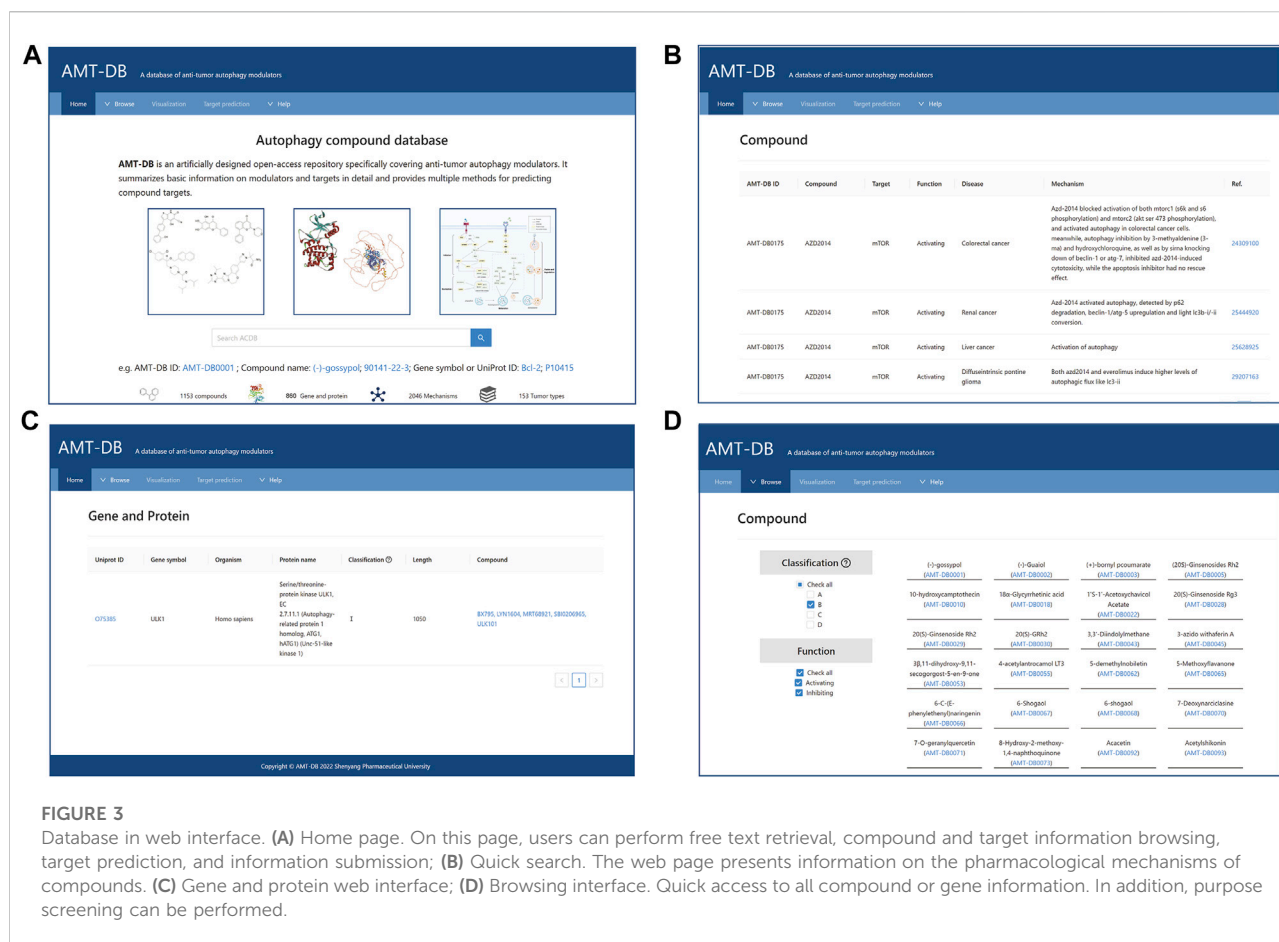
Data visualizations. (A) Stacking bars show the function of autophagy modulators in different tumors, with only the top 15 tumor types listed here; (B) Functional distribution diagram of autophagy regulator; (C) Classification of autophagy modulators in origin attributes; (D) Data distribution of autophagy targets contained in AMTDB.

organism, protein name, and length information of the autophagy target. To manage such data more clearly, classification criteria are strictly enforced. Targets proved by both the database and literature materials were identified as class I (70.5%); those that only existed in the database and were not supported by reference were class II (5.0%). Class III (24.5%) refers to some targets that have been reported in the literature but not included in the autophagy database, which are often the original targets of compounds but have been found to affect autophagy in later studies Figure 2.

According to statistics, 903 compounds induce autophagy as autophagy activators, 191 are autophagy inhibitors, and 59 compounds have different effects on autophagy in different tumors. Subsequently, during the data collection process, another classification was also placed in the AMTDB database. 1,153 autophagy modulators are meticulously divided into four categories according to their sources, 1) organic synthetic compounds (723, 62.7%); 2) monomer compounds derived from natural products (379, 32.9%); 3) derivatives and *in vivo* metabolites (37, 3.2%); 4) extraction Substances and compound preparations (14,

1.2%). In the autophagy modulators section, the basic information of the compounds is comprehensively compiled, including IUPAC Name, SMILES, CAS, target, disease, and molecular mechanism. Here, the disease refers specifically to tumors, especially cancer, such as breast cancer, ovarian cancer, oral squamous cell carcinoma, osteosarcoma, etc. are included. As an oral potent AMPK activator, ASP4132 was found in a recent non-small cell lung cancer study to induce AMPK phosphorylation and increase AMPK activity, thereby affecting the downstream mTORC1 inhibitory events, thereby inducing autophagy (Xia et al., 2021). It is worth noting that duplicate data has been excluded to avoid invalid and lengthy data from corrupting the reliability of the database. For example, Everolimus and RAD001 are the same compound but appear in different forms in different papers. To avoid data confusion, we unify the compound names (Avniel-Polak et al., 2018; Haas et al., 2019). Furthermore, 3-MA is an effective autophagy inhibitor, which has been reported in many references of breast cancer, but its molecular mechanism is widely used as a class III PI3K inhibitor to inhibit autophagy. Therefore, we give priority to retaining high-level articles and put others in the Ref.





column for reference. The above information can be displayed in the search and browse section.

Furthermore, the prediction function was adopted by AMTDB as an online tool for autophagy small molecule target prediction. Target prediction is essentially based on the principle of molecular similarity and is structured in two calculation modes, *Tanimoto Coefficient*, and *SHAFTS*, aiming to afford users with potential target information.

## Database usage instructions

AMTDB is composed of multiple functional sections such as retrieval, browse, predict, and upload, and has been published on webpage <https://amtdb.vercel.app/>, which implements various needs of users (Figure 3A).

### Retrieval

Users can quickly search for compounds or targets in the toolbar of the Home interface. AMTDB ID, CAS, and compound name were used to query autophagy regulator information. For example, by entering AZD 2014 (1009298-59-2), the web page provides chemical

information for the compound, including IUPAC Name, CAS, SMILES, and structure. Click on the AMT-ID on the report page, and detailed pharmacological information will appear, as shown in Figure 3B. It is worth mentioning that AMTDB ID is a custom numbering method of the database, which can be found in the sub-pages of retrieval and browsing, to facilitate the management of background data. Similarly, by entering a Gene symbol or UniProt ID, users can obtain gene/protein information and learn about compounds that modulate this target (Figure 3C).

### Browse

Under the browse module, the webpage lists all compounds or autophagy-related genes/proteins respectively. Users can categorize compounds or targets using the interactive filters provided on the left. For example, by selecting “b” on the compound browsing page, we obtain 379 monomeric compounds derived from natural products. Additionally, more detailed information can be achieved by hyperlinks (Figure 3D).

### Visualization

To reduce the user’s learning time cost, we have added a visualization function in AMTDB. The statistical results of tumor

**A**

**B**

**FIGURE 4**  
Web interface. (A) Target prediction; (B) The submit interface.

type, compound classification, and target classification are visually displayed, and users can click on the results to obtain the desired data.

### Target prediction

Under the sub-page of this section, two molecular similarity calculation methods are provided. As shown in Figure 4A, users can input the SMILES of small molecules, and the database will score the submitted molecules by *Tanimoto Coefficient* or *SHAFTS* and compare the similarity with the molecules in the library to predict potential targets. The calculation formulas of the two methods are shown in Table 1. Finally, users get target

information and similarity scores from web pages. Of course, compounds of the same target (listed in AMTDB) are also provided to the user for reference. The two prediction methods are different. *Tanimoto Coefficient* predicts at the 2D level, which is fast and widely used, while the *SHAFTS* algorithm calculates the similarity of spatial shapes. Although the latter is theoretically more accurate, the amount of computation is relatively large.

### Upload

The AMTDB database is based on massive text mining. We must admit that after the data collection is completed, some newly published documents have not been included yet. Herein, we provide an upload

TABLE 2 Comparisons of autophagy-related databases.

	Year	Topic	Compound	Target	Disease	Mechanism	Target prediction	Visualization	References
HADb	2011	Gene	–	234	–	+	–	–	–
ncRDeathDB	2015	ncRNA	–	+	–	+	–	–	+
ACDB	2017	Compound	357	+	+	+	–	–	+
THANATOS	2018	Regulation	–	4237	–	–	–	–	+
HAMdb	2018	Compound	841	796	+	+	–	–	+
AutophagySMDb	2019	Small molecules	~10000	71	+	+	–	–	+
ATdb	2019	Tumor	–	+	+	+	–	+	+
AMTDB	2022	Compound/target	1153	860	153	2046	+	+	+

function and welcome users to upload autophagy compounds and targets that are not in the database. Undoubtedly, we will update the data from time to time, aiming to provide users with a reliable and practical autophagy-related database (Figure 4B).

## Comparisons with other databases

After nearly a decade of efforts, autophagy has achieved considerable development, and increasing studies have prompted the generation of autophagy-related databases. At present, there are already some databases such as ACDB, and ATdb are opened. However, AMTDB focuses on both autophagy regulators and targets and is peculiar due to added visualization and target prediction capabilities. As shown in Table 2, HADb mainly includes human genes and proteins directly or indirectly involved in autophagy, while ncRDeathDB attempts to decipher the relationship between non-coding RNAs (ncRNAs) and programmed cell death (Moussay et al., 2011; Wu et al., 2015). ATdb, a powerful online database, provides a comprehensive introduction to autophagy and tumors, including 25 types of tumors, survival analysis, and DNA methylation (Chen et al., 2020). Nevertheless, the ATdb database lacks compound information and instead closely links autophagy to the clinic. Compared to compound databases (ACDB, HAMdb, and AutophagySMDb), the AMTDB database compiles compounds and autophagy targets and condenses all data. First of all, ncRNAs and endogenous regulators, such as angiotensin, heparin, and lipopolysaccharide, are not allowed (Deng et al., 2018; Wang et al., 2018; Nanduri et al., 2019). AMTDB contains more autophagic compounds than other databases such as ACDB, and the validity of the data is also an important reference rule for database data quality scores. Third, autophagy-related targets were provided, and confidence intervals were delineated based on target attributes and literature evidences, with a view to presenting a more reliable online resource. Of note, in autophagy-related database, we provide target prediction and visualization function innovatively, which have greatly enriched the database, providing clues for the development of antitumor drugs.

## Discussion

Autophagy, as we know, is an important biological function of maintaining the intracellular environment, which is strongly induced when lacking of oxygen, stress, and nutrients. Because of its key role in tumor cells, it has caused active intervene to become effective strategies for treating tumors, especially HCQ effective applications in tumor clinical experiments (Karasic et al., 2019). However, autophagy plays a complex and subtle role in tumors, showing both protective and killing functions of cancer cells. For example, casein kinase 1 alpha 1 activates PTEN/AKT/FOXO3A/ATG7 axis-mediated autophagy, inhibiting the growth of non-small cell lung cancer (Cai et al., 2018). Conversely, another study reported that inhibiting autophagy attenuated pancreatic stellate cell activation, thereby preventing pancreatic cancer cell growth and metastasis (Endo et al., 2017). Thus, both autophagy activators and autophagy inhibitors are potential therapeutic agents.

Considering the essential role of autophagy in tumors and the great therapeutic prospects of autophagy modulators, it is particularly important to construct a comprehensive database of compounds, autophagy targets, and molecular mechanisms. AMTDB includes 1,153 autophagy regulators, 153 diseases, 860 targets. Although AMTDB as an online resource related to autophagy is not proposed for the first time, its uniqueness is of great significance for the development of anti-tumor drugs. First, in order to provide users with a more practical and comprehensive database, the AMTDB database adds target prediction function and visualization, which facilitates the discovery of compound targets and provides a convincing path for the discovery of anti-tumor drugs. Secondly, it takes a bridge between autophagy regulators, autophagy-related genes, and tumors, highlights the complex mechanism relationship between the three. Third, AMTDB systematically classifies compounds and autophagy targets, effectively distinguishing natural products, organic synthetic compounds, extracts, and derivatives, which greatly ameliorates the convenience and purpose of retrieval. Finally, emerging articles has resulted in the accumulation of information on autophagy regulators and

targets, which requires a new database to be aggregated and updated. Indubitably, AMTDB still has some shortcomings, such as the role of ncRNA in manipulating autophagy cannot be underestimated (Zhao et al., 2020; Zhao et al., 2022). Therefore, we will continue to enrich the data information in later new versions. Although the existing data has been repeatedly checked and randomly verified, the efficiency and accuracy need to be further improved compared with rigorous algorithmic mining.

In conclusion, AMTDB, a comprehensive database dedicated to aggregating autophagic modulators and relevant targets, has been successfully established. In the future, the data in the AMTDB will be further expanded with the explosive growth of autophagy-related investigations, which is a foreseeable development trend. More advanced bioinformatics and artificial intelligence algorithms will be introduced by AMTDB, which would provide an unprecedented opportunity for the discovery of tumor drugs.

## Data availability statement

The original contributions presented in the study are included in the article/supplementary material, further inquiries can be directed to the corresponding authors.

## Author contributions

JF participates in project design, data collection and manuscript writing; LW, GH, QS, and RW participated in data collection and collation. LF, HY, and LZ gave guidance and support to the project. All authors approved the submitted version.

## References

- Aman, Y., Schmauck-Medina, T., Hansen, M., Morimoto, R. I., Simon, A. K., Bjedov, I., et al. (2021). Autophagy in healthy aging and disease. *Nat. Aging* 1 (8), 634–650. doi:10.1038/s43587-021-00098-4
- Avniel-Polak, S., Leibowitz, G., Doviner, V., Gross, D. J., and Grozinsky-Glasberg, S. (2018). Combining chloroquine with RAD001 inhibits tumor growth in a NEN mouse model. *Endocr. Relat. Cancer* 25 (6), 677–686. doi:10.1530/ERC-18-0121
- Bajusz, D., Rácz, A., and Héberger, K. (2015). Why is Tanimoto index an appropriate choice for fingerprint-based similarity calculations? *J. Cheminform.* 7, 20. doi:10.1186/s13321-015-0069-3
- Cai, J., Li, R., Xu, X., Zhang, L., Lian, R., Fang, L., et al. (2018). CK1 $\alpha$  suppresses lung tumour growth by stabilizing PTEN and inducing autophagy. *Nat. Cell Biol.* 20 (4), 465–478. doi:10.1038/s41556-018-0065-8
- Chen, K., Yang, D., Zhao, F., Wang, S., Ye, Y., Sun, W., et al. (2020). Autophagy and tumor database: ATdb, a novel database connecting autophagy and tumor. *Database.* 2020, baaa052. doi:10.1093/database/baaa052
- Deng, Y., Zhu, L., Cai, H., Wang, G., and Liu, B. (2018). Autophagic compound database: A resource connecting autophagy-modulating compounds, their potential targets and relevant diseases. *Cell Prolif.* 51 (3), e12403. doi:10.1111/cpr.12403
- Endo, S., Nakata, K., Ohuchida, K., Takesue, S., Nakayama, H., Abe, T., et al. (2017). Autophagy is required for activation of pancreatic stellate cells, associated with pancreatic cancer progression and promotes growth of pancreatic tumors in mice. *Gastroenterology* 152 (6), 1492–1506. doi:10.1053/j.gastro.2017.01.010
- Filomeni, G., De Zio, D., and Cecconi, F. (2015). Oxidative stress and autophagy: The clash between damage and metabolic needs. *Cell Death Differ.* 22 (3), 377–388. doi:10.1038/cdd.2014.150
- Fu, J., Yang, Y., Zhu, L., Chen, Y., and Liu, B. (2022). Unraveling the roles of protein kinases in autophagy: An update on small-molecule compounds for targeted therapy. *J. Med. Chem.* 65, 5870–5885. doi:10.1021/acs.jmedchem.1c02053
- Gong, J., Cai, C., Liu, X., Ku, X., Jiang, H., Gao, D., et al. (2013). ChemMapper: A versatile web server for exploring pharmacology and chemical structure association based on molecular 3D similarity method. *Bioinforma. Oxf. Engl.* 29 (14), 1827–1829. doi:10.1093/bioinformatics/btt270
- Haas, N. B., Appleman, L. J., Stein, M., Redlinger, M., Wilks, M., Xu, X., et al. (2019). Autophagy inhibition to augment mTOR inhibition: A phase I/II trial of Everolimus and hydroxychloroquine in patients with previously treated renal cell carcinoma. *Clin. Cancer Res.* 25 (7), 2080–2087. doi:10.1158/1078-0432.CCR-18-2204
- Karasic, T. B., O'Hara, M. H., Loaiza-Bonilla, A., Reiss, K. A., Teitelbaum, U. R., Borazanci, E., et al. (2019). Effect of gemcitabine and nab-paclitaxel with or without hydroxychloroquine on patients with advanced pancreatic cancer: A phase 2 randomized clinical trial. *JAMA Oncol.* 5 (7), 993–998. doi:10.1001/jamaoncol.2019.0684
- Li, Q., Ni, Y., Zhang, L., Jiang, R., Xu, J., Yang, H., et al. (2021). HIF-1 $\alpha$ -induced expression of m6A reader YTHDF1 drives hypoxia-induced autophagy and malignancy

## Funding

This work was supported by the National Key Research and Development Program of China (No: 2021YFE0203100), Natural Science Foundation of China (Grant No. 31970374), and Fundamental Research Funds for the Central Universities (Grant No. 2682021CX088).

## Acknowledgments

We are grateful to Prof. Heng Xu (Sichuan University) for his critical review on this manuscript.

## Conflict of interest

The authors declare that the research was conducted in the absence of any commercial or financial relationships that could be construed as a potential conflict of interest.

The reviewer XH declared a shared affiliation with the author(s) JF, QS, RW, LZ to the handling editor at the time of review.

## Publisher's note

All claims expressed in this article are solely those of the authors and do not necessarily represent those of their affiliated organizations, or those of the publisher, the editors and the reviewers. Any product that may be evaluated in this article, or claim that may be made by its manufacturer, is not guaranteed or endorsed by the publisher.

of hepatocellular carcinoma by promoting ATG2A and ATG14 translation. *Signal Transduct. Target. Ther.* 6 (1), 76. doi:10.1038/s41392-020-00453-8

Liu, X., Jiang, H., and Li, H. (2011). Shafts: A hybrid approach for 3D molecular similarity calculation. 1. Method and assessment of virtual screening. *J. Chem. Inf. Model.* 51 (9), 2372–2385. doi:10.1021/ci2000060s

Ma, C., and Chi, Y. H. (2022). Evaluation test and improvement of load balancing algorithms of nginx. *Ieee Access* 10, 14311–14324. doi:10.1109/Access.2022.3146422

Maggiore, G., Vogt, M., Stumpfe, D., and Bajorath, J. (2014). Molecular similarity in medicinal chemistry. *J. Med. Chem.* 57 (8), 3186–3204. doi:10.1021/jm401411z

Mathew, R., Karp, C. M., Beaudoin, B., Vuong, N., Chen, G., Chen, H.-Y., et al. (2009). Autophagy suppresses tumorigenesis through elimination of p62. *Cell* 137 (6), 1062–1075. doi:10.1016/j.cell.2009.03.048

Meyer, N., Henkel, L., Linder, B., Zielke, S., Tascher, G., Trautmann, S., et al. (2021). Autophagy activation, lipotoxicity and lysosomal membrane permeabilization synergize to promote pimozone- and loperamide-induced glioma cell death. *Autophagy* 17 (11), 3424–3443. doi:10.1080/15548627.2021.1874208

Moussay, E., Kaoma, T., Baginska, J., Muller, A., Van Moer, K., Nicot, N., et al. (2011). The acquisition of resistance to TNF $\alpha$  in breast cancer cells is associated with constitutive activation of autophagy as revealed by a transcriptome analysis using a custom microarray. *Autophagy* 7 (7), 760–770. doi:10.4161/auto.7.7.15454

Nanduri, R., Kalra, R., Bhagyaraj, E., Chacko, A. P., Ahuja, N., Tiwari, D., et al. (2019). AutophagySMD: A curated database of small molecules that modulate protein targets regulating autophagy. *Autophagy* 15 (7), 1280–1295. doi:10.1080/15548627.2019.1571717

Pavadai, E., Kaur, G., Wittlin, S., and Chibale, K. (2017). Identification of steroid-like natural products as antiplasmodial agents by 2D and 3D similarity-based virtual screening. *MedChemComm* 8 (6), 1152–1157. doi:10.1039/c7md00063d

Racz, A., Bajusz, D., and Heberger, K. (2018). Life beyond the Tanimoto coefficient: Similarity measures for interaction fingerprints. *J. Cheminform.* 10 (1), 48. doi:10.1186/s13321-018-0302-y

Wang, N.-N., Dong, J., Zhang, L., Ouyang, D., Cheng, Y., Chen, A. F., et al. (2018). HAMdb: A database of human autophagy modulators with specific

pathway and disease information. *J. Cheminform.* 10 (1), 34. doi:10.1186/s13321-018-0289-4

Wu, D., Huang, Y., Kang, J., Li, K., Bi, X., Zhang, T., et al. (2015). ncRDeathDB: A comprehensive bioinformatics resource for deciphering network organization of the ncRNA-mediated cell death system. *Autophagy* 11 (10), 1917–1926. doi:10.1080/15548627.2015.1089375

Xia, Y.-C., Zha, J.-H., Sang, Y.-H., Yin, H., Xu, G.-Q., Zhen, J., et al. (2021). AMPK activation by ASP4132 inhibits non-small cell lung cancer cell growth. *Cell Death Dis.* 12 (4), 365. doi:10.1038/s41419-021-03655-2

Zhang, L., Fu, L., Zhang, S., Zhang, J., Zhao, Y., Zheng, Y., et al. (2017). Discovery of a small molecule targeting ULK1-modulated cell death of triple negative breast cancer *in vitro* and *in vivo*. *Chem. Sci.* 8 (4), 2687–2701. doi:10.1039/c6sc05368h

Zhang, S.-F., Wang, X.-Y., Fu, Z.-Q., Peng, Q.-H., Zhang, J.-Y., Ye, F., et al. (2015). TXNDC17 promotes paclitaxel resistance via inducing autophagy in ovarian cancer. *Autophagy* 11 (2), 225–238. doi:10.1080/15548627.2014.998931

Zhang, Z., Qian, Q., Li, M., Shao, F., Ding, W.-X., Lira, V. A., et al. (2021). The unfolded protein response regulates hepatic autophagy by sXBP1-mediated activation of TFEB. *Autophagy* 17 (8), 1841–1855. doi:10.1080/15548627.2020.1788889

Zhao, R., Fu, J., Zhu, L., Chen, Y., and Liu, B. (2022). Designing strategies of small-molecule compounds for modulating non-coding RNAs in cancer therapy. *J. Hematol. Oncol.* 15 (1), 14. doi:10.1186/s13045-022-01230-6

Zhao, X., Su, L., He, X., Zhao, B., and Miao, J. (2020). Long noncoding RNA CA7-4 promotes autophagy and apoptosis via sponging MIR877-3P and MIR5680 in high glucose-induced vascular endothelial cells. *Autophagy* 16 (1), 70–85. doi:10.1080/15548627.2019.1598750

Zhuang, A., Chai, P., Wang, S., Zuo, S., Yu, J., Jia, S., et al. (2022). Metformin promotes histone deacetylation of optineurin and suppresses tumour growth through autophagy inhibition in ocular melanoma. *Clin. Transl. Med.* 12 (1), e660. doi:10.1002/ctm.2660



# Inhibiting Cytoprotective Autophagy in Cancer Therapy: An Update on Pharmacological Small-Molecule Compounds

## OPEN ACCESS

### Edited by:

Bo Liu,  
Sichuan University, China

### Reviewed by:

Gu He,  
Sichuan University, China  
Bo Han,  
Chengdu University of Traditional  
Chinese Medicine, China

### \*Correspondence:

Lan Zhang  
zhanglanx\_9@126.com  
Lu Chen  
lilychen2006@163.com

<sup>†</sup>These authors have contributed  
equally to this work

### Specialty section:

This article was submitted to  
Pharmacology of Anti-Cancer Drugs,  
a section of the journal  
Frontiers in Pharmacology

**Received:** 10 June 2022

**Accepted:** 21 June 2022

**Published:** 11 August 2022

### Citation:

Zhang L, Zhu Y, Zhang J, Zhang L and  
Chen L (2022) Inhibiting Cytoprotective  
Autophagy in Cancer Therapy: An  
Update on Pharmacological Small-  
Molecule Compounds.  
*Front. Pharmacol.* 13:966012.  
doi: 10.3389/fphar.2022.966012

Lijuan Zhang<sup>1,2†</sup>, Yuxuan Zhu<sup>1,2†</sup>, Jiahui Zhang<sup>3,4</sup>, Lan Zhang<sup>3\*</sup> and Lu Chen<sup>1,2\*</sup>

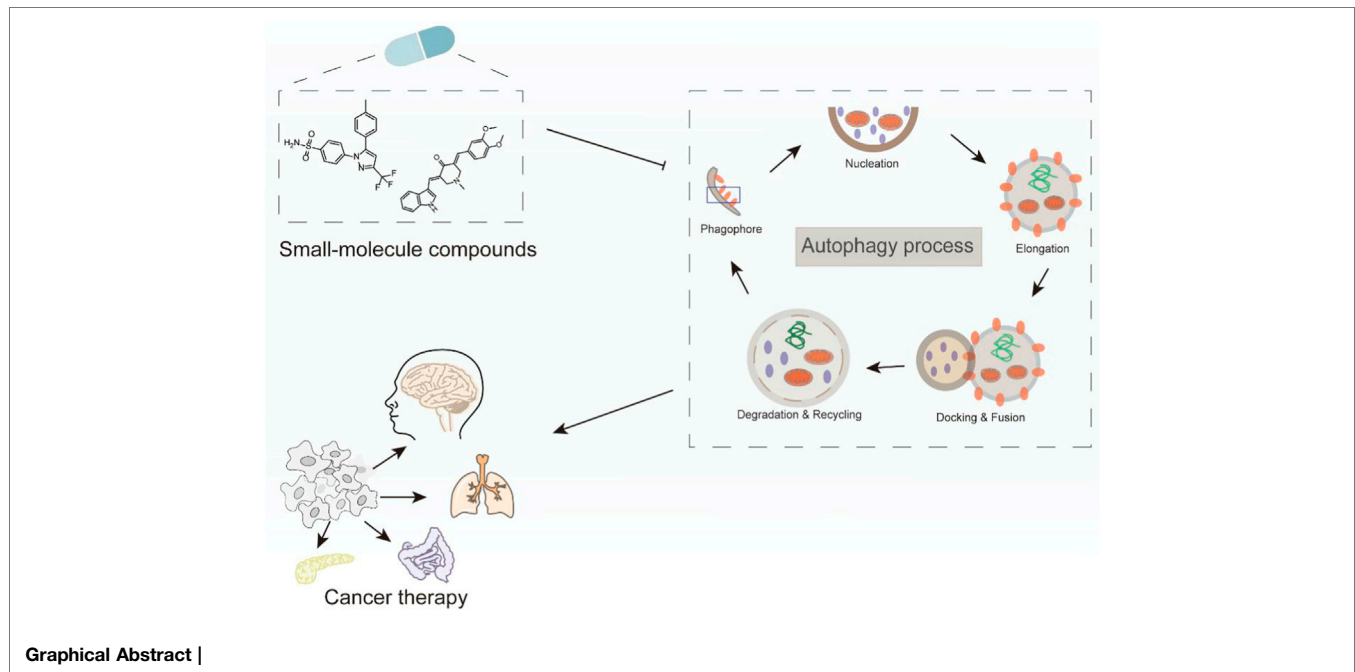
<sup>1</sup>Department of Pharmacy, Sichuan Academy of Medical Sciences & Sichuan Provincial People's Hospital, School of Medicine, University of Electronic Science and Technology of China, Chengdu, China, <sup>2</sup>Personalized Drug Therapy Key Laboratory of Sichuan Province, School of Medicine, University of Electronic Science and Technology of China, Chengdu, China, <sup>3</sup>Sichuan Engineering Research Center for Biomimetic Synthesis of Natural Drugs, School of Life Science and Engineering, Southwest Jiaotong University, Chengdu, China, <sup>4</sup>School of Traditional Chinese Materia Medica, Key Laboratory of Structure-Based Drug Design and Discovery of Ministry of Education, Shenyang Pharmaceutical University, Shenyang, China

Autophagy is a self-degradation process in which damaged proteins and organelles are engulfed into autophagosomes for digestion and eventually recycled for cellular metabolism to maintain intracellular homeostasis. Accumulating studies have reported that autophagy has the Janus role in cancer as a tumor suppressor or an oncogenic role to promote the growth of established tumors and developing drug resistance. Importantly, cytoprotective autophagy plays a prominent role in many types of human cancers, thus inhibiting autophagy, and has been regarded as a promising therapeutic strategy for cancer therapy. Here, we focus on summarizing small-molecule compounds inhibiting the autophagy process, as well as further discuss other dual-target small-molecule compounds, combination strategies, and other strategies to improve potential cancer therapy. Therefore, these findings will shed new light on exploiting more small-molecule compounds inhibiting cytoprotective autophagy as candidate drugs for fighting human cancers in the future.

**Keywords:** autophagy, cytoprotective autophagy, small-molecule compound, inhibitor, cancer therapy

**Abbreviations:** Atg, autophagy-related gene; 3-MA, 3-methyladenine; CQ, chloroquine; HCQ, hydroxychloroquine; PDK1, phosphoinositide-dependent protein kinase 1; mTOR, mammalian target of rapamycin; ULK1, Unc-51-like kinase 1; ER, endoplasmic reticulum; PI3K, phosphoinositide 3-kinases; CML, chronic myeloid leukemia; TNBC, triple negative breast cancer; CSCs, cancer stem cells; RCC, renal cell carcinoma; PPT1, palmitoyl-protein thioesterase 1; PAD4, peptidyl arginine deiminase 4; HMGB1, high mobility group box 1.





## INTRODUCTION

In eukaryotic cells, autophagy is an evolutionarily conserved process in which damaged or superfluous organelles, misfolded proteins, and invading microorganisms are degraded and removed by forming double-membrane autophagosomes and fusing with lysosomes (Mizushima, 2007). Autophagy has been reported to connect with multiple diseases, while the direct link between autophagy and cancer progress was proposed for the first time in 1999. In cancer cells, autophagy plays a dual role in promoting survival or inhibiting proliferation depending on the different contexts and stages of cancers (Singh et al., 2018). As a physiological process, autophagy can inhibit cancer by maintaining cell homeostasis, removing damaged organelles, and protecting normal cell growth. Once there is genetic damage that causes aberrant mutations, autophagy works to remove these aberrant mutations, thereby reducing the chance of cancer. (Barnard et al., 2016). In this case, the induction of autophagy by anticancer medications results in autophagic cell death acting as a cytotoxic process. On the contrary, as cancer progresses, autophagy is hijacked by cancer cells to provide the sufficient metabolic demands required for tumor survival and rapid proliferation. Thus, autophagy exerts a pro-survival mechanism contributing to cancer development and progression and protecting cancer cells from stress damage in advanced stages of cancer (Folkerts et al., 2019; Deng et al., 2020). Furthermore, autophagy involves in cancer cell resistance to chemotherapy/radiotherapy resulting in the mitigation of therapeutic effects (Das et al., 2018). Inhibition of cytoprotective autophagy sensitizes cancer cells to various treatments, enhancing the cytotoxicity of chemotherapeutic agents. Moreover, studies have reported that the genetic

knockdown of autophagy-related genes (*Atgs*) or pharmacological inhibition of autophagy can effectively promote the programmed death of tumor cells in preclinical models (Pan et al., 2019).

Despite the complex interaction between suppressive and supportive roles of autophagy in cancer, the majority of autophagy inhibitors have been proposed as a strategy for improving cancer therapies and considered in some clinical trials. Previous studies have shown that patients with BRAF mutant melanoma regressed after conventional anti-BRAF and chloroquine combination therapy (Awada et al., 2022). These compounds have been identified as cytoprotective autophagy inhibitors by targeting the classical PI3K complex, such as 3-methyladenine (3-MA), Wortmannin, and LY294002, which inhibit the early stage of autophagy, and autolysosomes, like chloroquine (CQ), hydroxychloroquine (HCQ), and bafilomycin A1, which primarily inhibit the late stage of autophagy (Bao et al., 2018; Collins et al., 2018; Wu et al., 2021). However, clinical trials have revealed that autophagy inhibitors have a limited efficacy as mono-therapies. The combination of anticancer drugs and autophagy inhibitors contributes to the effect of chemotherapy. For example, the combination of HCQ and MEK inhibitor binimetinib significantly suppresses the tumor development in both organoid and patient-derived xenograft (PDX) models of pancreatic ductal adenocarcinoma (PDAC) (Bryant et al., 2019). Inhibiting autophagy enhances the cytotoxicity and anti-angiogenic ability of anlotinib, and co-administration of anlotinib and CQ reduces VEGFA levels in the tumor supernatant even more, compared with anlotinib or CQ treatment alone (Liang et al., 2019). Although numerous compounds have been identified as autophagy inhibitors, a few compounds other than CQ/HCQ are clinically available, most



probably due to their toxicity and side effects due to the lack of specificity (Wang et al., 2016). Thus, the development of specific inhibitors targeting cytoprotective autophagy with potential clinical application becomes an urgent problem to be solved. In this review, we elaborate the molecular mechanisms that regulate autophagy and cytoprotective role of autophagy in cancer. Moreover, pharmacological small-molecule compounds blocking autophagy for cancer treatment are summarized, as well as combination therapies and dual-target small-molecule compounds involving autophagy modulators that can sensitize cancer cells to conventional therapies.

## THE CYTOPROTECTIVE ROLE OF AUTOPHAGY IN CANCER

### Mechanism and Process of Autophagy Induction

Autophagy mainly consists of four critical steps: initiation of autophagy, formation of autophagy, autophagosome docking and fusion, and autolysosome degradation (Li et al., 2020). The process of autophagy is controlled by a group of proteins encoded by the Atgs (Towers et al., 2020). Commonly, autophagy is triggered by nutrient deprivation or starvation condition, which results in Unc-51-like kinase1 (ULK1) complex activation. The ULK1 complex, consisting of ULK1, Atg13, FIP200, and Atg101, is negatively regulated by the mammalian target of rapamycin complex 1 (mTORC1) (Boya et al., 2013). Under nutrient starvation, mTORC1 is inhibited, which results in the subsequent induction of autophagy via dephosphorylating ULK1 (Zachari and Ganley, 2017). On the contrary, activated mTORC1 can phosphorylate ULK1 and suppress its kinase activity (Ganley et al., 2009). In addition to starvation, autophagy can also be activated by oxidative stress through the hypoxia-inducible factor 1- $\alpha$  (HIF- $\alpha$ ). The accumulation of HIF-1 $\alpha$  in hypoxic cells activates the BNIP/BNIP3L expression, which then dissociates the Bcl-2 and Beclin-1 (BECN1) complex to activate autophagy (Bellot et al., 2009). In the formation of autophagy, the ULK complex phosphorylates and activates the VPS34, part of PI3K complex including Beclin-1, VPS34, and other proteins, for preparing the membrane of the phagophore commonly from the endoplasmic reticulum (ER) (Behrends et al., 2010). In the final step of autophagy, autophagosome fuses with lysosomes to form autophagolysosome, and the cytoplasm-derived macromolecules can be degraded by enzymes in lysosomes (Li et al., 2020).

### The Functions of Cytoprotective Autophagy

Cytoprotective autophagy as a special type of autophagy plays a protective role in cancer cells via clearing damaged organelles, reducing DNA damage, and enhances the survival and resistance of the cancer cells, and finally promotes tumorigenesis and causes resistance to therapeutic agents. The process of cytoprotective autophagy provides energy and essential ingredients for cancer cells to survive via recycling cytoplasmic materials (Su et al., 2015; Vera-Ramirez et al., 2018). In addition, cytoprotective autophagy contributes to the aggressiveness of the cancers by facilitating

metastasis (Macintosh et al., 2012; Vera-Ramirez et al., 2018). Therefore, cytoprotective autophagy exerts significant effect in cancer development; the inhibition of cytoprotective autophagy may be a promising approach for the treatment of cancers. In autophagy process, cytoprotective autophagy is regulated by several upstream signaling pathways. The mainly PI3K/AKT/mTOR pathway is alive at the level of aerobic glycolysis in cancer cells. In this pathway, mTOR is sensitive to nutritional signals, involved in mRNA translation control, protein transport, and degradation in cells and playing an important role in cell growth and proliferation (Al-Bari and Xu, 2020). AKT is a main PI3K effector to trigger the mTORC1 signaling pathway for autophagy inhibition, while mTORC2 can phosphorylate AKT on a critical target site in other cell types, suggesting a close interaction between PI3K and mTOR signaling. Ras-Raf-MEK1/2-ERK1/2 pathway is another key important signaling to regulate autophagy in cancer cells. PI3K and Ras are both stimulated by growth factor combining with receptor tyrosine kinases to produce class I PtdIns3K (PI3K-I) and GTPase Ras, respectively (Yaeger and Corcoran, 2019). Then, PI3K-I activates the AKT via increasing membrane recruitment of AKT and phosphoinositide-dependent protein kinase 1 (PDK1). Furthermore, AKT and ERK1/2 can activate mTORC1 through phosphorylating and inhibiting the tuberous sclerosis complex 1/2 (TSC1/TSC2), causing inhibition of autophagy. In addition, activated ERK1/2 also stimulates autophagy through directly targeting downstream protein of autophagy (Inoki et al., 2002; Ma et al., 2005). The AMP-activated protein kinase (AMPK) signaling is another regulating pathway of autophagy. The decrease of ATP/AMP ratio can activate the AMPK pathway through the upstream proteins including LKB1, CaMKK $\beta$ , and TAK1 kinase. Then, active AMPK will phosphorylate and activate TSC1/TSC2, which lead to inactivation of mTORC1 and finally autophagy induction (Liang et al., 2007; Gwinn et al., 2008; Herrero-Martin et al., 2009). The p53 is a tumor suppressor playing dual roles in autophagy induction. In the aspect of nuclear p53, it can activate AMPK, which results in the activation of the TSC1/TSC2 complex and leading to the inhibition of the mTORC1 pathway and subsequent autophagy induction. On the contrary, cytoplasmic p53 exerts inhibitory function toward autophagy without mTOR (Feng et al., 2005; Tasdemir et al., 2008).

## SMALL-MOLECULE COMPOUNDS INHIBITING THE AUTOPHAGIC PROCESS

Autophagy is a complex physiological process exerting a significant role in maintaining intracellular homeostasis. In view of the pro-survival effect of autophagy in cancer cells, cytoprotective autophagy inhibition should be greatly beneficial to cancer therapy. In recent years, an increasing number of compounds for autophagy inhibition have been discovered with great potential clinical application (Figure 1). According to their effect on the major steps of autophagy, we classified these small-molecule compounds and elucidated their potential mechanism in cancer treatment (Table 1).

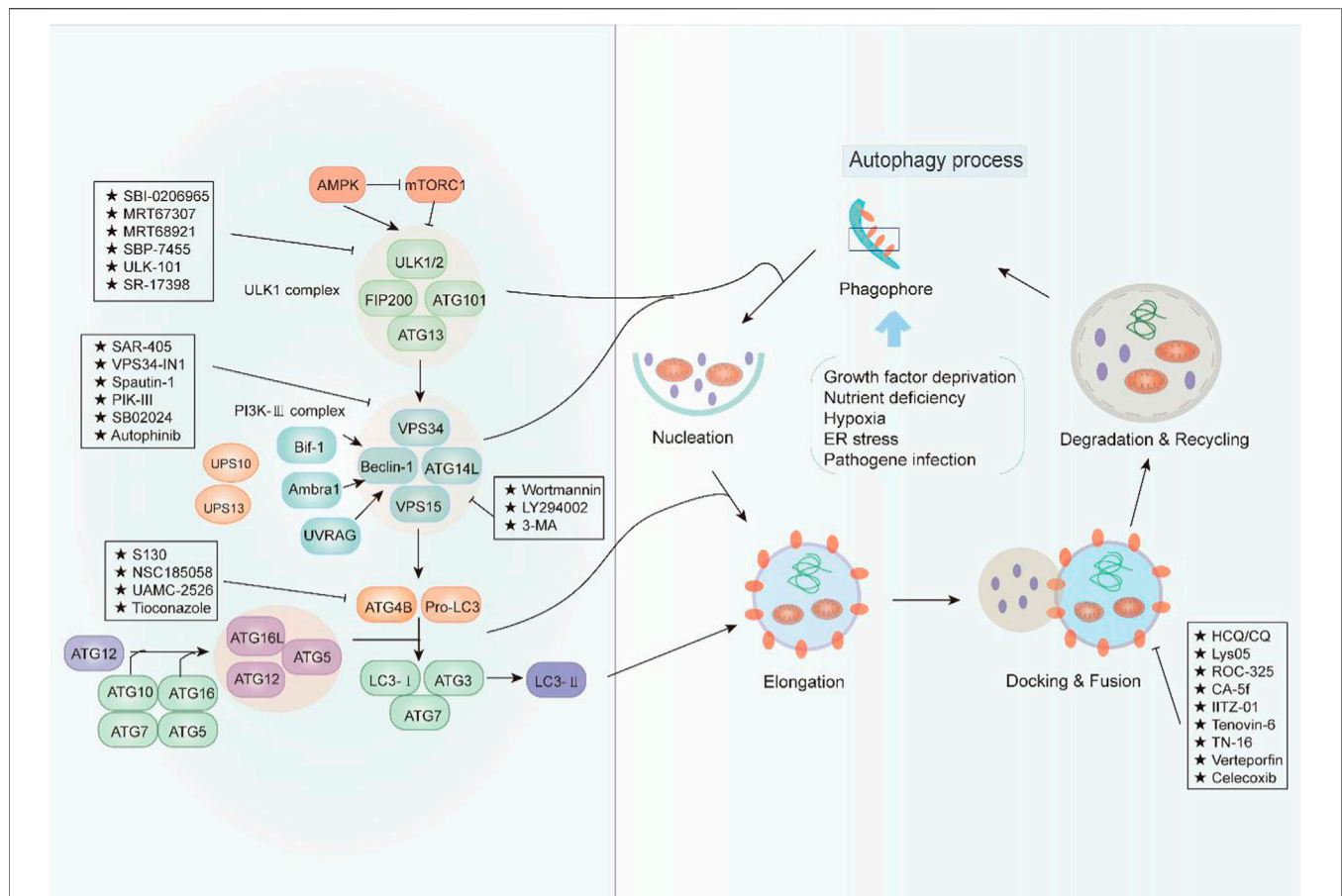


**FIGURE 1 |** An overview of the modulation of autophagy. The initiation of autophagy is controlled by the ULK1 kinase complex that integrates stress signals from mTORC1 and AMPK. When mTORC1 kinase activity is inhibited, ULK1 is activated and binding with multiple ATG proteins like ATG101, ATG13, and FIP200 to engage the formation of phagophore. Then, the ULK1 complex activates the autophagosome formation by the phosphorylation of VPS34 and Beclin-1, which forms a PI3K-III complex. Beclin 1 interacts with factors (Ambra1, Bif-1, UVRAG, and ATG14L) that modulate its binding to VPS34 whose lipid kinase activity is essential for autophagy. Cellular concentrations of the initiation complex are also under the control of an ubiquitination cascade regulated by the deubiquitination peptidases USP10 and USP13. In addition, the LC3 system is required for autophagosome transport and maturation. In the autophagosome maturation, pro-LC3 could be cleaved by ATG4B with assistance of ATG3 and ATG7 as well as ATG5, ATG12, and ATG16. Mature autophagosomes fuse with lysosomes to degrade their cargo, and recycle essential biomolecules. Some small-molecule compounds can suppress autophagy by targeting early or late stages in the pathway.

## Small-Molecule Inhibitors of ULK1

Initially, ULK1 as a serine/threonine kinase plays one of the most important autophagy-related genes in human cells (Tsukada and Ohsumi, 1993; Xiang et al., 2020). Commonly, ULK1 is able to combine with other proteins including FIP200, Atg13, and Atg101 to form the ULK1 complex, which functions as a key regulator for autophagy initiation under the downstream of mTOR (Chan, 2009). Moreover, it has been reported that ULK2 is the functional homologue of ULK1, exerting a critical effect for autophagy regulation. Therefore, ULK1/2 is a key regulator in the formation of the phagophore, making it an interesting target for drug discovery. Based on the structure of ULK1/2, several inhibitors have been discovered. For example, SBI0206965 (Figure 2, 1) is bound to the ATP binding site of ULK in the co-crystal structure of complex by forming a specific bidentate hydrogen bond between the trisubstituted pyrimidine scaffold and backbone residue Cys88 in the hinge region (Ren et al., 2020). SBI0206965 suppresses non-small cell lung cancer

cell (NSCLC) growth by modulating both autophagy and apoptosis pathways. In depth, SBI0206965 attenuates the drug resistance of cisplatin in NSCLC by inhibiting cytoprotective autophagy and promotes apoptosis independent of autophagy by destabilizing the pro-survival proteins Bcl-2/Bcl-xL (Tang et al., 2017). In addition, MRT67307 (Figure 2, 2) and MRT68921 (Figure 2, 3), previously identified as inhibitors of TANK binding protein 1 (TBK1), are also ULK1/2 inhibitors for their off-target effects on TBK1- and AMPK-related kinases. Both compounds require the key methionine 92 in the ATP binding pocket of ULK1 and probably disrupt the interaction between ULK1 and the scaffold proteins (Petherick et al., 2015). The experiment shows that these MRT compounds inhibit autophagy by reducing the transformation of LC3-I to LC3-II. Furthermore, MRT68921 is found to block ATG and suppress ovarian cancer development by targeting ULK1 kinase (Singha et al., 2020). In addition, a new optimized ULK1/2 inhibitor SBP-7455 (Figure 2, 4) displays improved target binding affinity compared

**TABLE 1 |** Small-molecule compounds for inhibiting autophagy in cancer therapy.

Target	Compound	Mechanism	Cancer	Biological activity	Ref.
ULK1/2 inhibitor	SBI-0206965	Inhibiting cytoprotective autophagy and promote apoptosis by destabilizing the pro-survival proteins Bcl-2/Bcl-xl	Lung cancer/triple-negative breast cancer	ULK1 IC <sub>50</sub> = 108 nM ULK2 IC <sub>50</sub> = 711 nM	Xiang et al. (2020)
	MRT67307	Blocking ATG through targeting ULK1	Cancer	ULK1 IC <sub>50</sub> = 45 nM ULK2 IC <sub>50</sub> = 38 nM	Chan, (2009)
	MRT68921	Inhibiting autophagy by reducing the transformation of LC3-I to LC3-II	High-grade serous ovarian cancer	ULK1 IC <sub>50</sub> = 2.9 nM ULK2 IC <sub>50</sub> = 1.1 nM	Ren et al. (2020)
	SBP-7455	Inhibiting autophagy by targeting ULK1	Triple-negative breast cancer	IC <sub>50</sub> = 13 nM	Tang et al. (2017)
	ULK-101	Inhibiting autophagy by targeting ULK1	Lung cancer	ULK1 IC <sub>50</sub> = 8.3 nM ULK2 IC <sub>50</sub> = 30 nM EC = 390 nM	Petherick et al. (2015)
	ULK-100	Inhibiting autophagy by targeting ULK1	Lung cancer	ULK1 IC <sub>50</sub> = 1.6 nM ULK2 IC <sub>50</sub> = 2.6 nM EC = 83 nM	Petherick et al. (2015)
	SR-17398	Inhibiting autophagy by targeting ULK1	Lung cancer	IC <sub>50</sub> = 22.4 μM	Singha et al. (2020)
Non-selective PI3K Inhibitor	Wortmannin	Inhibiting autophagy by targeting PI3K	Colon cancer	IC <sub>50</sub> = 20 nM	Zhang et al. (2020)
	3-Methyladenine	Inhibiting hypoxia-induced autophagy and increasing hypoxia-induced cell apoptosis	Cancer	IC <sub>50</sub> = 60 μM	Ihle et al. (2004)
	LY294002	Inhibiting autophagy, inducing apoptosis and cell cycle arrest	Pancreatic cancer	IC <sub>50</sub> = 0.5 μM	Wu et al. (2010), Wong et al. (2017), Dai et al. (2019), Andreidesz et al. (2021)
VPS34 inhibitor	SAR-405	Impeding autophagy through preventing autophagy vesicle trafficking	Renal tumor	IC <sub>50</sub> = 1.2 nM KD = 1.5 nM	Yang and Klionsky (2010), Ohashi et al. (2019)
	Compound 31	Inhibiting autophagy by targeting VPS34	Solid tumors	VPS34 IC <sub>50</sub> = 2 nM PI3Kα, β, δ, γ IC <sub>50</sub> > 2 μM mTOR IC <sub>50</sub> > 10 μM	Pasquier, (2015)
	VPS34-IN1	Impairing vesicular trafficking and mTORC1 signaling/inhibiting STAT5 phosphorylation downstream of FLT3-ITD signaling by targeting VPS34	Acute myeloid leukemia	IC <sub>50</sub> = 1.2 Nm KD = 1.5 nM	Ronan et al. (2014), Pasquier et al. (2015)
	Spautin-1	Activating GSK3β-induced apoptosis via inactivating PI3K/AKT pathway/suppressing melanoma growth via ROS-mediated DNA damage	Chronic myeloid leukemia/melanoma	IC <sub>50</sub> = 0.45–1.03 μM	Bago et al. (2014), Shao et al. (2014), Meunier et al. (2020)
	PIK-III	Enhancing VPS34-dependence in cancer cells by impairing iron mobilization via the VPS34–RAB7A axis	Chronic myeloid leukemia	VPS34 IC <sub>50</sub> = 18 nM mTOR IC <sub>50</sub> > 9.1 μM	Liu et al. (2011), Guo et al. (2020)
	SB02024	Potentiating cytotoxicity of Sunitinib and Erlotinib in breast cancer cell/inducing an infiltration of NK, CD8 <sup>+</sup> , and CD4 <sup>+</sup> T cells in melanoma and colorectal cancer	Breast cancer/colorectal cancer/melanoma	Kd = 4.5 μM	Dowdle et al. (2014), Kobylarz et al. (2020)
	Autophinib	Suppressing autophagy-mediated cell apoptosis via the AKT/mTOR pathway	Cancer	IC <sub>50</sub> = 19 nM	Dyczynski et al. (2018)
ATG4B inhibitor	S130	Attenuating the delipidation of LC3 through targeting ATG4B to inhibit autophagy via PI3K/mTOR pathway	Colorectal cancer	IC <sub>50</sub> = 3.24 μM Kd = 4.0 μM	Nakatogawa et al. 2012)
	NSC185058	Attenuating the delipidation of LC3 through targeting ATG4B to inhibit autophagy	Osteosarcoma/breast cancer	IC <sub>50</sub> = 51 μM	Bortnik et al. (2020)
	FMK-9a	Regulating cell autophagy through PI3K activation	Cervical cancer/glioblastoma	IC <sub>50</sub> = 260 nM Kd = 3.89 μM	Akin et al. (2014), Fu et al. (2019)
	UAMC-2526	Slowing down tumor growth and potentiating the effect of classical chemotherapy	Colorectal cancer	Plasma half-life = 126 min 70% metabolization after 30 min	Kurdi et al. (2017), Chu et al. (2018)
	Tioconazole	Suppressing autophagy and sensitizing cancer cells to chemotherapy	Breast cancer	ATG4A IC <sub>50</sub> = 1.3 μM ATG4B IC <sub>50</sub> = 1.8 μM	Tanc et al. (2019)

with SBI-0206965 and potently inhibits the ULK1/2 *in vitro* enzymatic activity, resulting in the reduction of viability in TNBC cells (Ren et al., 2020). Recently, two synthesized ULK1 inhibitors ULK-101 (Figure 2, 5) and ULK-100

(Figure 2, 6) also represent superior potency and selectivity to existing inhibitors in autophagy inhibition. Moreover, ULK-101 is demonstrated to sensitize KRAS mutant lung cancer cells to nutrient stress, indicating that nutrient-stressed cells may be

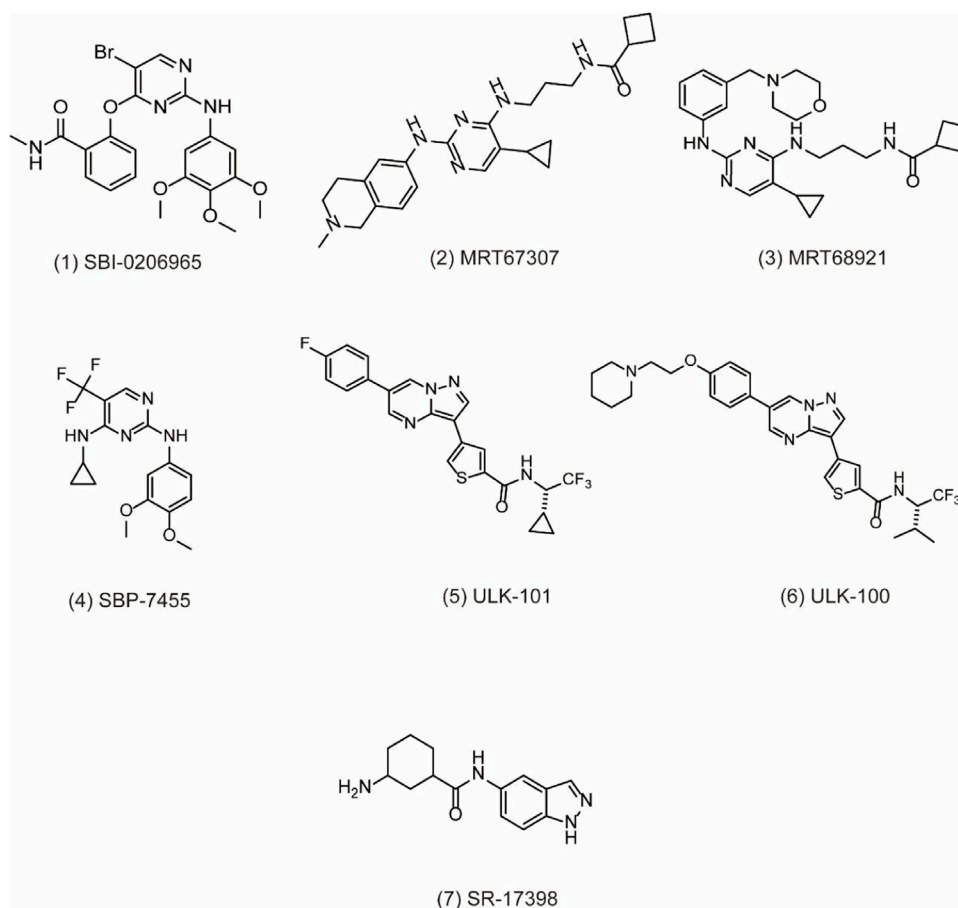


**FIGURE 2** | Chemical structures of **1–7** as inhibitors of autophagy by targeting ULK1.

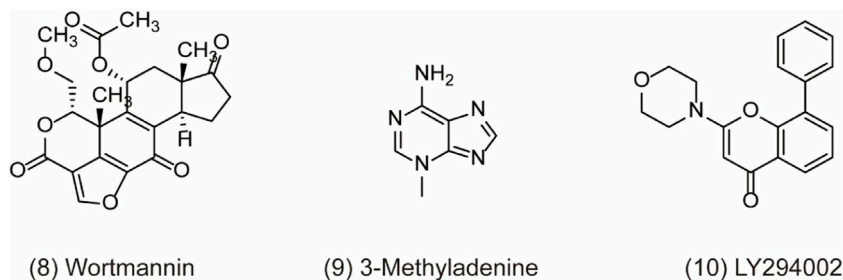


**FIGURE 3** | Chemical structures of **8–10** as inhibitors of autophagy by targeting PI3K-III.

particularly susceptible to ULK1 inhibition (Martin et al., 2018). SR-17398 (Figure 2, 7) is a new inhibitor discovered by in silico high-throughput screen (HTS) and optimization of a series of ULK1 inhibitors. Further optimization of SR-17398 generates significantly better potency than the original structure (Wood et al., 2017). In consideration of the functions of ULK1 in autophagy, more work is needed to discover the specific ULK1 inhibitors for potential cancer therapeutic effects in

animal models and clinical trials. The development of these more specific autophagy inhibitors provides for better anti-cancer treatment opportunities.

### Small-Molecule Inhibitors of PI3K

Recently, accumulating studies about PI3K (phosphoinositide 3-kinases) inhibitors have enriched tumor treatment methods due to the indication of the relationship between the PI3K/Akt/

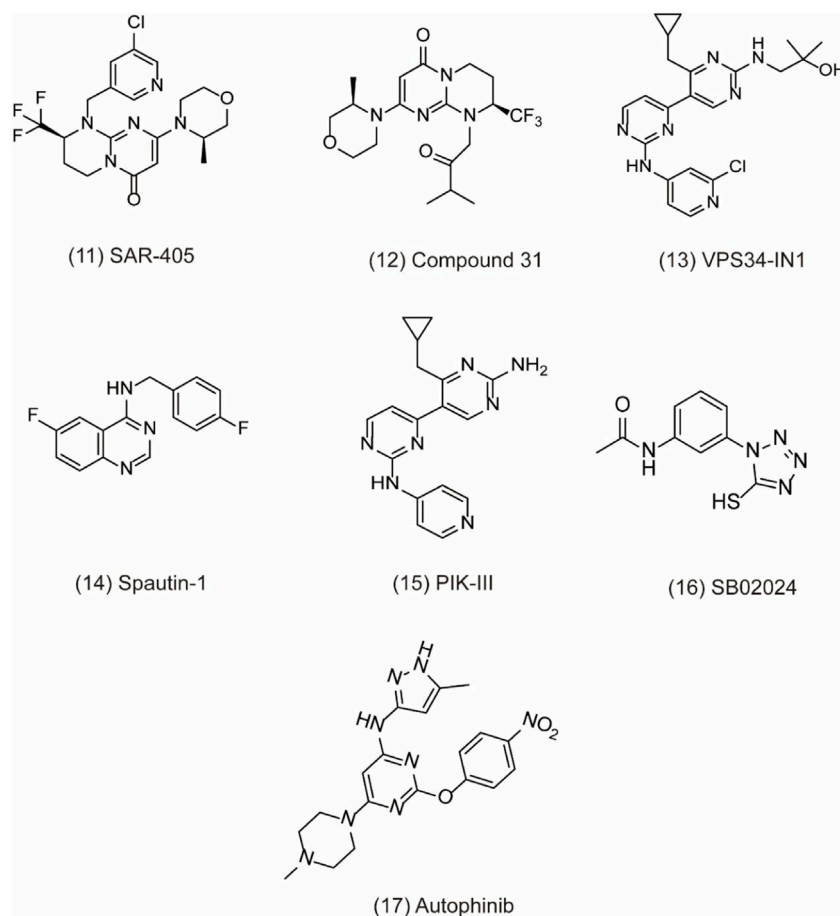


**FIGURE 4 |** Chemical structures of **11–17** as inhibitors of autophagy by targeting VPS34.

mTOR pathway and drug resistance and prognosis of tumor. However, there are still many issues to be discussed in terms of drug mechanism, clinical trials, and efficacy and safety about PI3K inhibitors in the real world (Dey et al., 2017). As we know, PI3K is the family of intracellular lipid kinases that are unique to eukaryotic cells and usually divided into three categories based on their structural features and substrate specificities, including class I, class II, and class III PI3K (also known as VPS34/PIK3C3) (Yu et al., 2015). More interestingly, it has been reported that these three classes of PI3Ks play distinct roles in autophagy. Class I PI3K is demonstrated as the inhibitor of autophagy, which is contrary to class III PI3K for the induction of autophagy (Petiot et al., 2000). In a study, PIK3C3 can combine with BECN1 and PIK3R4 to form a protein complex and produce phosphatidylinositol 3-phosphate (PtdIns3P), which is essential for the initiation and development of autophagy (Zhang et al., 2020). Therefore, class III PI3K comes into the focus as a potent drug target for autophagy inhibition. For example, pan-PI3K inhibitors like wortmannin (PX-866) (Figure 3, 8), 3-methyladenine (3-MA) (Figure 3, 9), and LY294002 (Figure 3, 10) are classical autophagy inhibitors. Wortmannin is derived from fungal metabolite and widely inhibits different classes of PI3K with good pharmacokinetics

in human tumor xenografts. Wortmannin shows an anti-tumor activity both alone and in combination with anti-cancer drugs like cisplatin to sensitizing radiation treatment (Ihle et al., 2004). In addition, the analogue 17-hydroxy Wortmannin decreases drug resistance by restoring TRAIL's response through ameliorating PIK3C3-beclin 1 (BECN1) complex and autophagy activity in colon cancer cells (Dai et al., 2019). However, 3-MA exerts a dual role in the modulation of autophagy via different temporal patterns of inhibition on class I and III PI3K (Wu et al., 2010). LY294002 is a synthetic compound like flavonoid quercetin and can inhibit autophagy via competing with ATP to bind PI3K active sites. According to the research, LY294002 shows promising therapeutic effects on proliferation inhibition through inducing cell cycle arrest and apoptosis in various types of cancer (Wong et al., 2017; Peng et al., 2020; Andreidesz et al., 2021). In addition, LY294002 combining with anticancer drugs promotes an anticancer effect on breast cancer cells (Abdallah et al., 2020). However, pan-PI3K inhibitors lack specificity and usually results in an off-target effect on other PI3K-related kinases such as mTOR, finally inducing unfavorable side effects in clinical trials. Therefore, the development of potent selective PI3K inhibitors holds the limelight in autophagy research.



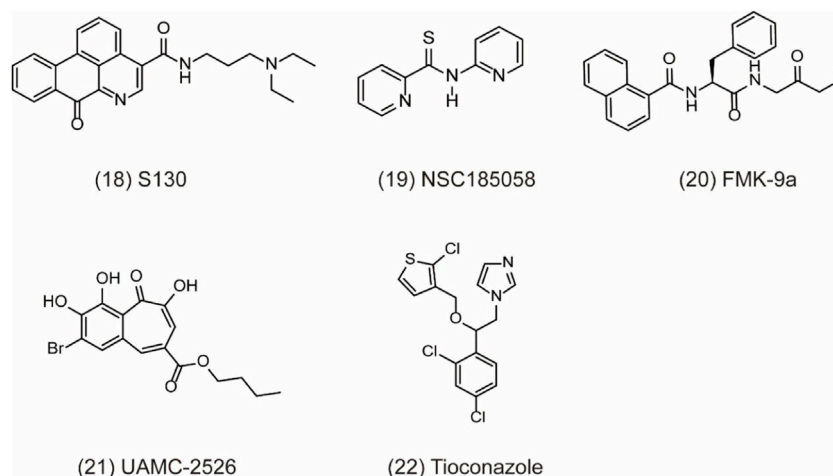


**FIGURE 5 |** Chemical structures of **18–22** as inhibitors of autophagy by targeting ATG4B.

### Small-Molecule Inhibitors of VPS34

VPS34 (vacuolar protein sorting 34) as a catalytic subunit of PI3K is originally discovered in yeast mutants and the only PI3K found in yeast (Yang and Klionsky, 2010). Based on the structure, VPS34 is mainly composed of C2 domain in the N-terminal, CCD domain, and phospholipid kinase domain in the C-terminal. The C2 domain can bind to beclin-1 without affecting the catalytic activity *in vitro*. However, the C-terminal is essential for its catalytic activity via suppressing the basal activity of the catalytic subunit. In addition, VPS34 regulates autophagosome synthesis and maturation by binding to Beclin1 and VPS15 as well as ATG14L/UVRAG to form three different PI3K complexes, which specifically phosphorylate the 3-hydroxyl of phosphatidylinositol (PI) to produce PIP<sub>3</sub>. Subsequently, PIP<sub>3</sub> recruits PIP<sub>3</sub> effector proteins containing FYVE or PX domains and regulates the formation of autophagosome membranes through a series of signal transduction (Ohashi et al., 2019). Therefore, the discovery of specific inhibitors for VPS34 may be potentially applied to treat cancer through autophagy pathway. For example, SAR405 (**Figure 4, 11**) is a highly selective VPS34 inhibitor, exerting autophagy inhibition effect by preventing autophagy vesicle trafficking from late endosomes to lysosomes but reserving the function of early endosomes (Pasquier, 2015). In recent study, the combination of SAR405 with mTOR inhibitor everolimus results in synergistic anti-proliferative activity in renal tumor cell lines, indicating its potential clinical application in cancer (Ronan et al., 2014). Recently, a new synthetic pyrimidinone derivative named compound 31 ((2S)-8-[(3R)-3-methylmorpholin-4-yl]-1-(3-methyl-2-oxo-butyl)-2-(trifluoromethyl)-3,4-dihydro-2H-pyrimido [1,2-a] pyrimidin-6-one)) (**Figure 4, 12**) also selectively inhibits VPS34. Based on the X-ray crystal structure in human VPS34, compound 31 specifically inhibits VPS34 due to its unique morpholine synthon (Pasquier et al., 2015). Another group of inhibitors are bis-aminopyrimidine derivatives including VPS34-IN1 (**Figure 4, 13**) and PIK-III (**Figure 4, 15**) by Novartis. VPS34-IN1 is found binding with the

hydrophobic region of the kinase ATP domain to inhibit VPS34. Moreover, VPS34-IN1 inhibits autophagy in acute myeloid leukemia (AML) cells via impairing vesicular trafficking and mTORC1 signaling in connection with STAT5 phosphorylation, downstream of FLT3-ITD signaling (Meunier et al., 2020). Owing to the phosphatidylinositol 3-phosphate-binding SGK3 protein kinase as the downstream target of VPS34, the target may be a therapeutic strategy to treat tumor cells (Bago et al., 2014). Spautin-1 (MBCQ) (**Figure 4, 14**) shows potent anticancer activity and improves the efficacy of imatinib mesylate by associating with GSK3 $\beta$  activation-induced apoptosis via inactivating the PI3K/AKT pathway in chronic myeloid leukemia (CML) (Shao et al., 2014). Moreover, Spautin-1 suppresses melanoma growth via damaging ROS-mediated DNA and promoting the degradation of PI3K complexes by inhibiting two ubiquitin-specific peptidases of USP10 and USP13 (Liu et al., 2011; Guo et al., 2020). PIK-III is also equipped with good selectivity over PIK3 and can be used to inhibit VPS34 enzymatic function with precision. PIK-III enhances VPS34-dependence in cancer cells by impairing iron mobilization via the VPS34-RAB7A (Kobylarz et al., 2020). In addition, NCOA4 is discovered as the substrate of PIK-III and can directly bind with ferritin heavy chain-1 (FTH1) to form an iron-binding ferritin complex for targeting autolysosomes (Dowdle et al., 2014). In addition, SB02024 (**Figure 4, 16**) is an ATP competitive inhibitor and binds in the active site of VPS34 to inhibit its catalytic function. SB02024 efficiently inhibits autophagy and *in vitro* or *in vivo* cell viability while enhances its cytotoxic effect in breast cancer cell lines by combining with Sunitinib (Dyczynski et al., 2018). Additionally, inhibiting VPS34 induces the infiltration of NK, CD8<sup>+</sup>, and CD4<sup>+</sup> T cells in melanoma and colorectal cancer (Noman et al., 2020). A novel potent VPS34 inhibitor named autophinib (**Figure 4, 17**) is discovered by phenotypic screening to monitor small molecule that induce autophagy damage (Robke et al., 2017). Autophinib shows structural advantages with chloro-substituent at the 6-position and smaller replacement of the pyrazole in the 4-position

**TABLE 2 |** Other small-molecule compounds for inhibiting autophagy in cancer therapy.

Compound	Mechanism	Cancer	Biological activity	Ref.
Hydroxychloroquine	Impairing autophagosome fusion with lysosomes	Breast cancer/pancreatic cancer/colon cancer/renal cancer/melanoma	IC <sub>50</sub> = 15–42 $\mu$ M	Takhsha et al. (2021)
Chloroquine	Impairing autophagosome fusion with lysosomes/ increasing cytotoxicity by decreasing proliferation and inducing cell apoptosis via the induction of p21WAF1/ CIP1 expression and autophagy inhibition	Pancreatic adenocarcinoma/ triple-negative breast cancer	EC = 15 $\mu$ M	Liu et al. (2018), Mauthe et al. (2018)
Mefloquine	Inhibiting glioblastoma angiogenesis via disrupting lysosomal function/inhibiting NF- $\kappa$ B signaling and inducing apoptosis	Breast cancer/glioblastoma/ colorectal cancer	EC = 0.5 $\mu$ M EC/EC <sub>CQ</sub> = 30	Hwang et al. (2020)
Lys05	Suppressing autophagy by phosphorylating p62 and AKT1S1	Lung cancer	IC <sub>50</sub> = 3.6 $\mu$ M	Sharma et al. (2012), Liang et al. (2016)
VATG-027	Sensitizing melanoma tumor to vemurafenib by lysosomal deacidification and disruption of autophagosome	Melanoma	IC <sub>50</sub> = 0.7 $\mu$ M EC = 0.1 $\mu$ M	McAfee et al. (2012); Ondrej et al. (2020)
VATG-032	Sensitizing melanoma tumor to vemurafenib by lysosomal deacidification and disruption of autophagosome	Melanoma	IC <sub>50</sub> = 27 $\mu$ M EC = 5 $\mu$ M	McAfee et al. (2012); Ondrej et al. (2020)
Nitazoxanide	Blocking late-stage lysosome acidification	Glioblastoma	IC <sub>50</sub> = 383.4–659.9 $\mu$ M	Goodall et al. (2014)
Dimeric quinacrine 661 (DQ661)	Inhibiting autophagy by targeting palmitoyl-protein thioesterase 1 (PPT1)	Melanoma/pancreatic cancer	IC <sub>50</sub> = 15 $\mu$ M	Zhao et al. (2020)
ROC-325	Inhibiting ATG5/7-dependent autophagic degradation and inducing apoptosis	Renal cell carcinoma	IC <sub>50</sub> = 4.9 $\mu$ M	Rebecca et al. (2017), Wang et al. (2018), Jones et al. (2019)
CA-5f	Suppressing autophagosome–lysosome fusion/ exhibiting strong cytotoxicity by increasing mitochondrial-derived reactive oxygen species (ROS) production	Lung cancer	IC <sub>50</sub> = 20 $\mu$ M	Carew et al. (2017)
IITZ-01	Potentiating TRAIL-induced apoptosis by DR5 upregulation and survivin downregulation via ubiquitin–proteasome pathway	Renal cancer/lung cancer/triple-negative breast cancer	IC <sub>50</sub> = 2.6 $\mu$ M	Carew and Nawrocki (2017), Zhang et al. (2019)
Tenovin-6	Affecting the acidification of autolysosomes and hydrolytic activity of lysosomes	Leukemia	IC <sub>50</sub> = 9.6 $\pm$ 0.8 $\mu$ M	Guntuku et al. (2019)
TN-16	Blocking autophagosome–lysosome fusion	Breast cancer	IC <sub>50</sub> = 0.4–1.7 $\mu$ M	Shahriyar et al. (2020)
Cepharanthine	Blocking autophagosome–lysosome fusion and inhibiting lysosomal cathepsin B and cathepsin D maturation	Non-small cell lung cancer/ breast cancer	IC <sub>50</sub> = 3.6 $\mu$ M	Yuan et al. (2017)
Verteporfin	Inhibiting PD-L1 through autophagy and the STAT1–IRF1–TRIM28 signaling axis/inducing p53 and impairing ubiquitin proteasomal degradation pathway (UPS)	Pancreatic ductal adenocarcinoma/osteosarcoma	IC <sub>50</sub> = 2.1–5.6 $\mu$ M	Donohue et al. (2011), Young et al. (2018), Hasanain et al. (2020)
PHY34	Inhibiting autophagy by targeting the ATP6V0A2 subunit while interacting with cellular apoptosis susceptibility and altering nuclear localization of proteins	Ovarian cancer/breast cancer	HGSOC cell IC <sub>50</sub> = 4 nM MDA-MB-435 IC <sub>50</sub> = 23 nM MDA-MB-231 IC <sub>50</sub> = 5.2 nM	Tang et al. (2018), Liang et al. (2020)
Celecoxib	Inhibiting cancer cell growth by modulating apoptosis and autophagy and reducing migration	Acute leukemia/osteosarcoma	IC <sub>50</sub> = 40 nM	Saini et al. (2021)
Bafilomycin A1	Preventing the fusion of autophagosome and lysosome/ suppressing the degradation of protein in autolysosome	Leukemia	IC <sub>50</sub> = 4–400 nM	Salvi et al. (2022)

and replacement of ether-oxygen in 2-position in the pyrimidine ring framework. With the emergence of these VPS34 specific inhibitors, autophagy inhibition has taken a new direction in cancer therapy, but further research is needed to reveal its role in tumor therapy.

## Small-Molecule Inhibitors of ATG4B

ATG4 is a pivotal autophagy-related cysteine protein family, which plays critical role in the autophagy process. Among the four homologs, ATG4B possesses superior efficiency. Hitherto, ATG4B has been discovered to form autophagic vesicles by promoting the activation of LC3-I through cleaving the

C-terminus of proLC3 (ATG8 family member) and exposure to ATG7. Then, LC3-I can be conjugated to phosphatidylethanolamine by ATG3 to form LC3-II and recruited to the autophagosome membranes to promote autophagic vesicle growth and expansion (Li et al., 2011; Skytte Rasmussen et al., 2017). Finally, ATG4B can provide enough LC3 to sustain autophagy by recycling the lipid LC3 in cells (Nakatogawa et al., 2012). Therefore, ATG4B is a requisite enzymatic component in the autophagy process and is becoming increasingly attractive target for cancer therapy. However, the development of specific antagonists of Atg4B is still at a very preliminary stage. In-depth exploration of the



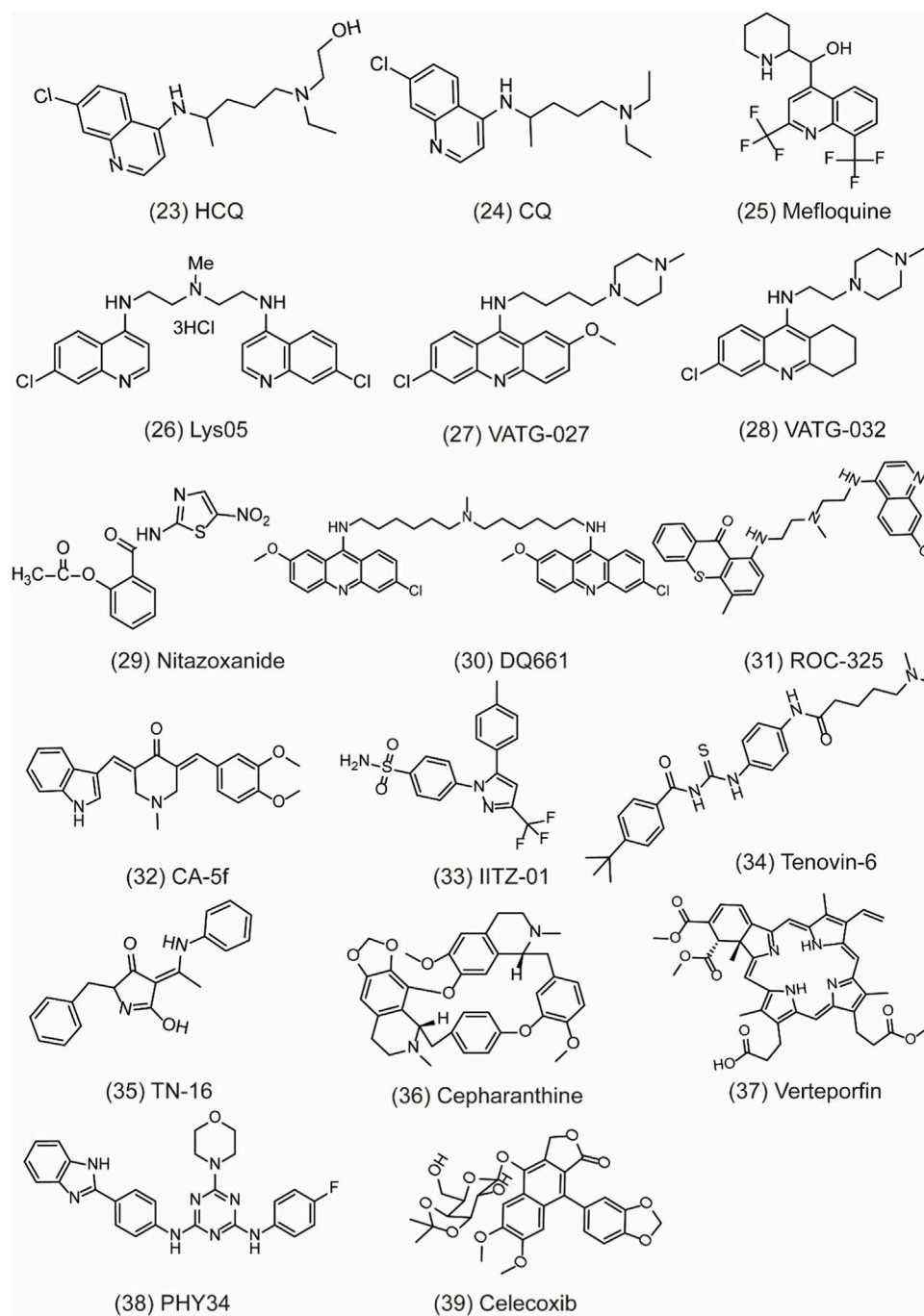


**FIGURE 6 |** Chemical structures of **23–39** as inhibitors of autophagy by targeting other targets.

interactions between Atg4B and LC3 is vital for the further discovery of more specific Atg4B antagonists. To date, increasing evidences confirm that ATG4B is overexpression in cancer cells, indicating that the ATG4B inhibition may be an effective approach for cancer treatment (Bortnik et al., 2020). Recently, considerable efforts have been made to identify small-molecule ATG4B inhibitors. For example, S130 (**Figure 5, 18**) is a potent ATG4B inhibitor discovered by in silico screening and

specifically suppresses the activity of ATG4B without affecting other proteases. S130 inhibits autophagy without causing the impairment of autophagosome fusion and dysfunction of lysosomes (Fu et al., 2019). Furthermore, S130 probably attenuates the delipidation of LC3-II to suppress the recycling of LC3-I. Therefore, S130 is an effective pharmacological agent to combine with ATG4B in autophagy for the treatment of cancer. NSC185058 (**Figure 5, 19**) is the inhibitor derived from the NCI

library. The mechanism of NSC185058 is like S130 to inhibit the delipidation of LC3, but not affect the mTOR or PI3K pathways. Furthermore, NSC185058 as an ATG4B antagonist can suppress tumor growth by autophagy inhibition (Akin et al., 2014). In addition, FMK-9a (Figure 5, 20) is also a potential ATG4B inhibitor and plays multiple roles in autophagy process. FMK-9a blocks the activation of pro-LC3 and delipidation of LC3 via inhibiting ATG4B, but phenotypically initiates cell autophagy through PI3K activation (Chu et al., 2018). However, autophagy levels are still increased in FMK-9a-treated cells, suggesting that FMK-9a induces autophagy independent of ATG4B. In addition, one study showed that FMK-9a could not inhibit Hela cell growth; thus, it could not yet be studied as an anticancer compound. In another study, small molecules with a benzotropolone backbone structure will be an effective approach to enhance the sensitivity to chemotherapy and attenuate tumor growth by the impairment of autophagy through targeting ATG4B (Kurdi et al., 2017). UAMC-2526 (Figure 5, 21) is the optimal compound for its fair plasma stability. This compound significantly inhibits tumor growth with the assistance of oxaliplatin and potentiates the chemotherapeutic effect of gemcitabine in pancreatic ductal adenocarcinoma (Tanc et al., 2019; Takhsha et al., 2021). Tioconazole (Figure 5, 22) used as a clinical antifungal drug approved by FDA is discovered as an ATG4/ATG4B inhibitor. Based on computational docking and molecular dynamics (MD) simulations, tioconazole can stably occupy the active site of ATG4 and transiently interact with the allosteric regulation site in LC3 to inhibit autophagy flux (Liu et al., 2018). In a word, ATG4B is a core autophagy-related protein and shows promising direction for cancer therapy by inhibiting autophagy.

## OTHER THERAPEUTIC STRATEGIES INHIBITING CYTOPROTECTIVE AUTOPHAGY

So far, there are little upstream autophagy inhibitors with well-defined targets successfully entering into clinical trials, but other inhibitors targeting proteins or pathways show the convincing *in vivo* activity (Table 2). For example, CQ/HCQ (Figure 6, 23) (Figure 6, 24) has been used clinically for cancer therapy by autophagy inhibition. CQ/HCQ mainly impairs autophagosome fusion with lysosomes due to the autophagy-independent severe disorganization of the Golgi and endo-lysosomal systems (Mauthe et al., 2018). At present, many clinical researchers continue to study chloroquine in various forms. Some scientists say this drug lacks specificity, but there are still many early trials underway. Moreover, there are plans to combine hydroxychloroquine with other anticancer drugs, which have shown promising results. For example, the combination of CQ and cisplatin (CDDP) can significantly increase cytotoxicity by decreasing proliferation and increasing cell apoptosis via the induction of p21<sup>WAF1/CIP1</sup> expression and autophagy inhibition in drug-resistant cells (Hwang et al., 2020). In another study, CQ is an effective adjunct to inhibit triple negative breast cancer (TNBC) cell metastasis and proliferation with carboplatin via targeting cancer

stem cells (CSCs) that is the character of TNBC (Liang et al., 2016). Recently, other quinoline analogs are synthesized to improve their anti-cancer efficacy. For example, mefloquine (MQ) (Figure 6, 25) shows the better potent efficacy in autophagy inhibition and produces unexpected anticancer effects in breast cancer (Sharma et al., 2012). Due to the limited effect of HCQ in clinical trials, the structural modification of CQ/HCQ is necessary. Synthesis of bisaminoquinoline can potently inhibit autophagy and impair *in vivo* tumor growth. In addition, CQ derivatives such as Lys01–Lys05 potently impair autophagy as the presence of two aminoquinoline rings and a triamine linker and C-7 chlorine (McAfee et al., 2012). Lys05 (Figure 6, 26) suppresses autophagy by the phosphorylation of sequestosome-1 (SQSTM1/p62) and proline-rich AKT1 substrate 1 (AKT1S1) (Ondrej et al., 2020). In addition, a novel series of acridine and tetrahydroacridine derivatives are synthesized as autophagy inhibitors. For example, VATG-027 (Figure 6, 27) and VATG-032 (Figure 6, 28) have therapeutic potential to sensitize oncogenic BRAF V600E mutant melanoma tumor to vemurafenib by lysosomal deacidification and disruption of autophagosome (Goodall et al., 2014). Likewise, prodigiosin also sensitizes colorectal cancer cells to 5-fluorouracil by impairing autophagosome–lysosome fusion (Zhao et al., 2020). Nitazoxanide (Figure 6, 29) is similar to VATGs in inhibiting autophagy through the blockage of late-stage lysosome acidification in glioblastoma (Wang et al., 2018). Moreover, a novel antimalarial named dimeric quinacrine 661 (DQ661) (Figure 6, 30) inhibits autophagy by targeting palmitoyl-protein thioesterase 1 (PPT1) and exerts anticancer effect in various tumors (Rebecca et al., 2017). Therefore, lysosomal-directed PPT1 inhibitors represent a novel approach to concurrently targeting late-autophagosomal process in cancer. DQ661 is found to block autophagy more than hydroxychloroquine, which is important for improving the efficacy and reducing off-target toxicity. ROC-325 (Figure 6, 31) is a very promising novel lysosomal autophagy inhibitor, exhibiting superior anticancer efficacy than HCQ in the preclinical study (Jones et al., 2019). The mechanism of ROC-325 is to antagonize renal cell carcinoma (RCC) growth and survival by inhibiting ATG5/7-dependent autophagic degradation and inducing apoptosis (Carew et al., 2017). Furthermore, the oral medication of ROC-325 exerts efficiency and is well tolerated in models of RCC rats (Carew and Nawrocki, 2017). A curcumin analog CA-5f (Figure 6, 32) is identified as a novel late-stage autophagy inhibitor with a potent anti-tumor effect against non-small cell lung cancer (Zhang et al., 2019). The s-triazine analogs such as IITZ-01 and IITZ-02 also act as potent lysosomotropic autophagy inhibitors for TNBC treatment (Guntuku et al., 2019). Moreover, IITZ-01 (Figure 6, 33) can potentiate TRAIL-induced apoptosis in cancer cells by DR5 upregulation and survivin downregulation via ubiquitin–proteasome pathway (Shahriyar et al., 2020). Tenovin-6 (Figure 6, 34) also impairs the autophagy in chronic lymphocytic leukemia cells by affecting the acidification of autolysosomes and hydrolytic activity of lysosomes (Yuan et al., 2017). TN-16 (Figure 6, 35) is also a potential autophagy inhibitor with the blockade of autophagosome–lysosome fusion at the later stage of autophagy (Hasanain et al., 2020). Other autophagy inhibitors like cepharanthine (CEP) (Figure 6, 36), verteporfin (Figure 6, 37), and PHY34 (Figure 6, 38) also exert an effect on different cancer cells

**TABLE 3 |** Dual and multiple targeted small-molecule compounds for inhibiting autophagy in cancer.

Target	Compound	Mechanism	Cancer	Biological activity	Ref.
PI3K/mTOR inhibitor	PKI-402	Suppressing cancer cell growth by degradation of Mcl-1 protein and disruption of the balance of Bcl-2 family protein	Ovarian cancer	IC <sub>50</sub> = 2–16 nM	Lu et al. (2016)
PI3K/mTOR inhibitor	CMG002	Inducing G0/G1 cell cycle arrest and enhancing apoptotic cell death	Gastric cancer	AGS IC <sub>50</sub> = 1.6 $\mu$ M NUGC3 IC <sub>50</sub> = 4.9 $\mu$ M	Fischer et al. (2020), Hu et al. (2020)
Hsp90 and late-autophagy inhibitor	DCZ5248	Inducing lysosomal acidification and lysosomal cathepsin activity/inducing G1-phase cell cycle arrest and apoptosis	Colon cancer	IC <sub>50</sub> = 0.5 $\mu$ M	Kim et al. (2019)
AMPK and Rab7 prenylation inhibitor	N6-isopentenyladenosine (iPA)	Impairing autophagic flux by blocking autophagosome-lysosome fusion through the defective function of Rab7	Melanoma	IC <sub>50</sub> = 2.5 $\mu$ M	Choi et al. (2019)
PI3K/mTOR inhibitor	NVP-BEZ235	Sensitizing cancer cells to radiotherapy through G2/M arrest and apoptotic cell death	Glioblastoma multiforme/thyroid cancer	IC <sub>50</sub> = 38.9 nM	Ranieri et al. (2018), Chen X. L. et al. (2021)
PI3K/Akt/mTOR inhibitor	PI103	Inducing apoptosis, reducing autophagy, suppressing NHEJ and HR repair pathways in prostate cancer	Cancer	IC <sub>50</sub> = 30 nM	Zhu et al. (2013)
HER2 inhibitor	TAK-165	Inhibiting autophagy in a HER2-independent manner	Acute myelocytic leukemia	IC <sub>50</sub> = 6 nM	Chang et al. (2013)
CDK7 inhibitor	THZ1	Enhancing cytotoxicity via autophagy suppression	Renal cell carcinoma	IC <sub>50</sub> = 3.2 nM	Chang et al. (2014)
CD13 inhibitor	Ubenimex	Sensitizing cancer cells to CDDP by autophagy through perturbing the CD13/EMP3/PI3K/AKT/NF- $\kappa$ B axis	Gastric cancer	IC <sub>50</sub> = 20 $\mu$ M	Huang et al. (2019)
JNK inhibitor	SP600125	Sensitizing cancer cells to oxaliplatin by inhibiting autophagy	Colorectal cancer	IC <sub>50</sub> = 40 nM	Chen H. et al. (2021)
Lysosome inhibitor	Trifluoperazine	Inhibiting autophagy flux by impairing lysosomes acidification and decreasing protein level of cathepsin L	Glioblastoma	IC <sub>50</sub> = 15 $\mu$ M	Guo et al. (2019)
MEK/ERK inhibition	Lycorine	Enhancing the degradation of high mobility group box 1 (HMGB1)/suppressing MEK-ERK pathway and increasing Bcl-2–Beclin-1 interaction	Multiple myeloma	IC <sub>50</sub> = 20 $\mu$ M	Vasilevskaya et al. (2016)

(Donohue et al., 2011; Tang et al., 2018; Young et al., 2018). Cepharanthine can enhance the anti-cancer property of dacomitinib (DAC) in non-small cell lung cancer by blocking the autophagosome-lysosome fusion and inhibiting lysosomal cathepsin B and cathepsin D maturation (Tang et al., 2018). Verteporfin suppresses basal and IFN-induced PD-L1 expression by disrupting multiple steps of autophagy and STAT1–IRF1–TRIM28 signaling axis (Liang et al., 2020). In a study, verteporfin sensitizes osteosarcoma cells to chemotherapy by inducing p53 and impairs ubiquitin proteasomal degradation pathway (UPS) by the accumulation of p62 under ROS stress (Saini et al., 2021). PHY34 significantly decreases tumor proliferation in ovarian cancer by inhibiting autophagy via targeting the ATP6V0A2 subunit of V (vacuolar)-ATPase and altering nuclear localization of proteins (Salvi et al., 2022). In addition, celecoxib (**Figure 6, 39**) is used as an anti-inflammatory agent, but has been discovered to have the antitumor effect in HL-60 acute leukemia cells by affecting lysosome function (Lu et al., 2016). Bafilomycin A1 is also an inhibitor of late autophagy inhibitor by preventing the fusion of autophagosome and lysosome, as well as suppressing the degradation of protein in autolysosome (Fischer et al., 2020). Although these lysosomal inhibitors show positive *in vivo* effect, their mechanism remains unclear as a lack of clear target. Therefore,

it is necessary to develop more potent, specific, and effective autophagy inhibitors for cancer treatment.

## DUAL-TARGET SMALL-MOLECULE COMPOUNDS INHIBITING CYTOPROTECTIVE AUTOPHAGY

Numerous autophagy inhibitors have been proved to exert different degrees of effect on tumor cells. However, the single-target compounds for cancers are not always aimed at the target protein and may develop the resistance to treatment. Thus, the occurrence of dual-target compounds and drug combination appears to be significant in tumor therapy (**Table 3**). The study indicates that the PI3K/AKT/mTOR signaling pathway is related to the cell proliferation, migration, and chemo-resistance. A few inhibitors can block both PI3K and mTOR to shut down the PI3K/Akt/mTOR pathway for the modulation of the autophagy process. For example, PKI-402 (**Figure 7, 40**) as a dual PI3K/mTOR inhibitor improves chemo-resistance in ovarian cancer cells by degrading Mcl-1 protein and disrupting the balance of Bcl-2 family protein through autophagy inhibition (Hu et al., 2020). CMG002 (**Figure 7, 41**) as a newly developed PI3K/mTOR dual inhibitor effectively

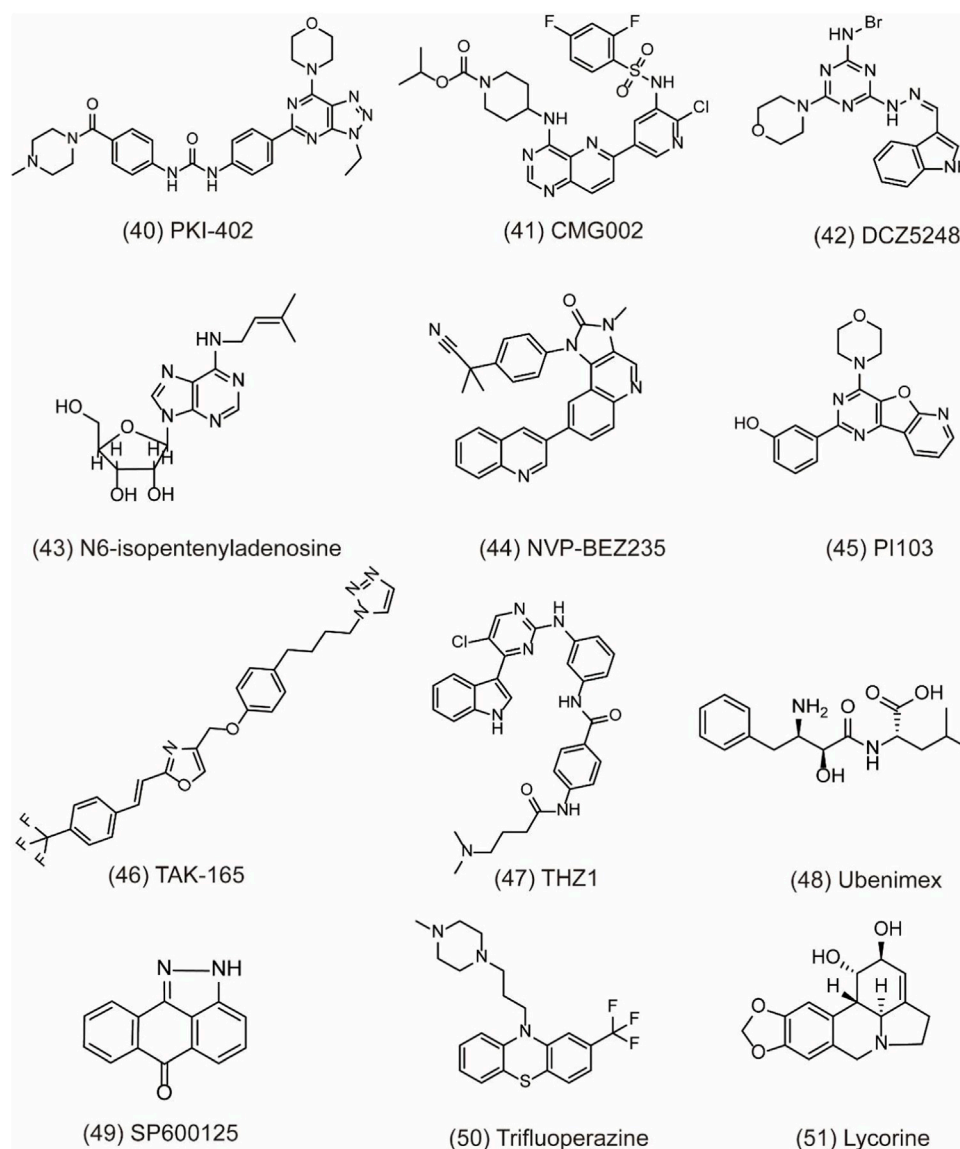


**FIGURE 7 |** Dual-target and combination strategies of small-molecule compounds of 40–51 as inhibitors of autophagy.

induces gastric cancer cell death when combined with CQ by inducing the G0/G1 cell cycle arrest and enhancing apoptotic cell death in AGS and NUGC3 cells (Kim et al., 2019). Additionally, CMG002 significantly improves the chemo-resistance in ovarian cancer as well (Choi et al., 2019). DCZ5248 (Figure 7, 42) is a novel dual inhibitor of Hsp90 and late-autophagy by inducing lysosomal acidification and lysosomal cathepsin activity. It shows antitumor activity by inducing the G1-phase cell cycle arrest and apoptosis in colon cancer cells. Therefore, DCZ5248 indicates that inhibiting both Hsp90 and autophagy provides a new therapeutic strategy for cancer treatment (Chen X. L. et al., 2021). N6-isopentenyladenosine (iPA) (Figure 7, 43) is a novel autophagic flux inhibitor, exerting an anti-proliferative activity in melanoma cells by dual targeting AMPK and Rab7 prenylation. Furthermore, iPA induces autophagosome accumulation through activating AMPK to

block mTOR pathway and impairs autophagic flux by blocking the autophagosome–lysosome fusion through the defective function of Rab7 (Ranieri et al., 2018).

## COMBINATION STRATEGIES OF SMALL-MOLECULE COMPOUNDS INHIBITING CYTOPROTECTIVE AUTOPHAGY

NVP-BEZ235 (Figure 7, 44) is a novel dual PI3K/mTOR inhibitor developed by Novartis Pharma. Preclinical studies have indicated that NVP-BEZ235 can induce autophagic cell death when autophagy inhibits the survival of cancer cells.



However, in advanced tumors, NVP-BEZ235 alone shows pro-survival effect but is totally reversed when combining with the autophagy inhibitor 3-MA. Therefore, the co-treatment of NVP-BEZ235 and autophagy inhibitors in cancer therapy by inhibiting autophagy is well documented. Notably, NVP-BEZ235 has been shown to sensitize cancer cells to radiotherapy through the G2/M arrest and apoptotic cell death (Chang et al., 2013; Zhu et al., 2013). PI103 (**Figure 7, 45**) is also a dual PI3K/mTOR inhibitor, sensitizing radio-therapy by inducing apoptosis, reducing autophagy, and suppressing NHEJ and HR repair pathways in prostate cancer (Chang et al., 2014). In addition, AC220 (Quizartinib), an FLT3 receptor tyrosine kinase inhibitor, is developed to treat AML in clinical trials. Through virtual screening, TAK-165 (Mubritinib) (**Figure 7, 46**), an autophagy inhibitor, is identified as a synergistic drug with AC220 at low doses. Further study indicates that a combination of TAK-165 with AC220 can potentially induce cancer cell death by HER2-independent autophagy (Ouchida et al., 2018). THZ1 (**Figure 7, 47**) used as a cyclin-dependent kinase 7 (CDK7) inhibitor reduces cell viability and induces apoptosis in human renal cell carcinoma. The combination of THZ1 and temsirolimus can potentially enhance cytotoxicity via autophagy suppression (Chow et al., 2020).

Particularly, some miRNAs can alter autophagy activities by regulating its downstream signaling like PI3K/AKT pathway and multiple autophagy regulators including Beclin-1, ATG5, ATG4B, and p62 (Huang et al., 2019). Autophagy modulation by miRNAs can sensitize cancer cells to chemotherapy and radiotherapy. Therefore, the discovery of miRNA regulators to inhibit autophagy is a novel and effective strategy for cancer treatment. In a study, peptidyl arginine deiminase 4 (PAD4) is identified as nasopharyngeal carcinoma (NPC) biomarker, negatively regulated by microRNA 3,164 (miR-3164). LINC00324 interacts with miR-3164 to modulate the PI3K/AKT pathway and suppress apoptosis and autophagy in carcinoma (Chen H. et al., 2021). CD13 is a transmembrane glycoprotein with metalloproteinase activity. It overexpresses in gastric cancer cells to improve cell invasion ability. Ubenimex (**Figure 7, 48**) as a CD13 inhibitor overcomes the resistance of cisplatin (CDDP) and improves the sensitivity of GC cells to CDDP by autophagy through perturbing the CD13/EMP3/PI3K/AKT/NF- $\kappa$ B axis (Guo et al., 2019). JNK belonging to the family of MAPK can regulate the activation of stress signaling to induce hypoxia-induced autophagy. Therefore, inhibiting JNK1 suppresses hypoxia-induced autophagy and sensitizes cancer cells to chemotherapy in HT29 cells. SP600125 (**Figure 7, 49**) is a JNK inhibitor and can sensitize HT29 cells to oxaliplatin by inhibiting autophagy (Vasilevskaya et al., 2016). Trifluoperazine (TFP) (**Figure 7, 50**) used as an antipsychotic drug treats cancer by enhancing the radio-sensitivity in glioblastoma (GBM) via impairing homologous recombination. Further study indicates that the treatment with TFP inhibits autophagy flux by impairing lysosome acidification and decreasing the protein level of cathepsin L, contributing to the radio-resistance of GBM cells (Zhang et al., 2017). In addition, lycorine (**Figure 7, 51**) is also an effective autophagy inhibitor and shows potential therapeutic effect alone or in combination

with bortezomib on multiple myeloma. Treatment with lycorine enhances the degradation of high mobility group box 1 (HMGB1), an important regulator of autophagy. MEK-ERK activation is then suppressed, and Bcl-2-Beclin-1 interactions are increased, leading to the inhibition of pro-survival autophagy and cell death (Roy et al., 2016).

In conclusion, pro-survival autophagy is the main cause of drug resistance and radiotherapy tolerance and severely impedes the tumor treatment in clinics. Therefore, numerous autophagy inhibitors have been studied for their anticancer potential. Aiming at the key protein targets in autophagy, plenty of effective anti-tumor autophagy inhibitors have been developed. In addition, some novel inhibitors targeting regulators of autophagy-related pathways are also regarded as a promising strategy. The dual-targeted drugs and drug combination also exert antitumor ability in cancer cells with potent cytotoxicity. In a word, discovery of novel autophagy inhibitors is valuable to cancer therapy, and more strives should be given to elucidate antitumor mechanism in the future.

## CONCLUSION AND PERSPECTIVES

As a highly conserved biological process, autophagy displays a dual role in cancer cells. In this review, we emphasize the pivotal role of autophagy as a cytoprotective and drug-resistant mechanism and propose the feasibility of research on autophagy inhibition in cancer treatment. Small-molecular compounds targeting key proteins in the autophagy process have been regarded as a promising strategy in tumor treatment. However, much of the studies focused on repositioning the antimalarial drug chloroquine and its derivatives, which are indirect autophagy inhibitors that are inexpensive, safe, and readily available for clinical trials. Studies show that when these agents are given in the right combinations, they can produce dramatic results. For example, CQ is found to improve vemurafenib sensitivity in resistant cell lines and provided for the first time in a patient harboring the V600E mutation (Levy et al., 2014). Additionally, a combination of CQ and gemcitabine enhances the antitumor activity for gallbladder cancer (Wang et al., 2020). Yet, other studies indicate that CQ and its derivative sensitization appears to be independent of autophagy inhibition as it offers only limited autophagy modulation. For example, a combination of ERK and autophagy inhibition is a treatment approach for pancreatic cancer. ERK inhibition enhances pancreatic ductal adenocarcinoma (PDAC) dependence on autophagy by the upregulation of autophagic processes, and autophagy inhibition enhances the ability of ERK inhibitors to mediate antitumor activity in KRAS-driven PDAC (Bryant et al., 2019). Therefore, the development of more selective and potent autophagy inhibitors must be essential to definitively promote the therapeutic benefit of targeting autophagy in cancer patients.

Currently, increasing compounds are developed to block the autophagy process by targeting the specific key proteins including ULK1 kinase, PI3K complex, VPS34, and ATG4B. Moreover, other compounds also contribute to the suppression of

cytoprotective autophagy. In addition, the drug combination and dual-targeted drugs can also promote sensitization of radio- or chemo-therapy. Importantly, additional factors functioning in autophagy process can also be considered as potential targets to inhibit autophagy and overcome therapy resistance, such as MAPK and AKT. Therefore, the inhibition of cytoprotective autophagy to enhance the therapeutic benefit of current anticancer therapies is an area for intense investigation. However, there still exist some challenges for these compounds in patient treatment, which greatly hinder the application of autophagy inhibitors in cancer treatment. Firstly, almost all of autophagy-related genes have non-autophagic functions resulting in hindrance to the study of the related mechanism (Xiao et al., 2021). To overcome this obstacle, the further mechanism of autophagy should be elaborated clearly and more endeavors should be put on the hunting of high-selective and effective compounds. In addition, autophagy appears to both activate and inhibit cell senescence, but long-term inhibition of autophagy seems to permanently increase the risk of cancer. Therefore, a novel strategy of drug combination between an inhibitor of autophagy with chemotherapy shows obvious clinical outcome in patients. Finally, several compounds remain unknown for their specific target in autophagy, which is also worthy of subsequent works for target recognition.

Previously, scientists have been trying to elucidate the role of autophagy in cancer, finding that the process can both inhibit the formation of new tumors and promote the growth of existing ones. These findings lead to dozens of trials combining chloroquine or hydroxychloroquine, with radio-/chemo-therapy drugs and targeted anticancer drugs for patients with refractory skin, brain, blood, and other cancers. But the results are not so good. Particularly, autophagy inhibitors have been shown to inhibit RAS-driven cancer growth, but this finding has been difficult to replicate in subsequent experiments. Therefore, studies for small-molecule inhibitors of autophagy, such as Sanofi's

VPS34 inhibitor SAR405 and Millennium's ATG7 small-molecule modulator, have been halted. Notably, growing evidences indicate that autophagy inhibition can also limit cancer growth through its effects on the tumor microenvironment and host immunity. Autophagy is a key immune escape mechanism; autophagy inhibitors promote inflammatory responses in the tumor micro-environment to enhance immune surveillance. Therefore, autophagy pathway is highly druggable and has multiple drug targets. In conclusion, autophagy inhibition is gaining focus as a potentially new therapeutic approach in cancer. The outlook for the clinical development of novel inhibitors that target upstream modulators of autophagy or lysosomal agents is studied right now, and small-molecule inhibitors are still promising for cancer treatment.

## AUTHOR CONTRIBUTIONS

LZ and LC conceived, formatted, and submitted this manuscript. LZ and YZ wrote the manuscript. LZ and JZ searched and archived the literature.

## FUNDING

This work was supported in part by grants from the National Key Research and Development Program of China (2020YFC2005500), Research Program of the Science and Technology Department of Sichuan Province (2021YJ0189), Research Program of the Science and Technology Department of Sichuan Province (2022NSFSC0630), Key research and Development Program of Science and Technology Department of Sichuan Province (2019YFS0514), and Research Program of the Science and Technology Department of Chengdu (2021-YF05-01034-SN).

## REFERENCES

- Abdallah, M. E., El-Readi, M. Z., Althubiti, M. A., Almaini, R. A., Ismail, A. M., Idris, S., et al. (2020). Tamoxifen and the PI3K inhibitor: LY294002 synergistically induce apoptosis and cell cycle arrest in breast cancer MCF-7 cells. *Molecules* 25 (15), E3355. doi:10.3390/molecules25153355
- Akin, D., Wang, S. K., Habibzadeh-Tari, P., Law, B., Ostrov, D., Li, M., et al. (2014). A novel ATG4B antagonist inhibits autophagy and has a negative impact on osteosarcoma tumors. *Autophagy* 10 (11), 2021–2035. doi:10.4161/autophagy.32229
- Al-Bari, M. A. A., and Xu, P. (2020). Molecular regulation of autophagy machinery by mTOR-dependent and -independent pathways. *Ann. N. Y. Acad. Sci.* 1467 (1), 3–20. doi:10.1111/nyas.14305
- Andreidesz, K., Koszegi, B., Kovacs, D., Bagone Vantus, V., Gallyas, F., Kovacs, K., et al. (2021). Effect of oxaliplatin, olaparib and LY294002 in combination on triple-negative breast cancer cells. *Int. J. Mol. Sci.* 22 (4), 2056. doi:10.3390/ijms22042056
- Awada, G., Schwarze, J. K., Tijtgat, J., Fasolino, G., Kruse, V., Neyns, B., et al. (2022). A lead-in safety study followed by a phase 2 clinical trial of dabrafenib, trametinib and hydroxychloroquine in advanced BRAFV600 mutant melanoma patients previously treated with BRAF-/MEK-inhibitors and immune checkpoint inhibitors. *Melanoma Res.* 32 (3), 183–191. doi:10.1097/cmr.0000000000000821
- Bago, R., Malik, N., Munson, M. J., Prescott, A. R., Davies, P., Sommer, E., et al. (2014). Characterization of VPS34-IN1, a selective inhibitor of Vps34, reveals that the phosphatidylinositol 3-phosphate-binding SGK3 protein kinase is a downstream target of class III phosphoinositide 3-kinase. *Biochem. J.* 463 (3), 413–427. doi:10.1042/BJ20140889
- Bao, J., Shi, Y., Tao, M., Liu, N., Zhuang, S., Yuan, W., et al. (2018). Pharmacological inhibition of autophagy by 3-MA attenuates hyperuricemic nephropathy. *Clin. Sci.* 132 (21), 2299–2322. doi:10.1042/CS20180563
- Barnard, R. A., Regan, D. P., Hansen, R. J., Maycotte, P., Thorburn, A., Gustafson, D. L., et al. (2016). Autophagy inhibition delays early but not late-stage metastatic disease. *J. Pharmacol. Exp. Ther.* 358 (2), 282–293. doi:10.1124/jpet.116.233908
- Behrends, C., Sowa, M. E., Gygi, S. P., and Harper, J. W. (2010). Network organization of the human autophagy system. *Nature* 466 (7302), 68–76. doi:10.1038/nature09204
- Bellot, G., Garcia-Medina, R., Gounon, P., Chiche, J., Roux, D., Pouyssegur, J., et al. (2009). Hypoxia-induced autophagy is mediated through hypoxia-inducible factor induction of BNIP3 and BNIP3L via their BH3 domains. *Mol. Cell. Biol.* 29 (10), 2570–2581. doi:10.1128/MCB.00166-09
- Bortnik, S., Tessier-Cloutier, B., Leung, S., Xu, J., Asleh, K., Burugu, S., et al. (2020). Differential expression and prognostic relevance of autophagy-related markers

- ATG4B, GABARAP, and LC3B in breast cancer. *Breast Cancer Res. Treat.* 183 (3), 525–547. doi:10.1007/s10549-020-05795-z
- Boya, P., Reggiori, F., and Codogno, P. (2013). Emerging regulation and functions of autophagy. *Nat. Cell Biol.* 15 (7), 713–720. doi:10.1038/ncb2788
- Bryant, K. L., Stalneck, C. A., Zeitouni, D., Klomp, J. E., Peng, S., Tikunov, A. P., et al. (2019). Combination of ERK and autophagy inhibition as a treatment approach for pancreatic cancer. *Nat. Med.* 25 (4), 628–640. doi:10.1038/s41591-019-0368-8
- Carew, J. S., Espitia, C. M., Zhao, W., Han, Y., Visconte, V., Phillips, J., et al. (2017). Disruption of autophagic degradation with ROC-325 antagonizes renal cell carcinoma pathogenesis. *Clin. Cancer Res.* 23 (11), 2869–2879. doi:10.1158/1078-0432.CCR-16-1742
- Carew, J. S., and Nawrocki, S. T. (2017). Drain the lysosome: Development of the novel orally available autophagy inhibitor ROC-325. *Autophagy* 13 (4), 765–766. doi:10.1080/15548627.2017.1280222
- Chan, E. Y. (2009). mTORC1 phosphorylates the ULK1-mAtg13-FIP200 autophagy regulatory complex. *Sci. Signal.* 2 (84), pe51. doi:10.1126/scisignal.284pe51
- Chang, L., Graham, P. H., Hao, J., Ni, J., Bucci, J., Cozzi, P. J., et al. (2013). Acquisition of epithelial-mesenchymal transition and cancer stem cell phenotypes is associated with activation of the PI3K/Akt/mTOR pathway in prostate cancer radioresistance. *Cell Death Dis.* 4, e875. doi:10.1038/cddis.2013.407
- Chang, L., Graham, P. H., Hao, J., Ni, J., Bucci, J., Cozzi, P. J., et al. (2014). PI3K/Akt/mTOR pathway inhibitors enhance radiosensitivity in radioresistant prostate cancer cells through inducing apoptosis, reducing autophagy, suppressing NHEJ and HR repair pathways. *Cell Death Dis.* 5, e1437. doi:10.1038/cddis.2014.415
- Chen, H., Wei, L., Luo, M., Wang, X., Zhu, C., Huang, H., et al. (2021). LINC00324 suppresses apoptosis and autophagy in nasopharyngeal carcinoma through upregulation of PAD4 and activation of the PI3K/AKT signaling pathway. *Cell Biol. Toxicol.* [Online ahead of print]. doi:10.1007/s10565-021-09632-x
- Chen, X. L., Liu, P., Zhu, W. L., and Lou, L. G. (2021). DCZ5248, a novel dual inhibitor of Hsp90 and autophagy, exerts antitumor activity against colon cancer. *Acta Pharmacol. Sin.* 42 (1), 132–141. doi:10.1038/s41401-020-0398-2
- Choi, H. J., Heo, J. H., Park, J. Y., Jeong, J. Y., Cho, H. J., Park, K. S., et al. (2019). A novel PI3K/mTOR dual inhibitor, CMG002, overcomes the chemoresistance in ovarian cancer. *Gynecol. Oncol.* 153 (1), 135–148. doi:10.1016/j.ygyno.2019.01.012
- Chow, P. M., Liu, S. H., Chang, Y. W., Kuo, K. L., Lin, W. C., Huang, K. H., et al. (2020). The covalent CDK7 inhibitor THZ1 enhances temsirolimus-induced cytotoxicity via autophagy suppression in human renal cell carcinoma. *Cancer Lett.* 471, 27–37. doi:10.1016/j.canlet.2019.12.005
- Chu, J., Fu, Y., Xu, J., Zheng, X., Gu, Q., Luo, X., et al. (2018). ATG4B inhibitor FMK-9a induces autophagy independent on its enzyme inhibition. *Arch. Biochem. Biophys.* 644, 29–36. doi:10.1016/j.abb.2018.03.001
- Collins, K. P., Jackson, K. M., and Gustafson, D. L. (2018). Hydroxychloroquine: a physiologically-based pharmacokinetic model in the context of cancer-related autophagy modulation. *J. Pharmacol. Exp. Ther.* 365 (3), 447–459. doi:10.1124/jpet.117.245639
- Dai, S., Yang, S., Hu, X., Sun, W., Tawa, G., Zhu, W., et al. (2019). 17-Hydroxy wortmannin restores TRAIL's response by ameliorating increased beclin 1 level and autophagy function in TRAIL-resistant colon cancer cells. *Mol. Cancer Ther.* 18 (7), 1265–1277. doi:10.1158/1535-7163.MCT-18-1241
- Das, C. K., Mandal, M., and Kogel, D. (2018). Pro-survival autophagy and cancer cell resistance to therapy. *Cancer Metastasis Rev.* 37 (4), 749–766. doi:10.1007/s10555-018-9727-z
- Deng, Z., Lim, J., Wang, Q., Purtell, K., Wu, S., Palomo, G. M., et al. (2020). ALS-FTLD-linked mutations of SQSTM1/p62 disrupt selective autophagy and NFE2L2/NRF2 anti-oxidative stress pathway. *Autophagy* 16 (5), 917–931. doi:10.1080/15548627.2019.1644076
- Dey, N., De, P., and Leyland-Jones, B. (2017). PI3K-AKT-mTOR inhibitors in breast cancers: From tumor cell signaling to clinical trials. *Pharmacol. Ther.* 175, 91–106. doi:10.1016/j.pharmthera.2017.02.037
- Donohue, E., Tovey, A., Vogl, A. W., Arns, S., Sternberg, E., Young, R. N., et al. (2011). Inhibition of autophagosome formation by the benzoporphyrin derivative verteporfin. *J. Biol. Chem.* 286 (9), 7290–7300. doi:10.1074/jbc.M110.139915
- Dowdle, W. E., Nyfeler, B., Nagel, J., Elling, R. A., Liu, S., Triantafellow, E., et al. (2014). Selective VPS34 inhibitor blocks autophagy and uncovers a role for NCOA4 in ferritin degradation and iron homeostasis *in vivo*. *Nat. Cell Biol.* 16 (11), 1069–1079. doi:10.1038/ncb3053
- Dyczynski, M., Yu, Y., Otrocka, M., Parpal, S., Braga, T., Henley, A. B., et al. (2018). Targeting autophagy by small molecule inhibitors of vacuolar protein sorting 34 (Vps34) improves the sensitivity of breast cancer cells to Sunitinib. *Cancer Lett.* 435, 32–43. doi:10.1016/j.canlet.2018.07.028
- Feng, Z., Zhang, H., Levine, A. J., and Jin, S. (2005). The coordinate regulation of the p53 and mTOR pathways in cells. *Proc. Natl. Acad. Sci. U. S. A.* 102 (23), 8204–8209. doi:10.1073/pnas.0502857102
- Fischer, T. D., Wang, C., Padman, B. S., Lazarou, M., and Youle, R. J. (2020). STING induces LC3B lipidation onto single-membrane vesicles via the V-ATPase and ATG16L1-WD40 domain. *J. Cell Biol.* 219 (12), e202009128. doi:10.1083/jcb.202009128
- Folkerts, H., Hilgendorf, S., Vellenga, E., Bremer, E., and Wiersma, V. R. (2019). The multifaceted role of autophagy in cancer and the microenvironment. *Med. Res. Rev.* 39 (2), 517–560. doi:10.1002/med.21531
- Fu, Y., Hong, L., Xu, J., Zhong, G., Gu, Q., Gu, Q., et al. (2019). Discovery of a small molecule targeting autophagy via ATG4B inhibition and cell death of colorectal cancer cells *in vitro* and *in vivo*. *Autophagy* 15 (2), 295–311. doi:10.1080/15548627.2018.1517073
- Ganley, I. G., Lam du, H., Wang, J., Ding, X., Chen, S., Jiang, X., et al. (2009). ULK1-ATG13-FIP200 complex mediates mTOR signaling and is essential for autophagy. *J. Biol. Chem.* 284 (18), 12297–12305. doi:10.1074/jbc.M900573200
- Goodall, M. L., Wang, T., Martin, K. R., Kortus, M. G., Kauffman, A. L., Trent, J. M., et al. (2014). Development of potent autophagy inhibitors that sensitize oncogenic BRAF V600E mutant melanoma tumor cells to vemurafenib. *Autophagy* 10 (6), 1120–1136. doi:10.4161/auto.28594
- Guntuku, L., Gangasani, J. K., Thummuri, D., Borkar, R. M., Manavathi, B., Ragampeta, S., et al. (2019). IITZ-01, a novel potent lysosomotropic autophagy inhibitor, has single-agent antitumor efficacy in triple-negative breast cancer *in vitro* and *in vivo*. *Oncogene* 38 (4), 581–595. doi:10.1038/s41388-018-0446-2
- Guo, J., Zhang, J., Liang, L., Liu, N., Qi, M., Zhao, S., et al. (2020). Potent USP10/13 antagonist spautin-1 suppresses melanoma growth via ROS-mediated DNA damage and exhibits synergy with cisplatin. *J. Cell. Mol. Med.* 24 (7), 4324–4340. doi:10.1111/jcmm.15093
- Guo, Q., Jing, F. J., Xu, W., Li, X., Li, X., Sun, J. L., et al. (2019). Ubenimex induces autophagy inhibition and EMT suppression to overcome cisplatin resistance in GC cells by perturbing the CD13/EMP3/PI3K/AKT/NF- $\kappa$ B axis. *Aging (Albany NY)* 12 (1), 80–105. doi:10.18632/aging.102598
- Gwinn, D. M., Shackelford, D. B., Egan, D. F., Mihaylova, M. M., Mery, A., Vasquez, D. S., et al. (2008). AMPK phosphorylation of raptor mediates a metabolic checkpoint. *Mol. Cell* 30 (2), 214–226. doi:10.1016/j.molcel.2008.03.003
- Hasanain, M., Sahai, R., Pandey, P., Maheshwari, M., Choyal, K., Gandhi, D., et al. (2020). Microtubule disrupting agent-mediated inhibition of cancer cell growth is associated with blockade of autophagic flux and simultaneous induction of apoptosis. *Cell Prolif.* 53 (4), e12749. doi:10.1111/cpr.12749
- Herrero-Martin, G., Hoyer-Hansen, M., Garcia-Garcia, C., Fumarola, C., Farkas, T., Lopez-Rivas, A., et al. (2009). TAK1 activates AMPK-dependent cytoprotective autophagy in TRAIL-treated epithelial cells. *EMBO J.* 28 (6), 677–685. doi:10.1038/emboj.2009.8
- Hu, X., Xia, M., Wang, J., Yu, H., Chai, J., Zhang, Z., et al. (2020). Dual PI3K/mTOR inhibitor PKI-402 suppresses the growth of ovarian cancer cells by degradation of Mcl-1 through autophagy. *Biomed. Pharmacother.* 129, 110397. doi:10.1016/j.biopha.2020.110397
- Huang, T., Wan, X., Alvarez, A. A., James, C. D., Song, X., Yang, Y., et al. (2019). MIR93 (microRNA -93) regulates tumorigenicity and therapy response of glioblastoma by targeting autophagy. *Autophagy* 15 (6), 1100–1111. doi:10.1080/15548627.2019.1569947
- Hwang, J. R., Kim, W. Y., Cho, Y. J., Ryu, J. Y., Choi, J. J., Jeong, S. Y., et al. (2020). Chloroquine reverses chemoresistance via upregulation of p21(WAF1/CIP1) and autophagy inhibition in ovarian cancer. *Cell Death Dis.* 11 (12), 1034. doi:10.1038/s41419-020-03242-x
- Ihle, N. T., Williams, R., Chow, S., Chew, W., Berggren, M. I., Paine-Murrieta, G., et al. (2004). Molecular pharmacology and antitumor activity of PX-866, a novel



- inhibitor of phosphoinositide-3-kinase signaling. *Mol. Cancer Ther.* 3 (7), 763–772. doi:10.1158/1535-7163.763.3.7
- Inoki, K., Li, Y., Zhu, T., Wu, J., and Guan, K. L. (2002). TSC2 is phosphorylated and inhibited by Akt and suppresses mTOR signalling. *Nat. Cell Biol.* 4 (9), 648–657. doi:10.1038/ncb839
- Jones, T. M., Espitia, C., Wang, W., Nawrocki, S. T., and Carew, J. S. (2019). Moving beyond hydroxychloroquine: the novel lysosomal autophagy inhibitor ROC-325 shows significant potential in preclinical studies. *Cancer Commun. (Lond.)* 39 (1), 72. doi:10.1186/s40880-019-0418-0
- Kim, M. Y., Kruger, A. J., Jeong, J. Y., Kim, J., Shin, P. K., Kim, S. Y., et al. (2019). Combination therapy with a PI3K/mTOR dual inhibitor and chloroquine enhances synergistic apoptotic cell death in epstein-barr virus-infected gastric cancer cells. *Mol. Cells* 42 (6), 448–459. doi:10.14348/molcells.2019.2395
- Kobylarz, M. J., Goodwin, J. M., Kang, Z. B., Annand, J. W., Hevi, S., O'Mahony, E., et al. (2020). An iron-dependent metabolic vulnerability underlies VPS34-dependence in RKO cancer cells. *PLoS One* 15 (8), e0235551. doi:10.1371/journal.pone.0235551
- Kurdi, A., Cleenewerck, M., Vangestel, C., Lyssens, S., Declercq, W., Timmermans, J. P., et al. (2017). ATG4B inhibitors with a benzotropolone core structure block autophagy and augment efficiency of chemotherapy in mice. *Biochem. Pharmacol.* 138, 150–162. doi:10.1016/j.bcp.2017.06.119
- Levy, J. M., Thompson, J. C., Griesinger, A. M., Amani, V., Donson, A. M., Birks, D. K., et al. (2014). Autophagy inhibition improves chemosensitivity in BRAF(V600E) brain tumors. *Cancer Discov.* 4 (7), 773–780. doi:10.1158/2159-8290.CD-14-0049
- Li, M., Hou, Y., Wang, J., Chen, X., Shao, Z. M., Yin, X. M., et al. (2011). Kinetics comparisons of mammalian Atg4 homologues indicate selective preferences toward diverse Atg8 substrates. *J. Biol. Chem.* 286 (9), 7327–7338. doi:10.1074/jbc.M110.199059
- Li, X., He, S., and Ma, B. (2020). Autophagy and autophagy-related proteins in cancer. *Mol. Cancer* 19 (1), 12. doi:10.1186/s12943-020-1138-4
- Liang, D. H., Choi, D. S., Ensor, J. E., Kaiparettu, B. A., Bass, B. L., Chang, J. C., et al. (2016). The autophagy inhibitor chloroquine targets cancer stem cells in triple negative breast cancer by inducing mitochondrial damage and impairing DNA break repair. *Cancer Lett.* 376 (2), 249–258. doi:10.1016/j.canlet.2016.04.002
- Liang, J., Shao, S. H., Xu, Z. X., Hennessy, B., Ding, Z., Larrea, M., et al. (2007). The energy sensing LKB1-AMPK pathway regulates p27(kip1) phosphorylation mediating the decision to enter autophagy or apoptosis. *Nat. Cell Biol.* 9 (2), 218–224. doi:10.1038/ncb1537
- Liang, J., Wang, L., Wang, C., Shen, J., Su, B., Marisetty, A. L., et al. (2020). Verteporfin inhibits PD-L1 through autophagy and the STAT1-IRF1-TRIM28 signaling Axis, exerting antitumor efficacy. *Cancer Immunol. Res.* 8 (7), 952–965. doi:10.1158/2326-6066.CIR-19-0159
- Liang, L., Hui, K., Hu, C., Wen, Y., Yang, S., Zhu, P., et al. (2019). Autophagy inhibition potentiates the anti-angiogenic property of multikinase inhibitor anlotinib through JAK2/STAT3/VEGFA signaling in non-small cell lung cancer cells. *J. Exp. Clin. Cancer Res.* 38 (1), 71. doi:10.1186/s13046-019-1093-3
- Liu, J., Xia, H., Kim, M., Xu, L., Li, Y., Zhang, L., et al. (2011). Beclin1 controls the levels of p53 by regulating the deubiquitination activity of USP10 and USP13. *Cell* 147 (1), 223–234. doi:10.1016/j.cell.2011.08.037
- Liu, P. F., Tsai, K. L., Hsu, C. J., Tsai, W. L., Cheng, J. S., Chang, H. W., et al. (2018). Drug repurposing screening identifies ticlozazole as an ATG4 inhibitor that suppresses autophagy and sensitizes cancer cells to chemotherapy. *Theranostics* 8 (3), 830–845. doi:10.7150/thno.22012
- Lu, Y., Liu, X. F., Liu, T. R., Fan, R. F., Xu, Y. C., Zhang, X. Z., et al. (2016). Celecoxib exerts antitumor effects in HL-60 acute leukemia cells and inhibits autophagy by affecting lysosome function. *Biomed. Pharmacother.* 84, 1551–1557. doi:10.1016/j.biopha.2016.11.026
- Ma, L., Chen, Z., Erdjument-Bromage, H., Tempst, P., and Pandolfi, P. P. (2005). Phosphorylation and functional inactivation of TSC2 by Erk implications for tuberous sclerosis and cancer pathogenesis. *Cell* 121 (2), 179–193. doi:10.1016/j.cell.2005.02.031
- Macintosh, R. L., Timpson, P., Thorburn, J., Anderson, K. I., Thorburn, A., Ryan, K. M., et al. (2012). Inhibition of autophagy impairs tumor cell invasion in an organotypic model. *Cell Cycle* 11 (10), 2022–2029. doi:10.4161/cc.20424
- Martin, K. R., Celano, S. L., Solitro, A. R., Gunaydin, H., Scott, M., O'Hagan, R. C., et al. (2018). A potent and selective ULK1 inhibitor suppresses autophagy and sensitizes cancer cells to nutrient stress. *iScience* 8, 74–84. doi:10.1016/j.isci.2018.09.012
- Mauthe, M., Orhon, I., Rocchi, C., Zhou, X., Luhr, M., Hijlkema, K. J., et al. (2018). Chloroquine inhibits autophagic flux by decreasing autophagosome-lysosome fusion. *Autophagy* 14 (8), 1435–1455. doi:10.1080/15548627.2018.1474314
- McAfee, Q., Zhang, Z., Samanta, A., Levi, S. M., Ma, X. H., Piao, S., et al. (2012). Autophagy inhibitor Lys05 has single-agent antitumor activity and reproduces the phenotype of a genetic autophagy deficiency. *Proc. Natl. Acad. Sci. U. S. A.* 109 (21), 8253–8258. doi:10.1073/pnas.1118193109
- Meunier, G., Birsén, R., Cazelles, C., Belhadj, M., Cantero-Aguilar, L., Kosmider, O., et al. (2020). Antileukemic activity of the VPS34-IN1 inhibitor in acute myeloid leukemia. *Oncogenesis* 9 (10), 94. doi:10.1038/s41389-020-00278-8
- Mizushima, N. (2007). Autophagy: process and function. *Genes Dev.* 21 (22), 2861–2873. doi:10.1101/gad.1599207
- Nakatogawa, H., Ishii, J., Asai, E., and Ohsumi, Y. (2012). Atg4 recycles inappropriately lipidated Atg8 to promote autophagosome biogenesis. *Autophagy* 8 (2), 177–186. doi:10.4161/auto.8.2.18373
- Noman, M. Z., Parpal, S., Van Moer, K., Xiao, M., Yu, Y., Viklund, J., et al. (2020). Inhibition of Vps34 reprograms cold into hot inflamed tumors and improves anti-PD-1/PD-L1 immunotherapy. *Sci. Adv.* 6 (18), eaax7881. doi:10.1126/sciadv.aax7881
- Ohashi, Y., Tremel, S., and Williams, R. L. (2019). VPS34 complexes from a structural perspective. *J. Lipid Res.* 60 (2), 229–241. doi:10.1194/jlr.R089490
- Ondrej, M., Cechakova, L., Fabrik, I., Klimentova, J., and Tichy, A. (2020). Lys05 - a promising autophagy inhibitor in the radiosensitization battle: Phosphoproteomic perspective. *Cancer Genomics Proteomics* 17 (4), 369–382. doi:10.21873/cgp.20196
- Ouchida, A. T., Li, Y., Geng, J., Najafav, A., Ofengeim, D., Sun, X., et al. (2018). Synergistic effect of a novel autophagy inhibitor and Quizartinib enhances cancer cell death. *Cell Death Dis.* 9 (2), 138. doi:10.1038/s41419-017-0170-9
- Pan, X., Chen, Y., Shen, Y., and Tantai, J. (2019). Knockdown of TRIM65 inhibits autophagy and cisplatin resistance in A549/DDP cells by regulating miR-138-5p/ATG7. *Cell Death Dis.* 10 (6), 429. doi:10.1038/s41419-019-1660-8
- Pasquier, B., El-Ahmad, Y., Filoche-Romme, B., Dureuil, C., Fassy, F., Abecassis, P. Y., et al. (2015). Discovery of (2S)-8-[(3R)-3-methylmorpholin-4-yl]-1-(3-methyl-2-oxobutyl)-2-(trifluoromethyl)-3,4-dihydro-2H-pyrimido[1,2-a]pyrimidin-6-one: a novel potent and selective inhibitor of Vps34 for the treatment of solid tumors. *J. Med. Chem.* 58 (1), 376–400. doi:10.1021/jm5013352
- Pasquier, B. (2015). SAR405, a PIK3C3/Vps34 inhibitor that prevents autophagy and synergizes with MTOR inhibition in tumor cells. *Autophagy* 11 (4), 725–726. doi:10.1080/15548627.2015.1033601
- Peng, X., Zhou, J., Li, B., Zhang, T., Zuo, Y., Gu, X., et al. (2020). Notch1 and PI3K/Akt signaling blockers DAPT and LY294002 coordinately inhibit metastasis of gastric cancer through mutual enhancement. *Cancer Chemother. Pharmacol.* 85 (2), 309–320. doi:10.1007/s00280-019-03990-4
- Petherick, K. J., Conway, O. J., Mpamhanga, C., Osborne, S. A., Kamal, A., Saxty, B., et al. (2015). Pharmacological inhibition of ULK1 kinase blocks mammalian target of rapamycin (mTOR)-dependent autophagy. *J. Biol. Chem.* 290 (18), 11376–11383. doi:10.1074/jbc.C114.627778
- Petiot, A., Ogier-Denis, E., Blommaert, E. F., Meijer, A. J., and Codogno, P. (2000). Distinct classes of phosphatidylinositol 3'-kinases are involved in signaling pathways that control macroautophagy in HT-29 cells. *J. Biol. Chem.* 275 (2), 992–998. doi:10.1074/jbc.275.2.992
- Ranieri, R., Ciaglia, E., Amodio, G., Picardi, P., Proto, M. C., Gazzero, P., et al. (2018). N6-isopentenyladenosine dual targeting of AMPK and Rab7 prenylation inhibits melanoma growth through the impairment of autophagic flux. *Cell Death Differ.* 25 (2), 353–367. doi:10.1038/cdd.2017.165
- Rebecca, V. W., Nicastri, M. C., McLaughlin, N., Fennelly, C., McAfee, Q., Ronghe, A., et al. (2017). A unified approach to targeting the lysosome's degradative and growth signaling roles. *Cancer Discov.* 7 (11), 1266–1283. doi:10.1158/2159-8290.CD-17-0741
- Ren, H., Bakas, N. A., Vamos, M., Chaikwad, A., Limpert, A. S., Wimer, C. D., et al. (2020). Design, synthesis, and characterization of an orally active dual-specific ULK1/2 autophagy inhibitor that synergizes with the PARP inhibitor olaparib for the treatment of triple-negative breast cancer. *J. Med. Chem.* 63 (23), 14609–14625. doi:10.1021/acs.jmedchem.0c00873

- Robke, L., Laraia, L., Carnero Corrales, M. A., Konstantinidis, G., Muroi, M., Richters, A., et al. (2017). Phenotypic identification of a novel autophagy inhibitor chemotype targeting lipid kinase VPS34. *Angew. Chem. Int. Ed. Engl.* 56 (28), 8153–8157. doi:10.1002/anie.201703738
- Ronan, B., Flamand, O., Vescovi, L., Dureuil, C., Durand, L., Fassy, F., et al. (2014). A highly potent and selective Vps34 inhibitor alters vesicle trafficking and autophagy. *Nat. Chem. Biol.* 10 (12), 1013–1019. doi:10.1038/nchembio.1681
- Roy, M., Liang, L., Xiao, X., Peng, Y., Luo, Y., Zhou, W., et al. (2016). Lycorine downregulates HMGB1 to inhibit autophagy and enhances bortezomib activity in multiple myeloma. *Theranostics* 6 (12), 2209–2224. doi:10.7150/thno.15584
- Saini, H., Sharma, H., Mukherjee, S., Chowdhury, S., and Chowdhury, R. (2021). Verteporfin disrupts multiple steps of autophagy and regulates p53 to sensitize osteosarcoma cells. *Cancer Cell Int.* 21 (1), 52. doi:10.1186/s12935-020-01720-y
- Salvi, A., Young, A. N., Huntsman, A. C., Pergande, M. R., Korkmaz, M. A., Rathnayake, R. A., et al. (2022). PHY34 inhibits autophagy through V-ATPase V0A2 subunit inhibition and CAS/CSE1L nuclear cargo trafficking in high grade serous ovarian cancer. *Cell Death Dis.* 13 (1), 45. doi:10.1038/s41419-021-04495-w
- Shahriyar, S. A., Seo, S. U., Min, K. J., Kubatka, P., Min, D. S., Chang, J. S., et al. (2020). Upregulation of DR5 and downregulation of survivin by IITZ-01, lysosomotropic autophagy inhibitor, potentiates TRAIL-mediated apoptosis in renal cancer cells via ubiquitin-proteasome pathway. *Cancers (Basel)* 12 (9), E2363. doi:10.3390/cancers12092363
- Shao, S., Li, S., Qin, Y., Wang, X., Yang, Y., Bai, H., et al. (2014). Spautin-1, a novel autophagy inhibitor, enhances imatinib-induced apoptosis in chronic myeloid leukemia. *Int. J. Oncol.* 44 (5), 1661–1668. doi:10.3892/ijo.2014.2313
- Sharma, N., Thomas, S., Golden, E. B., Hofman, F. M., Chen, T. C., Petasis, N. A., et al. (2012). Inhibition of autophagy and induction of breast cancer cell death by mefloquine, an antimalarial agent. *Cancer Lett.* 326 (2), 143–154. doi:10.1016/j.canlet.2012.07.029
- Singh, S. S., Vats, S., Chia, A. Y., Tan, T. Z., Deng, S., Ong, M. S., et al. (2018). Dual role of autophagy in hallmarks of cancer. *Oncogene* 37 (9), 1142–1158. doi:10.1038/s41388-017-0046-6
- Singha, B., Laski, J., Ramos Valdes, Y., Liu, E., DiMattia, G. E., Shepherd, T. G., et al. (2020). Inhibiting ULK1 kinase decreases autophagy and cell viability in high-grade serous ovarian cancer spheroids. *Am. J. Cancer Res.* 10 (5), 1384–1399.
- Skytte Rasmussen, M., Mouilleron, S., Kumar Shrestha, B., Wirth, M., Lee, R., Bowitz Larsen, K., et al. (2017). ATG4B contains a C-terminal LIR motif important for binding and efficient cleavage of mammalian orthologs of yeast Atg8. *Autophagy* 13 (5), 834–853. doi:10.1080/15548627.2017.1287651
- Su, Z., Yang, Z., Xu, Y., Chen, Y., and Yu, Q. (2015). Apoptosis, autophagy, necroptosis, and cancer metastasis. *Mol. Cancer* 14, 48. doi:10.1186/s12943-015-0321-5
- Takhsha, F. S., Vangestel, C., Tanc, M., De Bruycker, S., Berg, M., Pintelon, I., et al. (2021). ATG4B inhibitor UAMC-2526 potentiates the chemotherapeutic effect of gemcitabine in a Panc02 mouse model of pancreatic ductal adenocarcinoma. *Front. Oncol.* 11, 750259. doi:10.3389/fonc.2021.750259
- Tanc, M., Cleenewerck, M., Kurdi, A., Roelandt, R., Declercq, W., De Meyer, G., et al. (2019). Synthesis and evaluation of novel benzotropolones as Atg4B inhibiting autophagy blockers. *Bioorg. Chem.* 87, 163–168. doi:10.1016/j.bioorg.2019.03.021
- Tang, F., Hu, P., Yang, Z., Xue, C., Gong, J., Sun, S., et al. (2017). SBI206965, a novel inhibitor of Ulk1, suppresses non-small cell lung cancer cell growth by modulating both autophagy and apoptosis pathways. *Oncol. Rep.* 37 (6), 3449–3458. doi:10.3892/or.2017.5635
- Tang, Z. H., Cao, W. X., Guo, X., Dai, X. Y., Lu, J. H., Chen, X., et al. (2018). Identification of a novel autophagic inhibitor cepharanthine to enhance the anti-cancer property of daconitinib in non-small cell lung cancer. *Cancer Lett.* 412, 1–9. doi:10.1016/j.canlet.2017.10.001
- Tasdemir, E., Maiuri, M. C., Galluzzi, L., Vitale, I., Djavaheri-Mergny, M., D'Amelio, M., et al. (2008). Regulation of autophagy by cytoplasmic p53. *Nat. Cell Biol.* 10 (6), 676–687. doi:10.1038/ncb1730
- Towers, C. G., Wodetzki, D., and Thorburn, A. (2020). Autophagy and cancer: Modulation of cell death pathways and cancer cell adaptations. *J. Cell Biol.* 219 (1), e201909033. doi:10.1083/jcb.201909033
- Tsukada, M., and Ohsumi, Y. (1993). Isolation and characterization of autophagy-defective mutants of *Saccharomyces cerevisiae*. *FEBS Lett.* 333 (1–2), 169–174. doi:10.1016/0014-5793(93)80398-e
- Vasilevska, I. A., Selvakumaran, M., Roberts, D., and O'Dwyer, P. J. (2016). JNK1 inhibition attenuates hypoxia-induced autophagy and sensitizes to chemotherapy. *Mol. Cancer Res.* 14 (8), 753–763. doi:10.1158/1541-7786.MCR-16-0035
- Vera-Ramirez, L., Vodnala, S. K., Nini, R., Hunter, K. W., and Green, J. E. (2018). Autophagy promotes the survival of dormant breast cancer cells and metastatic tumour recurrence. *Nat. Commun.* 9 (1), 1944. doi:10.1038/s41467-018-04070-6
- Wang, C., Hu, Q., and Shen, H. M. (2016). Pharmacological inhibitors of autophagy as novel cancer therapeutic agents. *Pharmacol. Res.* 105, 164–175. doi:10.1016/j.phrs.2016.01.028
- Wang, F. T., Wang, H., Wang, Q. W., Pan, M. S., Li, X. P., Sun, W., et al. (2020). Inhibition of autophagy by chloroquine enhances the antitumor activity of gemcitabine for gallbladder cancer. *Cancer Chemother. Pharmacol.* 86 (2), 221–232. doi:10.1007/s00280-020-04100-5
- Wang, X., Shen, C., Liu, Z., Peng, F., Chen, X., Yang, G., et al. (2018). Nitazoxanide, an antiprotozoal drug, inhibits late-stage autophagy and promotes ING1-induced cell cycle arrest in glioblastoma. *Cell Death Dis.* 9 (10), 1032. doi:10.1038/s41419-018-1058-z
- Wong, Y. K., Xu, C., Kalesh, K. A., He, Y., Lin, Q., Wong, W. S. F., et al. (2017). Artemisinin as an anticancer drug: Recent advances in target profiling and mechanisms of action. *Med. Res. Rev.* 37 (6), 1492–1517. doi:10.1002/med.21446
- Wood, S. D., Grant, W., Adrados, I., Choi, J. Y., Alburger, J. M., Duckett, D. R., et al. (2017). *In silico* HTS and structure based optimization of indazole-derived ULK1 inhibitors. *ACS Med. Chem. Lett.* 8 (12), 1258–1263. doi:10.1021/acsmchemlett.7b00344
- Wu, M. X., Wang, S. H., Xie, Y., Chen, Z. T., Guo, Q., Yuan, W. L., et al. (2021). Interleukin-33 alleviates diabetic cardiomyopathy through regulation of endoplasmic reticulum stress and autophagy via insulin-like growth factor-binding protein 3. *J. Cell. Physiol.* 236 (6), 4403–4419. doi:10.1002/jcp.30158
- Wu, Y. T., Tan, H. L., Shui, G., Bauvy, C., Huang, Q., Wenk, M. R., et al. (2010). Dual role of 3-methyladenine in modulation of autophagy via different temporal patterns of inhibition on class I and III phosphoinositide 3-kinase. *J. Biol. Chem.* 285 (14), 10850–10861. doi:10.1074/jbc.M109.080796
- Xiang, H., Zhang, J., Lin, C., Zhang, L., Liu, B., Ouyang, L., et al. (2020). Targeting autophagy-related protein kinases for potential therapeutic purpose. *Acta Pharm. Sin. B* 10 (4), 569–581. doi:10.1016/j.apsb.2019.10.003
- Xiao, M., Benoit, A., Hasmim, M., Duhem, C., Vogin, G., Berchem, G., et al. (2021). Targeting cytoprotective autophagy to enhance anticancer therapies. *Front. Oncol.* 11, 626309. doi:10.3389/fonc.2021.626309
- Yaeger, R., and Corcoran, R. B. (2019). Targeting alterations in the RAF-MEK pathway. *Cancer Discov.* 9 (3), 329–341. doi:10.1158/2159-8290.CD-18-1321
- Yang, Z., and Klionsky, D. J. (2010). Mammalian autophagy: core molecular machinery and signaling regulation. *Curr. Opin. Cell Biol.* 22 (2), 124–131. doi:10.1016/j.ceb.2009.11.014
- Young, A. N., Herrera, D., Huntsman, A. C., Korkmaz, M. A., Lantvit, D. D., Mazumder, S., et al. (2018). Phyllanthusmin derivatives induce apoptosis and reduce tumor burden in high-grade serous ovarian cancer by late-stage autophagy inhibition. *Mol. Cancer Ther.* 17 (10), 2123–2135. doi:10.1158/1535-7163.MCT-17-1195
- Yu, X., Long, Y. C., and Shen, H. M. (2015). Differential regulatory functions of three classes of phosphatidylinositol and phosphoinositide 3-kinases in autophagy. *Autophagy* 11 (10), 1711–1728. doi:10.1080/15548627.2015.1043076
- Yuan, H., Tan, B., and Gao, S. J. (2017). Tenovin-6 impairs autophagy by inhibiting autophagic flux. *Cell Death Dis.* 8 (2), e2608. doi:10.1038/cddis.2017.25
- Zachari, M., and Ganley, I. G. (2017). The mammalian ULK1 complex and autophagy initiation. *Essays Biochem.* 61 (6), 585–596. doi:10.1042/EBC20170021
- Zhang, L., Qiang, P., Yu, J., Miao, Y., Chen, Z., Qu, J., et al. (2019). Identification of compound CA-5f as a novel late-stage autophagy inhibitor with potent anti-tumor effect against non-small cell lung cancer. *Autophagy* 15 (3), 391–406. doi:10.1080/15548627.2018.1511503
- Zhang, X., Xu, R., Zhang, C., Xu, Y., Han, M., Huang, B., et al. (2017). Trifluoperazine, a novel autophagy inhibitor, increases radiosensitivity in glioblastoma by impairing homologous recombination. *J. Exp. Clin. Cancer Res.* 36 (1), 118. doi:10.1186/s13046-017-0588-z
- Zhang, Y., Hu, B., Li, Y., Deng, T., Xu, Y., Lei, J., et al. (2020). Binding of Avibirnavirus VP3 to the PIK3C3-PDPK1 complex inhibits autophagy by activating the AKT-MTOR pathway. *Autophagy* 16 (9), 1697–1710. doi:10.1080/15548627.2019.1704118

- Zhao, C., Qiu, S., He, J., Peng, Y., Xu, H., Feng, Z., et al. (2020). Prodigiosin impairs autophagosome-lysosome fusion that sensitizes colorectal cancer cells to 5-fluorouracil-induced cell death. *Cancer Lett.* 481, 15–23. doi:10.1016/j.canlet.2020.03.010
- Zhu, W., Fu, W., and Hu, L. (2013). NVP-BEZ235, dual phosphatidylinositol 3-kinase/mammalian target of rapamycin inhibitor, prominently enhances radiosensitivity of prostate cancer cell line PC-3. *Cancer biother. Radiopharm.* 28 (9), 665–673. doi:10.1089/cbr.2012.1443

**Conflict of Interest:** The authors declare that the research was conducted in the absence of any commercial or financial relationships that could be construed as a potential conflict of interest.

**Publisher's Note:** All claims expressed in this article are solely those of the authors and do not necessarily represent those of their affiliated organizations, or those of the publisher, the editors, and the reviewers. Any product that may be evaluated in this article, or claim that may be made by its manufacturer, is not guaranteed or endorsed by the publisher.

Copyright © 2022 Zhang, Zhu, Zhang, Zhang and Chen. This is an open-access article distributed under the terms of the Creative Commons Attribution License (CC BY). The use, distribution or reproduction in other forums is permitted, provided the original author(s) and the copyright owner(s) are credited and that the original publication in this journal is cited, in accordance with accepted academic practice. No use, distribution or reproduction is permitted which does not comply with these terms.



## OPEN ACCESS

## EDITED BY

Bo Liu,  
Sichuan University, China

## REVIEWED BY

Haiyang Yu,  
Tianjin University of Traditional Chinese  
Medicine, China  
Xiaoxiao Huang,  
Shenyang Pharmaceutical University,  
China

## \*CORRESPONDENCE

Mingzhen Zhang,  
mzhang21@xjtu.edu.cn  
Kangsheng Tu,  
tks0912@foxmail.com

## SPECIALTY SECTION

This article was submitted to  
Pharmacology of Anti-Cancer Drugs,  
a section of the journal  
Frontiers in Pharmacology

RECEIVED 23 June 2022

ACCEPTED 08 July 2022

PUBLISHED 15 August 2022



## CITATION

Zhang Y, Zhao Y, Zhang Y, Liu Q,  
Zhang M and Tu K (2022), The crosstalk  
between sonodynamic therapy and  
autophagy in cancer.  
*Front. Pharmacol.* 13:961725.  
doi: 10.3389/fphar.2022.961725

## COPYRIGHT

© 2022 Zhang, Zhao, Zhang, Liu, Zhang  
and Tu. This is an open-access article  
distributed under the terms of the  
[Creative Commons Attribution License](https://creativecommons.org/licenses/by/4.0/)  
(CC BY). The use, distribution or  
reproduction in other forums is  
permitted, provided the original  
author(s) and the copyright owner(s) are  
credited and that the original  
publication in this journal is cited, in  
accordance with accepted academic  
practice. No use, distribution or  
reproduction is permitted which does  
not comply with these terms.

# The crosstalk between sonodynamic therapy and autophagy in cancer

Yujie Zhang<sup>1,2</sup>, Yuanru Zhao<sup>2</sup>, Yuanyuan Zhang<sup>2</sup>,  
Qingguang Liu<sup>1</sup>, Mingzhen Zhang <sup>1,2\*</sup> and  
Kangsheng Tu <sup>1,2\*</sup>

<sup>1</sup>Department of Hepatobiliary Surgery, The First Affiliated Hospital of Xi'an Jiaotong University, Xi'an, Shaanxi, China, <sup>2</sup>School of Basic Medical Sciences, Xi'an Jiaotong University Health Science Center, Xi'an, Shaanxi, China

As a noninvasive treatment approach for cancer and other diseases, sonodynamic therapy (SDT) has attracted extensive attention due to the deep penetration of ultrasound, good focusing, and selective irradiation sites. However, intrinsic limitations of traditional sonosensitizers hinder the widespread application of SDT. With the development of nanotechnology, nanoparticles as sonosensitizers or as a vehicle to deliver sonosensitizers have been designed and used to target tissues or tumor cells with high specificity and accuracy. Autophagy is a common metabolic alteration in both normal cells and tumor cells. When autophagy happens, a double-membrane autophagosome with sequestered intracellular components is delivered and fused with lysosomes for degradation. Recycling these cell materials can promote survival under a variety of stress conditions. Numerous studies have revealed that both apoptosis and autophagy occur after SDT. This review summarizes recent progress in autophagy activation by SDT through multiple mechanisms in tumor therapies, drug resistance, and lipid catabolism. A promising tumor therapy, which combines SDT with autophagy inhibition using a nanoparticle delivering system, is presented and investigated.

## KEYWORDS

sonodynamic therapy (SDT), sonosensitizers, autophagy, nanoparticles, cancer

## 1 Introduction

Ultrasound (US) has been widely used for both diagnostics and therapeutics in many fields, such as B-scan ultrasonography, bone repair, diabetic nephropathy, cancer therapy, immunotherapy, vaccination, and drug delivery (Cao et al., 2016; Escoffre et al., 2016; McHale et al., 2016; Padilla et al., 2016). Among these applications, the flexibility of US as an approach for noninvasively eradicating target solid tumors has recently drawn increasing attention (McHale et al., 2016). In cancer therapy, an ideal approach would be to apply a harmless stimulus that could lead to cytotoxic events at the target tumor tissue specifically and accurately. SDT, with its deep tissue penetration and high precision, has a great potential to become an ideal tumor therapy since

sonochemical or sonophotochemical reactions, which lead to cytotoxicity under a controlled US irradiation with the help of certain chosen sonosensitizers (Liu et al., 2015). The major limitations of the sonosensitizers used in the SDT include poor delivery accuracy and high toxicity (Pelt et al., 2018). With the development of nanotechnology, nanoparticles (NPs)-based sonosensitizers were designed, which made use of NPs to deliver the sonosensitizers to target tissues or tumor cells with high specificity (Chen et al., 2014; Qian et al., 2016; Feng et al., 2019; Qu et al., 2020). The other problem encountered is that SDT can promote autophagy in tumor cells, which influences the efficiency of SDT. In other words, autophagy can assist tumor cell survival by recycling damaged organelles and misfolded proteins under different stress conditions (Helgason et al., 2013; White et al., 2015; Levy et al., 2017). Researchers have proposed to inhibit the SDT-induced autophagy in order to improve the efficiency of SDT improvement (Chen et al., 2014; Mahalingam et al., 2014; Vogl et al., 2014; Song et al., 2018; Feng et al., 2019; Qu et al., 2020).

In this review, the mechanism and sonosensitizers of SDT are firstly summarized. Next, the recent progress in tumor therapies with emphasis on SDT is introduced. The relationship between SDT and autophagy in tumor therapies and other metabolic pathways is also reviewed. To better present this study, an introduction to autophagy is also detailed. Finally, a promising tumor therapy, which combines SDT with autophagy inhibition using a nanoparticle delivering system, is presented and investigated.

## 2 Sonodynamic therapy

Before the use of US for therapeutic purposes, the application of light was considered an option for non-invasive therapy, which was referred to as photodynamic therapy (PDT). PDT is the predecessor of SDT. PDT involves three constituent elements: a light source, a photosensitizer, and the local tissue oxygen. Reactive oxygen species (ROS) are formed in the tumor cells and tissues with porphyrins upon irradiation with light (Rkein and Ozog, 2014). PDT can interfere with cytokine-mediated responses in tumor progression and metastasis and play a pivot role (Kaleta-Richter et al., 2019). However, since the light has only a limited penetration depth, PDT cannot be effectively applied to deep-seated tumors (Huang, 2005). At the same time, PDT highly relies on the ability of specific photosensitizing agents to concentrate in tumor cells (Kessel and Oleinick, 2009). Therefore, lacking a suitable photosensitizing agent with high efficiency, good sensitivity, wide applicability, and low toxicity severely constrain the research on PDT. In addition, the study showed that autophagy induced by PDT treatment could act as a mode

of cell death after PDT (Buytaert et al., 2006; Kessel et al., 2006; Xue et al., 2007; Buytaert et al., 2008). However as a double-edged sword, autophagy can also promote tumor cell survival by compartmentalizing and recycling damaged tumor cell components after PDT, which significantly reduces the sensitivity and efficiency of PDT (Kessel et al., 2006; Kessel and Oleinick, 2009; Kaleta-Richter et al., 2019).

Based on PDT, SDT is gradually developed and optimized. The SDT is a new non-invasive tumor treatment method raised by Yumita et al. (1989) in 1989. When conducting research on PDT, they observed that some hematoporphyrin derivatives could also induce cell death under US irradiation (Yumita et al., 1989). It was then found that combined with US irradiation, some hematoporphyrin derivatives could act as sonosensitizers for tumor therapy, and this therapy was referred to as SDT. Research shows that most photosensitizers are sonosensitizers. Both PDT and SDT require the use of photosensitizer/sonosensitizers to trigger intracellular oxygen generation ROS to kill tumor cells. The SDT relies on the US and sonosensitizers present in the tumor tissue, with specific frequency and intensity, US irradiates the tumor site in deep tissue for a particular time, a lethal sono-damage such as necrosis and cell apoptosis by both mechanical stress and chemical reactions is caused and finally kills the tumor cells with high specificity and accuracy (Wang et al., 2013b; Parzych and Klionsky, 2014). Due to the deep penetration of US, SDT overcomes the major limitation of PDT. The SDT method is superior to the PDT method with deeper tissue penetration, higher precision, fewer side effects, and better patient compliance (Wang et al., 2013b; Pan et al., 2018b). The cytotoxic mechanisms of SDT in tumor treatment mainly include ultrasonic cavitation effect, singlet oxygen mechanism, mechanical damages, ultrasonic heating effect, apoptosis theory, and comprehensive effects of the mentioned mechanisms (Liu et al., 2015; Rengeng et al., 2017).

The major limitations of the sonosensitizers used in the SDT include poor delivery accuracy and high toxicity (Pelt et al., 2018). With the development of nanotechnology, nanoparticle-based sonosensitizers were designed, which make use of NPs to deliver the sonosensitizers to target tissues with high specificity (Chen et al., 2014; Qian et al., 2016; Feng et al., 2019; Qu et al., 2020). The other problem encountered is that SDT can promote autophagy in tumor cells, which inhibits the efficiency of SDT. It is because autophagy can assist tumor cell survival by recycling damaged organelles and misfolded proteins under different stress conditions (Helgason et al., 2013; White et al., 2015; Levy et al., 2017). Recently, the effect of autophagy induced by SDT in tumor treatment has drawn increasing attention (Wang et al., 2013b). Researchers have proposed to inhibit the SDT-induced autophagy in order to improve the efficiency of SDT (Chen et al., 2014; Mahalingam et al., 2014; Vogl et al., 2014; Song et al., 2018; Feng et al., 2019; Qu et al., 2020).



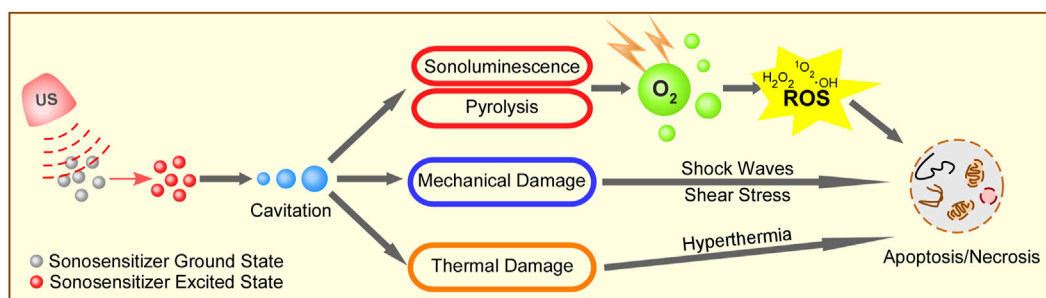


FIGURE 1

Schematic illustration of possible mechanisms of SDT. Ultrasound irradiation activates sonosensitizer from a ground state to an excited state to form cavitation around the surface of cancer cells. The energy from the collapse of cavitating bubbles can initiate sonoluminescent light, mechanical damage, and thermal damage to cancer cells. The energy can be transferred to the circumambient oxygen to produce a large amount of ROS, including singlet oxygen, peroxide, and hydroxyl radical, which subsequently mediate cell apoptosis and necrosis. At the same time, the cavitation also causes shock waves, shear stress, and hyperthermia to induce cell death.

## 2.1 Mechanism of sonodynamic therapy

The mechanisms of SDT include the generation of ROS, US mechanical damage, and thermal destruction. Figure 1 depicts the possible mechanisms of SDT.

### 2.1.1 Generation of reactive oxygen species

ROS generation is the most widely accepted mechanism of SDT, and this theory focuses on the cancer cell apoptosis caused by ROS production induced by cavitation and sonosensitizers (Nora Frulio et al., 2010). Under the irradiation of US, sonosensitizers can be activated from the ground state to the excited state to generate ROS, including singlet oxygen and hydroxyl radicals. Acoustic cavitation plays an important role in activating sonosensitizers to generate ROS during the interaction of US with an aqueous environment. The cavitation process involves the nucleation, growth, and implosive collapse of gas-filled bubbles under certain US conditions. Cavitation can be classified into stable cavitation and inertial cavitation based on its nature. In stable cavitation, gas-filled bubbles oscillate with the surrounding liquid to create a mixing of the surrounding media. In inertial cavitation, the gas-filled bubbles grow to a near resonance size and expand before collapsing violently (Suslick, 1990). A considerable amount of energy is released in the implosion, leading to very high temperature (up to 10,000 K) and pressure (up to 81 MPa) in the microenvironment (Cavalli et al., 2018). The resultant extreme temperature and pressure may act as sonochemical reactors and lead to tumor cell necrosis (Misik and Riesz, 2000).

Two kinds of ROS can be generated by different reactions. The sonosensitizers at excited state can react directly with adjacent oxygen to turn hydrogen atoms to free radicals. Alternatively, the energy released by the sonosensitizers from the excited state to the ground state can be absorbed by the adjacent oxygen to produce high active singlet oxygens ( $^1O_2$ ),

which account for the primary SDT toxicity. In addition, sonoluminescence, a phenomenon referring to that light is generated when a solution is irradiated with US, is identified as another significant mechanism in generating ROS (Suslick et al., 1990; Yin et al., 2016). The sonoluminescent light can motivate the energy-matching photoactive sonosensitizers to a short-lived singlet state, which would lead to photochemical reactions (Didenko et al., 2000; Yin et al., 2016). Pyrolysis can be another possible mechanism for generating ROS (Danno et al., 2008). The extreme temperature and pressure during the implosion of gas-filled bubbles could generate free radicals in the following two ways: direct sonosensitizer breakdown or sonosensitizer reactions with  $H^+$  or  $OH^-$  produced by the thermolysis of water (Danno et al., 2008). Irreversible damage to targeted tumor cells, including cell membrane damage, DNA fragmentation, and mitochondrial membrane potential disturbance, can be induced by the high concentration of ROS (Kwon et al., 2019). Studies have shown that ROS activate autophagy through a variety of pathways to mediate cell survival or death. Especially, it was found that ROS induced by SDT triggered autophagy in a mitochondria-dependent manner (Qu et al., 2020).

### 2.1.2 Ultrasound mechanical damages

The main factors causing US mechanical damage are cavitation effects and US radiation force (Yuan et al., 2015). It was reported that the mechanical pressure from US could lead to cell necrosis (Wang et al., 2003; Hiraoka et al., 2006). During the rapid collapsing of gas-filled bubbles under US irradiation, a considerable amount of energy is released to produce extreme temperature and pressure (Hiraoka et al., 2006). High shear stress and strong shock waves are generated, and they enhance the physical damage to cytomembranes, which ultimately lead to mechanical damage and tumor cell necrosis (Forbes et al., 2011).



TABLE 1 Summary of sonosensitizers and SDT conditions.

Sonosensitizer	Inorganic/ organic	Biological model	US parameters	Biological effects	References
5-ALA	Organic	C6 glioma cells in rat	1.0 MHz, 10.0 W/cm <sup>2</sup> , 5 min	Deep seated intracranial glioma tumor size decreased; selective anti-tumour effect	Ohmura et al. (2011)
ATX-70	Organic	Mammary tumor cells (DMBA) in Sprague–Dawley rat	1.92 MHz, 1.0–5.0 W/cm <sup>2</sup> , 15 min	Significant tumor growth inhibition; strong synergistic effect (Ohmura et al., 2011)	Yumita et al. (2007)
DCPH-P-Na(I)	Organic	MKN-45 cells in mice	1.0 MHz, 1.0 W/cm <sup>2</sup> , 10 min	Potent sonotoxicity on tumor cells under US irradiation; significant tumor growth inhibition; potential for clinical treatment of cancers located deep in the human body without inducing skin sensitivity	Hachimine et al. (2007)
Porfimer sodium	Organic	Mammary tumor cells (DMBA) in Sprague–Dawley rat	1.92 MHz, 1.0–5.0 W/cm <sup>2</sup> , 15 min	Significant tumor growth inhibition; US intensity showed a relatively sharp threshold for the synergistic antitumor effect	Yumita et al. (2004)
Hematoporphyrin	Organic	Hepatoma-22 cells in mice	1.43 MHz, 2.0 W/cm <sup>2</sup> , 1 min	Strong cytotoxic effects; significant lipid peroxidation in tumor cells; tumor volume and weight were remarkably decreased; tumor cell ultra-structure was significantly damaged	Wang et al. (2011)
SF1	Organic	S180 sarcoma cells in mice	1.0 MHz, 1.2 W/cm <sup>2</sup> , 3 min	Tumor growth inhibition effect was enhanced with increasing US intensity; coagulated necrosis or metamorphic tissue with inflammatory reactions	Xiaohuai et al. (2008)
Hematoporphyrin derivatives	Organic	S180 sarcoma cells in mice	1.1 MHz, 1.5 W/cm <sup>2</sup> , 3 min	SDT induced morphologic changes; important factors inhibiting the tumor cell growth and even inducing tumor cell death: damage of cell structure, change of cytochrome C oxidase activity, degradation and missing of DNA	Liu et al. (2003)
Sinoporphyrin sodium	Organic	4T1 mouse xenograft model	1.0 MHz, 1.0 W/cm <sup>2</sup> , 2 min	Increased intracellular ROS production; change of membrane permeability; tumor growth and metastatic spreading inhibitions	Liu et al. (2016)
Protoporphyrin IX	Organic	Oral squamous carcinoma in mice	1.0 MHz, 0.89 W/cm <sup>2</sup> , 20% duty cycle, 15 min	Cell cycle arrested at G2/M phase; activate Fas-mediated membrane receptor pathway (regulated by p53) to induce apoptosis	Lv et al. (2017)
Chlorin e6 (Ce6)	Organic	Human breast cancer MDA-MB-231 cells <i>in vitro</i>	1.0 MHz, 0.5–2.0 W/cm <sup>2</sup> , 1 min	Inhibition on the proliferation of cancer cells; dose-dependently	Gao et al. (2010)
Rose bengal (RB)	Organic	Human colorectal adenocarcinoma cell line (HT-29 cells) in mice	1.0 MHz, 1.0 W/cm <sup>2</sup> , 2 min	Suitable for detecting tumor location and size; higher drug accumulation at the tumor site; enhanced ROS generation efficiency; enhanced SDT therapeutic efficacy with minimal side effects	Hou et al. (2020)
TiO <sub>2</sub>	Inorganic	C32 melanoma cells in mice	1.0 MHz, 1.0 W/cm <sup>2</sup> , 2 min	Tumor cell viability was significantly decreased; significant inhibition of tumor growth	Harada et al. (2011)
PMCS	Inorganic	Human breast cancer cells <i>in vitro</i>	1.0 MHz, 2.5 W/cm <sup>2</sup> , 50% duty cycle, 5 min	High sonosensitization efficacy and good stability; high ROS production and induced cellular destruction; high tumor inhibition efficiency	Pan et al. (2018a)
PtCu <sub>3</sub>	Inorganic	4T1 breast cancer cells in mice	35 kHz, 3.0 W/cm <sup>2</sup> , 10 min	Highly efficient ROS generation in SDT; significantly enhanced sonotoxicity to cancer cells; minimal toxicity to normal tissues at therapeutic doses	Zhong et al. (2020)
BaTiO <sub>3</sub>	Inorganic	<i>In vitro</i> cellular level evaluation and <i>in vivo</i> tumor xenograft assessment	1.0 MHz, 1.0 W/cm <sup>2</sup> , 50% duty cycle, 1 min	Built-in electric field catalyzed the generation of ROS; US triggered cytotoxicity promoted tumor eradication; high therapeutic biosafety.	Zhu et al. (2020a)
Porous silicon NPs	Inorganic	Lung Lewis carcinoma in mice	1.0 MHz, 1.0 W/cm <sup>2</sup> , 3 min	Inhibition on the growth of primary tumor site; slowed down the metastasis process.	Sviridov et al. (2017)

(Continued on following page)

TABLE 1 (Continued) Summary of sonosensitizers and SDT conditions.

Sonosensitizer	Inorganic/ organic	Biological model	US parameters	Biological effects	References
Copper-cysteamine	Organic	4T1 breast cancer cells in mice	1.0 MHz, 2.0 W/cm <sup>2</sup> , 3 min	Efficient production of ROS; significant inhibition of tumor growth; enhanced cavitation for tumor destruction	Wang et al. (2018)
Double-layer hollow manganese silicate (DHMS)	Inorganic	4T1 breast cancer cells in mice	1.0 MHz, 1.0 W/cm <sup>2</sup> , 50% duty cycle, 1 min	Highly effective ROS yield; production of oxygen in the tumor micro-environment to overcome the hypoxia of the solid tumor; good tumor inhibition ability and biosafety	Pan et al. (2020)

### 2.1.3 Thermal destruction

The increase of tissue temperature through absorption and transformation of the US mechanical energy can also lead to tumor cell necrosis (Xiong et al., 2020). For example, under the irradiation of appropriate US, the sonosensitizer mesoporous silica NPs can cause hyperthermia to kill tumor cells. Due to the high penetration and high energy concentration capabilities of US, SDT can cause thermal destruction to deep-seated tumors (Xiong et al., 2020).

## 2.2 Sonosensitizers with nanoparticle delivery system

In SDT, the sonosensitizers can be classified into two groups: organic and inorganic (Table 1). The organic sonosensitizers have high SDT efficiency but with poor pharmacokinetics, skin sensitivity, low stability, and poor SDT efficiency. The inorganic sonosensitizers have superior physical and chemical properties and can be multifunctional. However, the poor SDT efficiency and potential biosafety problems are the main challenges for inorganic sonosensitizers (Liang et al., 2020a).

Currently, there are many limitations of sonosensitizers, which significantly influence the efficiency and sensitivity of SDT. The major challenges are the low drug delivery efficiency and limited generation of ROS (Hou et al., 2020). To make SDT practically applicable, thanks to the fast developing nanotechnology, nanoparticles-based sonosensitizers are introduced, which make use of nanoparticles to deliver the sonosensitizers to target tissues or tumor cells with high specificity and accuracy, and in the end, improve the outcomes of SDT (Pan et al., 2018b). Nano-sonosensitizers can be divided into two groups: nanoparticle as intrinsic sonosensitizer (TiO<sub>2</sub>, Ag/Pt, Si NPs, and polyhydroxy fullerene) and nanoparticle-assisted sonosensitizer (self-assembled, conjugated, embedded, or encapsulated) (Harada et al., 2011; Pan et al., 2018b; An et al., 2020a). Nano-sonosensitizers were summarized in Table 2 of Plenty of previous research has been conducted on NP-mediated SDT. As a typical semiconductor, TiO<sub>2</sub> has drawn much attention,

and TiO<sub>2</sub> NPs are shown to have positive anti-tumor effects both *in vitro* and *in vivo* under US irradiation (Harada et al., 2011). Harada et al. (2011) reported that compared to 1 MHz of US irradiation alone, combined US irradiation of mice injected with TiO<sub>2</sub> had a significant anti-tumor effect. However, the bio-distributions of traditional TiO<sub>2</sub> NPs are hard to manipulate, and the acute and long-run toxicity is unsatisfactory (Chen et al., 2014). Therefore, searching for an efficient and sensitive sonosensitizer is urgently needed.

Organic NP carriers for sonosensitizers are superior in high aqueous solubility, good bio-compatibility, satisfactory targeting specificity, and easy bio-degradation (Qian et al., 2016). Chen et al. (2017b) applied mitochondria targeting liposomes to carry hydrophobic sonosensitizer of hematoporphyrin monomethyl ether, which were released from the liposomes under US, and remarkably prevented the aggregation of sonosensitizers. Canaparo et al. (2013) reported that NPs delivered the sonosensitizers with high accuracy and enhanced the efficiency of carried sonosensitizers. Rui et al. (Hou et al., 2020) designed a sonosensitizer drug delivery system for rose bengal microbubbles. This drug delivery system was shown to have high drug loading content and good US imaging properties. Under US irradiation, the locations and sizes of the tumors were observed. More importantly, the rose bengal microbubbles were converted into rose bengal NPs through sonoporation effects *in situ* with US irradiation, which could bring many favorable effects, including high drug accumulation, and promoted generation efficiency of ROS. The high drug accumulation at the tumor site reduced the side effects, and the improved SDT efficiency showed great potential for cancer therapies.

The multifunctional NP systems with diagnostic and therapeutic functions have recently gained increasing attention in precision nanomedicine (Huang et al., 2018; Li et al., 2019). In the NP system investigated by Li et al. (2016a), the hydrophilic biodegradable polymeric NPs carried both sonosensitizer and a magnetic resonance contrast agent (Li et al., 2019). In order to target the tumor tissues with higher specificity and accuracy, the tumor-homing and penetrating peptide-F3 was used to decorate the surfaces of NPs. This designed F3 decorated poly lactic-co-glycolic acid NP showed a significantly higher tumor tissue concentration than non-targeted NP. More importantly, under

TABLE 2 Summary of nano-sonosensitizers.

NP	Drug carried/ combination drug	Biological models	Target cells	Biological effects	References
TiO <sub>2</sub>	None	C32 melanoma solid tumors in mice	C32 melanoma cells	Tumor cell viability significantly decreased; remarkable antitumor effect	Harada et al. (2011)
Fe <sub>3</sub> O <sub>4</sub> magnetic	Chitosan chloride (HTCC)/alginate	Gastric SGC7901/ADR tumor bearing mice	SGC7901/ADR gastric cancer cells	Excessive ROS accumulation and mitochondrial dysfunction; inhibition on the gastric tumor growth; reduced tumor volume	Li et al. (2016c)
Silver	Reduced graphene-oxide	Human cervical cancer (Hela CCL2) cell lines	Cervical cancer hela cells	Significant effects on the expressions of apoptotic and autophagy genes; accumulation of autophagosomes and autophagolysosomes; substantial generation of ROS	Yuan and Gurunathan (2017)
Gold	Protoporphyrin IX (PpIX)	Colon carcinoma tumor in male BALB/c mice	CT26 cancer cells	Higher tumor cell cellular uptake of PpIX; significant synergistic inhibitory effect on tumor growth; reduced tumor relative volume; increased average animal survival fraction	Shanei et al. (2012)
Porous silicon	Dextran (biopolymer)	Human lung cancer Hep2 cell lines	Hep2 cancer cells	Efficient uptake of the NPs by cancer cells; low cytotoxicity at high concentrations; the number of living cancer cells decreased	Sviridov et al. (2017)
Hollow polydopamine	Platinum NP, doxorubicin (DOX) and chlorine e6 (Ce6)	4T1 breast cancer cells in female Balb/C mice	4T1 cancer cells	Excellent biocompatibility with no toxicity to mice; effective delivery of drugs to target tumor cell mitochondria; relieved hypoxic state of the tumor site	An et al. (2020a)
Poly-methyl methacrylate	Meso-tetrakis (4-sulfonatophenyl) porphyrin (TPPS)	Human neuroblastoma SH-SY5Y cell lines	SH-SY5Y cells	Significant decrease in cancer cell proliferation; significant increase in necrotic and apoptotic cells; increased ROS production	Canaparo et al. (2013)
Poly (lactic-co-glycolic acid) (PLGA)	methylene blue (MB) and gadodiamide (Gd-DTPA-BMA)	MDA-MB-231 breast cancer cells in BALB/c nude mice	MDA-MB-231 cells	Combined therapeutic and diagnostic functionalities; better enrichment at the tumor site; promoted apoptosis triggered by US; good drug safety	Li et al. (2019)
Melanin	Folate and hematoporphyrin monomethyl ether	Human breast cancer MDA-MB-231 cells in female BALB/c nude mice	MDA-MB-231 cells	Enhanced photoacoustic imaging-guided SDT; accurate delivery of drugs to the tumor sites; engendered ROS-mediated cytotoxicity towards tumors	Huang et al. (2018)
Mesoporous silica	Doxorubicin (DOX) and Chlorin e6 (Ce6)	Breast cancer MDA-MB-2231 cells in female BALB/c nude mice	MDA-MB-2231 cells	High drug loading and delivery efficiency; targeted delivery and controllable activation potential; significant antitumor effect	Xu et al. (2020b)
Angiopep-2 peptide-modified liposomes	Ce6 and HCQ	GL261 glioma cells in female C57BL/6 mice	GL261 glioma cells	Selectively accumulated in the brain tumors during blood brain barrier opening; inhibited tumor growth and prolonged survival time	Qu et al. (2020)
Hollow mesoporous TiO <sub>2</sub>	HCQ and cancer cell membrane coating	Human breast cancer MCF-7 cells in nude mice	MCF-7 cells	Hide from macrophage phagocytosis; recognize and target the tumors by homologous targeting ability; elevated sensitivity of cancer cells to SDT	Feng et al. (2019)
Hollow mesoporous manganese trioxide (Mn <sub>2</sub> O <sub>3</sub> )	hyaluronic acid (HA) and HCQ	4T1 breast cancer cells in female BALB/c mice	4T1 cells	Significant lysosomal deacidification and autophagy blockade effects; selectively deliver HCQ to tumor sites; effective HCQ accumulation level at the target site	Zhang et al. (2019a)

satisfactory drug safety, the apoptosis caused by SDT with the designed multifunctional NP system was promoted. The results indicated a potential for further investigations and even clinical trials.

Huang et al (2018) carried out investigations on the combination of SDT with NP-assisted sonosensitizers under

the guidance of photoacoustic imaging, and this novel therapy was expected to eradicate tumor cells accurately. The designed NP-assisted sonosensitizer had a core-shell structure and was based on poly lactic-co-glycolic acid. The core was constructed by integrating melanin NPs for photoacoustic imaging, and the hematoporphyrin monomethyl ether was used to build the

TABLE 3 Category of combination therapy based on SDT in recent years.

Therapy	Materials	Sonosensitizers	<i>In vitro</i>	<i>In vivo</i>	US parameters	References
SDT/chemotherapy	Fe <sub>3</sub> O <sub>4</sub> -NaYF <sub>4</sub> @TiO <sub>2</sub>	TiO <sub>2</sub>	MCF-7	S180	1 W/cm <sup>2</sup> at different time durations (0, 0.5, 1, 3, and 5 min)	Song Shen et al. (2014)
	Fe <sub>3</sub> O <sub>4</sub> @TiO <sub>2</sub> -doxorubicin	TiO <sub>2</sub>	MCF-7	S180	1 W/cm <sup>2</sup> ; 3 min	Shen et al. (2015)
	MTN@DTX-CD	TiO <sub>2</sub>	MCF-7	S180	1 W/cm <sup>2</sup> ; 40 s	Shi et al. (2015)
	HPDF nanomicelle	Hematoporphyrin	MCF-7, MCF-7/ADR	—	1 MHz, 1.5 W/cm <sup>2</sup> ; 30 s	Wan et al. (2016a)
	HPDF nanoparticles	Hematoporphyrin	HepG2	HepG2	1.0 MHz, 1.5 W/cm <sup>2</sup> , 30 s	Liu et al. (2017)
	DOX@MSN-HA	MSN	MDA-MB-231	MDA-MB-231	30 s, 6 times of 5 s sonication, sonication interval = 1 min	Ding et al. (2017)
	O <sub>2</sub> MB-Gem	Rose Bengal	MIA PaCa-2, PANC-1	KPC mouse model	1 MHz, 30 s, 3 W/cm <sup>2</sup> , duty cycle = 50%, and PRF = 100 Hz	Nesbitt et al. (2018)
	DOX@HMONs-PpIX-RGD	PpIX	HCC	HCC	1.0 MHz, 50% duty cycle; 1 min	Li et al. (2018)
	DTX/X-NPs	Ce6	B16F10	B16F10	1.0 W/cm <sup>2</sup> for 1, 3 and 5 min	Liu et al. (2018)
	HPCID (ICG@PCH@Dox@HA)	ICG	4T1	4T1	1.2 MHz for 60 s at 1, 2, and 3 W,	Wu et al. (2019)
	CDP@HP-T	Ce6	4T1	4T1	1.0 W/cm <sup>2</sup> ; 3 min	An et al. (2020a)
	HPT-DOX	TiO <sub>2</sub>	4T1	4T1	1.0 MHz, 50% duty cycle, 0.5 W/cm <sup>2</sup> , 2 min	Liang et al. (2020b)
	O <sub>2</sub> MB-PTX-DOX and O <sub>2</sub> MB-PTX-RB	Rose Bengal	MCF-7	MCF-7	1 MHz, 30 s, 3 W/cm <sup>2</sup> , duty cycle = 50%, and PRF = 100 Hz	Logan et al. (2019)
	DOX@FeCPs	HMME	4T1, CT26	CT26	1.75 W/cm <sup>2</sup> at different time durations (0, 0.5, 1, 3, and 5 min)	Xu et al. (2020a)
	MSN-DOX-Ce6	Ce6	MDA-MB-231	MDA-MB-231	0.5 W/cm <sup>2</sup> ; 1 min	Xu et al. (2020b)
	CLH-5-ALA	5-ALA	4T1	4T1-luc cells	1 MHz, 3 W/cm <sup>2</sup> ; 3 min	Xiao et al. (2021)
	GMCDS-FA@CMC (Au@mSiO <sub>2</sub> /Ce6/DOX/SLB-FA@CMC)	Ce6	3T3, C26	orthotopic colorectal tumors	—	Zhang et al. (2021c)
	CPDP (Ce6/PFP/DTX/PLGA)	Ce6	4T1	4T1	1–2 W/cm <sup>2</sup> for different duration times	Zhang et al. (2021b)
	PCNP-DTX	Phycocyanin (PC)	MCF-7	S180	1 MHz, 0.75 W/cm; 2 min	Cao et al. (2021)
	DOX@PCN-224/Pt	TCPP	HUVEC, SKOV3 and CT26	CT26	1.0 MHz, 1.75 W/cm <sup>2</sup> ; 5 min	Ren et al. (2022)
	ZTC@M(ZIF-8@TPZ/Ce6@cytomembrane)	Ce6	AGS	AGS	1.0 MHz, 1.5 W/cm <sup>2</sup> ; 3 min	Yu et al. (2022)
SDT/immunotherapy	MFC (membrane-coated Fe-PDAP/Ce6)	Ce6	4T1	4T1	1.0 MHz, 2 W/cm <sup>2</sup> , 50% duty cycle; 1 min	Jiang et al. (2022)
	PFCE@THPP <sub>pr</sub> -COPs	THPP	CT26	CT26	40 kHz, 2 W; 10 min	Yang et al. (2022)
	PEG-CDM-aPD-L1/Ce6	Ce6	B16-F10	B16-F10	2 MHz, 2.0 W/cm <sup>2</sup> , 20% duty cycle; 5 min	Huang et al. (2021)
	TiO <sub>2</sub> -Ce6-CpG	TiO <sub>2</sub> -Ce6-CpG	Hepa1-6	Hepa1-6	1.0 MHz, duty cycle: 50%, 1.0 W/cm <sup>2</sup> ; 4 min	Lin et al. (2021)
	TIR@FITC-Nrf2-siRNA	IR780	CT26	CT26	1 MHz, 1.0 W/cm <sup>2</sup> , 50% duty cycle; 10 min	Wan et al. (2021)
SDT/PTT/Immunotherapy	CHINPs	HMME	4T1	4T1	1 MHz, 2.0 W/cm <sup>2</sup> , 50% duty cycle for different durations	Lin et al. (2022)
SDT-PDT	UCNPs@SiO <sub>2</sub> -RB	HMME	T24	—	2 W/cm <sup>2</sup> ; 10 min	Xu et al. (2017)
	Fe@UCNP-HMME	HMME	T24	—	2 W/cm <sup>2</sup> ; 5 min	Wang et al. (2019)
	UCNP@mSiO <sub>2</sub> (RB)-AgNPs	Rose Bengal (RB)	MRSA	—	2 W/cm <sup>2</sup> ; 5 min	Zhao et al. (2020)
	TiO <sub>2</sub>	TiO <sub>2</sub>	PC3	—	—	Aksel et al. (2021)
	NSGQDs	Doped graphene quantum dots	MCF7	—	1 MHz, 1 W/cm <sup>2</sup>	Nene and Nyokong. (2021)

(Continued on following page)

TABLE 3 (Continued) Category of combination therapy based on SDT in recent years.

Therapy	Materials	Sonosensitizers	<i>In vitro</i>	<i>In vivo</i>	US parameters	References
SDT/gas therapy	HMME/MCC-HA	HMME	MCF-7, NIH3T3	MCF-7	1 MHz, 1 W/cm <sup>2</sup> ; 1 min	Feng et al. (2018)
	Lip-AIPH	Bubble liposomal systems	MCF-7	MCF-7	1.0 MHz, 2 min, 50% duty cycle	Lin et al. (2019)
	GCZ@M (GSNO/Ce6@ZIF-8@Mem)	Ce6	4T1	4T1	1 W/cm <sup>2</sup> ; 3 min	An et al. (2020b)
	Au NR-mSiO <sub>2</sub> /AIPH	Au NR-mSiO <sub>2</sub> /AIPH	MCF-7	MCF-7	1.0 MHz, 0, 1.0, 1.5, 2.0, 2.5 W/cm <sup>2</sup> , duration (0, 3, 5, 7, 10 min)	Ye et al. (2021)
	OCN-PEG-(Ce6-Gd 3+)/BNN6	Ce6	4T1	4T1	1 W/cm <sup>2</sup> , duty cycle = 50%, pulse frequency = 100 Hz, and frequency = 1 MHz; 5 min	Zheng et al. (2021b)
	Re-Cy/Re-CHO	Re <sub>(I)</sub> tricarbonyl complexes	4T1	4T1	0.3 W/cm <sup>2</sup> , 3 MHz; 15 min	Zhu et al. (2022)
	T-mTNPs@L-Arg	TiO <sub>2</sub>	MCF-7	MCF-7	1 MHz, 1 W/cm <sup>2</sup> ; 1 min	Zuo et al. (2022)
	BPPL (BP-Pt-PEI-L-Arg)	Black phosphorus	4T1	4T1v	1.0 MHz, 50% duty cycle, 1.5 W/cm <sup>2</sup> ; 3 min	Cheng et al. (2022)
SDT/PTT	HMNCs (hematoporphyrin-melanin nanoconjugates)	Hematoporphyrin	4 T1	4 T1	US for 1, 3, 5, and 7 min	Zhang et al. (2021a)
	Cur-Au NPs-PEG	Cur-Au NPs-PEG	C540 (B16/F10)	C540 (B16/F10)	1.0 W/cm <sup>2</sup> ; 1 min	Kayani et al. (2021)
	TiN (ultra-small titanium nitride) nanodots	TiN	4T1	4T1	40 kHz, 3.0 W/cm <sup>2</sup>	Wang et al. (2021b)
	CD@Ti3C2Tx HJs	Ti3C2Tx	4T1, MG-63, hMSCs	4T1	50 kHz, 3.0 W/cm <sup>2</sup>	Geng et al. (2021)
	H-Ti3C2-PEG NSs	Ti3C2 NSs (Ti3C2 MXene nanosheets)	4T1	4T1	<1 W/cm <sup>2</sup> ; 10 min	Li et al. (2022)
SDT/CDT/chemotherapy	mZMD (mesoporous zeolitic-imidazolate framework@MnO <sub>2</sub> /doxorubicin)	mZM	HeLa	HeLa	1.0 MHz, 50% duty cycle 1.0 W/cm <sup>2</sup> ; 1 min	Guan et al. (2022)
SDT/PDT/chemotherapy	RBNs (RB-loaded peptido-nanomicelles)	Rose Bengal (RB)	CNE-2Z	CNE-2Z	1.5 W/cm <sup>2</sup> , 3 min	Liu et al. (2019)
	OC (oleanolic acid-Ce6)	Ce6	PC9, 4T1	4T1	400 mW/cm <sup>2</sup> , 2 min	Zheng et al. (2021a)
SDT/PDT/PTT	PAIN (peptide amphiphile-ICG nanomicelles)	PAIN	MDA MB-231	MDA MB-231	1.5 W/cm <sup>2</sup> , 5 min	Liu et al. (2020)
SDT/Gas therapy/Immunotherapy	iCRET NPs	iCRET NPs	CT26, 4T1, and 4T1-Luc	CT26	5 min (100 s × 3 points)	Jeon et al. (2022)
SDT/Autophagy	CCM-HMTNPs/HCQ	HMTNPs	MCF-7	MCF-7	1 W cm <sup>2</sup> ; 30 s	Feng et al. (2019)
	ACHL (angiopep-2 peptide-modified-liposomes co-loaded with Ce6 and HCQ)	Ce6	GL261	GL261	1.0 MHz, duty cycle: 20%, ultrasound power: 1 W, burst interval time: 1 s, duration time: 60 s	Qu et al. (2020)
	PpIX/3-MA@Lip	PpIX	MCF-7	MCF-7	1.0 MHz, 1.5 W/cm <sup>2</sup> , 50% duty cycle	Zhou et al. (2021)

shell to enhance photoacoustic imaging-guided SDT. Finally, tumor-targeting ligand folate was attached. The designed NP-assisted sonosensitizer had the following functions: high

photoacoustic imaging contrast enhancement capability, accurate delivery of melanin NPs to target tumor tissues, and enhanced SDT performance. Both *in vitro* and *in vivo*



experiments demonstrated the selective cytotoxicity effects of ROS induced by SDT on tumor cells with the assistance of NP-assisted sonosensitizer, which can promote the eradication of tumor tissues. Meanwhile, the toxicity of the designed NP-assisted sonosensitizer was evaluated, and this sonosensitizer was found to possess high biosafety.

Xu et al. (2020b) synthesized mesoporous silica NPs, and the NPs were loaded with doxorubicin and chlorin e6 as the sonosensitizer. Both *in vitro* and *in vivo* experiments were conducted to evaluate the anti-tumor effect of this NP-assisted sonosensitizer under SDT. The NPs were in the shapes of spheres with uniform sizes. The mesoporous structure led to high drug loading and delivery efficiency. On xenograft tumor-bearing mice, under US irradiation, the synthesized NP-assisted sonosensitizer showed a higher tumor suppression effect than doxorubicin combined with chlorin e6 or doxorubicin alone. The results suggested a potential for solid tumor therapy.

Zhang et al. (2019b) designed a mitochondria-targeted and US-activated NP delivery system for enhanced deep-penetration SDT. The built sonosensitizer IR780-based NPs showed effective surface-to-core diffusion *in vitro* and *in vivo*. With the guidance of US, the acoustic droplet vaporization effect significantly assisted the conveyance of IR780-NPs from the circulatory system to tumor tissues, and the acoustic wave force increased the penetration depth at the same time. Furthermore, the mitochondrial targeting capability of IR780-NPs improved the delivery accuracy. Following the mitochondrial targeting, the overproduction of ROS rendered cancer cells more susceptible to ROS-induced apoptosis. Meanwhile, IR780-NPs helped with photoacoustic and fluorescence imaging, which provided SDT guidance and monitoring potential.

## 2.3 Sonodynamic therapy combined with other therapy

Because of the advantages of SDT, it is an effective method for the treatment of a variety of diseases. Due to the complicated tumor microenvironment, many researchers have integrated SDT with other cancer treatment methods to achieve tumor eradication more effectively (Wan et al., 2016b). SDT can be applied as an adjunctive method to either chemotherapy, PDT, hyperthermotherapy, gas therapy, chemodynamic therapy, immunotherapy, or other therapies (Table 3) (Wan et al., 2016b; Liang et al., 2020a). Recent research suggested that favorable synergistic effects against tumor development and metastasis were achieved *in vitro* and *in vivo* when SDT was combined with other tumor therapies (Kondo and Kano, 1987; Gao et al., 2010; Wang et al., 2015b; Liang et al., 2020a).

### 2.3.1 Sonodynamic therapy with chemotherapy

As one of the commonly adopted clinical therapies against cancer, chemotherapy applies chemotherapeutic drugs with high

toxicity to tumor cells. However, severe systemic side effects caused by chemotherapy have always been the major challenge for this tumor therapy. It is suggested that combining chemotherapy with SDT can lead to significantly improved synergistic therapeutic effects with reduced systemic toxicity (Shen et al., 2015; Shi et al., 2015; Nesbitt et al., 2018; Logan et al., 2019; Liang et al., 2020a; Xu et al., 2020b). Chemotherapy often leads to multidrug resistance, which can cause tumor recurrence and metastasis. Combining SDT with chemotherapy has shown great advantages in overcoming drug resistance owing to controlling the release of drugs and increasing cell membrane permeability (Wan et al., 2016a; Chen et al., 2017a; Liu et al., 2017; Li et al., 2018; Liang et al., 2020b; Guan et al., 2022). Moreover, SDT was found to promote cancer cells' drug sensitivity by improving cellular internalization of chemotherapeutic drugs, activating the mitochondria-caspase signaling pathway, and down-regulating the expression of ATP-binding cassette transporters (Ding et al., 2017; Xu et al., 2020a; Ren et al., 2022). These functions enhanced the cytotoxicity of chemotherapeutic factors and therefore contributed to the promoted therapeutic efficiency (An et al., 2020a; Zhang et al., 2021b; Cao et al., 2021; Zhang et al., 2021c).

### 2.3.2 Sonodynamic therapy with photodynamic therapy

SDT can also be combined with photodynamic therapy, named sono-photodynamic therapy (SPDT). SPDT could enhance intracellular ROS generation, severe mitochondria damage, cell migration inhibition, nuclear condensation, cell membrane permeability, and significantly trigger cell apoptosis (Wang et al., 2013a; Li et al., 2014a; Li et al., 2014b; Wang et al., 2015a; Liu et al., 2016; Atmaca et al., 2021). Nene and Nyokong (2021) designed a nanoplatfrom in which phthalocyanines (Pcs) were conjugated to nitrogen (NGQDs) and nitrogen-sulfur (NSGQDs) graphene quantum dots. The nanoparticles were irradiated with light for photodynamic therapy (PDT), ultrasound for sonodynamic therapy, and the combination of both in photo-sonodynamic therapy (PSDT). They found that only  $^1\text{O}_2$  was detected for PDT treatment. In contrast, both the  $^1\text{O}_2$  and  $\cdot\text{OH}$  radicals were evident after SDT and PSDT treatments, and the combination therapy showed improved ROS generation efficacy compared to the monotherapies (Nene and Nyokong, 2021). Aksel et al. (2021) found that malondialdehyde (MDA) levels were increased while superoxide dismutase activity (SOD), catalase (CAT), and glutathione (GSH) levels were decreased after  $\text{TiO}_2$ -mediated SPDT (Aksel et al., 2021).

### 2.3.3 Sonodynamic therapy with gas therapy

Gas therapy has attracted much attention as a novel "green" cancer treatment strategy in recent years (Chen et al., 2019). To date, several gases, such as nitrogen ( $\text{N}_2$ ),

and nitric oxide (NO), carbon oxide (CO), carbon dioxide (CO<sub>2</sub>), have been involved in these therapeutic approaches (Chen et al., 2019). When SDT is combined with gas therapy for tumor treatment, the US triggers gas donors to release and produce highly toxic products or change the disease condition to promote the tumor suppression effects (An et al., 2020b; Cheng et al., 2022; Zhu et al., 2022; Zuo et al., 2022). The generated gas bubbles could be used as a powerful US contrast agent that greatly enhances the US contrast to guide cancer therapy. Some nanoplateforms, such as Lip-AIPH, Au NR-mSiO<sub>2</sub>/AIPH, OCN-PEG-(Ce6-Gd<sup>3+</sup>)/BNN6, and HMME/MCC-HA, have been explored, which integrated coordinated functions of diagnostics and therapy (Feng et al., 2018; Lin et al., 2019; Zheng et al., 2021b; Ye et al., 2021).

### 2.3.4 Sonodynamic therapy with immunotherapy

As a promising therapeutic modality for cancer treatment, immunotherapy, which stimulates the host tumor-specific innate and acquires systemic immune responses to attack cancer cells, is different from other traditional cancer therapies that directly target malignant cells (Li et al., 2021; Liang et al., 2021). Furthermore, immunotherapy can ablate localized tumors, inhibit distant tumors, and suppress tumor metastasis. After immunotherapy, the host can form long-term immune memory to prevent tumor recurrence (Li et al., 2021; Liang et al., 2021). SDT can motivate immune responses by eliciting ICD (immunogenic cell death) induced by the production of cytotoxic ROSs to suppress tumor growth and prevent tumor recurrence effectively (Li et al., 2020; Cheng et al., 2021; Yin et al., 2021). PFCE@THPP<sub>pr</sub>-COPs designed by Yang et al. (2022) can attenuate tumor hypoxia and suppress tumor growth by inducing ICD of cancer cells. After combining with anti-CD47 immunotherapy, this synergistic treatment exhibited potent protective memory antitumor immunity to prevent tumor recurrence (Yang et al., 2022). Some smart SDT platforms that induced potent antitumor immune responses were designed in recent years, such as MON-PpIX-LA-CO<sub>2</sub> (Yin et al., 2021), DYSP-C34 (Wang et al., 2021a), TiO<sub>2</sub>@CaP (Tan et al., 2021), membrane-coated Fe-PDAP/Ce6 (Jiang et al., 2022), Zn-TCPP/CpG (Zhu et al., 2020b), and so on. Immunotherapy has great potential to be combined with SDT to achieve more effective cancer treatments. Yue et al. (2019) combined noninvasive SDT with checkpoint blockade immunotherapy by the nanosensitizers HMME/R837@Lip to induce an anti-tumor response, and this combination arrested primary tumor progression and prevented lung metastasis. Other nanocarriers combining SDT with immunotherapy were also developed, such as TIR@FITC-Nrf2-siRNA (Wan et al., 2021), TiO<sub>2</sub>-Ce6-CpG (Lin et al., 2021), PEG-CDM-aPD-L1/Ce6 (Huang et al., 2021) and this combinatorial tumor therapeutics can robust anti-cancer immunity and long-term immune memory (Table 3).

### 2.3.5 Sonodynamic therapy with other therapies

Materials with high absorbance in the NIR-II region could be applied in photo-induced cancer therapy. The photothermal effect could prolong blood circulation and improve the O<sub>2</sub> supply, promoting ROS generation (Wang et al., 2021b; Geng et al., 2021; Li et al., 2022). The thermal effect in photothermal therapy can boost the efficiency of SDT and achieve synergistically enhanced therapeutic purposes (Zhang et al., 2021a; Kayani et al., 2021). At the same time, researchers have found that SDT can induce protective autophagy, which significantly reduces the efficiency of SDT, making it possible to combine SDT with autophagy to enhance the therapeutic efficacy (Feng et al., 2019; Liang et al., 2020a; Qu et al., 2020; Zhou et al., 2021).

## 3 Autophagy

### 3.1 Overview of autophagy pathway

Autophagy can be divided into three types according to the role of lysosomes, including macroautophagy, microautophagy, and chaperone-mediated autophagy. Macroautophagy (referred to as autophagy) is a process in which cells can form double-membraned autophagic vesicles named autophagosome that sequesters damaged organelles and misfold proteins and fuse with lysosome to form autolysosome for degradation (Figure 2) (Antonoli et al., 2017; Zhao et al., 2021). Microautophagy refers to a process in which misfolded proteins or damaged organelles are directly wrapped by lysosomal traps without forming autophagosomes. Molecular chaperone mediated autophagy refers to the process in which substrate protein is bound to lamp-2A receptor on lysosome by molecular chaperone such as HSP70, mediating its degradation (Bandyopachyay and Cuervo, 2008). Therefore, the autophagy process discussed in this paper is macroautophagy, referred to as autophagy.

#### 3.1.1 Initiation

Induction of autophagosome formation is regulated by the Unc-51-like kinase (ULK) complex, which is made up of a ULK family kinase (ULK1 and ULK2), autophagy-related gene 13 (ATG13), RB1-inducible coiled-coil 1 (RB1CC1/FIP200) and ATG101 (Hara et al., 2008; Chan, 2009; Zachari and Ganley, 2017).

#### 3.1.2 Nucleation, elongation, and maturation

The phosphatidylinositol 3-phosphate kinase (PI3K) complex consists of VPS34, BECN 1, ATG14L, and p150. Next, NRBF2 is recruited to the putative site of autophagosome formation (Matsunaga et al., 2009; Lu et al., 2014). Phosphatidylinositol (PI) in isolation membrane or omegasome is phosphorylated by the PI3K complex to produce phosphatidylinositol 3-phosphate (PtdIns3P), which

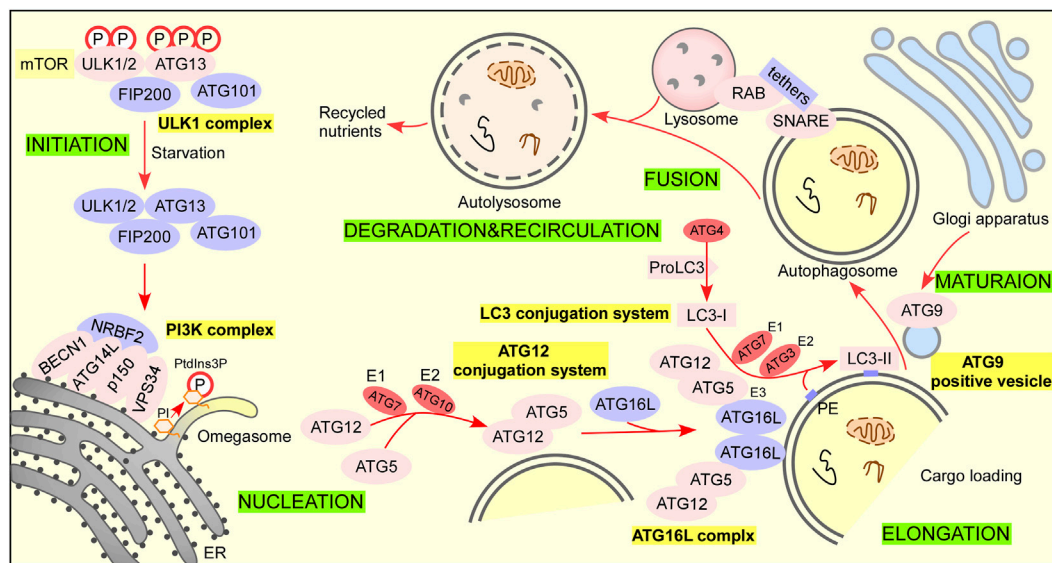


FIGURE 2

The autophagy pathway. There are 6 steps in the autophagy pathway. Step 1 Initiation: activation of ULK1 complex and multiple ATG proteins are engaged and localized to PAS. Under nutrient-rich conditions, mTORC1 phosphorylates ATG13 and ULK1/2 and blocks the interaction of ATG13 with ULK1/2, FIP200, and ATG101 to inactivate them (Hosokawa et al., 2009a; Hosokawa et al., 2009b; Park et al., 2016). When treated with rapamycin or under starvation conditions, mTORC1 dissociates from the complex and partially dephosphorylates these sites resulting in the complex anchors to a pre-autophagosomal structure (PAS) that recruits autophagy-related (ATG) proteins onto it to initial autophagy (Chan, 2009). Steps 2 Nucleation: ATG12 conjugation system and LC3 conjugation system are recruited to form phagophore. The ubiquitin-like protein ATG12 activated by the E1 enzyme ATG7 and E2 conjugating enzyme ATG 10 is irreversibly conjugated to ATG5 (Geng and Klionsky, 2008; Nakatogawa, 2013). The ATG12–ATG5 conjugate binds ATG16L1 with a lysine residue (K) in ATG5 to form the ATG16L1 complex (Hanada et al., 2007). The dimerization of ATG16L promotes membrane expansion (Ishibashi et al., 2011). ProLC3 is first cleaved by the cysteine protease ATG4 to expose their C termini glycine residue to form LC3-I (Satoo et al., 2009). LC3-I is activated by the E1 enzyme ATG7 and transferred to E2 enzyme ATG3, and the ATG16L complex exerts E3 enzyme activity that promotes the lipid conjugation of PE to LC3-I to form LC3-II for autophagosome formation (Kabeya et al., 2000; Fujita et al., 2008; Satoo et al., 2009; Nakatogawa, 2013). Step 3 Elongation: lipid enrichment supports a complex ubiquitin-like conjugation system that results in the conjugation of LC3 family members to the lipid phosphatidylethanolamine (PE) on phagophore. LC3 serves as a docking site for cargo adaptors that enable cargo loading into the AV. Step 4 Maturation: completion and transport of the autophagosome. ATG9-positive vesicles are delivered trans-Golgi apparatus, recycling endosome, and plasma membrane to contribute autophagosome maturation (Ravikumar et al., 2010; Takahashi et al., 2011; Orsi et al., 2012; Imai et al., 2016). Step 5 Fusion: autophagosome fuses lysosome to form autolysosome. Step 6 Degradation and recycling: degradation of cargo inside autolysosome and recycling of nutrients.

recruits multiple PtdIns3P-binding proteins to regulate autophagosome formation. ATG12 conjugation system and LC3 conjugation system are involved in elongation. The ATG12-conjugation system includes ATG12, ATG7, ATG10, ATG5, and ATG16L. The LC3-conjugation system includes ProLC3, ATG4, LC3-I, ATG7, ATG3, and LC3-II (LC3-I/PE). The ATG9A/ATG2-WIP1/2 trafficking system consisting of ATG9A, ATG2, and WIP1/2 is also involved in autophagosome precursor formation.

### 3.1.3 Fusion

The fusion of autophagosomes with functional endolysosomal compartments (early endosomes, late endosomes, and lysosomes) is required for autophagosome maturation, which is regulated by RABs, tethers (HOPS), and the SNARE complex (Itakura et al., 2012; Jiang et al., 2014; Tsuboyama et al., 2016; Shen et al., 2021).

### 3.1.4 Degradation and recirculation of autophagosomal contents

When autophagosome fuses with lysosomes to form autolysosome, autophagic cargo such as misfolded protein and damaged organelles are degraded by lysosomal hydrolases as well as the inner membrane of the autophagosome is degraded into amino acids or peptides for recycling by cells (Mony et al., 2016; Yim and Mizushima, 2020).

## 3.2 Relationships between autophagy and tumor

Research has shown that the occurrence and development of tumors are closely related to autophagy. Autophagy is deemed an evolutionarily conserved catabolic process in mammalian cells (Glick et al., 2010; Amaravadi et al., 2019). In the autophagy process, a

double-membrane autophagosome with a sequestered intracellular component is delivered and fused with lysosomes for degradation (Parzych and Klionsky, 2014). Recycling these materials can provide energy for the survival of cells under a variety of stress conditions (Glick et al., 2010; White et al., 2015; Kocaturk et al., 2019). The protein aggregates and damaged organelles are also removed to ensure cell homeostasis and quality control (Glick et al., 2010; Kocaturk et al., 2019). Autophagy regulates various physiological functions such as stress resistance, cell death determination, and tissue remodeling. For human cancers, large-scale genomic analysis reveals that it is uncommon to lose or mutate core autophagy genes (Amaravadi et al., 2016). However, oncogenic events that activate autophagy and lysosome biogenesis are identified (Amaravadi et al., 2016). In addition, autophagy can promote cellular senescence and cell surface antigen presentation, which prevents genome instability and necrosis and finally prevents cancer (Glick et al., 2010). Autophagy impacts the interaction between the tumor and the host by assisting stress adaption and eliminating activation of adaptive immune responses. In addition, autophagy helps the crosstalk between the tumor and the stroma, which assists tumor growth under different stress conditions. Therefore, the factors influencing autophagy in cancer include microenvironment stress, starvation level, and the immune system (Amaravadi et al., 2016).

The dichotomous role of autophagy in tumor cells is elaborated in detail. On the one hand, in normal cells, the basal level of autophagy is crucial in ensuring protein quality control by removing misfolded proteins and preventing the accumulation of damaged DNA from maintaining genetic stability. As a result, the autophagy process can suppress the formation of tumor cells. At the early stage some tumors can undergo autophagic cell death (ACD) through the induction of autophagy by some anticancer drugs, in which progress autophagy plays a pro-death role (Amaravadi et al., 2016). On the other hand, autophagy can help tumor cells adapt to diverse adverse environments by providing nutrients and removing cytotoxic substances under stress, thus assisting tumor cell survival. In these circumstances, autophagy plays a pivotal cytoprotective role in promoting malignant tumors' proliferation, invasion, and metastasis (White et al., 2015). In brief, autophagy acts as a double-edged sword (can have both pro-survival and pro-death effects) in tumor occurrence, development, and metastasis (Helgason et al., 2013; Levy et al., 2017; Yun and Lee, 2018; Amaravadi et al., 2019).

## 4 The crosstalk of sonodynamic therapy and autophagy

### 4.1 Sonodynamic therapy induced autophagy

SDT triggers autophagy (or macroautophagy), which can be divided into two conditions in cancer therapy and lipid metabolism,

as summarized in Figure 3. SDT-induced autophagy represents a double-edged sword, and a combination SDT with autophagy inhibition/activation strategies is summarized in Table 4.

#### 4.1.1 In cancer therapy

The ultimate target of all anti-tumor therapies is to kill the tumor cells effectively and specifically. Cell death is classified into three types: apoptosis, autophagy, and necrosis (Kitanaka and Kuchino, 1999). Up to now, the major method in anti-tumor therapy is to induce apoptosis. However, tumor cells can escape from apoptosis with multiple pathways triggered by the anti-tumor treatments, among which autophagy is a novel cellular response and is attracting increasing attention (Hsin et al., 2011). Autophagy protects tumor cells from various stimuli, including amino acid deficiency, hypoxia, DNA and mitochondrial damage, and oxidative stress (Amaravadi et al., 2016). With SDT, the tumor cells suffer from various environmental stresses, and therefore autophagy is promoted to assist the tumor cell survival. As a result, the efficiency of SDT is significantly reduced. Many researchers have carried out investigations on SDT-induced autophagy in different tumor cells.

Su et al. (2015) investigated the interplay between apoptosis and autophagy induced by SDT in leukemia K562 cells. Under the protoporphyrin IX (PpIX)-mediated SDT, with the techniques of morphological observation and biochemical analysis, the mitochondrial-dependent apoptosis was noted. At the same time, SDT was observed to promote Autophagy in K562 cells and caused an increase in EGFP-LC3 puncta cells, conversion of LC3 II/I, formation of autophagosome, and co-localization between LC3 and LAMP2 (a lysosome marker). It was proposed that the SDT-induced autophagy is a cytoprotective mechanism because the autophagy inhibitor 3-MA or bafilomycin A1 was shown to suppress autophagy and enhance the SDT-induced apoptosis and necrosis. Experimental data suggested that the ROS caused by PpIX-SDT treatment may play an important role in inducing autophagy. Wang et al. (2013b) investigated the potential inductions of autophagy. Many signaling pathways are involved in the SDT-induced autophagy, such as those related to the control of mitochondria damage and ROS generation. Mitochondria can be a source of ROS and a target of oxidative damage during oxidation stress. In the experiments, the generation of ROS after SDT diffuses the whole cells, including mitochondria, and the accumulated ROS significantly affects the normal functions of the mitochondria. The damaged mitochondria co-localized rapidly with the autophagosome marker, which suggested that mitochondria damage can be one of the triggers for the induction of autophagy. In addition, ROS was also found to be involved in SDT-induced autophagy. Song et al. (2018) proposed the PINK1/Parkin-dependent signaling pathway to initiate mitophagy and autophagy in the human breast adenocarcinoma cell line MCF-7 cells subjected to SDT. The 5-aminolevulinic acid was used as the sonosensitizer. Excessive productions of ROS caused by SDT, together with the PINK1/Parkin-dependent signaling pathway,



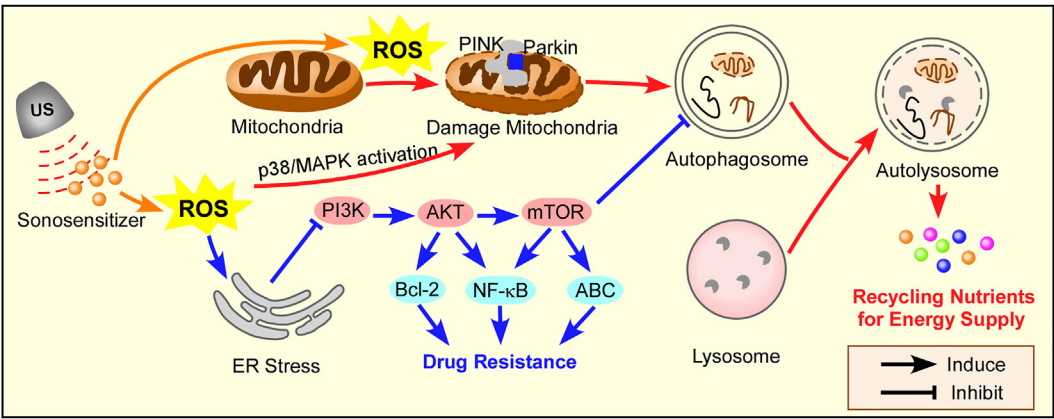


**FIGURE 3**  
The mechanism of autophagy induction by SDT. ROS triggers mitochondria-apoptosis, which induces protective autophagy through the PINK/ Parkin pathway in cancer therapy. SDT can inhibit chemotherapy sensitivity by ROS-induced ER stress, which activates autophagy in PI3K/AKT/mTOR pathway. Red arrow for cancer therapy, blue arrow for drug resistance in cancer therapy.

acted together to initiate mitophagy. The initiated mitophagy and autophagy helped protect the tumor cells against SDT-induced cell death. [Qu et al. \(2020\)](#) designed an “all-in-one” nanosensitizer platform that incorporated Ce6 and HCQ into angioprep-2 peptide-modified liposomes named ACHL. They found that SDT triggered mitophagy dependent on MAPK/p38 activation, which attenuated apoptosis in glioblastoma cells.

It is worth noting that SDT can enhance chemotherapy sensitivity and reverse drug resistance in tumor cells. At the same time, important clues have emerged that autophagy promotes tumor drug resistance by involves the changes of apoptotic signals ([Chang and Zou, 2020](#)). The inhibition of

Hedgehog (Hh) signaling pathway induces autophagy in BCR-ABL+ CML cells. Simultaneously inhibiting the Hh pathway and autophagy overcome CML drug resistance ([Zeng et al., 2015](#)). Many studies have shown that the addition of inhibitors of the PI3K/AKT/mTOR pathway can effectively enhance tumor therapy ([Chang et al., 2013](#); [Rangwala et al., 2014](#); [Zeng et al., 2015](#)). [Wu et al. \(2018\)](#) found that autophagy was induced in paclitaxel-resistant PC-3 cells after SDT treatment. A possible mechanism for promoting autophagy in paclitaxel-resistant PC-3 cells after SDT was the endoplasmic reticulum stress-mediated PI3K/AKT/mTOR signaling pathway. In the experiments, the observation of autophagy was realized by TEM and fluorescence

**TABLE 4** Summary the autophagy activation of SDT.

Type of cancer cell line	Sonosensitizer	Autophagy role	References
Murine leukemia L1210 cells	Protoporphyrin IX (PpIX)	Pro-survival	<a href="#">Wang et al. (2013b)</a>
4T1 cells	Ce6	Pro-survival	<a href="#">Li et al. (2014a)</a>
K562cells	Protoporphyrin IX (PpIX)	Pro-survival	<a href="#">Su et al. (2015)</a>
THP-1-derived macrophage	Hypericin	Pro-death	<a href="#">Li et al. (2016b)</a>
THP-1 macrophages	Berberin	Pro-death	<a href="#">Kou et al. (2017)</a>
THP-1 macrophages	Hydroxysafflor yellow A	Pro-death	<a href="#">Jiang et al. (2017)</a>
PTX-resistant PC-3 cells	—	Pro-survival	<a href="#">Wu et al. (2018)</a>
MCF-7 cells	5-ALA	Pro-survival	<a href="#">Song et al. (2018)</a>
MCF-7 cells	Hollow mesoporous titanium dioxide nanoparticles (HMTNPs)	Pro-survival	<a href="#">Feng et al. (2019)</a>
GL261 cells	Ce6	Pro-survival	<a href="#">Qu et al. (2020)</a>
4T1 cells	HMME@HMONS-3BP-PEG	Pro-death	<a href="#">Zou et al. (2021)</a>
MCF-7 cells	Protoporphyrin IX (PpIX)	Pro-survival	<a href="#">Zhou et al. (2021)</a>
B16-F0 mouse melanoma cells	Ce6	Pro-death	<a href="#">Zhang et al. (2022)</a>



TABLE 5 Summary of autophagy inhibitors.

Drugs	Target	Biological models	Status of the study	Biological effects	References
Chloroquine (CQ)	Lysosomal pH	Human breast cancer MCF-7 cells; human colorectal cancer cells	Approved by FDA; phase I clinical trial	Inhibition of protective autophagy by blocking autophagosome fusion and degradation; autophagy inhibition at the late stage of the pathway; evidence of preliminary antitumor activity	<a href="#">Sui et al. (2013)</a>
Hydroxychloroquine (HCQ)	Lysosomal pH	Human esophageal, hepatocellular carcinoma, lung, and pancreatic cancer cells	Approved by FDA; phase I clinical trial	Inhibition of autophagosome fusion with lysosomes and autophagosome degradation; autophagy inhibition at the late stage of the pathway; induction of autophagic tumor cell death; safely dose escalated in cancer patients	<a href="#">Sui et al. (2013)</a>
HCQ + tamoxifen	Lysosomes, estrogen receptor- $\alpha$ (ER $\alpha$ )	Human breast cancer cells in female athymic mice	<i>In vivo</i> models; cancer cell lines; phase I clinical trial	Reduced drug resistance; <i>In vitro</i> and <i>in vivo</i> promotion of antiestrogenic therapy	<a href="#">Cook et al. (2014)</a>
HCQ + temsirolimus	Lysosomes, mTOR pathway	Human renal carcinoma cell lines	Cancer cell lines	Induction of apoptosis and cell death; promotion of mitochondrial damage with mTOR down-regulation; tumor growth suppression	<a href="#">Lee et al. (2015)</a>
3- methyladenine (3-MA)	Autophagosome formation, class III PI3K inhibitor	Human chronic myelogenous leukemia K562 cell line	Cancer cell lines	Inhibition on the formation of autophagosomes; autophagy inhibition at the early stage of the pathway; aggravated chromatin condensation; enhanced SDT-induced apoptosis and necrosis	<a href="#">Su et al. (2015)</a>
Bafilomycin A1 (Ba A1)	Autophagolysosome formation, vacuolar-type H (+)-ATPase inhibitor	Murine sarcoma S180 cell line	Cancer cell lines	Inhibition on the fusion between autophagosomes and lysosomes; autophagy inhibition at the late stage of the pathway; enhanced SDT induced caspase-3 and PARP cleavage; enhanced SDT-induced cell death and anti-tumor effect	<a href="#">Wang et al. (2010a)</a>
Monensin	Endocytic and lysosomal pH	Human non-small lung cancer NCI-H1299 cell line	Cancer cell lines	Inhibition on the fusion between autophagosomes and lysosomes; autophagy inhibition at the late stage of the pathway; enhanced cell cycle arrest and apoptosis; tumor growth suppression	<a href="#">Choi et al. (2013)</a>
Wortmannin	Autophagosome formation, class III PI3K inhibitor	Hepatocytes from male wistar rats	Cells	Inhibition of autophagosome formation; potent inhibition of mammalian PtdIns 3-kinase; autophagy inhibition at the early stage of the pathway	<a href="#">Wang et al. (2010b)</a>
2- (4-morpholinyl)-8-phenyl-chromone (LY294002)	Autophagosome formation, class III PI3K inhibitor	Chinese hamster ovary (CHO) cell line	CHO cell lines	Inhibition of autophagosome formation; promotion of rolipram-induced PDE4A4 aggregate/foci formation; potent inhibition of autophagic sequestration; autophagy inhibition at the early stage of the pathway	<a href="#">Christian et al. (2010)</a>

microscopy. After SDT, the inhibition of PI3K/AKT/mTOR signaling pathway by endoplasmic reticulum stress-induced autophagy and autophagy reduced endoplasmic reticulum stress by eliminating the elimination of misfolded proteins and reactive oxygen species. It was further found that autophagy inhibition promoted endoplasmic reticulum stress, therefore down-regulating the PI3K/AKT/mTOR signaling pathway and finally leading to cell death ([Wu et al., 2018](#)).

## 4.2 Combining autophagy inhibition with sonodynamic therapy in cancer therapy

Considering the unfavorable effects of autophagy induced by SDT, many researchers suggested that the combination of SDT with autophagy inhibition can improve the efficiency of tumor therapy ([Wang et al., 2010a](#)). The role of autophagy in SDT-induced cytotoxicity in S180 cells was investigated by Wang et al., and an

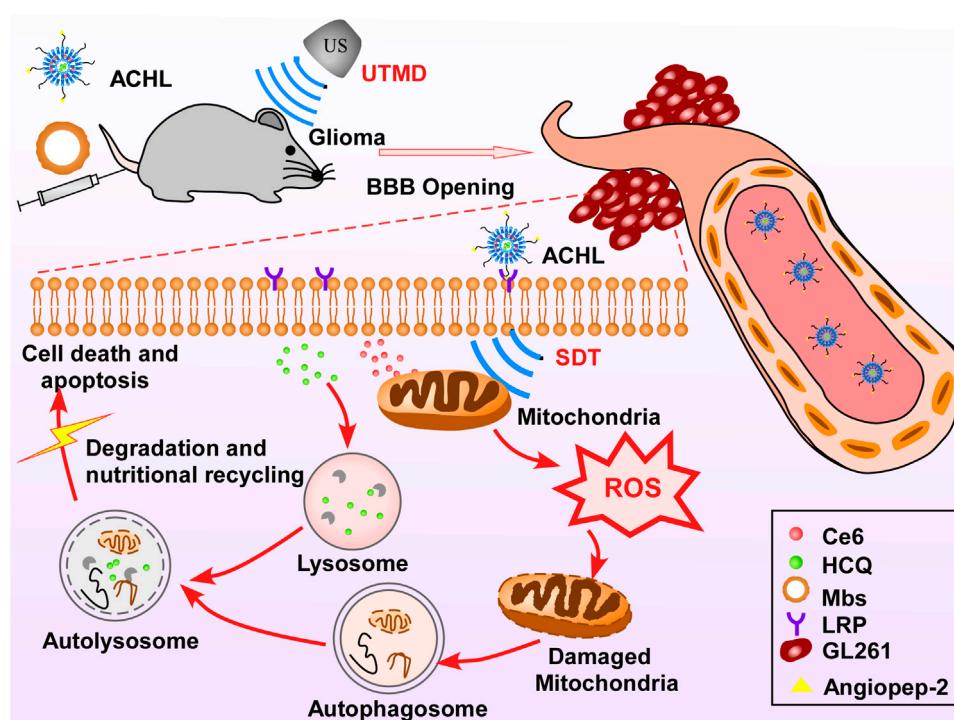


FIGURE 4

Schematic of "all-in-one" nanosensitizer platform. An "all-in-one" nanosensitizer platform by incorporating Ce6 and HCQ into angiopep-2 peptide-modified liposomes (designated ACHL) for orthotopic glioma theranostics was designed. An initial ultrasonic pulse (US1) destroyed the microbubbles and promoted the ACHL into the reversibly opened BBB, while a second ultrasonic stimulus (US2) generated the SDT effects. SDT-mediated mitophagy and its inhibition by HCQ were evaluated, along with the anti-glioma effects. The MAPK/p38 signaling pathway contributed to the progression of mitophagy induced by nanoCe6-SDT.

autophagy inhibitor study was performed. Through ample experiments, the autophagy inhibitors significantly promoted the SDT-induced cell death. Specifically, autophagy can participate in SDT-induced cell death, and the inhibition of autophagy at an early stage can promote the tumor treatment efficiency of SDT by the induced apoptosis and necrosis. Autophagy was detected in the S180 cells treated with SDT under TEM. Double membrane-enclosed vacuoles containing damaged cellular components were observed with TEM. The autophagosomes and autolysosomes involved in this process were further confirmed by the immunofluorescence method. Western blot analysis showed that after SDT, autophagy flux happened in the early stage of cell damage. Kessel and Oleinick raised a similar point that within 1 hour following PDT, the PDT-induced autophagy can be detected. The results showed that with the application of autophagy inhibitors 3-methyladenine or Bafilomycin A1, after 1 hour following SDT, the loss of mitochondria membrane potential greatly increased, and therefore inhibiting autophagy can accelerate SDT induced cell death (Kessel and Oleinick, 2009).

Su et al. (2015) reported that intensified autophagy in human chronic myelogenous leukemia K562 cells was induced by

protoporphyrin IX (PpIX) mediated SDT, and the induced autophagy was related to the up-regulation of Beclin-1 and the autophagic vacuoles observed in the SDT treated K562 cells. In the experiments, transfection of Beclin-1 shRNA inhibited the conversion of LC3 II/I and autophagic vacuoles significantly, which showed that autophagy was inhibited due to shRNA caused down-regulating of Beclin-1. In addition, compared with SDT only, the combined treatment with Beclin-1 shRNA led to more severe cytotoxicity. It was, therefore, demonstrated that SDT promoted autophagy of K562 cells significantly, autophagy might exert a self-protective effect against sonodamage for K562 cells, and finally, autophagy inhibition promoted cell apoptosis induced by SDT effectively.

The promising role of autophagy for drug development in cancer treatment was discussed. The state-of-art autophagy targeting methods and the potential role of autophagy in tumor immunity were thoroughly studied and reported. Autophagy suppressed tumor initiation but promoted advanced tumor growth. It was further found that autophagy inhibition could be sensitive and effective in advanced cancer therapy (Tanida, 2011). A variety of autophagy inhibitors in clinical trials and laboratory research were discussed, among which

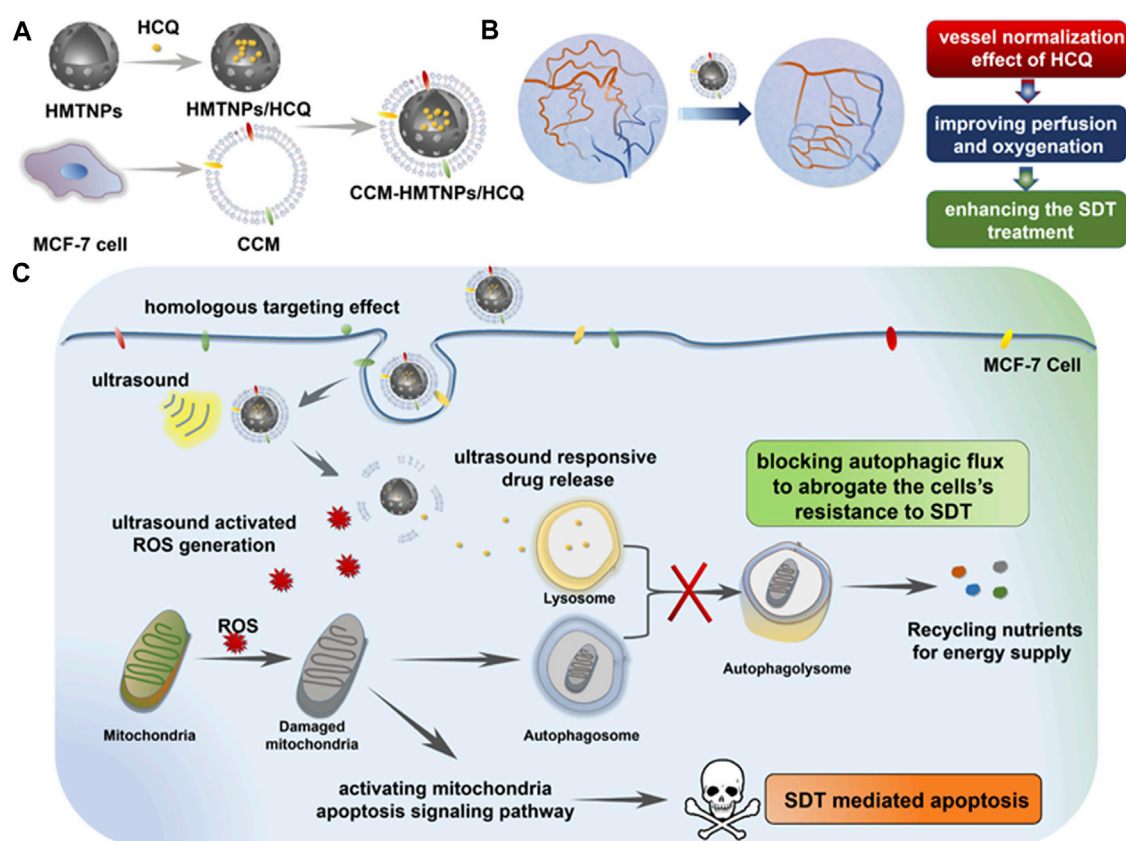


FIGURE 5

Schematic of the Cancer Cell Membrane Biomimetic Nanoplatform. (A) formulation of CCM-HMTNPs/HCQ, (B) vessel normalization effect of HCQ for enhancing the oxygen-dependent SDT treatment, and (C) schematic mechanism of CCM-HMTNPs/HCQ for enhanced SDT on breast cancer via autophagy regulation strategy. Copyright 2019, ACS Applied Materials & Interfaces.

hydroxychloroquine (HCQ) treatment was found to be effective in cancer treatment (Shi et al., 2017). The combination of HCQ with other chemicals as the autophagy inhibitor for cancer therapy was also discussed (Goldberg et al., 2012; Cook et al., 2014; Mahalingam et al., 2014; Rangwala et al., 2014; Rosenfeld et al., 2014; Vogl et al., 2014). To conclude, the autophagy inhibitor plays a promising role in tumor treatment. Autophagy inhibitors were summarized in Table 5. Still, research on a suitable autophagy inhibitor with superior targeting, high efficiency, good sensitivity, and low toxicity is further needed. The initiation of autophagy by protoporphyrin IX (PpIX) mediated SDT in murine leukemia L1210 cells was examined by Wang et al. (2013b). Experiments showed that autophagy was protective for tumor cells after SDT and therefore impairment of autophagy can enhance the anti-tumor effect. Experimental data suggested that autophagy inhibition accelerated apoptosis and necrosis of SDT-treated tumor cells. A treatment combining autophagy inhibitors with SDT promotes tumor cell death and will be a promising method for cancer therapy.

Based on the above literature review, it is clearly identified that both SDT and autophagy inhibition has great potential in tumor

therapy. To encounter the limitations of traditional sonosensitizers, the nanoparticles-based sonosensitizers, which make use of nanoparticles to deliver the sonosensitizers to target tissues or tumor cells, were introduced and investigated. The combination of SDT with nanoparticles-based sonosensitizers and autophagy inhibition proves to be a superior therapy with high specificity and accuracy and improves the outcomes of traditional tumor treatment methods. As an innovative tumor treatment concept, few researchers have carried out investigations in this field. However, as Qu et al. (2020) and Feng et al. (2019) suggested, this combinational tumor therapy method is sensitive, effective, and safe.

Qu et al. (2020) designed a novel "all-in-one" nanosensitizer and improved the SDT efficiency in glioma therapy. The "all-in-one" nanosensitizer incorporates the sonoactive chlorin e6 (Ce6) and hydroxychloroquine (HCQ) into angiopep-2 peptide-modified liposomes (APL), in which APL acts as the NP platform for drug delivery, Ce6 acts as the sonosensitizer, and HCQ acts as the autophagy inhibitor. APL can selectively accumulate in the glioma cells in the brain, which is a good strategy for precise drug delivery and can help minimize the side effects of the applied drugs on

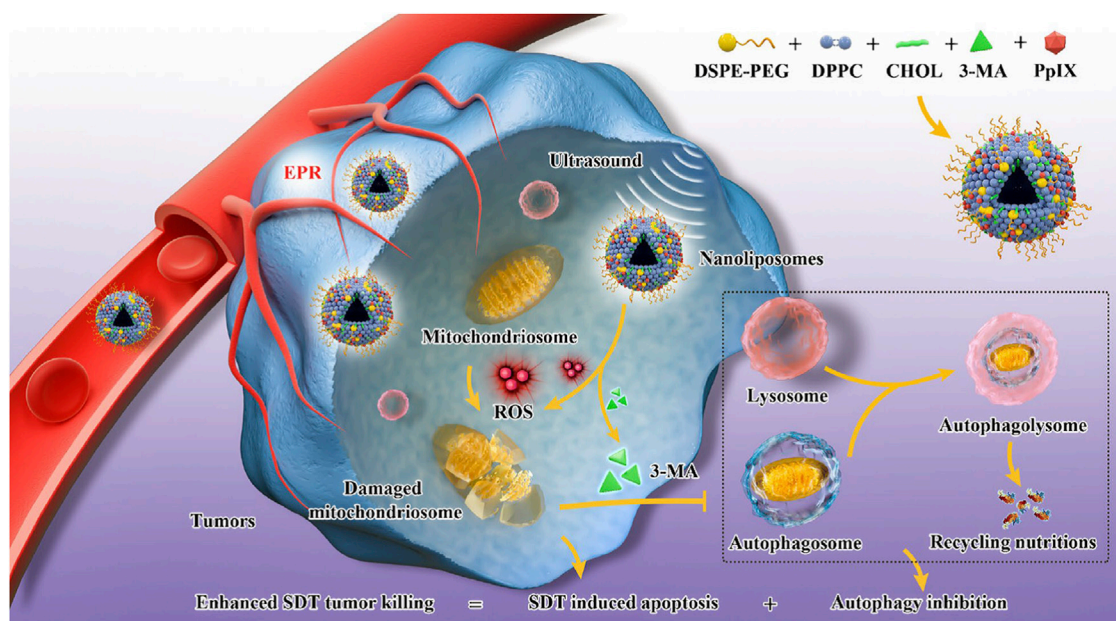


FIGURE 6

Engineering PpIX/3-MA@Lip nanosensitizer for synergistic SDT nanotherapeutics and autophagy blockage on combating cancer. The synthetic procedure of PpIX/3-MA@Lip nanosensitizers and schematic illustration of "all-in-one" strategy for cellular mechanism on SDT-induced cytoprotective autophagy and autophagy inhibition-enhanced antitumor efficacy of SDT. Enhanced production of intracellular ROS radicals by PpIX sonosensitizers-based SDT induced cytoprotective pro-survival autophagy. The integrated 3-MA inhibited the formation of autophagosomes in early-phase autophagy to eliminate the recycling nutrients for fulfilling the needs of cancer-cell adaptation and growth, which significantly induced the cancer-cell apoptosis and death. Copyright 2021, Journal of Nanobiotechnology.

orthotopic cells. As the autophagy helps tumor cells adapt to oxidative injury and other stress after SDT by recycling the damaged mitochondria, the autophagy inhibitor HCQ prevents the above process and significantly enhances the SDT therapeutic effect. The mechanism of autophagy inhibitor improving SDT efficiency was proposed in this review as the autophagy blockage can enhance oxidative damage and increase the apoptosis response (Figure 4).

A similar therapeutic method was reported by Feng et al. (2019), in which the sonosensitizer hollow mesoporous titanium dioxide NPs (HMTNPs), along with the autophagy inhibitor HCQ, were combined and coated with cancer cell membranes (CCM). The biomimetic CCM coating allowed the CCM-HMTNPs/HCQ drugs to be delivered to target tumor cells. Under US irradiation during SDT, HCQ was released to block the autophagy process. Moreover, the vessel normalization effect of HCQ improved the tumor cell hypoxia situation, which significantly promoted the oxygen-dependent HMTNPs-mediated SDT (Figure 5). It was concluded that the CCM-HMTNPs/HCQ drugs highly enhanced the sensitivity and efficiency of SDT on breast tumor cells (Feng et al., 2019).

Zhou et al. (2021) constructed an "all-in-one" nanoliposomes co-encapsulating sonosensitizers protoporphyrin IX (PpIX) and autophagy inhibitor 3-MA. It has been demonstrated that SDT induced cytoprotective pro-survival autophagy with alleviating

apoptosis through the MAPK signaling pathway. Combining SDT and autophagy blockage significantly decreased the cell resistance to intracellular oxidative stress and resulted in a remarkable synergistic effect on cancer therapy (Figure 6).

Therefore, applying autophagy inhibitors to improve the sensitivity of SDT in tumor therapy is expected to provide a new and promising strategy to increase the SDT efficiency and sensitivity.

## 5 Summary and outlook

Originated and developed from PDT, SDT is a novel non-invasive tumor therapy. The advantages of SDT include deep tissue penetration, high precision, low side effects, and good patient compliance. SDT refers to the "cavity effect" generated by the irradiation of ultrasound at a specific frequency on tumors in deep tissues. Under US irradiation, the sonosensitive accumulated by tumor cells changes them from the ground state to the excited state and reacts with surrounding oxygen molecules to produce a large number of ROS, resulting in tumor cell death. SDT has made great progress in the treatment of tumors, and there have been many studies on the treatment of pancreatic cancer, liver cancer, breast cancer and other deep tumors. How to improve the efficiency of SDT is still the focus and difficulty of sonodynamic research.



Firstly, the efficiency of SDT highly relies on the sonosensitizer, and the major challenge for the application of SDT lies in the poor sonosensitizer delivery accuracy. With the development of nanotechnology, NPs are introduced to deliver the sonosensitizers to target tissues or tumor cells with high specificity. Many researchers have investigated the suitable NPs to be used as target delivery carriers, which are reviewed in this paper. Secondly, the main mechanism of SDT is that US uses oxygen in tumor cells to produce a large number of ROS to destroy tumor cells. Increasing the production of ROS can fundamentally improve the efficacy of SDT. Studies have shown that reactive oxygen species can activate autophagy through a variety of pathways, degrade damaged proteins and organelles in cells, and mediate cell survival or death. Wang et al. (Wang et al., 2013a; Wang et al., 2013b) found that SDT activated autophagy while inducing apoptosis, and the activated autophagy inhibited apoptosis and protected tumor cells in 2013. Many successive studies have found that SDT-activated autophagy depends on ROS production, and activated autophagy helps tumor cells survive, which was summarized in this paper. It is speculated that avoiding the activation of protective autophagy during SDT can effectively improve the treatment sensitivity. State of the art therapeutic technique is the combination of SDT with nanoparticles-based sonosensitizers together with autophagy inhibition, which proves to be a superior therapy with high specificity and accuracy and improves the outcomes of traditional tumor treatment methods. Few investigations have been done in this area and are summarized in this review. Qu et al. (2020) used Angiopep-2 peptide modified liposomes to deliver Ce6, an acoustic sensitizer, and HCQ, an autophagy inhibitor, simultaneously to improve the acoustic dynamic therapy effect of glioma. Feng et al. (2019) used hollow mesoporous titanium dioxide nanoparticles to deliver the autophagy inhibitor HCQ and improve the SDT effect of breast cancer. Zhou et al. (2021) used liposomes to deliver acoustic sensitizer PpIX/autophagy inhibitor 3-MA synchronously, improving the therapeutic effect of acoustic dynamics on breast cancer.

Increasing the accumulation of sonosensitive agents in tumor sites using nanocarriers can increase the production of ROS, and then fundamentally improve the efficiency of sonodynamic therapy. The increase of ROS activated protective autophagy to inhibit the SDT efficacy. Therefore, it is speculated that the combination of targeted delivery of sonosensitizer and inhibition of autophagy can not only effectively kill tumor cells by increasing the production of ROS, but also avoid the

activation of protective-autophagy by ROS. The findings in this review suggest that this is a promising tumor therapy, and more investigations need to be carried out in this area.

## Author contributions

YjZ wrote the draft manuscript. YrZ, YyZ, and QL provided revised suggestions for this manuscript. MZ and KT supervised the manuscript and provided financial support.

## Funding

This work was supported by the National Natural Science Foundation of China (No. 82000523), the Natural Science Foundation of Shaanxi Province of China (No. 2020JQ-095), and the “Young Talent Support Plan” of Xi’an Jiaotong University, China (No. YX6J001).

## Acknowledgments

We would like to thank Shiwen Zhang for manuscript summarizing and editing work.

## Conflict of interest

The authors declare that the research was conducted in the absence of any commercial or financial relationships that could be construed as a potential conflict of interest.

## Publisher’s note

All claims expressed in this article are solely those of the authors and do not necessarily represent those of their affiliated organizations, or those of the publisher, the editors and the reviewers. Any product that may be evaluated in this article, or claim that may be made by its manufacturer, is not guaranteed or endorsed by the publisher.

## References

- Aksel, M., Kesmez, O., Yavas, A., and Bilgin, M. D. (2021). Titaniumdioxide mediated sonophotodynamic therapy against prostate cancer. *J. Photochem. Photobiol. B* 225, 112333. doi:10.1016/j.jphotobiol.2021.112333
- Amaravadi, R., Kimmelman, A. C., and White, E. (2016). Recent insights into the function of autophagy in cancer. *Genes Dev.* 30 (17), 1913–1930. doi:10.1101/gad.287524.116
- Amaravadi, R. K., Kimmelman, A. C., and Debnath, J. (2019). Targeting autophagy in cancer: Recent advances and future directions. *Cancer Discov.* 9 (9), 1167–1181. doi:10.1158/2159-8290.cd-19-0292
- An, J., Hu, Y. G., Cheng, K., Li, C., Hou, X. L., Wang, G. L., et al. (2020a). ROS-augmented and tumor-microenvironment responsive biodegradable nanoplatfor for enhancing chemo-sonodynamic therapy. *Biomaterials* 234, 119761. doi:10.1016/j.biomaterials.2020.119761
- An, J., Hu, Y. G., Li, C., Hou, X. L., Cheng, K., Zhang, B., et al. (2020b). A pH/ Ultrasound dual-response biomimetic nanoplatfor for nitric oxide gas-sonodynamic combined therapy and repeated ultrasound for relieving hypoxia. *Biomaterials* 230. doi:10.1016/j.biomaterials.2019.119636



- Antonoli, M., Di Rienzo, M., Piacentini, M., and Fimia, G. M. (2017). Emerging mechanisms in initiating and terminating autophagy. *Trends biochem. Sci.* 42 (1), 28–41. doi:10.1016/j.tibs.2016.09.008
- Atmaca, G. Y., Aksel, M., Keskin, B., Bilgin, M. D., and Erdoğan, A. (2021). The photo-physicochemical properties and *in vitro* sonophotodynamic therapy activity of Di-axially substituted silicon phthalocyanines on PC3 prostate cancer cell line. *Dyes Pigments* 184, 108760. doi:10.1016/j.dyepig.2020.108760
- Bandyopachay, U., and Cuervo, A. M. (2008). Entering the lysosome through a transient gate by chaperone-mediated autophagy. *Autophagy* 4 (8), 1101–1103. doi:10.4161/auto.7150
- Buytaert, E., Callewaert, G., Hendrickx, N., Scorrano, L., Hartmann, D., Missiaen, L., et al. (2006). Role of endoplasmic reticulum depletion and multidomain proapoptotic BAX and BAK proteins in shaping cell death after hypericin-mediated photodynamic therapy. *FASEB J.* 20 (6), 756–758. doi:10.1096/fj.05-4305fje
- Buytaert, E., Matroule, J. Y., Durinck, S., Close, P., Kocanova, S., Vandenheede, J. R., et al. (2008). Molecular effectors and modulators of hypericin-mediated cell death in bladder cancer cells. *Oncogene* 27 (13), 1916–1929. doi:10.1038/sj.onc.1210825
- Canaparo, R., Varchi, G., Ballestri, M., Foglietta, F., Sotgiu, G., Guerrini, A., et al. (2013). Polymeric nanoparticles enhance the sonodynamic activity of meso-tetrakis (4-sulfonatophenyl) porphyrin in an *in vitro* neuroblastoma model. *Int. J. Nanomedicine* 8, 4247–4263. doi:10.2147/ijn.s51070
- Cao, J., Pan, Q., Bei, S., Zheng, M., Sun, Z., Qi, X., et al. (2021). Concise nanoplateform of phycocyanin nanoparticle loaded with docetaxel for synergetic chemo-sonodynamic antitumor therapy. *ACS Appl. Bio Mater.* 4 (9), 7176–7185. doi:10.1021/acsabm.1c00745
- Cao, W. J., Matkar, P. N., Chen, H. H., Mofid, A., and Leong-Poi, H. (2016). Microbubbles and ultrasound: Therapeutic applications in diabetic nephropathy. *Adv. Exp. Med. Biol.* 880, 309–330. doi:10.1007/978-3-319-22536-4\_17
- Cavalli, R., Marano, F., Argenziano, M., Varese, A., Frairia, R., Catalano, M. G., et al. (2018). Combining drug-loaded nanobubbles and extracorporeal shock waves for difficult-to-treat cancers. *Curr. Drug Deliv.* 15 (6), 752–754. doi:10.2174/1567201814666171018120430
- Chan, E. Y. (2009). mTORC1 phosphorylates the ULK1-mAtg13-FIP200 autophagy regulatory complex. *Sci. Signal.* 2 (84), pe51. doi:10.1126/scisignal.284pe51
- Chang, H., and Zou, Z. (2020). Targeting autophagy to overcome drug resistance: Further developments. *J. Hematol. Oncol.* 13 (1), 159. doi:10.1186/s13045-020-01000-2
- Chang, Z., Shi, G., Jin, J., Guo, H., Guo, X., Luo, F., et al. (2013). Dual PI3K/mTOR inhibitor NVP-BE235-induced apoptosis of hepatocellular carcinoma cell lines is enhanced by inhibitors of autophagy. *Int. J. Mol. Med.* 31 (6), 1449–1456. doi:10.3892/ijmm.2013.1351
- Chen, H., Zhou, X., Gao, Y., Zheng, B., Tang, F., Huang, J., et al. (2014). Recent progress in development of new sonosensitizers for sonodynamic cancer therapy. *Drug Discov. Today* 19 (4), 502–509. doi:10.1016/j.drudis.2014.01.010
- Chen, L., Cong, D., Li, Y., Wang, D., Li, Q., Hu, S., et al. (2017a). Combination of sonodynamic with temozolomide inhibits C6 glioma migration and promotes mitochondrial pathway apoptosis by suppressing NHE-1 expression. *Ultrason. Sonochem.* 39, 654–661. doi:10.1016/j.ultsonch.2017.05.013
- Chen, L. C., Zhou, S. F., Su, L. C., and Song, J. B. (2019). Gas-mediated cancer bioimaging and therapy. *Acs Nano* 13 (10), 10887–10917. doi:10.1021/acsnano.9b04954
- Chen, M. J., Xu, A. R., He, W. Y., Ma, W. C., and Shen, S. (2017b). Ultrasound triggered drug delivery for mitochondria targeted sonodynamic therapy. *J. Drug Deliv. Sci. Technol.* 39, 501–507. doi:10.1016/j.jddst.2017.05.009
- Cheng, D., Wang, X., Zhou, X., and Li, J. (2021). Nanosonosensitizers with ultrasound-induced reactive oxygen species generation for cancer sonodynamic immunotherapy. *Front. Bioeng. Biotechnol.* 9, 761218. doi:10.3389/fbioe.2021.761218
- Cheng, L., Qiu, S., Wang, J., Chen, W., Wang, J., Du, W., et al. (2022). A multifunctional nanocomposite based on Pt-modified black phosphorus nanosheets loading with L-arginine for synergistic gas-sonodynamic cancer therapy. *Colloids Surfaces A Physicochem. Eng. Aspects* 638, 128284. doi:10.1016/j.colsurfa.2022.128284
- Choi, H. S., Jeong, E.-H., Lee, T.-G., Kim, S. Y., Kim, H.-R., Kim, C. H., et al. (2013). Autophagy inhibition with monensin enhances cell cycle arrest and apoptosis induced by mTOR or epidermal growth factor receptor inhibitors in lung cancer cells. *Tuberc. Respir. Dis.* 75 (1), 9–17. doi:10.4046/trd.2013.75.1.9
- Christian, F., Anthony, D. F., Vadrevu, S., Riddell, T., Day, J. P., McLeod, R., et al. (2010). p62 (SQSTM1) and cyclic AMP phosphodiesterase-4A4 (PDE4A4) locate to a novel, reversible protein aggregate with links to autophagy and proteasome degradation pathways. *Cell. Signal.* 22 (10), 1576–1596. doi:10.1016/j.cellsig.2010.06.003
- Cook, K. L., Wärr, A., Soto-Pantoja, D. R., Clarke, P. A., Cruz, M. I., Zwart, A., et al. (2014). Hydroxychloroquine inhibits autophagy to potentiate antiestrogen responsiveness in ER+ breast cancer. *Clin. Cancer Res.* 20 (12), 3222–3232. doi:10.1158/1078-0432.ccr-13-3227
- Danno, D., Kanno, M., Fujimoto, S., Feril, L. B., Kondo, T., Nakamura, S., et al. (2008). Effects of ultrasound on apoptosis induced by anti-CD20 antibody in CD20-positive B lymphoma cells. *Ultrason. Sonochem.* 15 (4), 463–471. doi:10.1016/j.ultsonch.2007.08.004
- Didenko, Y. T., McNamara, W. B., Iii, and Suslick, K. S. (2000). Molecular emission from single-bubble sonoluminescence. *Nature* 407 (6806), 877–879. doi:10.1038/35038020
- Ding, Y., Song, Z., Liu, Q., Wei, S., Zhou, L., Zhou, J., et al. (2017). An enhanced chemotherapeutic effect facilitated by sonication of MSN. *Dalton Trans.* 46 (35), 11875–11883. doi:10.1039/c7dt02600e
- Escoffier, J. M., Deckers, R., Bos, C., and Moonen, C. (2016). Bubble-assisted ultrasound: Application in immunotherapy and vaccination. *Adv. Exp. Med. Biol.* 880, 243–261. doi:10.1007/978-3-319-22536-4\_14
- Feng, Q., Yang, X., Hao, Y., Wang, N., Feng, X., Hou, L., et al. (2019). Cancer cell membrane-biomimetic nanoplateform for enhanced sonodynamic therapy on breast cancer via autophagy regulation strategy. *ACS Appl. Mat. Interfaces* 11 (36), 32729–32738. doi:10.1021/acsami.9b10948
- Feng, Q., Zhang, W., Yang, X., Li, Y., Hao, Y., Zhang, H., et al. (2018). pH/ultrasound dual-responsive gas generator for ultrasound imaging-guided therapeutic inertial cavitation and sonodynamic therapy. *Adv. Healthc. Mat.* 7 (5), 1700957. doi:10.1002/adhm.201700957
- Forbes, M. M., Steinberg, R. L., and O'Brien, W. D. (2011). Frequency-dependent evaluation of the role of definity in producing sonoporation of Chinese hamster ovary cells. *J. Ultrasound Med.* 30 (1), 61–69. doi:10.7863/jum.2011.30.1.61
- Fujita, N., Itoh, T., Omori, H., Fukuda, M., Noda, T., Yoshimori, T., et al. (2008). The Atg16L complex specifies the site of LC3 lipidation for membrane biogenesis in autophagy. *Mol. Biol. Cell* 19 (5), 2092–2100. doi:10.1091/mbc.e07-12-1257
- Gao, H. J., Zhang, W. M., Wang, X. H., and Zheng, R. N. (2010). Adriamycin enhances the sonodynamic effect of chlorin e6 against the proliferation of human breast cancer MDA-MB-231 cells *in vitro*. *Nan Fang. Yi Ke Da Xue Xue Bao* 30 (10), 2291–2294.
- Geng, B., Xu, S., Shen, L., Fang, F., Shi, W., Pan, D., et al. (2021). Multifunctional carbon dot/MXene heterojunctions for alleviation of tumor hypoxia and enhanced sonodynamic therapy. *Carbon* 179, 493–504. doi:10.1016/j.carbon.2021.04.070
- Geng, J., and Klionsky, D. J. (2008). The Atg8 and Atg12 ubiquitin-like conjugation systems in macroautophagy. 'Protein modifications: Beyond the usual suspects' review series. *EMBO Rep.* 9 (9), 859–864. doi:10.1038/embor.2008.163
- Glick, D., Barth, S., and Macleod, K. F. (2010). Autophagy: Cellular and molecular mechanisms. *J. Pathol.* 221 (1), 3–12. doi:10.1002/path.2697
- Goldberg, S. B., Supko, J. G., Neal, J. W., Muzikansky, A., Digumarthy, S., Fidias, P., et al. (2012). A phase I study of erlotinib and hydroxychloroquine in advanced non-small-cell lung cancer. *J. Thorac. Oncol.* 7 (10), 1602–1608. doi:10.1097/JTO.0b013e318262de4a
- Guan, S., Liu, X., Li, C., Wang, X., Cao, D., Wang, J., et al. (2022). Intracellular mutual amplification of oxidative stress and inhibition multidrug resistance for enhanced sonodynamic/chemodynamic/chemo therapy. *Small* 18, e2107160. doi:10.1002/smll.202107160
- Hachimine, K., Shibaguchi, H., Kuroki, M., Yamada, H., Kinugasa, T., Nakae, Y., et al. (2007). Sonodynamic therapy of cancer using a novel porphyrin derivative, DCPH-P-Na(I), which is devoid of photosensitivity. *Cancer Sci.* 98 (6), 916–920. doi:10.1111/j.1349-7006.2007.00468.x
- Hanada, T., Noda, N. N., Satomi, Y., Ichimura, Y., Fujioka, Y., Takao, T., et al. (2007). The Atg12-Atg5 conjugate has a novel E3-like activity for protein lipidation in autophagy. *J. Biol. Chem.* 282 (52), 37298–37302. doi:10.1074/jbc.C700195200
- Hara, T., Takamura, A., Kishi, C., Iemura, S., Natsume, T., Guan, J. L., et al. (2008). FIP200, a ULK-interacting protein, is required for autophagosome formation in mammalian cells. *J. Cell Biol.* 181 (3), 497–510. doi:10.1083/jcb.200712064
- Harada, Y., Ogawa, K., Irie, Y., Endo, H., Feril, L. B., Jr., Uemura, T., et al. (2011). Ultrasound activation of TiO2 in melanoma tumors. *J. Control. Release* 149 (2), 190–195. doi:10.1016/j.jconrel.2010.10.012
- Helgason, G. V., Holyoake, T. L., and Ryan, K. M. (2013). Role of autophagy in cancer prevention, development and therapy. *Essays Biochem.* 55, 133–151. doi:10.1042/bse0550133

- Hiraoka, W., Honda, H., Feril, L. B., Kudo, N., and Kondo, T. (2006). Comparison between sonodynamic effect and photodynamic effect with photosensitizers on free radical formation and cell killing. *Ultrason. Sonochem.* 13 (6), 535–542. doi:10.1016/j.ultrasonch.2005.10.001
- Hosokawa, N., Hara, T., Kaizuka, T., Kishi, C., Takamura, A., Miura, Y., et al. (2009a). Nutrient-dependent mTORC1 association with the ULK1-Atg13-FIP200 complex required for autophagy. *Mol. Biol. Cell* 20 (7), 1981–1991. doi:10.1091/mbc.e08-12-1248
- Hosokawa, N., Sasaki, T., Iemura, S., Natsume, T., Hara, T., Mizushima, N., et al. (2009b). Atg101, a novel mammalian autophagy protein interacting with Atg13. *Autophagy* 5 (7), 973–979. doi:10.4161/auto.5.7.9296
- Hou, R., Liang, X., Li, X., Zhang, X., Ma, X., Wang, F., et al. (2020). *In situ* conversion of rose bengal microbubbles into nanoparticles for ultrasound imaging guided sonodynamic therapy with enhanced antitumor efficacy. *Biomater. Sci.* 8 (9), 2526–2536. doi:10.1039/c9bm02046b
- Hsin, I. L., Ou, C. C., Wu, T. C., Jan, M. S., Wu, M. F., Chiu, L. Y., et al. (2011). GMI, an immunomodulatory protein from *Ganoderma microsporum*, induces autophagy in non-small cell lung cancer cells. *Autophagy* 7 (8), 873–882. doi:10.4161/auto.7.8.15698
- Huang, J., Liu, F., Han, X., Zhang, L., Hu, Z., Jiang, Q., et al. (2018). Nanosensitizers for highly efficient sonodynamic cancer theranostics. *Theranostics* 8 (22), 6178–6194. doi:10.7150/thno.29569
- Huang, J., Xiao, Z., An, Y., Han, S., Wu, W., Wang, Y., et al. (2021). Nanodrug with dual-sensitivity to tumor microenvironment for immuno-sonodynamic anti-cancer therapy. *Biomaterials* 269, 120636. doi:10.1016/j.biomaterials.2020.120636
- Huang, Z. (2005). A review of progress in clinical photodynamic therapy. *Technol. Cancer Res. Treat.* 4 (3), 283–293. doi:10.1177/153303460500400308
- Imai, K., Hao, F., Fujita, N., Tsuji, Y., Oe, Y., Araki, Y., et al. (2016). Atg9A trafficking through the recycling endosomes is required for autophagosome formation. *J. Cell Sci.* 129 (20), 3781–3791. doi:10.1242/jcs.196196
- Ishibashi, K., Fujita, N., Kanno, E., Omori, H., Yoshimori, T., Itoh, T., et al. (2011). Atg16L2, a novel isoform of mammalian Atg16L that is not essential for canonical autophagy despite forming an Atg12–5–16L2 complex. *Autophagy* 7 (12), 1500–1513. doi:10.4161/auto.7.12.18025
- Itakura, E., Kishi-Itakura, C., and Mizushima, N. (2012). The hairpin-type tail-anchored SNARE syntaxin 17 targets to autophagosomes for fusion with endosomes/lysosomes. *Cell* 151 (6), 1256–1269. doi:10.1016/j.cell.2012.11.001
- Jeon, J., Yoon, B., Song, S. H., Um, W., Song, Y., Lee, J., et al. (2022). Chemiluminescence resonance energy transfer-based immunostimulatory nanoparticles for sonoimmunotherapy. *Biomaterials* 283, 121466. doi:10.1016/j.biomaterials.2022.121466
- Jiang, P., Nishimura, T., Sakamaki, Y., Itakura, E., Hatta, T., Natsume, T., et al. (2014). The HOPS complex mediates autophagosome-lysosome fusion through interaction with syntaxin 17. *Mol. Biol. Cell* 25 (8), 1327–1337. doi:10.1091/mbc.E13-08-0447
- Jiang, Q., Qiao, B., Lin, X., Cao, J., Zhang, N., Guo, H., et al. (2022). A hydrogen peroxide economizer for on-demand oxygen production-assisted robust sonodynamic immunotherapy. *Theranostics* 12 (1), 59–75. doi:10.7150/thno.64862
- Jiang, Y., Kou, J., Han, X., Li, X., Zhong, Z., Liu, Z., et al. (2017). ROS-dependent activation of autophagy through the PI3K/Akt/mTOR pathway is induced by hydroxysafflor yellow A-sonodynamic therapy in THP-1 macrophages. *Oxid. Med. Cell. Longev.* 2017, 8519169. doi:10.1155/2017/8519169
- Kabeya, Y., Mizushima, N., Ueno, T., Yamamoto, A., Kirisako, T., Noda, T., et al. (2000). LC3, a mammalian homologue of yeast Apg8p, is localized in autophagosome membranes after processing. *Embo J.* 19 (21), 5720–5728. doi:10.1093/emboj/19.21.5720
- Kaleta-Richter, M., Kawczyk-Krupka, A., Aebischer, D., Bartusik-Aebischer, D., Czuba, Z., Cieřlar, G., et al. (2019). The capability and potential of new forms of personalized colon cancer treatment: Immunotherapy and Photodynamic Therapy. *Photodiagnosis Photodyn. Ther.* 25, 253–258. doi:10.1016/j.pdpdt.2019.01.004
- Kayani, Z., Dehdari Vais, R., Soratjahromi, E., Mohammadi, S., and Sattarahmady, N. (2021). Curcumin-gold-polyethylene glycol nanoparticles as a nanosensitizer for photothermal and sonodynamic therapies: *In vitro* and animal model studies. *Photodiagnosis Photodyn. Ther.* 33, 102139. doi:10.1016/j.pdpdt.2020.102139
- Kessel, D., and Oleinick, N. L. (2009). Initiation of autophagy by photodynamic therapy. *Methods Enzymol.* 453, 1–16. doi:10.1016/S0076-6879(08)04001-9
- Kessel, D., Vicente, M. G., and Reiners, J. J., Jr. (2006). Initiation of apoptosis and autophagy by photodynamic therapy. *Autophagy* 2 (4), 289–290. doi:10.4161/auto.2792
- Kitanaka, C., and Kuchino, Y. (1999). Caspase-independent programmed cell death with necrotic morphology. *Cell Death Differ.* 6 (6), 508–515. doi:10.1038/sj.cdd.4400526
- Kocaturk, N. M., Akkoc, Y., Kig, C., Bayraktar, O., Gozuacik, D., Kutlu, O., et al. (2019). Autophagy as a molecular target for cancer treatment. *Eur. J. Pharm. Sci.* 134, 116–137. doi:10.1016/j.ejps.2019.04.011
- Kondo, T., and Kano, E. (1987). Enhancement of hyperthermic cell killing by non-thermal effect of ultrasound. *Int. J. Radiat. Biol. Relat. Stud. Phys. Chem. Med.* 51 (1), 157–166. doi:10.1080/09553008714550591
- Kou, J. Y., Li, Y., Zhong, Z. Y., Jiang, Y. Q., Li, X. S., Han, X. B., et al. (2017). Berberine-sonodynamic therapy induces autophagy and lipid unloading in macrophage. *Cell Death Dis.* 8 (1), e2558. doi:10.1038/cddis.2016.354
- Kwon, S., Ko, H., You, D. G., Kataoka, K., and Park, J. H. (2019). Nanomedicines for reactive oxygen species mediated approach: An emerging paradigm for cancer treatment. *Acc. Chem. Res.* 52 (7), 1771–1782. doi:10.1021/acs.accounts.9b00136
- Lee, H. O., Mustafa, A., Hudes, G. R., and Kruger, W. D. (2015). Hydroxychloroquine destabilizes phospho-S6 in human renal carcinoma cells. *PLoS One* 10 (7), e0131464. doi:10.1371/journal.pone.0131464
- Levy, J. M. M., Towers, C. G., and Thorburn, A. (2017). Targeting autophagy in cancer. *Nat. Rev. Cancer* 17 (9), 528–542. doi:10.1038/nrc.2017.53
- Li, G., Zhong, X., Wang, X., Gong, F., Lei, H., Zhou, Y., et al. (2022). Titanium carbide nanosheets with defect structure for photothermal-enhanced sonodynamic therapy. *Bioact. Mat.* 8, 409–419. doi:10.1016/j.bioactmat.2021.06.021
- Li, J., Luo, Y., and Pu, K. (2021). Electromagnetic nanomedicines for combinational cancer immunotherapy. *Angew. Chem. Int. Ed. Engl.* 60 (23), 12682–12705. doi:10.1002/anie.202008386
- Li, Q., Liu, Q., Wang, P., Feng, X., Wang, H., Wang, X., et al. (2014a). The effects of Ce6-mediated sono-photodynamic therapy on cell migration, apoptosis and autophagy in mouse mammary 4T1 cell line. *Ultrasonics* 54 (4), 981–989. doi:10.1016/j.ultras.2013.11.009
- Li, Q., Wang, X., Wang, P., Zhang, K., Wang, H., Feng, X., et al. (2014b). Efficacy of chlorin e6-mediated sono-photodynamic therapy on 4T1 cells. *Cancer biother. Radiopharm.* 29 (1), 42–52. doi:10.1089/cbr.2013.1526
- Li, X. J., Feng, J., Zhang, R., Wang, J. D., Su, T., Tian, Z. H., et al. (2016c). Quaternized chitosan/alginate-Fe3O4 magnetic nanoparticles enhance the chemosensitization of multidrug-resistant gastric carcinoma by regulating cell autophagy activity in mice. *J. Biomed. Nanotechnol.* 12 (5), 948–961. doi:10.1166/jbn.2016.2232
- Li, X., Zhang, X., Zheng, L., Kou, J., Zhong, Z., Jiang, Y., et al. (2016a). Hypericin-mediated sonodynamic therapy induces autophagy and decreases lipids in THP-1 macrophage by promoting ROS-dependent nuclear translocation of TFEB. *Cell Death Dis.* 7 (12), e2527. doi:10.1038/cddis.2016.433
- Li, X., Zhang, X., Zheng, L., Kou, J., Zhong, Z., Jiang, Y., et al. (2016b). Hypericin-mediated sonodynamic therapy induces autophagy and decreases lipids in THP-1 macrophage by promoting ROS-dependent nuclear translocation of TFEB. *Cell Death Dis.* 7 (12), e2527. doi:10.1038/cddis.2016.433
- Li, Y., Hao, L., Liu, F., Yin, L., Yan, S., Zhao, H., et al. (2019). Cell penetrating peptide-modified nanoparticles for tumor targeted imaging and synergistic effect of sonodynamic/HIFU therapy. *Int. J. Nanomedicine* 14, 5875–5894. doi:10.2147/ijn.s212184
- Li, Y., Xie, J., Um, W., You, D. G., Kwon, S., Zhang, L., et al. (2020). Sono/photodynamic nanomedicine-elicited cancer immunotherapy. *Adv. Funct. Mat.* 31 (12), 2008061. doi:10.1002/adfm.202008061
- Li, Z., Han, J., Yu, L., Qian, X., Xing, H., Lin, H., et al. (2018). Synergistic sonodynamic/chemotherapeutic suppression of hepatocellular carcinoma by targeted biodegradable mesoporous nanosensitizers. *Adv. Funct. Mat.* 28 (26), 1800145. doi:10.1002/adfm.201800145
- Liang, J. L., Luo, G. F., Chen, W. H., and Zhang, X. Z. (2021). Recent advances in engineered materials for immunotherapy-involved combination cancer therapy. *Adv. Mat.* 33 (31), e2007630. doi:10.1002/adma.202007630
- Liang, S., Deng, X., Ma, P., Cheng, Z., and Lin, J. (2020a). Recent advances in nanomaterial-assisted combinational sonodynamic cancer therapy. *Adv. Mat.* 32, e2003214. doi:10.1002/adma.202003214
- Liang, S., Deng, X. R., Xu, G. Y., Xiao, X., Wang, M. F., Guo, X. S., et al. (2020b). A novel Pt-TiO2 heterostructure with oxygen-deficient layer as bilaterally enhanced sonosensitizer for synergistic chemo-sonodynamic cancer therapy. *Adv. Funct. Mat.* 30 (13), 1908598. doi:10.1002/adfm.201908598
- Lin, X., He, T., Tang, R., Li, Q., Wu, N., Zhou, Y., et al. (2022). Biomimetic nanoprobe-augmented triple therapy with photothermal, sonodynamic and checkpoint blockade inhibits tumor growth and metastasis. *J. Nanobiotechnology* 20 (1), 80. doi:10.1186/s12951-022-01287-y
- Lin, X. H., Qiu, Y., Song, L., Chen, S., Chen, X. F., Huang, G. M., et al. (2019). Ultrasound activation of liposomes for enhanced ultrasound imaging and synergistic gas and sonodynamic cancer therapy. *Nanoscale Horiz.* 4 (3), 747–756. doi:10.1039/c8nh00340h

- Lin, X., Huang, R., Huang, Y., Wang, K., Li, H., Bao, Y., et al. (2021). Nanosensitizer-Augmented sonodynamic therapy combined with checkpoint blockade for cancer immunotherapy. *Int. J. Nanomedicine* 16, 1889–1899. doi:10.2147/IJN.S290796
- Liu, M., Khan, A. R., Ji, J., Lin, G., Zhao, X., Zhai, G., et al. (2018). Crosslinked self-assembled nanoparticles for chemo-sonodynamic combination therapy favoring antitumor, antimetastasis management and immune responses. *J. Control. Release* 290, 150–164. doi:10.1016/j.jconrel.2018.10.007
- Liu, Q., Sun, S., Xiao, Y., Qi, H., Shang, Z., Zhang, J., et al. (2003). Study of cell killing and morphology on S180 by ultrasound activating hematoporphyrin derivatives. *Sci. China. C Life Sci.* 46 (3), 253–262. doi:10.1360/03yc9027
- Liu, X., Li, W., Geng, S., Meng, Q. G., and Bi, Z. G. (2015). Apoptosis induced by sonodynamic therapy in human osteosarcoma cells *in vitro*. *Mol. Med. Rep.* 12 (1), 1183–1188. doi:10.3892/mmr.2015.3479
- Liu, Y., Wan, G., Guo, H., Liu, Y., Zhou, P., Wang, H., et al. (2017). A multifunctional nanoparticle system combines sonodynamic therapy and chemotherapy to treat hepatocellular carcinoma. *Nano Res.* 10 (3), 834–855. doi:10.1007/s12274-016-1339-8
- Liu, Y., Wang, P., Liu, Q., and Wang, X. (2016). Sinoporphyrin sodium triggered sono-photodynamic effects on breast cancer both *in vitro* and *in vivo*. *Ultrason. Sonochem.* 31, 437–448. doi:10.1016/j.ultsonch.2016.01.038
- Liu, Z., Li, J., Chen, W., Liu, L., and Yu, F. (2020). Light and sound to trigger the pandora's box against breast cancer: A combination strategy of sonodynamic, photodynamic and photothermal therapies. *Biomaterials* 232, 119685. doi:10.1016/j.biomaterials.2019.119685
- Liu, Z., Wang, D., Li, J., and Jiang, Y. (2019). Self-assembled peptido-nanomicelles as an engineered formulation for synergy-enhanced combinational SDT, PDT and chemotherapy to nasopharyngeal carcinoma. *Chem. Commun.* 55 (69), 10226–10229. doi:10.1039/c9cc05463d
- Logan, K., Foglietta, F., Nesbitt, H., Sheng, Y., McKaig, T., Kamila, S., et al. (2019). Targeted chemo-sonodynamic therapy treatment of breast tumours using ultrasound responsive microbubbles loaded with paclitaxel, doxorubicin and Rose Bengal. *Eur. J. Pharm. Biopharm.* 139, 224–231. doi:10.1016/j.ejpb.2019.04.003
- Lu, J., He, L., Behrends, C., Araki, M., Araki, K., Jun Wang, Q., et al. (2014). NRB2F2 regulates autophagy and prevents liver injury by modulating Atg14L-linked phosphatidylinositol-3 kinase III activity. *Nat. Commun.* 5, 3920. doi:10.1038/ncomms4920
- Lv, Y., Zheng, J., Zhou, Q., Jia, L., Wang, C., Liu, N., et al. (2017). Antiproliferative and apoptosis-inducing effect of exo-protoporphyrin IX based sonodynamic therapy on human oral squamous cell carcinoma. *Sci. Rep.* 7, 40967. doi:10.1038/srep40967
- Mahalingam, D., Mita, M., Sarantopoulos, J., Wood, L., Amaravadi, R. K., Davis, L. E., et al. (2014). Combined autophagy and HDAC inhibition: a phase I safety, tolerability, pharmacokinetic, and pharmacodynamic analysis of hydroxychloroquine in combination with the HDAC inhibitor vorinostat in patients with advanced solid tumors. *Autophagy* 10 (8), 1403–1414. doi:10.4161/autophagy.29231
- Matsunaga, K., Saitoh, T., Tabata, K., Omori, H., Satoh, T., Kurotori, N., et al. (2009). Two Beclin 1-binding proteins, Atg14L and Rubicon, reciprocally regulate autophagy at different stages. *Nat. Cell Biol.* 11 (4), 385–396. doi:10.1038/ncb1846
- McHale, A. P., Callan, J. F., Nomikou, N., Fowley, C., and Callan, B. (2016). Sonodynamic therapy: Concept, mechanism and application to cancer treatment. *Adv. Exp. Med. Biol.* 880, 429–450. doi:10.1007/978-3-319-22536-4\_22
- Misik, V., and Riesz, P. (2000). Free radical intermediates in sonodynamic therapy. *Ann. N. Y. Acad. Sci.* 899, 335–348. doi:10.1111/j.1749-6632.2000.tb06198.x
- Mony, V. K., Benjamin, S., and O'Rourke, E. J. (2016). A lysosome-centered view of nutrient homeostasis. *Autophagy* 12 (4), 619–631. doi:10.1080/15548627.2016.1147671
- Nakatogawa, H. (2013). Two ubiquitin-like conjugation systems that mediate membrane formation during autophagy. *Essays Biochem.* 55, 39–50. doi:10.1042/bse0550039
- Nene, L. C., and Nyokong, T. (2021). Photo-sonodynamic combination activity of cationic morpholino-phthalocyanines conjugated to nitrogen and nitrogen-sulfur doped graphene quantum dots against MCF-7 breast cancer cell line *in vitro*. *Photodiagnosis Photodyn. Ther.* 36, 102573. doi:10.1016/j.pdpdt.2021.102573
- Nesbitt, H., Sheng, Y., Kamila, S., Logan, K., Thomas, K., Callan, B., et al. (2018). Gemcitabine loaded microbubbles for targeted chemo-sonodynamic therapy of pancreatic cancer. *J. Control. Release* 279, 8–16. doi:10.1016/j.jconrel.2018.04.018
- Nora Frulio, H. T., Deckers, R., Deckers, R., Lepreux, S., Moonen, C., and Quesson, B. (2010). Influence of ultrasound induced cavitation on magnetic resonance imaging contrast in the rat liver in the presence of macromolecular contrast agent. *Invest. Radiol.* 45 (5), 282–287. doi:10.1097/RLI.0b013e3181dac2a7
- Ohmura, T., Fukushima, T., Shibaguchi, H., Yoshizawa, S., Inoue, T., Kuroki, M., et al. (2011). Sonodynamic therapy with 5-aminolevulinic acid and focused ultrasound for deep-seated intracranial glioma in rat. *Anticancer Res.* 31 (7), 2527–2533.
- Orsi, A., Razi, M., Dooley, H. C., Robinson, D., Weston, A. E., Collinson, L. M., et al. (2012). Dynamic and transient interactions of Atg9 with autophagosomes, but not membrane integration, are required for autophagy. *Mol. Biol. Cell* 23 (10), 1860–1873. doi:10.1091/mbc.E11-09-0746
- Padilla, F., Puts, R., Vico, L., Guignandon, A., and Raum, K. (2016). Stimulation of bone repair with ultrasound. *Adv. Exp. Med. Biol.* 880, 385–427. doi:10.1007/978-3-319-22536-4\_21
- Pan, X., Bai, L., Wang, H., Wu, Q., Wang, H., Liu, S., et al. (2018a). Metal-organic-framework-Derived carbon nanostructure augmented sonodynamic cancer therapy. *Adv. Mat.* 30 (23), e1800180. doi:10.1002/adma.201800180
- Pan, X., Wang, H., Wang, S., Sun, X., Wang, L., Wang, W., et al. (2018b). Sonodynamic therapy (SDT): A novel strategy for cancer nanotheranostics. *Sci. China. Life Sci.* 61 (4), 415–426. doi:10.1007/s11427-017-9262-x
- Pan, X., Wang, W., Huang, Z., Liu, S., Guo, J., Zhang, F., et al. (2020). MOF-derived double-layer hollow nanoparticles with oxygen generation ability for multimodal imaging-guided sonodynamic therapy. *Angew. Chem. Int. Ed. Engl.* 59 (32), 13557–13561. doi:10.1002/anie.202004894
- Park, J. M., Jung, C. H., Seo, M., Otto, N. M., Grunwald, D., Kim, K. H., et al. (2016). The ULK1 complex mediates MTORC1 signaling to the autophagy initiation machinery via binding and phosphorylating ATG14. *Autophagy* 12 (3), 547–564. doi:10.1080/15548627.2016.1140293
- Parzych, K. R., and Klionsky, D. J. (2014). An overview of autophagy: Morphology, mechanism, and regulation. *Antioxid. Redox Signal.* 20 (3), 460–473. doi:10.1089/ars.2013.5371
- Pelt, J., Busatto, S., Ferrari, M., Thompson, E. A., Mody, K., Wolfram, J., et al. (2018). Chloroquine and nanoparticle drug delivery: A promising combination. *Pharmacol. Ther.* 191, 43–49. doi:10.1016/j.pharmthera.2018.06.007
- Qian, X., Zheng, Y., and Chen, Y. (2016). Micro/nanoparticle-Augmented sonodynamic therapy (SDT): Breaking the depth shallow of photoactivation. *Adv. Mat.* 28 (37), 8097–8129. doi:10.1002/adma.201602012
- Qu, F., Wang, P., Zhang, K., Shi, Y., Li, Y., Li, C., et al. (2020). Manipulation of Mitophagy by "All-in-One" nanosensitizer augments sonodynamic glioma therapy. *Autophagy* 16 (8), 1413–1435. doi:10.1080/15548627.2019.1687210
- Rangwala, R., Chang, Y. C., Hu, J., Algazy, K. M., Evans, T. L., Fecher, L. A., et al. (2014). Combined MTOR and autophagy inhibition: phase I trial of hydroxychloroquine and temsirolimus in patients with advanced solid tumors and melanoma. *Autophagy* 10 (8), 1391–1402. doi:10.4161/autophagy.29119
- Ravikumar, B., Moreau, K., Jahreiss, L., Puri, C., and Rubinsztein, D. C. (2010). Plasma membrane contributes to the formation of pre-autophagosomal structures. *Nat. Cell Biol.* 12 (8), 747–757. doi:10.1038/ncb2078
- Ren, Q., Yu, N., Wang, L., Wen, M., Geng, P., Jiang, Q., et al. (2022). Nanoarchitectonics with metal-organic frameworks and platinum nanozymes with improved oxygen evolution for enhanced sonodynamic/chemo-therapy. *J. Colloid Interface Sci.* 614, 147–159. doi:10.1016/j.jcis.2022.01.050
- Rengeng, L., Qianyu, Z., Yuehong, L., Zhongzhong, P., and Libo, L. (2017). Sonodynamic therapy, a treatment developing from photodynamic therapy. *Photodiagnosis Photodyn. Ther.* 19, 159–166. doi:10.1016/j.pdpdt.2017.06.003
- Rkein, A. M., and Ozog, D. M. (2014). Photodynamic therapy. *Dermatol. Clin.* 32 (3), 415–425. doi:10.1016/j.det.2014.03.009
- Rosenfeld, M. R., Ye, X., Supko, J. G., Desideri, S., Grossman, S. A., Brem, S., et al. (2014). A phase I/II trial of hydroxychloroquine in conjunction with radiation therapy and concurrent and adjuvant temozolomide in patients with newly diagnosed glioblastoma multiforme. *Autophagy* 10 (8), 1359–1368. doi:10.4161/autophagy.28984
- Satoo, K., Noda, N. N., Kumeta, H., Fujioka, Y., Mizushima, N., Ohsumi, Y., et al. (2009). The structure of Atg4B-LC3 complex reveals the mechanism of LC3 processing and delipidation during autophagy. *Embo J.* 28 (9), 1341–1350. doi:10.1038/emboj.2009.80
- Shanei, A., Sazgarnia, A., Tayyebi Meibodi, N., Eshghi, H., Hassanzadeh-Khayyat, M., Esmaily, H., et al. (2012). Sonodynamic therapy using protoporphyrin IX conjugated to gold nanoparticles: An *in vivo* study on a colon tumor model. *Iran. J. Basic Med. Sci.* 15 (2), 759–767.
- Shen, Q., Shi, Y., Liu, J., Su, H., Huang, J., Zhang, Y., et al. (2021). Acetylation of STX17 (syntaxin 17) controls autophagosome maturation. *Autophagy* 17 (5), 1157–1169. doi:10.1080/15548627.2020.1752471
- Shen, S., Wu, L., Liu, J., Xie, M., Shen, H., Qi, X., et al. (2015). Core-shell structured Fe3O4@TiO2-doxorubicin nanoparticles for targeted chemo-



- sonodynamic therapy of cancer. *Int. J. Pharm.* 486 (1–2), 380–388. doi:10.1016/j.ijpharm.2015.03.070
- Shi, J., Chen, Z., Wang, B., Wang, L., Lu, T., Zhang, Z., et al. (2015). Reactive oxygen species-manipulated drug release from a smart envelope-type mesoporous titanium nanovehicle for tumor sonodynamic-chemotherapy. *ACS Appl. Mat. Interfaces* 7 (51), 28554–28565. doi:10.1021/acsami.5b09937
- Shi, T. T., Yu, X. X., Yan, L. J., and Xiao, H. T. (2017). Research progress of hydroxychloroquine and autophagy inhibitors on cancer. *Cancer Chemother. Pharmacol.* 79 (2), 287–294. doi:10.1007/s00280-016-3197-1
- Song, L., Huang, Y., Hou, X., Yang, Y., Kala, S., Qiu, Z., et al. (2018). PINK1/Parkin-Mediated mitophagy promotes resistance to sonodynamic therapy. *Cell. Physiol. Biochem.* 49 (5), 1825–1839. doi:10.1159/000493629
- Song Shen, X. G., Wu, L., Wang, M., Wang, b. X., Wang, X., Kong, F., et al. (2014). Fenfen Kong, Haijun Shen, Meng Xie, Yanru Ge and Yi JinDual-core@shell-structured Fe<sub>3</sub>O<sub>4</sub>-NaYF<sub>4</sub>@TiO<sub>2</sub> nanocomposites as a magnetic targeting drug carrier for bioimaging and combined chemosonodynamic therapy. *J. Mat. Chem. B* 2, 5775–5784. doi:10.1039/C4TB00841C
- Su, X., Wang, P., Yang, S., Zhang, K., Liu, Q., Wang, X., et al. (2015). Sonodynamic therapy induces the interplay between apoptosis and autophagy in K562 cells through ROS. *Int. J. Biochem. Cell Biol.* 60, 82–92. doi:10.1016/j.biocel.2014.12.023
- Sui, X., Chen, R., Wang, Z., Huang, Z., Kong, N., Zhang, M., et al. (2013). Autophagy and chemotherapy resistance: A promising therapeutic target for cancer treatment. *Cell Death Dis.* 4 (10), e838. doi:10.1038/cddis.2013.350
- Suslick, K. S., Doktycz, S. J., and Flint, E. B. (1990). On the origin of sonoluminescence and sonochemistry. *Ultrasonics* 28 (5), 280–290. doi:10.1016/0041-624X(90)90033-K
- Suslick, K. S. (1990). Sonochemistry. *Sonochemistry. Sci.* 247(4949), 1439–1445. doi:doi:10.1126/science.247.4949.1439
- Sviridov, A. P., Osminkina, L. A., Kharin, A. Y., Gongalsky, M. B., Kargina, J. V., Kudryavtsev, A. A., et al. (2017). Cytotoxicity control of silicon nanoparticles by biopolymer coating and ultrasound irradiation for cancer theranostic applications. *Nanotechnology* 28 (10), 105102. doi:10.1088/1361-6528/aa5b7c
- Takahashi, Y., Meyerkord, C. L., Hori, T., Runkle, K., Fox, T. E., Kester, M., et al. (2011). Bif-1 regulates Atg9 trafficking by mediating the fission of Golgi membranes during autophagy. *Autophagy* 7 (1), 61–73. doi:10.4161/auto.7.1.14015
- Tan, X., Huang, J., Wang, Y., He, S., Jia, L., Zhu, Y., et al. (2021). Transformable nanosensitizer with tumor microenvironment-activated sonodynamic process and calcium release for enhanced cancer immunotherapy. *Angew. Chem. Int. Ed. Engl.* 60 (25), 14051–14059. doi:10.1002/anie.202102703
- Tanida, I. (2011). Autophagosome formation and molecular mechanism of autophagy. *Antioxid. Redox Signal.* 14 (11), 2201–2214. doi:10.1089/ars.2010.3482
- Tsuboyama, K., Koyama-Honda, I., Sakamaki, Y., Koike, M., Morishita, H., Mizushima, N., et al. (2016). The ATG conjugation systems are important for degradation of the inner autophagosomal membrane. *Science* 354 (6315), 1036–1041. doi:10.1126/science.aaf6136
- Vogl, D. T., Stadtmayer, E. A., Tan, K. S., Heitjan, D. F., Davis, L. E., Pontiggia, L., et al. (2014). Combined autophagy and proteasome inhibition: A phase 1 trial of hydroxychloroquine and bortezomib in patients with relapsed/refractory myeloma. *Autophagy* 10 (8), 1380–1390. doi:10.4161/auto.29264
- Wan, G., Chen, X., Wang, H., Hou, S., Wang, Q., Cheng, Y., et al. (2021). Gene augmented nuclear-targeting sonodynamic therapy via Nrf2 pathway-based redox balance adjustment boosts peptide-based anti-PD-L1 therapy on colorectal cancer. *J. Nanobiotechnology* 19 (1), 347. doi:10.1186/s12951-021-01094-x
- Wan, G., Liu, Y., Shi, S., Chen, B., Wang, Y., Wang, H., et al. (2016a). Hematoporphyrin and doxorubicin co-loaded nanomicelles for the reversal of drug resistance in human breast cancer cells by combining sonodynamic therapy and chemotherapy. *RSC Adv.* 6 (102), 100361–100372. doi:10.1039/c6ra22724d
- Wan, G. Y., Liu, Y., Chen, B. W., Liu, Y. Y., Wang, Y. S., Zhang, N., et al. (2016b). Recent advances of sonodynamic therapy in cancer treatment. *Cancer Biol. Med.* 13 (3), 325–338. doi:10.20892/j.issn.2095-3941.2016.0068
- Wang, H., Wang, X., Wang, P., Zhang, K., Yang, S., Liu, Q., et al. (2013a). Ultrasound enhances the efficacy of chlorin E6-mediated photodynamic therapy in MDA-MB-231 cells. *Ultrasound Med. Biol.* 39 (9), 1713–1724. doi:10.1016/j.ultrasmedbio.2013.03.017
- Wang, L., Li, G. Z., Cao, L., Dong, Y., Wang, Y., Wang, S. S., et al. (2021a). An ultrasound-driven immune-boosting molecular machine for systemic tumor suppression. *Sci. Adv.* 7 (43), eabj4796. doi:10.1126/sciadv.abj4796
- Wang, P., Li, C., Wang, X., Xiong, W., Feng, X., Liu, Q., et al. (2015a). Anti-metastatic and pro-apoptotic effects elicited by combination photodynamic therapy with sonodynamic therapy on breast cancer both *in vitro* and *in vivo*. *Ultrason. Sonochem.* 23, 116–127. doi:10.1016/j.ulsonch.2014.10.027
- Wang, P., Wang, X., Ma, L., Sahi, S., Li, L., Wang, X. B., et al. (2018). Nanosensitization by using copper-cysteamine nanoparticles augmented sonodynamic cancer treatment. *Part. Part. Syst. Charact.* 35 (4), 1700378. doi:10.1002/ppsc.201700378
- Wang, X., Jia, Y., Su, X., Wang, P., Zhang, K., Feng, X., et al. (2015b). Combination of protoporphyrin IX-mediated sonodynamic treatment with doxorubicin synergistically induced apoptotic cell death of a multidrug-resistant leukemia K562/DOX cell line. *Ultrasound Med. Biol.* 41 (10), 2731–2739. doi:10.1016/j.ultrasmedbio.2015.06.001
- Wang, X., Liu, Q., Wang, Z., Wang, P., Zhao, P., Zhao, X., et al. (2010a). Role of autophagy in sonodynamic therapy-induced cytotoxicity in S180 cells. *Ultrasound Med. Biol.* 36 (11), 1933–1946. doi:10.1016/j.ultrasmedbio.2010.06.022
- Wang, X., Liu, Q., Wang, Z., Wang, P., Zhao, P., Zhao, X., et al. (2010b). Role of autophagy in sonodynamic therapy-induced cytotoxicity in s180 cells. *Ultrasound Med. Biol.* 36 (11), 1933–1946. doi:10.1016/j.ultrasmedbio.2010.06.022
- Wang, X., Wang, P., Zhang, K., Su, X., Hou, J., Liu, Q., et al. (2013b). Initiation of autophagy and apoptosis by sonodynamic therapy in murine leukemia L1210 cells. *Toxicol. Vitro* 27 (4), 1247–1259. doi:10.1016/j.tiv.2012.12.023
- Wang, X., Wang, X., Yue, Q., Xu, H., Zhong, X., Sun, L., et al. (2021b). Liquid exfoliation of TiN nanodots as novel sonosensitizers for photothermal-enhanced sonodynamic therapy against cancer. *Nano Today* 39, 101170. doi:10.1016/j.nantod.2021.101170
- Wang, X., Wang, Y., Wang, P., Cheng, X., and Liu, Q. (2011). Sonodynamically induced anti-tumor effect with protoporphyrin IX on hepatoma-22 solid tumor. *Ultrasonics* 51 (5), 539–546. doi:10.1016/j.ultras.2010.12.001
- Wang, Z., Bai, J., Li, F., Du, Y., Wen, S., Hu, K., et al. (2003). Study of a "biological focal region" of high-intensity focused ultrasound. *Ultrasound Med. Biol.* 29 (5), 749–754. doi:10.1016/s0301-5629(02)00785-8
- Wang, Z., Liu, C., Zhao, Y., Hu, M., Ma, D., Zhang, P., et al. (2019). Photomagnetic nanoparticles in dual-modality imaging and photo-sonodynamic activity against bacteria. *Chem. Eng. J.* 356, 811–818. doi:10.1016/j.cej.2018.09.077
- White, E., Mehnert, J. M., and Chan, C. S. (2015). Autophagy, metabolism, and cancer. *Clin. Cancer Res.* 21 (22), 5037–5046. doi:10.1158/1078-0432.ccr-15-0490
- Wu, P., Sun, Y., Dong, W., Zhou, H., Guo, S., Zhang, L., et al. (2019). Enhanced anti-tumor efficacy of hyaluronic acid modified nanocomposites combined with sonotherapy against subcutaneous and metastatic breast tumors. *Nanoscale* 11 (24), 11470–11483. doi:10.1039/c9nr01691k
- Wu, Y., Liu, X., Qin, Z., Hu, L., and Wang, X. (2018). Low-frequency ultrasound enhances chemotherapy sensitivity and induces autophagy in PTX-resistant PC-3 cells via the endoplasmic reticulum stress-mediated PI3K/Akt/mTOR signaling pathway. *Onco. Targets. Ther.* 11, 5621–5630. doi:10.2147/ott.s176744
- Xiao, Z., Zhuang, B., Zhang, G., Li, M., and Jin, Y. (2021). Pulmonary delivery of cationic liposomal hydroxycamptothecin and 5-aminolevulinic acid for chemo-sonodynamic therapy of metastatic lung cancer. *Int. J. Pharm.* 601, 120572. doi:10.1016/j.ijpharm.2021.120572
- Xiaohuai, W., Lewis, T. J., and Mitchell, D. (2008). The tumoricidal effect of sonodynamic therapy (SDT) on S-180 sarcoma in mice. *Integr. Cancer Ther.* 7 (2), 96–102. doi:10.1177/1534735408319065
- Xiong, J., Jiang, B., Luo, Y., Zou, J., Gao, X., Xu, D., et al. (2020). Multifunctional nanoparticles encapsulating Astragalus polysaccharide and gold nanorods in combination with focused ultrasound for the treatment of breast cancer. *Int. J. Nanomedicine* 15, 4151–4169. doi:10.2147/IJN.S246447
- Xu, F., Hu, M., Liu, C., and Choi, S. K. (2017). Yolk-structured multifunctional up-conversion nanoparticles for synergistic photodynamic-sonodynamic antibacterial resistance therapy. *Biomater. Sci.* 5 (4), 678–685. doi:10.1039/c7bm00030h
- Xu, H., Yu, N., Zhang, J., Wang, Z., Geng, P., Wen, M., et al. (2020a). Biocompatible Fe-Hematoporphyrin coordination nanoplateforms with efficient sonodynamic-chemo effects on deep-seated tumors. *Biomaterials* 257, 120239. doi:10.1016/j.biomaterials.2020.120239
- Xu, P., Yao, J., Li, Z., Wang, M., Zhou, L., Zhong, G., et al. (2020b). Therapeutic effect of doxorubicin-chlorin E6-loaded mesoporous silica nanoparticles combined with ultrasound on triple-negative breast cancer. *Int. J. Nanomedicine* 15, 2659–2668. doi:10.2147/ijn.s243037
- Xue, L. Y., Chiu, S. M., Azizuddin, K., Joseph, S., and Oleinick, N. L. (2007). The death of human cancer cells following photodynamic therapy: Apoptosis competence is necessary for bcl-2 protection but not for induction of autophagy. *Photochem. Photobiol.* 83 (5), 1016–1023. doi:10.1111/j.1751-1097.2007.00159.x
- Yang, Z., Tao, D., Zhong, W., Liu, Z., Feng, L., Chen, M., et al. (2022). Perfluorocarbon loaded fluorinated covalent organic polymers with effective sonosensitization and tumor hypoxia relief enable synergistic sonodynamic-immunotherapy. *Biomaterials* 280, 121250. doi:10.1016/j.biomaterials.2021.121250

- Ye, J., Fu, Q., Liu, L., Chen, L., Zhang, X., Li, Q., et al. (2021). Ultrasound-propelled Janus Au NR-mSiO<sub>2</sub> nanomotor for NIR-II photoacoustic imaging guided sonodynamic-gas therapy of large tumors. *Sci. China Chem.* 64 (12), 2218–2229. doi:10.1007/s11426-021-1070-6
- Yim, W. W., and Mizushima, N. (2020). Lysosome biology in autophagy. *Cell Discov.* 6, 6. doi:10.1038/s41421-020-0141-7
- Yin, H., Chang, N., Xu, S., and Wan, M. (2016). Sonoluminescence characterization of inertial cavitation inside a BSA phantom treated by pulsed HIFU. *Ultrason. Sonochem.* 32, 158–164. doi:10.1016/j.ultsonch.2016.02.025
- Yin, Y., Jiang, X., Sun, L., Li, H., Su, C., Zhang, Y., et al. (2021). Continuous inertial cavitation evokes massive ROS for reinforcing sonodynamic therapy and immunogenic cell death against breast carcinoma. *Nano Today* 36, 101009. doi:10.1016/j.nantod.2020.101009
- Yu, Z., Cao, W., Han, C., Wang, Z., Qiu, Y., Wang, J., et al. (2022). Biomimetic metal-organic framework nanoparticles for synergistic combining of SDT-chemotherapy induce pyroptosis in gastric cancer. *Front. Bioeng. Biotechnol.* 10, 796820. doi:10.3389/fbioe.2022.796820
- Yuan, F., Yang, C., and Zhong, P. (2015). Cell membrane deformation and bioeffects produced by tandem bubble-induced jetting flow. *Proc. Natl. Acad. Sci. U. S. A.* 112 (51), E7039–E7047. doi:10.1073/pnas.1518679112
- Yuan, Y. G., and Gurunathan, S. (2017). Combination of graphene oxide-silver nanoparticle nanocomposites and cisplatin enhances apoptosis and autophagy in human cervical cancer cells. *Int. J. Nanomedicine* 12, 6537–6558. doi:10.2147/ijnm.s125281
- Yue, W. W., Chen, L., Yu, L. D., Zhou, B. G., Yin, H. H., Ren, W. W., et al. (2019). Checkpoint blockade and nanosensitizer-augmented noninvasive sonodynamic therapy combination reduces tumour growth and metastases in mice. *Nat. Com.* 10. doi:10.1038/s41467-019-09760-3
- Yumita, N., Nishigaki, R., Umemura, K., and Umemura, S. (1989). Hematoporphyrin as a sensitizer of cell-damaging effect of ultrasound. *Jpn. J. Cancer Res.* 80 (3), 219–222. doi:10.1111/j.1349-7006.1989.tb02295.x
- Yumita, N., Okuyama, N., Sasaki, K., and Umemura, S. (2007). Sonodynamic therapy on chemically induced mammary tumor: Pharmacokinetics, tissue distribution and sonodynamically induced antitumor effect of gallium-porphyrin complex ATX-70. *Cancer Chemother. Pharmacol.* 60 (6), 891–897. doi:10.1007/s00280-007-0436-5
- Yumita, N., Okuyama, N., Sasaki, K., and Umemura, S. (2004). Sonodynamic therapy on chemically induced mammary tumor: Pharmacokinetics, tissue distribution and sonodynamically induced antitumor effect of porphyrin sodium. *Cancer Sci.* 95 (9), 765–769. doi:10.1111/j.1349-7006.2004.tb03259.x
- Yun, C. W., and Lee, S. H. (2018). The roles of autophagy in cancer. *Int. J. Mol. Sci.* 19 (11), E3466. doi:10.3390/ijms19113466
- Zachari, M., and Ganley, I. G. (2017). The mammalian ULK1 complex and autophagy initiation. *Essays Biochem.* 61 (6), 585–596. doi:10.1042/ebc20170021
- Zeng, X., Zhao, H., Li, Y., Fan, J., Sun, Y., Wang, S., et al. (2015). Targeting Hedgehog signaling pathway and autophagy overcomes drug resistance of BCR-ABL-positive chronic myeloid leukemia. *Autophagy* 11 (2), 355–372. doi:10.4161/15548627.2014.994368
- Zhang, H., Ren, Y., Cao, F., Chen, J., Chen, C., Chang, J., et al. (2019a). *In situ* autophagy disruption generator for cancer theranostics. *ACS Appl. Mat. Interfaces* 11 (33), 29641–29654. doi:10.1021/acsami.9b10578
- Zhang, J., Shi, C., Shan, F., Shi, N., Ye, W., Zhuo, Y., et al. (2021a). From biology to biology: Hematoporphyrin-melanin nanoconjugates with synergistic sonodynamic-photothermal effects on malignant tumors. *Chem. Eng. J.* 408, 127282. doi:10.1016/j.cej.2020.127282
- Zhang, L., Yi, H., Song, J., Huang, J., Yang, K., Tan, B., et al. (2019b). Mitochondria-targeted and ultrasound-activated nanodroplets for enhanced deep-penetration sonodynamic cancer therapy. *ACS Appl. Mat. Interfaces* 11 (9), 9355–9366. doi:10.1021/acsami.8b21968
- Zhang, Q., Wang, W., Shen, H., Tao, H., Wu, Y., Ma, L., et al. (2021b). Low-intensity focused ultrasound-augmented multifunctional nanoparticles for integrating ultrasound imaging and synergistic therapy of metastatic breast cancer. *Nanoscale Res. Lett.* 16 (1), 73. doi:10.1186/s11671-021-03532-z
- Zhang, R. Y., Cheng, K., Xuan, Y., Yang, X. Q., An, J., Hu, Y. G., et al. (2021c). A pH/ultrasonic dual-response step-targeting enterosoluble granule for combined sonodynamic-chemotherapy guided via gastrointestinal tract imaging in orthotopic colorectal cancer. *Nanoscale* 13 (7), 4278–4294. doi:10.1039/d0nr08100k
- Zhang, Y., Kang, S., Lin, H., Chen, M., Li, Y., Cui, L., et al. (2022). Regulation of zeolite-derived upconversion photocatalytic system for near infrared light/ultrasound dual-triggered multimodal melanoma therapy under a boosted hypoxia relief tumor microenvironment via autophagy. *Chem. Eng. J.* 429, 132484. doi:10.1016/j.cej.2021.132484
- Zhao, Y. G., Codogno, P., and Zhang, H. (2021). Machinery, regulation and pathophysiological implications of autophagosomal maturation. *Nat. Rev. Mol. Cell Biol.* 22 (11), 733–750. doi:10.1038/s41580-021-00392-4
- Zhao, Y., Hu, M., Zhang, Y., Liu, J., Liu, C., Choi, S. K., et al. (2020). Multifunctional therapeutic strategy of Ag-synergized dual-modality upconversion nanoparticles to achieve the rapid and sustained cidal effect of methicillin-resistant *Staphylococcus aureus*. *Chem. Eng. J.* 385, 123980. doi:10.1016/j.cej.2019.123980
- Zheng, Y., Li, Z., Yang, Y., Shi, H., Chen, H., Gao, Y., et al. (2021a). A nanosensitizer self-assembled from oleanolic acid and chlorin e6 for synergistic chemo/sono-photodynamic cancer therapy. *Phytomedicine* 93, 153788. doi:10.1016/j.phymed.2021.153788
- Zheng, Y., Liu, Y., Wei, F., Xiao, H., Mou, J., Wu, H., et al. (2021b). Functionalized g-C<sub>3</sub>N<sub>4</sub> nanosheets for potential use in magnetic resonance imaging-guided sonodynamic and nitric oxide combination therapy. *Acta Biomater.* 121, 592–604. doi:10.1016/j.actbio.2020.12.011
- Zhong, X. Y., Wang, X. W., Cheng, L., Tang, Y. A., Zhan, G. T., Gong, F., et al. (2020). GSH-depleted PtCu<sub>3</sub> nanocages for chemodynamic-enhanced sonodynamic cancer therapy. *Adv. Funct. Mat.* 30 (4), 1907954. doi:10.1002/adfm.201907954
- Zhou, L., Huo, M., Qian, X., Ding, L., Yu, L., Feng, W., et al. (2021). Autophagy blockade synergistically enhances nanosensitizer-enabled sonodynamic cancer nanotherapeutics. *J. Nanobiotechnology* 19 (1), 112. doi:10.1186/s12951-021-00855-y
- Zhu, J., Ouyang, A., He, J., Xie, J., Banerjee, S., Zhang, Q., et al. (2022). An ultrasound activated cyanine-rhenium(I) complex for sonodynamic and gas synergistic therapy. *Chem. Commun.* 58 (20), 3314–3317. doi:10.1039/d1cc06769a
- Zhu, P., Chen, Y., and Shi, J. (2020a). Piezocatalytic tumor therapy by ultrasound-triggered and BaTiO<sub>3</sub>-mediated piezoelectricity. *Adv. Mat.* 32 (29), e2001976. doi:10.1002/adma.202001976
- Zhu, W., Chen, Q., Jin, Q., Chao, Y., Sun, L., Han, X., et al. (2020b). Sonodynamic therapy with immune modulatable two-dimensional coordination nanosheets for enhanced anti-tumor immunotherapy. *Nano Res.* 14 (1), 212–221. doi:10.1007/s12274-020-3070-8
- Zou, W., Hao, J., Wu, J., Cai, X., Hu, B., Wang, Z., et al. (2021). Biodegradable reduce expenditure bioreactor for augmented sonodynamic therapy via regulating tumor hypoxia and inducing pro-death autophagy. *J. Nanobiotechnology* 19 (1), 418. doi:10.1186/s12951-021-01166-y
- Zuo, S., Zhang, Y., Wang, Z., and Wang, J. (2022). Mitochondria-targeted mesoporous titanium dioxide nanoplateform for synergistic nitric oxide gas-sonodynamic therapy of breast cancer. *Int. J. Nanomedicine* 17, 989–1002. doi:10.2147/IJN.S348618





## OPEN ACCESS

## EDITED BY

Liang Ouyang,  
Sichuan University, China

## REVIEWED BY

Jianglong Yan,  
The University of Chicago, United States  
Chaoxing Zhang,  
University of California, Davis,  
United States

## \*CORRESPONDENCE

Shuangshuang Zeng,  
zengshuangshuang@csu.edu.cn  
Zhijie Xu,  
xzj1322007@csu.edu.cn

## SPECIALTY SECTION

This article was submitted to  
Pharmacology of Anti-Cancer Drugs,  
a section of the journal  
Frontiers in Pharmacology

RECEIVED 04 July 2022

ACCEPTED 25 July 2022

PUBLISHED 29 August 2022

## CITATION

Chen X, He Q, Zeng S and Xu Z (2022),  
Upregulation of nuclear division cycle  
80 contributes to therapeutic resistance  
via the promotion of autophagy-related  
protein-7-dependent autophagy in  
lung cancer.

Front. Pharmacol. 13:985601.  
doi: 10.3389/fphar.2022.985601

## COPYRIGHT

© 2022 Chen, He, Zeng and Xu. This is  
an open-access article distributed  
under the terms of the [Creative  
Commons Attribution License \(CC BY\)](#).  
The use, distribution or reproduction in  
other forums is permitted, provided the  
original author(s) and the copyright  
owner(s) are credited and that the  
original publication in this journal is  
cited, in accordance with accepted  
academic practice. No use, distribution  
or reproduction is permitted which does  
not comply with these terms.

# Upregulation of nuclear division cycle 80 contributes to therapeutic resistance *via* the promotion of autophagy-related protein-7-dependent autophagy in lung cancer

Xi Chen<sup>1</sup>, Qingchun He<sup>2,3</sup>, Shuangshuang Zeng<sup>1\*</sup> and  
Zhijie Xu<sup>4,5,6\*</sup>

<sup>1</sup>Department of Pharmacy, Xiangya Hospital, Central South University, Changsha, China, <sup>2</sup>Department of Emergency, Xiangya Hospital, Central South University, Changsha, China, <sup>3</sup>Department of Emergency, Xiangya Changde Hospital, Changde, China, <sup>4</sup>Department of Clinical Laboratory, Xiangya Hospital, Central South University, Changsha, China, <sup>5</sup>Department of Pathology, Xiangya Hospital, Central South University, Changsha, China, <sup>6</sup>Institute for Rational and Safe Medication Practices, National Clinical Research Center for Geriatric Disorders, Xiangya Hospital, Central South University, Changsha, China

Lung cancer remains the leading cause of malignant mortality worldwide. Hence, the discovery of novel targets that can improve therapeutic effects in lung cancer patients is an urgent need. In this study, we screened differentially expressed genes using isobaric tags for relative and absolute quantitation (iTRAQ) analysis and datasets from the cancer genome atlas database, and found that nuclear division cycle 80 (NDC80) might act as a novel prognostic indicator of lung cancer. The expression of NDC80 was significantly increased in lung cancer tissues, as compared to normal tissues, and high expression levels of NDC80 were correlated with unfavorable survival rates. Furthermore, an *in vitro* analysis showed that the stable knockdown of NDC80 decreased the cell viability and increased therapeutic sensitivity in two lung cancer cell lines, A549-IRR and H1246-IRR. Moreover, gene set enrichment analysis results showed that NDC80 was enriched in autophagy-related pathways. The downregulation of NDC80 inhibited the formation of autophagosomes, and reduced the expression of autophagy-related proteins such as LC3II, Beclin-1, and p62 in lung cancer cells. To further clarify the role of NDC80 as a downstream regulator of autophagy, we validated autophagic mediators through iTRAQ analysis and real-time polymerase chain reaction arrays. Autophagy-related protein7 (ATG7) was observed to be downregulated after the knockdown of NDC80 in lung cancer cells. Immunohistochemistry assay results revealed that both NDC80 and ATG7 were upregulated in an array of lung adenocarcinoma samples, compared to normal tissues, and the expression of NDC80 was identified to be positively associated with the levels of ATG7. Our findings suggest that NDC80 promotes the development of lung cancer by regulating autophagy, and might serve as a potential target for increasing the therapeutic sensitivity of lung cancer.

## KEYWORDS

NDC80, lung cancer, autophagy, ATG7, therapeutic target

## Introduction

As the leading cause of death worldwide, lung cancer is associated with low 5-years survival rates, which range from 4%–17% (Zhou et al., 2019; Ruiz-Cordero and Devine, 2020). Lung adenocarcinoma (LUAD) and lung squamous cell carcinoma (LUSC) are the most common subtypes of non-small lung cancer (NSCLC) and account for approximately 80%–85% of all cases (Yan et al., 2018; Alexander et al., 2020). Radiotherapy is one of the most effective approaches against lung cancer and is essential for the treatment of all stages of lung cancer through definitive or palliative treatment (Wei et al., 2019; Zhao et al., 2022). However, the advanced intrinsic resistance of lung cancer cells to ionizing radiation (IR) is a severe and frequently observed limitation in patients undergoing radiotherapy. It is critical to explore the mechanisms underlying radioresistance, to enhance treatment efficacy in lung cancer patients.

Autophagy, a process of intracellular catabolic self-digestion, involves the sequestration of dysfunctional proteins and damaged organelles within autophagosomes and the disposal of these components in lysosomes (Li et al., 2020). Recently, emerging studies have shown that radiation therapy can generate cellular stress, which induces autophagy with distinct functions in tumor cells. Autophagy could eliminate the misfolded proteins resulting from IR-induced endoplasmic reticulum stress and is considered to have a protective effect against radioresistance development in various types of cancer cells (Gao et al., 2020). For instance, membrane protein 1 was identified to competitively inhibit the interaction of Bcl-2 with Beclin1, thus increasing autophagy and cell survival after radiation treatment in nasopharyngeal carcinoma (Xu et al., 2021). In hepatocellular carcinoma cells, the knockdown of long non-coding RNA NEAT1 sensitized cells to IR via the downregulation of autophagy-related protein GABARAP (Sakaguchi et al., 2022). Autophagy may stimulate resistance to IR in lung cancer cells by moderating ROS under hypoxic conditions (Chen et al., 2017). Moreover, we had previously confirmed that caveolin-1 could confer IR resistance to NSCLC cells through M-protein-regulated autophagy in the GTPase family, which has immune-related functions (Chen et al., 2021). Even though various studies have reported the role of pro-survival autophagy on radioresistance, the underlying regulatory mechanism remains complex and still needs to be elucidated further.

Nuclear division cycle 80 (NDC80/Hec1), a subunit of a kinetochore complex (also called the NDC80 complex), constitutes and stabilizes microtubule-kinetochore attachment during the segregation of mitotic chromosomes (Saragapani et al., 2021). NDC80 is comprised of an

N-terminal microtubule-binding domain and a C-terminal domain that interacts with other components of the kinetochore complex (Wimbish and DeLuca, 2020). In recent times, interest has been focused on the role of NDC80 in tumor progression. The overexpression of NDC80 has been identified to be an oncogenic biomarker with poor prognosis in several cancers, including gastric and ovarian cancer, and osteosarcoma (Mo et al., 2013; Qu et al., 2014; Xu et al., 2017). Furthermore, the turnover of NDC80 is indispensable for maintaining the conditions necessary for meiosis, in which the loss of phosphorylation of NDC80 at ser-55 and ser-69 causes an erroneous kinetochore-microtubule interaction in colon, lung, and prostate cancers (Chen et al., 2020; Iemura et al., 2021). With regard to cancer treatment, NDC80 might become a novel target for increasing the sensitivity of pemigatinib used for the treatment of cholangiocarcinoma (Scheiter et al., 2021). Several reports obtained using bioinformatic analysis have shown that high expression levels of NDC80 resulted in poor survival in lung cancer patients (Sun et al., 2020; Gao et al., 2022). However, the regulatory effects of NDC80 on progression and radiotherapy efficacy in lung cancer still need to be clarified.

In the present study, we screened NDC80 as a potential biomarker involved in radioresistance development in lung cancer cells using isobaric tags for relative and absolute quantitation (iTRAQ) analysis and the cancer genome atlas (TCGA) database. We confirmed that NDC80 is expressed at high levels in the LUAD and LUSC samples, and is associated with poor prognosis in lung cancer patients. To further analyze the role of NDC80 in radioresistance of lung cancer, *in vitro* studies were performed to show that the knockdown of NDC80 inhibits the proliferation of cells, increases IR sensitivity, and reduces autophagy in lung cancer. Moreover, the upregulation of NDC80 promotes autophagy as it mediates the expression of autophagy-related protein7 (ATG7) in IR-resistant cells. Our data provide a novel prospect of using NDC80 for the regulation of radioresistance and suggest that NDC80 could be used as a novel therapeutic target for improving the sensitivity toward radiation therapy in lung cancer.

## Materials and methods

### Screening of DEGs in LUAD and lung squamous cell carcinoma using iTRAQ analysis and TCGA datasets

Isobaric tags for relative and absolute quantitation (iTRAQ) is a method used for the verification and quantification of

proteins *via* quantitative mass spectrometry (Moulder et al., 2018). iTRAQ is performed to identify differentially expressed proteins in A549 parental and IR-resistant cells using reagents from BGI Genomics (Guangzhou, China). The cancer genome atlas (TCGA) database is an open-access platform for the cataloging and discovery of gene expression and clinical prognosis data. Two expression profiling datasets of LUAD and LUSC were downloaded from the TCGA using GDC Application Programming Interface (<https://portal.gdc.cancer.gov/repository>). The LUAD dataset includes 406 cancerous and 55 non-neoplastic tissues. The LUSC dataset includes 350 cancerous and 42 non-neoplastic tissues. The differentially expressed genes (DEGs) between lung cancer and healthy specimens were identified based on the cut-off criteria ( $|\log FC| > 2.5$ ,  $p < 0.05$ ). Using TCGA datasets, LASSO Cox regression was implemented to construct a prognostic model of lung cancer. The LASSO algorithm was used for the normalization of gene expression profiles and shrinkage was performed with the “glmnet” R package (Friedman et al., 2010).

## Bioinformatic analysis of clinical characteristics and GSEA

The university of Alabama at Birmingham (UALCAN) was applied to acquire mRNA and protein data of lung cancer and healthy tissues from the TCGA and Clinical Proteomic Tumor Analysis Consortium (CPTAC) databases (<http://ualcan.path.uab.edu/analysis.html>) (Chandrashekar et al., 2022). Moreover, UALCAN was used to examine differential expression across cancer types, and perform subtype analysis of the stage and TP53 status. The Xiantao tool (<https://www.xiantao love/products>) is a comprehensive interactive web portal used to perform differential expression, survival, and enrichment analysis in various cancer types (Zhang et al., 2021). We used the XianTao tool to perform receiver operating characteristic (ROC) risk evaluation, survival analysis, univariate and multivariate Cox regression analysis, and construct a Nomogram plot. To further identify the prognostic role of NDC80, time-dependent (3-years, 5-years, and 8-years) ROCs were analyzed using the R package “survivalROC” in TCGA datasets (Friedman et al., 2010). For survival analysis, we divided lung cancer samples into high-and low-expression groups according to their median expression using the R “survival” package (Friedman et al., 2010). Moreover, to determine whether NDC80 plays a role in the autophagy process, we used the XianTao tool to perform enrichment using gene set enrichment analysis (GSEA). Furthermore, the gene expression omnibus (GEO) is an open-source platform that contains data regarding gene expression, chips, and microarrays (<http://www.ncbi.nlm.nih.gov/geo>).

Two expression profiling datasets (GSE102287 and GSE8894) were downloaded from the GEO database, for the analysis of the relationship between the expression of NDC80 and ATG7 (Lee et al., 2008; Mitchell et al., 2017). Kaplan-Meier Plotter ([www.kmplot.com](http://www.kmplot.com)) is an open-access database used for the storage of gene expression data and survival information of lung cancer patients. The Kaplan-Meier Plotter was used to analyze the correlation between ATG7 expression and the survival of patients with lung cancer.

## Cell cultures

The parental and IR-resistant NSCLC cell lines, including the LUAD (A549-P/A549-IRR) and LUSC (H1246-P/H1246-IRR) cell lines, were obtained from the Cancer Research Institute, Central South University, China. Parental and IR-resistant cells were cultured using 1,640 medium (8122374, Gibco™, United States) supplemented with 10% fetal bovine serum (04-001-1A/B, BioInd, Israel) and 1% penicillin and streptomycin under 37°C aseptic conditions in the presence of 5% CO<sub>2</sub>.

## NDC80 shRNA knockdown

The two lentiviral short hairpin RNAs (shRNAs) targeting NDC80 (shNDC80#1, 5'-CAAGGACCCGAG ACCACTTAA-3'; shNDC80#2, 5'-GAATTGCAGCAG ACTATTAAT-3') were custom synthesized by Sangon Biotech (Shanghai, China). Each lentiviral NDC80 shRNA was added to cultured IR-resistant cells for 48 h. Stable cells with the NDC80 shRNA were selected using puromycin (10 µg/ml, Sangon Biotech) for a total of 10 days. A scrambled shRNA purchased from Sigma-Aldrich (St. Louis, United States) was used for treating control cells. The protein expression of NDC80 was detected *via* Western blotting.

## RNA extraction and quantitative PCR

The total RNA sequences extracted from NSCLC cells were lysed with TRIzol reagent and then converted to cDNAs using a PrimeScript™ RT reagent kit (6,210, Takara, Japan). The qPCR assay was performed using the iTaq™ Universal SYBR green Supermix (1725121, Bio-Rad, United States), and β-actin was chosen as an internal control. The sequences of the forward and reverse primers are provided in [Supplementary Table S1](#). The relative expression levels were examined using the 2-ΔΔCT method, as shown in previous reports (Lu et al., 2022), and all the

detection-related processes were performed at least three times.

## Western blot analysis

NSCLC cells were collected and lysed using IP lysis buffer with protease inhibitor cocktails (B14012, Bimake, United States) at a ratio of 1:100. Equal amounts of 50 µg lysate samples were loaded onto 10% or 12% SDS-PAGE, and then transferred to PVDF membranes (0.22 µm: ISEQ00010; 0.45 µm: IPVH00010). Membranes were blocked with 5% skimmed milk for 1 h at room temperature, and incubated with primary antibodies diluted in 5% Bovine Serum Albumin (D620272, Sangon Biotech, China) overnight at 4°C. Primary antibodies included the NDC80 (1:1,000; 18932-1-AP, Proteintech, China), ATG7 (1:1,000; 10088-2-AP, Proteintech, China), LC3 A/B (1:1,000; 4108S, Cell Signaling Technology, USA), Beclin-1 (1:1,000; 3495S, Cell Signaling Technology, United States), p62 (1:500; sc-28359, Santa, United States) and β-actin (1:2000; sc-58673, Santa, United States) antibodies. Specific bands on membranes were visualized using Immobilon Western chemiluminescent reagents (WBKLS0500, Millipore, United States).

## CCK-8 assays

As reported in a previous study (Xu et al., 2018), cell viability was assessed using the CCK-8 assay. Summarily, cells were digested and seeded into 96-well plates ( $1 \times 10^3$  cells per well). After they were incubated for 24 h, cells were treated with different doses of IR using a gamma irradiator. Subsequently, the CCK-8 test solution (B34304, Bimake, United States) was added for 1 h at 37°C. The optical density (OD) at 450 nm was measured using a spectrometer.

## Colony formation assay

As described in our previous studies (Cui et al., 2019), IR-resistant cells were resuspended and seeded at a density of  $1 \times 10^3$  per well in a 6-well dish with a complete medium. Following the incubation of cells for 24 h, IR at different doses was used to provide treatment. After approximately 2 weeks of incubation, cells were fixed and stained with 0.3% w/v crystal violet/methanol for 20 min at room temperature.

## Transmission electron microscopy

Cells were digested and collected into 1.5 ml tubes. Then, 2.5% glutaraldehyde solution was used for cell fixation

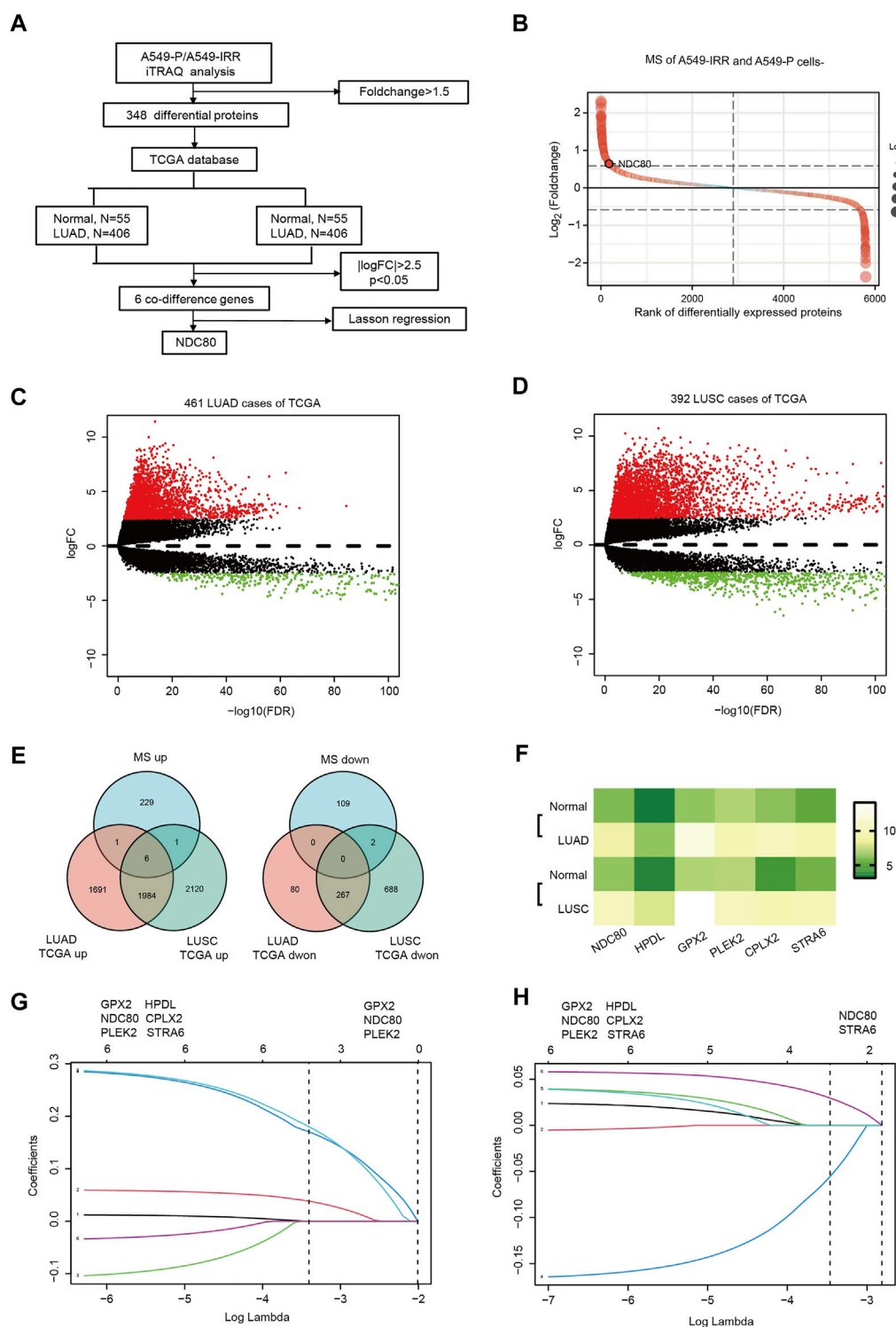
overnight at ambient temperature before being transited to the transmission electron microscopy (TEM) laboratory at the Pathology Department of Xiangya Hospital, Changsha, China, where cells were processed as described in our previous study (Chen et al., 2021). The cells were washed three times using Millonig's phosphate buffer and incubated for 1 h in 1% osmium tetroxide. The dehydration of the cells was performed using a graded series of 50%, 70%, and 90% acetone for 10 min for each step. Cells were then incubated two times in 100% acetone for 15 min. The process of resin soaking and embedding was performed using a 1:1 mix of acetone: resin for 12 h using samples, and polymerization was conducted with 100% resin overnight at 37°C. For the resin solidification process, cells were treated with 100% resin to allow polymerization to occur overnight at 37°C, and then incubated for 12 h at 60°C. Subsequently, 50–100 nm ultrathin sections of cells were made with an ultramicrotome and a diamond knife. After 3% uranyl acetate and lead nitrate double staining, the cells were examined and imaged on an electron microscope (HT-7700, Hitachi, Japan).

## Immunohistochemistry

The LUAD tissue array and clinical information regarding samples in the array were obtained from Outdo Biotech (Shanghai, China). The deparaffinization of specimens was performed in xylene and rehydration was performed in a graded series of alcohol solutions, as described previously (Xia et al., 2019). Endogenous peroxidase was blocked using 3% H<sub>2</sub>O<sub>2</sub> after the completion of the microwave antigen retrieval process. The samples were incubated with the primary antibody against the NDC80 antibody (1:500; 18932-1-AP, Proteintech, China) and ATG7 antibody (1:4000; 10088-2-AP, Proteintech, China). Two pathologists examined and differentially quantified the images of the sections. The evaluation of IHC intensity was performed and a score of 0 (negative), 1 (weak brown), 2 (moderate brown), or 3 (strong brown) was assigned, while the extent of staining was evaluated by assigning scores of 0 ( $\leq 10\%$ ), 1 (11%–25%), 2 (26%–50%), 3 (51%–75%), or 4 ( $> 75\%$ ). The final staining score was determined by multiplying the intensity score and extent score, and classified as weakly positive (1–3), positive (4–6), and strongly positive (7–12). All paraffin-embedded specimens were collected in accordance with the ethical standards of the human experimental committee.

## Statistical analysis

All experiments were performed in triplicate. The Student's t-test was performed to compare the differences

**FIGURE 1**

NDC80 is identified as a radioresistance-related gene in lung cancer. **(A)** The flowchart presents the process of identification of genes and their prognostic value in the LUAD and LUSC datasets. **(B)** iTRAQ analysis for the identification of differentially expressed proteins between A549-P and A549-IRR. **(C,D)** Identification of differentially expressed genes in LUAD **(C)** and LUSC **(D)** samples, as compared to paired healthy tissue samples from the TCGA database. **(E)** Visualization of the co-differences in genes from the results of iTRAQ analysis and the TCGA database. The 6 overlapping genes were upregulated in A549-IRR cells and tumor tissues. **(F)** The heatmap shows the expression of 6 overlapping genes in the LUAD and LUSC datasets. **(G,H)** Prognostic genes were identified using the least absolute shrinkage method and selection operator Cox regression model (LASSO) using datasets from TCGA in the LUAD **(G)** and LUSC **(H)** datasets. Coefficient distribution plots for the logarithmic (lambda) sequence for the selection of the best parameter (lambda).



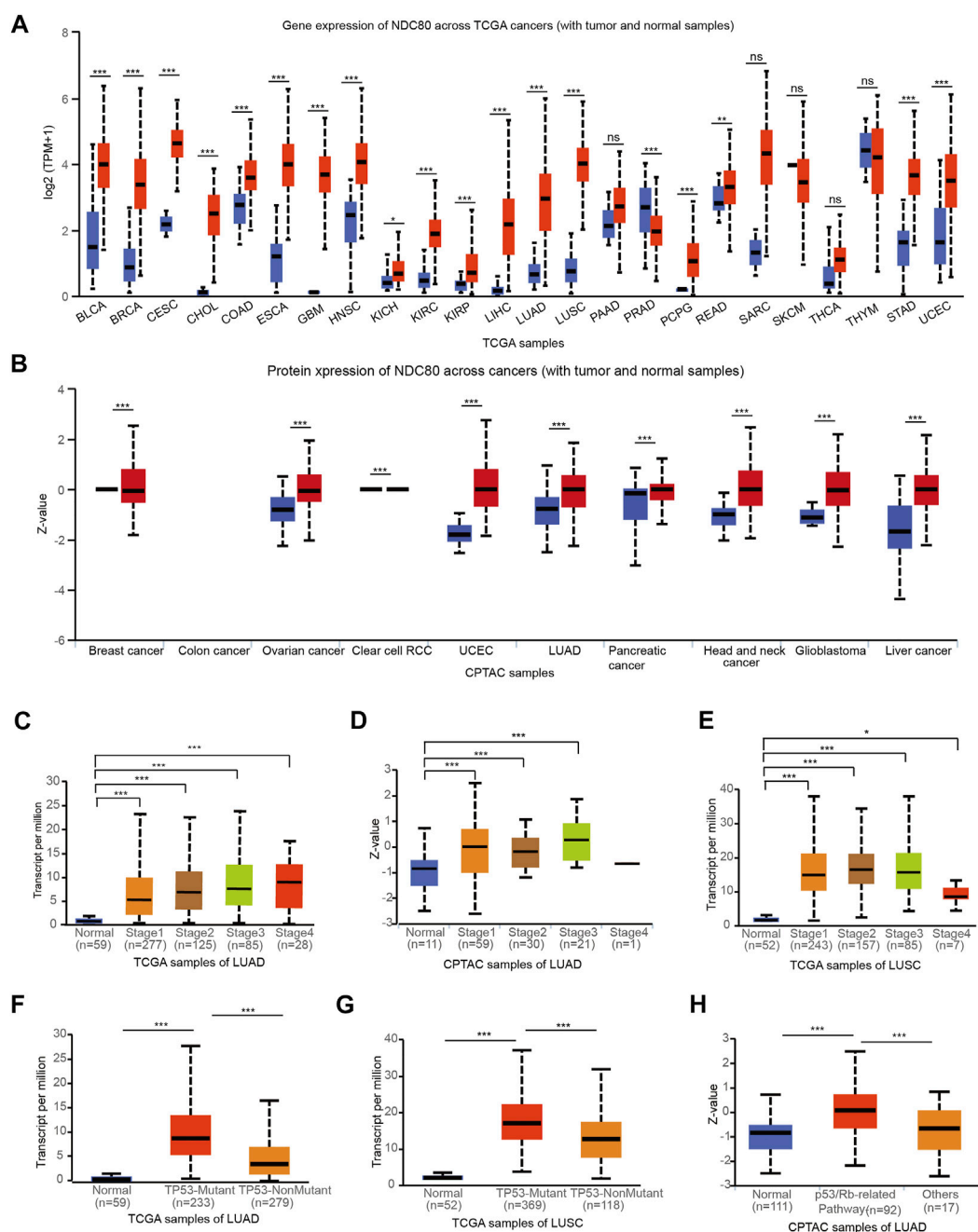


FIGURE 2

Validation of the expression level and clinical significance of NDC80. (A,B) A pan-cancer analysis for the comparison of the transcriptional and protein expression of NDC80 between cancerous and healthy control tissues through the TCGA (A) and CPTAC databases (B) from UALCAN platforms. (C–E) The correlation of the NDC80 expression level with stages of LUAD using the TCGA (C) and CPTAC (D) databases, and in the LUSC (E) dataset. (F–H) The association of NDC80 expression level with p53 mutations in the LUAD (F) and LUSC (G) datasets, and with the p53/Rb pathway in the LUAD (H) dataset. \* $p < 0.05$ ; \*\* $p < 0.01$ ; \*\*\* $p < 0.001$ .

between 2 data groups, and ANOVA was used for more than 2 data groups. Univariate and multivariate Cox regression was performed for survival analysis. Data analysis was performed

using GraphPad Prism 8 and SPSS 23.0. Significant differences were considered at \*,  $p < 0.05$ ; \*\*,  $p < 0.01$ ; \*\*\*,  $p < 0.001$  for all tests.

## Results

### Identification of NDC80 as a radioresistance-related gene in lung cancer

The flow diagram for the present study is shown in Figure 1A. To explore the potential proteins related to radioresistance regulation in lung cancer cells, iTRAQ analysis was performed, to examine the differentially expressed proteins in A549-P and A549-IRR cells. The IR-resistant characteristic of A549-IRR was verified as reported previously (Chen et al., 2021). As shown in Figure 1B and Supplementary Table S2, 5,796 proteins were analyzed, among which 348 proteins were differentially expressed between A549-P and A549-IRR cells (Foldchange>1.5). Two datasets that included 461 LUAD and 392 LUSC samples were selected from the TCGA database. A total of 4029–5,068 DEGs were identified in LUAD and LUSC samples, respectively, as compared to paired non-neoplastic samples (Figures 1C,D, Supplementary Table S3). Combined with information from iTRAQ analysis and two TCGA datasets, 6 co-different genes were identified to be upregulated in lung cancer (Figures 1E,F). Subsequently, we conducted LASSON regression to assess the best fitting variables from the two TCGA datasets. The results suggested that GPX2, NDC80, and PLEK2 represented suitable variables for survival analysis in LUAD datasets (Figure 1G), whereas NDC80 and STRA6 were applicable for use in LUSC datasets (Figure 1H). Intriguingly, only NDC80 was upregulated and related to prognosis in both LUAD and LUSC, and was considered to be the most suitable for further analysis.

### Clinical significance of NDC80 in lung cancer

To validate the clinical features of NDC80 in the progression of malignancies, pan-cancer analysis was performed using the TCGA and CPTAC datasets from the UALCAN platform. The results obtained using TCGA datasets showed that transcriptional expression levels of NDC80 were higher in 19 types of cancers, as compared to those for matched normal samples (Figure 2A). Meanwhile, the NDC80 expression level was significantly increased in 9 kinds of cancers from CPTAC datasets (Figure 2B). The combined results of pan-cancer analyses showed that the expression of NDC80 was notably elevated in LUAD and LUSC samples. The transcriptional and protein expression of NDC80 was increased in the I-IV and I-III stages of LUAD (Figures 2C,D), while the transcriptional expression of NDC80 was significantly enhanced in stages I-IV of LUSC, as compared to normal tissues (Figure 2E). TP53 mutations are frequent and

malignant alterations that are considered unfavorable prognostic biomarkers of lung cancer (Wadowska et al., 2020). We found that transcriptional NDC80 expression was significantly increased in LUAD and LUSC patients with TP53 mutations (Figures 2F,G). In addition, NDC80 was highly expressed in the p53/Rb-related pathways of LUAD patients (Figure 2H).

### Variations in the prognostic value of NDC80 in lung cancer

To understand the prognostic effect of NDC80 in lung cancer, we performed survival analysis in LUAD patients using the XianTao tool. The highest level of NDC80 was found in the dead patients of LUAD patients during overall survival (OS), disease-specific survival (DSS), and progression-free interval (PFI) events (Figures 3A–C). Moreover, the NDC80-based risk scores were obtained via time-dependent ROC, in which the AUC values for risk score predictions of 10-years OS, DSS, and PFI were 0.580, 0.611, and 0.555, respectively (Figures 3D–F). Similarly, a lower expression level of NDC80 was associated with an improved OS, DDS, and PFI in LUAD patients (Figures 3G–I). Additionally, the results of univariate and multivariate COX analysis also revealed that NDC80 was an independent risk factor of survival in LUAD (Table 1). In the nomogram model, the 10- and 15- year survivals were gradually decreased in patients with advanced TNM stage disease, pathologic stage, and high NDC80 expression levels (Figures 3J,K). Additionally, we further confirmed the prognostic role of NDC80 through datasets downloaded from the TCGA database. A similar tendency was observed for the risk scores of LUAD patients (Supplementary Figures S1A–C). With regard to LUSC patients, we found that the AUCs for patients with a 3-, 5-, and 8-year OS corresponded to 0.721, 0.723, and 0.708 (Supplementary Figures S1D–F). Furthermore, we stratified patients into groups, i.e., the high-risk and low-risk groups, based on variables such as gender, age, and TNM stages. All groups with lower risk scores revealed significantly favorable 3, 5, and 8-years overall survival values, in both LUAD and LUSC patients (Supplementary Figures S1G–L).

### Knockdown of NDC80 increases the radiosensitivity of lung cancer cells

To further investigate whether NDC80 was involved in radioresistance development in lung cancer cells, we determined the expression of NDC80 in A549 and H1246 parental and IR-resistant cells (Chen et al., 2021). The radioresistance feature of H1246-IRR was identified in Supplementary Figure S2. Through qPCR and western blot assays, mRNA and protein levels of NDC80 were found to be

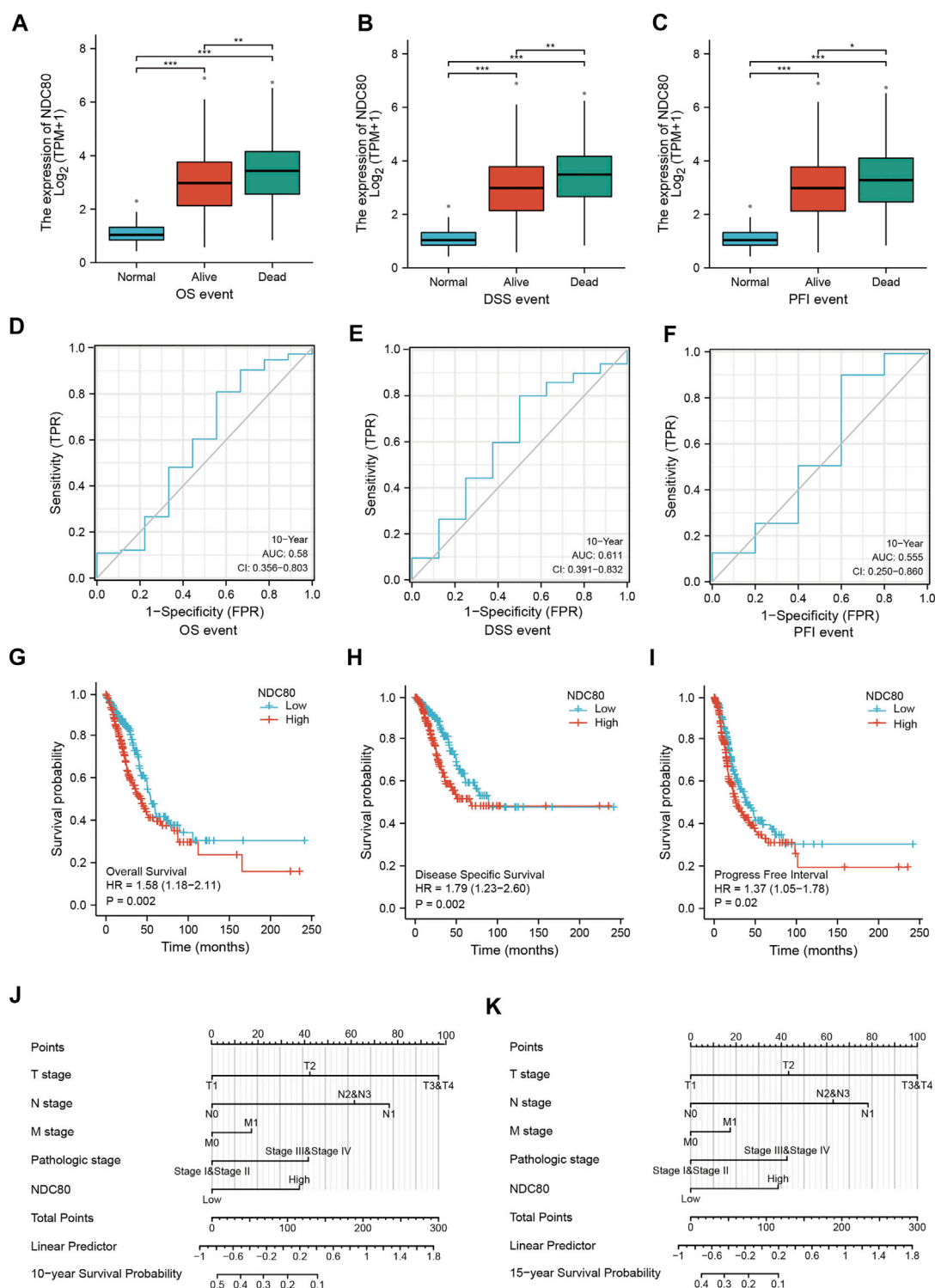


FIGURE 3

The prognostic value of NDC80 in LUAD. (A–C) Using the XianTao tool, the NDC80 expression level was compared among healthy control individuals, and surviving and dead LUAD patients with regard to their OS (A), DSS (B), and PFI (C). (D–F) The AUC values of time-dependent ROC curves were used to verify the 10-years prognostic risk score for OS (D), DSS (E), and PFI (F), based on NDC80 expression levels, using the XianTao tool. (G–I) Generation of survival curves for the OS (G), DSS (H), and PFI (I) of patients in the high-expression and low-expression groups using the XianTao tool. (J,K) The prognostic nomogram of LUAD for the 10-years (J) and 15-years (K) survival period is based on NDC80 expression levels using the XianTao tool. \**p* < 0.05; \*\**p* < 0.01; \*\*\**p* < 0.001.

TABLE 1 The univariate and multivariate Cox regression analysis and clinical features of NDC80.

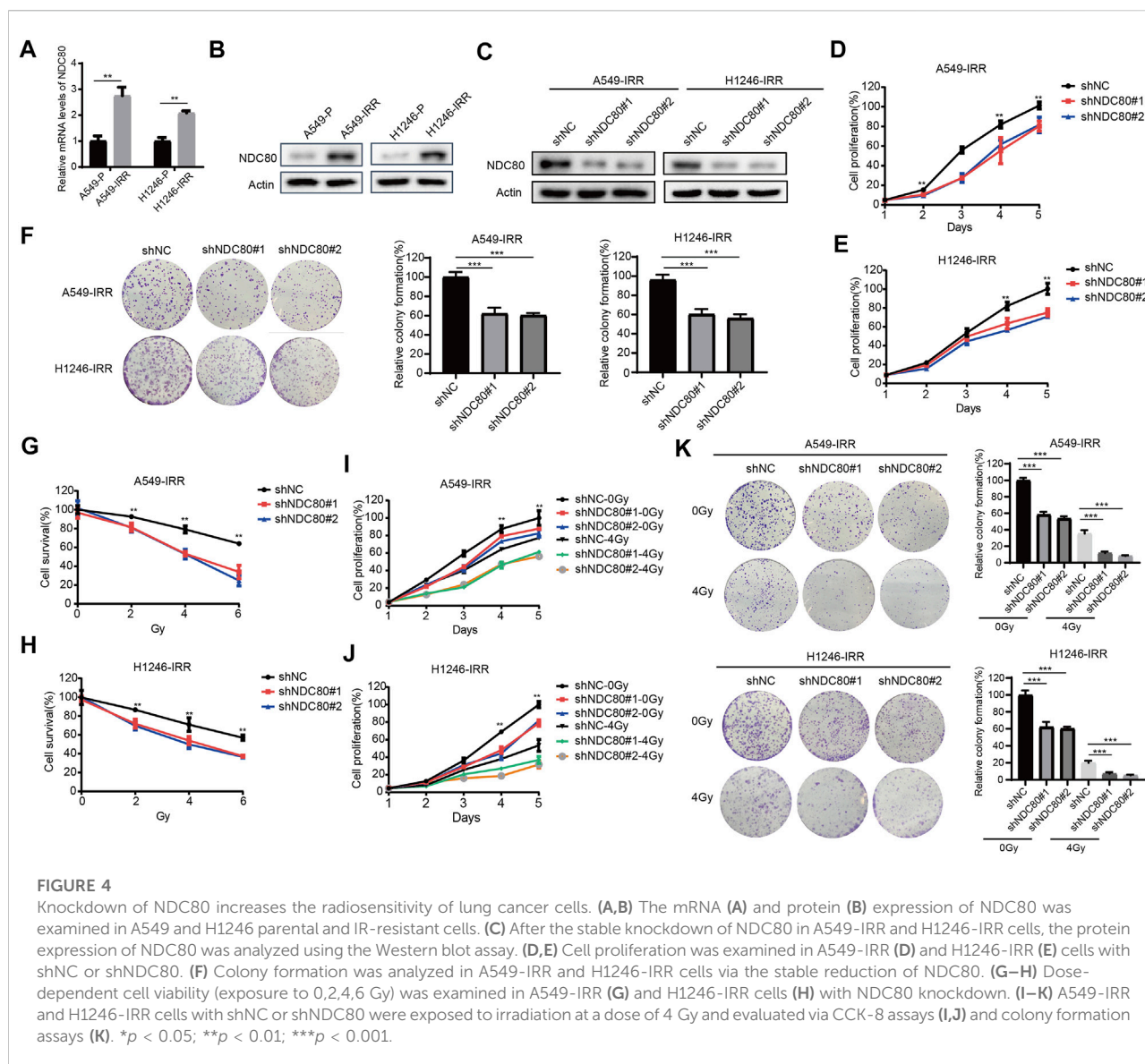
Characteristics	Univariate Cox analysis			Multivariate Cox analysis	
	Total(N)	HR(95% CI)	p value	HR(95% CI)	p value
T stage	523				
T1&T2	457	Reference			
T3&T4	66	2.317 (1.591–3.375)	<0.001	2.008 (1.254–3.216)	0.004
N stage	510				
N0	343	Reference			
N1&N2&N3	167	2.601 (1.944–3.480)	<0.001	2.061 (1.401–3.033)	<0.001
M stage	377				
M0	352	Reference			
M1	25	2.136 (1.248–3.653)	0.006	1.275 (0.670–2.426)	0.459
NDC80	526	1.269 (1.128–1.428)	<0.001	1.275 (1.107–1.469)	<0.001
Pathologic stage	518				
Stage I&Stage II	411	Reference			
Stage III&Stage IV	107	2.664 (1.960–3.621)	<0.001	1.288 (0.788–2.105)	0.313

notably upregulated in both A549-IRR and H1246-IRR cells, compared to their parental cells (Figures 4A,B). Subsequently, we established stably NDC80-depleted A549-IRR and H1246-IRR cells with two shRNAs (Figure 4C). Cell proliferation was significantly inhibited in A549-IRR and H1246-IRR cells after the knockdown of NDC80 (Figures 4D,E). Likewise, colony formation was notably reduced for shNDC80, compared to that observed for shNC (Figure 4F). To confirm the effects of NDC80 on radio-resistance in lung cancer cells, A549-IRR and H1246-IRR cells exhibiting stable NDC80 reduction were treated with IR. The results showed that the downregulation of NDC80 resulted in a dose-dependent inhibition of cell survival after treatment with 0, 2, 4, and 6 Gy IR (Figures 4G,H). Moreover, the knockdown of NDC80 enhanced the radiosensitivity of A549-IRR and H1246-IRR cells, in which the cell viability and colony formation were decreased by more than 50% after exposure to 4 Gy IR (Figures 4I–K). Collectively, these results suggest that the downregulation of NDC80 improved the sensitivity of lung cancer cells to IR.

## The role of NDC80 in the regulation of autophagy in lung cancer patients

Autophagy is a self-renewal process that devours cellular proteins and organelles, and was proposed as a protective mechanism for tumor cell survival in radiotherapy (Levy et al., 2017). In the present study, we performed GSEA using the information from iTRAQ analysis, and confirmed that autophagy might be affected by NDC80-affected biological functions (Figure 5A). Next, we assessed the NDC80-mediated autophagy in IR-resistant NSCLC cells. TEM results showed that

a number of autophagosomes exhibited a significant tendency to decrease in A549-IRR and H1246-IRR cells with NDC80 depletion (Figures 5B–D). We then determined the protein markers involved in the formation of autophagosomes, including Beclin-1, p62, and LC3 II *in vitro*. The protein expression levels of LC3-II, p62, and Beclin-1 were reduced in shNDC80, compared to shNC in A549-IRR and H1246-IRR cells (Figure 5E). To further unveil the molecular mechanisms underlying NDC80-regulated autophagy in lung cancer, the results from iTRAQ analysis were implemented to screen autophagic regulators. As shown in Supplementary Figure S3, autophagic regulators, including 12 upregulated and 2 downregulated proteins, were selected for further identification, according to their expression levels in iTRAQ analysis. Using the qPCR array, we examined the mRNA expression of these candidates in A549-IRR and H1246-IRR cells with stable NDC80 knockdown. The results showed that only ATG7 mRNA expression was markedly downregulated, after values were filtered using the criterion of foldchange >1.5 (Figure 5F). It is known that ATG7 acts as an E1-like activating enzyme and plays a vital role in mediating autophagy (Zhou et al., 2020). Therefore, we used two GEO datasets, GSE102287 and GSE8894, of which GSE102287 was comprised of NSCLC samples and GSE8894 was comprised of LUAD samples, for identifying the correlation between NDC80 and ATG7. The results showed that the expression of NDC80 was positively associated with the levels of ATG7 in lung cancer, using the GSE102287 and GSE8894 datasets (Figures 5G,H). Furthermore, we detected the protein expression level of ATG7 in NDC80-depleted IR-resistant NSCLC cells. The level of ATG7 was notably decreased, and this was accompanied by a reduction in the NDC80 levels in A549-IRR and H1246-IRR cells (Figure 5I). In addition, using Kaplan-Meier analysis, we found that patients with high expression levels of ATG7, and



especially those with LUAD, showed unfavorable survival in lung cancers (Figures 5J,K).

## Identification of correlation between expression of NDC80 and ATG7 by immunohistochemistry

The above findings indicated that the oncogenic effects of NDC80 might induce autophagy by mediating ATG7 in IR-resistant cells of lung cancer. Thus, we further validated the tumorigenic role of NDC80 and ATG7 in LUAD samples by IHC assays. As shown in Figures 6A–C, the staining intensity of NDC80 and ATG7 was stronger in LUAD samples than in healthy specimens. Furthermore, the expression of NDC80 in

Grade III pathological stage specimens was higher than that in Grade II and Grade I, respectively (Figure 6D). Consistently, the level of ATG7 was significantly increased in Grade III, as compared to that in Grade I (Figure 6E). Kaplan-Meier survival analysis suggested that LUAD patients with higher NDC80 or ATG7 expression levels had a poorer prognosis than those with lower expression levels (Figures 6F,G). We also found that the increased expression of NDC80 was concomitant with the elevated level of ATG7 (Figure 6H). Furthermore, targeted therapies for several oncogenic alterations, such as PD-L1-positive expression and ALK translocation have been incorporated during the clinical treatment of lung cancers (Imyanitov et al., 2021). Interestingly, higher expression levels of NDC80 were observed if PD-L1 > 50% LUAD than if it was < 50% PD-LI



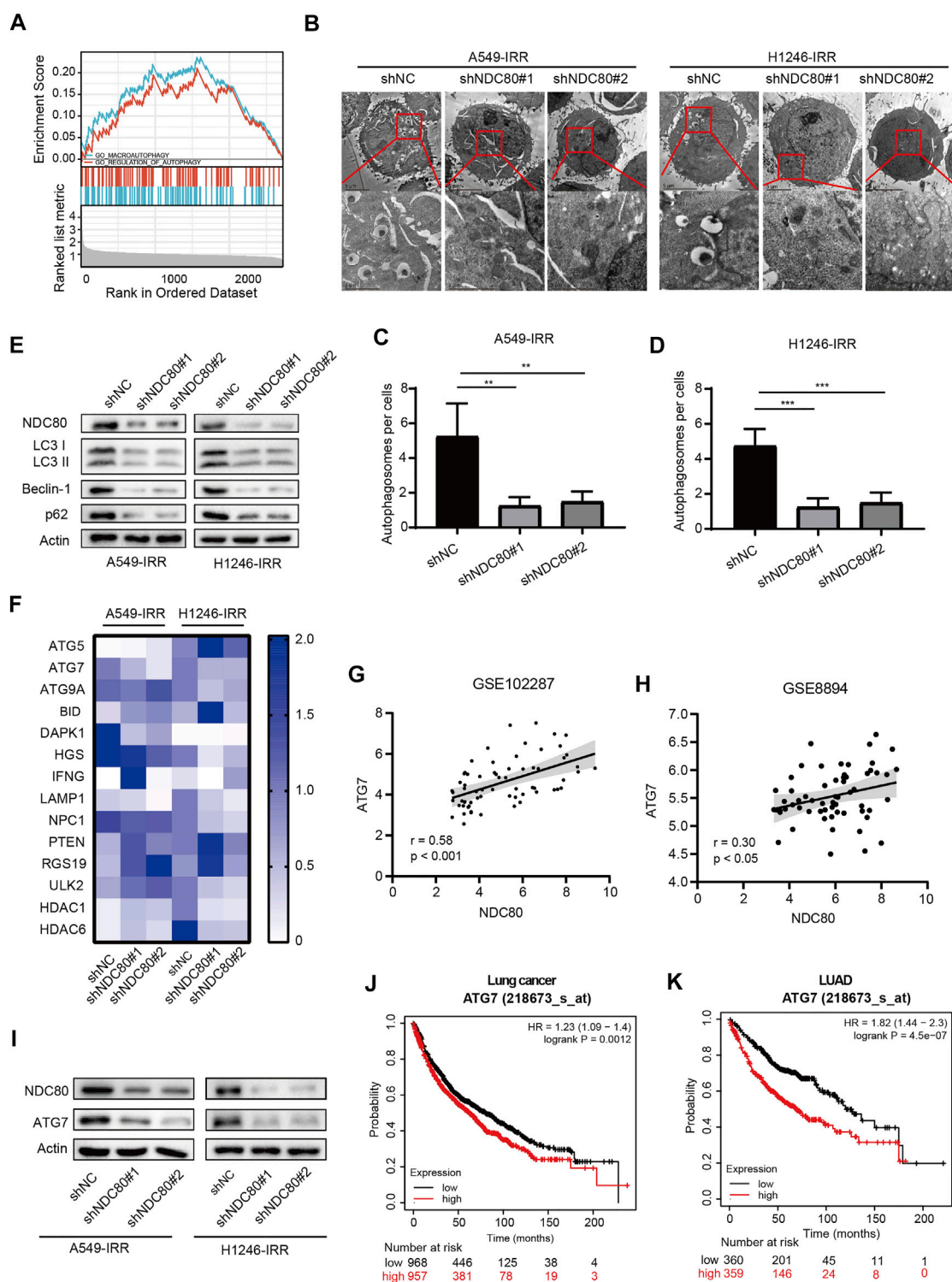


FIGURE 5

NDC80 regulates autophagy in lung cancer. (A) Analysis of the correlation between NDC80 and autophagy by GSEA analyses. (B–D) Autophagosome formation was detected by TEM analysis in A549-IRR and H1246-IRR cells with NDC80 knockdown. (E) After the knockdown of NDC80 in A549-IRR and H1246-IRR cells, LC3 II, Beclin-1, and p62 protein levels were detected. (F) The heatmap shows the mRNA levels of 14 autophagy-relevant genes identified in A549-IRR and H1246-IRR cells. (G,H) Validation of the correlation between NDC80 and ATG7 in two datasets, i.e., GSE102287 (G) and GSE8894 (H) in the GEO database. (I) Analysis of the protein expression level of ATG7 in NDC80-reduced A549-IRR and H1246-IRR cells. (J,K) Analysis of the prognostic value of ATG7 in lung cancer (J) and LUAD (K), through Kaplan-Meier analysis. \*\* $p < 0.01$ ; \*\*\* $p < 0.001$ .

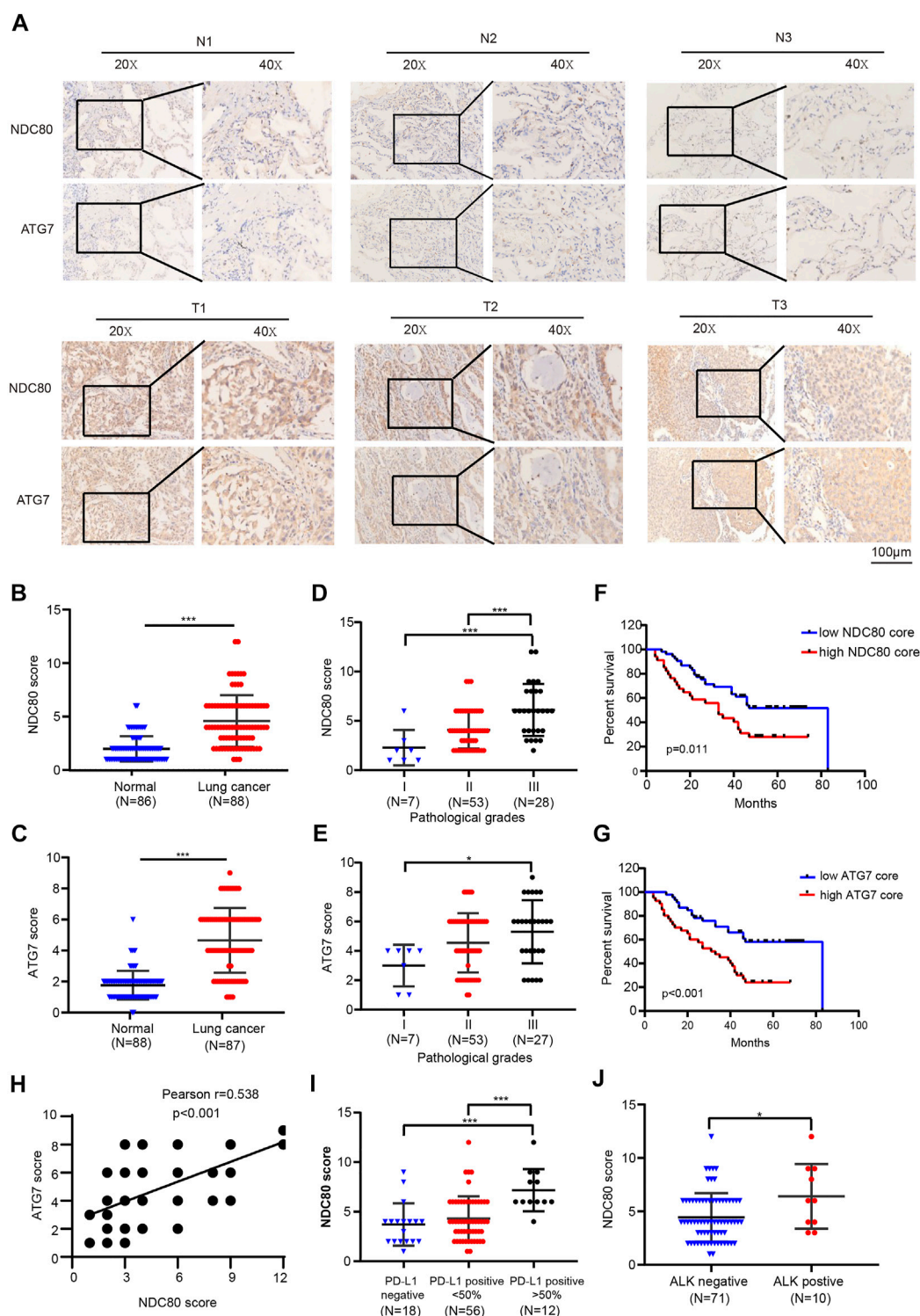


FIGURE 6

Identification of the correlation between the expression of NDC80 and ATG7 by IHC. (A–C) Determination of the expression levels of NDC80 and ATG7 in LUAD and healthy lung specimens by IHC analysis. (D,E) The comparison of NDC80 (D) and ATG7(E) expression in pathological stages. (F,G) The OS analysis of high- and low-expression levels of NDC80 (F) and ATG7(G). (H) The correlation between the expression of NDC80 and ATG7. (I,J) The correlation of NDC80 with PD-L1 expression (I) and ALK status (J). \* $p < 0.05$ ; \*\*\* $p < 0.001$ .

and negative tissues (Figure 6I). In addition, NDC80 expression was significantly enhanced in patients who were ALK-positive (Figure 6J). All these results suggest that NDC80 might become a potential biomarker for the treatment of lung cancer.

## Discussion

In this study, we showed that NDC80 served as a prognostic indicator of lung cancer. Furthermore, we found that NDC80 was associated with the expression of several diagnostic and therapeutic biomarkers of lung cancer, including TP53, PD-L1, and ALK. Moreover, we verified that NDC80 promoted cell growth and radioresistance in IR-resistant lung cancer cells by targeting autophagy. These findings suggest that the targeting of NDC80 might be a potential approach for overcoming the development of resistance in radioresistant NSCLCs.

Autophagy is a crucial and controversial process that helps maintain intracellular homeostasis as it plays dual functions in cell survival and death. Hence, the molecular mechanisms underlying autophagy-regulated radioresistance remain blurred and complicated. Several studies have shown that the blockade of autophagy signaling, including PI3K/mTOR, AMPK, and c-Jun signaling, has the potential to improve radiotherapeutic efficacy (Chaachouay et al., 2015; Zhang et al., 2016). In addition, we previously found that in IR-resistant NSCLC cells, LC3 II, Beclin-1, and p62 levels were notably higher than that of paired parental cells, while the knockdown of Cav1 decreased these protein levels and increased radiosensitivity (Chen et al., 2021). Our present study has revealed for the first time that NDC80-mediated has a cytoprotective role in autophagy in IR-resistant NSCLC cells. We observed that the downregulation of NDC80 in IR-resistant cells reduced the expression levels of LC3 II, Beclin-1, and p62 and the formation of autophagosomes. So far, there have been few reports on the relationship between NDC80 and autophagy. A study reported that NDC80, as a component of the KMN (KNL-1/Mis12/Ndc80) complex, could indirectly interact with Beclin-1, which is essential for kinetochore assembly in Hela cells (Fremont et al., 2013). This study shows that NDC80 could influence cell survival by affecting autophagy. Altogether, these data explain the mechanism by which NDC80 overcomes resistance to IR through pro-survival autophagic functions.

Furthermore, we elucidated that NDC80 regulates autophagy by targeting ATG7 in IR-resistant NSCLC cells. ATG7, an E1-like enzyme, is required for the conjugation of Atg12 to Atg5, which was coupled with phosphatidylethanolamine to LC3 (Collier et al., 2021). ATG7 has been observed to promote tumor development,

since the knockdown of ATG7 could inhibit the self-renewal and invasion of stem-like lung cancer cells (Zhou et al., 2021). Furthermore, ATG7 was reported to be overexpressed in lung cancer with cisplatin treatment, which causes resistance to apoptosis through cisplatin-induced hydroxyl radicals (Sumkhemthong et al., 2021). As for radiotherapy, ATG7 deficiency could sensitize cancer cells to IR (Schaaf et al., 2015). Moreover, the accumulation of autophagosomes with concomitantly elevated mRNA levels of ATG7 leads to radiation resistance in breast cancer under hypoxic exposure (He et al., 2012). These studies suggest that the effects of ATG7 on radiation treatment may be determined by the types of cancers and conditions. In the present study, we observed that the knockdown of NDC80 attenuated ATG7 expression in IR-resistant cells. Meanwhile, ATG7 was upregulated to a greater extent in LUAD samples than in normal tissues, and was positively correlated with the NDC80 expression level. These results indicate that the downregulation of NDC80 alleviates IR-resistant features in NSCLC cells through the regulation of ATG7-related autophagy.

In summary, in this study, we identified that NDC80 might be a diagnostic and prognostic indicator in lung cancer. Furthermore, elevated NDC80 expression was detected in IR-resistant NSCLC cells, and was found to induce radiation resistance. Our findings provide novel insights into the effect of NDC80 on radioresistance in cancer cells, and suggest that NDC80 could serve as a drug target for improving radiosensitivity.

## Data availability statement

The datasets presented in this study can be found in online repositories. The names of the repository/repositories and accession number(s) can be found in the article/Supplementary Material.

## Ethics statement

Ethical review and approval was not required for the study on human participants in accordance with the local legislation and institutional requirements. Written informed consent for participation was not required for this study in accordance with the national legislation and the institutional requirements.

## Author contributions

QH and ZX were responsible for the conception and design of the study; SZ provided administrative support;

XC provided the study materials; XC and SZ performed the collection and assembly of data; XC and SZ performed data analysis and interpretation; all the authors wrote and approved the manuscript.

## Funding

This study was supported by grants from the Natural Science Foundation of Hunan Province (2021JJ30904), the horizontal project (2021-021, 143010100), the Science and Technology Innovation Program of Hunan Province (2021RC3029), and the Youth Science Foundation of Xiangya Hospital (2019Q13), the Fundamental Research Funds for the Central Universities of Central South University (2022ZZTS0250).

## Acknowledgments

We thank Shanghai Keteng Educational Technology for assistance with language editing.

## References

- Alexander, M., Kim, S. Y., and Cheng, H. (2020). Update 2020: Management of non-small cell lung cancer. *Lung* 198 (6), 897–907. doi:10.1007/s00408-020-00407-5
- Chaachouay, H., Fehrenbacher, B., Toulany, M., Schaller, M., Multhoff, G., and Rodemann, H. P. (2015). AMPK-independent autophagy promotes radioresistance of human tumor cells under clinical relevant hypoxia *in vitro*. *Radiother. Oncol.* 116 (3), 409–416. doi:10.1016/j.radonc.2015.08.012
- Chandrashekar, D. S., Karthikeyan, S. K., Korla, P. K., Patel, H., Shovon, A. R., Athar, M., et al. (2022). Ualcan: An update to the integrated cancer data analysis platform. *Neoplasia* 25, 18–27. doi:10.1016/j.neo.2022.01.001
- Chen, J., Liao, A., Powers, E. N., Liao, H., Kohlstaedt, L. A., Evans, R., et al. (2020). Aurora B-dependent Ndc80 degradation regulates kinetochore composition in meiosis. *Genes Dev.* 34 (3–4), 209–225. doi:10.1101/gad.333997.119
- Chen, X., Wang, P., Guo, F., Wang, X., Wang, J., Xu, J., et al. (2017). Autophagy enhanced the radioresistance of non-small cell lung cancer by regulating ROS level under hypoxia condition. *Int. J. Radiat. Biol.* 93 (8), 764–770. doi:10.1080/09553002.2017.1325025
- Chen, X., Yan, Y. L., Zeng, S. S., Gong, Z. C., and Xu, Z. J. (2021). Caveolin-1 promotes radioresistance via IRGM-regulated autophagy in lung cancer. *Ann. Transl. Med.* 9 (1), 47. doi:10.21037/atm-20-3293
- Collier, J. J., Suomi, F., Olahova, M., McWilliams, T. G., and Taylor, R. W. (2021). Emerging roles of ATG7 in human health and disease. *EMBO Mol. Med.* 13 (12), e14824. doi:10.15252/emmm.202114824
- Cui, H., Wang, Q., Lei, Z., Feng, M., Zhao, Z., Wang, Y., et al. (2019). DTL promotes cancer progression by PDCD4 ubiquitin-dependent degradation. *J. Exp. Clin. Cancer Res.* 38 (1), 350. doi:10.1186/s13046-019-1358-x
- Fremont, S., Gerard, A., Galloux, M., Janvier, K., Karess, R. E., and Berlioz-Torrent, C. (2013). Beclin-1 is required for chromosome congression and proper outer kinetochore assembly. *EMBO Rep.* 14 (4), 364–372. doi:10.1038/embor.2013.23
- Friedman, J., Hastie, T., and Tibshirani, R. (2010). Regularization paths for generalized linear models via coordinate descent. *J. Stat. Softw.* 33 (1), 1–22. doi:10.18637/jss.v033.i01
- Gao, H., Pan, Q. Y., Wang, Y. J., and Chen, Q. F. (2022). Impact of KMN network genes on progression and prognosis of non-small cell lung cancer. *Anticancer. Drugs* 33 (1), e398–e408. doi:10.1097/CAD.0000000000001220
- Gao, L., Zheng, H., Cai, Q., and Wei, L. (2020). Autophagy and tumour radiotherapy. *Adv. Exp. Med. Biol.* 1207, 375–387. doi:10.1007/978-981-15-4272-5\_25
- He, W. S., Dai, X. F., Jin, M., Liu, C. W., and Rent, J. H. (2012). Hypoxia-induced autophagy confers resistance of breast cancer cells to ionizing radiation. *Oncol. Res.* 20 (5–6), 251–258. doi:10.3727/096504013x13589503483012
- Iemura, K., Natsume, T., Maehara, K., Kanemaki, M. T., and Tanaka, K. (2021). Chromosome oscillation promotes Aurora A-dependent Hec1 phosphorylation and mitotic fidelity. *J. Cell Biol.* 220 (7), e202006116. doi:10.1083/jcb.202006116
- Imyanitov, E. N., Iyevleva, A. G., and Levchenko, E. V. (2021). Molecular testing and targeted therapy for non-small cell lung cancer: Current status and perspectives. *Crit. Rev. Oncol. Hematol.* 157, 103194. doi:10.1016/j.critrevonc.2020.103194
- Lee, E. S., Son, D. S., Kim, S. H., Lee, J., Jo, J., Han, J., et al. (2008). Prediction of recurrence-free survival in postoperative non-small cell lung cancer patients by using an integrated model of clinical information and gene expression. *Clin. Cancer Res.* 14 (22), 7397–7404. doi:10.1158/1078-0432.CCR-07-4937
- Levy, J. M. M., Towers, C. G., and Thorburn, A. (2017). Targeting autophagy in cancer. *Nat. Rev. Cancer* 17 (9), 528–542. doi:10.1038/nrc.2017.53
- Li, X., He, S., and Ma, B. (2020). Autophagy and autophagy-related proteins in cancer. *Mol. Cancer* 19 (1), 12. doi:10.1186/s12943-020-1138-4
- Lu, C., Chen, X., Yan, Y., Ren, X., Wang, X., Peng, B., et al. (2022). Aberrant expression of ADAR1 facilitates temozolomide chemoresistance and immune infiltration in glioblastoma. *Front. Pharmacol.* 13, 768743. doi:10.3389/fphar.2022.768743
- Mitchell, K. A., Zingone, A., Toulabi, L., Boeckelman, J., and Ryan, B. M. (2017). Comparative transcriptome profiling reveals coding and noncoding RNA differences in NSCLC from african Americans and European Americans. *Clin. Cancer Res.* 23 (23), 7412–7425. doi:10.1158/1078-0432.CCR-17-0527
- Mo, Q. Q., Chen, P. B., Jin, X., Chen, Q., Tang, L., Wang, B. B., et al. (2013). Inhibition of Hec1 expression enhances the sensitivity of human ovarian cancer cells to paclitaxel. *Acta Pharmacol. Sin.* 34 (4), 541–548. doi:10.1038/aps.2012.197
- Moulder, R., Bhosale, S. D., Goodlett, D. R., and Lahesmaa, R. (2018). Analysis of the plasma proteome using iTRAQ and TMT-based Isobaric labeling. *Mass Spectrom. Rev.* 37 (5), 583–606. doi:10.1002/mas.21550

## Conflict of interest

The authors declare that the research was conducted in the absence of any commercial or financial relationships that could be construed as a potential conflict of interest.

## Publisher's note

All claims expressed in this article are solely those of the authors and do not necessarily represent those of their affiliated organizations, or those of the publisher, the editors and the reviewers. Any product that may be evaluated in this article, or claim that may be made by its manufacturer, is not guaranteed or endorsed by the publisher.

## Supplementary material

The Supplementary Material for this article can be found online at: <https://www.frontiersin.org/articles/10.3389/fphar.2022.985601/full#supplementary-material>



- Qu, Y., Li, J., Cai, Q., and Liu, B. (2014). Hec1/Ndc80 is overexpressed in human gastric cancer and regulates cell growth. *J. Gastroenterol.* 49 (3), 408–418. doi:10.1007/s00535-013-0809-y
- Ruiz-Cordero, R., and Devine, W. P. (2020). Targeted therapy and checkpoint immunotherapy in lung cancer. *Surg. Pathol. Clin.* 13 (1), 17–33. doi:10.1016/j.path.2019.11.002
- Sakaguchi, H., Tsuchiya, H., Kitagawa, Y., Tanino, T., Yoshida, K., Uchida, N., et al. (2022). NEAT1 confers radioresistance to hepatocellular carcinoma cells by inducing autophagy through GABARAP. *Int. J. Mol. Sci.* 23 (2), 711. doi:10.3390/ijms23020711
- Sarangapani, K. K., Koch, L. B., Nelson, C. R., Asbury, C. L., and Biggins, S. (2021). Kinetochore-bound Mps1 regulates kinetochore-microtubule attachments via Ndc80 phosphorylation. *J. Cell Biol.* 220 (12), e202106130. doi:10.1083/jcb.202106130
- Schaaf, M. B., Jutten, B., Keulers, T. G., Savelkoul, K. G., Peeters, H. J., van den Beucken, T., et al. (2015). Canonical autophagy does not contribute to cellular radioresistance. *Radiother. Oncol.* 114 (3), 406–412. doi:10.1016/j.radonc.2015.02.019
- Scheiter, A., Keil, F., Luke, F., Grosse, J., Verloh, N., Opitz, S., et al. (2021). Identification and in-depth analysis of the novel FGFR2-NDC80 fusion in a cholangiocarcinoma patient: Implication for therapy. *Curr. Oncol.* 28 (2), 1161–1169. doi:10.3390/curroncol28020112
- Sumkhemthong, S., Prompetchara, E., Chanvorachote, P., and Chaotham, C. (2021). Cisplatin-induced hydroxyl radicals mediate pro-survival autophagy in human lung cancer H460 cells. *Biol. Res.* 54 (1), 22. doi:10.1186/s40659-021-00346-2
- Sun, Z. Y., Wang, W., Gao, H., and Chen, Q. F. (2020). Potential therapeutic targets of the nuclear division cycle 80 (NDC80) complexes genes in lung adenocarcinoma. *J. Cancer* 11 (10), 2921–2934. doi:10.7150/jca.41834
- Wadowska, K., Bil-Lula, I., Trembecki, L., and Sliwinska-Mosson, M. (2020). Genetic markers in lung cancer diagnosis: A review. *Int. J. Mol. Sci.* 21 (13), E4569. doi:10.3390/ijms21134569
- Wei, J., Yan, Y., Chen, X., Qian, L., Zeng, S., Li, Z., et al. (2019). The roles of plant-derived triptolide on non-small cell lung cancer. *Oncol. Res.* 27 (7), 849–858. doi:10.3727/096504018X15447833065047
- Wimbish, R. T., and DeLuca, J. G. (2020). Hec1/Ndc80 tail domain function at the kinetochore-microtubule Interface. *Front. Cell Dev. Biol.* 8, 43. doi:10.3389/fcell.2020.00043
- Xia, T., Wu, X., Cao, M., Zhang, P., Shi, G., Zhang, J., et al. (2019). The RNA m6A methyltransferase METTL3 promotes pancreatic cancer cell proliferation and invasion. *Pathol. Res. Pract.* 215 (11), 152666. doi:10.1016/j.prp.2019.152666
- Xu, B., Wu, D. P., Xie, R. T., Liu, L. G., and Yan, X. B. (2017). Elevated NDC80 expression is associated with poor prognosis in osteosarcoma patients. *Eur. Rev. Med. Pharmacol. Sci.* 21 (9), 2045–2053.
- Xu, M., Chen, X., Lin, K., Zeng, K., Liu, X., Pan, B., et al. (2018). The long noncoding RNA SNHG1 regulates colorectal cancer cell growth through interactions with EZH2 and miR-154-5p. *Mol. Cancer* 17 (1), 141. doi:10.1186/s12943-018-0894-x
- Xu, S., Zhou, Z., Peng, X., Tao, X., Zhou, P., Zhang, K., et al. (2021). EBV-LMP1 promotes radioresistance by inducing protective autophagy through BNIP3 in nasopharyngeal carcinoma. *Cell Death Dis.* 12 (4), 344. doi:10.1038/s41419-021-03639-2
- Yan, Y., Xu, Z., Hu, X., Qian, L., Li, Z., Zhou, Y., et al. (2018). SNCA is a functionally low-expressed gene in lung adenocarcinoma. *Genes (Basel)* 9 (1), E16. doi:10.3390/genes9010016
- Zhang, X., Ji, J., Yang, Y., Zhang, J., and Shen, L. (2016). Stathmin1 increases radioresistance by enhancing autophagy in non-small-cell lung cancer cells. *Oncotargets. Ther.* 9, 2565–2574. doi:10.2147/OTT.S100468
- Zhang, Z., Qiu, X., Yan, Y., Liang, Q., Cai, Y., Peng, B., et al. (2021). Evaluation of ferroptosis-related gene AKR1C1 as a novel biomarker associated with the immune microenvironment and prognosis in breast cancer. *Int. J. Gen. Med.* 14, 6189–6200. doi:10.2147/IJGM.S329031
- Zhao, Y., Li, X., Zhang, H., Yan, M., Jia, M., and Zhou, Q. (2022). A transcriptome sequencing study on genome-wide gene expression differences of lung cancer cells modulated by fucoidan. *Front. Bioeng. Biotechnol.* 10, 844924. doi:10.3389/fbioe.2022.844924
- Zhou, B., Liu, J., Kang, R., Klionsky, D. J., Kroemer, G., and Tang, D. (2020). Ferroptosis is a type of autophagy-dependent cell death. *Semin. Cancer Biol.* 66, 89–100. doi:10.1016/j.semcancer.2019.03.002
- Zhou, Q., Cui, F., Lei, C., Ma, S., Huang, J., Wang, X., et al. (2021). ATG7-mediated autophagy involves in miR-138-5p regulated self-renewal and invasion of lung cancer stem-like cells derived from A549 cells. *Anticancer. Drugs* 32 (4), 376–385. doi:10.1097/CAD.0000000000000979
- Zhou, S., Yan, Y., Chen, X., Wang, X., Zeng, S., Qian, L., et al. (2019). Roles of highly expressed PAICS in lung adenocarcinoma. *Gene* 692, 1–8. doi:10.1016/j.gene.2018.12.064





## OPEN ACCESS

## EDITED BY

Ryszard Pluta,  
Laboratory of Ischemic and  
Neurodegenerative Brain Research,  
Mossakowski Medical Research Centre,  
Polish Academy of Sciences, Poland

## REVIEWED BY

Fangyi Long,  
Sichuan Provincial Maternity and Child  
Health Care Hospital, China  
Jianjun Chen,  
Southern Medical University, China

## \*CORRESPONDENCE

Wenqiu Zhang,  
zhangwenqiu@scu.edu.cn

<sup>†</sup>These authors have contributed equally  
to this work and share first authorship.

## SPECIALTY SECTION

This article was submitted to  
Pharmacology of Anti-Cancer Drugs,  
a section of the journal  
Frontiers in Pharmacology

RECEIVED 16 June 2022

ACCEPTED 01 August 2022

PUBLISHED 07 September 2022

## CITATION

Wei Y, Xiang H and Zhang W (2022),  
Review of various NAMPT inhibitors for  
the treatment of cancer.  
*Front. Pharmacol.* 13:970553.  
doi: 10.3389/fphar.2022.970553

## COPYRIGHT

© 2022 Wei, Xiang and Zhang. This is an  
open-access article distributed under  
the terms of the [Creative Commons  
Attribution License \(CC BY\)](https://creativecommons.org/licenses/by/4.0/). The use,  
distribution or reproduction in other  
forums is permitted, provided the  
original author(s) and the copyright  
owner(s) are credited and that the  
original publication in this journal is  
cited, in accordance with accepted  
academic practice. No use, distribution  
or reproduction is permitted which does  
not comply with these terms.

# Review of various NAMPT inhibitors for the treatment of cancer

Yichen Wei<sup>1,2†</sup>, Haotian Xiang<sup>3†</sup> and Wenqiu Zhang<sup>3\*</sup>

<sup>1</sup>West China School of Pharmacy, Sichuan University, Chengdu, China, <sup>2</sup>State Key Laboratory of Biotherapy and Cancer Center, Department of Respiratory and Critical Care Medicine, West China Hospital, Sichuan University, Chengdu, China, <sup>3</sup>Department of Ophthalmology, West China Hospital, Sichuan University, Chengdu, China

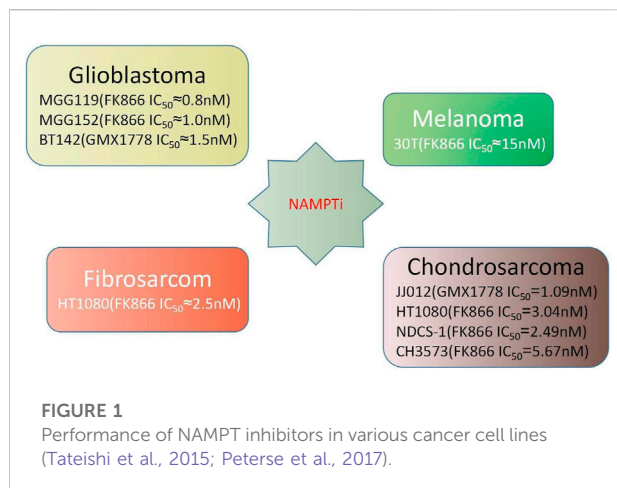
Nicotinamide phosphoribosyltransferase (NAMPT) is a rate-limiting enzyme in the NAD salvage pathway of mammalian cells and is overexpressed in numerous types of cancers. These include breast cancer, ovarian cancer, prostate cancer, gastric cancer, colorectal cancer, glioma, and b-cell lymphoma. NAMPT is also known to impact the NAD and NADPH pool. Research has demonstrated that NAMPT can be inhibited. NAMPT inhibitors are diverse anticancer medicines with significant anti-tumor efficacy in *ex vivo* tumor models. A few notable NAMPT specific inhibitors which have been produced include FK866, CHS828, and OT-82. Despite encouraging preclinical evidence of the potential utility of NAMPT inhibitors in cancer models, early clinical trials have yielded only modest results, necessitating the adaptation of additional tactics to boost efficacy. This paper examines a number of cancer treatment methods which target NAMPT, including the usage of individual inhibitors, pharmacological combinations, dual inhibitors, and ADCs, all of which have demonstrated promising experimental or clinical results. We intend to contribute further ideas regarding the usage and development of NAMPT inhibitors in clinical therapy to advance the field of research on this intriguing target.

## KEYWORDS

nicotinamide phosphoribosyltransferase, individual inhibitors, pharmacological combinations, dual inhibitors, antibody-drug conjugates

## 1 Introduction

One of the features of aggressive cancer is cellular metabolism reprogramming (Tennant et al., 2010; Loree and Kopetz, 2017). The regulation of these metabolic processes and the generation of adenosine triphosphate (ATP), which is constantly needed in both normal tissues and tumor cells, depends on nicotinamide adenine dinucleotide (NAD) and nicotinamide adenine dinucleotide phosphate (NADPH). In tumor cells, the half-life of NAD is only about 1 hour, so the synthesis of more NAD is necessary compensate for such rapid degradation, which in addition to the NAD required for ATP supply, makes their demand for this compound even greater (Rechsteiner et al., 1976; Schreiber et al., 2006). Based on these findings, it has been hypothesized that disrupting NAD homeostasis by interfering with NAD



biosynthesis processes, hence lowering the NAD pool in cancer cells, could be a promising technique in cancer therapy.

The three principal mechanisms for NAD synthesis are the Preiss-Handler pathway, the *de novo* pathway, and the salvage pathway. In the *de novo* pathway, we use tryptophan as a substrate to synthesize NAD in the organism through a series of enzymatic reactions. Because they hardly have all enzymes necessary to convert tryptophan to NAD, several cancer cell lines have been shown that they cannot utilize the *de novo* pathway (Heyes et al., 1997; Xiao et al., 2013). The Preiss-Handler pathway is commonly observed to be dysfunctional in cancer cells owing to the loss of expression of nicotinic acid phosphoribosyltransferase domain containing 1 (NAPRT1), which can help metabolize nicotinic acid (NA) to NAD (Watson et al., 2009; O'Brien et al., 2013; Shames et al., 2013). Because systemic NA levels are frequently insufficient to induce NAD synthesis, NAPRT1-expressing cancer cells cannot effectively utilize the NA-dependent salvage pathway (Kirkland, 2009). Tumor cells lacking NAPRT1, on the other hand, rely on NAMPT (the rate-limiting enzyme in salvage pathway) to create NAD and support cell survival, thus making them more vulnerable to NAMPT inhibitors (Olesen et al., 2010). This means modest changes in its activity can have a big impact on NAD metabolism and NAD-dependent cellular activities (Rongvaux et al., 2002; Revollo et al., 2004; Imai, 2009; Yaku et al., 2018).

NAMPT is found in all tissues of mammals, as well as lower species, such as insects, sponges, and prokaryotes, and its coding sequence is well conserved (McGlothlin et al., 2005). Nearly all of the human body's organs—including the cytoplasm, adipose tissue, blood, liver tissue, cerebrospinal fluid, pancreatic tissue—contain NAMPT (Sun et al., 2017). The binding site and biological function of this enzyme will be explained in detail later.

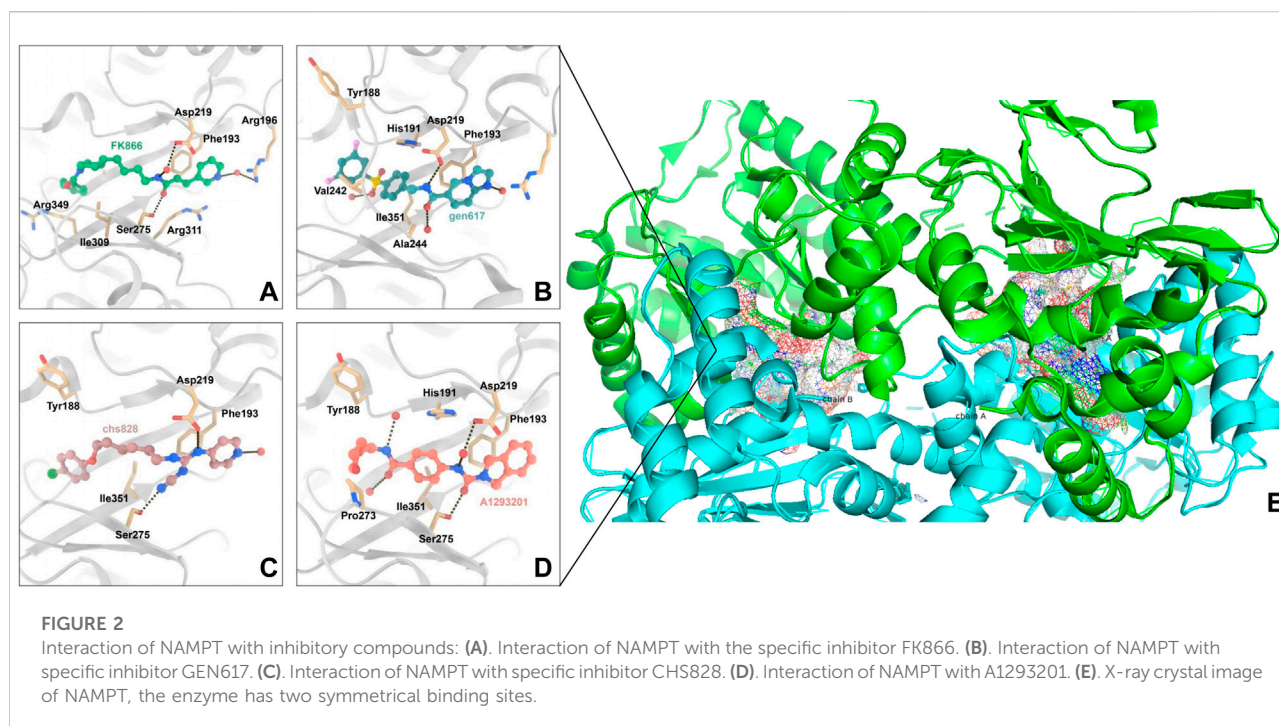
Elevated serum NAMPT levels are associated with non-alcoholic fatty liver disease, obesity, diabetes, and most significantly, malignancy (Figure 1) (Park et al., 2017; Pramono et al., 2020). In various malignancies like prostate cancer, ovarian cancer, colorectal

cancer, melanoma, breast cancer, myeloma, and gastric cancer, NAMPT is commonly increased, which has an impact on the NAD pool (Reddy et al., 2008; Bi et al., 2011; Olesen et al., 2011; Maldi et al., 2013; Shackelford et al., 2013; Zhang et al., 2013; Ju et al., 2016; Lucena-Cacace et al., 2017; Hesari et al., 2018; Lee et al., 2018; Lucena-Cacace et al., 2018; Vaupel et al., 2019). NAMPT inhibitors diminish NAD levels and, as a result, hamper the cellular growth of cancer (Barraud et al., 2016; Espindola-Netto et al., 2017; Hong et al., 2019). Conversely, boosting the NAD pool has been shown to exacerbate the overexpression of NAMPT and increase the occurrence of acquired resistance to chemotherapy medicines such as paclitaxel, adriamycin, fluorouracil, phenethyl isothiocyanate, and etoposide (Folgueira et al., 2005; Bi et al., 2011; Wang et al., 2011; Tome et al., 2012). In cancer cells, reducing NAMPT levels resulted in an increase in ROS and cell death. *In vitro* studies have demonstrated that employing NAMPT inhibitors to treat cancer cells, particularly cancer cell lines with IDH1/2 mutations, is considerably effective. Primary glioblastoma cell lines MGG119, MGG152, BT142, chondrosarcoma cell lines 30T, HT1080, SW1353, and gastric cancer cell lines MKN1, SNU668, Hs746T, SNU484, and SNU1750 with mutations have all been shown to be sensitive to NAMPT inhibition (Tateishi et al., 2015; Peterse et al., 2017). NAMPT inhibitors have not only showed promise as a monotherapy, but they have also been proven *in vitro* and *in vivo* investigations to prolong the therapeutic decline caused by cancer resistance to other medication treatment modalities. Such findings have led to drug combination and dual inhibitor studies (Nahimana et al., 2009; Sampath et al., 2015; Mitchell et al., 2019). More details about the relationship between NAMPT and cancer will be described later.

On the basis of the current understanding of NAMPT regulatory mechanisms and developing evidence for NAMPT's pathogenic functions in human cancer, the further study of NAMPT inhibitors is unquestionably significant for the treatment of cancer. However, as therapeutic demands grow, NAMPT inhibitor research and application tactics must always be adjusted. In this review, we will first present a comprehensive explanation of NAMPT's basic biological functions and its association with cancer, then we will talk about current clinical development status and observations. Last but not the least, this review summarizes the following research and application strategies for NAMPT inhibitors: specific inhibitors, dual inhibitors, pharmacological combinations, and NAMPTi-ADCs. From a chemical point of view, we will explain the research history of each type of inhibitor, and what the different types of inhibitors learn from each other in the development process.

## 2 Binding sites for Nicotinamide phosphoribosyltransferase

NAMPT's enzymatic activity was first discovered by Preiss and Handler in 1957 (Preiss et al., 1958). NAMPT has a molecular weight of around 55 kDa and primarily consists of 491 amino acids. Its x-ray



crystal structure has been recorded and it recognized as a dimeric class of type II phosphoribosyltransferases. NAMPT crystal structures bound to various ligands have been identified. These structures frequently contain a NAMPT homodimer with two similar active sites at the dimer interface. NAMPT inhibitors typically occupy the active site that NAM binds to, as well as a tunnel-shaped cavity which characteristically extends from an NAM binding site (Figure 2). Many NAMPT inhibitors are unique in that they rely on a nitrogen-containing heterocyclic component for cellular efficacy. When an NAMPT inhibitor binds to an NAMPT protein, the heterocyclic components protrude into the NAM binding site and mimic the covalent binding of the native substrate to PRPP (Khan et al., 2006).

Niacinamide mononucleotide (NMN) is created when NAMPT catalyzes the reversible addition of a ribosyl group from PRPP, which in terms of chemical structure is 5-phospho-D-ribosyl 1-pyrophosphate, to NAM (Garten et al., 2015). To speed up this process, NAMPT is autophosphorylated on H247, increasing the enzyme's activity 1,125 fold and its affinity for NAM 160,000 fold (Burgos et al., 2009). The transient autophosphorylation of NAMPT does, however, strengthen the bond between the two dimeric monomers that compose the active site, increasing the enzyme's affinity for PRPP by a factor of ten. When ATP is hydrolyzed and bound to it to create NAMN, NAMPT autophosphorylation increases catalytic efficiency 1,100 fold by lowering the  $K_m$  of NAM binding from 855 to 5 nM (Burgos and Schramm, 2008). Therefore, in the presence of adequate ATP,

NAMPT's  $K_m$  is 7 mM, and NAMPT is capable of efficiently converting NAM to NAMN.

### 3 Basic biological functions of Nicotinamide phosphoribosyltransferase

NAMPT has been demonstrated to play a role in the circadian clock (Figure 3). The recruitment of SIRT1 to the NAMPT promoter to boost NAMPT expression is controlled by the main component of the circadian clock mechanism. NAD production occurs next, and it triggers the activation of sirtuins and other NAD-dependent enzymes in turn. SIRT1 will suppress the component and subsequently NAMPT expression in a negative feedback loop. Through this mechanism, it is hypothesized that SIRT1 and NAMPT may be essential for metabolism circadian regulation (Nakahata et al., 2009; Ramsey et al., 2009). In the salvage pathway of NAD synthesis, its direct product, NAMN, may play a role in signaling (Wang et al., 2009; Yoshino et al., 2011). Similar to this, NAMPT can be thought of as a nicotinamide scavenger due to the fact that nicotinamide inhibits numerous NAD-utilizing enzymes.

In addition, NAMPT enhances the function of interleukin-7 and stem cell factor in the enhancement of normal human or mouse bone marrow pre-B colony formation (Dahl et al., 2012). Extracellular NAMPT functions as an immunomodulatory mediator that directly

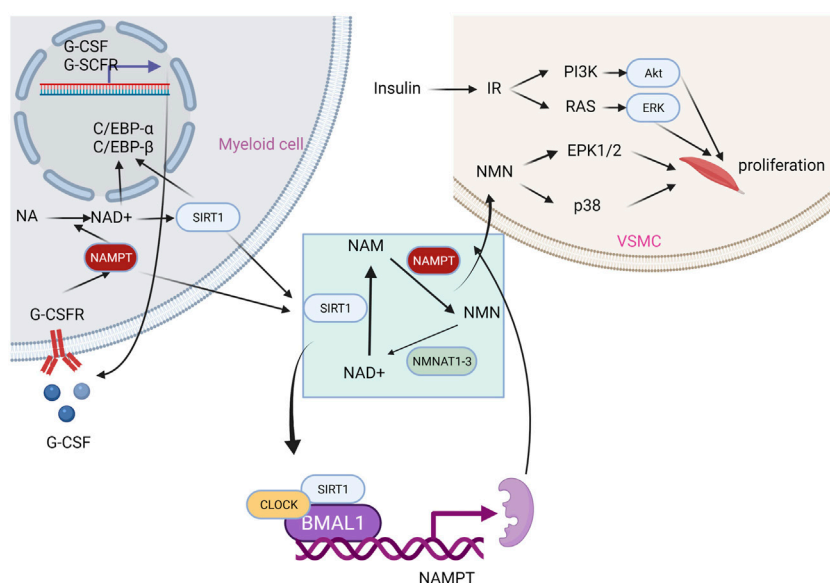


FIGURE 3

Effects of NAMPT on different physiological activities.

promotes inflammation in macrophages by elevating MMP production and activity; the treatment of extracellular NAMPT is dependent on MAPK signaling and induces cytokine production, monocyte chemo-taxis in human PBMCs (Moschen et al., 2007; Fan et al., 2011). In myelopoiesis, extracellular NAMPT induces granulocyte differentiation of CD34<sup>+</sup> hematopoietic progenitors by activating sirtuin and upregulating G-CSF and G-CSF receptors (Skokowa et al., 2009). Finally, there is ample evidence supporting the existence of crosstalk between the extracellular NAMPT signaling pathway and the insulin signaling pathway (Fukuhara et al., 2007).

## 4 Relationship with cancer

### 4.1 Crosstalk between Nicotinamide phosphoribosyltransferase and oncogenic signaling pathways

In a number of cancer models, crosstalk between oncogenic signaling pathways and NAMPT has been documented. Some oncogenic factors have been shown to control NAMPT expression and activity, such as the oncogenic transcription factor EWS-FLI1 in Ewing's sarcoma and the tumor suppressors FOXO1 (negatively controlling expression of NAMPT) as well as AKT (positively controlling NAMPT expression) in breast cancer (Mutz et al., 2017; Jeong et al., 2019). NAMPT can

control the activation of oncogenic signaling pathways in various circumstances. For instance, extracellular NAMPT (eNAMPT) released from melanoma cells and the overexpression of NAMPT in breast cancer cells have both been linked to the activation of AKT (Grolla et al., 2015; Ge et al., 2019). Additionally, it has been discovered that exogenous eNAMPT increases the proliferation of breast cancer cells by causing the activation of AKT and ERK1/2, which can be treated with AKT and ERK1/2 inhibitors (Gholinejad et al., 2017). In multiple cancer models, NAMPT inhibition was observed to decrease phosphorylation of ERK1/2, and NAMPT inhibitors and ERK1/2 blockers together increased cell death (Cea et al., 2012; Okumura et al., 2012; Zhang et al., 2012). Numerous cancers have been linked to the interaction between mTOR and NAMPT. NAMPT inhibition resulted in the elimination of mTOR activation, and an increase in AMPK $\alpha$  activation in hepatocellular carcinoma cells (Schuster et al., 2015). Pancreatic ductal adenocarcinoma cells, leukemic cells, and pancreatic neuroendocrine tumor cells all displayed comparable effects, and in both subtypes of pancreatic cancer, concurrent treatment with mTOR inhibitors enhanced the antiproliferative effects of NAMPT inhibition (Zucal et al., 2015; Mpilla et al., 2019). NAMPT inhibition has also been linked in multiple myeloma models to a decrease in mTOR activation, which is assumed to be a factor in autophagic death. The alterations in NAMPT expression that take place with the emergence of resistance to targeted therapy have been the subject of numerous



studies. BRAF inhibitor-resistant melanoma cells expressed more iNAMPT and eNAMPT than sensitive cells in both experimental models and clinical samples (Audrito et al., 2018a). Notably, the addition of NAMPT inhibitors can overcome resistance to BRAF inhibitors (Audrito et al., 2018b). Furthermore, inhibition of BRAF in susceptible cells results in downregulation of NAMPT transcription, whereas increase of NAMPT expression makes melanoma cells resistant to BRAF inhibitors (Ohanna et al., 2018). Based on data supporting the existence of crosstalk between NAMPT and oncogenic signaling pathways, co-targeting NAMPT with other signaling pathway molecules, such as ibrutinib, a BTK inhibitor for macroglobulinemic cells, may be a promising therapeutic strategy (Cea et al., 2016).

## 4.2 Nicotinamide phosphoribosyltransferase regulation of tumors

The expression and activity of NAMPT in malignancies are closely regulated by a number of transcriptional and post-transcriptional processes. Chowdhry and others described an NAMPT enhancer that regulates the expression and activity of NAMPT and is situated 65 kb upstream of the NAMPT transcriptional start site. Chromatin immunoprecipitation and additional research revealed that this H3K27 acetylated NAMPT enhancer binds to the transcription factors MAX and c-MYC, which control its activity, and performs substantially better exclusively in cancer cells that are dependent on the salvage pathway. An earlier work reported a c-MYC-NAMPT-SIRT1 positive feedback loop where c-MYC interacts with the NAMPT promoter and stimulates the expression of NAMPT, which in turn causes SIRT1 activation by increasing the supply of NAD. This is consistent with the involvement of c-MYC in NAMPT expression. By reducing p53 activity and blocking c-MYC-induced apoptosis, SIRT1 stabilizes c-MYC, increases its transcriptional activity, and stimulates cancer (Menssen et al., 2012). Inhibiting this loop, which is active in colorectal cancer, is thought to be a promising treatment approach (Brandl et al., 2018; Brandl et al., 2019). Another protein that is said to control the expression of NAMPT via several enhancer elements is the protein high mobility group A (HMGA1). It was shown that the HMGA1-NAMPT-NAD signaling axis drives a pro-inflammatory senescence-associated secretory phenotype (SASP) through enhancement of the activity of NF- $\kappa$ B, which is mediated by NAD, therefore encouraging an inflammatory environment and accelerating tumor growth (Nacarelli et al., 2019).

In fact, the overexpression of HMGA proteins in many cancer types is often associated with poor prognoses (Sumter et al., 2016). Contrarily, the tumor suppressor and

transcription factor Foxo1 binds to the NAMPT gene's 5' flanking region and reduces the expression of NAMPT in breast cancer cells, an action that is counteracted by the insulin-PI3K-AKT signaling pathway. In addition, expression of NAMPT in triple-negative breast cancer (TNBC) is epigenetically regulated by a new promoter-associated Lnc-RNA, NAMPT-AS "RP11-22N19.2". At both transcriptional and post-transcriptional stages, NAMPT-AS stimulates expression of NAMPT, which drives the tumor development process and enhances the aggressiveness of TNBC (Zhang et al., 2019). Another long-stranded non-coding RNA, gastric cancer-associated transcript 3 (GACAT3), promotes the development of gliomas by functioning as a molecular sponge for miR-135a, blocking its interaction with NAMPT, and controlling NAMPT production (Wang et al., 2019). According to various studies, microRNAs control NAMPT expression at the post-transcriptional level. Specifically, NAMPT mRNA is the target of miR-26b in colorectal cancer, miR-23b in melanoma, miR-381, miR-206, miR-494 and miR-154 in breast cancer cells, and miR-206 in pancreatic cancer (Bolandghamat Pour et al., 2019a; Bolandghamat Pour et al., 2019b; Ghorbanhosseini et al., 2019; Lv et al., 2020). In general, increased expression of these microRNAs can inhibit NAMPT expression and is associated with a decrease in cancer cell viability, suggesting that these microRNAs may have potential as anticancer drugs. From this discovery we know that the activity of NAMPT enzymes can be controlled by other enzymes in addition to being regulated at the gene level. Some research reported that SIRT6 specifically boosts NAMPT's enzymatic activity through direct protein deacetylation to shield cancer cells from oxidative stress (Sociali et al., 2019). Similar to this, a prior study discovered that SIRT1 deacetylates NAMPT, making it easy for adipocytes to secrete (Yoon et al., 2015). Through the transcription factor C/EBP- $\beta$ , mesenchymal glioblastoma stem cells selectively increase the expression of NAMPT and NNMT and interact with their gene regulatory areas. Notably, in these cell subtypes, NNMT downregulated DNA methyltransferase expression in a methionine-dependent way and generated a DNA hypomethylation condition (Jung et al., 2017).

## 4.3 Current clinical development status and observations

Following encouraging findings in preclinical research, the therapeutic safety and efficacy of NAMPTs have been assessed in people with cancer. There are ten NAMPT inhibitor trials registered on [clinicaltrials.gov](https://clinicaltrials.gov) as of January 2022 (Hjarnaa et al., 1999; Jonsson et al., 2000; Ekelund et al., 2001). The first human NAMPT inhibitor trial (NCT00003979) began in



TABLE 1 Clinical trials on NAMPT inhibitors (updated to January 2022).

Drug	Phase	Conditions	Status	Nut identifier	Outcome measures	Display of results on ClinicalTrials.gov
GMX1777	I	Solid Tumors and Lymphomas	Withdrawn	NCT00457574		No Results Posted
GMX1777+, Temozolomide	III	Metastatic Melanoma	Terminated	NCT00724841	<p>Primary Outcome Measures: Determine the recommended Phase II dose of GMX1777 in combination with temozolomide [ Time Frame: 2 years ] Learn more about the side effects of taking GMX1777 in combination with temozolomide [ Time Frame: Within the first 4 weeks ] Determine the disease response to treatment with GMX1777 in combination with temozolomide [ Time Frame: Within the first 8 weeks ]</p> <p>Secondary Outcome Measures: Learn more about how the body processes GMX1777 [ Time Frame: Within the first 30 days ]</p>	No Results Posted
CHS828	I	Unspecified Adult Solid Tumor, Protocol Specific	Withdrawn	NCT00003979		No Results Posted
APO866	I II	B-cell Chronic Lymphocytic Leukemia	Completed	NCT00435084	<p>Primary Outcome Measures: Safety and tolerability of APO866 in patients with refractory B-CLL not amenable to allogeneic HSCT [ Time Frame: 1 month]</p> <p>Secondary Outcome Measures: To determine the effect on the number of circulating leukemic after treatment as compared to baseline [Time Frame: 1 month]. To determine the effect on the number of CD38<sup>+</sup> after treatment as compared to baseline [Time Frame: 1 month]</p> <p>Correlative analysis on <i>in vivo</i> and <i>in vitro</i> sensitivity of leukemic cells, CD38 expression of leukemic cells and clinical outcome, immunophenotype and clinical outcome [Time Frame: 1 month]</p>	
APO866	II	Melanoma	Completed	NCT00432107	<p>Primary Outcome Measures: To determine the tumor response rate (according to Response Evaluation Criteria in Solid Tumors (RECIST) criteria) as the proportion of eligible patients with stage IV cutaneous melanoma or stage III not amenable to surgery. [Time Frame: Week 16]</p> <p>Secondary Outcome Measures: Safety and tolerability [Time Frame: Week 16 and 12 months follow-up]</p> <p>Time to response [Time Frame: Week 16]</p> <p>Duration of response [Time Frame: Week 16]</p> <p>Progression free survival [Time Frame: 12 months]</p> <p>Overall survival [Time Frame: 12 months]</p> <p>Evolution of serum VEGF and interleukin-8 (IL-8) during treatment [Time Frame: Week 16]</p>	No Results Posted
APO866	II	Cutaneous T-cell Lymphoma	Completed	NCT00431912	<p>Primary Outcome Measures: The proportion of eligible patients with refractory or relapsed CTCL whom have a complete response or partial response on cutaneous lesions (Tumor Burden Index) and extra-cutaneous disease. [Time Frame: Week 16]</p>	No Results Posted

(Continued on following page)

TABLE 1 (Continued) Clinical trials on NAMPT inhibitors (updated to January 2022).

Drug	Phase	Conditions	Status	Nut identifier	Outcome measures	Display of results on ClinicalTrials.gov
					Secondary Outcome Measures: Safety and tolerability, time to response, duration of overall response, duration of stable disease and time to treatment failure. [Time Frame: Week 16]	
KPT-9274	I	Acute Myeloid Leukemia Acute Myeloid Leukemia, in Relapse Acute Myeloid Leukemia Refractory	Recruiting	NCT04914845		No Results Posted
KPT-9274	I	Solid Tumors NHL	Terminated	NCT02702492	Primary Outcome Measures: Maximum tolerated dose (MTD) for KPT-9274 administered alone and with co-administration of niacin ER (extended release) (vitamin B3/nicotinic acid) [Time Frame: Approximately 4 weeks]	No Results Posted
KPT-9274&Niacin					Parts A and B: MTD will be based on the assessment of dose limiting toxicities (DLTs) during the first cycle of therapy and will be defined as the highest dose at which ≤1 participant out of 6 (or 0 out of 3) experiences DLTs within Cycle 1	
ER					Maximum tolerated dose (MTD) for KPT-9274 co-administered with nivolumab [Time Frame: Approximately 4 weeks]	
KPT-9274 + Nivolumab					Part C: MTD will be based on the assessment of dose limiting toxicities (DLTs) during the first cycle of therapy and will be defined as the highest dose at which ≤1 participant out of 6 (or 0 out of 3) experiences DLTs within Cycle 1	
ATG-019	I	Solid Tumor	Recruiting	NCT04281420		No Results Posted
ATG-019 + Niacin ER		Non-Hodgkin's Lymphoma				
OT-82 Dose Escalation	I	Lymphoma	Recruiting	NCT03921879		No Results Posted
OT-82 Dose Expansion		Lymphoma, Non-Hodgkin Lymphoma, B-Cell (and 4 more)				

1999 but was halted in 2012 due to serious side effects and poor clinical outcomes. Among the initial NAMPTis trials were phase I studies using CHS828, which is an NAMPT inhibitor which was developed in the early years of research on such compounds for solid tumors. They established the required dose of CHS828, but nevertheless, future trials were not recommended due to illness progression and major side events experienced by the participants in the study (Hovstadius et al., 2002a; Ravaud et al., 2005; Von Heideman et al., 2010). A clinical trial in Phase II for cutaneous T-cell lymphoma utilizing the NAMPT inhibitor FK866 was halted due to the failure to establish remission and the occurrence of substantial side effects (Goldinger et al., 2016). These poor outcomes were attributed to target off tumour toxicity as well as cellular uptake of NAD sources,

including nicotinic acid riboside, vitamin B3, and tryptophan (Table 1) (Grozio et al., 2013). More details are provided in the NAMPT Inhibitors section.

### 5 Nicotinamide phosphoribosyltransferase inhibitors

Using NAMPT as the target for oncology drugs, compounds with better inhibitory effects such as FK866, CHS828, GEN617, OT-82 and other cytotoxic compounds have been developed over the years. The development of NAMPT inhibitors with better therapeutic efficacy and dosing strategies will continue to be explored. This review will summarize the current research already conducted on NAMPT inhibitors, focusing upon

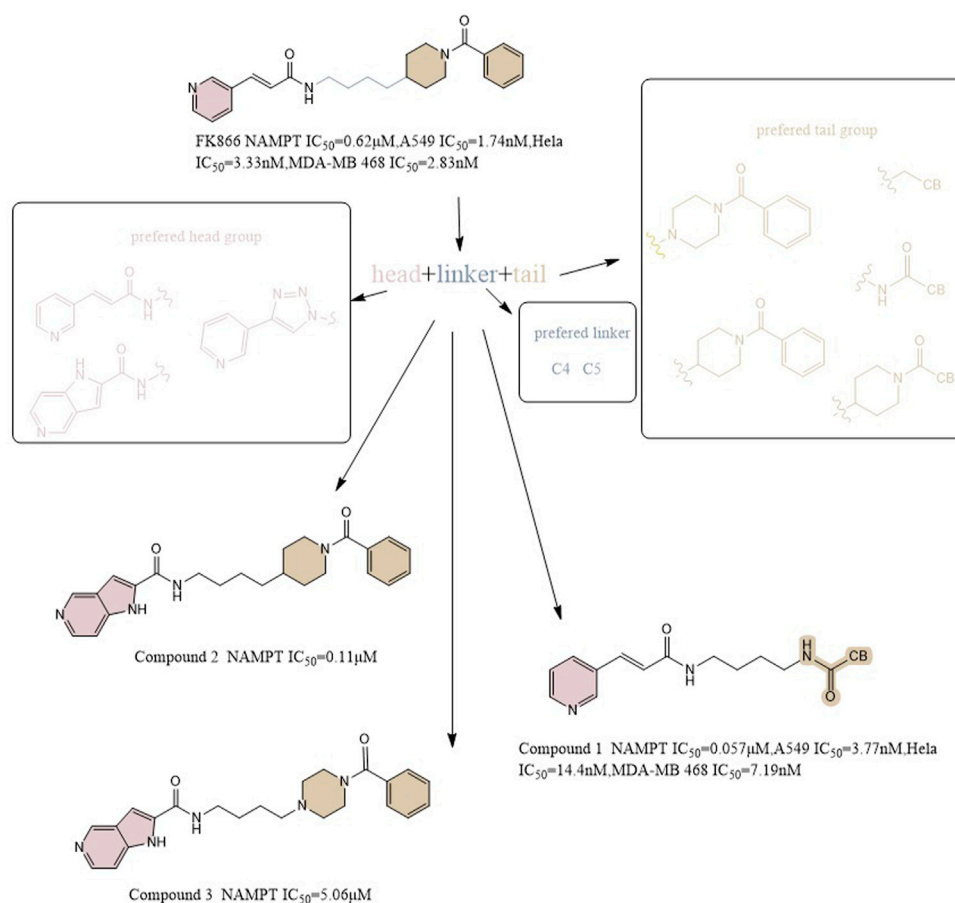


**FIGURE 4**  
Structural optimization of NAMPT inhibitors based on FK866 as a prototype.

specific inhibitors, drug combinations, dual inhibitors and NAMPTi-ADCs.

## 5.1 Specific inhibitors

### 5.1.1 FK866

Max Hasmann and Isabel Schemainda identified in 2002 a novel class of compounds with a characteristic induction of delayed cell death by high-throughput screening, by which (E)-N-[4-(1-benzoylpiperidin-4-yl) butyl]-3-(pyridin-3-yl) acrylamide (FK866) became the first reported NAMPT inhibitor, which could be a candidate anticancer drug with an  $IC_{50}$  of about 1 nM and which indirectly suppresses mitochondrial respiratory activity, but selectively inhibits NAPRT, causing gradual NAD depletion (Hasmann and Schemainda, 2003a). NAMPT is a homodimer with two unique tunnel-shaped cavities adjacent to each active site. Crystallographic studies of the complex of FK866 and

NAMPT revealed that FK866 binds to the tunnel cavity of NAMPT. The researchers divided the structural components of this family of NAMPT inhibitors into head (an aromatic moiety similar to pyridine), linker (a tunnel-interacting moiety), and tail components (a solvent-exposed group) based on the structure of FK866 (Figure 4) (Asawa et al., 2019). Subsequently, Sei-ichi Tanuma et al. performed substitutions for the head and tail groups and finally found that the head group with pyridinylacrylamide, the intermediate linker with a 4-carbon chain, and the tail group with p-carborane induced the best inhibitory activity, which was 10 times greater than that of FK866 ( $IC_{50}$  ~1 nM). The hydrogen bonding interactions between carborane amide and His191 can be used to explain these findings (Figure 2A) (Asawa et al., 2019; Tanuma et al., 2020).

### 5.1.2 CHS828 and GMX1777

CHS828, a pyridinyl cyanoguanidine anticancer drug which was developed by Leo PharmaAS, whose chemical structure can

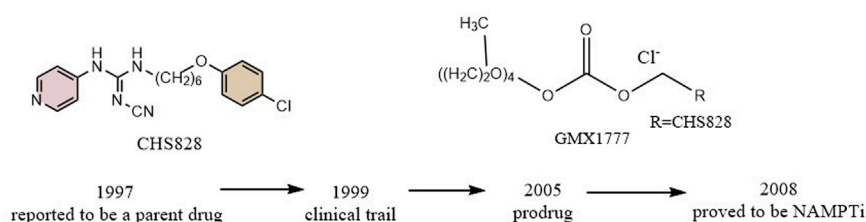


FIGURE 5

Discovery and research history of the NAMPT inhibitor CHS828.

also be divided into a head group, a linker and a tail group. It was reported upon by Schou and his colleagues in 1997. It showed strong anticancer activity in lung and breast cancer cell lines. In experiments with nude mice, treatment with CHS828 led to the regression of human lung and breast cancer tumors (Schou et al., 1997; Hjarnaa et al., 1999). CHS828 was examined in a clinical trial in 1999 (Hovstadius et al., 2002b), but it wasn't until 2008 that Olesen's research demonstrated that the compound can block NAMPT and kill cancer cells primarily by way of depleting NAD (Olesen et al., 2008). While attempting to address the solubility and pharmacokinetic issues which had been noted in the early clinical trials for CHS828, Ernst et al. created a number of prodrugs during this time that had improved properties. The best of these compounds was GMX1777, whose tetraethylene glycol portion was attached to the parent drug via a carbonate bond (Figure 5). Its solubility allows it to be rapidly released *in vivo* through intravenous injection. It exerts very strong inhibitory activity *in vivo* when used in combination with a cytostatic agent etoposide (Binderup et al., 2005). Crystallographic analysis revealed that CHS828, like FK866, exerts its activity by binding to the NAMPT tunneling cavity (Figure 2C).

### 5.1.3 GEN617 and LSN3154567

Through structure-guided design and the use of significant data from the eutectic structure of (thio) urea, Zheng et al. found a structurally unique NAMPT inhibitor which contains amide. Further optimization led to GEN617 ( $IC_{50} < 10$  nM vs. MiaPaCa2, PC3, HT1080, U251, and HCT116 lines), which has good *in vitro* and *in vivo* ADME qualities and single-digit nanomolar cellular semi-inhibitory doses against a number of human cancer cell lines, guided by the crystal structure of compound4 (NAMPT  $IC_{50} = 9$  nM and A2780  $IC_{50} = 10$  nM) with NAMPT complexes. In crystallographic analysis, Asp219 and the amide NH were observed to form a hydrogen link, and Ser275 and the amide carbon were seen to form a water-mediated hydrogen bond. In the NAM binding area,

GEN617's bicyclic imidazolopyridine ring is stacked between Tyr18 and Phe193 of the NAMPT residues, and the imidazole nitrogen points to the PRPP binding site (Figure 2B) (Zheng et al., 2013). However, GEN617 carries the risk of serious side effects, such as retina damage. NAMPT inhibitors' capacity to traverse the blood-retinal barrier is diminished by altering their polarity and permeability, which lowers the retina's exposure to the drugs. Using these findings for as a basis for further research, Genshi Zhao discovered a unique NAMPT inhibitor, LSN3154567 ( $IC_{50} = 3.1$  nM), which changed the ring of the tail group part to a hydrocarbon group, and did not cause retinal lesions in rats (Figure 6). The examined dogs' retinal and hematologic toxicity was fully removed by co-administrating NA without any appreciable reductions in effectiveness (Zhao et al., 2017).

### 5.1.4 A1293201

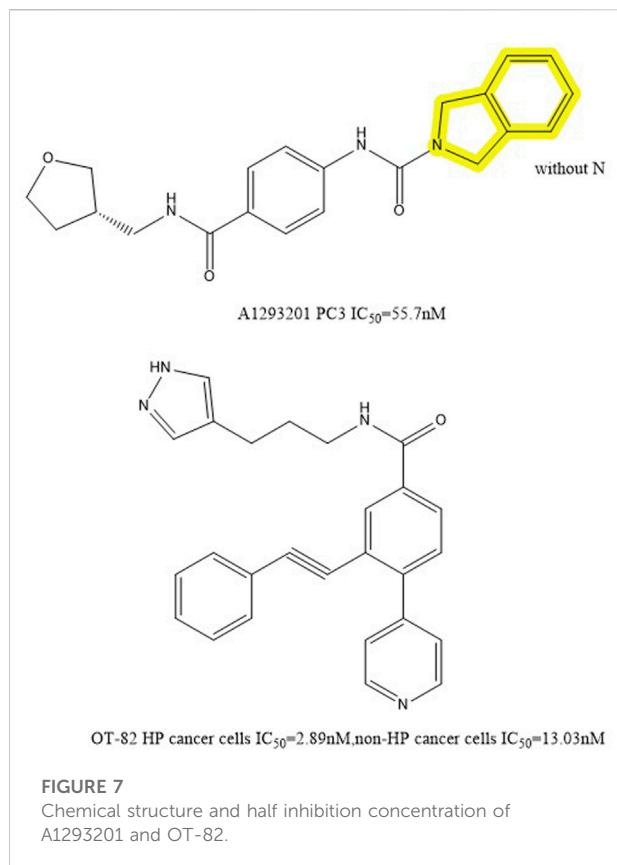
Through high-throughput cell screening and target identification, Julie et al. identified a series of novel non-substrate NAMPT inhibitors with robust preclinical efficacy and pharmacokinetic properties for oral administration. The candidate molecule in this series, A1293201 (PC3  $IC_{50} = 55.7$  nM), contains a heteroenopeptide "headgroup" that does not have the aromatic nitrogen of nicotinamide and nicotinamide-like compounds compared to previously identified inhibitors, such as FK866, GMX1777 and GNE617 (Figure 7). Crystallographic studies have shown that similar to FK866 and nicotinamide, A1293201 binds to the nicotinamide site and engages in crucial pi-stacking interactions with tyrosine 18; the central region of the compound passes through a narrow lipophilic tunnel to reach the distal opening of the active site (Figure 2D) (Wilsbacher et al., 2017).

According to Julie et al., the conventional wisdom that this property is necessary for cellular efficiency is challenged by powerful and selective NAMPT inhibitors like A1293201 which lack aromatic nitrogen in the nicotinamide moiety. Despite the lack of phosphorylation



The new NAMPT inhibitor OT-82 was created by OncoTaris and began Phase I clinical trials in 2019. A high-throughput cell-based screen of a chemical library of over 200,000 small





molecules led to the discovery of this lead compound, which was then validated and structurally improved (Figure 7). It inhibits NAMPT through NAD and ATP depletion and induces apoptotic cell death. It demonstrates higher action against hematopoietic malignancies ( $IC_{50} = 2.89 \pm 0.47$  nM) than against non-hematopoietic tumors ( $13.03 \pm 2.94$  nM) (Wilsbacher et al., 2017). OT-82 did not exhibit the same neurological, cardiac, or retinal toxicity as other NAMPTis in toxicological investigations in mice and non-human primates. The principal targets of OT-82 for dose-limiting toxicity in both species were found to be the lymphoid and hematopoietic organs.

## 5.2 Drug combinations

Although specific inhibitors have shown good cytotoxicity and targeting *in vivo* and *in vitro* experiments, they often face problems such as large toxic side effects in clinical trials, including the aforementioned neurological, cardiac and retinal toxicity. Additionally, single-target inhibitors become less effective over time with the development of drug resistance. Moreover, cancer is a multifactorial disease, so the application of only a single specific inhibitor has some inherent limitations. Although there is no clear literature or clinical data that the application of combinations of drugs carries a lower risk of toxic side effects than using a single specific inhibitor, it has been

documented that this strategy does have the potential to exert synergistic effects, enhance therapeutic effects, as well as delay and reduce the development of drug resistance (Figure 8).

### 5.2.1 PARPi + NAMPTi

Combinatorial drug matrix screening is an efficient method of identifying new therapies which show synergistic potential *in vitro*. Christine et al. performed drug combination screening for Ewing's sarcoma and identified several potentially effective combinations of drugs, including PARPis and NAMPTis (Heske et al., 2017). Using a multi-omics approach, this study also found that the apoptotic phenotypes and DNA damage which resulted from the combination were associated with NAD<sup>+</sup> and NMN loss, strengthened PARP suppression, and persistent activation of cellular stress pathways (Figure 9).

Currently there is an abundance of preclinical evidence which supports the theory that Ewing's sarcoma gene fusions depend on PARP1 activity and that tumor cell lines harboring these fusions are extremely vulnerable to PARP blocking (Brenner et al., 2012). Unfortunately, a xenograft model of Ewing's sarcoma cannot duplicate the single-agent efficacy of PARP inhibitors (Ordóñez et al., 2015; Smith et al., 2015). The addition of NAMPTis to PARPis is a potential combination therapy which would theoretically enable use of lower PARP inhibitors dosages by further reducing PARP activity, which may simultaneously make the therapy both more clinically effective and less toxic. Because the known toxicity profiles of both inhibitors seem to differ from one another, this kind of combination may be more tolerable for patients. In addition to Ewing's sarcoma, triple-negative breast cancer xenograft models have demonstrated that the combined inhibition of PARP and NAMPT slows tumor growth to some extent. Even in cases in which treatment has been delayed until the tumor becomes very large, this combined treatment still often results in tumor regression (Bajrami et al., 2012).

The study by Christine et al. may provide a new and complementary account of the mechanisms of this type of drug combination: the stress-activated protein kinases p38 MAPK and SAPK/JNK were co-activated by NAMPT and PARP inhibition, and PAR activity was considerably decreased both *in vitro* and *in vivo* following NAMPT and PARP inhibition (Heske et al., 2017).

### 5.2.2 NAMPTi + NAPRTi

Departing slightly from the previous combination, we might also consider another important pathway of NAD<sup>+</sup> production in order to identify and eliminate more NAMPT inhibitor resistance mechanisms. For this purpose we may shift our focus to another important target, nicotinic acid phosphoribosyltransferase (NAPRT). This is a second enzyme which produces NAD<sup>+</sup> and mediates the nicotinic

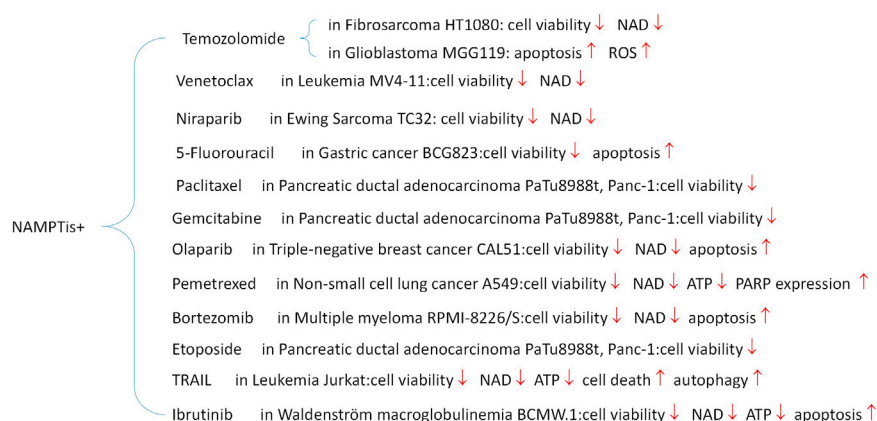


FIGURE 8

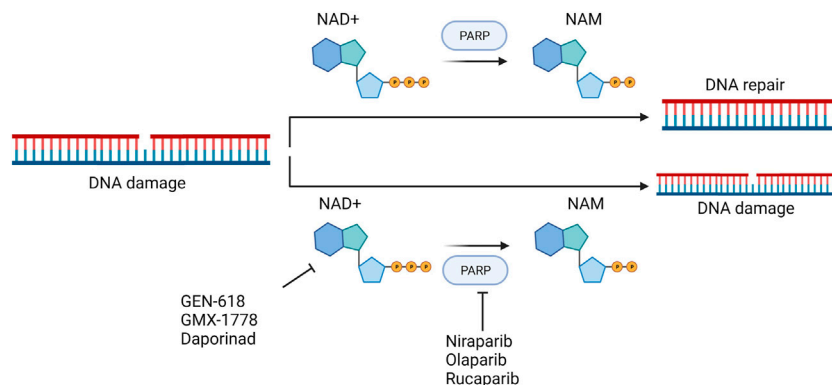
Performance of drug combination *in vitro*.

FIGURE 9

Theoretical basis of simultaneous targeting of PARP and NAMPT in tumor therapy.

acid (NA) to NAD<sup>+</sup> conversion. In a number of prevalent malignancies, the gene encoding is amplified and overexpressed, including ovarian cancer, where NAPRT expression correlates with the BRCAness gene expression profile.

Hara and his coworkers demonstrated that NAPRT is required for NA to raise cellular NAD<sup>+</sup> levels in human cells, that NAPRT and NAMPT both do the same for intracellular NAD<sup>+</sup> levels, as well as guard against the toxicity of hydrogen peroxide (Hara et al., 2007). In addition, Francesco's study on NAPRT shows that it plays previously undiscovered yet significant roles, demonstrating that in cancer cells which overexpress NAPRT, the compound also helps to maintain intracellular NAD<sup>+</sup> pools under basal conditions, and that, in a

subpopulation of tumors, NAPRT-dependent NAD<sup>+</sup> biogenesis aids DNA repair processes and tumor cellular metabolism. Francesco and his colleagues performed a series of validation experiments that yielded several intriguing results: 1) Cancer cells overexpressing NAPRT were insensitive to FK866. 2) NAPRT reduced DNA damage in cancer cells and regulated cytoplasmic and mitochondrial NAD<sup>+</sup> levels, oxidative phosphorylation and protein synthesis. 3) In cancer cells that overexpress NAPRT, inhibition of NAPRT by 2-hydroxynicotinic acid reduces OXPHOS and makes them sensitive to FK866. 4) NAPRT inhibition or silencing could lead to sensitization of ovarian cancer xenografts to FK866. These findings strongly suggest that 1) NAPRT genes are amplified and overexpressed in a subset of common cancers; 2) NAPRT plays a role in

cancer cells' (e.g., ovarian and pancreatic cancer cells) energy status, cell growth, metabolism, DNA repair processes, proliferation regulation and protein synthesis; 3) Resistance to NAMPT inhibitors in previously tried clinical trials may be overcome by NAMPT inhibition (Piacente et al., 2017).

### 5.2.3 VB3/other targeted agents + NAMPTi

Early studies on NAMPTi showed that exogenous addition of niacin (vitamin B3) could rescue cellular NAD + depletion and cytotoxicity via the PreissHandler pathway (Watson et al., 2009). This method depends only on the expression of NAMPT1 (Xiao et al., 2013). Because NAMPT1 is expressed in most mammalian tissues, this combination is generally an option for patients with NAMPT1-negative tumors. Combining NAMPTi's with niacin allows it to meet both clinical efficacy and safety requirements. Studies in mice have shown that when niacin is administered in combination with doses of NAMPTi which would otherwise be lethal, it can reduce the occurrence of problems related to mortality and toxicity, such as thrombocytopenia and lymphopenia. Using this tactic, several of the toxicities problems seen in human clinical trials were lessened. Coadministration with nicotinic acid significantly decreased histological evidence of toxicity to spleen, testicular, and lymphoid tissues and reversed damage to less afflicted kidney, liver, and gastrointestinal tissues (O'Brien et al., 2013).

In addition, NAMPTi was found to be effective in the following combinations: with Vorinostat for CLL and acute myeloid leukemia, with TRAIL for t-cell leukemia and CLL, with FX-11 for LDHA-dependent lymphomas, with Bortezomib for multiple myeloma, and with Rituxumab for B-cell lymphoma (Le et al., 2010; Zoppoli et al., 2010; Cea et al., 2011; Cagnetta et al., 2013; Nahimana et al., 2014).

We have found that combined drug therapy is more toxic to tumor cells not only in theory, but also *in vivo* and *in vitro* experiments, and that it can also solve the problem of drug resistance to some extent. However, the pharmacokinetic problems of two drugs in clinical trials are more demanding for modeling and difficult to control in practical applications.

## 5.3 Dual inhibitors

Although the strategy of drug combination solves to some degree the problems of drug resistance and greater toxicities that exist when treating with single drugs, the pharmacokinetic problems derived from the simultaneous use of two drugs are challenging to overcome in clinical practice. We want to take advantage of the efficacy of drug combinations and solve pharmacokinetic problems. Synthesizing hybrid molecules that can display two different balanced mechanisms of action, i.e., a dual

inhibitor, is a desirable strategy that can be adopted in drug development. Drugs with polypharmacological activities have now been shown to be more beneficial than combination therapy because they often have fewer severe side effects and provide doctors with a more flexible treatment approach.

### 5.3.1 PAK4-Nicotinamide phosphoribosyltransferase dual inhibition

A known  $\beta$ -catenin protein regulator, p21-activated kinase 4 (PAK4), a RhoGTPase (CDC42) effector, has been proven to control WNT signaling. In the cytoplasm, p21-activated kinase four phosphorylates  $\beta$ -catenin on Ser675, preventing its degradation and boosting its transcriptional activity. The changed cell polarity observed in several malignancies is caused by p21-activated kinase 4, which co-localizes with  $\beta$ -catenin at the cell membrane in the cell junctional region, phosphorylating it. Downstream effects of PAK4 inhibition include a reduction in G2-M transition, and downregulation of nuclear  $\beta$ -catenin, c-MYC and CyclinD1. In addition, inhibition of NAMPT resulted in significant depletion of NAD and downregulation of SIRT1 activity.

Based on preclinical evidence, it has been determined that combined inhibition of NAMPT and PAK4 may be a successful anticancer tactic. A broad-spectrum PAK inhibitor called PF-3758309 blocks both class A PAKs (PAKs 1, 2, and 3) and class B PAKs (PAKs 4,5,6) (Murray et al., 2010). It was discovered that FK866 is a very effective inhibitor of NAMPT (Hasmann and Schemainda, 2003b). Despite strong preclinical data for both compounds, both inhibitors were discontinued due to a lack of objective responses in phase I studies. In preclinical studies, the dual PAK4-NAMPT inhibitor KPT-9274 (NAMPT  $IC_{50}$  ~0.12  $\mu$ M, Caki-1 cells  $IC_{50}$  = 0.6  $\mu$ M, 786-O  $IC_{50}$  = 0.57  $\mu$ M) exhibited strong effectiveness against a variety of solid tumors and hematologic malignancies in both *in vivo* and *in vitro* settings (Figure 10) (Abu Aboud et al., 2016; Jiang et al., 2016; Aboukameel et al., 2017; Fulciniti et al., 2017; Rane et al., 2017). KPT-9274 has minimal cytotoxicity to normal primary kidney cells and when used in mice no significant weight loss was observed. The only known drug that targets both NAMPT and PAK4 is KPT-9274, which is the subject of NCT02702492 listed in Table 1. In this clinical trial, Gabriel et al. concluded that KPT-9274 could make pancreatic neuroendocrine tumor cells more sensitive to traditional mTOR inhibitors, resulting in better therapeutic outcomes (Mpilla et al., 2021). KPT-9274 has been demonstrated to modulate Wnt/ $\beta$ -linked protein signaling and decrease the growth of multiple tumor cell lines and subcutaneous xenograft models of mantle cell lymphoma. Non-Hodgkin's lymphoma cell lines are efficiently subjected to KPT-9274's dose-dependent induction of apoptosis (Azmi et al., 2017). KPT-9274 was well tolerated in subcutaneous non-Hodgkin's

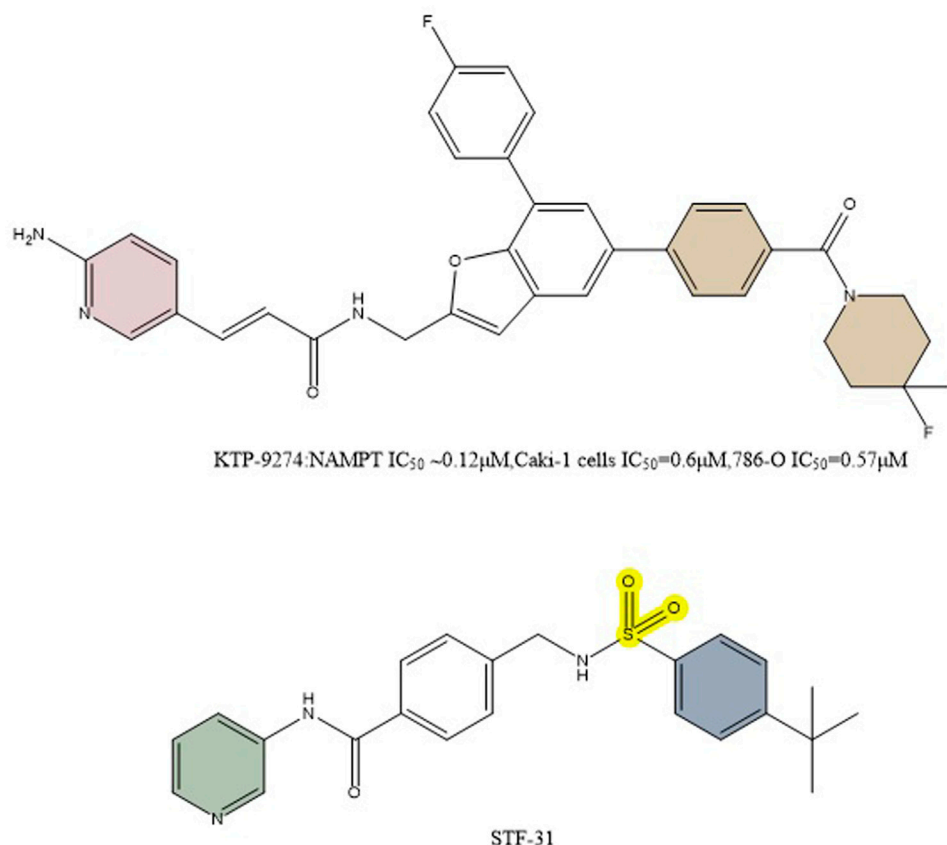


FIGURE 10  
Structure of dual inhibitors KPT-9274 and STF-31.

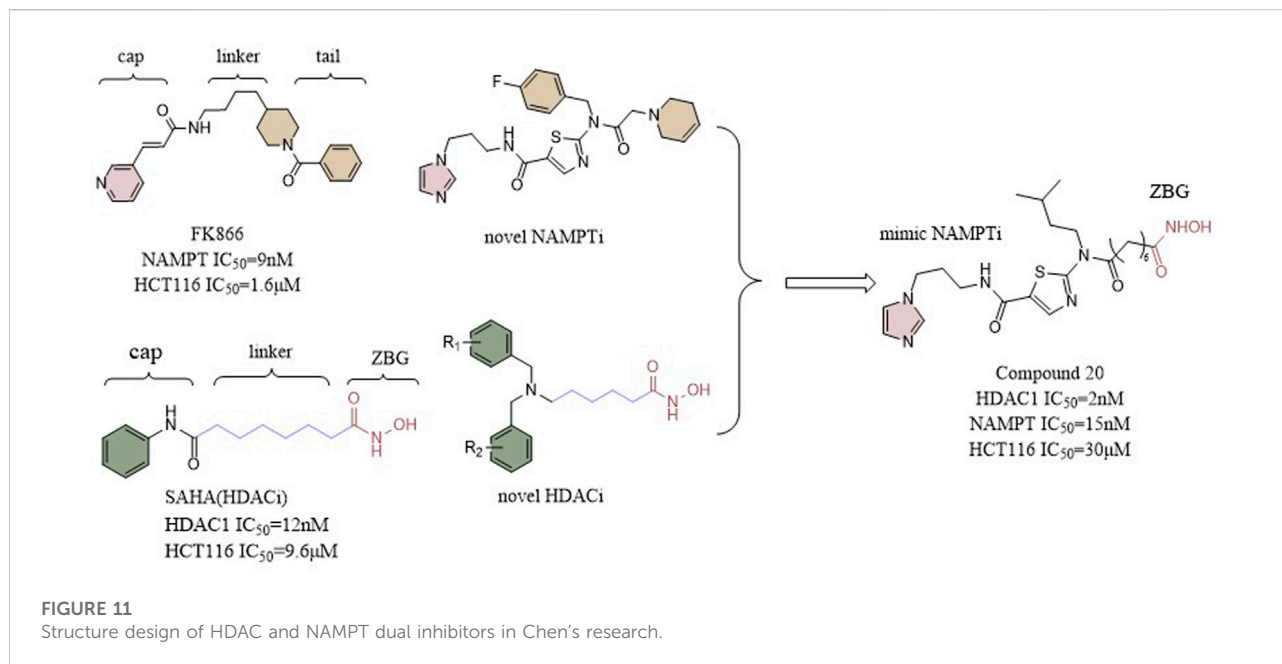
lymphoma xenografts in mice and exhibited significant antitumor activity.

### 5.3.2 GLUT1-Nicotinamide phosphoribosyltransferase dual inhibition

Currently, tumor therapy is thought to be made possible by the transfer of glucose during glycolysis and its metabolism (Porporato et al., 2011). Two distinct transporter molecules, the facilitated glucose transporter (GLUT), which facilitates energy-independent bidirectional transport, and the  $Na^+$ /glucose cotransporter (SGLT), which transports glucose actively, are involved in the uptake of glucose by cells. There are 13 structurally related members of the GLUT family in humans, and GLUT1 is the one that is most frequently expressed in primary tissues and cultured cells (Zhao and Keating, 2007). The predominant subtype of the glucose transporter that is overexpressed in cancer is GLUT1 (Moreno-Sánchez et al., 2007). After ingestion, glucose is metabolized to triphosphate via the glycolytic pathway, following additional oxidation. Trisaccharide-phosphate oxidation via glyceraldehyde 3-phosphate

dehydrogenase reduces  $NAD^+$ , which is needed for this step as an electron acceptor in the glycolytic pathway, to NADH. Without  $NAD^+$  + regeneration, glycolysis cannot be sustained. By converting pyruvate to lactate, which subsequently oxidizes NADH to  $NAD^+$ , which serves as an electron acceptor, this regeneration is accomplished.

STF-31's impact on  $NAD^+$  + metabolism and glucose transport was examined by Kraus et al. in comparison to GLUT inhibitors and NAMPT inhibitors. Unlike other GLUT mono-inhibitors, STF-31 exhibited some tumor suppression even in the low concentration range (below  $5 \mu M$ ), especially for the osteosarcoma MG-63 (Figure 10). Both STF-31 and GLUT inhibitors inhibited glucose uptake in tumor cells. Like the NAMPT monoinhibitors, STF-31 also significantly reduced cell viability. The findings suggest that STF-31 has a dual function and that the inhibitory effect is concentration-dependent, so a number of cancer cells studied appear to be more sensitive to its lethal effects as a given NAMPT inhibitor. Each inhibitory activity may have a different impact depending on the particular cellular setting. Cells with low expression levels of NAMPT may respond



better to the drug's inhibitory impact on NAMPT while cells with high expression levels of GLUT1 may be more sensitive to the drug's inhibitory effect on GLUT1 when they also have low expression levels of other GLUTs (Kraus et al., 2018).

### 5.3.3 HDAC-Nicotinamide phosphoribosyltransferase dual inhibition

The regulation of gene expression is greatly influenced by the post-translational alterations of chromatin histones. Histone acetyltransferases (HATs) and histone deacetylases (HDACs), two of the most extensively researched epigenetic changes, regulate balanced acetylation/deacetylation of lysines in the core histone tails. A regulated equilibrium between histone acetylation and deacetylation appears to be necessary for optimal cell proliferation (Yang and Seto, 2007). Many disorders, including neurodegenerative diseases, inflammatory diseases, and cancer, are thought to be influenced by the dysregulation of histone deacetylases (Oppermann, 2013). For example, in neuroblastoma, elevated expression of HDAC8 is linked to advanced illness and poor chances of survival. (Oehme et al., 2009); In patients with ovarian and gastric cancer, elevated expression levels of HDAC1, 2, and three have been linked to poor prognoses (Weichert et al., 2008a; Weichert et al., 2008b).

It has been demonstrated that NAMPT inhibitors increase the inhibitory effect of HDAC inhibitors, indicating that compounds with dual inhibition abilities may present potent antitumor activity. In a study by Chen et al. a potent inhibitor of NAMPT was bound to a zinc hydroxamic acid binding group via

a 6-carbon alkyl linker creating compound 20 ( $IC_{50} = 2 \text{ nM}$ ), which, in nanomolar range, demonstrated a better inhibitory effect against HDAC-1 than Vorinostat 1 ( $IC_{50} = 12 \text{ nM}$ ). Furthermore, compound 20 exhibited a considerably stronger inhibitory effect on NAMPT in comparison to FK866. *In vitro* anti-proliferative assays showed that compound 20 was no less potent than Vorinostat one and standard FK866 against the colon cancer HCT116 cell line. *In vivo* assays, the anti-tumor activity exhibited by compound 20 (TGI = 42%, T/C = 58%) was also higher than that of SAHA (T/C = 67%, TGI = 33%) and FK866 (T/C = 61%, TGI = 39%) (Figure 11) (Chen et al., 2018).

Dong et al. (2017) then replaced ZBG hydroxymethyl ester with 2-aminobenzamide, and their first designed dual inhibitor was prepared by linking MS0 (NAMPT inhibitor) with Tacedinaline (C994, HDAC inhibitor). Compared to MS0 and Tacedinaline, compound 21 exhibited weaker enzyme inhibition of NAMPT and HDAC1. To achieve balanced activity against both enzymes and improve the enzymatic efficiency, they created additional structural alterations. The HDAC inhibition activity was increased by introducing a 1,2,3-triazole ring in the linkage region, resulting in compound 22 ( $IC_{50} = 1.6 \mu\text{M}$ ), which exhibited better HDAC inhibition activity than Tacedinaline. In addition, compound 22 showed stronger NAMPT inhibitory activity compared to MS0. Compound 22 showed reduced antiproliferative activity against HCT-116 cell line cancer compared to compound 21. The TGI of compound 22 at the same dose (TGI = 69%) was far more higher than that of standard SAHA (TGI = 33%) and FK866 (TGI = 39%). These results make it a potential precursor for further structure-activity-relationship studies with the aim of



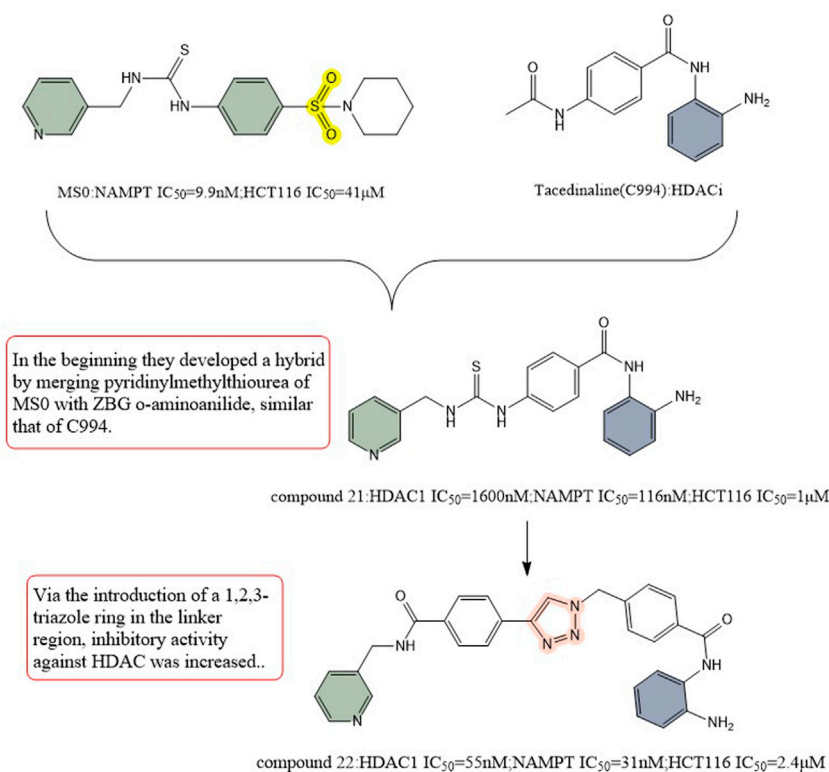


FIGURE 12

Structure design of HDAC and NAMPT dual inhibitors in Dong's research.

introducing more promising HDAC/NAMPT hybrid inhibitors (Figure 12).

#### 5.4 NAMPTi-antibody-drug conjugate

Efficacious medicinal medications are delivered by antibody-drug conjugates (ADC) to the targeted diseased spot while protecting healthy tissue from adverse side effects (Chari, 2016). Because problems related to targeting and dosage toxicity limit the clinical usage of NAMPT inhibitors, such as thrombocytopenia and gastrointestinal effects, targeted delivery to tumor tissues via the ADC pathway may significantly improve the therapeutic index. This method is expected to improve the therapeutic window for NAMPT inhibition.

Alexei et al. carried out a series of structural modifications using compounds 23 and 24 as lead payloads to detect their biological activities (Figure 13) (Palacios et al., 2018). Among them, compound 25 showed better tumor cytotoxicity as a payload (A2780  $IC_{50}$  = 5 nM), which demonstrated greater inhibitory activity against the following cells: NCI-H526 (high expression of c-kit antigen,  $IC_{50}$  = 2 nM), MDA-MB453 (high expression of HER2 antigen,  $IC_{50}$  = 0.4 nM) and NCI-N87 (high expression of HER2 antigen,  $IC_{50}$  = 1 nM). Five different cleavable and noncleavable linkers

were selected to be paired with c-kit, HER2, and IgG antibodies. The experimental results showed that L4 was the better linker. When targeting c-kit and when targeting HER2, data showed a lower  $IC_{50}$  (for the targeting of c-kit, the  $IC_{50}$  in NCI-H526, was 0.04nM; for HER2,  $IC_{50}$  was 0.006 nM in MDA-MB453 and 0.017 nM in NCI-N87) (Karpov et al., 2018). These conjugates showed *in vivo* effectiveness that was target-dependent while being well tolerated.

In another study, Christopher et al. designed the payload by structurally guided modification of the prototype inhibitor FK866 (Figure 14) (Neumann et al., 2018). They installed an amino group to the benzene ring of the tail group portion of FK866 and applied a pyridyl-cyanoguanidine group and a pyridylsquaramide group from the structure of CHS-828 in the head group portion to generate a new toxic payload, which retained cytotoxicity in cells. Among them, compound 26 has a lower  $EC_{50}$  (~5.2 nM for L540cy and ~5.9 nM for HEPG2) and greater cytotoxicity than FK866 (~6.7 nM for L540cy and ~6.8 nM for HEPG2). To increase the molecule's hydrophilicity on the linker side, a glucoside-based linker system was created. For the antibody side, CD19, CD30 and CD123 were chosen as targets for the design. The final result

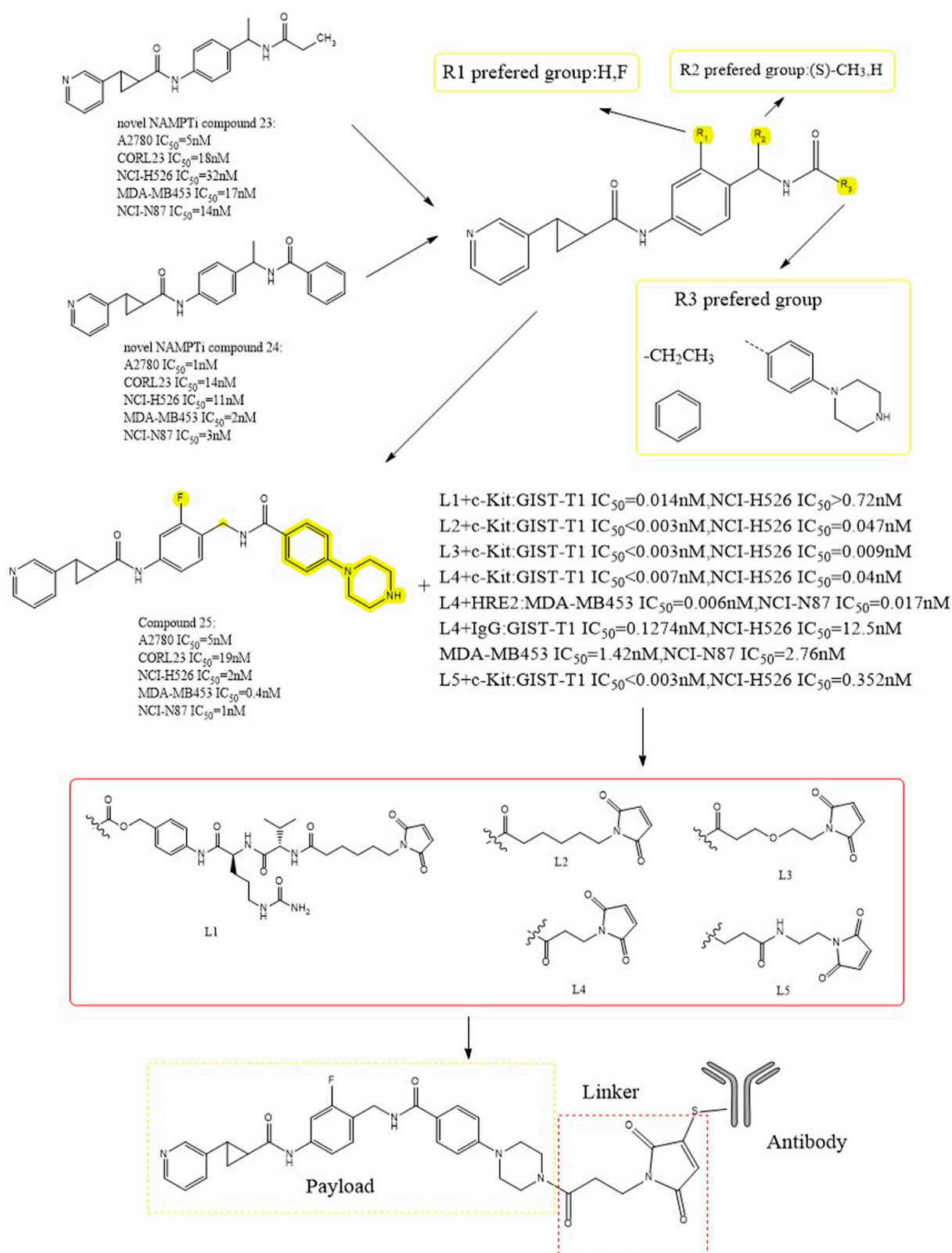
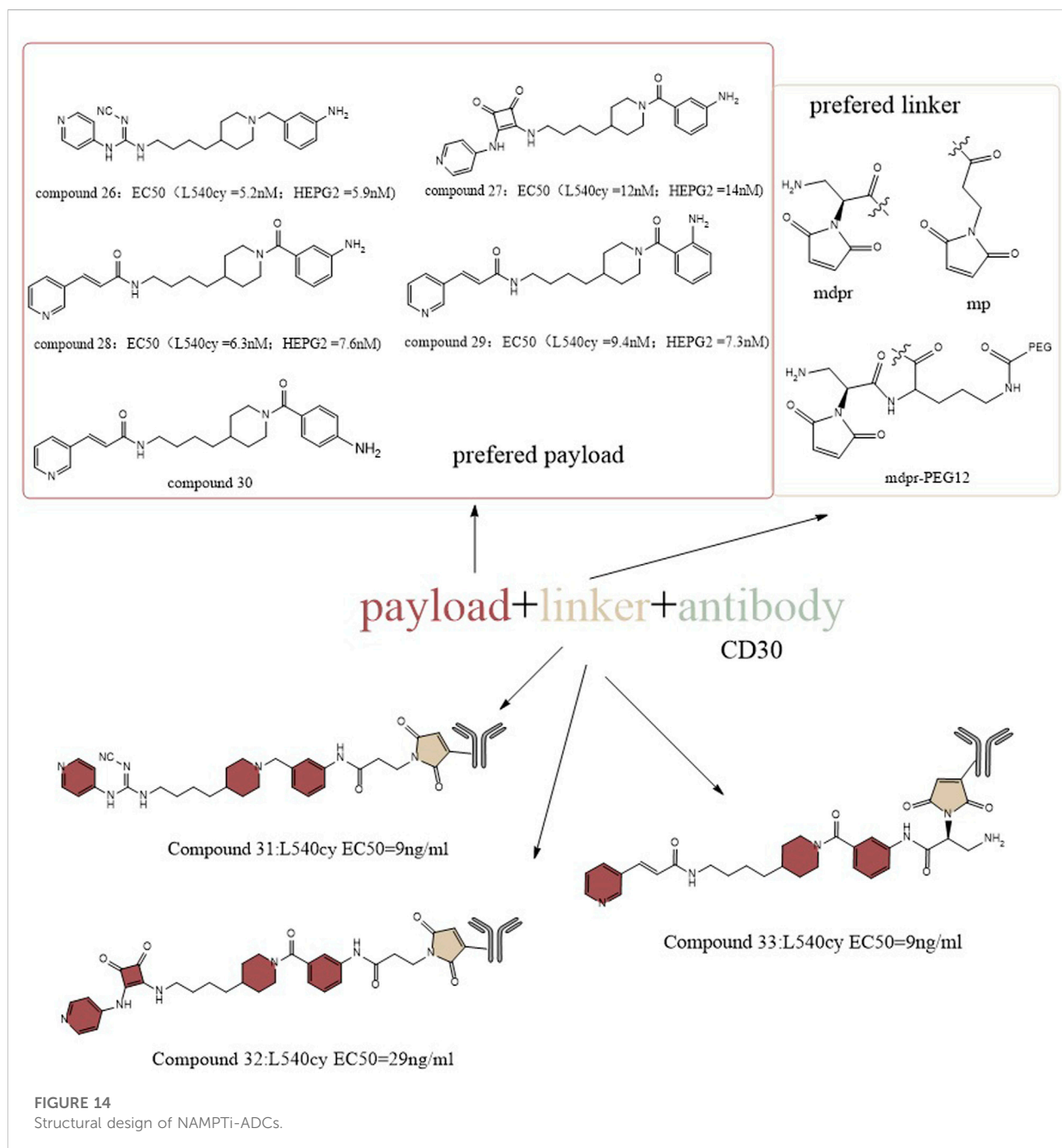


**FIGURE 13**  
 Structural design of NAMPTi-ADCs.



was a payload and a linker which worked together to give ADCs outstanding biophysical characteristics. From the activity point of view, they showed antigen-specific NAD depletion activity *in vitro*. After 96 h of treatment, ATP depletion was weak or absent in some cell lines, likely due to the kinetics of the drug release and internalization of the ADC. To achieve optimal action, rapid and persistent drug exposure could be required. As a result, the long circulation half-life of ADC *in vivo* may provide ongoing drug exposure

to antigen-positive target cells, making ADC administration an ideal method of NAMPT suppression. The *in vivo* anticancer efficacy of this group of ADC have been proven in numerous xenograft models of acute myeloid leukemia, non-Hodgkin's lymphoma (Burkitt lymphoma and follicular lymphoma, CD19 as antigen, 60%–100% of mice with tumor regression), and Hodgkin's lymphoma (CD30 as antigen, 80% of mice with tumor regression when administered at 10 mg/kg) (Neumann et al., 2018).

## 6 Conclusion

Cellular metabolism and signaling are affected by the production of NAD, the utilization of NAD as an ADPR donor, and the maintenance of NADPH homeostasis. Therefore, it is not surprising that activity within these pathways is frequently greater in patients with cancer. NAD-producing enzyme presents a set of targets that can be used to combat the proliferation of cancer. The salvage pathway is the main source of human NAD and is dependent on NAMPT, the rate-limiting enzyme in this cyclic pathway. Small alterations to its bio-activity can have a big impact on NAD-dependent cellular processes and NAD metabolism. Of the three NAD-producing pathways, it is currently the only one through which effective cancer therapy can be administered. Beginning with the study of CHS828 in 1997, we have seen many creative monomeric NAMPT inhibitors, such as GMX1777, CHS828, OT-82, and more. Lead compounds for small molecule NAMPT inhibitors are often obtained by fragment-based screening, virtual screening, and high-throughput screening. Even though NAMPT is the most frequently employed NAD-producing enzyme in chemical inhibitor applications, the low therapeutic efficacy and high toxicity of NAMPT inhibitors in clinical trials have slowed down the development of new such drugs. Cancer is a multifactorial disease, so manipulation of only a single target may fail to produce the desired therapeutic outcomes. Therefore, increasing the clinical availability of NAMPT inhibitors requires more drug designs and innovative drug delivery strategies. Drug combinations can, to some extent, reduce drug toxicity and side effects, exploit drug synergy and enhance therapeutic effects, as well as delay and reduce the development of drug resistance, but there are inherent pharmacokinetic problems when using two different drugs simultaneously that must be overcome. Therefore, using a single drug that influences two or more targets may be a more effective strategy. Currently, combination therapies have been shown to be more beneficial than drugs that exhibit polypharmacological activity because they have lower side effects and allow for more flexible treatment approaches. Dual-target-single-drug strategies have become a popular approach to cancer treatment, and more and more dual-target drugs which can target NAMPT are being developed. Currently the most common of these strategies include targeting PAK4 and NAMPT together, GLUT1 and NAMPT together, and HDAC and NAMPT together. Dual inhibitors, may in theory, solve to some extent the problems of

drug resistance, high toxicity and pharmacokinetic coordination of the two classes of drugs, but the actual efficacy of such therapeutic strategies is still yet to be seen in clinical trials. Thus, there is still a need for the development of new effective inhibitors based on new pairs of targets. Targeted delivery of cytotoxic payloads to tumor tissues via the ADC pathway may significantly improve therapeutic indices and is expected to improve the therapeutic window for NAMPT inhibition. In addition to determining the *in vivo* activity of such ADC payloads, meaningful advances to this type of therapy can only continue to pursue clinical applications if toxicity profiles are improved relative to the systemic administration of NAMPT inhibitors. This review briefly summarizes the practical application and experimental validation of the strategies using specific inhibitors, drug combinations, dual inhibitors, and ADCs, with the intention of aiding and inspiring future research on NAMPT-targeted oncology drugs. The further development and design of novel, selective, highly efficient, low toxicity and low molecular weight NAMPT inhibitors will not only help basic pathology research, but also bring great hope for the clinical treatment of tumors involving NAMPT to the benefit of more patients.

## Author contributions

YW was responsible for writing the article, HX was responsible for literature search and data collection, and WZ was responsible for drawing tables and pictures.

## Conflict of interest

The authors declare that the research was conducted in the absence of any commercial or financial relationships that could be construed as a potential conflict of interest.

## Publisher's note

All claims expressed in this article are solely those of the authors and do not necessarily represent those of their affiliated organizations, or those of the publisher, the editors and the reviewers. Any product that may be evaluated in this article, or claim that may be made by its manufacturer, is not guaranteed or endorsed by the publisher.

## References

Aboukameel, A., Muqbil, I., Senapedis, W., Baloglu, E., Landesman, Y., Shacham, S., et al. (2017). Novel p21-activated kinase 4 (PAK4) allosteric modulators

overcome drug resistance and stemness in pancreatic ductal adenocarcinoma. *Mol. Cancer Ther.* 16, 76–87. doi:10.1158/1535-7163.MCT-16-0205



- Abu Aboud, O., Chen, C. H., Senapedis, W., Baloglu, E., Argueta, C., and Weiss, R. H. (2016). Dual and specific inhibition of NAMPT and PAK4 By KPT-9274 decreases kidney cancer growth. *Mol. Cancer Ther.* 15, 2119–2129. doi:10.1158/1535-7163.MCT-16-0197
- Asawa, Y., Katsuragi, K., Sato, A., Yoshimori, A., Tanuma, S. I., and Nakamura, H. (2018). Structure-based drug design of novel carborane-containing nicotinamide phosphoribosyltransferase inhibitors. *Bioorg. Med. Chem.* 27 (13), 2832–2844. doi:10.1016/j.bmc.2019.05.013
- Audrito, V., Manago, A., La Vecchia, S., Zamporlini, F., Vitale, N., Baroni, G., et al. (2018). Synthetic lethality of PARP and NAMPT inhibition in triple-negative breast cancer cells. *EMBO Mol. Med.* 4, 1087–1096. doi:10.1002/emmm.201201250
- Barraud, M., Garnier, J., Loncle, C., Gayet, O., Lequeue, C., Vasseur, S., et al. (2016). A pancreatic ductal adenocarcinoma subpopulation is sensitive to FK866, an inhibitor of NAMPT. *Oncotarget* 7, 53783–53796. doi:10.18632/oncotarget.10776
- Bi, T. Q., Che, X. M., Liao, X. H., Zhang, D. J., Long, H. L., Li, H. J., et al. (2011). Overexpression of Nampt in gastric cancer and chemopotentiating effects of the Nampt inhibitor FK866 in combination with fluorouracil. *Oncol. Rep.* 26, 1251–1257. doi:10.3892/or.2011.1378
- Binderup, E., Björklund, F., Hjarnaa, P. V., Latini, S., Baltzer, B., Carlsen, M., et al. (2005). EB1627: A soluble prodrug of the potent anticancer cyanoguanidine CHS828. *Biol. Chem. Lett.* 15, 2491–2494. doi:10.1016/j.bmlcl.2005.03.064
- Bolandghamat Pour, Z., Nourbakhsh, M., Mousavizadeh, K., Madjd, Z., Ghorbanhosseini, S. S., Abdolvahabi, Z., et al. (2019). Suppression of nicotinamide phosphoribosyltransferase expression by MiR-154 reduces the viability of breast cancer cells and increases their susceptibility to doxorubicin. *BMC Cancer* 19, 1027. doi:10.1186/s12885-019-6221-0
- Bolandghamat Pour, Z., Nourbakhsh, M., Mousavizadeh, K., Madjd, Z., Ghorbanhosseini, S. S., Abdolvahabi, Z., et al. (2019). Up-regulation of MiR-381 inhibits NAD<sup>+</sup> salvage pathway and promotes apoptosis in breast cancer cells. *EXCLI J.* 18, 683–696. doi:10.17179/excli2019-1431
- Brandl, L., Kirstein, N., Neumann, J., Sendelhofert, A., Vieth, M., Kirchner, T., et al. (2018). The C-myc/NAMPT/SIRT1 feedback loop is activated in early classical and serrated route colorectal cancer and represents a therapeutic target. *Med. Oncol.* 36, 5. doi:10.1007/s12032-018-1225-1
- Brandl, L., Zhang, Y., Kirstein, N., Sendelhofert, A., Boos, S. L., Jung, P., et al. (2019). Targeting C-myc through interference with NAMPT and SIRT1 and their association to oncogenic drivers in murine serrated intestinal tumorigenesis. *Neoplasia* 21, 974–988. doi:10.1016/j.neo.2019.07.009
- Brenner, J. C., Feng, F. Y., Han, S., Patel, S., Goyal, S. V., Bou-Maroun, L. M., et al. (2012). PARP-1 inhibition as a targeted strategy to treat Ewing's sarcoma. *Cancer Res.* 72, 1608–1613. doi:10.1158/0008-5472.CAN-11-3648
- Burgos, E. S., Ho, M. -C., Almo, S. C., and Schramm, V. L. (2009). A phosphoenzyme mimic, overlapping catalytic sites and reaction coordinate motion for human NAMPT. *Proc. Natl. Acad. Sci. U. S. A.* 106, 13748–13753. doi:10.1073/pnas.0903898106
- Burgos, E. S., and Schramm, V. L. (2008). Weak coupling of ATP hydrolysis to the chemical equilibrium of human nicotinamide phosphoribosyltransferase. *Biochemistry* 47, 11086–11096. doi:10.1021/bi801198m
- Cagnetta, A., Cea, M., Calimeri, T., Acharya, C., Fulciniti, M., Tai, Y. T., et al. (2013). Intracellular NAD<sup>+</sup> depletion enhances bortezomib-induced anti-melanoma activity. *Blood* 122, 1243–1255. doi:10.1182/blood-2013-02-483511
- Cea, M., Cagnetta, A., Acharya, C., Acharya, P., Tai, Y. T., Yang, C., et al. (2016). Dual NAMPT and BTK targeting leads to synergistic killing of waldenstrom macroglobulinemia cells regardless of MYD88 and CXCR4 somatic mutation status. *Clin. Cancer Res.* 22, 6099–6109. doi:10.1158/1078-0432.CCR-16-0630
- Cea, M., Cagnetta, A., Fulciniti, M., Tai, Y. T., Hideshima, T., Chauhan, D., et al. (2012). Targeting NAD<sup>+</sup> salvage pathway induces autophagy in multiple myeloma cells via mTORC1 and extracellular signal-regulated kinase (ERK1/2) inhibition. *Blood* 120, 3519–3529. doi:10.1182/blood-2012-03-416776
- Cea, M., Soncini, D., Fruscione, F., Raffaghello, L., Garuti, A., Emionite, L., et al. (2011). Synergistic interactions between HDAC and sirtuin inhibitors in human leukemia cells. *PLoS One* 6, e22739. doi:10.1371/journal.pone.0022739
- Chari, R. V. J. (2016). Expanding the reach of antibody-drug conjugates. *ACS Med. Chem. Lett.* 7, 974–976. doi:10.1021/acsmedchemlett.6b00312
- Chen, W., Dong, G., Wu, Y., Zhang, W., Miao, C., and Sheng, C. (2018). Dual NAMPT/HDAC inhibitors as a new strategy for multitargeting antitumor drug discovery. *ACS Med. Chem. Lett.* 9 (1), 34–38. doi:10.1021/acsmedchemlett.7b00414
- Dahl, T. B., Holm, S., Aukrust, P., and Halvorsen, B. (2012). Visfatin/NAMPT: A multifaceted molecule with diverse roles in physiology and pathophysiology. *Annu. Rev. Nutr.* 32, 229–243. doi:10.1146/annurev-nutr-071811-150746
- Dong, G., Chen, W., Wang, X., Yang, X., Xu, T., Wang, P., et al. (2017). Small molecule inhibitors simultaneously targeting cancer metabolism and epigenetics: Discovery of novel nicotinamide phosphoribosyltransferase (NAMPT) and histone deacetylase (HDAC) dual inhibitors. *J. Med. Chem.* 60 (19), 7965–7983. doi:10.1021/acs.jmedchem.7b00467
- Ekelund, S., Sjöholm, A., Nygren, P., Binderup, L., and Larsson, R. (2001). Cellular pharmacodynamics of the cytotoxic guanidino-containing drug CHS-828. Comparison with methylglyoxal-bis(guanylhydrazine). *Eur. J. Pharmacol.* 418, 39–45. doi:10.1016/s0014-2999(01)00944-x
- Espindola-Netto, J. M., Chini, C. C. S., Tarrago, M., Wang, E., Dutta, S., Pal, K., et al. (2017). Preclinical efficacy of the novel competitive NAMPT inhibitor STF-118804 in pancreatic cancer. *Oncotarget* 8, 85054–85067. doi:10.18632/oncotarget.18841
- Fan, Y., Meng, S., Wang, Y., Cao, J., and Wang, C. (2011). Visfatin/PBEF/Nampt induces EMMPRIN and MMP-9 production in macrophages via the NAMPT-MAPK (p38, ERK1/2)-NF- $\kappa$ B signaling pathway. *Int. J. Mol. Med.* 27, 607–615. doi:10.3892/ijmm.2011.621
- Folgueira, M. A., Carraro, D. M., Brentani, H., Patrão, D. F., Barbosa, E. M., Netto, M. M., et al. (2005). Gene expression profile associated with response to doxorubicin-based therapy in breast cancer. *Clin. Cancer Res.* 11, 7434–7443. doi:10.1158/1078-0432.CCR-04-0548
- Fukuhara, A., Matsuda, M., Nishizawa, M., Segawa, K., Tanaka, M., Kishimoto, K., et al. (2007). *Science* 318, 565. doi:10.1126/science.318.5850.565b
- Fulciniti, M., Martinez-Lopez, J., Senapedis, W., Oliva, S., Lakshmi Bandi, R., Amodio, N., et al. (2017). Functional role and therapeutic targeting of p21-associated kinase 4 (PAK4) in multiple myeloma. *Blood* 129, 2233–2245. doi:10.1182/blood-2016-06-724831
- Garten, A., Schuster, S., Penke, M., Gorski, T., de Giorgis, T., and Kiess, W. (2015). Physiological and pathophysiological roles of NAMPT and NAD metabolism. *Nat. Rev. Endocrinol.* 11, 535–546. doi:10.1038/nrendo.2015.117
- Ge, X., Zhao, Y., Dong, L., Seng, J., Zhang, X., and Dou, D. (2019). NAMPT regulates PKM2 nuclear location through 14-3-3 $\zeta$ : Conferring resistance to tamoxifen in breast cancer. *J. Cell. Physiol.* 234, 23409–23420. doi:10.1002/jcp.28910
- Gholinejad, Z., Kheiripour, N., Nourbakhsh, M., Ilbeigi, D., Behroozfar, K., Hesari, Z., et al. (2017). Extracellular NAMPT/Visfatin induces proliferation through ERK1/2 and AKT and inhibits apoptosis in breast cancer cells. *Peptides* 92, 9–15. doi:10.1016/j.peptides.2017.04.007
- Ghorbanhosseini, S. S., Nourbakhsh, M., Zangoeei, M., Abdolvahabi, Z., Bolandghamatpour, Z., Hesari, Z., et al. (2019). MicroRNA-494 induces breast cancer cell apoptosis and reduces cell viability by inhibition of nicotinamide phosphoribosyltransferase expression and activity. *EXCLI J.* 18, 838–851. doi:10.17179/excli2018-1748
- Golding, S. M., Gobbi Bischof, S., Fink-Puches, R., Klemke, C. D., Dreno, B., Bagot, M., et al. (2016). Efficacy and safety of APO866 in patients with refractory or relapsed cutaneous T-cell lymphoma: A phase 2 clinical trial. *JAMA Dermatol.* 152, 837–839. doi:10.1001/jamadermatol.2016.0401
- Grolla, A. A., Torretta, S., Gnemmi, I., Amoroso, A., Orsomando, G., Gatti, M., et al. (2015). Nicotinamide phosphoribosyltransferase (NAMPT/PBEF/visfatin) is a tumoural cytokine released from melanoma. *Pigment. Cell Melanoma Res.* 28, 718–729. doi:10.1111/pcmr.12420
- Grozio, A., Sociali, G., Sturla, L., Caffa, I., Soncini, D., Salis, A., et al. (2013). CD73 protein as a source of extracellular precursors for sustained NAD<sup>+</sup> biosynthesis in FK866-treated tumor cells. *J. Biol. Chem.* 288, 25938–25949. doi:10.1074/jbc.M113.470435
- Hara, N., Yamada, K., Shibata, T., Osago, H., Hashimoto, T., and Tsuchiya, M. (2007). Elevation of cellular NAD levels by nicotinic acid and involvement of nicotinic acid phosphoribosyltransferase in human cells. *J. Biol. Chem.* 282, 24574–24582. doi:10.1074/jbc.M610357200



- Hasmann, M., and Schemainda, I. (2003). FK866, a highly specific noncompetitive inhibitor of nicotinamide phosphoribosyltransferase, represents a novel mechanism for induction of tumor cell apoptosis. *Cancer Res.* 63, 7436–7442.
- Hasmann, M., and Schemainda, I. (2003). FK866, a highly specific noncompetitive inhibitor of nicotinamide phosphoribosyltransferase, represents a novel mechanism for induction of tumor cell apoptosis. *Cancer Res.* 63, 7436–7442.
- Hesari, Z., Nourbakhsh, M., Hosseinkhani, S., Abdolvahabi, Z., Alipour, M., Tavakoli-Yaraki, M., et al. (2018). Down-regulation of NAMPT expression by mir-206 reduces cell survival of breast cancer cells. *Gene* 673, 149–158. doi:10.1016/j.gene.2018.06.021
- Heske, C. M., Davis, M. I., Baumgart, J. T., Wilson, K., Gormally, M. V., Chen, L., et al. (2017). Matrix screen identifies synergistic combination of PARP inhibitors and nicotinamide phosphoribosyltransferase (NAMPT) inhibitors in ewing sarcoma. *Clin. Cancer Res.* 23 (23), 7301–7311. doi:10.1158/1078-0432.CCR-17-1121
- Heyes, M. P., Chen, C. Y., Major, E. O., and Saito, K. (1997). Different kynurenine pathway enzymes limit quinolinic acid formation by various human cell types. *Biochem. J.* 326, 351–356. doi:10.1042/bj3260351
- Hjarna, P. J., Jonsson, E., Latini, S., Dhar, S., Larsson, R., Bramm, E., et al. (1999). CHS 828, a novel pyridyl cyanoguanidine with potent antitumor activity *in vitro* and *in vivo*. *Cancer Res.* 59, 5751–5757.
- Hong, S. M., Hwang, S. W., Wang, T., Park, C. W., Ryu, Y. M., Jung, J. H., et al. (2019). Increased nicotinamide adenine dinucleotide pool promotes colon cancer progression by suppressing reactive oxygen species level. *Cancer Sci.* 110, 629–638. doi:10.1111/cas.13886
- Hovstadius, P., Larsson, R., Jonsson, E., Skov, T., Kissmeyer, A.-M., Krasilnikoff, K., et al. (2002). A phase I study of CHS 828 in patients with solid tumor malignancy. *Clin. Cancer Res.* 8, 2843–2850.
- Hovstadius, P., Larsson, R., Jonsson, E., Skov, T., Kissmeyer, A. M., Krasilnikoff, K., et al. (2002). A Phase I study of CHS 828 in patients with solid tumor malignancy. *Clin. Cancer Res.* 8, 2843–2850.
- Imai, S. (2009). Nicotinamide phosphoribosyltransferase (nampt): A link between NAD biology, metabolism, and diseases. *Curr. Pharm. Des.* 15, 20–28. doi:10.2174/138161209787185814
- Jeong, B., Park, J. W., Kim, J. G., and Lee, B. J. (2019). FOXO1 functions in the regulation of nicotinamide phosphoribosyltransferase (Nampt) expression. *Biochem. Biophys. Res. Commun.* 511, 398–403. doi:10.1016/j.bbrc.2019.02.069
- Jiang, Y. Y., Lin, D. C., Mayakonda, A., Hazawa, M., Ding, L. W., Chien, W. W., et al. (2016). Targeting super-enhancer-associated oncogenes in oesophageal squamous cell carcinoma. *Gut* 66, 1358–1368. doi:10.1136/gutjnl-2016-311818
- Jonsson, E., Friberg, L. E., Karlsson, M. O., Hassan, S. B., Freij, A., Hansen, K., et al. (2000). Determination of drug effect on tumour cells, host animal toxicity and drug pharmacokinetics in a hollow-fibre model in rats. *Cancer Chemother. Pharmacol.* 46, 493–500. doi:10.1007/s002800000181
- Ju, H. Q., Zhuang, Z. N., Li, H., Tian, T., Lu, Y. X., Fan, X. Q., et al. (2016). Regulation of the Nampt-mediated NAD salvage pathway and its therapeutic implications in pancreatic cancer. *Cancer Lett.* 379, 1–11. doi:10.1016/j.canlet.2016.05.024
- Jung, J., Kim, L. J., Wang, X., Wu, Q., Sanvoranart, T., Hubert, C. G., et al. (2017). Nicotinamide metabolism regulates glioblastoma stem cell maintenance. *JCI Insight* 2, 90019. doi:10.1172/jci.insight.90019
- Karpov, A. S., Abrams, T., Clark, S., Raikar, A., D'Alessio, J. A., Dillon, M. P., et al. (2018). Nicotinamide phosphoribosyltransferase inhibitor as a novel payload for antibody-drug conjugates. *ACS Med. Chem. Lett.* 9 (8), 838–842. doi:10.1021/acsmchemlett.8b00254
- Khan, J. A., Tao, X., and Tong, L. (2006). Molecular basis for the inhibition of human NMPRTase, a novel target for anticancer agents. *Nat. Struct. Mol. Biol.* 13 (7), 582–588. doi:10.1038/nsmb1105
- Kirkland, J. B. (2009). Niacin status, NAD distribution and ADP-ribose metabolism. *Curr. Pharm. Des.* 15, 3–11. doi:10.2174/138161209787185823
- Kraus, D., Reckenbeil, J., Veit, N., Kuerpig, S., Meisenheimer, M., Beier, I., et al. (2018). Targeting glucose transport and the NAD pathway in tumor cells with STF-31: A re-evaluation. *Cell. Oncol.* 41 (5), 485–494. doi:10.1007/s13402-018-0385-5
- Le, A., Cooper, C. R., Gouw, A. M., Dinavahi, R., Maitra, A., Deck, L. M., et al. (2010). Inhibition of lactate dehydrogenase A induces oxidative stress and inhibits tumor progression. *Proc. Natl. Acad. Sci. U. S. A.* 107, 2037–2042. PMID:20133848. doi:10.1073/pnas.0914433107
- Lee, J., Kim, H., Lee, J. E., Shin, S. J., Oh, S., Kwon, G., et al. (2018). Selective cytotoxicity of the NAMPT inhibitor FK866 toward gastric cancer cells with markers of the epithelial-mesenchymal transition, due to loss of NAPRT. *Gastroenterology* 155, 799–814. doi:10.1053/j.gastro.2018.05.024
- Loree, J. M., and Kopetz, S. (2017). Recent developments in the treatment of metastatic colorectal cancer. *Ther. Adv. Med. Oncol.* 9, 551–564. doi:10.1177/1758834017714997
- Lucena-Cacace, A., Otero-Albiol, D., Jimenez-Garcia, M. P., Munoz-Galvan, S., and Carnero, A. (2018). NAMPT is a potent oncogene in colon cancer progression that modulates cancer stem cell properties and resistance to therapy through Sirt1 and PARP. *Clin. Cancer Res.* 24, 1202–1215. doi:10.1158/1078-0432.CCR-17-2575
- Lucena-Cacace, A., Otero-Albiol, D., Jimenez-Garcia, M. P., Peinado-Serrano, J., and Carnero, A. (2017). NAMPT overexpression induces cancer stemness and defines a novel tumor signature for glioma prognosis. *Oncotarget* 8, 99514–99530. doi:10.18632/oncotarget.20577
- Lv, R., Yu, J., and Sun, Q. (2020). Anti-angiogenic role of microRNA-23b in melanoma by disturbing NF- $\kappa$ B signaling pathway via targeted inhibition of NAMPT. *Future Oncol.* 16, 541–458. doi:10.2217/fon-2019-0699
- Maldi, E., Travelli, C., Caldarelli, A., Agazzone, N., Cintura, S., Galli, U., et al. (2013). Nicotinamide phosphoribosyltransferase (NAMPT) is over-expressed in melanoma lesions. *Pigment. Cell Melanoma Res.* 26, 144–146. doi:10.1111/pcmr.12037
- McGlothlin, J. R., Gao, L., Lavoie, T., Simon, B. A., Easley, R. B., Ma, S. F., et al. (2005). Molecular cloning and characterization of canine pre-B-cell colony-enhancing factor. *Biochem. Genet.* 43, 127–141. doi:10.1007/s10528-005-1505-2
- Menssen, A., Hydring, P., Kapelle, K., Vervoorts, J., Diebold, J., Luscher, B., et al. (2012). The C-myc oncoprotein, the NAMPT enzyme, the SIRT1-inhibitor DBC1, and the SIRT1 deacetylase form a positive feedback loop. *Proc. Natl. Acad. Sci. U. S. A.* 109, E187–E196. doi:10.1073/pnas.1105304109
- Mitchell, S. R., Larkin, K., Grieselhuber, N. R., Lai, T. H., Cannon, M., Orwick, S., et al. (2019). Selective targeting of NAMPT by KPT-9274 in acute myeloid leukemia. *Blood Adv.* 3, 242–255. doi:10.1182/bloodadvances.2018024182
- Moreno-Sánchez, R., Rodríguez-Enríquez, S., Marín-Hernández, A., and Saavedra, E. (2007). Energy metabolism in tumor cells. *FEBS J.* 274, 1393–1418. doi:10.1111/j.1742-4658.2007.05686.x
- Moschen, A. R., Kaser, A., Enrich, B., Mosheimer, B., Theurl, M., Niederegger, H., et al. (2007). Visfatin, an adipocytokine with proinflammatory and immunomodulating properties. *J. Immunol.* 178, 1748–1758. doi:10.4049/jimmunol.178.3.1748
- Mpilla, G., Aboukameel, A., Muqbil, I., Kim, S., Beydoun, R., Philip, P. A., et al. (2019). PAK4-NAMPT dual inhibition as a novel strategy for therapy resistant pancreatic neuroendocrine tumors. *Cancers* 11, 1902. doi:10.3390/cancers11121902
- Mpilla, G. B., Uddin, M. H., Al-Hallak, M. N., Aboukameel, A., Li, Y., Kim, S. H., et al. (2021). PAK4-NAMPT dual inhibition sensitizes pancreatic neuroendocrine tumors to everolimus. *Mol. Cancer Ther.* 20, 1836–1845. doi:10.1158/1535-7163.MCT-20-1105
- Murray, B. W., Guo, C., Piraino, J., Westwick, J. K., Zhang, C., Lamerdin, J., et al. (2010). Small-molecule p21-activated kinase inhibitor PF-3758309 is a potent inhibitor of oncogenic signaling and tumor growth. *Proc. Natl. Acad. Sci. U. S. A.* 107, 9446–9451. doi:10.1073/pnas.0911863107
- Mutz, C. N., Schwentner, R., Aryee, D. N., Bouchard, E. D., Mejia, E. M., Hatch, G. M., et al. (2017). EWS-FLI1 confers exquisite sensitivity to NAMPT inhibition in Ewing sarcoma cells. *Oncotarget* 8, 24679–24693. doi:10.18632/oncotarget.14976
- Nacarelli, T., Lau, L., Fukumoto, T., Zundell, J., Fatkhutdinov, N., Wu, S., et al. (2019). NAD<sup>+</sup> metabolism governs the proinflammatory senescence-associated secretome. *Nat. Cell Biol.* 21, 397–407. doi:10.1038/s41556-019-0287-4
- Nahimana, A., Aubry, D., Breton, C. S., Majjigapu, S. R., Sordat, B., Vogel, P., et al. (2014). The anti-lymphoma activity of APO866, an inhibitor of nicotinamide adenine dinucleotide biosynthesis, is potentiated when used in combination with anti-CD20 antibody. *Leuk. Lymphoma* 55, 2141–2150. doi:10.3109/10428194.2013.869325
- Nahimana, A., Attinger, A., Aubry, D., Greaney, P., Ireson, C., Thougard, A. V., et al. (2009). The NAD biosynthesis inhibitor APO866 has potent antitumor activity against hematologic malignancies. *Blood* 113, 3276–3286. doi:10.1182/blood-2008-08-173369
- Nakahata, Y., Sahar, S., Astarita, G., Kaluzova, M., and SassoneCorsi, P. (2009). Circadian control of the NAD<sup>+</sup> salvage pathway by CLOCK/SIRT1. *Science* 324, 654–657. doi:10.1126/science.1170803
- Neumann, C. S., Olivas, K. C., Anderson, M. E., Cochran, J. H., Jin, S., Li, F., et al. (2018). Targeted delivery of cytotoxic NAMPT inhibitors using antibody-drug conjugates. *Mol. Cancer Ther.* 17 (12), 2633–2642. doi:10.1158/1535-7163.MCT-18-0643

- O'Brien, T., Oeh, J., Xiao, Y., Liang, X., Vanderbilt, A., Qin, A., et al. (2013). Supplementation of nicotinic acid with NAMPT inhibitors results in loss of *in vivo* efficacy in NAPRT1-deficient tumor models. *Neoplasia* 15, 1314–1329. doi:10.1593/neo.131718
- Oehme, I., Deubzer, H. E., Wegener, D., Pickert, D., Linke, J. P., Hero, B., et al. (2009). Histone deacetylase 8 in neuroblastoma tumorigenesis. *Clin. Cancer Res.* 15 (1), 91–99. doi:10.1158/1078-0432.CCR-08-0684
- Ohanna, M., Cerezo, M., Nottet, N., Bille, K., Didier, R., Beranger, G., et al. (2018). Pivotal role of NAMPT in the switch of melanoma cells toward an invasive and drug-resistant phenotype. *Genes Dev.* 32, 448–461. doi:10.1101/gad.305854.117
- Okumura, S., Sasaki, T., Minami, Y., and Ohsaki, Y. (2012). Nicotinamide phosphoribosyltransferase: A potent therapeutic target in non-small cell lung cancer with epidermal growth factor receptor-gene mutation. *J. Thorac. Oncol.* 7, 49–56. doi:10.1097/JTO.0b013e318233d686
- Olesen, U. H., Christensen, M. K., Björklund, F., Jäätelä, M., Jensen, P. B., Sehested, M., et al. (2008). Anticancer agent CHS-828 inhibits cellular synthesis of NAD. *Biochem. Biophys. Res. Commun.* 367, 799–804. doi:10.1016/j.bbrc.2008.01.019
- Olesen, U. H., Hastrup, N., and Sehested, M. (2011). Expression patterns of nicotinamide phosphoribosyltransferase and nicotinic acid phosphoribosyltransferase in human malignant lymphomas. *APMIS* 119, 296–303. doi:10.1111/j.1600-0463.2011.02733.x
- Olesen, U. H., Petersen, J. G., Garten, A., Kiess, W., Yoshino, J., Imai, S. -I., et al. (2010). Target enzyme mutations are the molecular basis for resistance towards pharmacological inhibition of nicotinamide phosphoribosyltransferase. *BMC Cancer* 10, 677–690. doi:10.1186/1471-2407-10-677
- Oppermann, U. (2013). Why is epigenetics important in understanding the pathogenesis of inflammatory musculoskeletal diseases? *Arthritis Res. Ther.* 15 (2), 209. doi:10.1186/ar4186
- Ordonez, J. L., Amaral, A. T., Carcaboso, A. M., Herrero-Martin, D., del Carmen Garcia-Macias, M., Sevillano, V., et al. (2015). The PARP inhibitor olaparib enhances the sensitivity of Ewing sarcoma to trabectedin. *Oncotarget* 6, 18875–18890. doi:10.18632/oncotarget.4303
- Palacios, D. S., Meredith, E., Kawanami, T., Adams, C., Chen, X., Darsigny, V., et al. (2018). Structure based design of nicotinamide phosphoribosyltransferase (NAMPT) inhibitors from a phenotypic screen. *Bioorg. Med. Chem. Lett.* 28, 365–370. doi:10.1016/j.bmcl.2017.12.037
- Park, S. M., Li, T., Wu, S., Li, W. Q., Weinstock, M., Qureshi, A. A., et al. (2017). Niacin intake and risk of skin cancer in US women and men. *Int. J. Cancer* 140, 2023–2031. doi:10.1002/ijc.30630
- Peterse, E. F. P., van den Akker, B., Niessen, B., Oosting, J., Suijker, J., de Jong, Y., et al. (2017). NAD synthesis pathway interference is a viable therapeutic strategy for chondrosarcoma. *Mol. Cancer Res.* 15, 1714–1721. doi:10.1158/1541-7786.MCR-17-0293
- Piacente, F., Caffa, I., Ravera, S., Sociali, G., Passalacqua, M., Vellone, V. G., et al. (2017). Nicotinic acid phosphoribosyltransferase regulates cancer cell metabolism, susceptibility to NAMPT inhibitors, and DNA repair. *Cancer Res.* 77 (14), 3857–3869. doi:10.1158/0008-5472.CAN-16-3079
- Porporato, P. E., Dhup, S., Dadhich, R. K., Copetti, T., and Sonveaux, P. (2011). Anticancer targets in the glycolytic metabolism of tumors: A comprehensive review. *Front. Pharmacol.* 2, 49. doi:10.3389/fphar.2011.00049
- Pramono, A. A., Rather, G. M., Herman, H., Lestari, K., and Bertino, J. R. (2020). NAD- and NADPH-contributing enzymes as therapeutic targets in cancer: An overview. *Biomolecules* 10 (3), 358. doi:10.3390/biom10030358
- Preiss, J., Handler, P., and Biosynthesis of diphosphopyridine nucleotide, I. (1958). Biosynthesis of diphosphopyridine nucleotide. *J. Biol. Chem.* 233, 488–492. doi:10.1016/s0021-9258(18)64789-1
- Ramsey, K. M., Yoshino, J., Brace, C. S., Abrassart, D., Kobayashi, Y., Marcheva, B., et al. (2009). Circadian clock feedback cycle through NAMPT-mediated NAD+ biosynthesis. *Science* 324, 651–654. doi:10.1126/science.1171641
- Rane, C., Senapedis, W., Baloglu, E., Landesman, Y., Crochiere, M., Das-Gupta, S., et al. (2017). A novel orally bioavailable compound KPT-9274 inhibits PAK4, and blocks triple negative breast cancer tumor growth. *Sci. Rep.* 7, 42555. doi:10.1038/srep42555
- Ravaud, A., Cerny, T., Terret, C., Wanders, J., Bui, B. N., Hess, D., et al. (2005). Phase I study and pharmacokinetic of CHS-828, a guanidino-containing compound, administered orally as a single dose every 3 weeks in solid tumours: An ECGS/EORTC study. *Eur. J. Cancer* 41, 702–707. doi:10.1016/j.ejca.2004.12.023
- Rechsteiner, M., Hillyard, D., and Olivera, B. M. (1976). Magnitude and significance of NAD turnover in human cell line D98/AH2. *Nature* 259, 695–696. doi:10.1038/259695a0
- Reddy, P. S., Umesh, S., Thota, B., Tandon, A., Pandey, P., Hegde, A. S., et al. (2008). PBEF1/NAMPTase/Visfatin: A potential malignant astrocytoma/glioblastoma serum marker with prognostic value. *Cancer Biol. Ther.* 7, 663–668. doi:10.4161/cbt.7.5.5663
- Revollo, J. R., Grimm, A. A., and Imai, S. (2004). The NAD biosynthesis pathway mediated by nicotinamide phosphoribosyltransferase regulates Sir2 activity in mammalian cells. *J. Biol. Chem.* 279, 50754–50763. doi:10.1074/jbc.M408388200
- Rongvaux, A., Shea, R. J., Mulks, M. H., Gigot, D., Urbain, J., Leo, O., et al. (2002). Pre-B-cell colony-enhancing factor, whose expression is up-regulated in activated lymphocytes, is a nicotinamide phosphoribosyltransferase, a cytosolic enzyme involved in NAD biosynthesis. *Eur. J. Immunol.* 32, 3225–3234. doi:10.1002/1521-4141(200211)32:11<3225::AID-IMMU3225>3.0.CO;2-L
- Sampath, D., Zabka, T. S., Misner, D. L., O'Brien, T., and Dragovich, P. S. (2015). Inhibition of nicotinamide phosphoribosyltransferase (NAMPT) as a therapeutic strategy in cancer. *Pharmacol. Ther.* 151, 16–31. doi:10.1016/j.pharmthera.2015.02.004
- Schou, C., Ottosen, E. R., Petersen, H. J., Björklund, F., Latini, S., Hjarnaa, P. V., et al. (1997). Novel cyanoguanidines with potent oral antitumor activity. *Bioorg. Med. Chem. Lett.* 7, 3095–3100. doi:10.1016/s0960-894x(97)10152-4
- Schreiber, V., Dantzer, F., Ame, J. C., and De Murcia, G. (2006). Poly (ADP-ribose): Novel functions for an old molecule. *Nat. Rev. Mol. Cell Biol.* 7, 517–528. doi:10.1038/nrm1963
- Schuster, S., Penke, M., Gorski, T., Gebhardt, R., Weiss, T. S., Kiess, W., et al. (2015). FK866-induced NAMPT inhibition activates AMPK and downregulates mTOR signaling in hepatocarcinoma cells. *Biochem. Biophys. Res. Commun.* 458, 334–340. doi:10.1016/j.bbrc.2015.01.111
- Shackelford, R. E., Mayhall, K., Maxwell, N. M., Kandil, E., and Coppola, D. (2013). Nicotinamide phosphoribosyltransferase in malignancy: A review. *Genes Cancer* 4, 447–456. doi:10.1177/1947601913507576
- Shames, D. S., Elkins, K., Walter, K., Holcomb, T., Du, P., Mohl, D., et al. (2013). Loss of NAMPT1 expression by tumor-specific promoter methylation provides a novel predictive biomarker for NAMPT inhibitors. *Clin. Cancer Res.* 19, 6912–6923. doi:10.1158/1078-0432.CCR-13-1186
- Skokowa, J., Lan, D., Thakur, B. K., Wang, F., Gupta, K., Cario, G., et al. (2009). NAMPT1 is essential for the GCSF-induced myeloid differentiation provides a NAD(+)-sirtuin-1-dependent pathway. *Nat. Med.* 15, 151–158. doi:10.1038/nm.1913
- Smith, M. A., Hampton, O. A., Reynolds, C. P., Kang, M. H., Maris, J. M., Gorlick, R., et al. (2015). Initial testing (stage 1) of the PARP inhibitor BMN 673 by the pediatric preclinical testing program: PALB2 mutation predicts exceptional *in vivo* response to BMN 673. *Pediatr. Blood Cancer* 62, 91–98. doi:10.1002/pbc.25201
- Sociali, G., Grozio, A., Caffa, I., Schuster, S., Becherini, P., Damonte, P., et al. (2019). SIRT6 deacetylase activity regulates NAMPT activity and NAD(P)(H) pools in cancer cells. *FASEB J. Off. Publ. Fed. Am. Soc. Exp. Biol.* 33, 3704–3717. doi:10.1096/fj.201800321R
- Sumter, T. F., Xian, L., Huso, T., Koo, M., Chang, Y.-T., Almasri, T. N., et al. (2016). The high mobility group A1 (HMGA1) transcriptome in cancer and development. *Curr. Mol. Med.* 16, 353–393. doi:10.2174/1566524016666160316152147
- Sun, Y., Zhu, S., Wu, Z., Huang, Y., Liu, C., Tang, S., et al. (2017). Elevated serum visfatin levels are associated with poor prognosis of hepatocellular carcinoma. *Oncotarget* 8, 23427–23435. doi:10.18632/oncotarget.15080
- Tanuma, S. I., Katsuragi, K., Oyama, T., Yoshimori, A., Shibasaki, Y., Asawa, Y., et al. (2020). Structural basis of beneficial design for effective nicotinamide phosphoribosyltransferase inhibitors. *Molecules* 25 (16), 3633. doi:10.3390/molecules25163633
- Tateishi, K., Wakimoto, H., Iafrate, A. J., Tanaka, S., Loebel, F., Lelic, N., et al. (2015). Extreme vulnerability of IDH1 mutant cancers to NAD+ depletion. *Cancer Cell* 28, 773–784. doi:10.1016/j.ccell.2015.11.006
- Tennant, D. A., Durán, R. V., and Gottlieb, E. (2010). Targeting metabolic transformation for cancer therapy. *Nat. Rev. Cancer* 10, 267–277. doi:10.1038/nrc2817
- Tome, M. E., Frye, J. B., Coyle, D. L., Jacobson, E. L., Samulitis, B. K., Dvorak, K., et al. (2012). Lymphoma cells with increased anti-oxidant defenses acquire chemoresistance. *Exp. Ther. Med.* 3, 845–852. doi:10.3892/etm.2012.487
- Vaupel, P., Schmidberger, H., and Mayer, A. (2019). The Warburg effect: Essential part of metabolic reprogramming and central contributor to cancer progression. *Int. J. Radiat. Biol.* 95, 912–919. doi:10.1080/09553002.2019.1589653
- Von Heideman, A., Berglund, A., Larsson, R., and Nygren, P. (2010). Safety and efficacy of NAD depleting cancer drugs: Results of a phase I clinical trial of CHS 828 and overview of published data. *Cancer Chemother. Pharmacol.* 65, 1165–1172. doi:10.1007/s00280-009-1125-3

- Wang, B., Hasan, M. K., Alvarado, E., Yuan, H., Wu, H., and Chen, W. Y. (2011). NAMPT overexpression in prostate cancer and its contribution to tumor cell survival and stress response. *Oncogene* 30, 907–921. doi:10.1038/onc.2010.468
- Wang, J., Zhang, M., and Lu, W. (2019). Long noncoding RNA GACAT3 promotes glioma progression by sponging MiR-135a. *J. Cell. Physiol.* 234, 10877–10887. doi:10.1002/jcp.27946
- Wang, P., Xu, T. Y., Guan, Y. F., Su, D. F., Fan, G. R., and Miao, C. Y. (2009). Perivascular adipose tissue-derived visfatin is a vascular smooth muscle cell growth factor: Role of nicotinamide mononucleotide. *Cardiovasc. Res.* 81, 370–380. doi:10.1093/cvr/cvn288
- Watson, M., Roulston, A., Bélec, L., Billot, X., Marcellus, R., Bédard, D., et al. (2009). The small molecule GMX1778 is a potent inhibitor of NAD<sup>+</sup> biosynthesis: Strategy for enhanced therapy in nicotinic acid phosphoribosyltransferase 1-deficient tumors. *Mol. Cell. Biol.* 29, 5872–5888. doi:10.1128/MCB.00112-09
- Weichert, W., Denkert, C., Noske, A., Darb-Esfahani, S., Dietel, M., Kalloger, S. E., et al. (2008). Expression of class I histone deacetylases indicates poor prognosis in endometrioid subtypes of ovarian and endometrial carcinomas. *Neoplasia* 10 (9), 1021–1027. doi:10.1593/neo.08474
- Weichert, W., Röske, A., Gekeler, V., Beckers, T., Ebert, M. P., Pross, M., et al. (2008). Association of patterns of class I histone deacetylase expression with patient prognosis in gastric cancer: A retrospective analysis. *Lancet. Oncol.* 9 (2), 139–148. doi:10.1016/S1470-2045(08)70004-4
- Wilsbacher, J. L., Cheng, M., Cheng, D., Trammell, S. A. J., Shi, Y., Guo, J., et al. (2017). Discovery and characterization of novel nonsubstrate and substrate NAMPT inhibitors. *Mol. Cancer Ther.* 16, 1236–1245. doi:10.1158/1535-7163.MCT-16-0819
- Xiao, Y., Elkins, K., Durieux, J. K., Lee, L., Oeh, J., Yang, L. X., et al. (2013). Dependence of tumor cell lines and patient-derived tumors on the NAD salvage pathway renders them sensitive to NAMPT inhibition with GNE-618. *Neoplasia* 15, 1151–1160. doi:10.1593/neo.131304
- Yaku, K., Okabe, K., Hikosaka, K., and Nakagawa, T. (2018). NAD metabolism in cancer therapeutics. *Front. Oncol.* 8, 622. doi:10.3389/fonc.2018.00622
- Yang, X. J., and Seto, E. (2007). HATs and HDACs: From structure, function and regulation to novel strategies for therapy and prevention. *Oncogene* 26 (37), 5310–5318. doi:10.1038/sj.onc.1210599
- Yoon, M. J., Yoshida, M., Johnson, S., Takikawa, A., Usui, I., Tobe, K., et al. (2015). SIRT1-Mediated ENAMPT secretion from adipose tissue regulates hypothalamic NAD<sup>+</sup> and function in mice. *Cell Metab.* 21, 706–717. doi:10.1016/j.cmet.2015.04.002
- Yoshino, J., Mills, K. F., Yoon, M. J., and Imai, S. (2011). Nicotinamide mononucleotide, a key NAD(+) intermediate, treats the pathophysiology of diet- and age-induced diabetes in mice. *Cell Metab.* 14, 528–536. doi:10.1016/j.cmet.2011.08.014
- Zhang, C., Tong, J., and Huang, G. (2013). Nicotinamide phosphoribosyl transferase (Namt) is a target of microRNA-26b in colorectal cancer cells. *PLoS ONE* 8, e69963. doi:10.1371/journal.pone.0069963
- Zhang, H., Zhang, N., Liu, Y., Su, P., Liang, Y., Li, Y., et al. (2019). Epigenetic regulation of NAMPT by NAMPT-AS drives metastatic progression in triple-negative breast cancer. *Cancer Res.* 79, 3347–3359. doi:10.1158/0008-5472.CAN-18-3418
- Zhang, L. Y., Liu, L. Y., Qie, L. L., Ling, K. N., Xu, L. H., Wang, F., et al. (2012). Antiproliferation effect of APO866 on C6 glioblastoma cells by inhibiting nicotinamide phosphoribosyltransferase. *Eur. J. Pharmacol.* 674, 163–170. doi:10.1016/j.ejphar.2011.11.017
- Zhao, F. Q., and Keating, A. F. (2007). Functional properties and genomics of glucose transporters. *Curr. Genomics* 8, 113–128. doi:10.2174/138920207780368187
- Zhao, G., Green, C. F., Hui, Y.-H., Prieto, L., Shepard, R., Dong, S., et al. (2017). Discovery of a highly selective NAMPT inhibitor that demonstrates robust efficacy and improved retinal toxicity with nicotinic acid coadministration. *Mol. Cancer Ther.* 16, 2677–2688. doi:10.1158/1535-7163.MCT-16-0674
- Zheng, X., Bauer, P., Baumeister, T., Buckmelter, A. J., Caligiuri, M., Clodfelter, K. H., et al. (2013). Structure-based discovery of novel amide-containing nicotinamide phosphoribosyltransferase (nampt) inhibitors. *J. Med. Chem.* 56, 6413–6433. doi:10.1021/jm4008664
- Zoppoli, G., Cea, M., Soncini, D., Fruscione, F., Rudner, J., Moran, E., et al. (2010). Potent synergistic interaction between the Nampt inhibitor APO866 and the apoptosis activator TRAIL in human leukemia cells. *Exp. Hematol.* 38, 979–988. doi:10.1016/j.exphem.2010.07.013
- Zucal, C., D'Agostino, V. G., Casini, A., Mantelli, B., Thongon, N., Soncini, D., et al. (2015). EIF2A-dependent translational arrest protects leukemia cells from the energetic stress induced by NAMPT inhibition. *BMC Cancer* 15, 855. doi:10.1186/s12885-015-1845-1



## OPEN ACCESS

## EDITED BY

Bo Liu,  
Sichuan University, China

## REVIEWED BY

Lingjuan Zhu,  
Shenyang Pharmaceutical University,  
China  
Haiyang Yu, Tianjin University of  
Traditional Chinese Medicine,  
China

## \*CORRESPONDENCE

Guangfu Jiang  
huaxi\_jgf@outlook.com

<sup>†</sup>These authors have contributed  
equally to this work

## SPECIALTY SECTION

This article was submitted to  
Pharmacology of Anti-Cancer Drugs,  
a section of the journal  
Frontiers in Oncology

RECEIVED 30 July 2022

ACCEPTED 19 August 2022

PUBLISHED 12 September 2022

## CITATION

Qiang L, Li H, Wang Z, Wan L and  
Jiang G (2022) Deconvoluting the  
complexity of autophagy in colorectal  
cancer: From crucial pathways to  
targeted therapies.  
*Front. Oncol.* 12:1007509.  
doi: 10.3389/fonc.2022.1007509

## COPYRIGHT

© 2022 Qiang, Li, Wang, Wan and Jiang.  
This is an open-access article  
distributed under the terms of the  
[Creative Commons Attribution License](#)  
(CC BY). The use, distribution or  
reproduction in other forums is  
permitted, provided the original  
author(s) and the copyright owner(s)  
are credited and that the original  
publication in this journal is cited, in  
accordance with accepted academic  
practice. No use, distribution or  
reproduction is permitted which does  
not comply with these terms.

# Deconvoluting the complexity of autophagy in colorectal cancer: From crucial pathways to targeted therapies

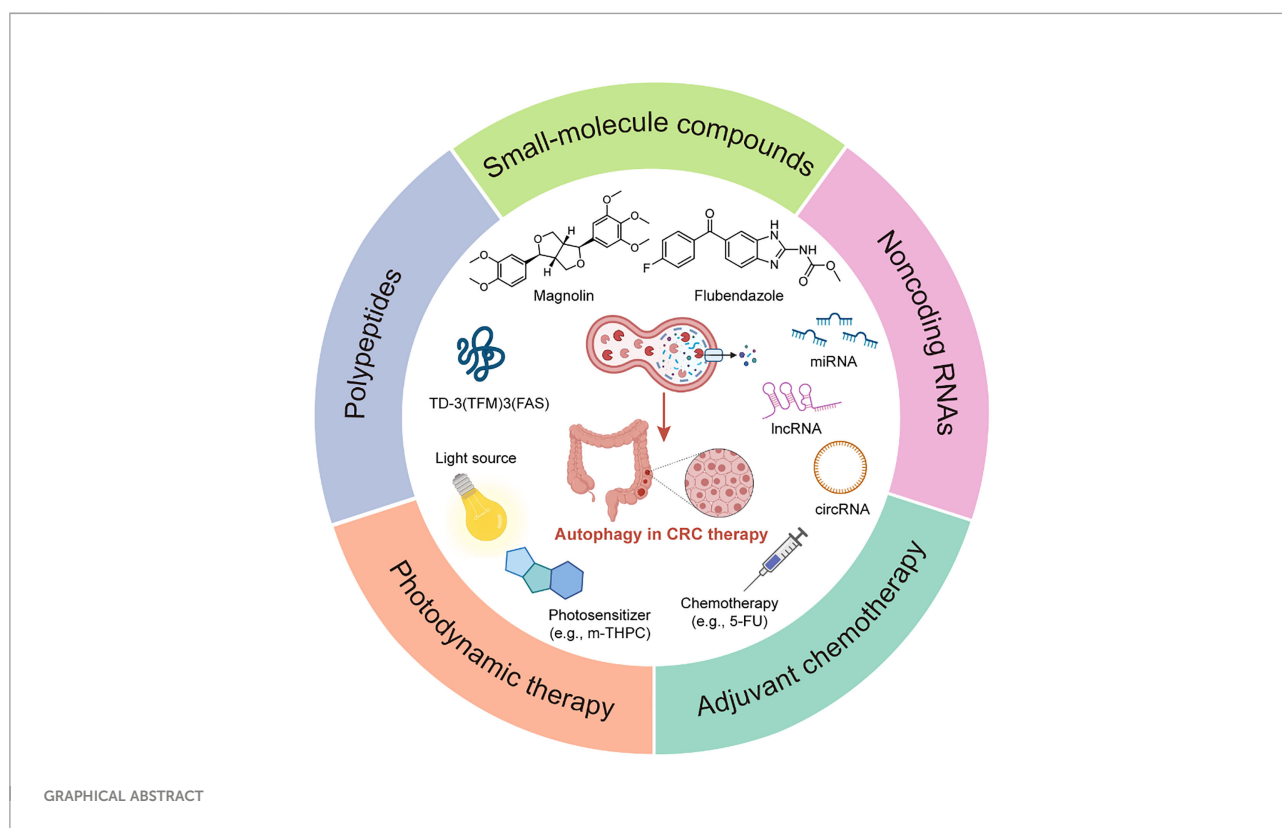
Liming Qiang<sup>1†</sup>, Hongpeng Li<sup>2†</sup>, Zhaohui Wang<sup>2</sup>,  
Lin Wan<sup>2</sup> and Guangfu Jiang<sup>2\*</sup>

<sup>1</sup>Department of Gastroenterology Ward, Guang'an People's Hospital, Guang'an, China, <sup>2</sup>Department of Gastrointestinal Surgery, Guang'an People's Hospital, Guang'an, China

Colorectal cancer (CRC) is a common gastrointestinal tumor with a high degree of malignancy, and most clinical cases are diagnosed at an advanced stage, which has unfortunately missed an opportunity for surgery; therefore, elucidation of the crucial pathways of CRC development and discovery of targeted therapeutic strategies should be anticipated. Autophagy, which is an evolutionarily highly conserved catabolic process, may promote tumorigenesis and development of CRC. On the contrary, autophagy can trigger programmed cell death to inhibit CRC progression. Correspondingly, several targeted therapeutic strategies have been reported in CRC, including small-molecule compounds, polypeptides, non-coding RNAs, photodynamic, and adjuvant therapies. Thus, in this review, we focus on summarizing the crucial pathways of autophagy in CRC, and further discuss the current therapeutic strategies targeting autophagy. Together, these findings may shed light on the key regulatory mechanisms of autophagy and provide more promising therapeutic approaches for the future CRC therapies.

## KEYWORDS

colorectal cancer (CRC), autophagy, crucial pathway, therapeutic strategy, targeted therapy



## Introduction

Colorectal cancer (CRC) is well-known as the most common malignant gastrointestinal tumor in the world, with about 1.9 million new cases in 2020, accounting for about 10% of the global cancer incidence, ranking third among all cancers (1). And, CRC mortality constantly remains at a relatively high level, with about 940,000 new deaths in 2020, accounting for 9.4% of global cancer deaths, which is the second leading cause of cancer death followed by lung cancer (1, 2). The 5-year survival rate of CRC patients is approximately 60%-70% with distant stage diagnosis is only 14% (2, 3). Unfortunately, the majority of CRC cases are usually detected in the advanced clinical stage and diagnosed as the distant stage with a poor prognosis (3, 4). Hitherto, the current treatment of CRC has still been limited to the traditional surgery combined with chemoradiotherapy (5); however, chemotherapy drugs, including the most classic 5-Fluorouracil (5-FU), will inevitably develop chemotherapy resistance after long-term treatment, weakening the efficacy and causing tumor recurrence (6). Due to the severe side effects of chemoradiotherapy and the inability of surgical treatment for patients diagnosed at an advanced stage, most patients, especially those with poor prognosis, still lack effective targeted therapy, resulting in a high annual mortality rate of CRC (1, 2, 7). Thus, in-depth exploration of the pathogenesis of CRC and searching for effective targeted therapeutic approaches are urgent to be solved.

Of note, autophagy is an evolutionarily highly conserved catabolic process that regulates the expression of various oncogenes and tumor suppressor genes, which is a double-edged sword in many types of human cancers, such as CRC (8). On one hand, autophagy plays a cytoprotective role by removing misfolded proteins, damaged organelles, and reactive oxygen species, limiting tumorigenesis; on the other hand, autophagy provides energy through catabolism to help tumor cells cope with stress stimuli, such as insufficient oxygen, nutrient deficiencies, or cancer treatment, which leads to tumor progression (9, 10). Currently, there are some small-molecule compounds as autophagic modulators (e.g., chloroquine or hydroxychloroquine) have shown a promising tumor therapeutic potential in clinical trials, and targeting autophagy has gradually been recognized as one of new strategies for potential therapeutic purposes (11). As mentioned above, in this review, we summarize several crucial pathways of autophagy in CRC progression, and further discuss some therapeutic strategies targeting autophagy to improve CRC treatment.

## Crucial pathways for autophagy regulation in CRC

It is well-known that there are five critical stages in the canonical autophagy process, including autophagy initiation,



phagophore nucleation, phagophore elongation and maturation, autophagosome and lysosome fusion, autolysosome degradation and recycling (12).

## Autophagy initiation: ULK1-ATG13-FIP200-ATG101

UNC-51-like autophagy-activating kinase 1 (ULK1), as the homologous protein of yeast Atg1, plays a vital role in the autophagy initiation stage. As a conserved promoter of the autophagy process, ULK1 forms ULK complex with autophagy-related gene (ATG) 13, RB1-inducible coiled-coil 1 (RB1CC1; FIP200), and ATG101, which transmit autophagy signals and initiate the formation of autophagosome when they are activated (13). Recently, there is a study has shown that ULK1 is the most frequently mutated gene in The Cancer Genome Atlas (TCGA)-colorectal adenocarcinoma dataset, implying that ULK1 and its regulatory network may be closely related to colorectal carcinogenesis (14). Notably, the upregulation of ULK1 significantly induces autophagy-dependent cell death in RKO human CRC cells, which exerts excellent antiproliferative potency (15).

The mechanistic target of rapamycin (mTOR), the most widely studied negative regulator of autophagy, is usually activated by PI3K-Akt and directly inhibits ULK1 to inhibit autophagy (16). In CRC, FAT tumor suppressor homolog 4 (FAT4) inhibits the PI3K-Akt-mTOR pathway, promoting autophagy and inhibiting migration and invasion in SW480, HCT116 and LOVO human CRC cells (17); similarly, downregulation of pleckstrin homology like domain family A member 2 (PHLDA2) inhibits the PI3K-Akt-mTOR pathway, inducing autophagy and inhibiting proliferation in SW480, HCT116 human CRC cells (18).

AMP-activated protein kinase (AMPK) is also a critical regulator upstream of ULK1, which directly phosphorylates ULK1 to activate autophagy. In addition, activated AMPK also phosphorylates downstream tuberous sclerosis complex 1 and 2 (TSC1/2) to enhance inhibition of Rheb, thereby inhibiting mTOR and inducing autophagy (19). In HCT116 and HT29 human CRC cells, knockdown of AMPK restricted tumor autophagy-dependent cell death, leading to tumor progression (20) (Figure 1).

## Phagophore nucleation: BECN1-VPS34-VPS15-ATG14-AMBRA1-UVRAG

Coiled-coil myosin-like BCL2-interacting protein (BECN1), as the homologous protein of yeast Atg6, forms the class III phosphoinositide 3-kinase (PI3K) complex with phosphatidylinositol 3-kinase catalytic subunit type 3 (PIK3C3; VPS34), phosphoinositide 3-kinase regulatory subunit 4 (PIK3R4; VPS15), ATG14, autophagy and beclin 1 regulator

1 (AMBRA1) and UV radiation resistance-associated (UVRAG), which is responsible for the phagophore nucleation; specifically, it is usually phosphorylated by activated ULK1 and acts as an integral scaffold for the PI3K complex, recruiting autophagy-related proteins such as ATG9 to localize to phagophore (21). Interestingly, a recent study has shown that the transcription factor sex-determining region Y-box2 (SOX2) can bind to the promoter of BECN1 to induce its transcription and activate autophagy in SW480 and SW620 human CRC cells, resulting in tumor progression (22); and, interleukin-6 (IL-6), independently of its substrate signal transducer and activator of transcription 3 (STAT3), induces Janus kinase 2 (JAK2) to phosphorylate the tyrosine residue at position 333 of BECN1 in LoVo human CRC cells, enhancing BECN1-VPS34 interaction and autophagy significantly, which leading to a poor prognosis of CRC patients (23). In addition, the inhibition of VPS34 also strongly reduces the level of autophagy in Caco-2 human CRC cells (24) (Figure 1).

## Phagophore elongation and maturation: ATG5-ATG12-ATG16L1/ATG4B-ATG7-LC3

There are two important ubiquitination modifications in phagophore elongation and maturation, one of which is that ATG5, ATG12 and ATG16L1 are catalyzed by ATG7 and ATG10 to form a complex and localize to the autophagosome membrane (25). In CRC, patients with high ATG5 expression generally have a poorer prognosis and are more likely to cause tumor recurrence (26). Interestingly, the *ATG16L1*<sup>T300A</sup> variant elicits a defect of autophagy, which is closely associated with better patient prognosis (27). Notably, ATG16L2, as a paralog of ATG16L1, which N-terminal region also binds to the ATG5-ATG12 complex like ATG16L1, but is not recruited to the autophagosome membrane, possibly acting as a potential competitive ATG16L1 inhibitor to inhibit autophagy; in CRC, its overexpression inhibits tumor proliferation *in vitro* and *in vivo*, and is associated with usually a long survival rate (28). The other ubiquitination modification is that ATG4B and ATG7 cleave the LC3 precursor protein to generate LC3-I, and the ATG5-ATG12-ATG16L1 complex catalyzes the coupling of LC3-I to phosphatidylethanolamine (PE) to form LC3-II (MAP1LC3B) (29). In HCT116 and Caco2 human CRC cells, silencing of ATG4B increases autophagy levels (30). ATG7 is usually highly expressed in CRC cells and has nothing to do with the survival of intestinal epithelial cells, but affects the survival of tumors, which is a potential target in CRC (31) (Figure 1).

## Autophagosome and lysosome fusion, autolysosome degradation and recycling

Ras-related protein Rab-7a (RAB7A) is a critical small GTPase that promotes autophagosome-lysosome fusion, which

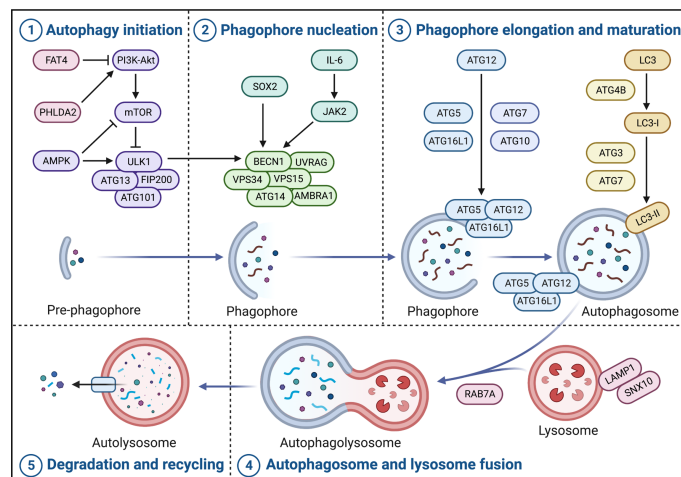


FIGURE 1

Crucial pathways of autophagy in CRC. Autophagy in CRC broadly contains five stages, namely autophagy initiation, phagophore nucleation, phagophore elongation and maturation, autophagosome and lysosome fusion, and autolysosome degradation and recycling. The ULK complex (ULK1-ATG13-FIP200-ATG101) triggers autophagy initiation and the PI3K complex (BECN1-VPS34-VPS15-ATG14-AMBRA1-UVRAG) promotes phagophore nucleation. Moreover, phagophore elongation and maturation contain two important ubiquitination modifications, one of which is the formation of complexes and localization of ATG5, ATG12, and ATG16L1 to the autophagosome membrane catalyzed by ATG7 and ATG10; the other is the cleavage of LC3 precursor protein by ATG4B and ATG7 to generate LC3-I, and the ATG5-ATG12-ATG16L1 complex catalyzes LC3-I coupling with PE to form LC3-II. Subsequently, RAB7A and LAMP1 are involved in autophagosome and lysosome fusion to form autolysosome. Finally, the contents of the autolysosome are degraded and recycled into the cytoplasm to re-engage in cellular metabolism.

together with lysosome-associated membrane protein 1 (LAMP1), participates in autophagosome-lysosome fusion to form autolysosome. Subsequently, the contents of the autolysosome are degraded and recycled into the cytoplasm to re-engage in cellular metabolism (25). Currently, sorting nexin 10 (SNX10) has been reported to interact with ATG12-ATG5 conjugates and LAMP1 to promote autophagosome-lysosome fusion, inhibiting the occurrence and progression of CRC (32) (Figure 1).

## Therapeutic strategies targeting autophagy for CRC therapy

Currently, the therapeutic strategies for CRC are mainly traditional tumor treatment approaches, namely surgery, radiotherapy, and chemotherapy. However, for patients whose conditions are not suitable for conventional treatment approaches, such as patients with recurrent, metastatic tumors or locally advanced inoperable treatment, targeting autophagy with small-molecule compounds has shown solid therapeutic potential. Notably, some emerging therapeutic strategies such as polypeptide and non-coding RNAs (ncRNAs) that modulate autophagy for CRC therapy also have achieved promising preclinical results. Additionally, autophagy-targeting of photodynamic therapy and autophagy adjuvant chemotherapy strategies demonstrate the broad prospects of autophagy in CRC therapy.

## Small-molecule compounds targeting autophagy

Hitherto, a variety of small-molecule compounds have demonstrated compelling efficacy in CRC therapy *via* modulating autophagy. For instance, Fangchinoline, an alkaloid monomer with anti-inflammatory activity derived from the *Stephaniae tetrandrine* S. Moore, is a novel autophagy agonist in CRC that activates the AMPK-mTOR-ULK1 pathway to induce autophagy-dependent cell death in HT29 and HCT116 human CRC cells and also exerts an effective growth inhibition of tumors *in vivo* (33). Similarly, Chaetochin J, an alkaloid monomer derived from *Chaetomium* sp, activates AMPK and inhibits PI3K-Akt-mTOR to induce autophagy, manifesting a solid antiproliferative effect in RKO, HCT116 and SW480 human CRC cells with  $IC_{50}$ s of 0.56, 0.61 and 0.65  $\mu$ M (34). Celastrol, contained in *Tripterygium wilfordii*, inhibits the transcription factor Nur77 and upregulates ATG7 to induce autophagy, achieving favorable antitumor effects in HCT116 and SW480 human CRC cells and the HCT116 xenograft mouse model (35). Magnolin, a lignan monomer with anti-inflammatory and antioxidant activity derived from *Magnolia biondii*, significantly upregulates LC-3B and downregulates p62 by inhibiting leukemia inhibitory factor (LIF)-STAT3-Mcl-1 to induce autophagy in HCT116 and SW480 human CRC cells and HCT116 xenograft model, which showing excellent anticancer potential (36). Notably, Dehydrodiisoeugenol, a traditional Chinese medicine monomer composition derived from nutmeg,

inhibits the late stage of autophagy by inducing endoplasmic reticulum (ER) stress, which greatly restricts the growth and proliferation of tumors; it exhibits convincing antiproliferative activity not only in HCT116 and SW620 human CRC cells with  $IC_{50}$ s of 54.32  $\mu$ M and 46.74  $\mu$ M but also in cell-derived xenograft (CDX) and patient-derived tumor xenograft (PDX) models with lower toxicity (37). In addition to natural products, there are several repositioning small-molecule compounds that contribute to CRC therapy *via* modulating autophagy. For instance, lomitapide, a clinical drug approved by the Food and Drug Administration (FDA) for the treatment of hypercholesterolemia, is recently reported to upregulate AMPK phosphorylation and promote the formation of BECN1-VPS34-ATG14 complex, thereby inducing autophagy in HCT116 and HT29 human CRC cells, which significantly inhibits tumor proliferation *in vitro* and *in vivo* (20). Similarly, flubendazole, an anthelmintic drug approved by FDA, downregulates STAT3 phosphorylation levels, mTOR and p62, and upregulates Beclin 1 and LC3-I/II in HCT116, RKO and SW480 human CRC cells, which promoting the initiation of autophagy to prevent tumor progression without substantially affecting normal cell proliferation (38). Currently, a series of dual-target inhibitors of bromodomain-containing protein 4 (BRD4) and histone deacetylases (HDAC) based on the structure design and optimization have been reported, among which compound 17c is the most potent inhibitor of BRD4 and HDAC, induces autophagy *via* BRD4-AMPK-mTOR-ULK1 pathway, showing promising antiproliferative activities *in vitro* and *in vivo* (39) (Figure 2A).

## Polypeptides targeting autophagy

Notably, compared with small-molecule compounds, polypeptides usually have higher selectivity and stability *in vivo* with a low probability of immune system rejection and are expected to achieve higher efficacy. Recently, TD-3(TFM)3 (FAS), a novel DNA tetrahedron (TD) with two types of therapeutic peptides (FAS peptides and FK-16 peptides) has been designed; among them, FK-16 is delivered to the cytoplasm of HT-29 human CRC cells by cell-penetrating peptide, further upregulating the expression of p53, ATG5, and ATG7, inducing autophagy-dependent cell death and exerting strong and specific tumor-suppressive efficacy (40) (Figure 2B). In addition, LL-37, an antimicrobial peptide, is closely related to cellular processes such as apoptosis and autophagy, inhibiting the carcinogenesis of intestinal cells. However, due to the complex pathogenesis of CRC, whether LL-37 can treat CRC by regulating autophagy still need to explore (41).

## Noncoding RNAs targeting autophagy

In recent years, ncRNA has been found to play critical roles in various cellular physiological processes and is closely related

to the occurrence and progression of diseases, especially cancer. Currently, there are a series of regulatory strategies have been applied to tumor diagnosis and clinical trials (42). Notably, autophagy regulated by ncRNAs can affect multiple core processes involved in tumor survival, including proliferation, apoptosis, invasion, and metastasis (43). Therefore, in-depth exploration of the mechanism of ncRNAs regulating autophagy is expected to provide new directions for CRC therapy.

Of note, microRNAs (miRNAs) are short ncRNAs that are extensively studied in cancer due to their modulation of various downstream mRNAs, which have been reported as novel specific biomarkers in multiple cancers. For instance, miR-338-5p is often highly expressed in the more malignant CRC phenotype, implying that it could serve as a promising potential biomarker for CRC diagnosis; it inhibits PIK3C3 and suppresses autophagy to promote tumor invasion and migration (44). Similarly, miR-27b-3p has also been reported as a potential therapeutic target for CRC that suppresses autophagy by inhibiting ATG10, which also helps reverse the resistance developed by long-term chemotherapy (45) (Figure 2C).

Notably, long non-coding RNAs (lncRNAs) modulate various biological processes, which are closely related to the occurrence and development of multiple diseases, and as a current research hotspot in cancer pathology. Metastasis-associated lung adenocarcinoma transcript 1 (MALAT1), one of the first lncRNAs reported to be involved in cancer metastasis, is aberrantly expressed in multiple human malignancies and can act as a sponge for various miRNAs. In CRC, MALAT1 acts as a sponge for miR-101 to activate autophagy, promoting proliferation and inhibiting apoptosis in HCT116 and SW620 human CRC cells; therefore, the high expression of MALAT1 is closely related to poor prognosis in CRC patients (46). Interestingly, MALAT1 can also act as a sponge for miR-26a-5p, reversing the inhibition of Smad1 by miR-26a-5p to elicit Smad1 upregulation; Smad1 can bind to the ATG5 promoter, induce the transcription of ATG5 to activate autophagy, promoting proliferation and metastasis in HT29 and SW1116 human CRC cells (47). Similarly, lncRNA small nucleolar RNA host gene 6 (SNHG6) acts as a sponge for miR-26a-5p, upregulating ULK1 and activating autophagy in RKO, HT29 and HCT116 human CRC cells (48). In addition, lncRNA small nucleolar RNA host gene 14 (SNHG14) is often highly expressed in a variety of cancers, leading to poor progression; in CRC, SNHG14 suppresses miR-186 to upregulate ATG14, inducing autophagy in SW620 and SW480 human CRC cells (49). Cancer susceptibility candidate 9 (CASC9) is a lncRNA highly expressed in CRC in both TCGA and The Encyclopedia of RNA Interactomes (ENCORI) datasets, which high expression is associated with poor patient prognosis. Inhibition of CASC9 upregulates the phosphorylation level of AMPK and suppresses Akt-mTOR signaling, inhibiting tumor growth and inducing autophagy in HCT116 and SW480 human CRC cells, which is a promising strategy for CRC therapy (50). Moreover, lncRNA

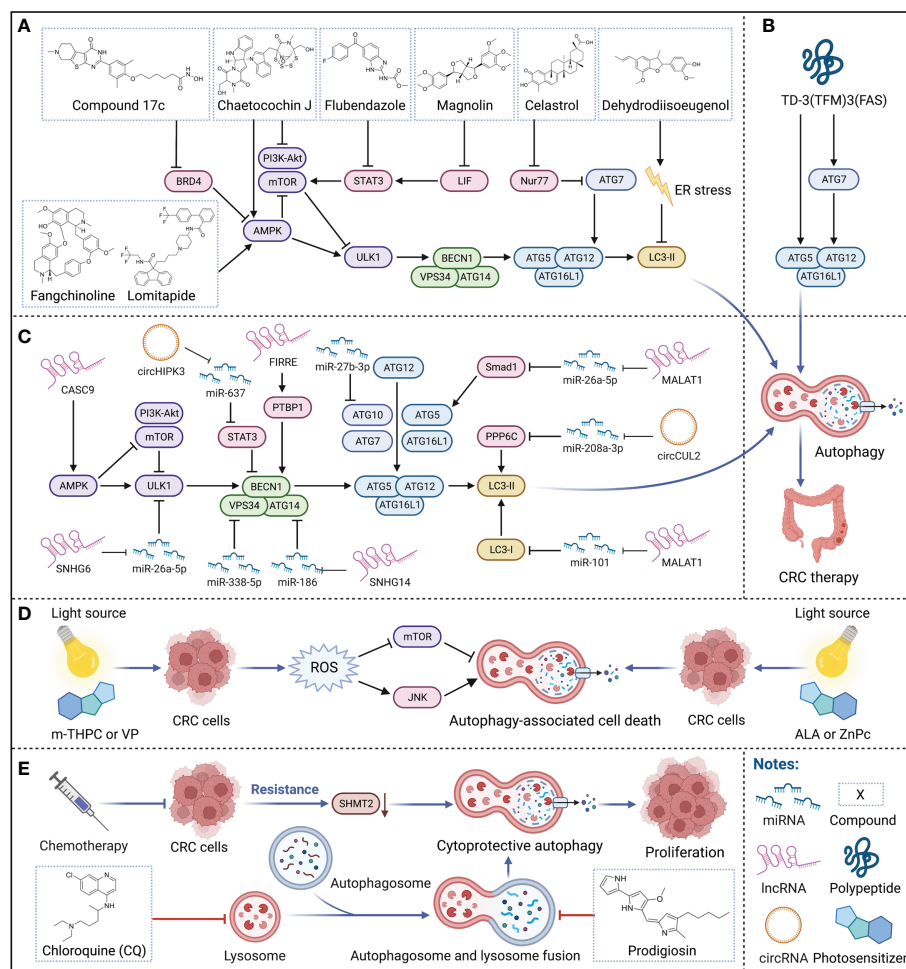


FIGURE 2

Therapeutic strategies targeting autophagy for CRC therapy. (A–C) Small-molecule compounds, polypeptide, and ncRNAs for targeting autophagy in CRC therapy. Various small-molecule compounds, the polypeptide, and multiple ncRNAs modulate critical regulators of autophagy to treat CRC. (D) Photodynamic therapy targeting autophagy in CRC therapy. Multiple photosensitizers with specific wavelength light source irradiation induce autophagy-associated cell death, participating in CRC therapy. (E) Adjuvant chemotherapy by autophagy for CRC therapy. Autophagy inhibitors can effectively suppress the cytoprotective autophagy triggered by long-term chemotherapy and restore the sensitivity of tumors to chemotherapy drugs, enhancing the effectiveness of chemotherapy.

functional intergenic repeating RNA element (FIRRE) is often located in the nucleus and can bind PTBP1 to promote its translocation to the cytoplasm to stabilize the cytoplasmic mRNA BECN1, increasing the level of autophagy in RKO human CRC cells (51) (Figure 2C).

Importantly, circular RNAs (circRNAs) are a special class of ncRNAs that often function as competing endogenous RNAs (ceRNAs) for miRNAs, which implied an emerging strategy in cancer therapy. For instance, circCUL2 acts as a sponge for miR-208a-3p to inhibit tumor proliferation *via* upregulating protein phosphatase 6 catalytic subunit (PPP6C), which induces autophagy in SW480 and SW620 human CRC cells and the SW480 xenograft model (52). Similarly, circHIPK3 acts as a sponge for miR-637 to upregulate STAT3, activating

downstream Bcl-2 to suppress beclin1 to inhibit autophagy *in vitro* and *in vivo* (53) (Figure 2C). Although the application of ncRNAs in tumor diagnosis and treatment is still in the early stage, as more and more mechanisms are discovered, we believe that the clinical application of ncRNAs is just around the corner.

## Photodynamic therapy targeting autophagy

Photodynamic therapy (PDT), an emerging minimally invasive procedure for cancer therapy, relies on specific wavelength light source irradiation to activate photosensitizers in tumors to generate biotoxic singlet oxygen and other highly



reactive oxygen species (ROS), which in turn oxidatively damages tumors, and exerts therapeutic effects by inducing various forms of cell death such as apoptosis or autophagy (54, 55). Compared with traditional treatment strategies for cancer, PDT is less invasive, has better selectivity and a broader range of applications, and can be repeated multiple times without drug resistance or toxicity (55). Currently, PDT to induce autophagy has achieved a series of progress in CRC therapy. For instance, treatment of HCT116 and SW480 human CRC cells with the second-generation photosensitizers meta-tetrahydroxyphenylchlorin (m-THPC) and verteporfin (VP) produces a large amount of ROS, induces autophagy by activating c-Jun N-terminal kinase (JNK) and inhibiting the phosphorylation of mTOR; in addition, m-THPC and VP also effectively suppress the tumor progression of HCT116 xenografts (56). Importantly, both high-speed and short-term acute PDT (aPDT) and low-speed and long-term metronomic PDT (mPDT) with the photosensitizer 5-aminolevulinic acid (ALA) can induce autophagy in SW837 human CRC cells, and ALA-mPDT induces autophagy earlier and exhibits stronger antitumor effect than ALA-aPDT (57). Similarly, PDT with the photosensitizer zinc phthalocyanine (ZnPc) at a light flux of 12 J/cm<sup>2</sup> or 24 J/cm<sup>2</sup> induces autophagy in SW480 human CRC cells (58) (Figure 2D).

## Adjuvant chemotherapy targeting autophagy

5-FU is the first drug recognized as an effective chemotherapy drug for CRC, which has been widely used in CRC clinical therapy since 1957. Unfortunately, long-term treatment inevitably develops chemoresistance, resulting in tumor relapse; notably, autophagy plays a critical role in its drug resistance mechanism. Once 5-FU gives tumors stress, autophagy can provide additional nutrients to meet the metabolic needs of tumors, resulting in abnormal proliferation and weakening the effectiveness of chemotherapy (6). Therefore, the therapeutic strategy of 5-FU combined with autophagy inhibition may considerably improve the survival rate of CRC patients. For instance, the treatment of 5-FU decreases the expression of serine hydroxymethyltransferase-2 (SHMT2), which promotes autophagy and triggers 5-FU resistance, resulting in poor prognosis of CRC patients; while 5-FU combined with the autophagy inhibitor chloroquine (CQ) reverses the insensitivity to 5-FU in CRC cells with low SHMT2 expression *in vitro* and *in vivo*, thereby enhancing the effect of chemotherapy (59). Prodigiosin, a secondary metabolite synthesized by bacteria such as *Serratia marcescens*, inhibits autophagy by blocking the fusion of autophagosome and lysosome and suppressing the activity of lysosomal hydrolase, further triggers the accumulation of LC3B-II and SQSTM, enhances the sensitivity of tumors to 5-FU, synergizing with 5-FU to inhibit CRC progression in HCT116 and SW480 human CRC cells and HCT116 cells nude mice

xenografts (60). In addition, knockdown of ATG7 resensitizes SW480 and HT29 human CRC cells to Irinotecan and 5-FU, overcoming chemoresistance, again confirming the feasibility of autophagy inhibitors to alleviate chemoresistance (31). Similarly, inhibition of autophagy also increases radiosensitivity, which implies a potential CRC therapeutic strategy. For instance, downregulation of long non-coding RNA homeobox transcript antisense intergenic RNA (HOTAIR) upregulates miR-93 to downregulate ATG12, improving the effect of radiotherapy *via* inhibiting autophagy in SW480 and HCT116 human CRC cells and CRC xenograft models (61) (Figure 2E).

## Conclusions and perspectives

CRC is a common malignant tumor with a high global incidence and mortality rate, and its therapeutic strategies have been mainly dependent on surgery, radiotherapy, and chemotherapy so far. Unfortunately, some patients are already at an advanced stage of CRC when they are detected and cannot be treated surgically. Therefore, development of some new emerging therapeutic approaches should be urgent. On one hand, autophagy removes damaged nucleic acids and cellular organelles to protect cells from stress damage, effectively reducing the probability of CRC occurrence. On the other hand, autophagy may help CRC respond to the therapeutic stimuli, provides the energy required for tumor proliferation through catabolism, and even resists drug stimuli to resistance.

Notably, the crucial pathway for autophagy regulation is one of the current research hotspots in CRC pathology. Many canonical regulators of autophagy processes (e.g., ULK1, ATG5, ATG16L1) are aberrantly expressed in CRC patients. In addition, some studies knocked down or overexpressed critical regulators in each stage of autophagy to rationally utilize its two sides, initially showing favorable antitumor effects. In short, an in-depth exploration of crucial pathways for autophagy regulation in CRC and the corresponding effective interventions will considerably improve CRC therapy.

Currently, several small-molecule compounds targeting autophagy (e.g., Fangchinoline, Chaetochin J, and Celastrol) have been achieving some promising preclinical results and exerted a great potential on potential CRC therapies. Notably, compared with small-molecule compounds, polypeptides [e.g., TD-3(TFM)3(FAS)] generally have higher selectivity and stability *in vivo*, and are less susceptible to rejection by the immune system, exhibiting high therapeutic potential for CRC. In addition, some key regulatory factors (e.g., microRNA miR-338-5p, lncRNA MALAT1, and circRNA circCUL2) have also been continuously identified as autophagy-related biomarkers in CRC, providing accumulating evidence for the availability of clinical diagnosis and treatment. As a new emerging therapeutic strategy, photodynamic therapy also achieved inspiring stage results in CRC therapy by inducing autophagy, which provides



more options for CRC patients. Interestingly, autophagy reverses long-term chemotherapy-induced resistance and sensitize tumors to chemotherapeutic drugs.

In summary, modulating autophagy has been emerging as a promising strategy for CRC therapy, which can benefit the patients who are not suitable for traditional treatment, and can be used as adjuvant chemotherapy to overcome drug resistance. Importantly, the rapid development of new technologies, such as artificial intelligence (AI) seems to be delineated the intricate dynamic balance of autophagy between CRC progression and treatment (62). With the continuous exploration of the relationship between autophagy and CRC, we believe that the Janus roles of autophagy would be subtly manipulated, and more effectively therapeutic strategies will be exploited to greatly improve potential CRC therapies in the future.

## Author contributions

LQ, HL participates in manuscript writing and figure drawing; ZW, LW participates in references collection and manuscript formatting adjustments. GJ reviewed and edited the manuscript. All the authors approved the submitted version.

## References

1. Sung H, Ferlay J, Siegel RL, Laversanne M, Soerjomataram I, Jemal A, et al. Global cancer statistics 2020: Globocan estimates of incidence and mortality worldwide for 36 cancers in 185 countries. *CA: Cancer J Clin* (2021) 71(3):209–49. doi: 10.3322/caac.21660
2. Siegel RL, Miller KD, Goding Sauer A, Fedewa SA, Butterly LF, Anderson JC, et al. Colorectal cancer statistics, 2020. *CA Cancer J Clin* (2020) 70(3):145–64. doi: 10.3322/caac.21601
3. Li N, Lu B, Luo C, Cai J, Lu M, Zhang Y, et al. Incidence, mortality, survival, risk factor and screening of colorectal cancer: A comparison among China, Europe, and northern America. *Cancer Lett* (2021) 522:255–68. doi: 10.1016/j.canlet.2021.09.034
4. Dang Y, Hu D, Xu J, Li C, Tang Y, Yang Z, et al. Comprehensive analysis of 5-hydroxymethylcytosine in ZW10 kinetochore protein as a promising biomarker for screening and diagnosis of early colorectal cancer. *Clin Trans Med* (2020) 10(3):e125. doi: 10.1002/ctm2.125
5. Bijelic L, Ramos I, Goeré D. The landmark series: Surgical treatment of colorectal cancer peritoneal metastases. *Ann Surg Oncol* (2021) 28(8):4140–50. doi: 10.1245/s10434-021-10049-3
6. Blondy S, David V, Verdier M, Mathonnet M, Perraud A, Christou N. 5-fluorouracil resistance mechanisms in colorectal cancer: From classical pathways to promising processes. *Cancer Sci* (2020) 111(9):3142–54. doi: 10.1111/cas.14532
7. Li C, Li Z, Zhang T, Wei P, Li N, Zhang W, et al. (1)H nmr-based metabolomics reveals the antitumor mechanisms of triptolide in Balb/C mice bearing Ct26 tumors. *Front Pharmacol* (2019) 10:1175. doi: 10.3389/fphar.2019.01175
8. Xia H, Green DR, Zou W. Autophagy in tumour immunity and therapy. *Nat Rev Cancer* (2021) 21(5):281–97. doi: 10.1038/s41568-021-00344-2
9. Amaravadi RK, Kimmelman AC, Debnath J. Targeting autophagy in cancer: Recent advances and future directions. *Cancer Discov* (2019) 9(9):1167–81. doi: 10.1158/2159-8290.CD-19-0292
10. Yun CW, Jeon J, Go G, Lee JH, Lee SH. The dual role of autophagy in cancer development and a therapeutic strategy for cancer by targeting autophagy. *Int J Mol Sci* (2020) 22(1):179. doi: 10.3390/ijms22010179
11. Mulcahy Levy JM, Thorburn A. Autophagy in cancer: Moving from understanding mechanism to improving therapy responses in patients. *Cell Death Differ* (2020) 27(3):843–57. doi: 10.1038/s41418-019-0474-7

## Funding

This work was supported by grants from the fund of the high-quality development of Guang 'an People's Hospital (Grant No. 21FZ008).

## Conflict of interest

The authors declare that the research was conducted in the absence of any commercial or financial relationships that could be construed as a potential conflict of interest.

## Publisher's note

All claims expressed in this article are solely those of the authors and do not necessarily represent those of their affiliated organizations, or those of the publisher, the editors and the reviewers. Any product that may be evaluated in this article, or claim that may be made by its manufacturer, is not guaranteed or endorsed by the publisher.

12. Galluzzi L, Bravo-San Pedro JM, Levine B, Green DR, Kroemer G. Pharmacological modulation of autophagy: Therapeutic potential and persisting obstacles. *Nat Rev Drug Discov* (2017) 16(7):487–511. doi: 10.1038/nrd.2017.22
13. Zachari M, Ganley IG. The mammalian Ulk1 complex and autophagy initiation. *Essays Biochem* (2017) 61(6):585–96. doi: 10.1042/ebc20170021
14. Zhang P, Holowatyj AN, Roy T, Pronovost SM, Marchetti M, Liu H, et al. An Sh3px1-dependent endocytosis-autophagy network restrains intestinal stem cell proliferation by counteracting egfr-erk signaling. *Dev Cell* (2019) 49(4):574–89.e5. doi: 10.1016/j.devcel.2019.03.029
15. Hu Y, Qian Y, Wei J, Jin T, Kong X, Cao H, et al. The Disulfiram/Copper complex induces autophagic cell death in colorectal cancer by targeting Ulk1. *Front Pharmacol* (2021) 12:752825. doi: 10.3389/fphar.2021.752825
16. Peng Y, Wang Y, Zhou C, Mei W, Zeng C. Pi3k/Akt/mTOR pathway and its role in cancer therapeutics: Are we making headway? *Front Oncol* (2022) 12:819128. doi: 10.3389/fonc.2022.819128
17. Wei R, Xiao Y, Song Y, Yuan H, Luo J, Xu W. Fat4 regulates the emt and autophagy in colorectal cancer cells in part Via the Pi3k-akt signaling axis. *J Exp Clin Cancer Res* (2019) 38(1):112. doi: 10.1186/s13046-019-1043-0
18. Ma Z, Lou S, Jiang Z. Phlda2 regulates emt and autophagy in colorectal cancer Via the Pi3k/Akt signaling pathway. *Aging (Albany N Y)* (2020) 12(9):7985–8000. doi: 10.18632/aging.103117
19. Yuan J, Dong X, Yap J, Hu J. The mapk and ampk signalings: Interplay and implication in targeted cancer therapy. *J Hematol Oncol* (2020) 13(1):113. doi: 10.1186/s13045-020-00949-4
20. Zuo Q, Liao L, Yao ZT, Liu YP, Wang DK, Li SJ, et al. Targeting Pp2a with lomitapide suppresses colorectal tumorigenesis through the activation of Ampk/Beclin1-mediated autophagy. *Cancer Lett* (2021) 521:281–93. doi: 10.1016/j.canlet.2021.09.010
21. Levy JMM, Towers CG, Thorburn A. Targeting autophagy in cancer. *Nat Rev Cancer* (2017) 17(9):528–42. doi: 10.1038/nrc.2017.53
22. Zhu Y, Huang S, Chen S, Chen J, Wang Z, Wang Y, et al. Sox2 promotes chemoresistance, cancer stem cells properties, and epithelial-mesenchymal transition by B-catenin and Beclin1/Autophagy signaling in colorectal cancer. *Cell Death Dis* (2021) 12(5):449. doi: 10.1038/s41419-021-03733-5

23. Hu F, Song D, Yan Y, Huang C, Shen C, Lan J, et al. Il-6 regulates autophagy and chemotherapy resistance by promoting Becn1 phosphorylation. *Nat Commun* (2021) 12(1):3651. doi: 10.1038/s41467-021-23923-1
24. Kumar B, Ahmad R, Sharma S, Gowrikumar S, Primeaux M, Rana S, et al. Ptk3c3 inhibition promotes sensitivity to colon cancer therapy by inhibiting cancer stem cells. *Cancers (Basel)* (2021) 13(9):2168. doi: 10.3390/cancers13092168
25. Galluzzi L, Green DR. Autophagy-independent functions of the autophagy machinery. *Cell* (2019) 177(7):1682–99. doi: 10.1016/j.cell.2019.05.026
26. Hu WH, Yang WC, Liu PF, Liu TT, Morgan P, Tsai WL, et al. Clinicopathological association of autophagy related 5 protein with prognosis of colorectal cancer. *Diagnostics (Basel Switzerland)* (2021) 11(5):782. doi: 10.3390/diagnostics11050782
27. Foerster EG, Mukherjee T, Cabral-Fernandes L, Rocha JDB, Girardin SE, Philpott DJ. How autophagy controls the intestinal epithelial barrier. *Autophagy* (2022) 18(1):86–103. doi: 10.1080/15548627.2021.1909406
28. Don Wai Luu L, Kaakoush NO, Castaño-Rodríguez N. The role of Atg16l2 in autophagy and disease. *Autophagy [Preprint]* (2022) 1–10. Available at: <https://www.tandfonline.com/doi/abs/10.1080/15548627.2022.2042783> (Accessed Aug 30, 2022).
29. Lystad AH, Carlsson SR, Simonsen A. Toward the function of mammalian Atg12-Atg5-Atg16l1 complex in autophagy and related processes. *Autophagy* (2019) 15(8):1485–6. doi: 10.1080/15548627.2019.1618100
30. Liu PF, Leung CM, Chang YH, Cheng JS, Chen JJ, Weng CJ, et al. Atg4b promotes colorectal cancer growth independent of autophagic flux. *Autophagy* (2014) 10(8):1454–65. doi: 10.4161/auto.29556
31. Scherr AL, Jassowicz A, Pató A, Ellsner C, Ismail L, Schmitt N, et al. Knockdown of Atg7 induces nuclear-Lc3 dependent apoptosis and augments chemotherapy in colorectal cancer cells. *Int J Mol Sci* (2020) 21(3):1099. doi: 10.3390/ijms21031099
32. Zhang S, Yang Z, Bao W, Liu L, You Y, Wang X, et al. Snx10 (Sorting nexin 10) inhibits colorectal cancer initiation and progression by controlling autophagic degradation of src. *Autophagy* (2020) 16(4):735–49. doi: 10.1080/15548627.2019.1632122
33. Xiang X, Tian Y, Hu J, Xiong R, Bautista M, Deng L, et al. Fangchinoline exerts anticancer effects on colorectal cancer by inducing autophagy via regulation Ampk/Mtor/Ulk1 pathway. *Biochem Pharmacol* (2021) 186:114475. doi: 10.1016/j.bcp.2021.114475
34. Hu S, Yin J, Yan S, Hu P, Huang J, Zhang G, et al. An epipolythiodioxopiperazine alkaloid, induces apoptosis and autophagy in colorectal cancer via ampk and Ptk3/Akt/Mtor pathways. *Bioorg Chem* (2021) 109:104693. doi: 10.1016/j.bioorg.2021.104693
35. Zhang W, Wu Z, Qi H, Chen L, Wang T, Mao X, et al. Celastrol upregulated Atg7 triggers autophagy via targeting Nur77 in colorectal cancer. *Phytomedicine* (2022) 104:154280. doi: 10.1016/j.phymed.2022.154280
36. Yu H, Yin S, Zhou S, Shao Y, Sun J, Pang X, et al. Magnolin promotes autophagy and cell cycle arrest via blocking Lif/Stat3/Mcl-1 axis in human colorectal cancers. *Cell Death Dis* (2018) 9(6):702. doi: 10.1038/s41419-018-0660-4
37. Li C, Zhang K, Pan G, Ji H, Li C, Wang X, et al. Dehydrodiisoeugenol inhibits colorectal cancer growth by endoplasmic reticulum stress-induced autophagic pathways. *J Exp Clin Cancer Res* (2021) 40(1):125. doi: 10.1186/s13046-021-01915-9
38. Lin S, Yang L, Yao Y, Xu L, Xiang Y, Zhao H, et al. Flubendazole demonstrates valid antitumor effects by inhibiting Stat3 and activating autophagy. *J Exp Clin Cancer Res* (2019) 38(1):293. doi: 10.1186/s13046-019-1303-z
39. Pan Z, Li X, Wang Y, Jiang Q, Jiang L, Zhang M, et al. Discovery of Thieno [2,3-D]Pyrimidine-Based hydroxamic acid derivatives as bromodomain-containing protein 4/Histone deacetylase dual inhibitors induce autophagic cell death in colorectal carcinoma cells. *J Medicinal Chem* (2020) 63(7):3678–700. doi: 10.1021/acs.jmedchem.9b02178
40. Zhang N, Yang Y, Wang Z, Yang J, Chu X, Liu J, et al. Polypeptide-engineered DNA tetrahedrons for targeting treatment of colorectal cancer via apoptosis and autophagy. *J Control Release* (2019) 309:48–58. doi: 10.1016/j.jconrel.2019.07.012
41. Porter RJ, Murray GI, Alnabulsi A, Humphries MP, James JA, Salto-Tellez M, et al. Colonic epithelial cathelicidin (LI-37) expression intensity is associated with progression of colorectal cancer and presence of Cd8(+) T cell infiltrate. *J Pathol Clin Res* (2021) 7(5):495–506. doi: 10.1002/cjp.2222
42. Slack FJ, Chinnaiyan AM. The role of non-coding rnas in oncology. *Cell* (2019) 179(5):1033–55. doi: 10.1016/j.cell.2019.10.017
43. Liang J, Zhang L, Cheng W. Non-coding rna-mediated autophagy in cancer: A protumor or antitumor factor? *Biochim Biophys Acta Rev Cancer* (2021) 1876(2):188642. doi: 10.1016/j.bbcan.2021.188642
44. Chu CA, Lee CT, Lee JC, Wang YW, Huang CT, Lan SH, et al. Mir-338-5p promotes metastasis of colorectal cancer by inhibition of phosphatidylinositol 3-kinase, catalytic subunit type 3-mediated autophagy pathway. *EBioMedicine* (2019) 43:270–81. doi: 10.1016/j.ebiom.2019.04.010
45. Sun W, Li J, Zhou L, Han J, Liu R, Zhang H, et al. The c-Myc/Mir-27b-3p/Atg10 regulatory axis regulates chemoresistance in colorectal cancer. *Theranostics* (2020) 10(5):1981–96. doi: 10.7150/thno.37621
46. Si Y, Yang Z, Ge Q, Yu L, Yao M, Sun X, et al. Long non-coding rna Malat1 activated autophagy, hence promoting cell proliferation and inhibiting apoptosis by sponging mir-101 in colorectal cancer. *Cell Mol Biol Lett* (2019) 24:50. doi: 10.1186/s11658-019-0175-8
47. Zhou J, Wang M, Mao A, Zhao Y, Wang L, Xu Y, et al. Long noncoding rna Malat1 sponging mir-26a-5p to modulate Smad1 contributes to colorectal cancer progression by regulating autophagy. *Carcinogenesis* (2021) 42(11):1370–9. doi: 10.1093/carcin/bgab069
48. Wang X, Lan Z, He J, Lai Q, Yao X, Li Q, et al. Lncrna Snhg6 promotes chemoresistance through Ulk1-induced autophagy by sponging mir-26a-5p in colorectal cancer cells. *Cancer Cell Int* (2019) 19:234. doi: 10.1186/s12935-019-0951-6
49. Han Y, Zhou S, Wang X, Mao E, Huang L. Snhg14 stimulates cell autophagy to facilitate cisplatin resistance of colorectal cancer by regulating mir-186/Atg14 axis. *BioMed Pharmacother* (2020) 121:109580. doi: 10.1016/j.biopha.2019.109580
50. Islam Khan MZ, Law HKW. Cancer susceptibility candidate 9 (Casc9) promotes colorectal cancer carcinogenesis via mtor-dependent autophagy and epithelial-mesenchymal transition pathways. *Front Mol Biosci* (2021) 8:627022. doi: 10.3389/fmolb.2021.627022
51. Wang Y, Li Z, Xu S, Li W, Chen M, Jiang M, et al. Lncrna firre functions as a tumor promoter by interaction with Ptbp1 to stabilize Becn1 mrna and facilitate autophagy. *Cell Death Dis* (2022) 13(2):98. doi: 10.1038/s41419-022-04509-1
52. Yang BL, Liu GQ, Li P, Li XH. Circular rna Cul2 regulates the development of colorectal cancer by modulating apoptosis and autophagy via mir-208a-3p/Ppp6c. *Aging (Albany N Y)* (2022) 14(1):497–508. doi: 10.18632/aging.203827
53. Zhang Y, Li C, Liu X, Wang Y, Zhao R, Yang Y, et al. Circchipk3 promotes oxaliplatin-resistance in colorectal cancer through autophagy by sponging mir-637. *EBioMedicine* (2019) 48:277–88. doi: 10.1016/j.ebiom.2019.09.051
54. Martins WK, Belotto R, Silva MN, Grasso D, Suriani MD, Lavor TS, et al. Autophagy regulation and photodynamic therapy: Insights to improve outcomes of cancer treatment. *Front Oncol* (2020) 10:610472. doi: 10.3389/fonc.2020.610472
55. Kwiatkowski S, Knap B, Przysupski D, Sackzo J, Kędzierska E, Knap-Czop K, et al. Photodynamic therapy - mechanisms, photosensitizers and combinations. *BioMed Pharmacother* (2018) 106:1098–107. doi: 10.1016/j.biopha.2018.07.049
56. Song C, Xu W, Wu H, Wang X, Gong Q, Liu C, et al. Photodynamic therapy induces autophagy-mediated cell death in human colorectal cancer cells via activation of the Ros/Jnk signaling pathway. *Cell Death Dis* (2020) 11(10):938. doi: 10.1038/s41419-020-03136-y
57. Shi X, Zhang H, Jin W, Liu W, Yin H, Li Y, et al. Metronomic photodynamic therapy with 5-aminolevulinic acid induces apoptosis and autophagy in human Sw837 colorectal cancer cells. *J Photochem Photobiol B* (2019) 198:111586. doi: 10.1016/j.jphotobiol.2019.111586
58. Gholizadeh M, Doustvandi MA, Mohammadnejad F, Shadbad MA, Tajalli H, Brunetti O, et al. Photodynamic therapy with zinc phthalocyanine inhibits the stemness and development of colorectal cancer: Time to overcome the challenging barriers? *Molecules* (2021) 26(22):6877. doi: 10.3390/molecules26226877
59. Chen J, Na R, Xiao C, Wang X, Wang Y, Yan D, et al. The loss of Shmt2 mediates 5-fluorouracil chemoresistance in colorectal cancer by upregulating autophagy. *Oncogene* (2021) 40(23):3974–88. doi: 10.1038/s41388-021-01815-4
60. Zhao C, Qiu S, He J, Peng Y, Xu H, Feng Z, et al. Prodigiosin impairs autophagosome-lysosome fusion that sensitizes colorectal cancer cells to 5-Fluorouracil-Induced cell death. *Cancer Lett* (2020) 481:15–23. doi: 10.1016/j.canlet.2020.03.010
61. Liu Y, Chen X, Chen X, Liu J, Gu H, Fan R, et al. Long non-coding rna hotair knockdown enhances radiosensitivity through regulating microrna-93/Atg12 axis in colorectal cancer. *Cell Death Dis* (2020) 11(3):175. doi: 10.1038/s41419-020-2268-8
62. Bhinder B, Gilvary C, Madhukar NS, Elemento O. Artificial intelligence in cancer research and precision medicine. *Cancer Discov* (2021) 11(4):900–15. doi: 10.1158/2159-8290.Cd-21-0090

## Glossary

5-FU	5-Fluorouracil
AI	artificial intelligence
ALA	5-aminolevulinic acid
AMBRA1	autophagy and beclin 1 regulator 1
AMPK	AMP-activated protein kinase
aPDT	acute PDT
ATG	autophagy-related gene
BECN1	coiled-coil myosin-like BCL2-interacting protein
BRD4	bromodomain-containing protein 4
CASC9	cancer susceptibility candidate 9
CDX	cell-derived xenograft
ceRNA	competing endogenous RNA
circRNA	circular RNA
CQ	chloroquine
CRC	colorectal cancer
ENCORI	The Encyclopedia of RNA Interactomes
ER	endoplasmic reticulum
FAT4	FAT tumor suppressor homolog 4
FDA	Food and Drug Administration
FIRRE	functional intergenic repeating RNA element
HDAC	histone deacetylases
HOTAIR	homeobox transcript antisense intergenic RNA
IL-6	interleukin-6
JAK2	Janus kinase 2
JNK	c-Jun N-terminal kinase
LAMP1	lysosome-associated membrane protein 1
LIF	leukemia inhibitory factor

(Continued)

## Continued

lncRNA	long non-coding RNA
MALAT1	metastasis-associated lung adenocarcinoma transcript 1
miRNAs	microRNAs
mPDT	metronomic PDT
mTOR	mechanistic target of rapamycin
m-THPC	meta-tetrahydroxyphenylchlorin
ncRNA	non-coding RNA
PDT	photodynamic therapy
PDX	patient-derived tumor xenograft
PE	phosphatidylethanolamine
PHLDA2	pleckstrin homology like domain family A member 2
PI3K	phosphoinositide 3-kinase
PIK3C3	phosphatidylinositol 3-kinase catalytic subunit type 3
PIK3R4	phosphoinositide 3-kinase regulatory subunit 4
PPP6C	protein phosphatase 6 catalytic subunit
RAB7A	Ras-related protein Rab-7a
RB1CC1	RB1-inducible coiled-coil 1
ROS	reactive oxygen species
SHMT2	serine hydroxymethyltransferase-2
SNHG6	small nucleolar RNA host gene 6
SNHG14	small nucleolar RNA host gene 14
SNX10	sorting nexin 10
SOX2	sex-determining region Y-box2
STAT3	signal transducer and activator of transcription 3
TCGA	The Cancer Genome Atlas
TD	tetrahedron
TSC1/2	tuberous sclerosis complex 1 and 2
ULK1	UNC-51-like autophagy-activating kinase 1
UVRAG	UV radiation resistance-associated
VP	verteporfin
ZnPc	zinc phthalocyanine.



## OPEN ACCESS

## EDITED BY

Guan Wang,  
Sichuan University, China

## REVIEWED BY

Yunlong Lei,  
Chongqing Medical University, China  
Donglai Ma,  
Hebei University of Chinese Medicine,  
China  
Lin Wang,  
Shandong Agricultural University, China

## \*CORRESPONDENCE

Jian Pan,  
panjian2019@suda.edu.cn  
Jian Wang,  
szuwj2022@163.com

## SPECIALTY SECTION

This article was submitted to  
Pharmacology of Anti-Cancer Drugs,  
a section of the journal  
Frontiers in Pharmacology

RECEIVED 24 June 2022

ACCEPTED 05 September 2022

PUBLISHED 16 September 2022

## CITATION

Yang R, Ma S, Zhuo R, Xu L, Jia S, Yang P,  
Yao Y, Cao H, Ma L, Pan J and Wang J  
(2022), Suppression of endoplasmic  
reticulum stress-dependent autophagy  
enhances cynaropicrin-induced  
apoptosis via attenuation of the P62/  
Keap1/Nrf2 pathways in neuroblastoma.  
*Front. Pharmacol.* 13:977622.  
doi: 10.3389/fphar.2022.977622

## COPYRIGHT

© 2022 Yang, Ma, Zhuo, Xu, Jia, Yang,  
Yao, Cao, Ma, Pan and Wang. This is an  
open-access article distributed under  
the terms of the [Creative Commons  
Attribution License \(CC BY\)](https://creativecommons.org/licenses/by/4.0/). The use,  
distribution or reproduction in other  
forums is permitted, provided the  
original author(s) and the copyright  
owner(s) are credited and that the  
original publication in this journal is  
cited, in accordance with accepted  
academic practice. No use, distribution  
or reproduction is permitted which does  
not comply with these terms.

# Suppression of endoplasmic reticulum stress-dependent autophagy enhances cynaropicrin-induced apoptosis via attenuation of the P62/Keap1/Nrf2 pathways in neuroblastoma

Randong Yang<sup>1,2</sup>, Shurong Ma<sup>1,2</sup>, Ran Zhuo<sup>1,2</sup>, Lingqi Xu<sup>1,2</sup>,  
Siqi Jia<sup>2</sup>, Pengcheng Yang<sup>2</sup>, Ye Yao<sup>2</sup>, Haibo Cao<sup>2</sup>, Liya Ma<sup>1,2</sup>,  
Jian Pan<sup>2\*</sup> and Jian Wang<sup>1,2\*</sup>

<sup>1</sup>Institute of Pediatric Research, Children's Hospital of Soochow University, Suzhou, China,

<sup>2</sup>Department of Pediatric Surgery, Children's Hospital of Soochow University, Suzhou, China

Autophagy has dual roles in cancer, resulting in cellular adaptation to promote either cell survival or cell death. Modulating autophagy can enhance the cytotoxicity of many chemotherapeutic and targeted drugs and is increasingly considered to be a promising cancer treatment approach. Cynaropicrin (CYN) is a natural compound that was isolated from an edible plant (artichoke). Previous studies have shown that CYN exhibits antitumor effects in several cancer cell lines. However, its anticancer effects against neuroblastoma (NB) and the underlying mechanisms have not yet been investigated. More specifically, the regulation of autophagy in NB cells by CYN has never been reported before. In this study, we demonstrated that CYN induced apoptosis and protective autophagy. Further mechanistic studies suggested that ER stress-induced autophagy inhibited apoptosis by activating the p62/Keap1/Nrf2 pathways. Finally, *in vivo* data showed that CYN inhibited tumor growth in xenografted nude mice. Overall, our findings suggested that CYN may be a promising candidate for the treatment of NB, and the combination of pharmacological inhibitors of autophagy may hold novel therapeutic potential for the treatment of NB. Our paper will contribute to the rational utility and pharmacological studies of CYN in future anticancer research.

## KEYWORDS

cynaropicrin, apoptosis, autophagy, p62/Keap1/Nrf2, neuroblastoma

## Introduction

Neuroblastoma (NB), a malignant cancer originating from sympathetic nerves, is known to be the most common extracranial solid cancer in childhood, accounting for approximately 15% of all cancer-related paediatric deaths (Matthay et al., 2016; Youlden et al., 2020). Currently, there are multimodal strategies to treat NB, including surgery, radiotherapy, induction chemotherapy, immunotherapy and autologous stem cell transplantation either in combination or separately depending on the clinical features and disease stage (Cañete, 2020; Tas et al., 2020). However, the treatment of NB remains unsatisfactory, and the prognosis of advanced NB in children is poor, with a 5-year survival rate below 40% (Xu et al., 2018). Thus, there is a continuing need to develop new treatment strategies and drugs for NB.

Presently, there is mounting interest in the development of alternative medicines from plant-derived natural products with few side effects (Feng et al., 2011; Newman and Cragg, 2012; Fridlender et al., 2015). It has been estimated that roughly half of the drugs used in clinical practice have been derived from natural substances in recent years due to their anticancer activity (Kingston, 2011). Cynaropicrin (CYN), a sesquiterpene lactone, is a natural compound isolated from an edible plant (artichoke) (Zaib and Khan, 2020). Previous studies have reported that CYN exhibits phenomenal versatile biological and pharmacological abilities, including anti-inflammatory, antihepatitis C, antiparasitic, antibacterial, anti-photoaging, and antihyperlipidaemic properties and so on (Elsebai et al., 2016). More recently, the literature has proposed the antitumour efficacy of CYN, such as against colorectal cancer (Zheng et al., 2020), human melanoma (De Cicco et al., 2021), anaplastic thyroid cancer (Lepore et al., 2019), and lung carcinoma (Ding et al., 2021). However, to date, there are no studies on CYN with respect to NB, and the possible effects and underlying mechanisms of CYN on NB are still elusive.

It is currently well established from research that natural compounds possessing anticancer properties can induce apoptosis by modulating various intracellular pathways, including endoplasmic reticulum (ER) stress and autophagy (Elmore 2007; Nikolettou et al., 2013; Hasima and Ozpolat, 2014). Notably, the functional association between apoptosis, ER stress and autophagy is an extensive crosstalk network (Song et al., 2017). The ER is an organelle that is responsible for protein folding and calcium homeostasis maintenance. ER stress occurs when homeostatic processes are disrupted and primarily results in the activation of the unfolded protein response (UPR). There are three distinct pathways in the UPR: ATF6, PERK-eIF2 $\alpha$ -ATF4 and IRE1 (Healy et al., 2009). Furthermore, accumulating evidence has demonstrated the vital role of ER stress in apoptosis and autophagy in various tumour cells. Therefore, targeting the ER stress response is an effective

anticancer strategy. To date, recent studies have not revealed the relationship between CYN and ER stress.

Autophagy, commonly referred to as macroautophagy, can be triggered by ER stress (Radogna et al., 2015). The autophagic pathway includes vesicle elongation, autophagosome formation, maturation, autophagosome-lysosome fusion, and degradation (Choi et al., 2013). Autophagy acts as a double-edged sword that facilitates or inhibits apoptosis induction in cancer cells under stress conditions (Su et al., 2015; Song et al., 2017). Increasing evidence has indicated that inhibiting autophagy induced by chemotherapy or targeted therapeutic drugs can lead to favourable conditions in anticancer therapy by promoting cancer cell apoptosis (Rangwala et al., 2014; Datta et al., 2019). Similarly, nuclear factor-erythroid 2-related factor 2 (Nrf2) is another cellular protective signalling pathway conferring adaptive protection against proteotoxic stress. Under physiological conditions, Nrf2 is carried to the proteasome by Keap1 and is maintained at a low level through degradation by the ubiquitin proteasome system (Schmoll et al., 2017). Under stress conditions, Nrf2 is released from the Keap1-Nrf2 complex and translocates into the nucleus (Itoh et al., 2003). In addition to this classical pathway, in the p62-dependent noncanonical Keap1-Nrf2 pathway, p62 persistently activates Nrf2 through competitive interaction with Keap1 (Celesia et al., 2020; Dash et al., 2020). Evidence has shown that the Nrf2 signal pathway is related to the regulation of autophagy in cells under ER stress. Therefore, in this study, we investigated the anticancer efficacy of CYN against NB and further elucidated the role and potential mechanisms of CYN on ER stress, autophagy and the Nrf2 pathway in NB cells.

## Materials and methods

### Reagents and antibodies

CYN (97% purity) was purchased from Chengdu Biopurify Phytochemicals Ltd. (Chengdu, China), and a stock solution (100 mM) in dimethyl sulfoxide (DMSO;  $\geq 99.7\%$ , Sigma-Aldrich, St. Louis, MO, United States) was stored at  $-20^{\circ}\text{C}$ . The final concentrations of DMSO in all experiments were lower than 0.1% (V/V). RAPA (100 nM), 3-Methyladenine (3-MA, 2 mM), chloroquine (CQ, 10  $\mu\text{M}$ ) and TUDCA (2  $\mu\text{M}$ ) were purchased from MCE (Monmouth Junction, NJ, United States). Triton X-100, 4% paraformaldehyde and a bicinchoninic acid (BCA) protein assay kit were purchased from Beyotime Biotechnology (Shanghai, China). Primary antibodies against Bax, Bcl-2, Beclin-1, LC3B, p62/SQSTM1, Atg5, CHOP, GRP78, ATF6, p-eIF2 $\alpha$ , IRE1 $\alpha$  and LAMP-2 were purchased from Abcam (Cambridge, United Kingdom). Primary antibodies against PARP, cleaved caspase-3, caspase-3, Ki-67 and GAPDH were purchased from Cell Signaling Technology (Danvers, MA, United States).



## Cell culture

The human NB cell lines (SK-N-BE(2) and SH-SY5Y) and human 293FT cells were obtained from the National Collection of Authenticated Cell Cultures (Shanghai, China). Cells were cultured in DMEM/F12 supplemented with 10% FBS (all from Gibco-BRL, Grand Island, NY, United States) and 1% penicillin–streptomycin (Beyotime Biotechnology, Shanghai, China) at 37°C in a humidified atmosphere containing 5% CO<sub>2</sub>.

## Cell viability assay

SK-N-BE(2) and SH-SY5Y cells were seeded into 96-well plates ( $2 \times 10^4$  cells per well) and incubated overnight. Then, the cells were treated with different concentrations of CYN or DMSO. After stimulation, cell proliferation was determined using CCK-8 reagent (Dojindo Laboratories, Kumamoto, Japan) every 24 h for four consecutive days. The absorbance at 450 nm was measured with a microplate reader (Thermo Fisher Scientific, Grand Island, NY). The viability of control cells was taken as 100%.

## EdU experiment

An EdU kit (Beyotime, Shanghai, China) was used for the EdU staining assay. According to the manufacturer's instructions, the reaction solution was added to each well for 2 h of incubation in the dark. Afterwards, the cells were fixed with 4% paraformaldehyde for 30 min, and 0.3% Triton X-100 was added for 15 min at room temperature. After staining the nuclei with Hoechst 33342, the cells were collected under a fluorescence microscope (Olympus, Tokyo, Japan).

## Colony formation assay

NB cells were inoculated in six-well plates (1000 cells/well) and treated with different concentrations (0, 5, and 10  $\mu$ M) of CYN. After culturing for 14 days, cell colonies were immobilized with 4% paraformaldehyde for 30 min and stained with 0.5% crystal violet (Boster, Wuhan, Boster) for 15 min.

## Lentivirus preparation and infection

For the downregulation of CHOP and Nrf2, shRNA sequences were synthesized by IGE Biotechnology (Guangzhou, China). For lentivirus preparation, the packaging plasmid psPAX2 and envelope plasmid pMD2.G were purchased from IGE Biotechnology (Guangzhou, China). 293FT cells were

cotransfected with pMD2.G, psPAX2 and CHOP or Nrf2 plasmids for 6 h, and then the cell medium was removed for cell culture in fresh medium for 48 h. The viral supernatant was collected, filtered, and concentrated by PEG-8000 (Beyotime, Shanghai, China) precipitation. After incubation of the lentivirus with NB cells for 24 h, puromycin (Sigma–Aldrich, St. Louis, MO, United States) was used to screen for stable cell lines.

## Cell cycle analysis

Flow cytometry was used to perform cell cycle analysis. NB cells were trypsinized after CYN treatment for 24 h, fixed with 75% ethanol at 4°C overnight, and then incubated with 50  $\mu$ g/ml PI for 30 min at room temperature in the dark. Subsequently, the cells stained with PI fluorescence were detected with flow cytometry.

## Annexin V/PI staining

The extent of apoptosis was determined using an Annexin V/PI detection apoptosis kit (BD Biosciences, Heidelberg, Germany). After CYN treatment for 24 h, NB cells were trypsinized with trypsin solution without EDTA, harvested, washed with ice-cold PBS, and then resuspended in binding buffer. Subsequently, the cells were incubated with Annexin V and PI for 15 min at room temperature. After incubation, the results were assessed by flow cytometry (BD Biosciences, Heidelberg, Germany).

## Western blotting analysis

Total protein was lysed in RIPA buffer (Beyotime Biotechnology, Shanghai, China), and the cytoplasmic and nuclear proteins were extracted with a nuclear and cytoplasmic protein extraction kit (Beyotime Biotechnology, Shanghai, China). The protein samples were separated *via* SDS–PAGE and transferred to PVDF membranes. The membranes were blocked with TBST containing 5% skim milk for 1.5 h and subsequently incubated with primary antibodies at 4°C overnight, followed by incubation with secondary antibodies at room temperature for 1 h. Finally, images of the western blot bands were analysed using an ECL system (Perkin Elmer, Waltham, MA, United States).

## Immunofluorescence assay

After the designated treatments, NB cells were fixed in 4% paraformaldehyde for 30 min, permeabilized with 0.3% Triton X-100 for 15 min, incubated in 5% BSA for 1 h (all the above steps

were conducted at room temperature), and incubated with primary antibodies overnight at 4°C. The next day, Alexa Fluor 594 goat anti-rabbit IgG (Jackson, West Grove, PA, United States) or Alexa Fluor 488 goat anti-mouse IgG (Jackson, West Grove, PA, United States) was used as the secondary antibody. After incubation with the secondary antibody at room temperature for 1 h in the dark, the nuclei were stained with DAPI (Biosharp, Shanghai, China) for 5 min. Finally, the images were photographed by fluorescence microscopy (Olympus, Tokyo, Japan).

## Analysis of autophagy flux

NB cells were transfected with the mRFP-GFP-LC3 adenovirus (IGE Biotechnology, Guangzhou, China) for subsequent experimental studies for 24 h in DMEM/F12 supplemented with 10% FBS and 1% p/s. After washing with PBS, the cells were immediately fixed with 4% paraformaldehyde for 30 min, and 0.3% Triton X-100 was added for 15 min at room temperature. Subsequently, the nuclei were stained with DAPI for 5 min at room temperature. Autophagic flux measurements were performed with laser scanning confocal microscopes (Olympus, Tokyo, Japan).

## Coimmunoprecipitation assay

After treatment with CYN, the total cellular proteins were harvested by centrifugation and incubated with p62 or Keap1 antibody at 4°C overnight. Next, the cell lysates were incubated with protein A/G agarose beads for 4 h at 4°C. After elution from the bead-bound immunocomplexes, western blotting, as described for the western blot assay, was carried out to determine the protein levels.

## Transmission electron microscopy

Transmission electron microscopy (TEM) was used to visualize the autophagosomes and autolysosomes. NB cells were harvested by trypsinization, fixed with 2.5% glutaraldehyde overnight at 4°C, and postfixated with 1% OsO<sub>4</sub> (pH 7.4) for 2 h at room temperature. After OsO<sub>4</sub> removal, the samples were dehydrated in a graded ethanol series (30–100%), infiltrated, and embedded in resin. After polymerization of the resin at 55°C for 36 h, serial sections were cut with a Leica EM UC7 ultramicrotome (Leica, Nussloch, Germany). Sections were stained with uranyl acetate and alkaline lead citrate and then examined under a Gatan SC1000 (Model 832) CCD camera (Gatan, Pleasanton, CA, United States).

## In Vivo experiments

Female BALB/c nude mice (4 weeks old) received a subcutaneous injection of NB cells ( $2 \times 10^6$  cells per mouse) suspended in 100  $\mu$ l of extracellular matrix gel (Corning, NY, United States) into their front flanks. The mice were randomly divided into two groups ( $n = 5$ ) and treated with CYN once a day for 3 weeks (0 or 5 mg/kg, i.g.). This concentration was referred to the article by Zhang et al. (Zheng et al., 2020). Tumour volumes and mouse weights were measured every 3 days. Tumour volumes were calculated with the formula (length  $\times$  width  $\times$  height)/2. After 3 weeks, all the mice were sacrificed by euthanasia, and afterwards, the tumours were quickly collected for weight measurements and then embedded in paraffin for immunohistochemistry.

## Immunohistochemistry

Tumour tissues were fixed in 4% paraformaldehyde and embedded in paraffin for sectioning. The sections were dewaxed in xylene and rehydrated in graded alcohol solutions. Primary antibodies (anti-Ki-67, anti-cleaved caspase-3, anti-Bec1-1, and anti-CHOP) were added for overnight incubation at 4°C, followed by staining with a secondary antibody (Thermo Fisher Scientific, Grand Island, NY) for 30 min at 37°C. An ultrasensitive SP (Mouse/Rabbit) IHC Kit and DAB Plus Kit (MXB Biotechnologies, China) were used following the manufacturer's protocols. Before dehydration and mounting, the sections were counterstained with haematoxylin. Finally, images were examined using an Olympus microscope camera (Tokyo, Japan).

## Statistical analysis of data

All experiments were repeated at least three times, and the data are expressed as the mean  $\pm$  SD. Statistical significance was analysed using *t* test (two groups) or one-way ANOVA (multiple groups), and a *p* value <0.05 was considered statistically significant.

## Results

### CYN inhibited the proliferation of NB cells

The chemical structure of CYN is shown in Figure 1A. To determine the effect of CYN on the proliferation of NB cells, the viability of NB cells treated with different concentrations of CYN (0, 2.5, 5, 10, 20 and 40  $\mu$ M) for 24, 48, 72 and 96 h was

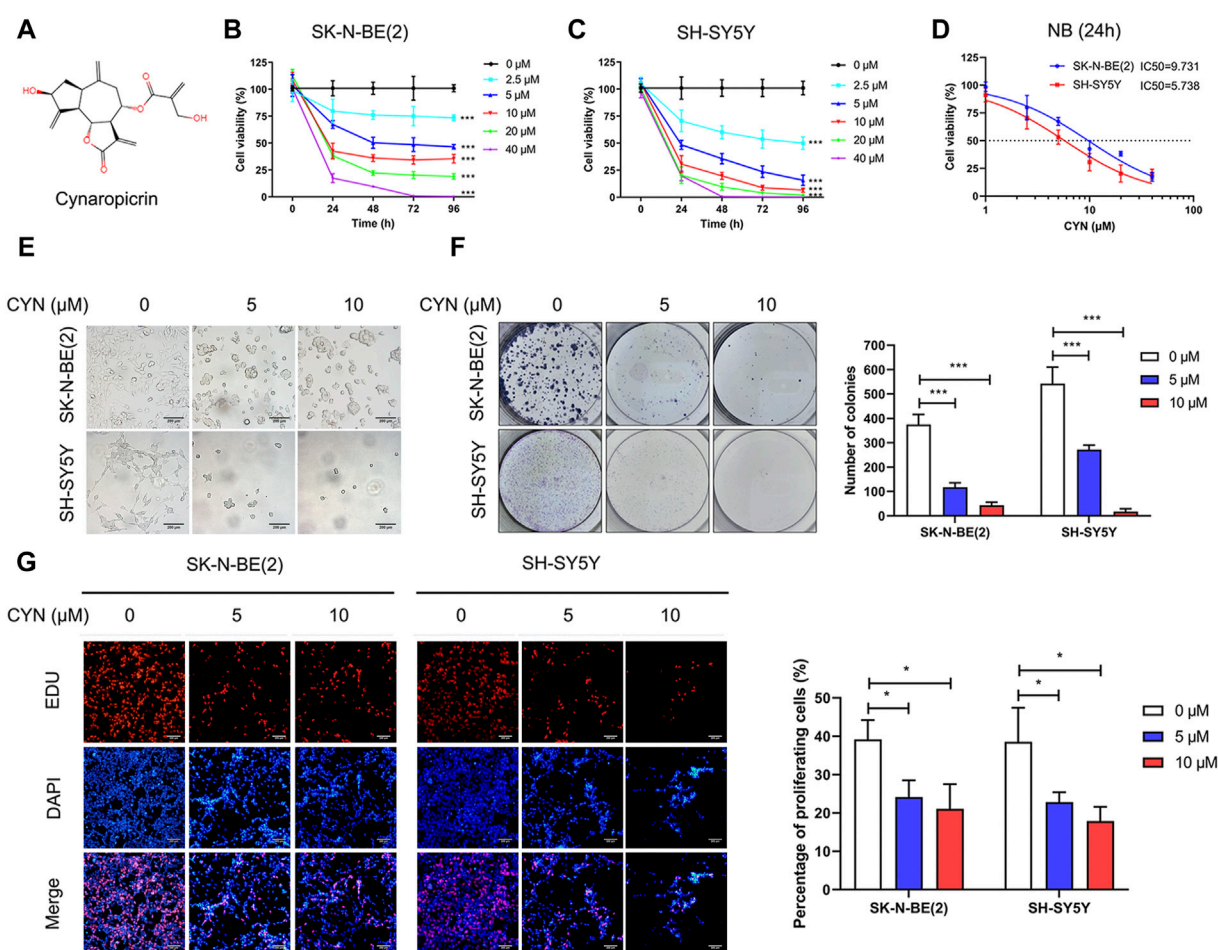


FIGURE 1

Effects of CYN on cell viability in NB cells. (A) The structure of cynaropicrin. (B,C) Cell viability was evaluated by CCK-8 assay. (D) IC<sub>50</sub> was analyzed via the cell viability assay. (E) Morphological changes of NB cells (Scale bar = 200  $\mu$ m). (F) Colony formation assay of NB cells treated with CYN. (G) EdU incorporation assay of NB cells treated with CYN (Scale bar = 200  $\mu$ m). \* $p < 0.05$ , \*\*\* $p < 0.001$  versus the control group.

investigated by CCK-8 assay. The results showed that CYN inhibited NB cell proliferation in a time- and dose-dependent manner (Figures 1B,C). Further analysis showed that the IC<sub>50</sub> values for SK-N-BE(2) and SH-SY5Y cells were 9.731 and 5.738  $\mu$ M at 24 h, respectively (Figure 1D). Therefore, concentrations of 5 and 10  $\mu$ M were selected for the following experiments. Compared with the control, an increase in the number of floating dead cells and cell shrinkage, which are suggestive of cell death, were observed 24 h after CYN treatment (Figure 1E). Subsequently, a colony formation assay was performed to further examine the CYN-mediated inhibition of NB cell proliferation, and the results showed that CYN significantly inhibited colony formation (Figure 1F). Next, an EdU assay was used to examine the antiproliferative activities of CYN against NB cells. As shown in Figure 1G, CYN significantly suppressed DNA replication

in NB cells. Collectively, these data proved that CYN had a significant inhibitory effect on the proliferation of NB cells.

## CYN induced cell cycle arrest and NB cell apoptosis

To further determine whether cell cycle distribution and apoptosis participate in the inhibition of NB cell proliferation, we first investigated the effect of CYN on cell cycle distribution by flow cytometry. The results showed that CYN treatment markedly arrested NB cells at the G2 phase (Figure 2A). We next explored the effect of CYN on the apoptosis of NB cells using Annexin V/PI staining and flow cytometry. The flow cytometry data revealed that CYN significantly increased the apoptosis rates in NB cells with increasing dosage (Figure 2B). In addition,

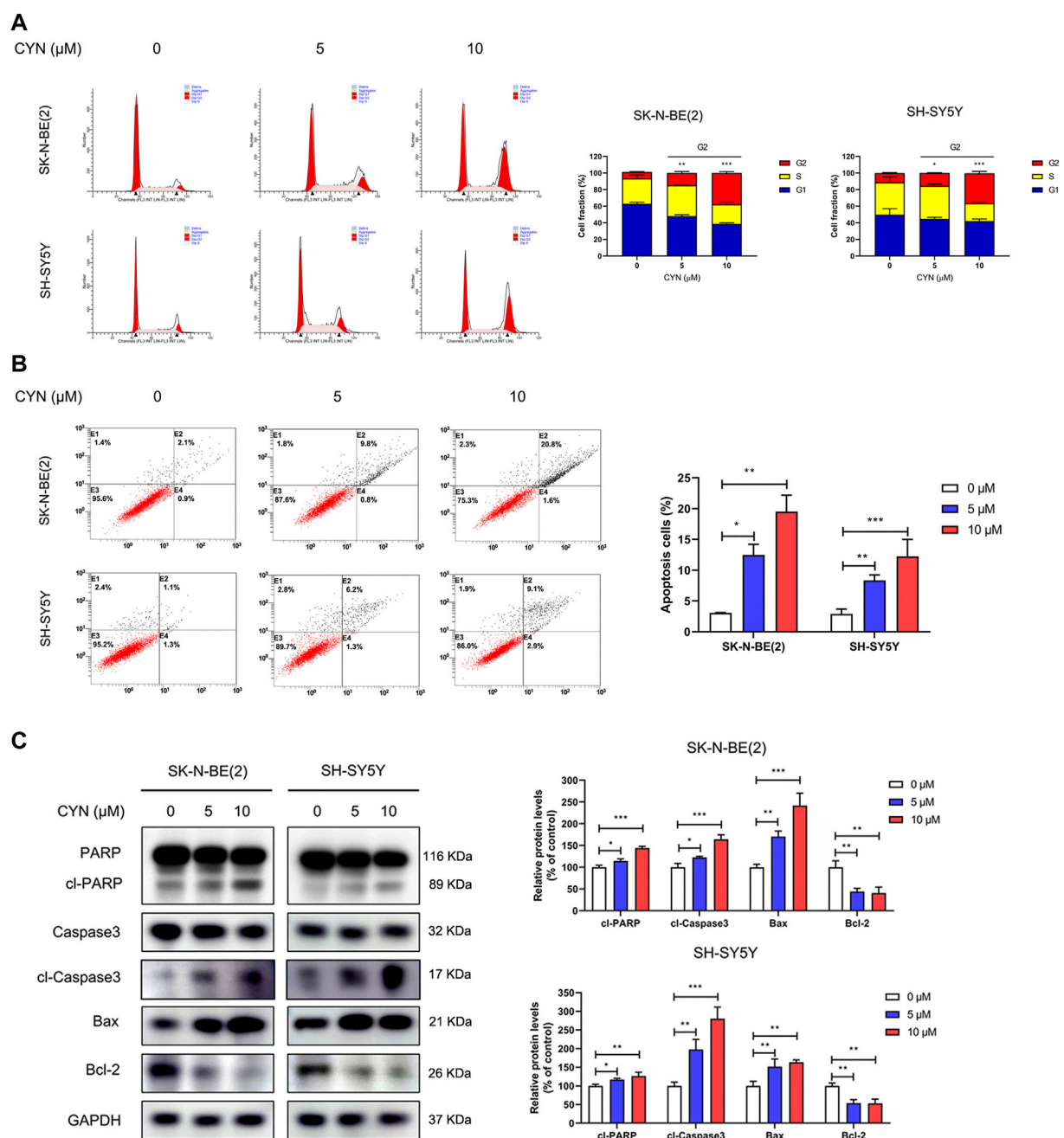


FIGURE 2

Effects of CYN on the cell cycle and apoptosis in NB cells. (A) Cell cycle was analyzed by flow cytometry. (B) Annexin V-FITC/PI staining and flow cytometry were used to measure and analyze apoptotic NB cells treated with CYN for 24 h. (C) The expression levels of apoptosis markers were measured by western blot analysis. \* $p < 0.05$ , \*\* $p < 0.01$ , \*\*\* $p < 0.001$  versus the control group.

western blot analysis showed that the expression levels of cleaved PARP, cleaved caspase-3, and Bax were considerably upregulated, while the expression level of Bcl-2 was downregulated after treatment with CYN (Figure 2C). Thus, the above evidence illustrated that CYN affected the proliferation of NB cells by inducing cell cycle arrest and apoptosis.

## CYN initiated autophagy and inhibited autophagic flux in NB cells

The correlation between autophagy and apoptosis in tumour cells has been previously reported (Rangwala et al., 2014; Su et al., 2015; Song et al., 2017; Datta et al., 2019). To assess CYN-



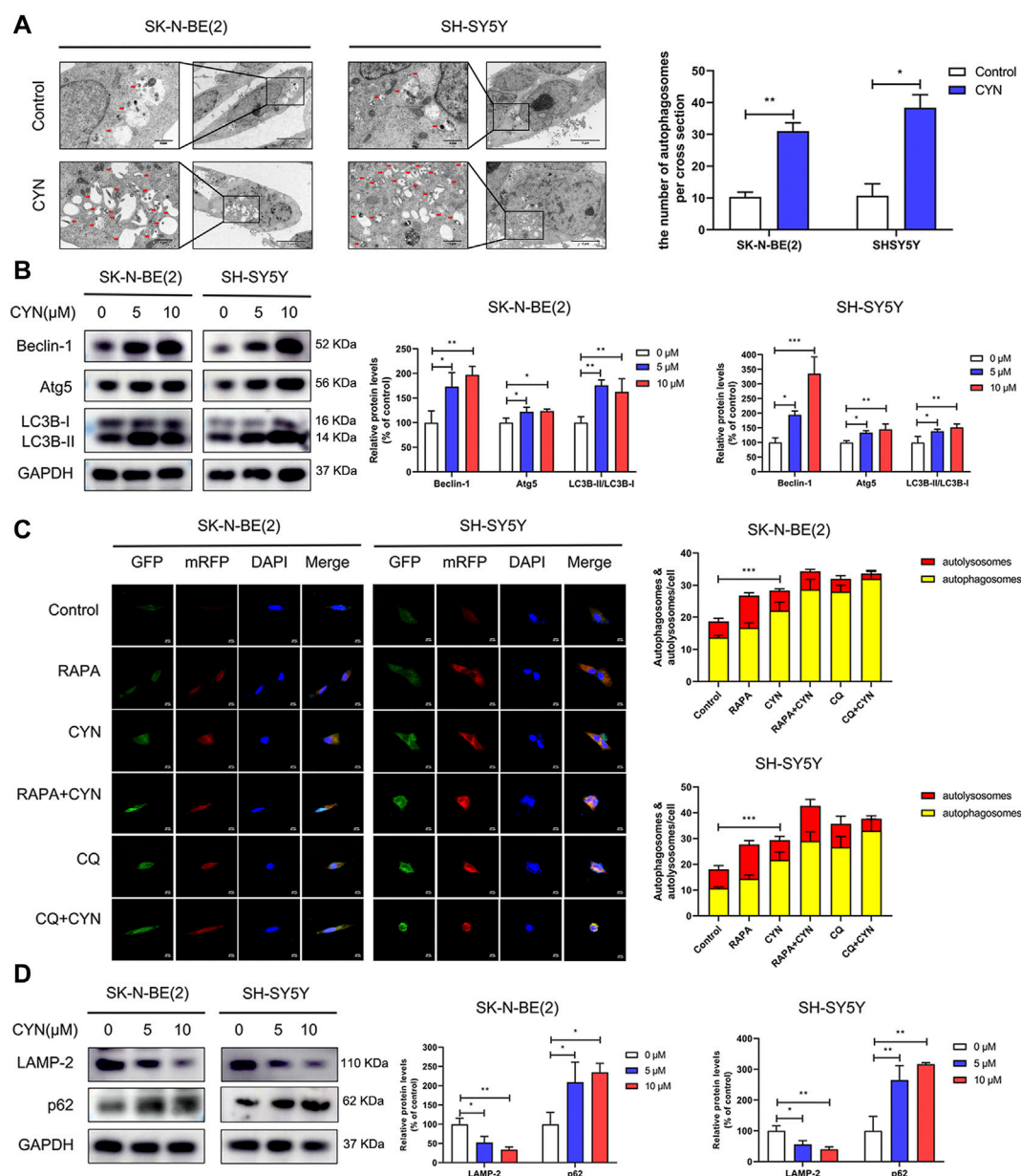


FIGURE 3

Effects of CYN on the autophagy level in NB cells. (A) Transmission electron microscopy (TEM) was utilized to observe the ultrastructure of NB cells, and the arrows indicate autophagosomes. (B) The expression levels of autophagy markers were analyzed by western blotting. (C) Confocal microscopy was utilized to detect fluorescence of mRFP-GFP-LC3. (D) Western blotting analysis of LAMP-2 and p62 protein expression. \* $p < 0.05$ , \*\* $p < 0.01$ , \*\*\* $p < 0.001$  versus the control group.

induced autophagy, transmission electron microscopy (TEM) was used. The TEM images showed a notably increased number of autophagic vacuoles (Figure 3A, red arrow) in the cytoplasmic area of CYN-treated NB cells compared with the control group. We also evaluated the expression levels of autophagy-related proteins by western blotting. As shown in Figure 3B, CYN increased Beclin-1, Atg5 and LC3B-II protein levels and the LC3B-II/LC3B-I ratio.

Furthermore, autophagic flux, as a dynamic process, manifests as autophagosome formation and autophagic degradation. Blocking the fusion of autophagosomes and lysosomes impairs autophagic degradation (Mizushima et al., 2010). Thus, NB cells transfected with mRFP-GFP-LC3 adenovirus were applied to distinguish autophagosomes and autolysosomes. The GFP-tag in the mRFP-GFP-LC3 fusion protein is quenched, while the mRFP-tag remains



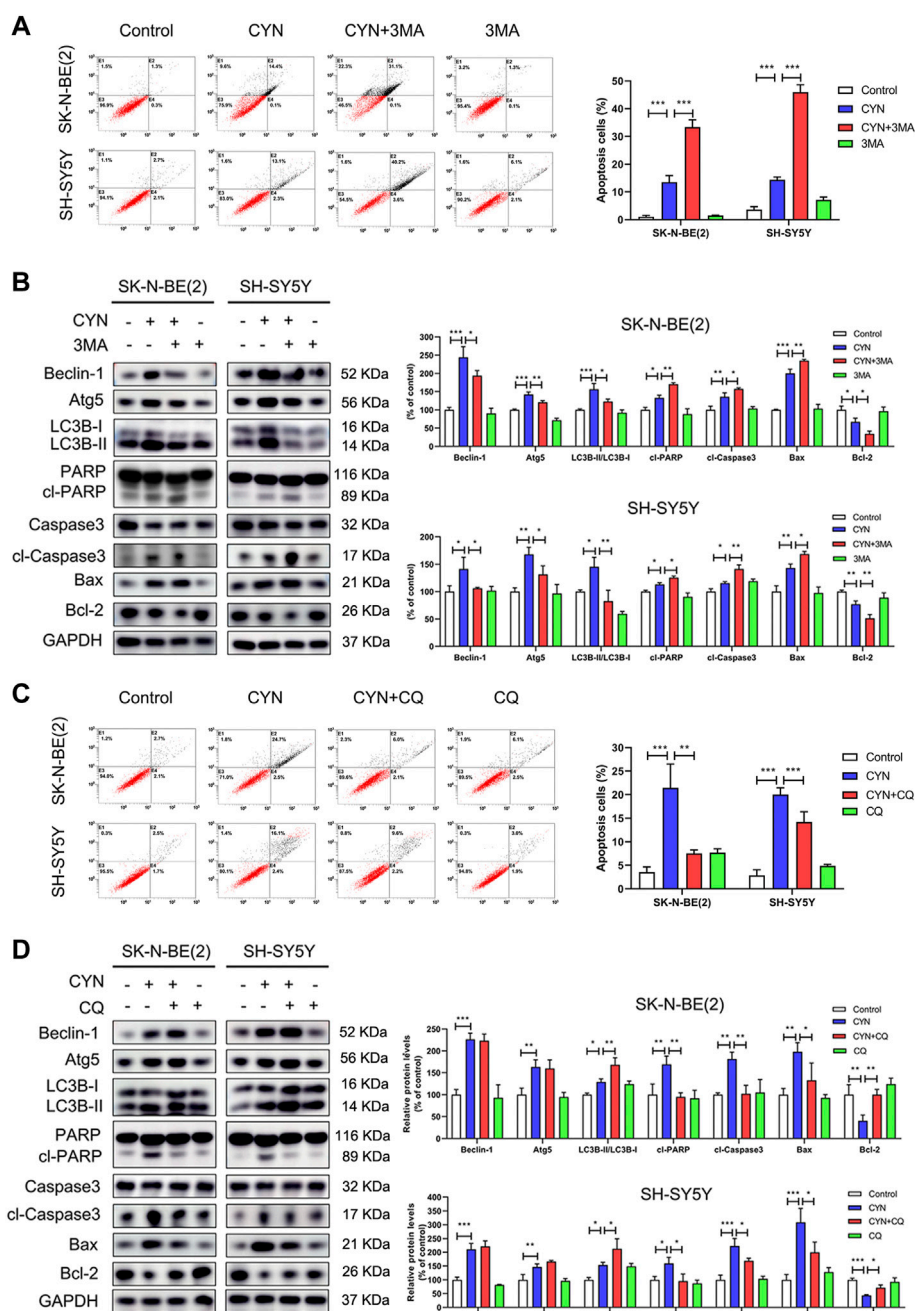


FIGURE 4

Relationship between apoptosis and autophagy in NB cells treated by CYN. (A) Apoptosis of NB cells was measured and analyzed by flow cytometry. (B) The expression levels of autophagy and apoptosis markers were analyzed by western blotting. (C) The number of apoptotic cells was assessed by Annexin V-FITC/PI staining and flow cytometry. (D) The expression levels of apoptosis markers were measured by western blot analysis.  $*p < 0.05$ ,  $**p < 0.01$ ,  $***p < 0.001$  versus the control group.  $*p < 0.05$ ,  $**p < 0.01$ ,  $***p < 0.001$  versus the CYN group.

in the acidic pH environment of autolysosomes. Therefore, in early autophagosomes, the red puncta overlaid with the green puncta and appeared yellow in the merged images, while in the autolysosomes, the free red puncta did not cover the green puncta and appeared red in the merged images. As shown in

Figure 3C, RAPA (100 nM, an autophagy inducer) enhanced the formation of both green and red puncta, and colocalization gave rise to more yellow and red-only puncta, suggesting the accumulation of autophagosomes and the maturation of autolysosomes. Conversely, both CYN and CQ (10  $\mu$ M, an

inhibitor of autophagosome-lysosome fusion) dramatically increased the number of red and green puncta. After colocalization, yellow fluorescence significantly increased instead of red fluorescence, indicating that CYN autophagic flux blocked the autophagosome-autolysosome fusion process, similar to CQ. Next, we examined the fluorescence colocalization of LC3B and LAMP-2. LAMP-2, as an autophagosome-lysosomal fusion marker, can reflect the maturation of autolysosomes. Minimal colocalization of LC3B and LAMP-2 was found after CYN treatment (Supplementary Figure S1), which further confirmed that CYN can block autophagosome-lysosome fusion. Additionally, stimulation of autophagic flux can cause the depletion of p62, an autophagy adapter protein. The implication is that upon the impairment of autophagic degradation, p62 accumulates within cells. Herein, we found that CYN suppressed the expression of LAMP-2 and increased the expression of p62 in a dose-dependent manner (Figure 3D). Taken together, these results suggested that CYN-induced autophagosome accumulation was due to both the initiation of autophagy and the inhibition of autophagic flux.

## Autophagy stimulated by CYN partially attenuated apoptotic cell death in NB cells

Having clearly established that CYN activated autophagy in NB cells, we then attempted to determine the functional relationship between autophagy and apoptosis after CYN treatment. In our studies, the protein level of Atg5 was significantly increased in NB cells after CYN treatment (Figure 3B). To validate the relationship between CYN-induced autophagy and apoptosis, we silenced Atg5 by siRNA and used Annexin V-FITC/PI staining by flow cytometry and western blotting to examine apoptosis. The results showed that silencing of Atg5 significantly attenuated LC3-II accumulation and increased apoptosis in NB cells (Supplementary Figure S2). Additionally, Either 3 MA (2 mM, a specific early-phase autophagy inhibitor) or CQ (10  $\mu$ M, a specific late-phase autophagy inhibitor) was used in NB cells. As illustrated in Figure 4A, cotreatment with CYN and 3-MA resulted in markedly more apoptosis than treatment with CYN (10  $\mu$ M) alone. In addition, the western blot data showed that CYN and 3 MA cotreatment attenuated the effects of CYN on the expression levels of autophagy-related proteins (Beclin-1, Atg5 and LC3B) and increased the expression of apoptotic markers compared with CYN treatment (Figure 4B). The above results suggested that inhibiting autophagy with 3 MA enhanced the apoptotic effects of CYN in NB cells. Contrary to the above results, CQ partly abolished the induction of cell apoptosis induced by CYN (Figure 4C). Consistent with the results from flow cytometry, CQ effectively inhibited the CYN-induced upregulation of the expression of apoptotic markers

(Figure 4D). In addition, CQ enhanced the effect of CYN on the expression level of LC3B but had no effect on Beclin-1 and Atg5. These data suggested that CYN played a protective role in CYN-induced NB cell apoptosis by initiating autophagy and blocking autophagosome-lysosomal fusion.

## NB cell apoptosis induced by CYN could Be partially abrogated by autophagy mediated by triggering ER stress

Increasing evidence has indicated that ER stress is related to autophagy and apoptosis (Song et al., 2017). Considering the mutual connection among autophagy, apoptosis and ER stress, we explored the effects of CYN on ER stress components and its relationship with autophagy and apoptosis. First, we used western blotting to examine the expression levels of the ER stress markers CHOP, BIP, ATF6, p-eIF2 $\alpha$  and IRE1 $\alpha$ . As shown in Figure 5A, CYN (10  $\mu$ M) treatment upregulated ER stress-associated proteins in a dose-dependent manner. Next, we ascertained the relationship among autophagy, apoptosis and ER stress in NB cells. CHOP is the downstream target for three branches of ER stress signalling, namely, eIF2 $\alpha$ , ATF6 and IRE1 $\alpha$  (Datta et al., 2019). Thus, shRNA targeting CHOP was used to inhibit ER stress, and autophagy and apoptosis were examined by flow cytometry and western blotting. The western blot results revealed that CHOP shRNA effectively reversed the expression levels of ER stress- and autophagy-associated proteins upregulated by CYN while further enhancing the expression levels of apoptotic proteins (Figure 5B). Moreover, the flow cytometry results showed that the apoptotic cell rate was increased in the CHOP shRNA and CYN cotreatment group compared with the CYN group (Figure 5C). To support the above results, we repeated the above experiments with the ER stress inhibitor TUDCA and obtained the same results (Supplementary Figure S3). Taken together, these results indicated that CYN triggered ER stress, which subsequently induced protective autophagy.

## CYN-induced autophagy inhibited apoptosis by promoting Nrf2 nuclear translocation and the P62-Keap1 interaction

Data from earlier studies have indicated that the Nrf2 pathway is involved in the antitumor activity of CYN in cancer cells (Takei et al., 2015; Ding et al., 2021). Given that p62 is an activator of the Nrf2-Keap1 pathway (Schmoll et al., 2017) and that the expression of p62 was upregulated by CYN stimulation (Figure 3D), we proposed that CYN could activate Nrf2 signalling in NB cells. Consistent with previous results (Takei et al., 2015; Ding et al., 2021), CYN (10  $\mu$ M) treatment

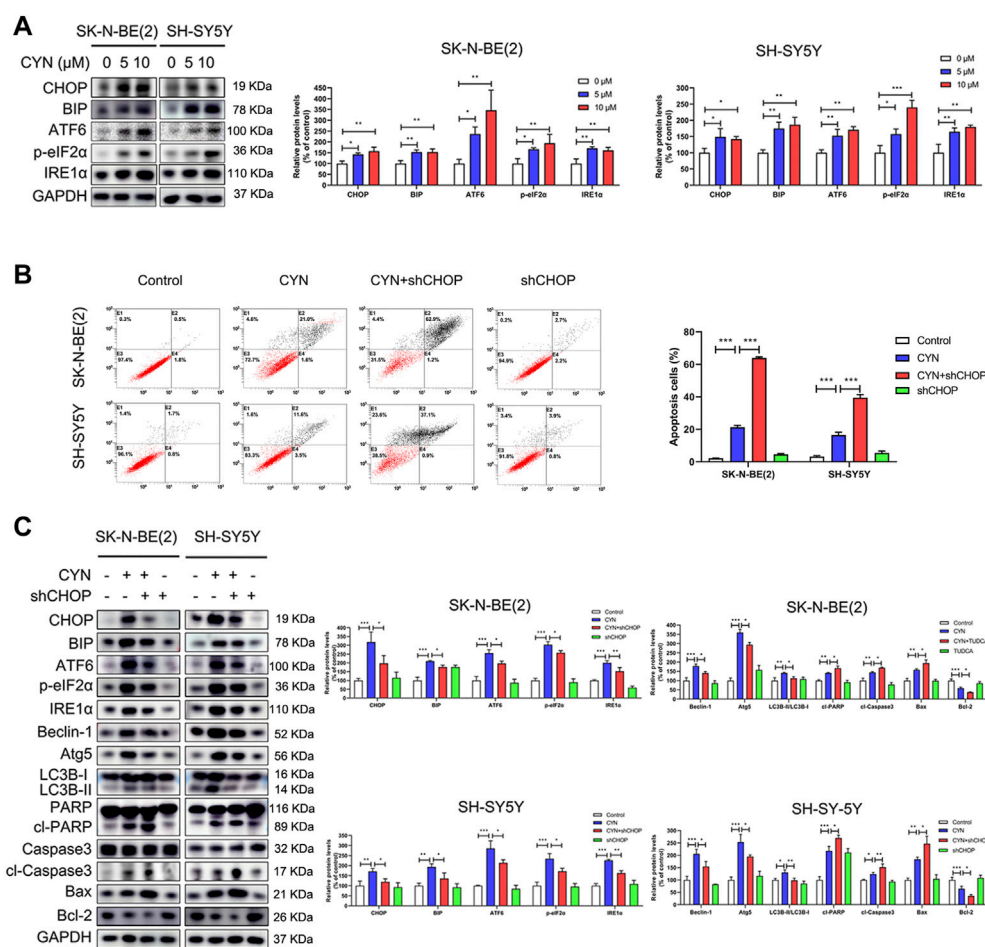


FIGURE 5

Relationship between ER stress, apoptosis and autophagy in NB cells treated by CYN. **(A)** Levels of ER stress-related proteins were analyzed by western blot. **(B)** Cell apoptotic ratio was measured and analyzed by flow cytometry. **(C)** Western blotting analysis detected the expression of ER stress-, autophagy- and apoptosis-related proteins. \* $p < 0.05$ , \*\* $p < 0.01$ , \*\*\* $p < 0.001$  versus the control group. \* $p < 0.05$ , \*\* $p < 0.01$ , \*\*\* $p < 0.001$  versus the CYN group.

significantly increased Nrf2 expression in a dose-dependent manner (Figure 6A). The mRNA expressions of Nrf2 did not significantly change after CYN treatment (Supplementary Figure S4). Nrf2 plays a pivotal role in controlling redox balance, which attributed to the anti-cancer effects of drugs. Therefore, we detected the changes of reactive oxygen species (ROS) levels by flow cytometry to verify whether they are consistent with the trend of Nrf2 changes. As shown in Supplementary Figure S5, CYN induced the accumulation of ROS. To investigate whether there was an intrinsic link between autophagy and the Nrf2 pathway in CYN-treated NB cells, the protein level of Nrf2 was detected by western blotting. The results showed that treatment with shBeclin-1 reversed the increase in the expression of Nrf2 in CYN-treated NB cells (Figure 6B). Activation of Nrf2 signalling, indicated by Nrf2 nuclear translocation, has a critical role in autophagy. To illuminate

whether CYN mediates the nuclear translocation of Nrf2, we observed the nuclear translocation of Nrf2 and monitored the subcellular localization of the Nrf2 protein by western blot analysis. Herein, we found that Nrf2 translocated from the cytosol to the nucleus after CYN treatment (Figure 6C), and the abundant accumulation of nuclear Nrf2 in CYN-treated NB cells was then confirmed by western blot analysis (Figure 6D). Under normal conditions, p62 competes with Keap1 for the same binding site on Nrf2; subsequently, Nrf2 is released from the Nrf2-Keap1 complex and translocates into the nucleus. As illustrated in Figure 6E, the immunofluorescence signal of p62 (green) was localized in the nucleus and cytoplasm, while the signal for Keap1 (red) was mainly distributed in the cytoplasm. Additionally, colocalization of p62 and Keap1 (yellow) was detected almost exclusively in the cytoplasm and the immunofluorescence intensity of p62 was

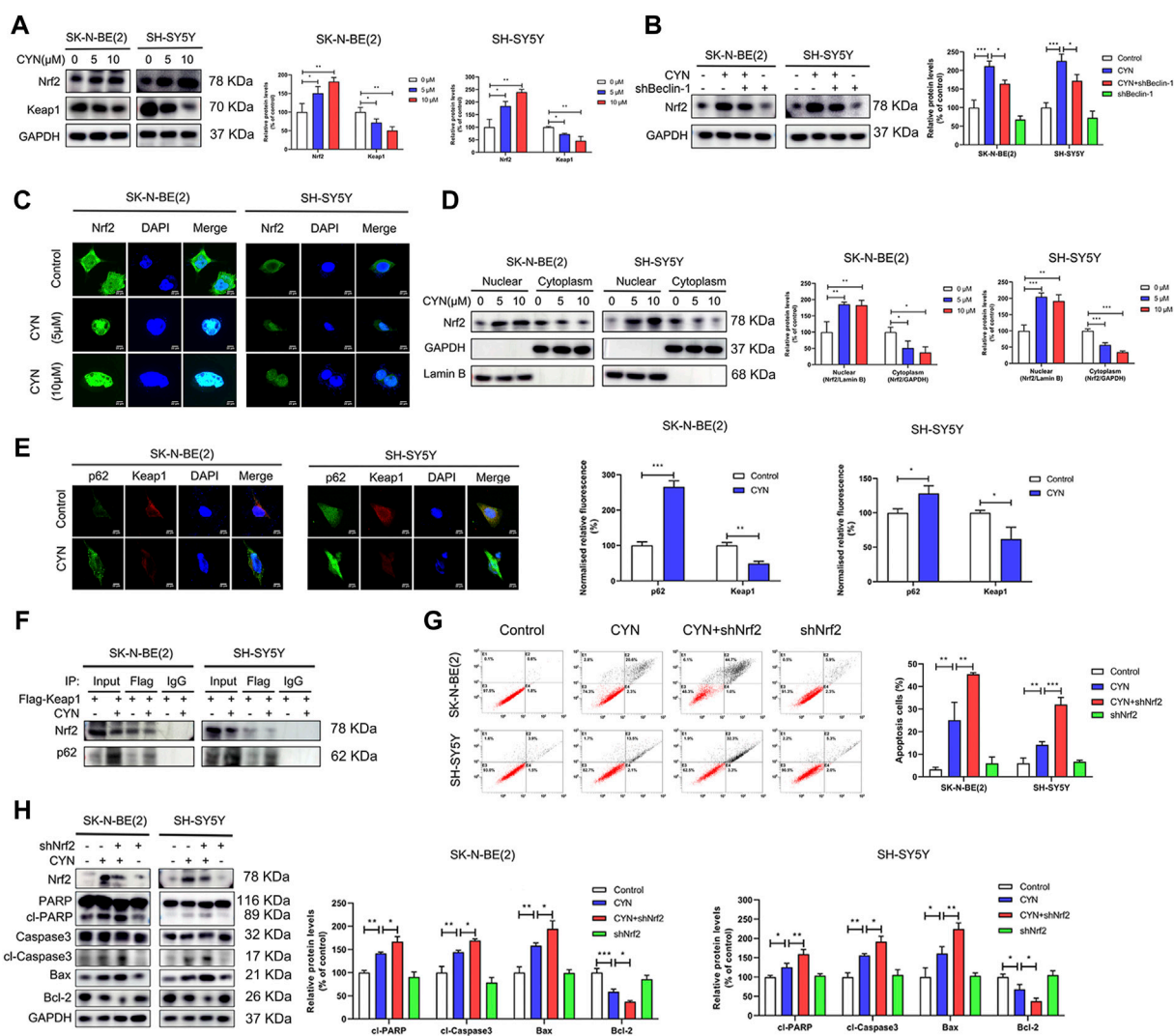


FIGURE 6

Relationship between the p62-Keap1-Nrf2 pathway and apoptosis in NB cells treated by CYN. (A) The Nrf2 and Keap1 protein level were determined by western blot. (B) Level of Nrf2 was analyzed by western blot. (C) CYN-treated NB cells were immunostained with anti-Nrf2 antibody (green) and counterstained with DAPI (blue). Scale bar: 20 μm. (D) The cytosolic and nuclear expressions of Nrf2 were determined by western blotting. (E) Immunofluorescence images and quantitative analysis of p62 and Keap1. Scale bars: 20 μm. (F) Nrf2 and p62 were detected by western blot after IP with anti-Flag. (G) Apoptosis of NB cells was measured and analyzed by flow cytometry. (H) Western blotting analysis detected the expression of apoptosis-related proteins. \* $p < 0.05$ , \*\* $p < 0.01$ , \*\*\* $p < 0.001$  versus the control group. \* $p < 0.05$ , \*\* $p < 0.01$ , \*\*\* $p < 0.001$  versus the CYN group.

enhanced, while that of Keap1 was weakened (Figure 6E). In addition, Co-IP showed that CYN stimulation increased the interaction between endogenous p62 and Keap1 but decreased the interaction between endogenous Nrf2 and Keap1 (Figure 6F). Next, we investigated the crosstalk between Nrf2 signalling and apoptosis, and the results showed that knockdown of Nrf2 significantly blocked the CYN-induced apoptosis (Figures 6G,H). Collectively, these data suggested that CYN-induced autophagy inhibited apoptosis through the p62/Keap1/Nrf2 pathways.

## CYN inhibited NB growth *in vivo*

To investigate the antitumor properties of CYN *in vivo*, we subcutaneously inoculated SK-N-BE(2) cells into athymic nude mice, and after 1 week, the mice were intraperitoneally treated with 2.5 mg/kg CYN once a day for three consecutive weeks. Our results showed that CYN markedly decreased the tumour volumes and weights compared to the vehicle group (Figures 7A–D), with no effect on the mouse body weight (Figure 7E). Mouse



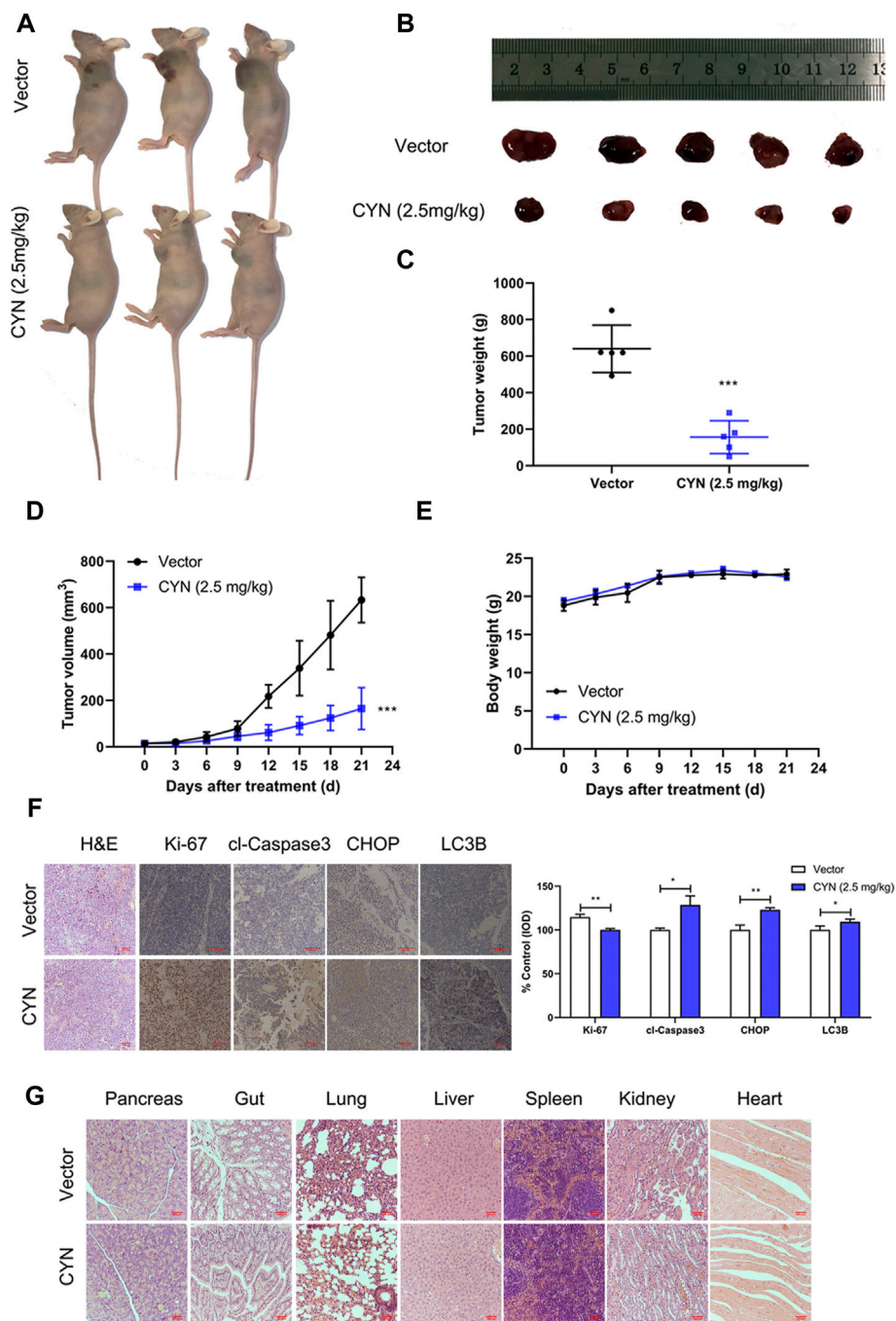


**FIGURE 7**

Effects of CYN on the NB tumor growth in athymic nude mice. **(A,B)** Representative images of xenograft tumors were shown. **(C)** Tumor weight after 3 weeks of treatment with CYN. **(D)** Tumor volume during administration of CYN. **(E)** The weight of mice was monitored during the experiment. **(F)** IHC staining results detected and analyzed the expression of Ki-67, cl-Caspase3, CHOP and LC3B. **(G)** HE stains examined the histopathologic characteristics of pancreas, gut, lung, liver, spleen, kidney and heart. \* $p < 0.05$ , \*\* $p < 0.01$ , \*\*\* $p < 0.001$  versus the vector group.

tumour tissues were collected for IHC staining to confirm whether the results *in vivo* agreed with those *in vivo*. The data indicated that CYN treatment significantly upregulated the expression levels of cleaved caspase-3, CHOP and LC3B and

downregulated the expression of Ki-67 compared with the vehicle group (Figure 7F). The H&E staining results revealed no notable pathological lesions in the pancreas, gut, lung, liver, spleen, kidney or heart tissues in the CYN treatment group



(Figure 7G). Overall, these results demonstrated that CYN exerted potent antitumor properties with low toxicity in animals.

## Discussion

Currently, a large number of natural dietary compounds have attracted considerable attention because of their promising anticancer activity and good safety characteristics. CYN, a characteristic sesquiterpene lactone found in nutritious artichokes, has been shown to exhibit anticancer activity in cancer cell lines (Zheng et al., 2020; Ding et al., 2021). However, no previous study has reported the effect and underlying mechanisms of CYN in NB. In our study, we verified that CYN could significantly and concentration-dependently suppress the growth of NB SK-N-BE(2) and SH-SY5Y cells (Figure 1) with IC<sub>50</sub> values of 9.731  $\mu$ M in SK-N-BE(2) cells and 5.738  $\mu$ M in SH-SY5Y cells (Figure 1D). Compared with other cancer cell lines, the IC<sub>50</sub> values of CYN in NB cells were lower, suggesting that NB cells were much more sensitive to CYN than other cells (Ding et al., 2021). Our data showed that CYN suppressed the growth of NB cells by inducing G2 phase cell cycle arrest and apoptosis. Moreover, CYN treatment induced ER stress-dependent autophagy against apoptosis through the p62/Keap1/Nrf2 pathways.

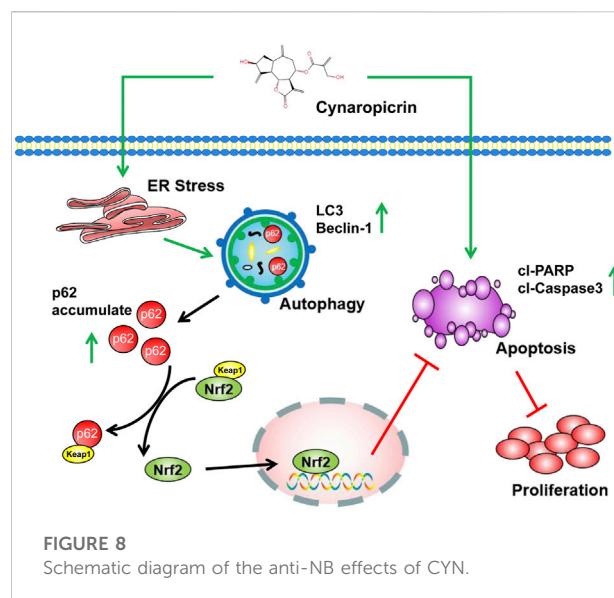
CYN has been reported to induce apoptosis in various cancers (Zheng et al., 2020; Ding et al., 2021). Here, we found through flow cytometry analysis that, similar to the above results, CYN arrested the cell cycle at G2 phase, resulting NB cell apoptosis (Figure 2). Apoptosis, a type of programmed cell death, is regarded as a potential target for the antitumor actions of many anticancer drugs (Guicciardi and Gores, 2009). Moreover, apoptosis can be triggered in a caspase-dependent or a caspase-independent manner. In caspase-dependent apoptosis, apoptotic signalling occurs *via* two different pathways: the mitochondrial (endogenous) pathway and the death receptor (exogenous) pathway (Xiong et al., 2014). Notably, CYN appeared to induce apoptosis in NB cells through the mitochondrial apoptotic pathway, as evidenced by the activation of caspase-3 and PARP, the increased Bax protein level, and decreased Bcl-2 protein level (Figure 2C). Of course, it is worth noting that apoptosis is a type of RCD (regulated cell death), and it is extremely meaningful to add an omics part in future studies to systematically understand the molecular mechanism for studying the anticancer effect of CYN. Moreover, autophagy, as an evolutionarily conserved catabolic process, helps to maintain cellular homeostasis (Li et al., 2016). Given that autophagy is closely associated with apoptosis, we examined whether CYN affected autophagy in NB cells. We found that CYN significantly activated autophagy by

increasing its initiation and blocking the fusion of autophagosomes and lysosomes (Figure 3). In a previous study, Cristiane et al. found that incubating bloodstream trypomastigotes with CYN induced autophagy (da Silva et al., 2013). However, there has been no report regarding the effect of CYN on autophagy in cancer, and further studies are needed. Autophagy is a highly dynamic multistep process, and both increasing the rate of autophagosome formation and decreasing the rate of autophagic degradation can promote the accumulation of autophagosomes. In this study, early-stage autophagy in CYN-treated NB cells was evidenced by an increased number of autophagosomes by TEM and increased protein expression of the autophagy markers LC3B-II, Atg5 and Beclin-1 (Figures 3A,B). On the other hand, with the aid of the mRFP-GFP-LC3B constructs, we demonstrated that CYN blocked autophagosome-lysosome fusion in these cells (Figure 3C). In addition, autophagic flux disruption by CYN through inhibition of autophagosome-lysosome fusion can be explained by the colocalization of LC3B with LAMP-2 (Supplementary Figure S1) and the p62 and LAMP-2 results (Figure 3D). Therefore, our study demonstrated that CYN promoted autophagy by initiating autophagy and inhibiting autophagic flux. ER stress is considered a common feature in several types of cancers (Bhardwaj et al., 2020; Xia et al., 2021). Additionally, previous evidence has suggested that various natural compounds and their derivatives can trigger ER stress to exert anticancer effects (Huang et al., 2021). Here, we showed for the first time that CYN activate ER stress in human cancer cells (Figure 5A). Based on the findings above, we were curious about the relationship among ER stress, apoptosis and autophagy after CYN treatment in NB cells.

There is a close relationship among ER stress, apoptosis and autophagy (Mizushima 2007; Cheng et al., 2015; Song et al., 2017). Our aim was to clarify the relationship among the three distinct processes, as it is essential during CYN treatment. First, we aimed to clarify the relationship between autophagy and apoptosis in CYN-treated NB cells. In recent years, increasing evidence has suggested that, inconsistent with apoptosis, autophagy plays contradictory roles in cancer and functions as a prosurvival or antisurvival mechanism depending on the tumour type or microenvironment (Healy et al., 2009; Song et al., 2017). In our study, we confirmed that inhibiting autophagy using siAtg5 and 3-MA (an early-phase autophagy inhibitor) increased apoptosis (Figures 4A,B). This observation suggests that autophagy plays a cytoprotective role in NB cells treated with CYN. In addition, we used chloroquine (CQ) to further investigate the relationship between autophagy and apoptosis. CQ, as a specific late-phase autophagy inhibitor, inhibits the fusion of lysosomes with autophagosomes (Boya et al., 2005). Our results demonstrated that the combination of CYN with CQ treatment reduced apoptosis compared with CYN

treatment alone (Figures 4C,D). These results indicated that CYN-triggered blockade of autophagic lysosomal fusion played a crucial role in cytoprotective autophagy. Next, we aimed to clarify the relationship among ER stress, autophagy and apoptosis in CYN-treated NB cells. Accumulating evidence has suggested that ER stress plays a vital role in inducing apoptosis and autophagy in various tumour cells (Shen et al., 2017; Zheng et al., 2018). Moreover, ER stress can regulate autophagy alone or both autophagy and apoptosis (Shen et al., 2017; Zheng et al., 2018). In this study, the relationship among ER stress, apoptosis and autophagy was investigated after transfecting cells with CHOP-specific shRNA (Figure 5) or co-treated with ER stress inhibitor TUDCA (Supplementary Figure S3). Zheng et al. reported that the activation of ER stress could cause melanoma cell apoptosis and inhibit autophagy (Zheng et al., 2018). In contrast to previous studies, our results suggested that ER stress induced only protective autophagy in NB cells but did not participate in CYN-induced apoptosis. In line with our results, Shen et al. demonstrated that ER stress participated in only autophagy, not apoptosis, in sarcoma cells (Shen et al., 2017). These results indicated that CYN-triggered ER stress might induce protective autophagy in NB cells and then impair the antitumor effects of CYN. Therefore, it was necessary to further clarify the pro-autophagy mechanism of CYN treatment to improve the antitumour effects on NB.

In the present study, we observed that CYN increased the protein expression of p62 (Figure 3D). p62 acts as not only an autophagy receptor protein but also an activator of the noncanonical Keap1-Nrf2 pathway (Komatsu et al., 2010). It has also been documented that Nrf2 is activated in cancers, and the high activity of Nrf2 can play a protective role in tumour cells (Zhang et al., 2015; Rojo de la Vega et al., 2018). The interrelation between Nrf2 and p62 is well known; that is, p62 competitively binds with Keap1, which results in Nrf2 release from the Nrf2-Keap1 complex and Nrf2 translocation into the nucleus (Itoh et al., 2003; Schmoll et al., 2017; Dash et al., 2020). Our results showed that CYN improved Nrf2 transactivation by enhancing Nrf2 nuclear translocation, suggesting that CYN promoted Nrf2 activation by enhancing the binding of p62 to Keap1 in the cytoplasm (Figures 6C–F). It is noted that CYN enhanced the protein level of Nrf2 but not that of the mRNA. Thus, possibility exists that CYN may have enhanced Nrf2 protein expression *via* post-transcriptional mechanisms that deserve further study. Nrf2 signalling and autophagy crosstalk is complex and controversial. The study conducted by Xu et al. revealed that Nrf2 acted as a downstream regulator of autophagy in gastric cancer cells (Xu et al., 2022). In contrast, other findings from the study by Xu et al. reported a negative interaction between autophagy and the Nrf2 pathway (Li et al., 2018). Our findings were in agreement with Xu et al.'s results (Li et al., 2018), and the meaningful downregulation of Nrf2 protein expression following the inhibition of autophagy induced by



shBeclin-1 (Figure 6B) suggested that Nrf2 signalling could be partly activated by autophagy in CYN-treated NB cells. The association between autophagy, apoptosis and NRF2 pathway has been gradually concerned and studied in recent years (Arab et al., 2021; Lu et al., 2021). To verify that CYN-induced autophagy inhibits apoptosis through the Nrf2 pathway, we investigated the crosstalk between the two signalling pathways. Our findings were in agreement with Xu et al.'s results (Xu et al., 2022), in which Nrf2 knockdown inhibited apoptosis in CYN-treated NB cells (Figures 6G,H), indicating that Nrf2 signalling might be a disadvantageous element for the antitumor effects of CYN on NB. Furthermore, we preliminarily detected the changes of ROS after CYN treatment (Supplementary Figure S5), suggesting that there may be an exploratory association between antioxidant response and autophagy in neuroblastoma treated with CYN, which is worthy of further study in the future.

In summary, the current study indicated that CYN inhibited NB cell growth *in vitro* and *in vivo*, and the mechanism specifically involved ER stress/autophagy/Nrf2 signalling/apoptosis. We provided insights into the molecular mechanisms by which CYN induces apoptosis and ER stress-mediated protective autophagy. That is, ER stress-mediated autophagy triggers the p62/Keap1/Nrf2 pathways, followed by attenuation of CYN-induced apoptosis in NB; the interplay is summarized in Figure 8. Our study indicated that CYN may be a potential antitumor agent for NB prevention and treatment. This is the first study to examine the crosstalk between CYN-induced apoptosis and autophagy, which involves the activation of the p62/Keap1/Nrf2 signalling pathway. Therefore, we provided a basis for future preclinical and clinical trial exploration to improve the efficacy of CYN in NB treatment.

## Data availability statement

The original contributions presented in the study are included in the article/Supplementary Material, further inquiries can be directed to the corresponding authors.

## Ethics statement

The animal study was reviewed and approved by The animal experiments are complied with the requirements of the Animal Care and Use Committee at Children's Hospital of Soochow University.

## Author contributions

Conception and design: RY, JW, and JP. Acquisition of data: SM and LX. Analysis and interpretation of data: YY, SJ, LM, and PY. Writing, review, and/or revision of the manuscript: RY, RZ, and HC.

## Funding

This work was supported by grants from the Postgraduate Research & Practice Innovation Program of Jiangsu Province (KYCX21\_2982); Jiangsu Province Key R&D Program (Social Development) Projects (BE2020659); the Science and Technology

Project of Suzhou (SS2019011); Suzhou Introduced Project of Clinical Medical Expert Team (SZYJTD201706); Suzhou Clinical Medical Center (Szlcyxzx202104).

## Conflict of interest

The authors declare that the research was conducted in the absence of any commercial or financial relationships that could be construed as a potential conflict of interest.

## Publisher's note

All claims expressed in this article are solely those of the authors and do not necessarily represent those of their affiliated organizations, or those of the publisher, the editors and the reviewers. Any product that may be evaluated in this article, or claim that may be made by its manufacturer, is not guaranteed or endorsed by the publisher.

## Supplementary material

The Supplementary Material for this article can be found online at: <https://www.frontiersin.org/articles/10.3389/fphar.2022.977622/full#supplementary-material>

## References

- Arab, H. H., Al-Shorbagy, M. Y., and Saad, M. A. (2021). Activation of autophagy and suppression of apoptosis by dapagliflozin attenuates experimental inflammatory bowel disease in rats: Targeting AMPK/mTOR, HMGB1/RAGE and Nrf2/HO-1 pathways. *Chem. Biol. Interact.* 335, 109368. doi:10.1016/j.cbi.2021.109368
- Bhardwaj, M., Leli, N. M., Koumenis, C., and Amaravadi, R. K. (2020). Regulation of autophagy by canonical and non-canonical ER stress responses. *Semin. Cancer Biol.* 66, 116–128. doi:10.1016/j.semcancer.2019.11.007
- Boya, P., González-Polo, R. A., Casares, N., Perfettini, J. L., Dessen, P., Larochette, N., et al. (2005). Inhibition of macroautophagy triggers apoptosis. *Mol. Cell. Biol.* 25, 1025–1040. doi:10.1128/mcb.25.3.1025-1040.2005
- Cañete, A., and CAñete, A. (2020). High-risk neuroblastoma: where do we go? *Ann. Oncol.* 31, 326–327. doi:10.1016/j.annonc.2019.12.003
- Celesia, A., Morana, O., Fiore, T., Pellerito, C., D'Anneo, A., Lauricella, M., et al. (2020). ROS-dependent ER stress and autophagy mediate the anti-tumor effects of tributyltin (IV) ferulate in colon cancer cells. *Int. J. Mol. Sci.* 21, E8135. doi:10.3390/ijms21218135
- Cheng, Y. C., Chang, J. M., Chen, C. A., and Chen, H. C. (2015). Autophagy modulates endoplasmic reticulum stress-induced cell death in podocytes: a protective role. *Exp. Biol. Med.* 240, 467–476. doi:10.1177/1535370214553772
- Choi, A. M., Ryter, S. W., and Levine, B. (2013). Autophagy in human health and disease. *N. Engl. J. Med.* 368, 1845–1846. doi:10.1056/NEJMc1303158
- da Silva, C. F., Batista Dda, G., De Araújo, J. S., Batista, M. M., Lionel, J., de Souza, E. M., et al. (2013). Activities of psilostachyin A and cynaropicrin against *Trypanosoma cruzi* in vitro and in vivo. *Antimicrob. Agents Chemother.* 57, 5307–5314. doi:10.1128/aac.00595-13
- Dash, S., Aydin, Y., and Wu, T. (2020). Integrated stress response in hepatitis C promotes nrf2-related chaperone-mediated autophagy: A novel mechanism for host-microbe survival and HCC development in liver cirrhosis. *Semin. Cell Dev. Biol.* 101, 20–35. doi:10.1016/j.semcdb.2019.07.015
- Datta, S., Choudhury, D., Das, A., Mukherjee, D. D., Dasgupta, M., Bandopadhyay, S., et al. (2019). Autophagy inhibition with chloroquine reverts paclitaxel resistance and attenuates metastatic potential in human nonsmall lung adenocarcinoma A549 cells via ROS mediated modulation of  $\beta$ -catenin pathway. *Apoptosis* 24, 414–433. doi:10.1007/s10495-019-01526-y
- De Cicco, P., Busà, R., Ercolano, G., Formisano, C., Allegra, M., Taglialatela-Scafati, O., et al. (2021). Inhibitory effects of cynaropicrin on human melanoma progression by targeting MAPK, NF- $\kappa$ B, and Nrf-2 signaling pathways in vitro. *Phytother. Res.* 35, 1432–1442. doi:10.1002/ptr.6906
- Ding, Z., Xi, J., Zhong, M., Chen, F., Zhao, H., Zhang, B., et al. (2021). Cynaropicrin induces cell cycle arrest and apoptosis by inhibiting PKM2 to cause DNA damage and mitochondrial fission in A549 cells. *J. Agric. Food Chem.* 69, 13557–13567. doi:10.1021/acs.jafc.1c05394
- Elmore, S. (2007). Apoptosis: a review of programmed cell death. *Toxicol. Pathol.* 35, 495–516. doi:10.1080/01926230701320337
- Elsebai, M. F., Mocan, A., and Atanasov, A. G. (2016). Cynaropicrin: A comprehensive research review and therapeutic potential as an anti-hepatitis C virus agent. *Front. Pharmacol.* 7, 472. doi:10.3389/fphar.2016.00472
- Feng, Y., Wang, N., Zhu, M., Feng, Y., Li, H., and Tsao, S. (2011). 'Recent progress on anticancer candidates in patents of herbal medicinal products. *Recent Pat. Food Nutr. Agric.* 3, 30–48. doi:10.2174/2212798411103010030
- Fridlender, M., Kapulnik, Y., and Koltai, H. (2015). Plant derived substances with anti-cancer activity: From folklore to practice. *Front. Plant Sci.* 6, 799. doi:10.3389/fpls.2015.00799
- Guicciardi, M. E., and Gores, G. J. (2009). Life and death by death receptors. *Faseb J.* 23, 1625–1637. doi:10.1096/fj.08-111005
- Hasima, N., and Ozpolat, B. (2014). Regulation of autophagy by polyphenolic compounds as a potential therapeutic strategy for cancer. *Cell Death Dis.* 5, e1509. doi:10.1038/cddis.2014.467

- Healy, S. J., Gorman, A. M., Mousavi-Shafaei, P., Gupta, S., and Samali, A. (2009). Targeting the endoplasmic reticulum-stress response as an anticancer strategy. *Eur. J. Pharmacol.* 625, 234–246. doi:10.1016/j.ejphar.2009.06.064
- Huang, Y., Yuan, K., Tang, M., Yue, J., Bao, L., Wu, S., et al. (2021). Melatonin inhibiting the survival of human gastric cancer cells under ER stress involving autophagy and Ras-Raf-MAPK signalling. *J. Cell. Mol. Med.* 25, 1480–1492. doi:10.1111/jcmm.16237
- Itoh, K., Wakabayashi, N., Katoh, Y., Ishii, T., O'Connor, T., and Yamamoto, M. (2003). Keap1 regulates both cytoplasmic-nuclear shuttling and degradation of Nrf2 in response to electrophiles. *Genes cells.* 8, 379–391. doi:10.1046/j.1365-2443.2003.00640.x
- Kingston, D. G. (2011). Modern natural products drug discovery and its relevance to biodiversity conservation. *J. Nat. Prod.* 74, 496–511. doi:10.1021/np100550t
- Komatsu, M., Kurokawa, H., Waguri, S., Taguchi, K., Kobayashi, A., Ichimura, Y., et al. (2010). The selective autophagy substrate p62 activates the stress responsive transcription factor Nrf2 through inactivation of Keap1. *Nat. Cell Biol.* 12, 213–223. doi:10.1038/ncb2021
- Lepore, S. M., Maggiano, V., Lombardo, G. E., Maiuolo, J., Mollace, V., Bulotta, S., et al. (2019). Antiproliferative effects of cynaropicrin on anaplastic thyroid cancer cells. *Endocr. Metab. Immune Disord. Drug Targets* 19, 59–66. doi:10.2174/1871530318666180928153241
- Li, H., Peng, X., Wang, Y., Cao, S., Xiong, L., Fan, J., et al. (2016). Atg5-mediated autophagy deficiency in proximal tubules promotes cell cycle G2/M arrest and renal fibrosis. *Autophagy* 12, 1472–1486. doi:10.1080/15548627.2016.1190071
- Li, X., Liang, M., Jiang, J., He, R., Wang, M., Guo, X., et al. (2018). Combined inhibition of autophagy and Nrf2 signaling augments bortezomib-induced apoptosis by increasing ROS production and ER stress in pancreatic cancer cells. *Int. J. Biol. Sci.* 14, 1291–1305. doi:10.7150/ijbs.26776
- Lu, Z., Ren, Y., Yang, L., Jia, A., Hu, Y., Zhao, Y., et al. (2021). Inhibiting autophagy enhances sulforaphane-induced apoptosis via targeting NRF2 in esophageal squamous cell carcinoma. *Acta Pharm. Sin. B* 11, 1246–1260. doi:10.1016/j.apsb.2020.12.009
- Matthay, K. K., Maris, J. M., Schleiermacher, G., Nakagawara, A., Mackall, C. L., Diller, L., et al. (2016). Neuroblastoma. *Nat. Rev. Dis. Prim.* 2, 16078. doi:10.1038/nrdp.2016.78
- Mizushima, N., Yoshimori, T., and Levine, B. (2010). Methods in mammalian autophagy research. *Cell* 140, 313–326. doi:10.1016/j.cell.2010.01.028
- Mizushima, N. (2007). Autophagy: Process and function. *Genes Dev.* 21, 2861–2873. doi:10.1101/gad.1599207
- Newman, D. J., and Cragg, G. M. (2012). Natural products as sources of new drugs over the 30 years from 1981 to 2010. *J. Nat. Prod.* 75, 311–335. doi:10.1021/np200906s
- Nikolietopoulou, V., Markaki, M., Palikaras, K., and Tavernarakis, N. (2013). Crosstalk between apoptosis, necrosis and autophagy. *Biochim. Biophys. Acta* 1833, 3448–3459. doi:10.1016/j.bbamcr.2013.06.001
- Radogna, F., Dicato, M., and Diederich, M. (2015). Cancer-type-specific crosstalk between autophagy, necroptosis and apoptosis as a pharmacological target. *Biochem. Pharmacol.* 94, 1–11. doi:10.1016/j.bcp.2014.12.018
- Rangwala, R., Chang, Y. C., Hu, J., Algazy, K. M., Evans, T. L., Fecher, L. A., et al. (2014). Combined MTOR and autophagy inhibition: phase I trial of hydroxychloroquine and temsirolimus in patients with advanced solid tumors and melanoma. *Autophagy* 10, 1391–1402. doi:10.4161/auto.29119
- Rojo de la Vega, M., Chapman, E., and Zhang, D. D. (2018). NRF2 and the hallmarks of cancer. *Cancer Cell* 34, 21–43. doi:10.1016/j.ccell.2018.03.022
- Schmoll, D., Engel, C. K., and Glombik, H. (2017). The keap1-nrf2 protein-protein interaction: A suitable target for small molecules. *Drug Discov. Today. Technol.* 24, 11–17. doi:10.1016/j.ddtec.2017.10.001
- Shen, S., Zhou, M., Huang, K., Wu, Y., Ma, Y., Wang, J., et al. (2017). Blocking autophagy enhances the apoptotic effect of 18 $\beta$ -glycyrrhetic acid on human sarcoma cells via endoplasmic reticulum stress and JNK activation. *Cell Death Dis.* 8, e3055. doi:10.1038/cddis.2017.441
- Song, S., Tan, J., Miao, Y., Li, M., and Zhang, Q. (2017). Crosstalk of autophagy and apoptosis: Involvement of the dual role of autophagy under ER stress. *J. Cell. Physiol.* 232, 2977–2984. doi:10.1002/jcp.25785
- Su, Z., Yang, Z., Xu, Y., Chen, Y., and Yu, Q. (2015). Apoptosis, autophagy, necroptosis, and cancer metastasis. *Mol. Cancer* 14, 48. doi:10.1186/s12943-015-0321-5
- Takei, K., Hashimoto-Hachiya, A., Takahara, M., Tsuji, G., Nakahara, T., and Furue, M. (2015). Cynaropicrin attenuates UVB-induced oxidative stress via the AhR-Nrf2-Nqo1 pathway. *Toxicol. Lett.* 234, 74–80. doi:10.1016/j.toxlet.2015.02.007
- Tas, M. L., Reedijk, A. M. J., Karim-Kos, H. E., Kremer, L. C. M., van de Ven, C. P., Dierselhuis, M. P., et al. (2020). Neuroblastoma between 1990 and 2014 in the Netherlands: Increased incidence and improved survival of high-risk neuroblastoma. *Eur. J. Cancer* 124, 47–55. doi:10.1016/j.ejca.2019.09.025
- Xia, Y., Chen, J., Yu, Y., Wu, F., Shen, X., Qiu, C., et al. (2021). Compensatory combination of mTOR and TrxR inhibitors to cause oxidative stress and regression of tumors. *Theranostics* 11, 4335–4350. doi:10.7150/thno.52077
- Xiong, S., Mu, T., Wang, G., and Jiang, X. (2014). Mitochondria-mediated apoptosis in mammals. *Protein Cell* 5, 737–749. doi:10.1007/s13238-014-0089-1
- Xu, D. Q., Toyoda, H., Yuan, X. J., Qi, L., Chelakkot, V. S., Morimoto, M., et al. (2018). Anti-tumor effect of AZD8055 against neuroblastoma cells in vitro and in vivo. *Exp. Cell Res.* 365, 177–184. doi:10.1016/j.yexcr.2018.02.032
- Xu, F., Xie, Q., Li, Y. W., Jing, Q. Q., Liu, X. J., Xu, Y. C., et al. (2022). Suppression of JNK/ERK dependent autophagy enhances Jaspine B derivative-induced gastric cancer cell death via attenuation of p62/Keap1/Nrf2 pathways. *Toxicol. Appl. Pharmacol.* 438, 115908. doi:10.1016/j.taap.2022.115908
- Youlten, D. R., Jones, B. C., Cundy, T. P., Karpelowsky, J., Aitken, J. F., and McBride, C. A. (2020). Incidence and outcomes of neuroblastoma in Australian children: A population-based study (1983–2015). *J. Paediatr. Child. Health* 56, 1046–1052. doi:10.1111/jpc.14810
- Zaib, S., and Khan, I. (2020). Synthetic and medicinal chemistry of phthalazines: Recent developments, opportunities and challenges. *Bioorg. Chem.* 105, 104425. doi:10.1016/j.bioorg.2020.104425
- Zhang, M., Zhang, C., Zhang, L., Yang, Q., Zhou, S., Wen, Q., et al. (2015). Nrf2 is a potential prognostic marker and promotes proliferation and invasion in human hepatocellular carcinoma. *BMC Cancer* 15, 531. doi:10.1186/s12885-015-1541-1
- Zheng, Y., Wang, K., Wu, Y., Chen, Y., Chen, X., Hu, C. W., et al. (2018). Pinocembrin induces ER stress mediated apoptosis and suppresses autophagy in melanoma cells. *Cancer Lett.* 431, 31–42. doi:10.1016/j.canlet.2018.05.026
- Zheng, D., Zhu, Y., Shen, Y., Xiao, S., Yang, L., Xiang, Y., et al. (2020). Cynaropicrin shows antitumor progression potential in colorectal cancer through mediation of the LIFR/STATs Axis. *Front. Cell Dev. Biol.* 8, 605184. doi:10.3389/fcell.2020.605184



## OPEN ACCESS

EDITED BY  
Chen Yi,  
Sichuan University, China

REVIEWED BY  
Lan Zhang,  
Southwest Jiaotong University, China  
Jin Zhang,  
Shenzhen University, China

\*CORRESPONDENCE  
Ling-Li Zheng,  
zhenglingli@cmc.edu.cn  
Haixia Huang,  
Alicehhx123@163.com

SPECIALTY SECTION  
This article was submitted to  
Pharmacology of Anti-Cancer Drugs,  
a section of the journal  
Frontiers in Pharmacology

RECEIVED 15 July 2022  
ACCEPTED 02 September 2022  
PUBLISHED 03 October 2022

CITATION  
Gou Q, Zheng L-L and Huang H (2022),  
Unravelling the roles of Autophagy in  
OSCC: A renewed perspective from  
mechanisms to potential applications.  
*Front. Pharmacol.* 13:994643.  
doi: 10.3389/fphar.2022.994643

COPYRIGHT  
© 2022 Gou, Zheng and Huang. This is  
an open-access article distributed  
under the terms of the [Creative  
Commons Attribution License \(CC BY\)](#).  
The use, distribution or reproduction in  
other forums is permitted, provided the  
original author(s) and the copyright  
owner(s) are credited and that the  
original publication in this journal is  
cited, in accordance with accepted  
academic practice. No use, distribution  
or reproduction is permitted which does  
not comply with these terms.

# Unravelling the roles of Autophagy in OSCC: A renewed perspective from mechanisms to potential applications

Qiutong Gou<sup>1</sup>, Ling-Li Zheng<sup>2\*</sup> and Haixia Huang<sup>1\*</sup>

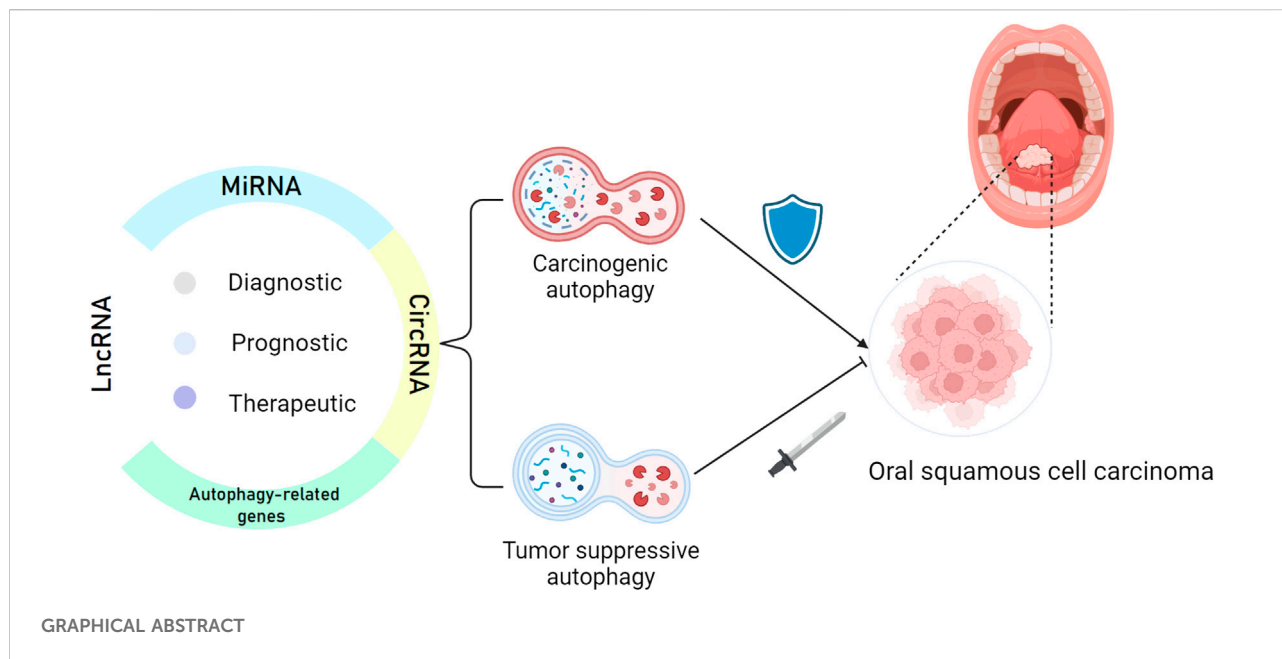
<sup>1</sup>Luzhou Key Laboratory of Oral and Maxillofacial Reconstruction and Regeneration, The Affiliated Stomatology Hospital of Southwest Medical University, Southwest Medical University, Luzhou, China, <sup>2</sup>Department of Pharmacy, The First Affiliated Hospital of Chengdu Medical College, Chengdu, China

Oral squamous cell carcinoma (OSCC) is associated with a low survival rate and a high disability rate, making it a serious health burden, particularly in Southeast Asian countries. Therefore, improvements in the diagnosis, treatment, and prognosis prediction of OSCC are highly warranted. Autophagy has a significant impact on cancer development. Studies on autophagy in various human cancers have made outstanding contributions; however, the relationship between autophagy and OSCC remains to be explored. This review highlights the roles of autophagy in OSCC and discusses the relationship between autophagy and Epithelial–mesenchymal transition. Considering the lack of OSCC biomarkers, we focus on the studies involving OSCC-related bioinformatics analysis and molecular targets. Based on some classical targets, we summarize several key autophagy-related biomarkers with a considerable potential for clinical application, which may become the hotspot of OSCC research. In conclusion, we elaborate on the interrelationship between autophagy and OSCC and highlight the shortcomings of current studies to provide insights into the potential clinical strategies.

## KEYWORDS

oral squamous cell carcinoma (OSCC), autophagy, epithelial–mesenchymal transition (EMT), biomarker, diagnosis, treatment, prognosis





## Introduction

Oral squamous cell carcinoma (OSCC) exhibits a low survival rate and a high deformity rate due to its ability to metastasize and disrupt the upper digestive tract and respiratory tract functions (Ho et al., 2017). The scarcity of clinical diagnosis indices of OSCC often leads to a late diagnosis. Chemoradiotherapy combined with surgery is critical to patients in late stages (stage III and stage IV) or with metastasis (Moratin et al., 2020). However, chemotherapeutic drugs such as cisplatin (CDDP) and 5-fluorouracil fail to produce a satisfactory outcome due to OSCC cell chemoresistance (Li et al., 2019). Moreover, the prognosis of OSCC is mainly predicted by the macroscopic tumor-node-metastasis (TNM)-based staging in clinical practice, where supportive detection at the molecular level is needed. Therefore, new biomarkers are urgently required to improve the diagnosis, treatment, and prognosis prediction of OSCC patients.

Autophagy is an evolutionarily conserved process that leads to the degradation of damaged organelles and recycling of energy sources. Research has contributed to major breakthroughs in autophagy in cancer (Xia et al., 2021). Some critical biological processes in cancer, such as invasion and metastasis, are regulated by the modulation of autophagy and Epithelial-mesenchymal transition (EMT) (Chen H.T et al., 2019). Additionally, the homeostasis of cancer cells is significantly modulated by the crosstalk between autophagy and apoptosis pathways (Das et al., 2021). Hence, targeting autophagy has become a hotspot in OSCC research. However,

the roles of autophagy in OSCC remain controversial. On the one hand, the stemness and malignancy of OSCC cells were enhanced by increasing autophagy (Naik et al., 2018). On the other hand, apoptosis was promoted when upregulated autophagy was present in OSCC (Huang et al., 2018). Further discussion on the roles of autophagy in OSCC is required to understand the occurrence and progression of OSCC, which might provide us information for more in-depth studies. The present review summarizes the autophagy-related biomarkers, which possess the potential for clinical applications, and sheds light on the roles of autophagy in OSCC, hence providing clues for new treatment options.

## Targeting Autophagy in OSCC

Autophagy protects cells by maintaining metabolic homeostasis under multiple threats including energy stress and hypoxia stress (Xiang et al., 2020). This biological process is usually presented in three forms, namely macroautophagy, microautophagy, and chaperone-mediated autophagy (Fleming et al., 2022). Among these forms, macroautophagy (commonly known as autophagy), which relies on autophagosomes to deliver autophagic cargo such as damaged organelles and unfolded proteins, is most closely related to cancer progression (Zhang et al., 2018). Classical autophagy involves five consecutive steps: (a) initiation of autophagy, (b) nucleation in vesicles, (c) vesicle formation, (d) docking and fusion, and (e) degradation and recycling of autophagic cargo. Targeting autophagy in some cancers (such as breast cancer) has been proven to be a

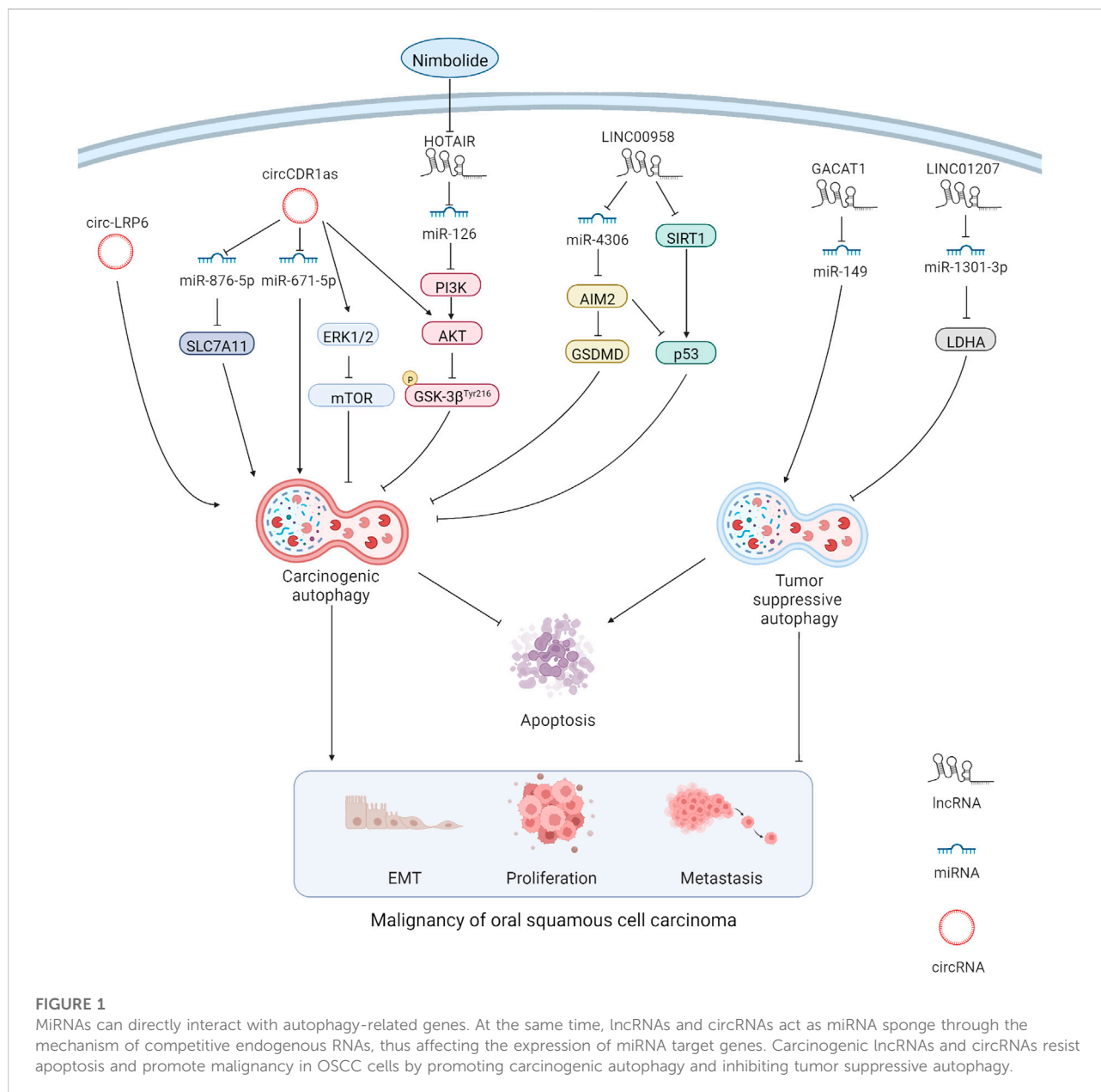
TABLE.1 Autophagy-related biomarkers in OSCC.

Biomarker	Type	Role in OSCC	Mechanism/Pathway	Experimental verification	Application	Ref
EGFR	Autophagy-related genes	Carcinogenic	Apoptosis Human cytomegalovirus infection Human papillomavirus infection	NO	Prognostic	<a href="#">Yang et al. (2020)</a>
HSPB8	Autophagy-related genes	Tumor suppressive	Apoptosis Human cytomegalovirus infection Human papillomavirus infection	NO	Prognostic	<a href="#">Yang et al. (2020)</a> ; <a href="#">Jin and Qin (2020)</a>
PRKN	Autophagy-related genes	Carcinogenic	Apoptosis Human cytomegalovirus infection Human papillomavirus infection	NO	Prognostic	<a href="#">Yang et al. (2020)</a>
CDKN2A	Autophagy-related genes	Tumor suppressive	Apoptosis Human cytomegalovirus infection Human papillomavirus infection	NO	Prognostic	<a href="#">Yang et al. (2020)</a> ; <a href="#">Jin and Qin (2020)</a>
FADD	Autophagy-related genes	Carcinogenic	Apoptosis Human cytomegalovirus infection Human papillomavirus infection	NO	Prognostic	<a href="#">Yang et al. (2020)</a> ; <a href="#">Jin and Qin (2020)</a>
ITGA3	Autophagy-related genes	Carcinogenic	Apoptosis Human cytomegalovirus infection Human papillomavirus infection	NO	Prognostic	<a href="#">Yang et al. (2020)</a> ; <a href="#">Jin and Qin (2020)</a>
BAK1	Autophagy-related genes	Carcinogenic	Apoptosis Human cytomegalovirus infection Human papillomavirus infection	NO	Prognostic	<a href="#">Jin and Qin (2020)</a> ; <a href="#">Zhu et al. (2020)</a>
NKX2-3	Autophagy-related genes	Tumor suppressive	Apoptosis Human cytomegalovirus infection Human papillomavirus infection	YES	Prognostic	<a href="#">Jin and Qin (2020)</a> ; <a href="#">Zhu et al. (2020)</a>
CXCR4	Autophagy-related genes	Tumor suppressive	Apoptosis Human cytomegalovirus infection	NO	Prognostic	<a href="#">Jin and Qin, (2020)</a>

(Continued on following page)

TABLE.1 (Continued) Autophagy-related biomarkers in OSCC.

Biomarker	Type	Role in OSCC	Mechanism/Pathway	Experimental verification	Application	Ref
			Human papillomavirus infection			
ATG12	Autophagy-related genes	Carcinogenic	Apoptosis ErbB pathway	YES	Prognostic; Diagnostic; and Therapeutic	Huang et al. (2021)
BID	Autophagy-related genes	Carcinogenic	Apoptosis ErbB pathway	YES	Prognostic; Diagnostic; and Therapeutic	Huang et al. (2021); Zhu et al. (2020)
SPHK1	Autophagy-related genes	Tumor suppressive	Apoptosis Human cytomegalovirus infection Human papillomavirus infection	YES	Prognostic	Zhu et al. (2020)
LINC00958	lncRNA	Carcinogenic	Inhibiting miR-4306/AIM2 Inhibiting SIRT1/p53	YES	Therapeutic	Jiang L et al. (2021)
AL354733.3	lncRNA	Tumor suppressive	—	YES	Prognostic	Jiang Q et al. (2021)
PTCSC2	lncRNA	Tumor suppressive	—	YES	Prognostic	Jiang L et al. (2021)
UBAC2-AS1	lncRNA	Carcinogenic	—	YES	Prognostic	Jiang L et al. (2021)
LINC01963	lncRNA	Tumor suppressive	—	YES	Prognostic	Jiang L et al. (2021)
MIR600HG	lncRNA	Carcinogenic	—	YES	Prognostic	Jiang L et al. (2021)
AP002884.1	lncRNA	Carcinogenic	—	YES	Prognostic	Jiang L et al. (2021)
RTCA-AS1	lncRNA	Tumor suppressive	—	YES	Prognostic	Jiang L et al. (2021)
AC099850.3	lncRNA	Carcinogenic	—	YES	Prognostic	Jiang L et al. (2021)
AL512274.1	lncRNA	Tumor suppressive	—	YES	Prognostic	Jiang L et al. (2021)
HOTAIR	lncRNA	Carcinogenic	Inhibiting miR-126/PI3K/AKT/GSK-3 $\beta$	YES	Therapeutic	Sophia et al. (2018)
GACAT1	lncRNA	Carcinogenic	Inhibiting miR-149	YES	Therapeutic	Chen et al. (2021)
LINC01207	lncRNA	Carcinogenic	Inhibiting miR-1301-3p/LDHA	YES	Therapeutic	Lu et al. (2021)
miR-126	MiRNA	Tumor suppressive	Inhibiting PI3K/AKT/GSK-3 $\beta$	YES	Diagnostic and Therapeutic	Sophia et al. (2018)
miR-149	MiRNA	Tumor suppressive	Inducing tumor-suppressive autophagy	YES	Diagnostic and Therapeutic	Chen et al. (2021)
miR-1301-3p	MiRNA	Tumor suppressive	Inhibiting LDHA	YES	Diagnostic and Therapeutic	Lu et al. (2021)
circ-LRP6	CircRNA	Carcinogenic	Activating-carcinogenic autophagy	YES	Therapeutic	Zhang et al. (2021)
circ-CDR1as	CircRNA	Carcinogenic	Activating-AKT/ERK 1/2/mTOR Inhibiting miR-671-5p Inhibiting miR-876-5p/SLC7A11	YES	Therapeutic	Gao et al. (2019); Cui et al. (2021)



successful strategy (Xu et al., 2020), providing new inspiration for OSCC studies, which has helped us achieve encouraging results. For instance, cordycepin strengthened the radiosensitivity of OSCC cells by inducing autophagy and apoptosis (Ho et al., 2019). Moreover, enteromorpha compressa extract was predicted to exert a therapeutic effect against OSCC by regulating autophagy and apoptosis (Pradhan et al., 2020). Nevertheless, the specific mechanism through which these compounds modulate autophagy remains to be elucidated. Identification of precise autophagy-related targets and the underlying mechanism/

pathway is essential to make targeting autophagy in OSCC a promising approach. Meanwhile, there seem to be divergent views on the role of autophagy in OSCC. Several studies showed that autophagy promotes OSCC progression and inhibiting autophagy may be an effective means to treat OSCC (Chen et al., 2018; Dong et al., 2020), while other studies reached the conclusion that autophagy kills OSCC cells and inhibits cancer metastasis (Yang et al., 2019; Kong et al., 2020). A closer look at the roles of autophagy in OSCC is essential for how to target autophagy (activation or inhibition) in OSCC.

## Autophagy-related biomarkers in OSCC

The identification of specific biomarkers is of great significance for the diagnosis, treatment, and prognosis prediction of cancers. Bioinformatics is a reliable tool to clarify the biological significance of massive biological data, which can help accurately predict biomarkers in cancers. In addition to mining online databases and sequencing alone, genomics, transcriptomics, proteomics, and other omics methods are often combined to improve prediction accuracy (Chen Y et al., 2019). Autophagy-related biomarkers associated with the diagnosis, treatment, and prognosis prediction of OSCC, including autophagy-related genes and non-coding RNAs, such as long non-coding RNAs (lncRNAs), micro RNAs (miRNAs), and circular RNAs (circular RNAs), have been identified.

### Autophagy-related genes

Eight of the 12 anatomical sites of head and neck squamous cell carcinoma (HNSCC) also belong to OSCC, such as tongue, buccal mucosa, and floor of mouth. Therefore, research on HNSCC has great overlap with that on OSCC, providing meaningful references for OSCC study. Autophagy-related genes are involved in many phases of autophagy, especially in autophagosome formation. Thirty-eight autophagy-related genes, which are differentially expressed in HNSCC tissues relative to normal tissues, were screened out in a recent study mining of HNSCC data from The Cancer Genome Atlas (TCGA). Six genes, namely heat shock protein B 8 (HSPB8), epidermal growth factor receptor (EGFR), integrin alpha-3 (ITGA3), fas-associated protein with death domain (FADD), cyclin-dependent kinase inhibitor 2 A (CDKN2A), and PINK1-Parkin RBR E3 ubiquitin-protein ligase (PRKN), were used to establish a risk model, which proved the practical value of these six genes in predicting HNSCC prognosis. The Kyoto Encyclopedia of Genes and Genomes (KEGG) pathway enrichment analysis indicated that these genes were obviously related to apoptosis, human cytomegalovirus infection, and human papillomavirus infection (Yang et al., 2020). Similar conclusions were obtained in another HNSCC study (Jin and Qin, 2020) using similar methods, wherein seven autophagy-related genes in HNSCC, namely ITGA3, FADD, CDKN2A, HSPB8, NK2 homeobox 3 (NKX2-3), BCL2 antagonist/killer 1 (BAK1), and C-X-C motif chemokine receptor 4 (CXCR4), were screened out. The prognostic value of these genes was confirmed through Kaplan–Meier analysis and receiver operating characteristic curve analysis. Additionally, the top three pathways identified through the KEGG pathway enrichment analysis were the apoptosis-related pathway, human cytomegalovirus infection, and human papillomavirus infection, followed by the epidermal growth factor receptor

(ErbB) pathway and hypoxia-inducible factor-1 (HIF-1) pathway. HSPB8, FADD, ITGA3, and CDKN2A are the repeatable targets in HNSCC. In an OSCC study, 37 differentially expressed autophagy-related genes, almost similar to those in HNSCC, were screened out. However, only autophagy-related 12 homolog 12 (ATG12) and BH3 interacting domain death agonist (BID) were confirmed as prognostic biomarkers, unlike those in HNSCC. Interestingly, the KEGG pathway analysis of these genes indicated their enrichment in apoptosis accompanied by the ErbB pathway, platinum drug resistance, and tumor necrosis factor (TNF) pathway (Huang et al., 2021). Moreover, the conclusions of other OSCC studies have been consistent. BAK1, BID, NKX2-3, and sphingosine kinase 1 (SPHK1) were selected as the targets by analyzing OSCC samples, and the downregulation of SPHK1 expression was verified in OSCC pathological tissues through immunohistochemistry (Zhu et al., 2020). These results suggested that HSPB8, FADD, ITGA3, and CDKN2A are repeatable targets in HNSCC, which may also play a role in OSCC, and FADD and NKX2-3 may have high prognostic and therapeutic value in OSCC. However, the bioinformatics analysis of these autophagy-related genes lacks experimental validation (Table 1).

### Autophagy-related non-coding RNAs (lncRNAs, miRNAs, and circRNAs)

lncRNAs are a type of non-coding RNA with a length of more than 200 nucleotides, and accumulating evidence suggests their indispensable role in cancers (McCabe and Rasmussen, 2021). The lncRNA/miRNA/mRNA axis alters the biological behaviors of cancer cells, such as the ability to undergo EMT and metastasis and show chemoresistance, wherein lncRNAs act as competitive endogenous RNAs (ceRNAs) by sponging miRNAs and changing the expression of their downstream target genes. The similar mechanism exists in OSCC (Figure 1). For example, overexpression of the lncRNA JPX transcript (JPX) was detected in OSCC cells, and JPX silencing could attenuate OSCC malignancy. The internal mechanism might be explained as the binding of JPX to miR-944 and the subsequent augmentation of Cadherin 2 (CDH2) via ceRNAs (Yao et al., 2021). lncRNAs also show carcinogenicity when autophagy is involved. The lncRNA long intergenic non-protein coding RNA 958 (LINC00958) was overexpressed in multiple OSCC cell lines compared with that in normal oral epithelial cells, and increased cell death and inhibition of cell proliferation were observed after LINC00958 silencing, which was accompanied by the decreased autophagy level. Further investigation indicated that LINC00958 sponged miR-4306 to activate the pyroptosis pathway, which was mediated by absent in melanoma 2 (AIM2), and promoted the survival rate of OSCC cells. In addition, sirtuin-1 (SIRT1) expression was



downregulated by LINC00958, which, in turn, reduced p53 expression (Jiang L et al., 2021). In a large-scale bioinformatics analysis, a series of autophagy-related lncRNAs, including AL354733.3, papillary thyroid carcinoma susceptibility candidate 2 (PTCSC2), UBAC2 antisense RNA 1 (UBAC2-AS1), long intergenic non-protein coding RNA 1963 (LINC01963), MIR600 host gene (MIR600HG), AP002884.1, RTCA antisense RNA 1 (RTCA-AS1), AC099850.3, and AL512274.1, were predicted to have prognostic values in OSCC, and the results were verified through quantitative reverse transcription polymerase chain reaction (RT-qPCR) and analysis of clinical samples. However, functional annotations were only performed through gene set enrichment analysis (GSEA), and the underlying mechanisms or pathways were not identified (Jiang Q et al., 2021). Although a series of autophagy-related lncRNAs were identified in the aforementioned bioinformatics analysis, the lncRNA HOX transcript antisense RNA (HOTAIR), which can modulate autophagy in various cancers, did not appear in the aforementioned list. HOTAIR overexpression was detected in OSCC cells, and HOTAIR knockdown could suppress the viability, migration, and invasion of OSCC cells by inhibiting autophagy. In addition, the sensitivity of OSCC cells to CDDP was increased, which indicates the therapeutic potential of HOTAIR in OSCC (Wang et al., 2018) (Table 1).

MiRNAs are non-coding, single-stranded RNA molecules with a length of approximately 22 nucleotides encoded by endogenous genes, and they are involved in the regulation of post transcriptional gene expression (Davey et al., 2021). In multiple cancers, the phosphoinositide 3-kinase (PI3K)/protein kinase B (AKT) pathway is obviously regulated by miRNAs, which affects the proliferation and invasion ability of cancer cells (Zhao et al., 2022). The interaction among lncRNAs, miRNAs, and PI3K/AKT pathway-mediated autophagy in OSCC was confirmed in a study using nimbolide, which provided us a new therapeutic target of OSCC, namely miR-126. The upregulation of miR-126 expression was measured after treating SCC-131 and SCC-4 OSCC cell lines with nimbolide. Additionally, protective autophagy was inhibited through inactivation of the PI3K/AKT/glycogen synthase kinase 3 (GSK3) pathway. The apoptosis rate of OSCC cells was also increased (Sophia et al., 2018). Additionally, miR-149 expression was downregulated by the sponge effect of the lncRNA gastric cancer-associated transcript 1 (GACAT1) in OSCC. Furthermore, GACAT1 knockdown promoted autophagy and apoptosis while inhibiting proliferation and metastasis in OSPECAPJ41 and HSC-4CC OSCC cell lines. Interestingly, when the miR-149 inhibitor was applied, the results were reversed, indicating that the lncRNA GACAT1 and miR-149

are promising therapeutic targets in OSCC (Chen et al., 2021). Similarly, in HSC-3 and HSC-4 OSCC cell lines, autophagy and proliferation were inhibited by the effect of miR-1301-3p on the carcinogenic gene lactate dehydrogenase A (LDHA), and apoptosis was promoted. The lncRNA long intergenic non-protein coding RNA 1207 (LINC01207), which is overexpressed in OSCC tissues, could sponge miR-1301-3p to liberate LDHA and cause an unfavorable prognosis (Lu et al., 2021) (Table 1).

CircRNAs are widely existing endogenous non-coding RNAs with a closed ring structure. Unlike traditional linear RNAs, circRNAs are not easily degraded because they are not affected by RNA exonucleases (Kristensen et al., 2022). Similar to lncRNAs, circRNAs act as a miRNA sponge through the mechanism of ceRNA, thus affecting the expression of miRNA target genes (Shi D. et al., 2021) (Figure 1). The circRNA LDL receptor-related protein 6 (LRP6) is highly expressed in OSCC tissues, and its knockdown reduced the autophagy flux and EMT in SCC-15 OSCC cell lines. Notably, the attenuated EMT caused by the knockdown of circ-LRP6 or autophagy related 5 homolog (ATG5) was partially restored by the autophagy agonist rapamycin, revealing the possible interaction between autophagy and EMT in OSCC (Zhang et al., 2021). In addition, the highly-expressed circRNA cerebellar degeneration-related protein 1 antisense (CDR1as) contributed to a higher survival rate of OSCC cells by enhancing autophagy and suppressing apoptosis under hypoxia environment. This phenomenon is associated with miR-671-5p sponging by circCDR1as, which inhibits the mammalian target of the rapamycin (mTOR) pathway and activates the AKT/extracellular signal-regulated kinase 1/2 (ERK1/2) pathway (Gao et al., 2019). Such conclusions provide us with a novel treatment strategy by targeting circCDR1as to reduce the tolerance of OSCC cells to hypoxia. Moreover, circCDR1as modulated solute carrier family 7 member 11 (SLC7A11) by sponging miR-876-5p to enhance autophagy-related metastasis and inhibit apoptosis (Cui et al., 2021). This finding confirms the oncogenic role of circCDR1as in OSCC, suggesting that circCDR1as suppression or relieving the inhibitory effect of circCDR1as on downstream targets could be promising in OSCC treatment. At present, there are few studies on circRNA in OSCC autophagy. According to the current results, autophagy-related circRNAs play a carcinogenic role in OSCC; however, more detailed studies are needed to confirm the finding (Table 1). Studies on non-autophagy-related circRNAs have shown that many circRNAs also inhibit OSCC progression; however, the relationship of circRNAs with autophagy remains to be further explored.

## Autophagy as a double-edged sword in OSCC

### Autophagy promotes OSCC progression

The epithelium of the oral cavity mainly originates from the ectoderm, whereas the epithelium of the tongue originates from the endoderm and mesoderm, and these processes are regulated by the Notch pathway. The dysregulation of Notch expression promotes cells to produce stem cell markers such as cluster of differentiation 44 (CD44) and accelerates OSCC progression (Porcheri and Mitsiadis, 2021). Coincidentally, high CD44 levels were detected in OSCC tissues and CDDP-resistant cells under a high autophagic flux, and the inhibition of autophagy could reduce stemness and CD44 expression of OSCC cells (Naik et al., 2018). Furthermore, in OSCC tissues and cell lines, the overexpression of recombinant human retinol-binding protein 1 (RBP1) triggered increased proliferation, migration, and invasiveness of OSCC cells, which was accompanied by abnormally elevated autophagy mediated via the RBP1-cytoskeleton-associated protein 4 (CKAP4) axis; these malignant phenotypes were suppressed after autophagy inhibition (Gao et al., 2020).

Environmental stresses such as hypoxia, energy stress, and damage factors are crucial to cancer progression. The stimulatory effect of autophagy on cancers is partly related to these environmental stresses. For instance, autophagy induced by HIF1- $\alpha$  can help cancer cells resist hypoxia-induced apoptosis. Specifically, the proliferation, migration, and invasion of SCC-9 OSCC cell lines were enhanced by the oncogene special AT-rich sequence-binding protein 2 (SATB2). In addition, hypoxia-induced autophagy and stemness were increased. Intriguingly, SATB2 knockdown reversed this chain action by causing the accumulation of autophagosomes and blockage of the autophagy flux (Dong et al., 2020). Cancer progression requires adequate energy supply. Autophagy can protect OSCC cells by saving energy and recycling sources under starvation. Increased autophagy prevented the OSCC cells from undergoing cell death and apoptosis, whereas 3-methyladenine (3-MA) attenuated autophagy triggered by malnutrition and weakened this protective effect (Abd El-Aziz et al., 2021). In addition, the underlying mechanism of hyperthermia in OSCC was investigated. Hypoxia and starvation caused by hyperthermia could increase the autophagy flux. Interestingly, the inhibition of autophagy in such situations could attenuate cell migration and strengthen hyperthermia-induced apoptosis in OSCC cells (Shi F. et al., 2021). Damage factors such as reactive oxygen species (ROS) can slow down cancer progression. ROS levels increase dramatically under ambient pressure, which may cause serious damage to the cellular structure, a condition known as oxidative stress. Mitophagy is utilized to resist oxidative stress. In OSCC, the terminalia bellirica (TB) extract gallic acid was introduced to promote the accumulation of mitochondrial ROS, causing DNA damage. Consequently, proliferation was inhibited and apoptosis was promoted in OSCC

cells. Moreover, autophagy inhibitors 3-MA and chloroquine reinforced TB extract-induced apoptosis in OSCC (Patra et al., 2020). This finding suggests that the inhibition of autophagy might enhance the sensitivity of OSCC cells to anti-cancer drugs.

EMT is a process in which epithelial cells gradually lose their own characteristics and acquire the characteristics of mesenchymal cells. Cells undergoing EMT are usually in a state of transition between epithelium and mesenchymal cells, thereby showing higher apoptosis tolerance and oncogenic potential (Kröger et al., 2019). EMT worsened the lesions by promoting the proliferation and metastasis of cancer cells (Pastushenko and Blanpain, 2019). The expression of the key glycolytic enzyme phosphofructokinase-platelet (PFKP) is significantly increased in OSCC patients, which leads to the increased starvation-induced autophagy and promotes EMT in OSCC cell lines. The abnormally increased autophagy and EMT were blocked after PFKP knockdown (Chen et al., 2018), indicating that a parallel relationship exists between autophagy and EMT in OSCC. More recently, the direct interaction between autophagy and EMT was confirmed by the inhibition of proliferation, migration, invasion, and EMT in OSCC cells following cudraxanthone D (CD) treatment. To investigate the underlying mechanism, the autophagy inhibitor 3-MA and the autophagy agonist resveratrol were applied, which inhibited and promoted EMT of OSCC cells, respectively. Moreover, resveratrol-induced autophagy and the corresponding EMT were suppressed by CD, thus rescuing OSCC cells from acquiring the malignant phenotype, thereby supporting the idea that autophagy promotes EMT in OSCC (Yu et al., 2019). This conclusion is also supported by a more recent study. As previously described, knockdown of circ-LRP6 or ATG5 reduced autophagy and impaired EMT, while application of rapamycin activated autophagy and restored EMT (Zhang et al., 2021).

### Autophagy suppresses OSCC progression

Despite playing a role in promoting OSCC progression, autophagy has been reported to inhibit OSCC progression. The PI3K/AKT/mTOR pathway is closely related to autophagy dysregulation in cancers (Liu et al., 2022). Knockdown of the lncRNA cancer susceptibility candidate 9 (CASC9) in SCC-15 and CAL-27 OSCC cell lines resulted in an obvious downregulation of p-AKT, p-mTOR, p62, and B cell lymphoma/leukemia-2 (Bcl-2), thereby promoting autophagy and apoptosis. Intriguingly, CASC9 knockdown-induced autophagy and apoptosis were reversed by the AKT activator SC79 (Yang et al., 2019). Similarly, a study reported that honokiol could suppress OSCC by increasing autophagy and apoptosis, and inactivation of the AKT/mTOR pathway was also reported (Huang et al., 2018). The relationship between inflammation and cancer has long been studied, and autophagy can inhibit cancer progression through the crosstalk between inflammatory pathways. The nuclear factor-kappa B (NF- $\kappa$ B) pathway in

most cancers is overactivated. Toll-like receptor 4 (TLR4) protein promotes cervical lymph node metastasis in OSCC by activating the NF- $\kappa$ B pathway, resulting in a poor prognosis. Autophagy could partially inhibit TLR4-mediated invasiveness by suppressing the NF- $\kappa$ B pathway in SCC-9 OSCC cell lines (Kong et al., 2020). The inverse relationship between autophagy and the NF- $\kappa$ B pathway was further clarified. Ursolic acid was found to increase autophagy and promote apoptosis by inhibiting the AKT/mTOR/NF- $\kappa$ B pathway, resulting in the abrogation of migration/invasion in CA-922 and SCC-2095 OSCC cell lines (Lin et al., 2019). Whether autophagy plays a role in promoting chemoresistance in OSCC is another controversial topic. The sensitivity of OSCC cells (CAL-27 and SCC-9) was enhanced after the inhibition of autophagy, which led the authors to draw the conclusion that autophagy helps OSCC cells acquire chemoresistance (Xu et al., 2017). However, this study used areca nut extract to induce autophagy. Areca nut is the main contributor for OSCC initiation, implying that the increased chemoresistance of OSCC cells may be mainly due to the oncogenic effect of carcinogens, and the role of autophagy in OSCC chemoresistance remains to be explored. More recently, obviously increased autophagy was found in SCC-4 OSCC cells but not in the novel CDDP-resistant OSCC cell line (SCC-4cisR), indicating that autophagy was probably not associated with the acquisition of cisplatin resistance in OSCC cells (Magnano et al., 2021). Probably, the study of inducing drug resistance first, followed by the analysis of the autophagy level in normal and drug-resistant OSCC cells, would yield more convincing results.

## Conclusion and perspectives

This review unraveled the intimate relationship between autophagy and OSCC. On the one hand, autophagy promotes OSCC by maintaining the viability of cancer stem cells, resisting microenvironmental stress, and promoting EMT. On the other hand, autophagy suppresses OSCC by inducing apoptosis and inhibiting invasion and migration of OSCC cells. These contrasting effects may be attributed to differences in the stages of OSCC examined in different studies. Comprehensive studies at specific OSCC stages are needed to explore the exact roles of autophagy in the long process from OSCC initiation to tumor formation and malignant progression. Autophagy-related biomarkers such as autophagy-related genes, lncRNAs, miRNAs, and circRNAs have been reported. These biomarkers regulate multiple biological processes of OSCC through autophagy and exhibit a great potential for clinical application. In terms of diagnosis, the analysis of salivary miRNAs is simpler than that of salivary mRNAs, and miRNAs are not affected by the high digestive sensitivity of RNase, using miRNAs as a biomarker for early diagnosis of OSCC is a feasible option. At the same time,

saliva samples are easy to collect and non-invasive for detection, which is easier to be accepted, and is suitable for a wide range of early OSCC screening. Regarding the prognosis prediction, sequencing the tumor tissues resected from patients and establishing and continuously improving the risk model through these autophagy-related biomarkers to predict the 1-, 3-, and 5-year survival rates of patients in combination with clinical indicators, such as tumor grade, may assist clinicians in adjusting treatment plans and communicating with patients. Moreover, further study on the relationship between EMT and autophagy may give instructions to the prediction of OSCC metastasis possibility and lymph node dissection. For OSCC treatment, some existing compounds such as TB and CD have been proven to inhibit OSCC by modulating the autophagy level. Additionally, developing specially designed drugs for the aforementioned autophagy-related biomarkers through molecular docking, high-throughput screening, and molecular dynamic simulation may be promising in improving OSCC treatment. Notably, reliability of some of the biomarkers has not been confirmed through experiments. Experimental verification of the repeatable targets might provide guidance for developing an effective clinical strategy for OSCC treatment.

In summary, this review presents a series of autophagy-related biomarkers and discusses the roles of autophagy in OSCC progression. Further exploration is required in the field of autophagy in OSCC for the improvement of clinical therapy.

## Author contributions

L-LZ and HH conceived, formatted, revised extensively, and submitted this manuscript. QG wrote the manuscript.

## Funding

This work was supported by the South West Medical University (Grant No. 2021ZKMS013).

## Conflict of interest

The authors declare that the research was conducted in the absence of any commercial or financial relationships that could be construed as a potential conflict of interest.

## Publisher's note

All claims expressed in this article are solely those of the authors and do not necessarily represent those of their affiliated

organizations, or those of the publisher, the editors, and the reviewers. Any product that may be evaluated in this article, or

claim that may be made by its manufacturer, is not guaranteed or endorsed by the publisher.

## References

- Abd El-Aziz, Y. S., Leck, L. Y. W., Jansson, P. J., and Sahni, S. (2021). Emerging role of autophagy in the development and progression of oral squamous cell carcinoma. *Cancers (Basel)* 13 (24), 6152. doi:10.3390/cancers13246152
- Chen, G., Liu, H., Zhang, Y., Liang, J., Zhu, Y., Zhang, M., et al. (2018). Silencing PFKFB3 inhibits starvation-induced autophagy, glycolysis, and epithelial-mesenchymal transition in oral squamous cell carcinoma. *Exp. Cell Res.* 370 (1), 46–57. doi:10.1016/j.yexcr.2018.06.007
- Chen, H. T., Liu, H., Mao, M. J., Tan, Y., Mo, X. Q., Meng, X. J., et al. (2019). Crosstalk between autophagy and epithelial-mesenchymal transition and its application in cancer therapy. *Mol. Cancer* 18 (1), 101. doi:10.1186/s12943-019-1030-2
- Chen, J., Chen, X., Fu, L., Chen, J., Chen, Y., and Liu, F. (2021). LncRNA GACAT1 targeting miRNA-149 regulates the molecular mechanism of proliferation, apoptosis and autophagy of oral squamous cell carcinoma cells. *Aging (Albany NY)* 13 (16), 20359–20371. doi:10.18632/aging.203416
- Chen, Y., Wang, G., Cai, H., Sun, Y., Ouyang, L., and Liu, B. (2019). Deciphering the rules of *in silico* autophagy methods for expediting medicinal research. *J. Med. Chem.* 62 (15), 6831–6842. doi:10.1021/acs.jmedchem.8b01673
- Cui, L., Huang, C., and Zhou, D. (2021). Overexpression of circCDR1as drives oral squamous cell carcinoma progression. *Oral Dis.* (Online ahead of print) doi:10.1111/odi.14085
- Das, S., Shukla, N., Singh, S. S., Kushwaha, S., and Shrivastava, R. (2021). Mechanism of interaction between autophagy and apoptosis in cancer. *Apoptosis* 26 (9–10), 512–533. doi:10.1007/s10495-021-01687-9
- Davey, M. G., Lowery, A. J., Miller, N., and Kerin, M. J. (2021). MicroRNA expression profiles and breast cancer chemotherapy. *Int. J. Mol. Sci.* 22 (19), 10812. doi:10.3390/ijms221910812
- Dong, W., Chen, Y., Qian, N., Sima, G., Zhang, J., Guo, Z., et al. (2020). SATB2 knockdown decreases hypoxia-induced autophagy and stemness in oral squamous cell carcinoma. *Oncol. Lett.* 20 (1), 794–802. doi:10.3892/ol.2020.11589
- Fleming, A., Bourdenx, M., Fujimaki, M., Karabiyik, C., Krause, G. J., Lopez, A., et al. (2022). The different autophagy degradation pathways and neurodegeneration. *Neuron* 110 (6), 935–966. doi:10.1016/j.neuron.2022.01.017
- Gao, L., Dou, Z. C., Ren, W. H., Li, S. M., Liang, X., and Zhi, K. Q. (2019). CircCDR1as upregulates autophagy under hypoxia to promote tumor cell survival via AKT/ERK(1/2)/mTOR signaling pathways in oral squamous cell carcinomas. *Cell Death Dis.* 10 (10), 745. doi:10.1038/s41419-019-1971-9
- Gao, L., Wang, Q., Ren, W., Zheng, J., Li, S., Dou, Z., et al. (2020). The RBP1-CKAP4 axis activates oncogenic autophagy and promotes cancer progression in oral squamous cell carcinoma. *Cell Death Dis.* 11 (6), 488. doi:10.1038/s41419-020-2693-8
- Ho, A. S., Kim, S., Tighiouart, M., Gudino, C., Mita, A., Scher, K. S., et al. (2017). Metastatic lymph node burden and survival in oral cavity cancer. *J. Clin. Oncol.* 35 (31), 3601–3609. doi:10.1200/jco.2016.71.1176
- Ho, S. Y., Wu, W. S., Lin, L. C., Wu, Y. H., Chiu, H. W., Yeh, Y. L., et al. (2019). Cordycepin enhances radiosensitivity in oral squamous carcinoma cells by inducing autophagy and apoptosis through cell cycle arrest. *Int. J. Mol. Sci.* 20 (21), E5366. doi:10.3390/ijms20215366
- Huang, G. Z., Lu, Z. Y., Rao, Y., Gao, H., and Lv, X. Z. (2021). Screening and identification of autophagy-related biomarkers for oral squamous cell carcinoma (OSCC) via integrated bioinformatics analysis. *J. Cell. Mol. Med.* 25 (9), 4444–4454. doi:10.1111/jcmm.16512
- Huang, K. J., Kuo, C. H., Chen, S. H., Lin, C. Y., and Lee, Y. R. (2018). Honokiol inhibits *in vitro* and *in vivo* growth of oral squamous cell carcinoma through induction of apoptosis, cell cycle arrest and autophagy. *J. Cell. Mol. Med.* 22 (3), 1894–1908. doi:10.1111/jcmm.13474
- Jiang, L., Ge, W., Cui, Y., and Wang, X. (2021). The regulation of long non-coding RNA 00958 (LINC00958) for oral squamous cell carcinoma (OSCC) cells death through absent in melanoma 2 (AIM2) depending on microRNA-4306 and Sirtuin1 (SIRT1) *in vitro*. *Bioengineered* 12 (1), 5085–5098. doi:10.1080/21655979.2021.1955561
- Jiang, Q., Xue, D., Shi, F., and Qiu, J. (2021). Prognostic significance of an autophagy-related long non-coding RNA signature in patients with oral and oropharyngeal squamous cell carcinoma. *Oncol. Lett.* 21 (1), 29. doi:10.3892/ol.2020.12290
- Jin, Y., and Qin, X. (2020). Development of a prognostic signature based on autophagy-related genes for head and neck squamous cell carcinoma. *Arch. Med. Res.* 51 (8), 860–867. doi:10.1016/j.arcmed.2020.09.009
- Kong, Q., Liang, Y., He, Q., You, Y., Wu, L., Liang, L., et al. (2020). Autophagy inhibits TLR4-mediated invasiveness of oral cancer cells via the NF- $\kappa$ B pathway. *Oral Dis.* 26, 1165–1174. doi:10.1111/odi.13355
- Kristensen, L. S., Jakobsen, T., Hager, H., and Kjems, J. (2022). The emerging roles of circRNAs in cancer and oncology. *Nat. Rev. Clin. Oncol.* 19 (3), 188–206. doi:10.1038/s41571-021-00585-y
- Kröger, C., Afeyan, A., Mraz, J., Eaton, E. N., Reinhardt, F., Khodor, Y. L., et al. (2019). Acquisition of a hybrid E/M state is essential for tumorigenicity of basal breast cancer cells. *Proc. Natl. Acad. Sci. U. S. A.* 116 (15), 7353–7362. doi:10.1073/pnas.1812876116
- Li, X., Guo, S., Xiong, X. K., Peng, B. Y., Huang, J. M., Chen, M. F., et al. (2019). Combination of quercetin and cisplatin enhances apoptosis in OSCC cells by downregulating xIAP through the NF- $\kappa$ B pathway. *J. Cancer* 10 (19), 4509–4521. doi:10.7150/jca.31045
- Lin, C. W., Chin, H. K., Lee, S. L., Chiu, C. F., Chung, J. G., Lin, Z. Y., et al. (2019). Ursolic acid induces apoptosis and autophagy in oral cancer cells. *Environ. Toxicol.* 34 (9), 983–991. doi:10.1002/tox.22769
- Liu, W., Jin, W., Zhu, S., Chen, Y., and Liu, B. (2022). Targeting regulated cell death (RCD) with small-molecule compounds in cancer therapy: A revisited review of apoptosis, autophagy-dependent cell death and necroptosis. *Drug Discov. Today* 27 (2), 612–625. doi:10.1016/j.drudis.2021.10.011
- Lu, X., Chen, L., Li, Y., Huang, R., Meng, X., and Sun, F. (2021). Long non-coding RNA LINC01207 promotes cell proliferation and migration but suppresses apoptosis and autophagy in oral squamous cell carcinoma by the microRNA-1301-3p/lactate dehydrogenase isoform A axis. *Bioengineered* 12 (1), 7780–7793. doi:10.1080/21655979.2021.1972784
- Magnano, S., Hannon Barroeta, P., Duffy, R., O'Sullivan, J., and Zisterer, D. M. (2021). Cisplatin induces autophagy-associated apoptosis in human oral squamous cell carcinoma (OSCC) mediated in part through reactive oxygen species. *Toxicol. Appl. Pharmacol.* 427, 115646. doi:10.1016/j.taap.2021.115646
- McCabe, E. M., and Rasmussen, T. P. (2021). LncRNA involvement in cancer stem cell function and Epithelial-mesenchymal transition. *Semin. Cancer Biol.* 75, 38–48. doi:10.1016/j.semcancer.2020.12.012
- Moratin, J., Horn, D., Metzger, K., Ristow, O., Flechtenmacher, C., Engel, M., et al. (2020). Squamous cell carcinoma of the mandible - patterns of metastasis and disease recurrence in dependence of localization and therapy. *J. Craniomaxillofac. Surg.* 48 (12), 1158–1163. doi:10.1016/j.jcms.2020.10.006
- Naik, P. P., Mukhopadhyay, S., Panda, P. K., Sinha, N., Das, C. K., Mishra, R., et al. (2018). Autophagy regulates cisplatin-induced stemness and chemoresistance via the upregulation of CD44, ABCB1 and ADAM17 in oral squamous cell carcinoma. *Cell Prolif.* 51 (1). doi:10.1111/cpr.12411
- Pastushenko, I., and Blanpain, C. (2019). EMT transition states during tumor progression and metastasis. *Trends Cell Biol.* 29 (3), 212–226. doi:10.1016/j.tcb.2018.12.001
- Patra, S., Panda, P. K., Naik, P. P., Panigrahi, D. P., Praharaj, P. P., Bhol, C. S., et al. (2020). Terminalia bellirica extract induces anticancer activity through modulation of apoptosis and autophagy in oral squamous cell carcinoma. *Food Chem. Toxicol.* 136, 111073. doi:10.1016/j.fct.2019.111073
- Porcheri, C., and Mitsiadis, T. A. (2021). Notch in head and neck cancer. *Adv. Exp. Med. Biol.* 1287, 81–103. doi:10.1007/978-3-030-55031-8\_7
- Pradhan, B., Patra, S., Behera, C., Nayak, R., Patil, S., Bhutia, S. K., et al. (2020). Enteromorpha compressa extract induces anticancer activity through apoptosis and autophagy in oral cancer. *Mol. Biol. Rep.* 47 (12), 9567–9578. doi:10.1007/s11033-020-06010-4
- Shi, D., Li, H., Zhang, J., and Li, Y. (2021a). CircGDI2 regulates the proliferation, migration, invasion and apoptosis of OSCC via miR-454-3p/FOXF2 Axis. *Cancer Manag. Res.* 13, 1371–1382. doi:10.2147/cmar.s277096
- Shi, F., Luo, D., Zhou, X., Sun, Q., Shen, P., and Wang, S. (2021b). Combined effects of hyperthermia and chemotherapy on the regulate autophagy of oral

squamous cell carcinoma cells under a hypoxic microenvironment. *Cell Death Discov.* 7 (1), 227. doi:10.1038/s41420-021-00538-5

Sophia, J., Kowshik, J., Dwivedi, A., Bhutia, S. K., Manavathi, B., Mishra, R., et al. (2018). Nimbolide, a neem limonoid inhibits cytoprotective autophagy to activate apoptosis via modulation of the PI3K/Akt/GSK-3 $\beta$  signalling pathway in oral cancer. *Cell Death Dis.* 9 (11), 1087. doi:10.1038/s41419-018-1126-4

Wang, X., Liu, W., Wang, P., and Li, S. (2018). RNA interference of long noncoding RNA HOTAIR suppresses autophagy and promotes apoptosis and sensitivity to cisplatin in oral squamous cell carcinoma. *J. Oral Pathol. Med.* 47 (10), 930–937. doi:10.1111/jop.12769

Xia, H., Green, D. R., and Zou, W. (2021). Autophagy in tumour immunity and therapy. *Nat. Rev. Cancer* 21 (5), 281–297. doi:10.1038/s41568-021-00344-2

Xiang, H., Zhang, J., Lin, C., Zhang, L., Liu, B., and Ouyang, L. (2020). Targeting autophagy-related protein kinases for potential therapeutic purpose. *Acta Pharm. Sin. B* 10 (4), 569–581. doi:10.1016/j.apsb.2019.10.003

Xu, J., Patel, N. H., and Gewirtz, D. A. (2020). Triangular relationship between p53, autophagy, and chemotherapy resistance. *Int. J. Mol. Sci.* 21 (23), E8991. doi:10.3390/ijms21238991

Xu, Z., Huang, C. M., Shao, Z., Zhao, X. P., Wang, M., Yan, T. L., et al. (2017). Autophagy induced by areca nut extract contributes to decreasing cisplatin toxicity in oral squamous cell carcinoma cells: Roles of reactive oxygen species/AMPK signaling. *Int. J. Mol. Sci.* 18 (3), E524. doi:10.3390/ijms18030524

Yang, C., Mei, H., Peng, L., Jiang, F., Xie, B., and Li, J. (2020). Prognostic correlation of an autophagy-related gene signature in patients with head and neck squamous cell carcinoma. *Comput. Math. Methods Med.* 2020, 7397132. doi:10.1155/2020/7397132

Yang, Y., Chen, D., Liu, H., and Yang, K. (2019). Increased expression of lncRNA CASC9 promotes tumor progression by suppressing autophagy-mediated cell apoptosis via the AKT/mTOR pathway in oral squamous cell carcinoma. *Cell Death Dis.* 10 (2), 41. doi:10.1038/s41419-018-1280-8

Yao, Y., Chen, S., Lu, N., Yin, Y., and Liu, Z. (2021). LncRNA JPX overexpressed in oral squamous cell carcinoma drives malignancy via miR-944/CDH2 axis. *Oral Dis.* 27 (4), 924–933. doi:10.1111/odi.13626

Yu, S. B., Kang, H. M., Park, D. B., Park, B. S., and Kim, I. R. (2019). Cudraxanthone D regulates Epithelial–mesenchymal transition by autophagy inhibition in oral squamous cell carcinoma cell lines. *Evid. Based. Complement. Altern. Med.* 2019, 5213028. doi:10.1155/2019/5213028

Zhang, J., Wang, G., Zhou, Y., Chen, Y., Ouyang, L., and Liu, B. (2018). Mechanisms of autophagy and relevant small-molecule compounds for targeted cancer therapy. *Cell. Mol. Life Sci.* 75 (10), 1803–1826. doi:10.1007/s00018-018-2759-2

Zhang, Q., Jiang, C., Ren, W., Li, S., Zheng, J., Gao, Y., et al. (2021). Circ-LRP6 mediates Epithelial–mesenchymal transition and autophagy in oral squamous cell carcinomas. *J. Oral Pathol. Med.* 50 (7), 660–667. doi:10.1111/jop.13163

Zhao, R., Fu, J., Zhu, L., Chen, Y., and Liu, B. (2022). Designing strategies of small-molecule compounds for modulating non-coding RNAs in cancer therapy. *J. Hematol. Oncol.* 15 (1), 14. doi:10.1186/s13045-022-01230-6

Zhu, L., Yan, D., Chen, Y., Chen, S., Chen, N., and Han, J. (2020). The identification of autophagy-related genes in the prognosis of oral squamous cell carcinoma. *Oral Dis.* 26 (8), 1659–1667. doi:10.1111/odi.13492



## Glossary

<b>3-MA</b> 3-methyladenine	<b>JPX</b> JPX transcript
<b>AIM2</b> absent in melanoma 2	<b>LDHA</b> lactate dehydrogenase A
<b>AKT</b> protein kinase B	<b>LINC00958</b> long intergenic non-protein coding RNA 958
<b>ATG5</b> autophagy-related 5 homolog	<b>LINC01207</b> long intergenic non-protein coding RNA 1207
<b>ATG12</b> autophagy-related 12 homolog	<b>LINC01963</b> long intergenic non-protein coding RNA 1963
<b>BAK1</b> BCL2 antagonist/killer 1	<b>LncRNA</b> long non-coding RNA
<b>Bcl-2</b> B-cell lymphoma/leukemia-2	<b>LRP6</b> LDL receptor-related protein 6
<b>BID</b> BH3 interacting domain death agonist	<b>MIR600HG</b> MIR600 host gene
<b>CASC9</b> cancer susceptibility candidate 9	<b>miRNA</b> MicroRNA
<b>CD</b> cudraxanthone D	<b>mTOR</b> mammalian target of rapamycin
<b>CD44</b> cluster of differentiation 44	<b>NF-<math>\kappa</math>B</b> nuclear factor kappa B
<b>CDDP</b> cisplatin	<b>NKX2-3</b> NK2 Homeobox 3
<b>CDH2</b> cadherin 2	<b>OSCC</b> oral squamous cell carcinoma
<b>CDKN2A</b> cyclin-dependent kinase inhibitor 2 A	<b>PFKP</b> phosphofructokinase-platelet;
<b>CDR1as</b> cerebellar degeneration-related protein 1 antisense	<b>PI3K</b> phosphoinositide 3-kinase
<b>CircRNA</b> circular RNA	<b>PRKN</b> Parkin RBR E3 ubiquitin protein ligase
<b>CKAP4</b> cytoskeleton-associated protein 4	<b>PTCSC2</b> papillary thyroid carcinoma susceptibility candidate 2
<b>CXCR4</b> C-X-C motif chemokine receptor 4	<b>RBPI</b> recombinant human retinol-binding protein 1
<b>EGFR</b> epidermal growth factor receptor	<b>ROS</b> reactive oxygen species
<b>EMT</b> Epithelial–mesenchymal transition	<b>RTCA-AS1</b> RTCA antisense RNA 1
<b>ErbB</b> epidermal growth factor receptor	<b>RT-qPCR</b> quantitative reverse-transcription polymerase chain reaction
<b>ERK1/2, extracellular signal-regulated kinase 1/2</b>	<b>SATB2</b> special AT-rich sequence-binding protein 2
<b>FADD</b> Fas-associated protein with death domain;	<b>SIRT1</b> Sirtuin-1
<b>GACAT1</b> gastric cancer-associated transcript 1	<b>SLC7A11</b> solute carrier family 7 member 11
<b>GSEA</b> Gene set enrichment analysis	<b>SPHK1</b> sphingosine kinase 1
<b>HIF-1</b> hypoxia-inducible factor-1	<b>TB</b> <i>Terminalia</i> bellirica
<b>HNSCC</b> Head and neck squamous cell carcinoma	<b>TCGA</b> The Cancer Genome Atlas
<b>HOTAIR</b> HOX transcript antisense RNA	<b>TLR4</b> Toll-like receptor 4
<b>HSPB8</b> heat shock protein B 8	<b>TNF</b> tumor necrosis factor
<b>ITGA3</b> integrin alpha-3	<b>TNM</b> tumor-node-metastasis
	<b>UBAC2-AS1</b> UBAC2 antisense RNA 1.



## OPEN ACCESS

## EDITED BY

Ryszard Pluta,  
Mossakowski Medical Research Institute  
(PAS), Poland

## REVIEWED BY

Amr Ahmed El-Arabey,  
Al-Azhar University, Egypt  
Gulam M. Rather,  
The State University of New Jersey,  
United States

## \*CORRESPONDENCE

Yang Yu,  
1018yuyang@jnu.edu.cn  
Danfeng Shi,  
shidf18@jnu.edu.cn

## SPECIALTY SECTION

This article was submitted to  
Pharmacology of Anti-Cancer Drugs,  
a section of the journal  
Frontiers in Pharmacology

RECEIVED 23 August 2022

ACCEPTED 13 October 2022

PUBLISHED 24 October 2022

## CITATION

Shi D, Pang Q, Qin Q, Yao X, Yao X and  
Yu Y (2022), Discovery of novel anti-  
tumor compounds targeting PARP-1  
with induction of autophagy through *in*  
*silico* and *in vitro* screening.  
*Front. Pharmacol.* 13:1026306.  
doi: 10.3389/fphar.2022.1026306

## COPYRIGHT

© 2022 Shi, Pang, Qin, Yao, Yao and Yu.  
This is an open-access article  
distributed under the terms of the  
[Creative Commons Attribution License](#)  
(CC BY). The use, distribution or  
reproduction in other forums is  
permitted, provided the original  
author(s) and the copyright owner(s) are  
credited and that the original  
publication in this journal is cited, in  
accordance with accepted academic  
practice. No use, distribution or  
reproduction is permitted which does  
not comply with these terms.

# Discovery of novel anti-tumor compounds targeting PARP-1 with induction of autophagy through *in silico* and *in vitro* screening

Danfeng Shi<sup>1\*</sup>, Qianqian Pang<sup>1</sup>, Qianyu Qin<sup>1</sup>, Xinsheng Yao<sup>1</sup>,  
Xiaojun Yao<sup>2</sup> and Yang Yu<sup>1\*</sup>

<sup>1</sup>Guangdong Province Key Laboratory of Pharmacodynamic Constituents of TCM and New Drugs Research, International Cooperative Laboratory of Traditional Chinese Medicine Modernization and Innovative Drug Development of Ministry of Education (MOE) of China, Institute of Traditional Chinese Medicine and Natural Products, College of Pharmacy, Jinan University, Guangzhou, China, <sup>2</sup>State Key Laboratory of Quality Research in Chinese Medicine, Macau Institute for Applied Research in Medicine and Health, Macau University of Science and Technology, Taipa, Macau, China

Poly (ADP-ribose) polymerase 1 (PARP-1) is a critical enzyme involved in DNA damage repair and recombination, and shows great potential for drug development in the treatment of cancers with defective DNA repair. The anti-tumor activities of PARP-1 inhibitors are regulated by both inhibition activities and allosteric mechanisms of PARP-1, and may also be involved in an autophagy-mediated process. Screening PARP-1 inhibitors with potential allosteric mechanisms and induced autophagy process could achieve elevated potency toward cancer cell killing. In this study, we tried to discover novel anti-tumor compounds targeting PARP-1 by computer simulations and *in vitro* screening. In order to filter PARP-1 inhibitors that could affect the folding state of the helix domain (HD) on PARP-1, the free energy contribution of key residues on HD were systematically analyzed using the ligand-binding crystal structures and integrated into *in silico* screening workflow for the selection of 20 pick-up compounds. Four compounds (Chemdiv codes: 8012-0567, 8018-6529, 8018-7168, 8018-7603) were proved with above 40% inhibitory ratio targeting PARP-1 under 20  $\mu$ M, and further performed binding mode prediction and dynamic effect evaluation by molecular dynamics simulation. Further *in vitro* assays showed that compounds 8018-6529 and 8018-7168 could inhibit the growth of the human colorectal cancer cell (HCT-116) with IC<sub>50</sub> values of 4.30 and 9.29  $\mu$ M and were accompanied with an induced autophagy process. Taken together, we discover two novel anti-tumor compounds that target PARP-1 with an induced autophagy process and provide potential hit compounds for the anti-cancer drug development.

## KEYWORDS

PARP-1 inhibitor, anti-tumor, *in silico* screening, autophagy, allosteric

## 1 Introduction

Poly (ADP-ribose) polymerase 1 (PARP-1) is a critical enzyme in the cell nucleus that responds to the damage repair of single- and double-stranded DNA breaks (SSBs and DSBs) (Ame et al., 2004). Upon relocating and binding to DNA damage sites, PARP-1 could activate the poly (ADP-ribosyl)ation by transforming ADP-ribose unit from nicotinamide adenine dinucleotide (NAD<sup>+</sup>) to various substrate proteins or nucleic acids (Langelier et al., 2018a). This post-translational modification (PTM) process on PARP-1 itself or histones in nucleosomes proximal to the break could rebuild the connection between DNA damage and chromatin modification. It has been found that the lacking of both PARP-dependent SSB repair and BRCA-dependent DSB repair is not tolerable for cell survival (Helleday, 2011), which is also known as a phenomenon of synthetic lethality (O'Neil et al., 2017). The PARP-1 inhibitors can selectively kill the cancer cells with homologous recombination (HR) defect caused by BRCA1/2 mutations, and have been approved for the therapy of cancers such as ovarian cancer, prostate cancer and breast cancer, etc (Rouleau et al., 2010; Lin and Kraus, 2017; Lord and Ashworth, 2017). Clinically, these PARP inhibitors have been mainly applied for the maintenance therapy of malignancies or the treatment for recurrent cancer, and the combination therapies with other kind of inhibitors also show great potential for the overcome of tumor resistance (Rose et al., 2020; Tung and Garber, 2022).

PARP-1 inhibitors with distinct scaffolds exhibit vastly different anti-tumor efficacy in the clinic (Shen et al., 2013). Basically, all PARP-1 inhibitors were engaged in a competitive manner to the nicotinamide portion of NAD<sup>+</sup> by forming hydrogen bonding with the backbone amide of Gly863 and the side chain oxygen of Ser904. The typical scaffold-hopping optimization of benzamide and cyclic lactam scaffolds has generated a variety of active scaffolds with excellent inhibitory activities (Wang et al., 2016). Recently, it is validated that PARP-1 inhibitors could confer its cellular toxicity through two ways simultaneously, inhibiting poly (ADP-ribosyl)ation by the occupancy of the ADP-ribosyl transferase (ART) domain and prolonging the retention of PARP-1 on DNA damage (Langelier et al., 2018b; Zandarashvili et al., 2020). The retention of PARP-1 on DNA damage is dependent on an allosteric regulatory effect which is engaged in the conformational unfolding of the helix domain (HD) adjacent to the ART domain. The mechanistic studies also showed that the cellular toxicities of PARP-1 inhibitors could be elevated with the stronger abilities to destabilize the conformation of HD (Langelier et al., 2018b; Zandarashvili et al., 2020; Rouleau-Turcotte et al., 2022). It is indicated that the inhibitors with contacts with HD could trap PARP-1 on DNA damage and show enhanced killing ability against cancer cells. Therefore, the discovery and design of novel PARP-1 inhibitors can be optimized in view of the effect on the HD.

In addition to the direct targeted regulation effects on DNA repair process, PARP-1 inhibitors also have shown great potential to intervene the autophagy process which was induced by the DNA damage (Zhang et al., 2018) and shows great potential for synergistic therapeutic effect (Munoz-Gomez et al., 2009; Arun et al., 2015; Jiang et al., 2018; Casili et al., 2020). Typically, PARP-1 inhibitors have been reported to induce autophagy in a variety of tumor models, including ovarian cancer (Santiago-O'Farrill et al., 2020), chronic myeloid leukemia (Liu et al., 2019) and hepatocellular carcinoma (Zai et al., 2020), and the cotreatment with an autophagy inhibitor (chloroquine) may further expand the therapeutic efficacy of PARP inhibitors. The induction of autophagy by PARP-1 inhibitors may further provide an opportunity to improve the efficacy against tumors.

Methods like molecular docking and molecular dynamics simulation have provided a series of ways to analyze the interactions between the ligand and binding sites (Liu et al., 2018). It is hypothesized that a systematic analysis of different conformational states of complex will provide valuable information about the ligand binding before the screening process (Cooper et al., 2011; Maveyraud and Mourey, 2020). The different conformational states of domains or residues around the binding site have significant effect on the binding mode of ligands and will further affect the docking-based screening (Chen et al., 2006). Currently, more than 40 crystal structures of PARP-1 complex were reported in the PDB database (Sussman et al., 1998), providing abundant information about binding modes and conformational changes upon ligand binding. By decomposing the total binding affinity to the contribution of every single residue, the key residues around the binding sites could be effectively recognized. In order to discover novel PARP-1 inhibitor, the systematic analysis of the residues around ART domain and the HD were performed before *in silico* screening process. The reveal of the dynamic and energetic characters of PARP-1 complex may improve the performance of *in silico* screening.

In this study, an integrated approach of *in silico* and *in vitro* screening was performed to discover novel PARP-1 inhibitors. In order to enhance the effectiveness of virtual screening and find molecules with potential allosteric effect, the pocket residues on ART domain and HD were analyzed by their effect on the binding free energy with PARP-1 inhibitors. Multiple linear regression was applied to re-weight the contribution of these key residues and applied in the virtual screening. Then, a protocol of virtual screening workflow is evaluated and designed for the discovery of novel scaffolds of PARP-1 inhibitors, and 20 compounds were purchased from the Chemdiv database for *in vitro* assays. The inhibition ratio was evaluated by chemiluminescent PARP Assay Kit assay, and four hit compounds were found at micromolar level. Molecular dynamics simulation combined with binding free energy calculation revealed the binding modes, and further cell experiments also validated the potential anti-tumor effect of these compounds and

the process of inducing autophagy. These compounds can provide new scaffolds for developing novel PARP-1 inhibitors applicable to cancer therapy using further hit-to-lead structural modification strategies.

## 2 Materials and methods

### 2.1 Crystal structure collection and binding mode analysis

A series of crystal structures of the PARP-1 in complex with structurally diverse inhibitors were retrieved from the PDB database (<https://www.rcsb.org/>). The crystal structures with the existence of the HD in crystal structures of complex (Supplementary Table S1) were further selected for binding mode analysis. The crystal structures were prepared in the Protein Preparation Wizard module in Schrödinger Software Suite (Schrödinger, LLC: New York, NY, 2015). The crystalline water molecules and ions in each crystal structure were removed, while the ligand and protein were prepared by adding hydrogens, filling in missing side chains, and assigning the protonation state of residues at pH value of 7.0. Then, the mass centroids of the native ligands in the crystal structures were defined as the centers of the binding pockets. All the ligands were extracted from the crystal structures and prepared using MMFFs force field, with a target pH of  $7.0 \pm 2.0$  in the LigPrep module. Then, all the ligands were redocked into the corresponding complex structures with restriction of all heavy atoms to the reference position. And the interactive free energy contributions of residues within 10 Å of the mass centroids of the native ligands were derived out and analyzed. The experimental values of affinities for PARP-1 ligands were estimated by the referring IC<sub>50</sub> values.

According to the free energy contributions and electrostatic properties, residues at the active binding site of PARP-1 were further clustered into three groups, namely electrostatic group, non-electrostatic group and other group. The total free energy contributions of residues in three groups were summed as energy terms of  $E_{ele}$ ,  $E_{nonele}$ ,  $E_{other}$  for complex structures respectively. Then, a multiple linear regression model was applied to fit these energy terms to the experimental affinities of the corresponding ligand. The binding affinities ( $y$ ) was depicted as follows:

$$y = c_1 \times E_{ele} + c_2 \times E_{nonele} + c_3 \times E_{other} + c_0$$

### 2.2 Evaluation of molecular docking

The crystal structure in complex with Niraparib (PDB ID: 4R6E) was selected as the receptor for the docking-based virtual screening process. To evaluate the screening power of the receptor, a compound dataset containing both actives and decoys was constructed. 40 ligands of PARP-1 were extracted

from the complex crystal structures as the actives. The decoys with structural similarity to actives were generated with an active-to-decoy ratio of 1:50 in the DUD-E server (Mysinger et al., 2012) (<http://dude.docking.org/generate>) as shown in Supplementary Table S2, and a total of 1990 decoys were generated by deleting the duplicates. Firstly, the docking ability of the Glide module was evaluated by redocking the native ligands (Niraparib) into its binding site using HTVS, SP and XP protocol respectively, and the binding poses with the best docking score were selected for conformational superposition to the original crystal structures. The root mean square deviation (RMSD) was calculated focusing on all heavy atoms of ligands. In order to further evaluate the virtual screening (VS) performance of the receptor (Empereur-Mot et al., 2015), the receiver operating characteristics (ROC) curve with the calculation of area under curve (AUC) was applied to evaluate the discrimination capability between actives and decoys for different docking protocols (Florkowski, 2008).

### 2.3 The workflow of virtual screening and the purchase of selected compounds

The Chemdiv database (<https://www.chemdiv.com/>) that contains over 1.5 million compounds was applied for the screening of PARP-1 inhibitors. All the compounds were prepared using MMFFs force field, with a target pH of  $7.0 \pm 2.0$ , in the LigPrep module. The pocket grid was generated from the crystal structure (PDB ID: 4R6E) and applied in the Virtual Screening Workflow module. All the compounds were firstly prefiltered by Linpinski's Rules and step-by-step filtered by the docking protocol of high throughput virtual screening (HTVS), standard precision (SP), and extra precision (XP) protocol. The retaining ratios of HTVS, SP, and XP protocol were set as 10%, 10%, and 20% respectively. The top-ranked 2,000 compounds with the best XP docking scores were finally applied for further affinity evaluation by the above multiple linear regression model involved in energy terms of  $E_{ele}$ ,  $E_{nonele}$ ,  $E_{other}$ . In order to select the diverse scaffold types, the top 500 compounds with the best predicted affinities were clustered by the  $k$ -means clustering in Canvas. The representative compounds were picked out for subsequent novelty check in the SciFinder Scholar (<https://scifinder.cas.org/>). Finally, 20 compounds with proper binding modes and unknown reports of PARP1 inhibitory activities were selected and purchased from the Taosu Bio-Technique Co., Ltd. (Shanghai, China).

### 2.4 PARP-1 enzyme assays

The ability of 20 selected compounds to inhibit PARP-1 enzyme activity was assessed using Trevigen's PARP-1 assay kit (Trevigen, cat. No. 4676-096-K) following the manufacturer's instruction. For PARP inhibitor determination, enzyme assays

were conducted in 96-wells FlashPlate (PerkinElmer) with 0.5 U/μl of PARP-1 enzyme, 0.5× activated DNA, 0.5× PARP Cocktail, in a final volume of 50 μl by 1× PARP Buffer. Reactions were initiated by adding NAD<sup>+</sup> to the PARP reaction mixture with or without inhibitors and incubated for 60 min at room temperature. 50 μl of 1× Strep-HRP was added to each well to quench the reaction. The plate was sealed and shaken for a further 60 min. Finally, PeroxyGlow<sup>TM</sup> A and PeroxyGlow<sup>TM</sup> B were equal volumes and added 100 μl per well. Immediately take chemiluminescent readings by Synergy<sup>TM</sup> HT (Bio Tek, United States).

## 2.5 The binding mode and energy analysis by molecular dynamics simulation

The initial binding modes of four hit compounds were predicted by docking protocol of XP. A total of four complex conformations were applied in the molecular dynamics (MD) simulation. The geometry optimization and partial charges calculation of hit compounds were performed in Gaussian09 program using HF/6–31G\* basis set. The restrained electrostatic potentials (RESP) were assigned using the general AMBER force field (GAFF) (Bhadra and Siu, 2019). Then, all four complex systems were neutralized with sodium ions or chloride ions and immersed in a rectangular TIP3P water box at least 10 Å away from the proteins. All complex systems were parameterized using ff14SB force field (Maier et al., 2015) and performed all-atom molecular simulations in AMBER14 package (Case et al., 2014). The molecular dynamics simulation process was performed in four steps. Firstly, the initial structures were minimized by 2,500 cycles of steepest descent and 2,500 cycles of conjugate gradient. Secondly, the temperature for each system was gradually upgraded from 0 K to 300 K within a period of 100 ps. Thirdly, all the heavy atoms of protein and compound were equilibrated with gradually decreasing restraining force constants from 2.0, to 1.5, to 1.0, to 0.5, to 0.1, to 0 kcal mol<sup>-1</sup> Å<sup>-2</sup> and the simulation time was 100 ps for each restraining force constant. Finally, the molecular dynamics simulations were performed with all the restraints released in the isothermal isobaric (NPT) ensemble with a temperature of 300 K and a pressure of 1 atm. During the simulation, particle mesh Ewald (PME) was used to compute electrostatics in periodic boundary condition and the bonds involving hydrogen atoms were constrained using the SHAKE algorithm. The time step was set as 2 fs, and the trajectories for each system was generated with a production time of 100 ns. The MM/GBSA method were further performed to evaluate the binding free energy between the receptor and ligand. 200 snapshots were extracted from the last 20 ns trajectories and used for MM/

GBSA calculation, and the parameter settings were referred to the previous works published by our group (Shi et al., 2018; Shi et al., 2019). Then, the per-residue free energy decomposition and root mean square fluctuation were calculated to evaluate the dynamics effect of hit compounds on the binding site of PARP-1 in the complex systems.

## 2.6 Cell proliferation inhibition assay

The human colorectal cancer cells line HCT-116, RKO were obtained from ATCC and cultured in Dulbecco's modified Eagle medium (DMEM) containing 10% fetal bovine serum (FBS, Gibco), 100 U/ml penicillin (Hyclone) and 100 μg/ml streptomycin (Hyclone). Both cell lines were grown in a humidified atmosphere with 5% CO<sub>2</sub>/95% air at 37°C. The cytotoxic effects of PARP-1 inhibitors were measured by CCK-8. Cells in the logarithmic growth phase were plated in 96-well culture plates. After treatment with Niraparib, compound 8018-7168 and 8018-6529 at indicated concentrations. CCK-8 was added to each well for 4 h at 37°C. Then the optical density value was detected at 450 nm using a microplate reader (Bio Tek). The inhibition rate was calculated from the following equation:

$$\text{Inhibition ratio} = \left(1 - \frac{OD_{\text{compound}}}{OD_{\text{control}}}\right) \times 100\%$$

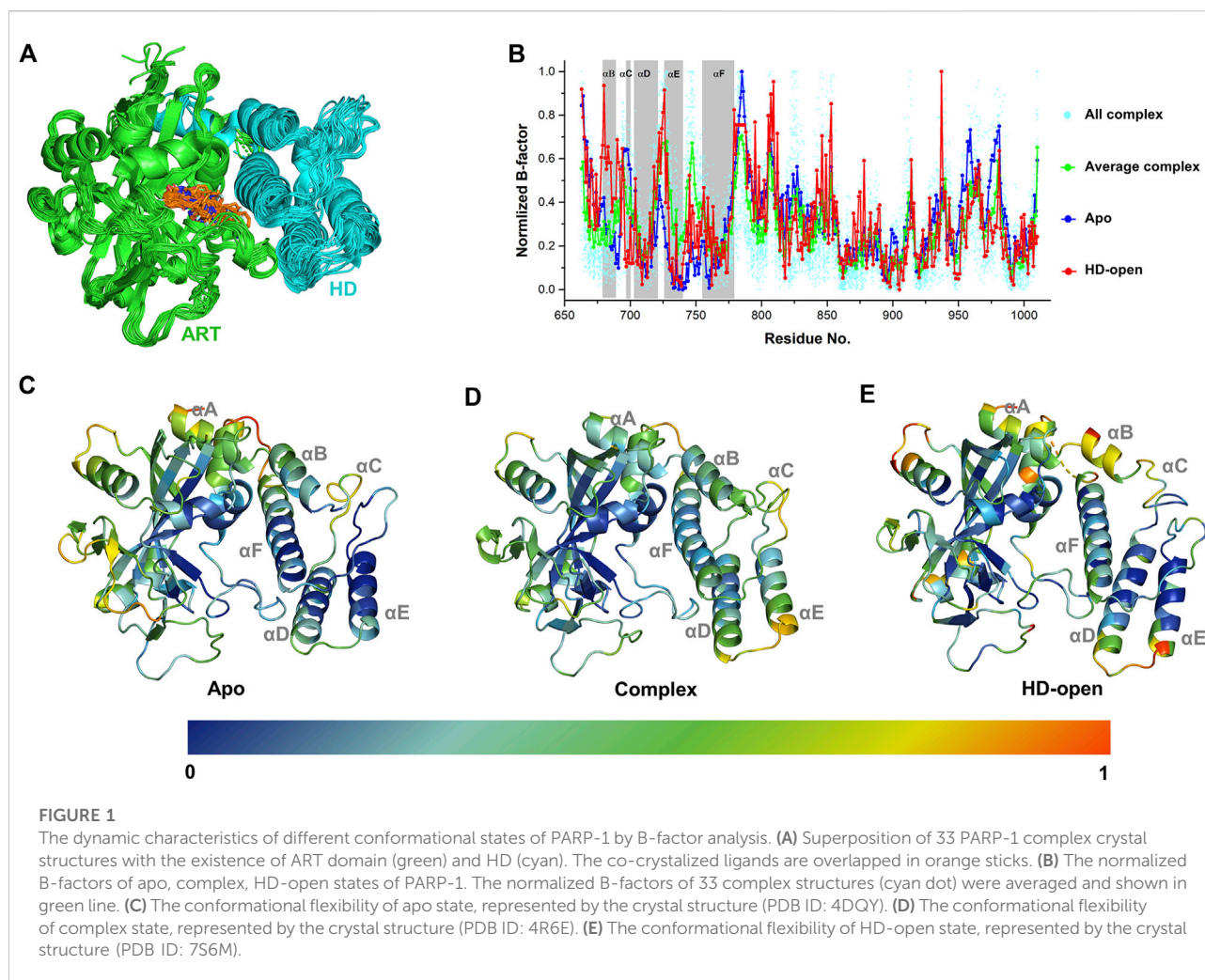
## 2.7 Western blot analysis

After treatment with the corresponding IC<sub>50</sub> concentration of Niraparib, compound 8018-6529, 8018-7168 for 48 h, HCT-116 cells were subjected to protein extracted extraction and equivalent amounts of the extraction were separated by SDS-PAGE and transferred onto PVDF membranes. Following blockage of nonspecific sites with 5% skimmed milk powder in TBST, the membranes were incubated with primary antibodies and subsequently subjected to secondary antibodies. ImageJ Software was used to quantify the resulting bands.

## 2.8 Transmission electron microscopy analysis

HCT-116 cells were treated with Niraparib, compound 8018-6529, 8018-7168 at the corresponding IC<sub>50</sub> concentration for 48 h. Then the samples were harvested and processed under the instructions. A transmission electron microscope (TEM, JEM-





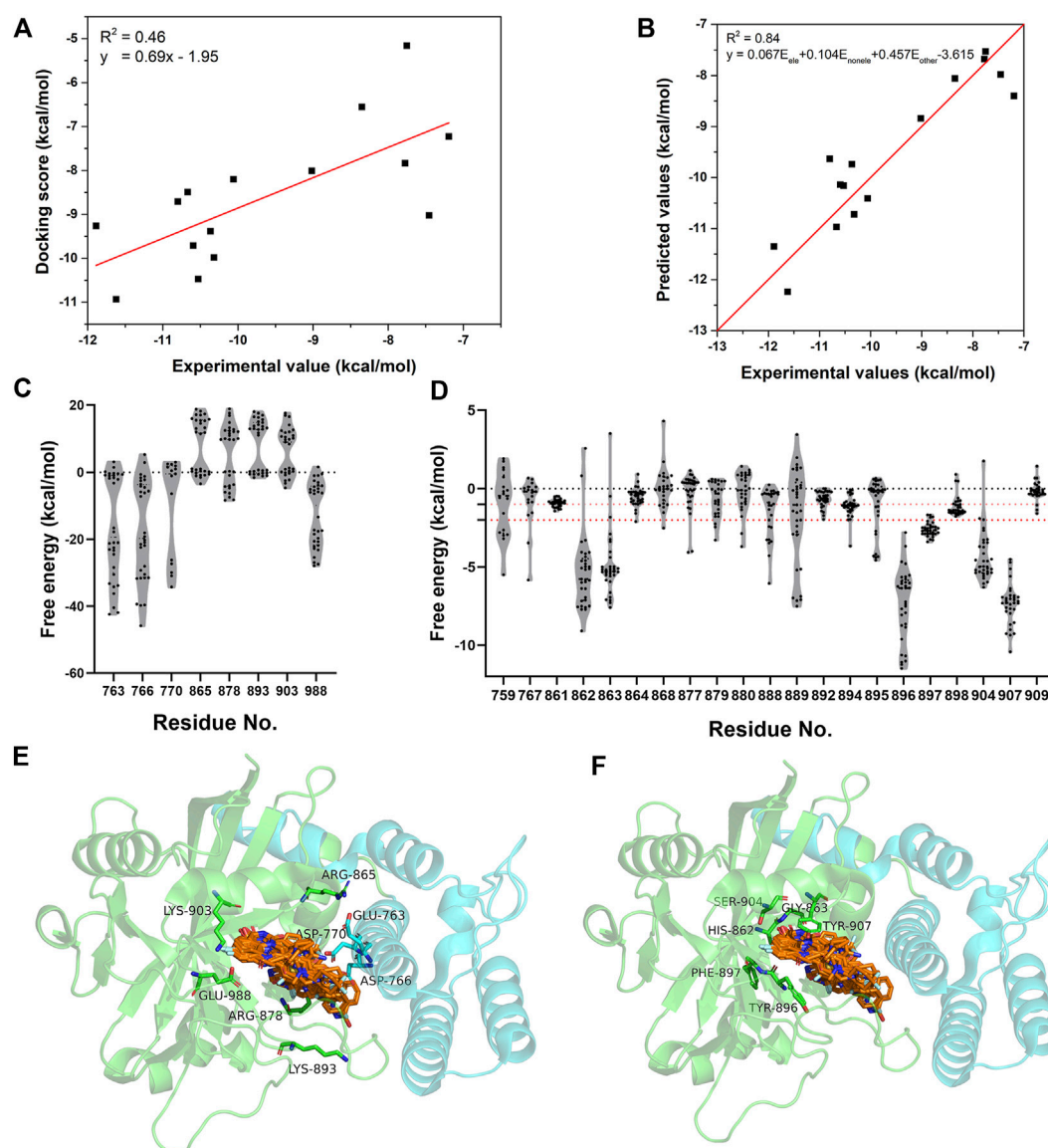
2100) was used to detect the sliced samples. Micrographs were obtained at the magnification of  $\times 25000$ ,  $n = 3$ .

### 3 Results

#### 3.1 The dynamic and energetic characteristics of PARP-1 complex

A complete catalytic domain for PARP-1 is consisted of the ART domain and the helix domain (HD). Recently, the HD-open state has been captured in the crystal structures, which shows an active conformation that could prolong interactions with the DNA damage and accounts for allosteric mechanism of PARP-1 (Rouleau-Turcotte et al., 2022). In order to analyze the ligand's effect on the dynamics and energetic characteristics of the catalytic domain, 33 PARP-1 complex structures with the existence of the HD were selected and analyzed. As shown in Figure 1A, it can be seen that the location superposition of all

ligands with diverse binding poses forms a good occupation at the binding site between the ART domain and HD, despite of the minor conformational fluctuation of protein. Different complex structures showed an obvious fluctuation in the distribution of B-factors, and the average value was calculated to reflect the general characteristics of ligand binding (Figure 1B). The dynamics characteristics were further compared between the apo, complex and HD-open states using the normalized B-factors. It can be seen that the main dynamics difference among these states occurs at the HD, and the apo state turns to be more stable comparing to the complex and HD-open states. The normalized B-factors were further projected to different helices of the HD as shown in Figures 1C–E. The  $\alpha D$ ,  $\alpha E$ ,  $\alpha F$  of HD turn out to be more dynamics in complex state than apo state, suggesting that the binding of ligands could change the conformational flexibility of HD. As a conformational state that binds to DNA damage, the HD-open state shows a conformational shift of HD and a more flexible  $\alpha A$  and  $\alpha B$ . The conformational association between  $\alpha A/\alpha B$  and  $\alpha F$  seems to

**FIGURE 2**

The energetic characteristics of PARP-1 complex by per-residue energy decomposition in molecular docking. **(A)** The linear relationship between the docking scores and experimental activities for 15 PARP-1 ligands. **(B)** The linear relationship between the predicted activities and experimental activities by a multiple linear regression model. **(C,E)** The per-residue energy distribution and location of electrostatic residue group on PARP-1. **(D,F)** The per-residue energy distribution and location of non-electrostatic residue group on PARP-1.

be the main switch for HD-open state and the interaction with  $\alpha F$  could be a useful approach to intervene allosteric effect of PARP-1.

The energetic characteristics of PARP-1 complex were further analyzed by molecular docking. All ligands were redocked with a conformational constraint to the native poses and the corresponding docking scores were applied for binding free energy analysis. As the experimental activities for some ligands were missing or inconsistent among different reports, the ligands were applied only if their activities exist at the same

level of magnitude in different reports and the experimental values were depicted by the average of IC<sub>50</sub> values. As shown in Figure 2A, a total of 15 ligands with valid activities showed linear correlation with their docking scores with R<sup>2</sup> of 0.46. The per-residue free energy decomposition was further performed for all complex structures, and the energy contributions of the pocket residues were evaluated by the distribution probabilities of values. As shown in Figures 2C,E, eight electrostatic residues show obvious energetic perturbation for the binding free energies of PARP-1 ligands. The negative-charged residues including

TABLE 1 The calculated energy contribution of three residue groups and the predicted activities by a multiple linear regression model.

PDB	Eele <sup>a</sup>	Enonele <sup>b</sup>	Eother <sup>c</sup>	Predicted <sup>d</sup>	Experimental <sup>e</sup>
1UK0	-27.60	-31.85	-1.51	-9.47	-10.80
2RD6	-27.05	-37.99	0.12	-9.33	—
3GN7	-21.43	-38.54	-1.28	-9.64	—
3L3M	-16.65	-48.90	0.07	-9.78	—
4GV7	-3.40	-32.29	-1.71	-7.98	-7.46
4HHY	-24.67	-45.16	-3.04	-11.35	-11.89
4HHZ	-11.12	-42.76	-2.97	-10.16	-10.53
4L6S	-56.25	-40.28	-1.47	-12.24	-11.62
4OPX	-7.78	-27.32	-1.53	-7.68	-7.77
4OQA	-1.74	-30.47	-2.54	-8.06	-8.35
4OQB	-8.30	-21.89	-2.37	-7.53	-7.75
4R5W	-8.32	-43.07	-1.75	-9.45	—
4R6E	-33.44	-50.87	0.08	-11.11	—
4RV6	-36.45	-38.64	0.62	-9.79	—
4UND	-8.50	-37.30	-1.67	-8.83	—
4UXB	-15.81	-37.64	4.25	-6.65	—
4ZZZ	-3.87	-35.54	-1.81	-8.40	-7.19
5A00	-32.98	-45.02	1.68	-9.74	-10.37
5HA9	-25.28	-20.94	-2.15	-8.47	—
5KPN	-21.31	-51.57	-1.94	-11.29	—
5KPO	-20.21	-52.82	-1.96	-11.36	—
5KPP	-15.33	-54.20	-1.79	-11.10	—
5KPQ	-12.84	-50.57	-2.14	-10.71	—
5WRQ	-52.56	-47.39	-2.40	-13.16	—
5WRY	-49.05	-54.66	-1.85	-13.43	—
5WRZ	-31.97	-34.18	1.15	-8.78	—
5WS0	-37.67	-38.08	-0.68	-10.41	-10.06
5WS1	-35.74	-39.50	-1.86	-10.97	-10.67
5WTC	-16.65	-52.36	-1.63	-10.92	—
5XSR	-39.98	-43.86	1.56	-10.14	-10.59
5XST	-40.52	-51.08	2.02	-10.72	-10.32
5XSU	-32.63	-40.62	2.60	-8.84	-9.02
6GHK	-4.84	-50.47	-1.82	-10.02	—

<sup>a</sup>The sum of the residue energy terms for residues in the electrostatic group.<sup>b</sup>The sum of the residue energy terms for residues in the non-electrostatic group.<sup>c</sup>The sum of the residue energy terms for the other residues except the electrostatic group and non-electrostatic group.<sup>d</sup>The predicted binding free energies calculated by the multiple-linear regression model for the native ligand in the corresponding complex.<sup>e</sup>The experimental binding free energies calculated by the average IC<sub>50</sub> according to the following equation:  $\Delta G = -RT \ln (1/IC_{50})$ .

Glu763, Asp766, Asp770, and Glu988 have positive effect for binding, while the positive-charged residues including Arg865, Arg878, Lys893, and Lys903 have negative effect. This electrostatic interaction preference may account for the fact that most ligands of PARP-1 are positive-charged. It can be seen that Glu763, Asp766, Asp770 are all located on  $\alpha F$  of HD, suggesting the electrostatic attraction between the ligands and these residues could affect the interaction and stability of HD. The other non-electrostatic residues also show great effect on the binding free energies (Figures 2D,F). It can be seen that His862,

Gly863, Tyr896, Phe897, Ser904, Tyr907 have key interactions for almost all complex structures, while other hydrophobic or polar residues at the binding site show different interactions among different ligands. According to the electrostatic property, the residues involved in the ligand binding were classified into three groups, namely the electrostatic group, the non-electrostatic group and the others. To evaluate the effect of different residue groups, the energy contribution of each group was calculated as shown in Table 1. A multiple linear regression model was built with R<sup>2</sup> of 0.84 as follows:

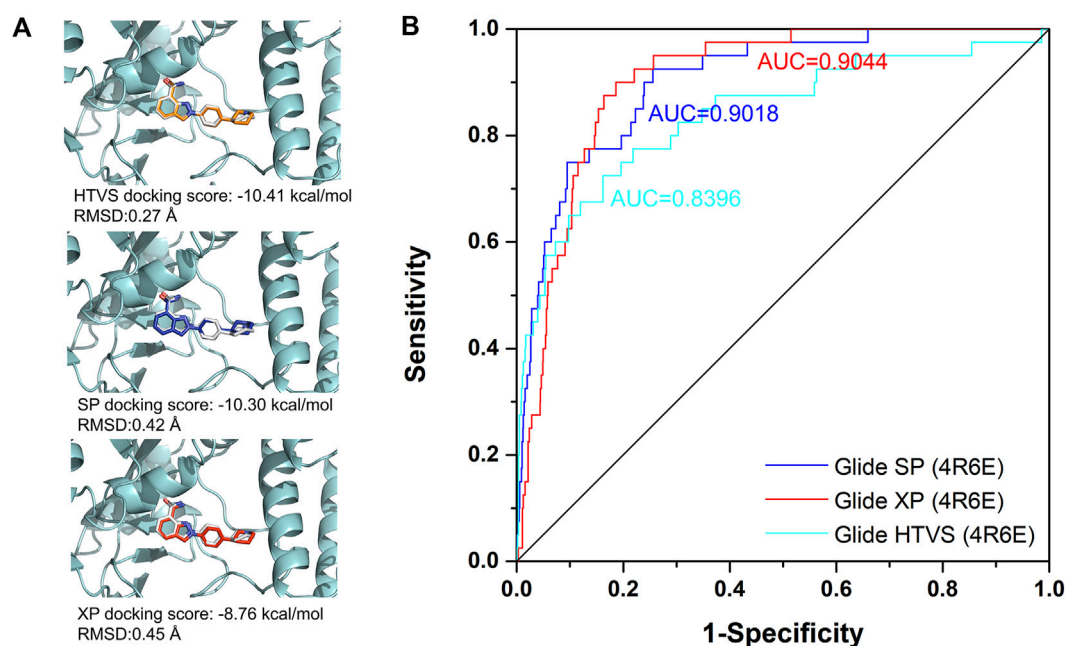


FIGURE 3

The evaluation of docking power and screening power for crystal structure in complex with Niraparib (PDB ID: 4R6E). (A) The evaluation of the docking power of crystal structure of 4R6E by HTVS, SP, and XP protocol respectively. (B) The screening power of the crystal structure of 4R6E by HTVS, SP, and XP protocol.

$y = 0.067 E_{ele} + 0.104 E_{nonele} + 0.457 E_{other} - 3.615$ , and the predicted activities showed a good consistency with the experimental activities (Figure 2B). It is suggested that the residue classification and multiple linear regression are useful approach to improve the accuracy of predicted values by molecular docking method, and could be further applied for the affinity predicted during the virtual screening.

### 3.2 The virtual screening workflow and discovery of new hit compounds

Among all the complex states, the crystal structure in complex with Niraparib (PDB ID: 4R6E) was selected for the docking-based virtual screening. The docking power of different docking protocols (HTVS, SP, XP) in Schrödinger 2015 were firstly evaluated by redocking the native ligands into the original crystal structures. As shown in Figure 3A, Niraparib were redocked into the pocket of PARP-1 with a good overlapping to the native pose with RMSD lower than 2 Å, indicating that the native pose could be successfully predicted by different docking protocols. Then, the screening power of different docking protocols were further tested. A dataset of 2030 compounds (including 40 actives and 1990 decoys) were built and applied to perform molecular docking. The screening power was evaluated by area under curve (AUC) of the receiver operating

characteristics (ROC) curve. As shown in Figure 3B, the AUC values for HTVS, SP, XP were 0.8396, 0.9018, 0.9044 respectively and large enough for the docking-based virtual screening process. Specially, with the improvement of docking accuracy from HTVS to SP to XP, there is an increasing trend in screening capacity. Therefore, the docking protocols with crystal structure of 4R6E for was suitable for the following docking-based virtual screening workflow.

Then, an integrated *in silico* screening workflow was performed to get the candidate compounds targeting PARP-1. As shown in Figure 4A, over 1.5 million compounds in Chemdiv database were firstly pre-filtered by the Linpinski's Rules, and the left compounds were successively screened by the docking protocols of HTVS, SP and XP with the retain ratio of top 10%, 20%, 20% respectively. A total 2,000 compounds were selected with the top-ranking XP docking scores. A per-residue free energy evaluation was further performed to predict the binding affinity of those compounds, and the top 500 compounds were retained. In order to ensure as much structural diversity as possible with the fewest compounds, the structural clustering was performed and 20 candidate compounds were finally selected and purchased for *in vitro* assay (Figure 4B). The inhibitory activities *in vitro* were performed using Trevigen's PARP-1 assay kit. As shown in Figure 4C, the inhibition ratios of two positive controls (Olaparib and Niraparib) were firstly tested under 10 nM with



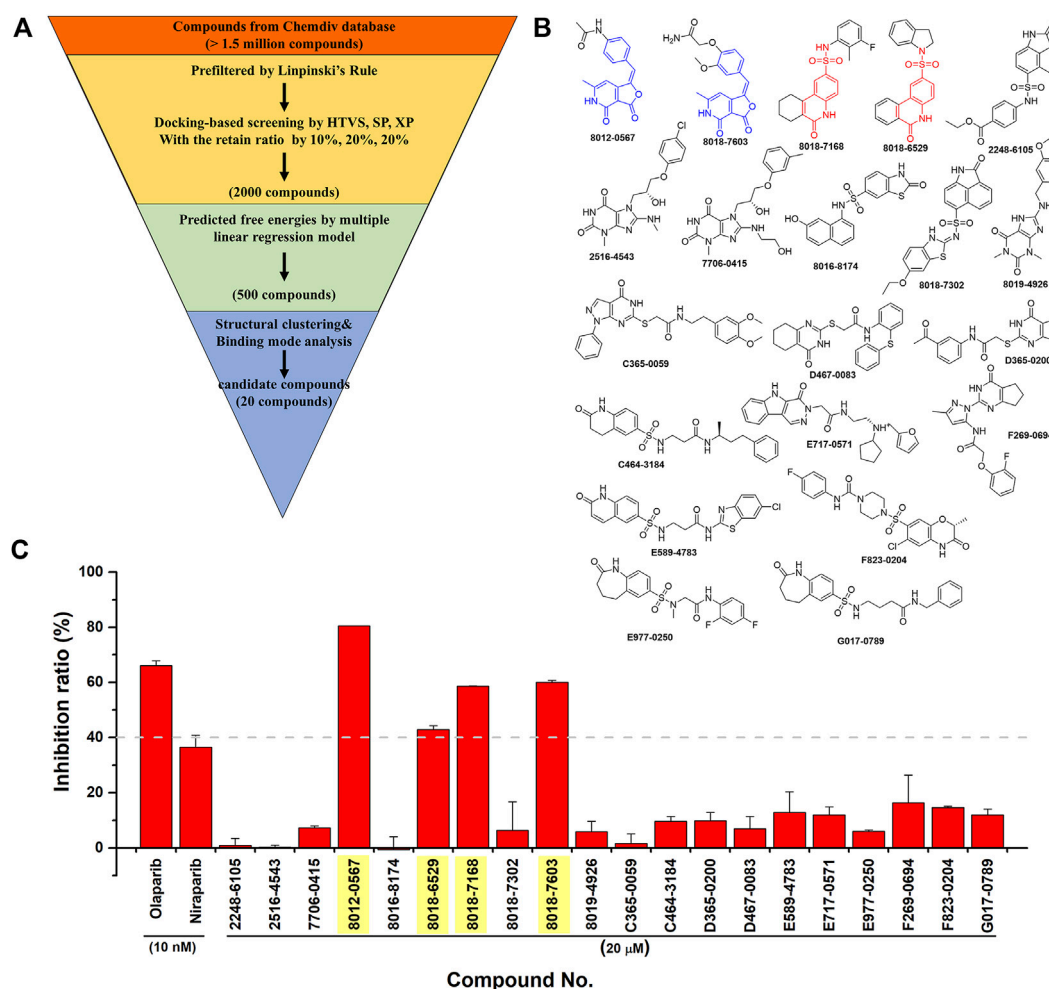


FIGURE 4

The integrated *in silico* screening workflow and *in vitro* inhibitory activity assay of candidate compounds. (A) The *in silico* screening workflow. (B) The chemical formula of 20 compounds selected for *in vitro* assay. The scaffolds of four hit compounds are labeled out with arylidenefuopyridinediones (compound 8012-0567 and 8018-7603) in blue and 1,2-Dihydro-2-oxo-6-quinolinesulfonamide (compound 8018-7168 and 8018-6529) in red. (C) The inhibitory activities of two positive controls and 20 candidate compounds.

values of 66.1% and 36.7%, which were consistent with the corresponding range of IC<sub>50</sub> activities. Then, the inhibition ratios of all candidate compounds were evaluated under 20  $\mu$ M, and a cutoff value of 40% were set to select the potential hit compounds. Four compounds (Chemdiv codes: 8012-0567, 8018-6529, 8018-7168, 8018-7603) showed obvious inhibitory activities against PARP-1 than other compounds with values of 80.5%, 42.9%, 58.7%, 60.0% respectively. The corresponding chemical formulas can be found in Figure 4B. It can be seen that 8012-0567 and 8018-7603 have the same scaffold unit of arylidenefuopyridinediones, while 8018-6529 and 8018-7168 have the same structural fragments of 1,2-Dihydro-2-oxo-6-quinolinesulfonamide. All these hit compounds have no report of PARP-1 inhibition activity before.

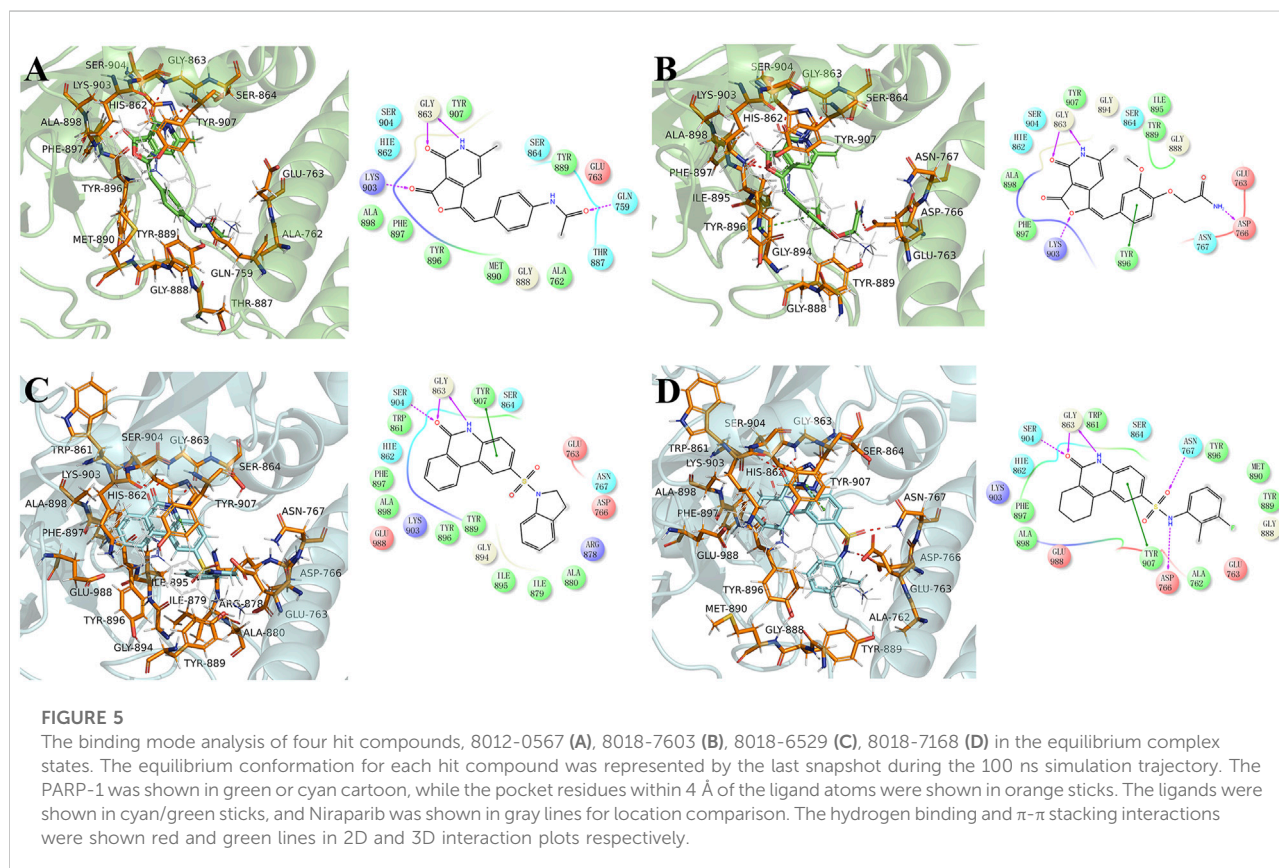
### 3.3 The energetic and dynamic effect of hit compounds on PARP-1

The binding free energies of the equilibrium complex states for four hit compounds were evaluated by the conformational sampling of last 20 ns trajectories of molecular dynamics simulation and further calculated by the MM/GBSA method as shown in Table 2. It can be found that the calculated binding free energies ( $\Delta H$ ) have a good consistency with the experimental inhibition ratio for 8012-0567/8018-7603 and 8012-6529/8018-7168. The  $\Delta H$  was then split into polar parts ( $\Delta E_{\text{ele}}$ ,  $\Delta E_{\text{ele,sol}}$ ) and non-polar parts ( $\Delta E_{\text{vdw}}$ ,  $\Delta E_{\text{nonpl,sol}}$ ). For all the four hit compound systems, the energy terms  $\Delta E_{\text{ele}}$ ,  $\Delta E_{\text{vdw}}$ ,  $\Delta E_{\text{nonpl,sol}}$  were favorable for ligand binding while the polar interaction contribution by solvent ( $\Delta E_{\text{ele,sol}}$ ) was adverse. The electrostatic



TABLE 2 The binding free energies of four hit compounds evaluated by MM/GBSA.

Terms (kcal/mol)	8012-0567	8018-7603	$\Delta^a$	8018-7168	8018-6529	$\Delta^b$
$\Delta E_{ele}^c$	$-48.00 \pm 5.58$	$-41.18 \pm 10.34$	$-6.82 \pm 10.75$	$-25.15 \pm 5.51$	$-24.84 \pm 4.16$	$-0.31 \pm 6.90$
$\Delta E_{vdw}^d$	$-43.96 \pm 2.53$	$-43.62 \pm 2.95$	$-0.34 \pm 3.89$	$-46.63 \pm 2.98$	$-44.75 \pm 2.67$	$-1.88 \pm 4.00$
$\Delta E_{ele,sol}^e$	$54.42 \pm 3.89$	$54.53 \pm 7.34$	$-0.11 \pm 8.31$	$38.43 \pm 3.74$	$40.04 \pm 2.97$	$-1.61 \pm 4.78$
$\Delta E_{nonpl,sol}^f$	$-5.33 \pm 0.11$	$-5.69 \pm 0.18$	$0.36 \pm 0.21$	$-6.08 \pm 0.14$	$-5.82 \pm 0.12$	$-0.26 \pm 0.18$
$\Delta H^g$	$-42.88 \pm 2.84$	$-35.96 \pm 3.68$	$-6.92 \pm 4.65$	$-39.44 \pm 2.93$	$-35.36 \pm 2.65$	$-4.08 \pm 3.95$
Inhibition ratio	$80.5 \pm 0.1\%$	$60.0 \pm 0.8\%$		$58.7 \pm 0.1\%$	$42.9 \pm 1.4\%$	

<sup>a</sup>The energy difference between compound 8012-0567 and 8018-7603.<sup>b</sup>The energy difference between compound 8018-7168 and 8018-6529.<sup>c</sup>The electrostatic energy term.<sup>d</sup>The Van der Waals energy term.<sup>e</sup>The polar solvation free energy term.<sup>f</sup>The non-polar solvation free energy term.<sup>g</sup>The total binding free energy as the sum of  $\Delta E_{ele}$ ,  $\Delta E_{vdw}$ ,  $\Delta E_{ele,sol}$ ,  $\Delta E_{nonpl,sol}$ .

interaction ( $\Delta E_{ele}$ ) was much stronger in 8012-0567 complex than 8018-7603 complex, which mainly accounts for the free energy difference between these two compounds. As for 8012-6529/8018-7168 complex systems, the van der Waals interaction ( $\Delta E_{vdw}$ ) and electrostatic interaction by solvent ( $\Delta E_{ele,sol}$ ) in 8018-7168 system were both optimized than 8012-6529.

The equilibrium complex states for four hit compounds were achieved from the last snapshot in the molecular dynamics. The binding modes were further characterized by the interactions between ligands and the adjacent residues as shown in Figure 5. Compounds 8012-0567 and 8018-7603 have similar location superposition with the binding pose of Niraparib. The scaffold

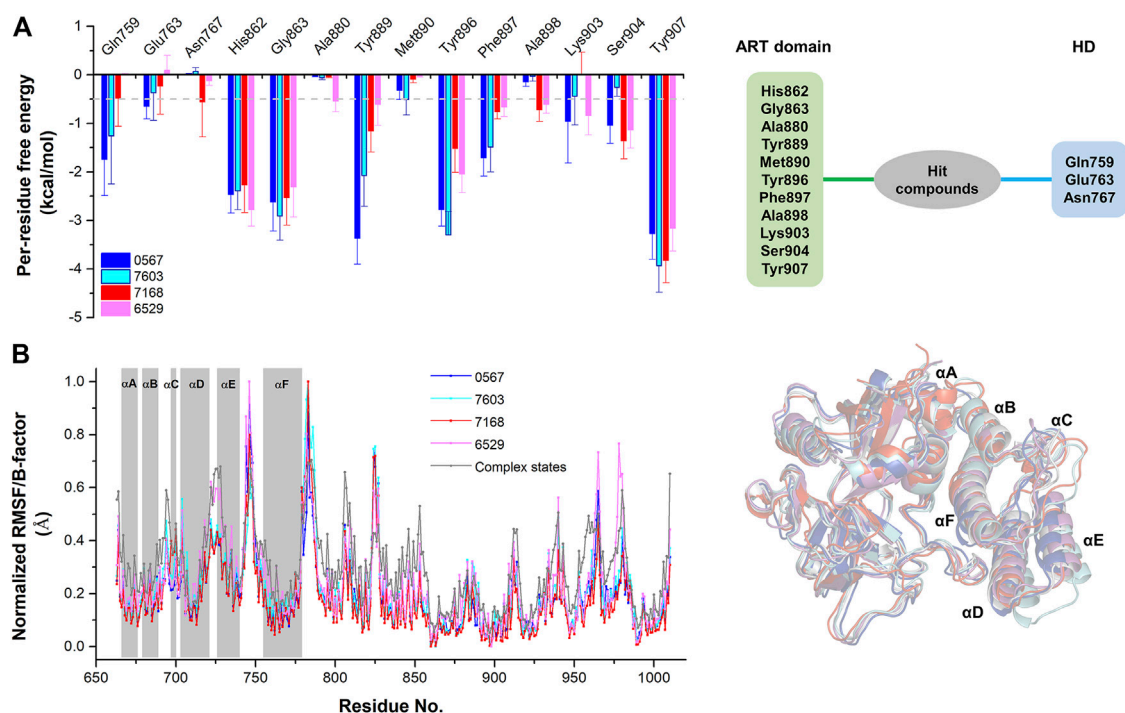


FIGURE 6

The per-residue free energy decomposition and conformational analysis of the equilibrium conformations of four hit compounds by molecular dynamics. (A) The per-residue free energy decomposition of the key residues on ART domain and HD. (B) The normalized RMSF analysis of the equilibrium conformations of four hit compounds compared to the average B-factors of the complex states. The equilibrium conformations of four hit compounds were superposed with the crystal structures (PDB ID: 4R6E).

of 8012-0567/8018-7603 forms three hydrogen bonds with the backbone atoms of Gly863 and the sidechain of Lys903 in the ART domain. The different substituted groups on the benzene ring affect the minor conformational shift of the ring and different interactions with the residues in  $\alpha$ F of HD. 8012-0567 has a hydrogen bonding with Gln759, while 8018-7603 has  $\pi$ - $\pi$  stacking with Tyr896 and hydrogen bonding with Asp766 (Figures 5A,B). However, compounds 8012-6529 and 8018-7168 have quite different location superposition comparing to binding pose of Niraparib. The scaffold of 8012-6529/8018-7168 also form three hydrogen bonds with the backbone atoms of Gly863 and the sidechain of Ser904, and a  $\pi$ - $\pi$  stacking interaction with the scaffold benzene ring in the ART domain. The binding poses of 8012-0567/8018-7603 are also affected by the substituted groups. The sulfonamide group of 8012-7168 forms hydrogen bonds with Asp766 and Asn767 in  $\alpha$ F of HD, while sulfonamide group of 8018-6529 forms no hydrogen bonds. (Figures 5C,D). The further per-residue energy decomposition in Figure 6A shows that His862, Gly863, Ala880, Tyr889, Met890, Tyr896, Phe897, Ala898, Lys903, Ser904, Tyr907 in ART domain and Gln759, Glu763, Asn767 in HD have the significant energy contribution for the binding of four hit compounds. Consistent with the

known inhibitors, His862, Gly863, Tyr889, Tyr896, Phe897, Tyr907 act as the core residues with the main energy contributions for all hit compounds, while other residues provide different energy contribution based on the difference of substitutions. When interacting with the HD, Gln759 and Glu763 have obvious contribution for the binding of 8012-0567/8018-7603, while Gln759 and Asn767 benefit for the binding of 8012-7168. The dynamic effect of the equilibrium complex states induced by hit compounds were further characterized by the normalized root mean square fluctuation (RMSF). The equilibrium complex state predicted by molecular dynamics has the similar dynamic profile with the complex crystal structures as shown in Figure 6B. It can be seen that the main conformational fluctuations occur at the  $\alpha$ D- $\alpha$ E loop and  $\alpha$ E- $\alpha$ F loop of the HD upon the ligand binding, which shows obvious conformational shift among the equilibrium complex states.

### 3.4 The anti-tumor activity evaluation and autophagy mechanism

To validate the anti-tumor activities of these hit compounds of PARP-1, HCT-116 (BRCA-deficient colorectal carcinoma

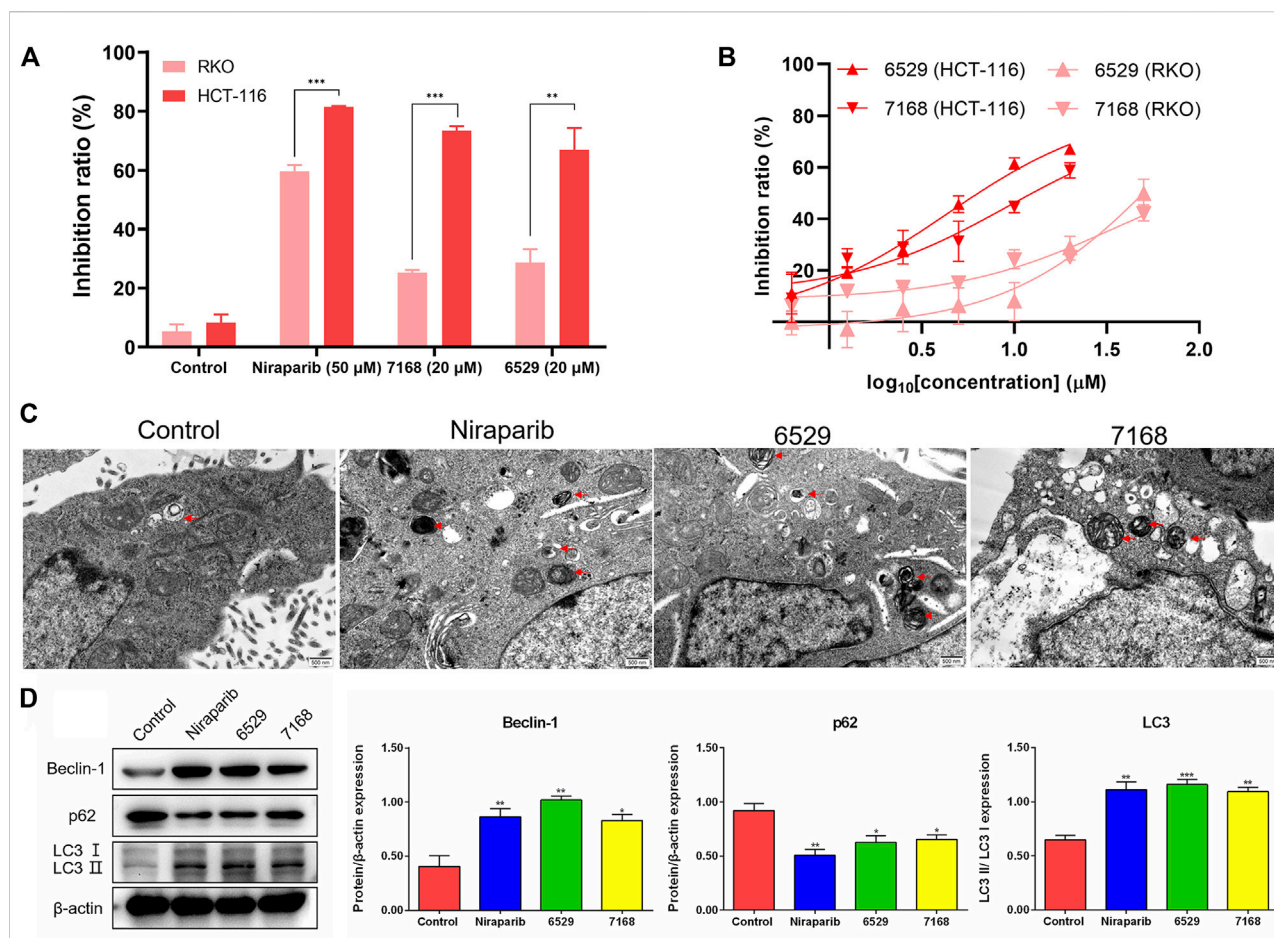


FIGURE 7

Discovered hit compounds inhibit cell survival and induced the autophagy in a human colorectal carcinoma cell line HCT-116. (A) The inhibition ratio of two hit compounds (8012-0567, 8018-7603) at 20 μM against the cell survival of human colorectal carcinoma cell lines (HCT-116, RKO), Niraparib at 50 μM as the positive control. Cell viability was determined by the CCK-8 assay ( $n = 3$ ). ( $*p < 0.05$ ,  $**p < 0.01$ ,  $***p < 0.001$ ) (B) the human colorectal carcinoma cell lines (HCT-116, RKO) were treated with different concentrations of 8018-6529 and 8018-7168. The IC<sub>50</sub> values were predicted by utilizing the GraphPad<sup>®</sup> program. (C) TEM detection of autophagosomes accumulation in HCT-116 cells treated with compound 8018-6529 and 8018-7168 for 24 h, Niraparib as the positive control. (D) Western blot analysis was performed after treatment of compound 8018-6529 and 8018-7168 to demonstrate the expression of Beclin-1, p62, and LC3 II/I protein, markers for autophagy, Niraparib as the positive control. Densitometric values of Beclin-1, p62 and LC3 compared with their respective total proteins were evaluated via ImageJ software and are presented as the mean  $\pm$  SD ( $n = 3$ ) ( $*p < 0.05$ ,  $**p < 0.01$ ,  $***p < 0.001$ ).

cells), RKO (BRCA-proficient colorectal carcinoma cells) were applied for the cell survival assay. As shown in Figure 7A, compounds 8018-7168 and 8018-6529 out of the four hit compounds have significant inhibition effect against the cell growth for both cell lines at 20 μM. Considering the synthetic lethality of PARP-1 inhibitors against BRCA-deficient cells, it can be seen that the inhibition ratio of these two compounds is significantly higher in HCT-116 than RKO in the colorectal carcinoma cell lines, which is also consistent with the results of Niraparib. Specially, compounds 8018-7168 and 8018-6529 show obvious anti-tumor activities against HCT-116 cell lines and the IC<sub>50</sub> were further tested as 9.29 μM and 4.30 μM respectively, which showed better inhibitory effect than Niraparib (Figure 7B; Table 3; Supplementary Figure S1). The previous studies

TABLE 3 The IC<sub>50</sub> values of anti-tumor activities of compound 8018-7168, 8018-6529 and Niraparib against HCT-116 and RKO cell lines. The unit of concentration is μM.

Cell lines	8018-7168	8018-6529	Niraparib
HCT116	4.30	9.30	33.09
RKO	73.27	35.03	40.89

demonstrated that autophagy was initiated in a series of cancer cell lines after the treatment of PARP-1 inhibitors, but no report for HCT-116 cell lines. To further demonstrate the induction of autophagy, we firstly investigated the ultrastructure



by transmission electron microscopy (TEM) before and after the treatment of compounds 8018-7168 and 8018-6529. TEM images clearly demonstrate that these two compounds could induce the process of autophagy by generating more autophagosomes compared with untreated cells (Figure 7C). Then, the level of three autophagy-related proteins, Beclin 1, sequestosome 1 (SQSTM1/p62) and microtubule-associated protein 1 light chain3 (LC3) were detected in HCT-116 with the treatment of compounds 8018-7168 and 8018-6529 (Niraparib for positive control) by immunoblot analysis. Figure 7D showed that compounds 8018-7168 and 8018-6529 obviously increased the level of Beclin 1 and LC3 II/I, and reduced the level of p62 in HCT-116 cells, which further proved the induction of autophagy.

## 4 Discussion

The clinical efficacy of small molecule compounds is affected by a series of factors and mechanisms, which is even pronounced for the targeted inhibitors of PARP-1 (Rose et al., 2020). In addition to competitive binding to the substrate binding site of NAD<sup>+</sup>, some PARP-1 inhibitors can also affect the conformational state of PARP-1 through allosteric regulation mechanism, thereby affecting its retention time binding to the damaged DNA (Zandarashvili et al., 2020). It has been confirmed that the allosteric effect has a close and direct relationship with the helix domain (HD), and small-molecule inhibitors can affect the conformational state and dynamic characteristics of HD through the interaction with HD residues (Rouleau-Turcotte et al., 2022). In this study, we tried to analyze energetic and dynamic effect of reported small-molecule inhibitors on the HD, so as to reveal the allosteric regulatory effect of small-molecule binding. We preliminarily studied the residue energy contribution and B-factor in the complex states by a systematic analysis of crystal structures with the existence of the HD. It is found that the interactions with HD are mainly related to the electrostatic residues including Glu763, Asp766, Asp770 on  $\alpha$ F helix of HD, and the mutual interactions might further cause the conformational changes of other helices on HD, thus eventually result in the HD-open state. These results provide the initial hint for the following *in silico* and *in vitro* screening.

In the process of per-residue energy analysis by molecular docking, it was found that there was a better multiple-linear relationship between three energy terms (Eele, Enonele, Eother) and the experimental activities of the reported inhibitors, when comparing to the linear relationship between the docking scores and the experimental activities. These energy terms were achieved by classifying the pocket residues of PARP-1 according to electrostatic properties, and summing the contributions of residues in each group. Meanwhile, we applied this multiple-linear model for *in silico* screening process. Since the high false positive rate is always a big problem in virtual screening (Adeshina et al., 2020; Bender

et al., 2021), other strategies were also designed to ensure the reliability of virtual screening during the whole process, including the evaluation of docking and screening abilities, structural diversity analysis and the inspection of binding modes. Trevigen's PARP-1 assay kit assays confirmed that the *in silico* screening process was quite successful, with a hit ratio of 20%, despite that the inhibitory activities was still at the micromolar level. For the further investigation of active scaffolds of four hit compounds, it was found that the PARP-1 inhibitory activity had never been reported for these compounds before. What's more, the scaffold unit of arylidenefuopyridinediones for 8012-0567 and 8018-7603 was previously reported to show Topoisomerase 1 (LdTop1) (Mamidala et al., 2016) and  $\alpha$ -glucosidase (Bathula et al., 2015) inhibition activities. As PARP-1 has broad synergistic effect with other targets in anti-tumor studies (Chang et al., 2021; Wei et al., 2021), these compounds also provide the alternative active scaffold for the further multi-targeting drug design by combining PARP-1 with LdTop1 or  $\alpha$ -glucosidase.

In the course of the binding mode and energy analysis of the hit compounds by molecular dynamics, we found that four compounds have strong interaction with key residues including His862, Gly863, Tyr889, Tyr896, Phe897, Tyr907, which is consistent with the known inhibitors (Jagtap and Szabo, 2005; Curtin and Szabo, 2020). It was also noticed that these compounds could form hydrogen bonding with residues like Gln759, Asp766, Asn767 on the HD, which was also shown correspondingly in the energy analysis. The effect of these hit compounds on HD was not quite significant from the energetic aspect, and the overall dynamic characteristics were similar to the conformations of known small-molecule complexes of PARP-1. One possible reason is that the substituent groups of the compounds, especially the structural part interacting with the HD is not big enough to form strong interactions. Therefore, the further structural modification against substituent groups of the compounds may effectively improve the interactions with HD. From the per-residue energy decomposition, it was found that further improving the electrostatic interaction ( $\Delta E_{ele}$ ) for arylidenefuopyridinedione of 8012-0567 and 8018-7603 or further improving the van der Waals interaction ( $\Delta E_{vdw}$ ) or electrostatic interaction by solvent ( $\Delta E_{ele,sol}$ ) for 1,2-Dihydro-2-oxo-6-quinolinesulfonamide of 8012-6529 and 8018-7168 might be able to optimize the inhibitory activities of the corresponding derivatives.

The cell experiments were further applied to confirm the anti-tumor abilities of the four hit compounds, specially by the colorectal carcinoma cell lines with BRCA deficiency or not. The results showed that two out of four hit compounds had validated inhibitory effect against two human colorectal carcinoma cell lines (HCT-116, RKO), and the better inhibitory effect of these compounds against HCT-116 than RKO was consistent with the results of Niraparib. As the signaling pathways of tumor growth are quite complex and may be regulated by a series of factors, the

detailed mechanism of the anti-tumor specificity for two hit compounds for HCT-116 still need further investigation in the future. Compounds 8012-6529 and 8018-7168 showed significant concentration-dependent inhibitory effect against HCT-116, and the IC<sub>50</sub> values both reached the micromolar level. Previously, the induced autophagy by PARP-1 inhibitors was reported in other tumor cells (Arun et al., 2015; Liu et al., 2019; Santiago-O'Farrill et al., 2020; Zai et al., 2020), but not in HCT-116. Further western blot analysis and transmission electron microscopy analysis of 8012-6529 and 8018-7168 confirmed the induction of autophagy. It was suggested that the anti-tumor effect of PARP-1 inhibitors could be further enhanced by combination use with autophagy inhibitors. The results of this study also suggested the possibility of 8012-6529 and 8018-7168 for combination use against the killing of HCT-116.

Overall, four hit compounds with obvious inhibitory activities targeting PARP-1 were discovered through *in silico* and *in vitro* screening. Further cell assays showed that compounds 8018-6529 and 8018-7168 could inhibit the growth of the human colorectal cancer cell (HCT-116) with IC<sub>50</sub> values of 4.30 and 9.29  $\mu$ M and were accompanied with induced autophagy process. The suggestions on the structural modification of these compounds were also provided by the binding mode and energy analysis. The results in this study could provide potential hit compounds for the development of anti-cancer drug.

## Data availability statement

The original contributions presented in the study are included in the article/Supplementary material, further inquiries can be directed to the corresponding authors.

## Author contributions

Conceptualization: DS, YY, and XSY. Data curation: DS. Formal analysis: DS, QP, and QQ. Molecular docking analysis and molecular dynamics: DS. Computational software: XJY.

## References

- Adeshina, Y. O., Deeds, E. J., and Karanicolas, J. (2020). Machine learning classification can reduce false positives in structure-based virtual screening. *P Natl. Acad. Sci. U. S. A.* 117 (31), 18477–18488. doi:10.1073/pnas.2000585117
- Ame, J. C., Spenlehauer, C., and de Murcia, G. (2004). The PARP superfamily. *Bioessays* 26 (8), 882–893. doi:10.1002/bies.20085
- Arun, B., Akar, U., Gutierrez-Barrera, A. M., Hortobagyi, G. N., and Ozpolat, B. (2015). The PARP inhibitor AZD2281 (Olaparib) induces autophagy/mitophagy in BRCA1 and BRCA2 mutant breast cancer cells. *Int. J. Oncol.* 47 (1), 262–268. doi:10.3892/ijo.2015.3003
- Bathula, C., Mamidala, R., Thulluri, C., Agarwal, R., Jha, K. K., Munshi, P., et al. (2015). Substituted furopyridinediones as novel inhibitors of  $\alpha$ -glucosidase. *RSC Adv.* 5 (110), 90374–90385. doi:10.1039/C5RA19255B
- Bender, B. J., Gahbauer, S., Luttens, A., Lyu, J., Webb, C. M., Stein, R. M., et al. (2021). A practical guide to large-scale docking. *Nat. Protoc.* 16 (10), 4799–4832. doi:10.1038/s41596-021-00597-z
- Bhadra, P., and Siu, S. W. I. (2019). Refined empirical force field to model protein-self-assembled monolayer interactions based on AMBER14 and GAFF. *Langmuir* 35 (29), 9622–9633. doi:10.1021/acs.langmuir.9b01367
- Case, D. A., Babin, V., Berryman, J., Betz, R., Cai, Q., Cerutti, D., et al. (2014). Amber 14.
- Casili, G., Campolo, M., Lanza, M., Filippone, A., Scuderi, S., Messina, S., et al. (2020). Role of ABT888, a novel poly(ADP-ribose) polymerase (PARP) inhibitor in countering autophagy and apoptotic processes associated to spinal cord injury. *Mol. Neurobiol.* 57 (11), 4394–4407. doi:10.1007/s12035-020-02033-x

Funding acquisition: DS. Methodology: DS, QP, and QQ. Drafting the manuscript: DS and QP. Review and editing: DS and YY.

## Funding

This research was funded by the National Natural Science Foundation of China (Grant No. 81903426).

## Acknowledgments

We are grateful for the high-performance computing platform at Jinan University, China, which was used to carry out this study.

## Conflict of interest

The authors declare that the research was conducted in the absence of any commercial or financial relationships that could be construed as a potential conflict of interest.

## Publisher's note

All claims expressed in this article are solely those of the authors and do not necessarily represent those of their affiliated organizations, or those of the publisher, the editors and the reviewers. Any product that may be evaluated in this article, or claim that may be made by its manufacturer, is not guaranteed or endorsed by the publisher.

## Supplementary material

The Supplementary Material for this article can be found online at: <https://www.frontiersin.org/articles/10.3389/fphar.2022.1026306/full#supplementary-material>



- Chang, X., Sun, D., Shi, D., Wang, G., Chen, Y., Zhang, K., et al. (2021). Design, synthesis, and biological evaluation of quinazolin-4(3H)-one derivatives co-targeting poly(ADP-ribose) polymerase-1 and bromodomain containing protein 4 for breast cancer therapy. *Acta Pharm. Sin. B* 11 (1), 156–180. doi:10.1016/j.apsb.2020.06.003
- Chen, H., Lyne, P. D., Giordanetto, F., Lovell, T., and Li, J. (2006). On evaluating molecular-docking methods for pose prediction and enrichment factors. *J. Chem. Inf. Model.* 46 (1), 401–415. doi:10.1021/ci0503255
- Cooper, D. R., Porebski, P. J., Chruszcz, M., and Minor, W. (2011). X-ray crystallography: Assessment and validation of protein-small molecule complexes for drug discovery. *Expert Opin. Drug Discov.* 6 (8), 771–782. doi:10.1517/17460441.2011.585154
- Curtin, N. J., and Szabo, C. (2020). Poly(ADP-ribose) polymerase inhibition: Past, present and future. *Nat. Rev. Drug Discov.* 19 (10), 711–736. doi:10.1038/s41573-020-0076-6
- Empereur-Mot, C., Guillemin, H., Latouche, A., Zagury, J. F., Viallon, V., and Montes, M. (2015). Predictiveness curves in virtual screening. *J. Cheminform.* 7, 52. doi:10.1186/s13321-015-0100-8
- Florkowski, C. M. (2008). Sensitivity, specificity, receiver-operating characteristic (ROC) curves and likelihood ratios: Communicating the performance of diagnostic tests. *Clin. Biochem. Rev.* 29, S83–S87.
- Helleday, T. (2011). The underlying mechanism for the PARP and BRCA synthetic lethality: Clearing up the misunderstandings. *Mol. Oncol.* 5 (4), 387–393. doi:10.1016/j.molonc.2011.07.001
- Jagtap, P., and Szabo, C. (2005). Poly(ADP-ribose) polymerase and the therapeutic effects of its inhibitors. *Nat. Rev. Drug Discov.* 4 (5), 421–440. doi:10.1038/nrd1718
- Jiang, H. Y., Yang, Y., Zhang, Y. Y., Xie, Z., Zhao, X. Y., Sun, Y., et al. (2018). The dual role of poly(ADP-ribose) polymerase-1 in modulating parthanatos and autophagy under oxidative stress in rat cochlear marginal cells of the stria vascularis. *Redox Biol.* 14, 361–370. doi:10.1016/j.redox.2017.10.002
- Langelier, M. F., Eisemann, T., Riccio, A. A., and Pascal, J. M. (2018a). PARP family enzymes: Regulation and catalysis of the poly(ADP-ribose) posttranslational modification. *Curr. Opin. Struct. Biol.* 53, 187–198. doi:10.1016/j.sbi.2018.11.002
- Langelier, M. F., Zandarashvili, L., Aguiar, P. M., Black, B. E., and Pascal, J. M. (2018b). NAD(+) analog reveals PARP-1 substrate-blocking mechanism and allosteric communication from catalytic center to DNA-binding domains. *Nat. Commun.* 9 (1), 844. doi:10.1038/s41467-018-03234-8
- Lin, K. Y., and Kraus, W. L. (2017). PARP inhibitors for cancer therapy. *Cell.* 169 (2), 183. doi:10.1016/j.cell.2017.03.034
- Liu, X., Shi, D., Zhou, S., Liu, H., Liu, H., and Yao, X. (2018). Molecular dynamics simulations and novel drug discovery. *Expert Opin. Drug Discov.* 13 (1), 23–37. doi:10.1080/17460441.2018.1403419
- Liu, Y., Song, H., Song, H., Feng, X., Zhou, C., and Huo, Z. (2019). Targeting autophagy potentiates the anti-tumor effect of PARP inhibitor in pediatric chronic myeloid leukemia. *Amb. Express* 9 (1), 108. doi:10.1186/s13568-019-0836-z
- Lord, C. J., and Ashworth, A. (2017). PARP inhibitors: Synthetic lethality in the clinic. *Science* 355 (6330), 1152–1158. doi:10.1126/science.aam7344
- Maier, J. A., Martinez, C., Kasavajhala, K., Wickstrom, L., Hauser, K. E., and Simmerling, C. (2015). ff14SB: Improving the accuracy of protein side chain and backbone parameters from ff99SB. *J. Chem. Theory Comput.* 11 (8), 3696–3713. doi:10.1021/acs.jctc.5b00255
- Mamidala, R., Majumdar, P., Jha, K. K., Bathula, C., Agarwal, R., Chary, M. T., et al. (2016). Identification of Leishmania donovani Topoisomerase I inhibitors via intuitive scaffold hopping and bioisosteric modification of known Top 1 inhibitors. *Sci. Rep.* 6, 26603. doi:10.1038/srep26603
- Maveyraud, L., and Mourey, L. (2020). Protein X-ray crystallography and drug discovery. *Molecules* 25 (5), E1030. doi:10.3390/molecules25051030
- Munoz-Gomez, J. A., Rodriguez-Vargas, J. M., Quiles-Perez, R., Aguilar-Quesada, R., Martin-Oliva, D., de Murcia, G., et al. (2009). PARP-1 is involved in autophagy induced by DNA damage. *Autophagy* 5 (1), 61–74. doi:10.4161/auto.5.1.7272
- Mysinger, M. M., Carchia, M., Irwin, J. J., and Shoichet, B. K. (2012). Directory of useful decoys, enhanced (DUD-E): Better ligands and decoys for better benchmarking. *J. Med. Chem.* 55 (14), 6582–6594. doi:10.1021/jm300687e
- O'Neil, N. J., Bailey, M. L., and Hieter, P. (2017). Synthetic lethality and cancer. *Nat. Rev. Genet.* 18 (10), 613–623. doi:10.1038/nrg.2017.47
- Rose, M., Burgess, J. T., O'Byrne, K., Richard, D. J., and Bolderson, E. (2020). PARP inhibitors: Clinical relevance, mechanisms of action and tumor resistance. *Front. Cell. Dev. Biol.* 8, 564601. doi:10.3389/fcell.2020.564601
- Rouleau, M., Patel, A., Hendzel, M. J., Kaufmann, S. H., and Poirier, G. G. (2010). PARP inhibition: PARP1 and beyond. *Nat. Rev. Cancer* 10 (4), 293–301. doi:10.1038/nrc2812
- Rouleau-Turcotte, E., Krastev, D. B., Pettitt, S. J., Lord, C. J., and Pascal, J. M. (2022). Captured snapshots of PARP1 in the active state reveal the mechanics of PARP1 allostery. *Mol. Cell.* 82, 2939–2951.e5. doi:10.1016/j.molcel.2022.06.011
- Santiago-O'Farrill, J. M., Weroha, S. J., Hou, X., Oberg, A. L., Heinzen, E. P., Maurer, M. J., et al. (2020). Poly(adenosine diphosphate ribose) polymerase inhibitors induce autophagy-mediated drug resistance in ovarian cancer cells, xenografts, and patient-derived xenograft models. *Cancer* 126 (4), 894–907. doi:10.1002/cncr.32600
- Shen, Y., Rehman, F. L., Feng, Y., Boshuizen, J., Bajrami, I., Elliott, R., et al. (2013). BMN 673, a novel and highly potent PARP1/2 inhibitor for the treatment of human cancers with DNA repair deficiency. *Clin. Cancer Res.* 19 (18), 5003–5015. doi:10.1158/1078-0432.CCR-13-1391
- Shi, D. F., An, X. L., Bai, Q. F., Bing, Z. T., Zhou, S. Y., Liu, H. X., et al. (2019). Computational insight into the small molecule intervening PD-L1 dimerization and the potential structure-activity relationship. *Front. Chem.* 7, 764. doi:10.3389/fchem.2019.00764
- Shi, D. F., Bai, Q. F., Zhou, S. Y., Liu, X. W., Liu, H. X., and Yao, X. J. (2018). Molecular dynamics simulation, binding free energy calculation and unbinding pathway analysis on selectivity difference between FKBP51 and FKBP52: Insight into the molecular mechanism of isoform selectivity. *Proteins* 86 (1), 43–56. doi:10.1002/prot.25401
- Sussman, J. L., Lin, D., Jiang, J., Manning, N. O., Prilusky, J., Ritter, O., et al. (1998). Protein Data bank (PDB): Database of three-dimensional structural information of biological macromolecules. *Acta Crystallogr. D. Biol. Crystallogr.* 54, 1078–1084. doi:10.1107/s0907444498009378
- Tung, N., and Garber, J. E. (2022). PARP inhibition in breast cancer: Progress made and future hopes. *NPJ Breast Cancer* 8, 47. doi:10.1038/s41523-022-00411-3
- Wang, Y. Q., Wang, P. Y., Wang, Y. T., Yang, G. F., Zhang, A., and Miao, Z. H. (2016). An update on poly(ADP-ribose)polymerase-1 (PARP-1) inhibitors: Opportunities and challenges in cancer therapy. *J. Med. Chem.* 59 (21), 9575–9598. doi:10.1021/acs.jmedchem.6b00055
- Wei, L., Wang, M., Wang, Q., and Han, Z. (2021). Dual targeting, a new strategy for novel PARP inhibitor discovery. *Drug Discov. Ther.* 15 (6), 300–309. doi:10.5582/ddt.2021.01100
- Zai, W., Chen, W., Han, Y., Wu, Z., Fan, J., Zhang, X., et al. (2020). Targeting PARP and autophagy evoked synergistic lethality in hepatocellular carcinoma. *Carcinogenesis* 41 (3), 345–357. doi:10.1093/carcin/bgz104
- Zandarashvili, L., Langelier, M. F., Velagapudi, U. K., Hancock, M. A., Steffen, J. D., Billur, R., et al. (2020). Structural basis for allosteric PARP-1 retention on DNA breaks. *Science* 368 (6486), eaax6367. doi:10.1126/science.aax6367
- Zhang, J., Wang, G., Zhou, Y., Chen, Y., Ouyang, L., and Liu, B. (2018). Mechanisms of autophagy and relevant small-molecule compounds for targeted cancer therapy. *Cell. Mol. Life Sci.* 75 (10), 1803–1826. doi:10.1007/s00018-018-2759-2



## OPEN ACCESS

EDITED BY  
Guan Wang,  
Sichuan University, China

REVIEWED BY  
Wanli Yang,  
Fourth Military Medical University,  
China  
Siddharth Mehra,  
University of Miami Health System,  
United States

\*CORRESPONDENCE  
Ioannis Serafimidis  
iseraf@bioacademy.gr

†These authors have contributed  
equally to this work and share  
first authorship

SPECIALTY SECTION  
This article was submitted to  
Pharmacology of Anti-Cancer Drugs,  
a section of the journal  
Frontiers in Oncology

RECEIVED 20 September 2022  
ACCEPTED 09 November 2022  
PUBLISHED 24 November 2022

CITATION  
Troumpoukis D, Papadimitropoulou A,  
Charalampous C, Kogionou P,  
Palamaris K, Sarantis P and  
Serafimidis I (2022) Targeting  
autophagy in pancreatic cancer: The  
cancer stem cell perspective.  
*Front. Oncol.* 12:1049436.  
doi: 10.3389/fonc.2022.1049436

COPYRIGHT  
© 2022 Troumpoukis,  
Papadimitropoulou, Charalampous,  
Kogionou, Palamaris, Sarantis and  
Serafimidis. This is an open-access  
article distributed under the terms of  
the [Creative Commons Attribution  
License \(CC BY\)](#). The use, distribution  
or reproduction in other forums is  
permitted, provided the original  
author(s) and the copyright owner(s)  
are credited and that the original  
publication in this journal is cited, in  
accordance with accepted academic  
practice. No use, distribution or  
reproduction is permitted which does  
not comply with these terms.

# Targeting autophagy in pancreatic cancer: The cancer stem cell perspective

Dimitrios Troumpoukis<sup>1†</sup>, Adriana Papadimitropoulou<sup>1†</sup>,  
Chrysanthi Charalampous<sup>1</sup>, Paraskevi Kogionou<sup>1</sup>,  
Kostas Palamaris<sup>2</sup>, Panagiotis Sarantis<sup>3</sup>  
and Ioannis Serafimidis<sup>1\*</sup>

<sup>1</sup>Center of Basic Research, Biomedical Research Foundation of the Academy of Athens, Athens, Greece, <sup>2</sup>First Department of Pathology, Medical School, National and Kapodistrian University of Athens, Athens, Greece, <sup>3</sup>Molecular Oncology Unit, Department of Biological Chemistry, Medical School, National and Kapodistrian University of Athens, Athens, Greece

Pancreatic cancer is currently the seventh leading cause of cancer-related deaths worldwide, with the estimated death toll approaching half a million annually. Pancreatic ductal adenocarcinoma (PDAC) is the most common (>90% of cases) and most aggressive form of pancreatic cancer, with extremely poor prognosis and very low survival rates. PDAC is initiated by genetic alterations, usually in the oncogene KRAS and tumor suppressors CDKN2A, TP53 and SMAD4, which in turn affect a number of downstream signaling pathways that regulate important cellular processes. One of the processes critically altered is autophagy, the mechanism by which cells clear away and recycle impaired or dysfunctional organelles, protein aggregates and other unwanted components, in order to achieve homeostasis. Autophagy plays conflicting roles in PDAC and has been shown to act both as a positive effector, promoting the survival of pancreatic tumor-initiating cells, and as a negative effector, increasing cytotoxicity in uncontrollably expanding cells. Recent findings have highlighted the importance of cancer stem cells in PDAC initiation, progression and metastasis. Pancreatic cancer stem cells (PaCSCs) comprise a small subpopulation of the pancreatic tumor, characterized by cellular plasticity and the ability to self-renew, and autophagy has been recognised as a key process in PaCSC maintenance and function, simultaneously suggesting new strategies to achieve their selective elimination. In this review we evaluate recent literature that links autophagy with PaCSCs and PDAC, focusing our discussion on the therapeutic implications of pharmacologically targeting autophagy in PaCSCs, as a means to treat PDAC.

## KEYWORDS

autophagy, pancreas, pancreatic cancer, PDAC - pancreatic ductal adenocarcinoma, Cancer Stem Cell (CSC), pancreatic cancer stem cells, hydroxychloroquine

## Introduction

Pancreatic Ductal Adenocarcinoma (PDAC) is the most common form of pancreatic cancer and is expected to become the second-leading cause of cancer-related deaths worldwide by 2030 (1, 2). PDAC origin remains a controversial issue but most studies support the notion that it arises from the uncontrollable proliferation of the ductal cells of the exocrine compartment, resulting in the development of a highly aggressive neoplasm (3). The molecular profiling of PDAC includes multiple gene expression alterations and copy number aberrations with KRAS (Kirsten rat sarcoma viral oncogene homolog) mutations accounting for more than 90% of the cases. However, further cancer progression requires additional mutations including tumor suppressor protein p53 (TP53), cyclin-dependent kinase inhibitor 2A (CDKN2A) and SMAD family member 4 (SMAD4) (4, 5). Treatment strategies for PDAC include tumor resection in combination with chemo/radio therapies but the efficacy is very limited as most patients relapse and eventually die from metastasis within 5 years (2).

In PDAC, approximately 1% of the total tumor mass consists of Pancreatic Cancer Stem Cells (PaCSCs) that feature auto-renewal and differentiation characteristics that allow them to generate multiple and genetically diverse cancer cell lineages (6). PaCSCs were initially described by Li et al. as cells that uniquely express a combination of CD24/CD44/EpCAM surface markers, and display enriched tumor initiating capacity when transplanted in immunocompromised mice (7). Over the last few years, investigation of the PaCSC population has attracted significant attention and is now being recognised as the main source of tumor heterogeneity and plasticity, and a niche of major importance for pancreatic tumor initiation and progression (8). In addition to CD44, CD24 and EpCAM (ESA), other markers that have been subsequently employed to characterise PaCSCs include CD133, ALDH1, CXCR4 and DCLK1, however, expression of these proteins is not restricted to PaCSCs exclusively (9–12). Many diverse signaling pathways have been found to operate in PaCSCs, including Notch, WNT, Hippo, Sonic-Hedgehog, mTOR and PI3K/Akt. These pathways actively maintain stemness and ensure an increased metastatic potential, but at the same time promote chemoprevention and resistance to conventional therapies (13).

A major cellular process that was found to be critically altered during PDAC initiation and progression is autophagy (14). Autophagy is a highly conserved “self-digestion” process that involves the catabolism of dysfunctional compounds, damaged organelles and engulfed pathogens to maintain cellular integrity and survival. Autophagy is achieved by the enclosure of this cytoplasmic “waste” cargo inside double-membrane vesicles and their concomitant translocation to lysosomes for degradation. Normally, autophagy acts as a major regulator of homeostasis, however under stressful

conditions (hypoxia, starvation etc) mainly induced by disease (including cancer), the degradation of subcellular elements is accelerated in order to recycle the macromolecules and render them available to fulfill energy requirements (15–17). Major autophagic signals and regulators include the mammalian target of rapamycin (mTOR), AMP-activated protein kinase (AMPK), WNT and TGF $\beta$  (18–20).

In this concise review, we evaluate the literature, outline current evidence on the role of autophagy in PaCSCs, and discuss how this knowledge can lead to more effective therapies against PDAC.

## Autophagy in PDAC – A double-edged sword

Increased autophagic activity in PDAC has long been recognized as a major contributing factor in tumor survival, progression and metastasis. Through autophagy, PDAC tumors gain vital resources for the maintenance of their integrity, and this is achieved *via* mechanisms that have been expertly reviewed in great detail elsewhere (more recently by Gillson et al, 2022) (14). Our intention here is to focus on the seemingly contradictory and often debated dual (positive and negative) role of autophagy in PDAC. In this context, autophagy has been shown to attenuate the development of preneoplastic lesions in early pancreatic carcinogenesis, whereas, at more advanced stages, it was shown to promote tumor development. Disruption of the vital autophagy related genes *atg7* or *atg5* induces the development of benign pancreatic intraepithelial neoplasia (PanIN) in mice harboring the oncogenic Kras<sup>G12D</sup> mutation. However, despite the fact that spontaneous adenomas do occur, these are not able to progress to a more malignant state (21–23). Autophagy is up-regulated in various PDAC cell lines and is found to be elevated in PanINs as they progress towards PDAC. Consequently, inhibition of autophagy with the use of chloroquine or with shRNA against *atg5* suppresses their growth *in vitro* and attenuates tumor development in pancreatic cancer mouse models (24). This effect was attributed to elevation of ROS (Reactive Oxygen Species) levels, increased DNA damage and impaired mitochondrial function. Resulting tumors retain their benign character and do not evolve to a more malignant state, indicating that autophagy assists tumor initiation at first but then acts as tumor suppressor, blocking progression to more advanced stages. Similar observations were made with the loss of *atg5* or *atg7* in mice harboring oncogenic KRAS mutations. Biallelic loss of *atg5/7* reinforced tumor initiation but repressed the transition of PanINs to PDAC in mice carrying a wild-type *p53* allele. On the contrary, when *p53* is deleted, loss of *atg5/7* results in accelerated tumor progression indicating that *p53* status can determine whether autophagy will act as a tumor suppressor or accelerate tumor development (22, 23). In a later

study, Görgülü et al, showed that biallelic deletion of *atg5* in the presence of oncogenic KRAS stimulated acinar-to-ductal metaplasia (ADM), which progressed to PanIN stage 1 but did not eventually lead to PDAC. In contrast, mice carrying just one wild-type copy of the *atg5* gene were able to develop PDAC and exhibited increased invasive capacity with a higher frequency than their wild-type (KRAS : ATG5+/+) counterparts (25).

Interesting results regarding the cumulative role of autophagy in PDAC were also extracted from two mouse models, in which hallmark KRAS<sup>G12D</sup> mutation was combined with two distinct heterozygous Trp53 loss-of-function mutations, frequently encountered in human pancreatic carcinomas (Trp53R172, Trp53R172H) (26, 27). In these models, one Trp53 allele is inactivated *via* a loss-of-function mutation, while the second one is subsequently lost *via* loss of heterozygosity (LOH), at a later stage of tumor progression (28). These models do not bear a complete deletion of Trp53, and therefore emulate human disease pathology more faithfully, thus enabling the investigation of the complex interplay between mutant Trp53 and autophagy regulation. In both models, pancreas-specific autophagy inhibition was achieved *via* a Cre-mediated genetic ablation of ATG7 with conflicting results. While in KRasG12D/+; Trp53R172H/+ animals, ATG7 ablation impeded tumorigenesis, by reducing incidence of both pre-invasive and terminal PDAC lesions (27), KRasG12D/+; Trp53R172/+ mice were characterized by an increased abundance of both acinar-to-ductal metaplasia (ADM) and pancreatic-intraepithelial neoplasia (PanIN) foci as well as more foci of invasive pancreatic tumors (26). The contradictory data derived from the above studies confirm the context-dependent role of autophagy in tumor evolutionary routes, which seems to be largely affected by the genetic background of the tumor-initiating cells.

The dual role of autophagy in PDAC biology has highlighted the importance of deciphering whether this process has a predominantly positive or negative effect in tumor development. Clarification of this important point will determine whether autophagy should be pharmacologically stimulated or inhibited in order to provide an effective treatment option for PDAC, with consensus so far favoring the later hypothesis.

## Autophagy in pancreatic cancer stem cells

Cancer stem cells have been shown to rely heavily on autophagic processes for the maintenance of their stemness, their survival under hypoxic and other stress conditions and the development of resistance to therapies (29). The study of autophagy in PaCSCs has been attracting increasing attention over the last decade due to the realization of its crucial involvement in PDAC development and its potential role in

PDAC therapies (Figure 1). Rausch et al. was the first to demonstrate an interaction between PaCSCs, hypoxia and autophagy, initially by studying fixed patient-derived PDAC samples where he revealed strong co-expression of markers for CSCs (CD44, CD24), hypoxia (CA-IX) and autophagy (BECLIN1, LC3) (30). During hypoxia, cells from the established cell line MIA-PaCa2 that features high CSC properties are able to survive and migrate, whereas BxPc-3 cells with limited CSC properties cannot respond efficiently and eventually undergo apoptosis (30). The higher stemness of MIA-PaCa2 cells is due to several key mutations that they carry. These include amino-acid substitutions in KRAS and TP53 (G12D and R248W, respectively) and a complete loss of CDKN2A (31, 32). On the contrary, BxPc-3 cells appear to have physiological KRAS while they carry a different amino-acid substitution in TP53 (Y220C) and display complete loss of both CDKN2A and SMAD4 proteins. These genotypic differences are considered to be responsible for the higher stemness of MIA-PaCa2 cells, indirectly leading to the suppression of non-canonical Wnt signaling (33). In this context, autophagosomes and expression of autophagy-related genes (beclin1, atg3, atg4b, and atg12) were found to be significantly elevated in CSCs of the MIA-PaCa2 cell-line but not in BxPc-3 cells. Similarly, Zhu et al. has shown that in the stressful environment of hypoxia, pancreatic cancer cells with stem cell-like properties (isolated by means of CD133 expression) displayed a significant degree of metastatic potential, self-renewal ability and elevated expression of the autophagy-related proteins LC3-II and BECLIN1 (34). Moreover, HIF-1 $\alpha$  has been positively correlated with autophagy (35) as migrating cells with stem cell features exhibited concurrent up-regulation of HIF-1 $\alpha$  and autophagy-related genes (ATGs). This correlation was further confirmed by evidence that HIF-1 $\alpha$  down-regulation by RNA silencing results in reduced autophagy (34). Co-expression of the autophagy marker LC3 with stem cell markers CD133, CD44 and ALDH1 in pancreatic cancer tissue samples is another example in support of the positive correlation between autophagy and cancer cell stemness (36). Interestingly, the same study showed that pancreatic cancer patients with increased co-expression of LC3 and ALDH1 correlated with poor Progression Free Survival (PFS) and worse Overall Survival (OS). PANC-1 cells transfected with lentivirus carrying shRNA against *atg5*, *atg7* and *becn1* exhibited a significant decrease in CD44, CD133 and ALDH1 expression. Reduced levels of expression of these CSC markers concomitantly affected the stem cell properties of the transfected cells. Their self-renewal capacity and their proliferation potential were reduced, as these cells formed less spheres and exhibited impaired growth in culture compared to their control counterparts (36). Furthermore, when the transfected cells were transplanted into NOD/SCID mice, tumor volume was consistently lower compared to control mice and displayed resistance to gemcitabine. These results were further confirmed by pharmacological regulation of autophagy with the addition of



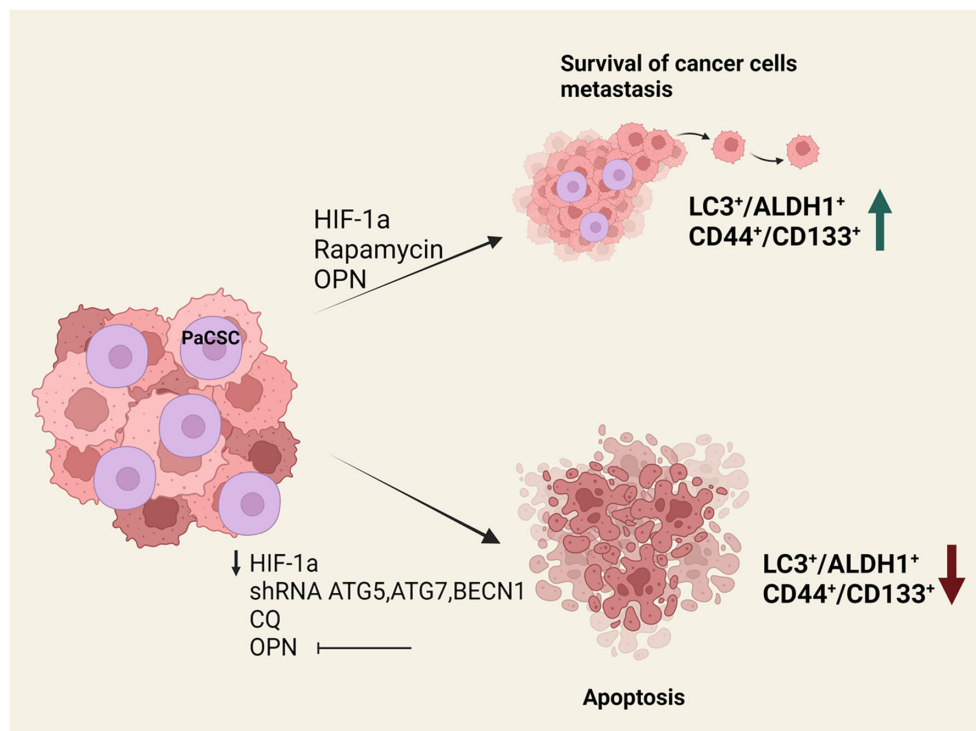


FIGURE 1

Effects of autophagy perturbation in PaCSCs maintenance and function. *In vitro* and *in vivo* experiments have shown that the presence of HIF-1a, rapamycin or osteopontin increase the survival of cancer stem cells and help metastasis. This is associated with an increase in LC3+/ALDH1+ and CD44+/CD133+ surface marker expression. On the contrary, when there is a reduction of HIF-1a or osteopontin, when *atg5*, *atg7* and *becn1* are silenced, or in the presence of chloroquine, cancer stem cells undergo apoptosis.

the autophagy inhibitor chloroquine (CQ) and the inducer rapamycin. Levels of LC3/ALDH1 and CD44/CD133 expression were reduced by CQ treatment but showed significant increase in the presence of rapamycin (36). Additionally, osteopontin (OPN), which was previously reported to positively regulate sphere forming ability of cancer cells, was found to increase the levels of CD44, CD133, ALDH1 and LC3-II in various pancreatic cell lines, an effect that can be reversed by attenuating osteopontin activity or blocking autophagy altogether. After suppression of the OPN-mediated signaling pathways, it was revealed that NF- $\kappa$ B is a major contributor of OPN-stimulated autophagy and CSC activity. This observation is in agreement with other studies that have identified NF- $\kappa$ B as an inducer of autophagy under stressful environmental conditions such as heat shock (37). Finally, recent studies by Qin et al. showed that the stem cell-like properties of pancreatic cancer cells were reduced after the inhibition of the Nutrient-deprivation Autophagy Factor-1 (NAF-1), an autophagy-related protein localized in the outer mitochondrial membrane that is mainly involved in the maintenance of mitochondrial integrity (38–41). Pancreatic CSCs display an increased sensitivity to defects in mitochondrial homeostasis

due to their predominant dependence on oxidative phosphorylation (OXPHOS) for their survival (42). NAF-1 inhibition therefore significantly affects stem cell properties of PaCSCs and mitigates their invasive capacity (41).

## Targeting autophagy in PDAC

The majority of patients with PDAC are diagnosed in advanced stages of the disease, when the tumor is inoperable and surgery is no longer a viable treatment option. Chemotherapy and radiotherapy are first-line palliative treatments for PDAC patients and the standard chemotherapeutic drug commonly used was Gemcitabine until Folfirinox (a combination of 5-fluorouracil, folinic acid, irinotecan and oxaliplatin) proved to be more efficient in increasing OS (43).

Targeting autophagy in combination with chemotherapy has emerged as an attractive and very promising strategy in confronting PDAC. A variety of autophagy inhibitors, with distinct substrate specificities, have been developed and evaluated *in vitro* on cancer cell-lines, as well as *in vivo* on mouse models of PDAC. Based on their target molecules, the



existing inhibitors can be segregated into two main classes: those that aim at constraining the initial step of autophagosome formation (44, 45) and those that block the merging of autophagosomes with lysosomes by altering the acidic environment of lysosomes (46, 47). The first class encompasses agents that impede the generation of the two core autophagy initiation multi-protein complexes, ULK1 and PI3KC3-C1 (48, 49). The main representatives of this class are MRT68921 (50, 51), SBI-0206965 (52–54) and SBI-7455 (55), which selectively target ULK1 kinase, and Spautin-1 (56, 57) and SAR405 (58, 59), which selectively suppress the PI3KC3-C1 complex. To this day, none of these compounds have progressed further into clinical studies on human patients.

On the contrary, the compound Hydroxychloroquine (HCQ) -a derivative of chloroquine and the major representative of the second class of autophagy inhibitors (60) - has been assessed in a number of clinical trials for PDAC, either as a monotherapy, or in combination with standard chemotherapy regimens or novel classes of anti-proliferative drugs (Table 1). Initially, a clinical trial investigated the effect of monotherapy using daily administrations of Hydroxychloroquine, however the drug yielded no significant responses (61). On the contrary, two phase 1/phase 1b/2 clinical trials that used a combination of gemcitabine and HCQ, provided encouraging data as there was reduction of the CA19.9 tumor marker, an increase in LC3-II staining and an improved PFS. Despite these very promising observations however, no safe conclusions could be drawn by these two studies due to the small number of patients and the lack of randomization (62, 63). More recently, a randomized phase II clinical trial was conducted using Gemcitabine together with nab-paclitaxel, with or without HCQ, in patients with advanced pancreatic cancer. Although the OS or PFS were not significantly improved, the study showed that the response rate was improved in HCQ-treated patients, therefore it was proposed that HCQ be included at the preoperative stage (61, 64).

Many attempts have been made in order to combine autophagy inhibition with novel cancer immunotherapy protocols that are currently under development. Yamamoto

et al. showed that autophagy inhibition increases expression of MHC-I molecules on the surface of PDAC cells, leading to increased infiltration of immune cells, thus demonstrating that autophagy inhibition combined with immunotherapy could be a promising therapeutic option against PDAC (65). Nevertheless, the sole study to this day performed on pancreatic cancer patients treated with a combination of HCQ, gemcitabine, nab-paclitaxel and avelumab (an anti-PD-L1 antibody) was terminated due to undesirable side effects. Further clinical trials that combine HCQ with MAPK inhibitors for advanced and metastatic pancreatic cancer are currently under way (66).

In addition to the synthetic agents mentioned above, a number of natural derivatives have demonstrated a capacity to interact in multiple ways with the autophagic pathways, and can potentially be used in PDAC treatment. Even though their exact mechanism of action is unclear, they seem to converge to a common path of apoptosis inhibition. Fudan-Yueyang-Ganoderma lucidum (FYGL; a proteoglycan extracted from Ganoderma lucidum) and Alantolactone demonstrated inhibitory effect in late-stage of autophagy along with increased apoptotic potential, mediated by elevated ROS production and suppression of STAT3 and Bcl-2 respectively (67–70). Curcumin is also capable of inducing pro-apoptotic effects, by increasing the BAX/Bcl-2 ratio (71), while ursolic acid (UA) downregulated autophagy, predominantly *via* inducing cell cycle arrest (72).

## Discussion – prospects of targeting autophagy in PaCSCs

The destruction of CSC niches is essential in order to achieve PDAC therapy and avoid cancer recurrence, however CSC niches in PDAC tumors are protected by the low-oxygen tumor environment and this is a major contributing factor to anti-cancer therapy resistance (29). Possible treatments could arise from the targeting of autophagy in PaCSCs and several preclinical studies are exploring the possibility of eliminating PaCSC niches

TABLE 1 Clinical trials for PDAC that include targeting of autophagy.

CLINICAL TRIAL	REGIMEN	PHASE	RESULTS	REFERENCE
NCT01273805	Hydroxychloroquine (HCQ)	Phase II	No significant responses	Wolpin et al. 2014 (61)
NCT01128296	HCQ with Gemcitabine	Phase I/II	Decrease in CA19-9 Surgical oncologic outcomes were encouraging	Boone et al. 2015 (62)
NCT01777477	HCQ with Gemcitabine	Phase I	No dose-limiting toxicities Median time to progression was 4 months Median overall survival was 7.6 months	Samaras et al., 2017 (63)
NCT01506973	Gemcitabine hydrochloride and nab-paclitaxel (GA) ± HCQ	Phase II	Overall survival at 12 months was 41% in the HCQ group and 49% in the non-HCQ group Overall response rate was 38.2% in the HCQ group and 21.1% in the non-HCQ group	Karasic et al., 2019 (64)

by perturbing autophagy. Signaling pathways that are active in PaCSCs, such as NOTCH, WNT and SHH, are being explored as possible targets for impairing pluripotency in combination with autophagy targeting (9). On the other hand, the fact that PaCSCs reside in the anatomically distinct regions of a niche, which is often pharmacologically inaccessible, necessitates the exploration of alternative properties of PaCSCs as targets for therapy. Cancer dormancy is characterized by attenuation of cell proliferation and the transition to a quiescence-like state. It has been shown that dormancy contributes significantly to cancer relapse and induction of metastasis. Conventional anticancer therapies usually target proliferating cells hence the acquisition of a dormant phenotype results to the evasion of treatments and worse overall survival. The biological mechanisms and signaling pathways regulating the dormant phenotype of tumor cells also apply to CSC behavior, and recent studies indicate that autophagy plays a vital role in the entrance of CSCs to a dormant state, the maintenance of their survival and their reactivation under specific conditions (73).

In addition to the pre-clinical studies, efforts to effectively tackle PDAC currently explore the clinical use of small molecules that target autophagy, in combination with chemotherapy and/or immunotherapy (14). Targeting cancer stemness is currently the basis of ongoing clinical trials on Phase III with paclitaxel/nab paclitaxel and gemcitabine with the addition of napabucasin, a small molecule that inhibits STAT3-mediated gene transcription. The results from phase 1b/2 achieved a Partial Response (PR) of almost 42% and approximate 3% of Complete Response (CR) (74). This enhanced chemotherapy scheme could be complemented with selected compounds that target key components of the autophagic process, in order not only to eliminate tumor-cells but also to eradicate hidden and evading PaCSCs.

Despite the undoubted benefits of autophagy inhibition in cancer treatment, the complex role of this “self-digestion” process in tumorigenesis, coupled with the capacity of tumor stem cells to utilize alternative nutrient sources under starvation conditions, could impose some restrictions to the clinical efficacy of this therapeutic approach. While in the majority of cases autophagy is considered a cytoprotective mechanism that serves as an adaptation system of neoplastic cells in conditions of nutrient scarcity, there is still controversy regarding its overall effects in cancer initiation and progression. Recent experimental evidence, from both *in vitro* and *in vivo* studies, suggests a context-dependent anti-tumor effect of autophagy, mediated by a detrimental effect on cancer stem cell survival and metastasis. Even though autophagy is a process antagonistic to apoptosis, overt autophagic influx can in fact trigger apoptosis under certain conditions by activation of caspase-8 and the diminution of endogenous apoptosis inhibitors (75). Moreover, genetic ablation of ATG5 in a KRAS-driven mouse model of PDAC enhances the metastatic potential of tumor stem cells, implying an anti-metastatic effect of autophagy under certain circumstances, especially during the initial stages of tumor

development (25). It has also been shown that neoplastic cells are equipped with an intrinsic ability to circumvent dependency on autophagy and exploit compensatory signal transduction systems, such as Nrf2 signalling and deployment of complementary nutritional sources through the process of micropinocytosis (76). These strategies enable cancer stem cells to survive nutrient stress conditions arising from starvation, thus ensuring their survival and growth. It is therefore implied that potential anti-PDAC pharmacotherapy schemes relying on autophagy targeting in PaCSCs should carefully consider both the tumor-suppressive and the tumor-promoting effects of this action.

## Author contributions

DT, AP and IS wrote the first draft of the manuscript. All authors contributed to the article, reviewed and edited the final manuscript and approved the submitted version.

## Funding

Work in the senior author’s laboratory is supported by funding provided by Boehringer Ingelheim GmbH (CRA: 493341) and the Greek General Secretariat of Research and Innovation (GSRI) (Code: T1EDK-03532). The funders had no role in study design, data collection and analysis, decision to publish, or manuscript preparation.

## Acknowledgments

The authors thank all members of the Stem Cell and Cancer Biology laboratory at BRFAA for critical discussions over the manuscript and wish to apologise to all investigators whose work has not been cited here due to space restrictions.

## Conflict of interest

The authors declare that the research was conducted in the absence of any commercial or financial relationships that could be construed as potential conflict of interest.

## Publisher’s note

All claims expressed in this article are solely those of the authors and do not necessarily represent those of their affiliated organizations, or those of the publisher, the editors and the reviewers. Any product that may be evaluated in this article, or claim that may be made by its manufacturer, is not guaranteed or endorsed by the publisher.

# References

1. Quante AS, Ming C, Rottmann M, Engel J, Boeck S, Heinemann V, et al. Projections of cancer incidence and cancer-related deaths in Germany by 2020 and 2030. *Cancer Med* (2016) 5(9):2649–56. doi: 10.1002/cam4.767
2. Sung H, Ferlay J, Siegel RL, Laversanne M, Soerjomataram I, Jemal A, et al. Global cancer statistics 2020: GLOBOCAN estimates of incidence and mortality worldwide for 36 cancers in 185 countries. *CA Cancer J Clin* (2021) 71(3):209–49. doi: 10.3322/caac.21660
3. Adamska A, Domenichini A, Falasca M. Pancreatic ductal adenocarcinoma: Current and evolving therapies. *Int J Mol Sci* (2017) 18(7):1338. doi: 10.3390/ijms18071338
4. Mizrahi JD, Surana R, Valle JW, Shroff RT. Pancreatic cancer. *Lancet* (2020) 395(10242):2008–20. doi: 10.1016/S0140-6736(20)30974-0
5. Qian Y, Gong Y, Fan Z, Luo G, Huang Q, Deng S, et al. Molecular alterations and targeted therapy in pancreatic ductal adenocarcinoma. *J Hematol Oncol* (2020) 13(1):130. doi: 10.1186/s13045-020-00958-3
6. Lee CJ, Dosch J, Simeone DM. Pancreatic cancer stem cells. *J Clin Oncol* (2008) 26(17):2806–12. doi: 10.1200/JCO.2008.16.6702
7. Li C, Heidt DG, Dalerba P, Burant CF, Zhang L, Adsay V, et al. Identification of pancreatic cancer stem cells. *Cancer Res* (2007) 67(3):1030–7. doi: 10.1158/0008-5472.CAN-06-2030
8. Subramaniam D, Kaushik G, Dandawate P, Anant S. Targeting cancer stem cells for chemoprevention of pancreatic cancer. *Curr Med Chem* (2018) 25(22):2585–94. doi: 10.2174/0929867324666170127095832
9. Barman S, Fatima I, Singh AB, Dhawan P. Pancreatic cancer and therapy: Role and regulation of cancer stem cells. *Int J Mol Sci* (2021) 22(9):4765. doi: 10.3390/ijms22094765
10. Hong SP, Wen J, Bang S, Park S, Song SY. CD44-positive cells are responsible for gemcitabine resistance in pancreatic cancer cells. *Int J Cancer* (2009) 125(10):2323–31. doi: 10.1002/ijc.24573
11. Maréchal R, Demetter P, Nagy N, Berton A, Decaestecker C, Polus M, et al. High expression of CXCR4 may predict poor survival in resected pancreatic adenocarcinoma. *Br J Cancer* (2009) 100(9):1444–51. doi: 10.1038/sj.bjc.6605020
12. Ito H, Tanaka S, Akiyama Y, Shimada S, Adikrisna R, Matsumura S, et al. Dominant expression of DCLK1 in human pancreatic cancer stem cells accelerates tumor invasion and metastasis. *PLoS One* (2016) 11(1):e0146564. doi: 10.1371/journal.pone.0146564
13. Hermann PC, Sainz B. Pancreatic cancer stem cells: A state or an entity? *Semin Cancer Biol* (2018) 53:223–31. doi: 10.1016/j.semcancer.2018.08.007
14. Gillson J, Abd El-Aziz YS, Leck LYW, Jansson PJ, Pavlakis N, Samra JS, et al. Autophagy: A key player in pancreatic cancer progression and a potential drug target. *Cancers (Basel)* (2022) 14(14):3528. doi: 10.3390/cancers14143528
15. Hermann PC, Huber SL, Herrler T, Aicher A, Ellwart JW, Guba M, et al. Distinct populations of cancer stem cells determine tumor growth and metastatic activity in human pancreatic cancer. *Cell Stem Cell* (2007) 1(3):313–23. doi: 10.1016/j.stem.2007.06.002
16. Ikenaga N, Ohuchida K, Mizumoto K, Yu J, Kayashima T, Hayashi A, et al. Characterization of CD24 expression in intraductal papillary mucinous neoplasms and ductal carcinoma of the pancreas. *Hum Pathol* (2010) 41(10):1466–74. doi: 10.1016/j.humpath.2010.04.004
17. Hou YC, Chao YJ, Tung HL, Wang HC, Shan YS. Coexpression of CD44-positive/CD133-positive cancer stem cells and CD204-positive tumor-associated macrophages is a predictor of survival in pancreatic ductal adenocarcinoma. *Cancer* (2014) 120(17):2766–77. doi: 10.1002/cncr.28774
18. Shang L, Chen S, Du F, Li S, Zhao L, Wang X. Nutrient starvation elicits an acute autophagic response mediated by Ulk1 phosphorylation and its subsequent dissociation from AMPK. *Proc Natl Acad Sci U.S.A.* (2011) 108(12):4788–93. doi: 10.1073/pnas.1100844108
19. Kroemer G, Mariño G, Levine B. Autophagy and the integrated stress response. *Mol Cell* (2010) 40(2):280–93. doi: 10.1016/j.molcel.2010.09.023
20. Tan VP, Miyamoto S. Nutrient-sensing mTORC1: Integration of metabolic and autophagic signals. *J Mol Cell Cardiol* (2016) 95:31–41. doi: 10.1016/j.jmcc.2016.01.005
21. Takamura A, Komatsu M, Hara T, Sakamoto A, Kishi C, Waguri S, et al. Autophagy-deficient mice develop multiple liver tumors. *Genes Dev* (2011) 25(8):795–800. doi: 10.1101/gad.2016211
22. Rosenfeldt MT, O'Prey J, Morton JP, Nixon C, MacKay G, Mrowinska A, et al. p53 status determines the role of autophagy in pancreatic tumour development. *Nature* (2013) 504(7479):296–300. doi: 10.1038/nature12865
23. Yang A, Rajeshkumar NV, Wang X, Yabuuchi S, Alexander BM, Chu GC, et al. Autophagy is critical for pancreatic tumor growth and progression in tumors with p53 alterations. *Cancer Discovery* (2014) 4(8):905–13. doi: 10.1158/2159-8290.CD-14-0362
24. Yang S, Wang X, Contino G, Liesa M, Sahin E, Ying H, et al. Pancreatic cancers require autophagy for tumor growth. *Genes Dev* (2011) 25(7):717–29. doi: 10.1101/gad.2016111
25. Görgülü K, Diakopoulos KN, Ai J, Schoeps B, Kabacaoglu D, Karpathaki AF, et al. Levels of the autophagy-related 5 protein affect progression and metastasis of pancreatic tumors in mice. *Gastroenterology* (2019) 156(1):203–217.e20. doi: 10.1053/j.gastro.2018.09.053
26. Long JS, Kania E, McEwan DG, Barthet VJA, Brucoli M, Ladds MJGW, et al. ATG7 is a haploinsufficient repressor of tumor progression and promoter of metastasis. *Proc Natl Acad Sci U.S.A.* (2022) 119(28):e2113465119. doi: 10.1073/pnas.2113465119
27. Mainz L, Sarhan MAF, Roth S, Sauer U, Maurus K, Hartmann EM, et al. Autophagy blockage reduces the incidence of pancreatic ductal adenocarcinoma in the context of mutant. *Front Cell Dev Biol* (2022) 10:785252. doi: 10.3389/fcell.2022.785252
28. Sabapathy K, Lane DP. Therapeutic targeting of p53: all mutants are equal, but some mutants are more equal than others. *Nat Rev Clin Oncol* (2018) 15(1):13–30. doi: 10.1038/nrclinonc.2017.151
29. Nazio F, Bordin M, Cianfanelli V, Locatelli F, Cecconi F. Autophagy and cancer stem cells: molecular mechanisms and therapeutic applications. *Cell Death Differ* (2019) 26(4):690–702. doi: 10.1038/s41418-019-0292-y
30. Rausch V, Liu L, Apel A, Rettig T, Gladkikh J, Labsch S, et al. Autophagy mediates survival of pancreatic tumour-initiating cells in a hypoxic microenvironment. *J Pathol* (2012) 227(3):325–35. doi: 10.1002/path.3994
31. Sun C, Yamato T, Furukawa T, Ohnishi Y, Kijima H, Horii A, et al. Characterization of the mutations of the K-ras, p53, p16, and SMAD4 genes in 15 human pancreatic cancer cell lines. *Oncol Rep* (2001) 8(1):89–92. doi: 10.3892/or.8.1.89
32. Deer EL, González-Hernández J, Coursen JD, Shea JE, Ngatia J, Scaife CL, et al. Phenotype and genotype of pancreatic cancer cell lines. *Pancreas* (2010) 39(4):425–35. doi: 10.1097/MPA.0b013e3181c15963
33. Wang MT, Holderfield M, Galeas J, Delrosario R, To MD, Balmain A, et al. K-Ras promotes tumorigenicity through suppression of non-canonical wnt signaling. *Cell* (2015) 163(5):1237–51. doi: 10.1016/j.cell.2015.10.041
34. Zhu H, Wang D, Zhang L, Xie X, Wu Y, Liu Y, et al. Upregulation of autophagy by hypoxia-inducible factor-1 $\alpha$  promotes EMT and metastatic ability of CD133+ pancreatic cancer stem-like cells during intermittent hypoxia. *Oncol Rep* (2014) 32(3):935–42. doi: 10.3892/or.2014.3298
35. Wang P, Long M, Zhang S, Cheng Z, Zhao X, He F, et al. Hypoxia inducible factor-1 $\alpha$  regulates autophagy via the p27-E2F1 signaling pathway. *Mol Med Rep* (2017) 16(2):2107–12. doi: 10.3892/mmr.2017.6794
36. Yang MC, Wang HC, Hou YC, Tung HL, Chiu TJ, Shan YS. Blockade of autophagy reduces pancreatic cancer stem cell activity and potentiates the tumoricidal effect of gemcitabine. *Mol Cancer* (2015) 14:179. doi: 10.1186/s12943-015-0449-3
37. Nivon M, Richet E, Codogno P, Arrigo AP, Kretz-Remy C. Autophagy activation by NF $\kappa$ B is essential for cell survival after heat shock. *Autophagy* (2009) 5(6):766–83. doi: 10.4161/auto.8788
38. Lin CC, Lin MS. New insight into curcumin-based therapy in spinal cord injuries: Cisd2 regulation. *Neural Regener Res* (2016) 11(2):222–3. doi: 10.4103/1673-5374.177718
39. Paddock ML, Wiley SE, Axelrod HL, Cohen AE, Roy M, Abresch EC, et al. MitoNEET is a uniquely folded 2Fe 2S outer mitochondrial membrane protein stabilized by pioglitazone. *Proc Natl Acad Sci U.S.A.* (2007) 104(36):14342–7. doi: 10.1073/pnas.0707189104
40. Chen YF, Kao CH, Chen YT, Wang CH, Wu CY, Tsai CY, et al. Cisd2 deficiency drives premature aging and causes mitochondria-mediated defects in mice. *Genes Dev* (2009) 23(10):1183–94. doi: 10.1101/gad.1779509
41. Qin T, Cheng L, Xiao Y, Qian W, Li J, Wu Z, et al. NAF-1 inhibition by resveratrol suppresses cancer stem cell-like properties and the invasion of pancreatic cancer. *Front Oncol* (2020) 10:1038. doi: 10.3389/fonc.2020.01038
42. Sancho P, Burgos-Ramos E, Tavera A, Bou Kheir T, Jagust P, Schoenhals M, et al. MYC/PGC-1 $\alpha$  balance determines the metabolic phenotype and plasticity of pancreatic cancer stem cells. *Cell Metab* (2015) 22(4):590–605. doi: 10.1016/j.cmet.2015.08.015

43. Chandana S, Sabiker HM, Mahadevan D. Therapeutic trends in pancreatic ductal adenocarcinoma (PDAC). *Expert Opin Investig Drugs* (2019) 28(2):161–77. doi: 10.1080/13543784.2019.1557145
44. Hamacher-Brady A. Autophagy regulation and integration with cell signaling. *Antioxid Redox Signal* (2012) 17(5):756–65. doi: 10.1089/ars.2011.4410
45. Shang L, Wang X. AMPK and mTOR coordinate the regulation of Ulk1 and mammalian autophagy initiation. *Autophagy* (2011) 7(8):924–6. doi: 10.4161/aut.7.8.15860
46. Gonzalez-Noriega A, Grubb JH, Talkad V, Sly WS. Chloroquine inhibits lysosomal enzyme pinocytosis and enhances lysosomal enzyme secretion by impairing receptor recycling. *J Cell Biol* (1980) 85(3):839–52. doi: 10.1083/jcb.85.3.839
47. Yavon A, Cabantchik ZI, Ginsburg H. Susceptibility of human malaria parasites to chloroquine is pH dependent. *Proc Natl Acad Sci U.S.A.* (1985) 82(9):2784–8. doi: 10.1073/pnas.82.9.2784
48. Itakura E, Kishi C, Inoue K, Mizushima N. Beclin 1 forms two distinct phosphatidylinositol 3-kinase complexes with mammalian Atg14 and UVRAG. *Mol Biol Cell* (2008) 19(12):5360–72. doi: 10.1091/mbc.e08-01-0080
49. Russell RC, Tian Y, Yuan H, Park HW, Chang YY, Kim J, et al. ULK1 induces autophagy by phosphorylating beclin-1 and activating VPS34 lipid kinase. *Nat Cell Biol* (2013) 15(7):741–50. doi: 10.1038/ncb2757
50. Petherick KJ, Conway OJ, Mpmhanga C, Osborne SA, Kamal A, Saxty B, et al. Pharmacological inhibition of ULK1 kinase blocks mammalian target of rapamycin (mTOR)-dependent autophagy. *J Biol Chem* (2015) 290(48):28726. doi: 10.1074/jbc.A114.627778
51. Singha B, Laski J, Ramos Valdés Y, Liu E, DiMattia GE, Shepherd TG. Inhibiting ULK1 kinase decreases autophagy and cell viability in high-grade serous ovarian cancer spheroids. *Am J Cancer Res* (2020) 10(5):1384–99. Available at: <https://e-century.us/files/ajcr/10/5/ajcr0108592.pdf>.
52. Egan DF, Chun MG, Vámos M, Zou H, Rong J, Miller CJ, et al. Small molecule inhibition of the autophagy kinase ULK1 and identification of ULK1 substrates. *Mol Cell* (2015) 59(2):285–97. doi: 10.1016/j.molcel.2015.05.031
53. Lu J, Zhu L, Zheng LP, Cui Q, Zhu HH, Zhao H, et al. Overexpression of ULK1 represents a potential diagnostic marker for clear cell renal carcinoma and the antitumor effects of SBI-0206965. *EBioMedicine* (2018) 34:85–93. doi: 10.1016/j.ebiom.2018.07.034
54. Tang F, Hu P, Yang Z, Xue C, Gong J, Sun S, et al. SBI0206965, a novel inhibitor of Ulk1, suppresses non-small cell lung cancer cell growth by modulating both autophagy and apoptosis pathways. *Oncol Rep* (2017) 37(6):3449–58. doi: 10.3892/or.2017.5635
55. Ren H, Bakas NA, Vámos M, Chaikwad A, Limpert AS, Wimer CD, et al. Design, synthesis, and characterization of an orally active dual-specific ULK1/2 autophagy inhibitor that synergizes with the PARP inhibitor olaparib for the treatment of triple-negative breast cancer. *J Med Chem* (2020) 63(23):14609–25. doi: 10.1021/acs.jmedchem.0c00873
56. Liu J, Xia H, Kim M, Xu L, Li Y, Zhang L, et al. Beclin1 controls the levels of p53 by regulating the deubiquitination activity of USP10 and USP13. *Cell* (2011) 147(1):223–34. doi: 10.1016/j.cell.2011.08.037
57. Xiao J, Feng X, Huang XY, Huang Z, Huang Y, Li C, et al. Spautin-1 ameliorates acute pancreatitis via inhibiting impaired autophagy and alleviating calcium overload. *Mol Med* (2016) 22:643–52. doi: 10.2119/molmed.2016.00034
58. Ronan B, Flamand O, Vescovi L, Dureuil C, Durand L, Fassy F, et al. A highly potent and selective Vps34 inhibitor alters vesicle trafficking and autophagy. *Nat Chem Biol* (2014) 10(12):1013–9. doi: 10.1038/nchembio.1681
59. Zhou P, Li Y, Li B, Zhang M, Xu C, Liu F, et al. Autophagy inhibition enhances celecoxib-induced apoptosis in osteosarcoma. *Cell Cycle* (2018) 17(8):997–1006. doi: 10.1080/15384101.2018.1467677
60. Pan Y, Gao Y, Chen L, Gao G, Dong H, Yang Y, et al. Targeting autophagy augments in vitro and in vivo antimyeloma activity of DNA-damaging chemotherapy. *Clin Cancer Res* (2011) 17(10):3248–58. doi: 10.1158/1078-0432.CCR-10-0890
61. Wolpin BM, Robinson DA, Wang X, Chan JA, Cleary JM, Enzinger PC, et al. Phase II and pharmacodynamic study of autophagy inhibition using hydroxychloroquine in patients with metastatic pancreatic adenocarcinoma. *Oncologist* (2014) 19(6):637–8. doi: 10.1634/theoncologist.2014-0086
62. Boone BA, Bahary N, Zureikat AH, Moser AJ, Normolle DP, Wu WC, et al. Safety and biologic response of pre-operative autophagy inhibition in combination with gemcitabine in patients with pancreatic adenocarcinoma. *Ann Surg Oncol* (2015) 22(13):4402–10. doi: 10.1245/s10434-015-4566-4
63. Samaras P, Tusup M, Nguyen-Kim TDL, Seifert B, Bachmann H, von Moos R, et al. Phase I study of a chloroquine-gemcitabine combination in patients with metastatic or unresectable pancreatic cancer. *Cancer Chemother Pharmacol* (2017) 80(5):1005–12. doi: 10.1007/s00280-017-3446-y
64. Karasic TB, O'Hara MH, Loaiza-Bonilla A, Reiss KA, Teitelbaum UR, Borazanci E, et al. Effect of gemcitabine and nab-paclitaxel with or without hydroxychloroquine on patients with advanced pancreatic cancer: A phase 2 randomized clinical trial. *JAMA Oncol* (2019) 5(7):993–8. doi: 10.1001/jamaoncol.2019.0684
65. Yamamoto K, Venida A, Yano J, Biancur DE, Kakiuchi M, Gupta S, et al. Autophagy promotes immune evasion of pancreatic cancer by degrading MHC-I. *Nature* (2020) 581(7806):100–5. doi: 10.1038/s41586-020-2229-5
66. Reyes-Castellanos G, Abdel Hadi N, Carrier A. Autophagy contributes to metabolic reprogramming and therapeutic resistance in pancreatic tumors. *Cells* (2022) 11(3):426. doi: 10.3390/cells11030426
67. Bao S, Zheng H, Ye J, Huang H, Zhou B, Yao Q, et al. Dual targeting EGFR and STAT3 with erlotinib and alantolactone Co-loaded PLGA nanoparticles for pancreatic cancer treatment. *Front Pharmacol* (2021) 12:625084. doi: 10.3389/fphar.2021.625084
68. He R, Shi X, Zhou M, Zhao Y, Pan S, Zhao C, et al. Alantolactone induces apoptosis and improves chemosensitivity of pancreatic cancer cells by impairment of autophagy-lysosome pathway via targeting TFEB. *Toxicol Appl Pharmacol* (2018) 356:159–71. doi: 10.1016/j.taap.2018.08.003
69. Wu X, Jiang L, Zhang Z, He Y, Teng Y, Li J, et al. Pancreatic cancer cell apoptosis is induced by a proteoglycan extracted from. *Oncol Lett* (2021) 21(1):34. doi: 10.3892/ol.2020.12295
70. Zheng H, Yang L, Kang Y, Chen M, Lin S, Xiang Y, et al. Alantolactone sensitizes human pancreatic cancer cells to EGFR inhibitors through the inhibition of STAT3 signaling. *Mol Carcinog* (2019) 58(4):565–76. doi: 10.1002/mc.22951
71. Zhu Y, Bu S. Curcumin induces autophagy, apoptosis, and cell cycle arrest in human pancreatic cancer cells. *Evid Based Complement Alternat Med* (2017) 2017:5787218. doi: 10.1155/2017/5787218
72. Lin JH, Chen SY, Lu CC, Lin JA, Yen GC. Ursolic acid promotes apoptosis, autophagy, and chemosensitivity in gemcitabine-resistant human pancreatic cancer cells. *Phytother Res* (2020) 34(8):2053–66. doi: 10.1002/ptr.6669
73. Akkoc Y, Peker N, Akcay A, Gozuacik D. Autophagy and cancer dormancy. *Front Oncol* (2021) 11:627023. doi: 10.3389/fonc.2021.627023
74. Wang S, Zheng Y, Yang F, Zhu L, Zhu XQ, Wang ZF, et al. The molecular biology of pancreatic adenocarcinoma: translational challenges and clinical perspectives. *Signal Transduct Target Ther* (2021) 6(1):249. doi: 10.1038/s41392-020-00422-1
75. Lim J, Murthy A. Targeting autophagy to treat cancer: Challenges and opportunities. *Front Pharmacol* (2020) 11:590344. doi: 10.3389/fphar.2020.590344
76. Su H, Yang F, Fu R, Li X, French R, Mose E, et al. Cancer cells escape autophagy inhibition via NRF2-induced macropinocytosis. *Cancer Cell* (2021) 39(5):678–693.e11. doi: 10.1016/j.ccell.2021.02.016

# Frontiers in Pharmacology

Explores the interactions between chemicals and living beings

The most cited journal in its field, which advances access to pharmacological discoveries to prevent and treat human disease.

## Discover the latest Research Topics

[See more →](#)

### Frontiers

Avenue du Tribunal-Fédéral 34  
1005 Lausanne, Switzerland  
[frontiersin.org](https://frontiersin.org)

### Contact us

+41 (0)21 510 17 00  
[frontiersin.org/about/contact](https://frontiersin.org/about/contact)



### Frontiers in Pharmacology

